British Geological Survey
NATURAL ENVIRONMENT RESEARCH COUNCIL

Ghana Airborne Geophysics Project in the Volta and Keta Basins: BGS Final Report

Financed by the 8th European Development Fund to the Government of Ghana, Project No. 8 ACP GH 027/13, under the Mining Sector Support Programme

Geophysical Baselines Programme

Commissioned Report CR/09/02 N

BRITISH GEOLOGICAL SURVEY

GEOPHYSICAL BASELINES PROGRAMME
COMMISSIONED REPORT CR/09/02N

Ghana Airborne Geophysics Project in the Volta and Keta Basin: BGS Final Report

C J Jordan, J N Carney, C W Thomas, P McDonnell

Contributor

P Turner, K McManus, F M McEvoy

Keywords

Ghana, Volta, Keta, remote sensing, geophysics, minerals, EU.

Front cover

A typical roadside exposure, also note the dip slopes in the distance.

Bibliographical reference

JORDAN CJ, CARNEY JN, THOMAS CW, MCDONNELL P, TURNER P, MCMANUS K, MCEVOY FM. 2009. Ghana Airborne Geophysics Project: BGS Final Report. *British Geological Survey Commissioned Report*, CR/09/02. 325pp.

Keyworth, Nottingham British Geological Survey 2009

BRITISH GEOLOGICAL SURVEY

The full range of our publications is available from BGS shops at Nottingham, Edinburgh, London and Cardiff (Welsh publications only) see contact details below or shop online at www.geologyshop.com

The London Information Office also maintains a reference collection of BGS publications, including maps, for consultation.

We publish an annual catalogue of our maps and other publications; this catalogue is available online or from any of the BGS shops.

The British Geological Survey carries out the geological survey of Great Britain and Northern Ireland (the latter as an agency service for the government of Northern Ireland), and of the surrounding continental shelf, as well as basic research projects. It also undertakes programmes of technical aid in geology in developing countries.

The British Geological Survey is a component body of the Natural Environment Research Council.

British Geological Survey offices

BGS Central Enquiries Desk

Tel 0115 936 3143 Fax 0115 936 3276

email enquiries@bgs.ac.uk

Kingsley Dunham Centre, Keyworth, Nottingham NG12 5GG

Tel 0115 936 3241 Fax 0115 936 3488

email sales@bgs.ac.uk

Murchison House, West Mains Road, Edinburgh EH9 3LA

Tel 0131 667 1000 Fax 0131 668 2683

email scotsales@bgs.ac.uk

London Information Office at the Natural History Museum Cromwell Road, London SW7 5BD

Tel 020 7589 4090 Fax 020 7584 8270

Tel 020 7942 5344/45 email bgslondon@bgs.ac.uk

Columbus House, Greenmeadow Springs, Tongwynlais, Cardiff CF15 7NE

Tel 029 2052 1962 Fax 029 2052 1963

Forde House, Park Five Business Centre, Harrier Way, Sowton EX2 7HU

Tel 01392 445271 Fax 01392 445371

Maclean Building, Crowmarsh Gifford, Wallingford OX10 8BB

Tel 01491 838800 Fax 01491 692345

Geological Survey of Northern Ireland, Colby House, Stranmillis Court, Belfast BT9 5BF

Tel 028 9038 8462 Fax 028 9038 8461

www.bgs.ac.uk/gsni/

Parent Body

Natural Environment Research Council, Polaris House, North Star Avenue, Swindon SN2 1EU

Tel 01793 411500 Fax 01793 411501

www.nerc.ac.uk

Website www.bgs.ac.uk

Shop online at www.geologyshop.com

Foreword

This is the final report derived from a study by the British Geological Survey (BGS) working in collaboration with Fugro Airborne Surveys Ltd in the Volta and Keta Basins of Ghana. Outputs from the project include geological and topographic maps, processed satellite imagery, training manuals, a differential GPS survey, a fully attributed GIS, and a series of abstracts and excursion guide published in the Voltaian Basin Workshop Proceedings (Kalsbeek, 2008). A detailed report was produced following the completion of Phase 1 (Jordan et al., 2006) while this document summarises all of the project deliverables.

The mineral sector in Ghana has shown significant growth in the past decade, thanks to an investor-friendly environment created by the Government since the mid 1980s. However, the success of the sector, which represents 38% of the total export value and employs more than 36,000 people, is unlikely to be sustainable, due to both internal (weak regulatory institutions and geological support organisations) and external (limited exploration funds and fierce international competition) factors. The rapid depletion of known resources through recently introduced intensive mining methods and the lack of discovery of new deposits implies that mineral output may decline substantially over the next 5 to 7 years. Private sector mining operations cannot be sustained, unless the mining institutions improve their operations, provide up-to-date geological and geophysical information to discover new resources and formulate and implement new policies.

The European Union has provided funding to the Government of Ghana, under the Mining Sector Support Programme (MSSP), to support these interventions. The MSSP overall objectives are to sustain the country's mining sector economic performance, to alleviate poverty by increasing employment and to mitigate the mines' negative environmental impacts. Its specific purpose is to enhance institutional capacities to effectively promote and regulate the mineral resources sector in order to reverse the current trend of reduced private-sector mineral exploration, while facilitating the development of sustainable medium-term projects.

The main beneficiaries of the Programme are the institutions such as the Geological Survey Department (GSD), the Ministry of Mines (MOM), the Minerals Commission (MC), and the Mines Department (MD). The MC is the Executing Agency of the programme and the finance is provided through the Ministry of Finance and the National Authorising Officer (NAO). The other stakeholders that will benefit from the programme implementation are the various mining communities, i.e. local population, mineworkers, mining and exploration companies and the country at large.

Acknowledgements

A large number of individuals in Ghana and the UK have contributed to the success of this project. This assistance has been received at all stages of the study. In addition to supplying data, many individuals have freely given their advice, and provided local knowledge. Of the many individuals who have contributed to the project we would particularly like to thank the following:

Mr Philip Amoako and Mr Agyei Duodo (successive Directors of the GSD)

Ms Akua Appiah-Akuramaa and Mr Joehida Quaye (GSD remote sensing counterparts)

Dr Per Kalvig (GEUS)

Mr Paul Asante, Mr Amos Essel and Mr Branson (GSD drivers)

Mr Jerome Vidal, Mr Harald van der Berg & Mr George Asiamah (successive Fugro Project Managers, Ghana)

Dr Warwick Crowe, Ms Shonny Jackson-Hicks, Dr Steve Batty, Dr Craig Buchan & Helen Anderson (Fugro Airborne Surveys, Perth)

Dr Thorkild Maack Rasmussen and Mr Leif Thorning (GEUS QC Project)

Mr Kwame Odame Boamah (Head, Information Management Division, GSD)

Dr John Acquah Asabir (MSSP, PMU)

BGS Cartographic staff, including Kathy Arbon, Bob Cooper, Ian Longhurst, Sheila Myers, Tony Myers and Simon Ward.

Contents

FIGURES

TABLES

Summary

This report describes the work undertaken by BGS between November 2006 and March 2009 in collaboration with Fugro Airborne Surveys Pty Ltd on an airborne geophysical survey and ground reconnaissance mapping of the Volta River and Keta Basins, Ghana. The project was supported by the EU as part of the Mining Sector Support Programme, Project Number 8ACP GH 027/13. The initial contract duration was three years, but this was extended by five months to account for acquisition of gravity data by another project.

Some parts of Ghana have been airborne surveyed as part of the Mining Sector Development and Environmental Project, co-funded by the World Bank and the Nordic Development Fund, but no work was carried out on the Volta River and Keta basins, which together form a major portion of the Ghanaian territory.

The approximate areas covered by the surveys are estimated at 98,000 km² for the satellite imagery and the airborne geophysics, except for the Time Domain Electromagnetic (TDEM) survey which was limited to 60,000 km².

The main beneficiary of this project is the Geological Survey Department, GSD. The work enhanced its geological infrastructure and its personnel received hands-on training on modern geological mapping technology. Indirect beneficiaries were the mining and exploration companies that can follow up the reconnaissance work with detailed exploration work.

The project was conducted in five phases, and this document reports on the BGS input to Phase 1, 4 and 5, with no inputs required in Phases 2 and 3:

- Phase1: geological outline through Radar and optical satellite imageries.
- Phase 2: airborne geophysical survey over the two basins for magnetics and Gamma Ray spectrometry (Fugro survey).
- Phase 3: airborne electromagnetic and magnetic geophysical survey of specific areas, following the completion and interpretation of phase 2, using fixed wing time domain technology (Fugro survey).
- Phase 4: interpretation of the combined geology and geophysics.
- Phase 5: production of factual and interpretation maps.

The full list of BGS products is outlined in Table 1 below, while Jordan et al. (2006) describe the products delivered on schedule in Phase 1.

	Deliverables / Products	Delivered
Phase 1	Acquire and process optical and microwave imagery	✓
	Acquire and process a Digital Terrain Model, including extracting 30m contours	✓
	Conduct a Differential GPS survey	✓
	Produce 1:100,000 scale topographic maps	✓
	Produce 1:100,000 scale preliminary geology maps	✓
	Fully attributed GIS	✓
	Formal training courses in Remote Sensing and Geophysics	✓
Phase 2	No BGS input required	
Phase 3	No BGS input required	
Phase 4	Work alongside project geophysicists to interpret new datasets	✓
	Integrate geophysics with the revised geology and imagery to define exploration models	✓
	Test the exploration models using prospectivity analysis	✓
	Field verification and acquisition of samples for verification of targets	✓
	Input to Final Report	✓
Phase 5	Fully attributed GIS with updated linework, point observations and potential mineral occurrences (for inclusion in the final maps produced by Fugro)	✓

Table 1 BGS project deliverables listed by Phase.

As well as the five phases listed above, BGS staff also played a major part in the Voltaian Stratigraphic Workshop (10 – 17th March 2008) that was organised by Dr Per Kalvig of GEUS. BGS staff gave five presentations, chaired a session and led the field excursion (including producing the field guide). An agreed outcome of Workshop discussions was that a BGS representative would sit on the Voltaian stratigraphic committee.

In order to complete the contract deliverables, and attend the Workshop, BGS teams made five visits to Ghana as listed below:

1. Compilation trip to review and collect all relevant datasets and to meet counterparts and local experts (e.g. University academics and topographic survey departments)
2. Differential GPS survey
3. First geological fieldwork season, with two field teams
4. Second geological fieldwork season, with two field teams
5. Voltaian Stratigraphy Workshop and excursion.

1 Introduction

The Volta and Keta Basins were defined in the contract using a table of WGS84 Datum UTM 30N coordinates as well as a diagrammatic representation, as follows (Table 2 and Figure 1). The remote sensing datasets acquired by BGS extend for a minimum of 1km beyond the given boundary in order to provide a context for the interpretations, and also importantly, so that the algorithms (such as contouring) that were applied to the data were not truncated unnaturally at the project area boundary.

WGS84 Datum, UTM30N			LATITUDE			LONGITUDE		
#	X	Y	DD	MM	SS.s	DD	MM	SS.s
Volta Basin Survey Area								
A	820762.0E	1191975.2N	10	46	08.48N	0	04	02.13W
B	815175.7E	1189991.2N	10	45	05.69N	0	07	06.45W
C	622451.8E	1056695.0N	09	33	27.27N	01	53	03.25W
D	622954.7E	843746.3N	07	37	54.29N	01	53	07.07W
E	614465.6E	843593.7N	07	37	50.02N	01	57	44.11W
F	720934.3E	742281.1N	06	42	40.56N	01	00	04.71W
G	722423.2E	738209.8N	06	40	27.86N	0	59	16.78W
H	746543.4E	724716.8N	06	33	05.40N	0	46	13.66W
I	747899.3E	725571.8N	06	33	33.03N	0	45	29.42W
J	816338.1E	675939.7N	06	06	27.39N	0	08	31.90W
K	855332.0E	730025.4N	06	35	38.83N	0	12	45.91E
L	860060.1E	729930.2N	06	35	34.73N	0	15	19.61E
M	857671.5E	1042598.8N	09	25	00.53N	0	15	22.49E
Point M to Point A follows the country border								
A	820762.0E	1191975.2N	10	46	08.48N	0	04	02.13W

WGS84 Datum, UTM30N			LATITUDE			LONGITUDE		
#	X	Y	DD	MM	SS.s	DD	MM	SS.s
Keta Basin Survey Area								
N	914137.2E	726699.1N	06	33	37.40N	0	44	36.60E
O	911503.8E	724083.1N	06	32	13.02N	0	43	10.39E
P	858956.0E	636100.7N	05	44	44.19N	0	14	25.15E
Point P to Point N follows the country border								
N	914137.2E	726699.1N	06	33	37.40N	0	44	36.60E

Table 2 Survey boundaries of the Volta and Keta Basins in UTM 30N coordinates.

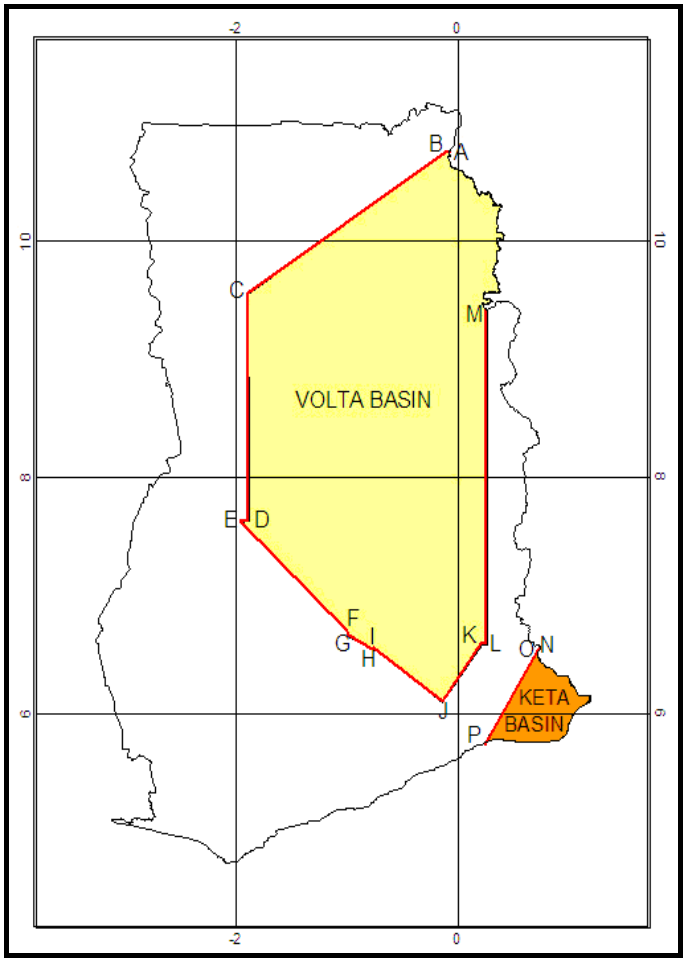

Figure 1 Geographical location of the Volta and Keta Basins, Ghana.

A report has already been published that details the BGS methodology and results from Phase 1 of the project (Jordan *et al.*, 2006). This document briefly summarises that work along with progress made in the successive phases. An outline of the methodology for the project is shown in Figure 2, divided for ease of explanation into three stages. The methodology is described briefly in this section and expanded upon in later sections of this document.

The first stage (outlined in blue) involved compiling and assessing any available appropriate information, which was collected during a visit to Ghana as well as from UK institutions and other European collections. These data were assessed before those deemed reliable were used to produce an outline geological model, *i.e.* a conceptual model of the geology of the Volta and Keta Basins. A Geographic Information System (GIS) was used to compile, compare and collect all spatially-enabled datasets throughout the project, as well as for image interpretation, prospectivity modelling and map production.

As shown in Figure 2 the early steps in Stage 2 run concurrently with Stage 1, so while existing geological publications were collected and analysed, the BGS also acquired a range of remote sensing datasets including Landsat TM and ETM optical imagery, Radarsat microwave imagery and a Digital Terrain Model (DTM). These were geocorrected using ephemeris data from the satellite sensors along with Ground Control Points (GCPs) from the differential GPS survey. Following manipulation in digital image processing software to highlight geological features, the imagery was interpreted in light of the geological model, then 'traditional' reconnaissance fieldwork was undertaken before a GIS was used to produce preliminary geological and topographical maps at 1:100,000 scale. These were delivered in both hardcopy and digital formats.

The importance of the imagery and its interpretation cannot be overstated. We were limited to one month in the field for each of the two field seasons, and had to cover an area approximately

100,000km^2, the equivalent of Scotland and Wales combined. It was therefore necessary to use the imagery to interpret as much of the geology as possible prior to and after fieldwork.

Stage 3 (outlined in red below) consisted of integrating the newly-acquired Fugro geophysical datasets and re-evaluating the interpretation during a second season of fieldwork. Additional rock samples were collected in the second field season and the most appropriate from the two field seasons underwent multi-element and fire assay analyses. The results are described in the mineral prospectivity section of this report.

The second field season enabled BGS to update the geological model and the GIS, and subsequently to deliver linework, including mineral potential zones to Fugro and the GSD. Dr Warwick Crowe and Ms Shonny Jackson-Hicks (Fugro) were in the field area at the same time and this allowed the teams to meet occasionally and to have fruitful discussions on the geology and potential mineral resources. Whereas the first set of geological and topographic maps were published by BGS at 1:100,000 scale, the second set were published by Fugro at 1:250,000 scale using the BGS linework merged with the Fugro geophysics interpretations.

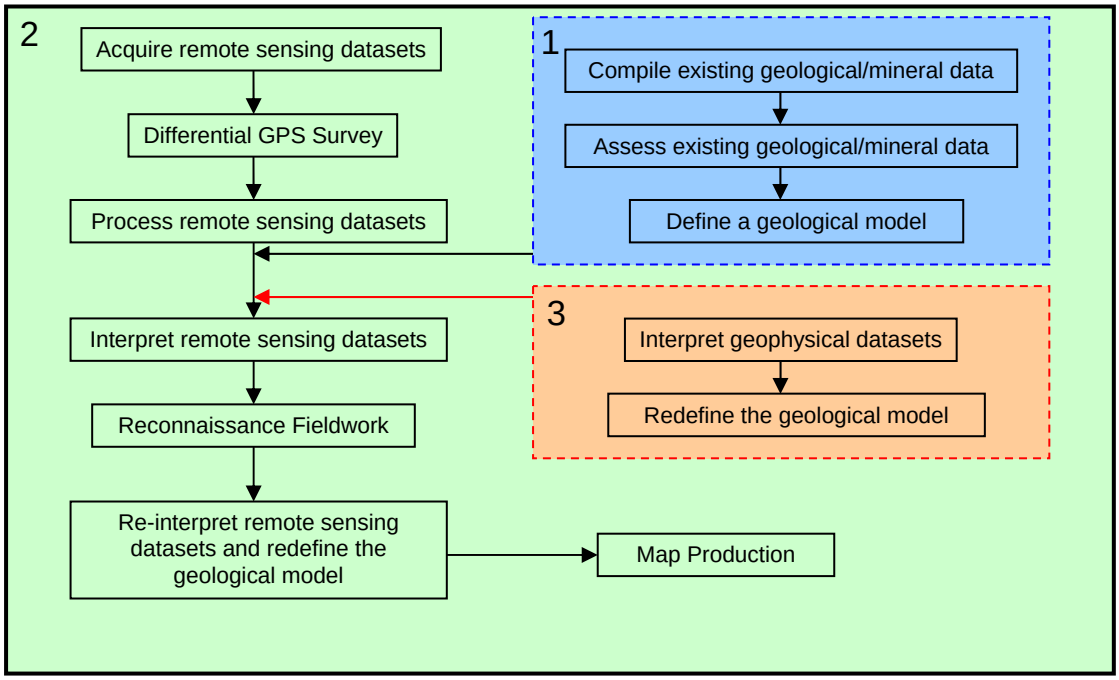

Figure 2 Flowchart for BGS project methodology.

Dr Per Kalvig (GEUS) organised a workshop in Ghana to discuss the stratigraphy of the Voltaian, held from 10 – 17th March 2008. BGS gave five presentations, chaired a session and led the field excursion. Participation in this workshop was a useful exercise as it enabled us to meet staff from other organisations working in the area and to discuss and review their geological models. It also resulted in the invitation for a BGS representative to sit on a Voltaian stratigraphic committee.

2 Data Sources and Processing

Three satellite remote sensing datasets were acquired by BGS; optical Landsat, Radarsat and a Digital Terrain Model (DTM), as specified in the contract. These datasets and their processing are described in detail in Jordan *et al.*, (2006). Copies of both the raw and processed data were transferred onto GSD computers, along with the image processing software, ERMapper 7.0. All of the data were referenced to the WGS84 UTM projection so that they can be easily referenced in the GSD GIS.

2.1 LANDSAT IMAGERY

Landsat data is optical and is therefore susceptible to interference from haze, clouds and other types of atmospheric interference. Furthermore, the satellite passes over the same place every 16 days due to its orbital parameters, so it is necessary to have cloud/haze-free conditions at the time when the sensor passes overhead in order to acquire suitable imagery. A combination of scenes from different dates is therefore often required in order to compile a cloud-free mosaic.

Two sets of Landsat imagery were used in this project; Thematic Mapper (TM) from the Landsat-5 platform, and Enhanced Thematic Mapper (ETM) from the Landsat-7 platform. Twelve scenes (each measuring 180km by 180km) were needed for complete coverage of the Volta and Keta Basins, as listed in Table 3 and shown in Figure 3. Each scene required approximately 750Mb of disk space

	Landsat Thematic Mapper		**Landsat Enhanced Thematic Mapper**	
Path / Row Designation	**Date of acquisition**	**Spectral bands**	**Date of acquisition**	**Spectral bands**
192 56	13/01/1986	1-7	04/04/2001	1-8
193 53	30/10/1987	1-7	04/12/2000	1-8
193 54	10/01/1991	1-7	04/12/2000	1-8
193 55	10/01/1991	1-7	07/12/2001	1-8
193 56	25/12/1990	1-7	04/02/2000	1-8
194 53	11/11/1989	1-7	07/11/1999	1-8
194 54	11/11/1986	1-7	07/11/1999	1-8
194 55	11/01/1986	1-7	20/03/2002	1-8
194 56	29/12/1986	1-7	15/01/2002	1-8
195 53	18/01/1986	1-7	03/11/2001	1-8
195 54	02/11/1986	1-7	02/02/2000	1-8
195 55	18/01/1986	1-7	02/02/2000	1-8

Table 3 Landsat images listed both by Path/Row and date of acquisition by the sensor.

The Landsat-5 satellite is older than Landsat-7, and the spatial resolution is lower, ranging from 30 to 120 m for TM and from 15 to 60 m for ETM. A combination of both image types was useful to ensure cloud-free coverage and also because the images are from different times of year so vegetation differences could be used to highlight geological features.

Ephemeris data, which is extracted from the satellite sensor at the time of image acquisition, was used initially to position the imagery in geographical space – in this case the client requested us to use WGS84 with the appropriate UTM zone (North 30 and North 31). Following geocorrection all the imagery was displayed in a single viewer to ensure that the overlap between scenes is accurate and to confirm that we had full coverage for both basins in the project area. Once the differential GPS survey was completed, and the data processed, they were used to validate the geocorrection accuracy of the Landsat data. All of the GPS points were plotted within 1 pixel of their location on the imagery, proving the rectification to be accurate.

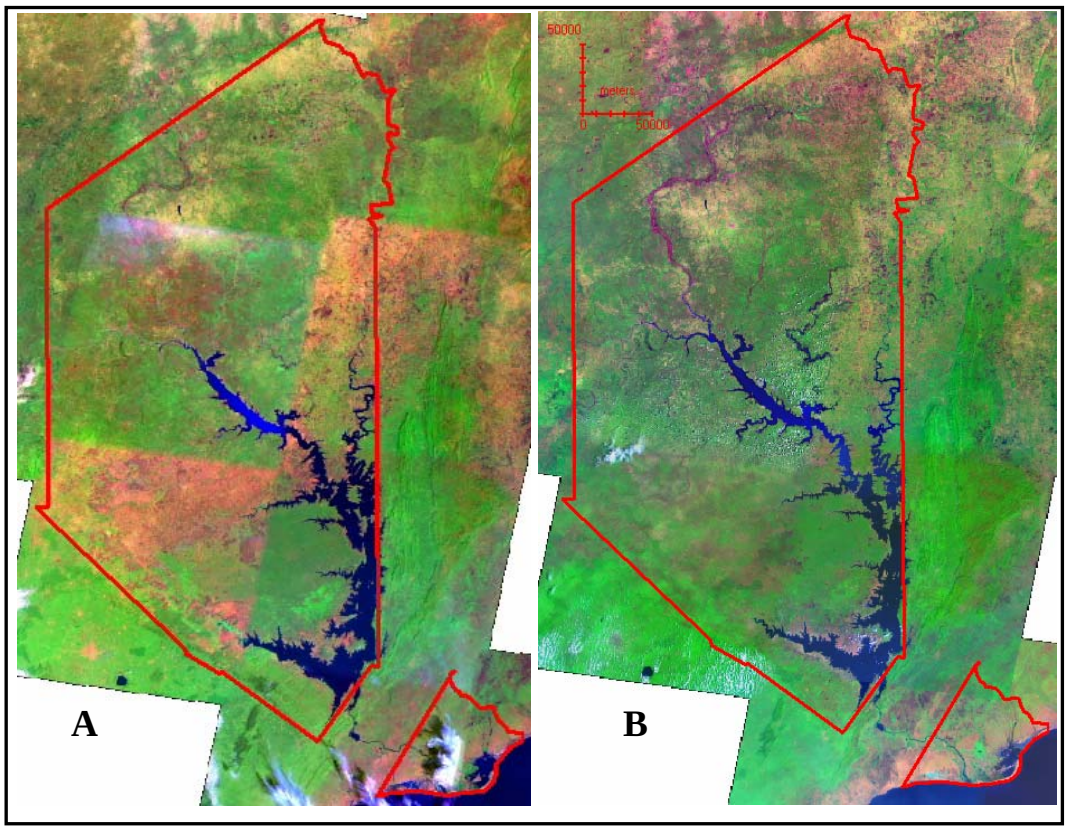

Figure 3 Landsat image mosaics, band combination 7,4,1 A) TM data; B) ETM data.

Regional digital image processing techniques were applied to the Landsat imagery to highlight the geological information, followed by advanced image processing in specific areas of interest, as described below.

Experience has shown that certain band combinations provide the most useful information for geological and topographical feature extraction from Landsat imagery. The band combinations 741 and 457, displayed as Red, Green, and Blue (R,G,B) were selected for the Volta and Keta Basins with contrast stretches applied to each scene to optimise the level of information that can be extracted. The individual scenes were then combined into a single seamless mosaic for ease of use in the GIS. The mosaic was also saved in an ECW compressed format which retains the spatial and spectral information of the imagery, but the smaller file size enables it to be opened in lower specification PCs. The raw Landsat ETM data require up to 7.5 GB of disk space while the compressed data were reduced to 30 MB.

Advanced processing included band ratioing to emphasise spectral contrasts between iron minerals and clays, and Principal Components Analysis (PCA) to reveal more subtle spectral features. These techniques were used to generate enhanced image products prior to interpretation.

Band ratioing was used to create mineral composite images using the following inputs

i. Input 1 (red) = 5/4 Ferrous

ii. Input 2 (green) = 5/7 Clay

iii. Input 3 (blue) = 3/1 Iron oxide

The resulting images are displayed as R,G,B where red areas relate to ferrous minerals, green areas indicate the presence of clays and blue areas are indicative of iron oxides. The mineral ratio images required 3.75 GB of file space. Advanced processing methods such as the ‘Crosta technique’ were applied to the Landsat ETM data in an effort to distinguish gossans and areas of alteration. Unfortunately the thickness of superficial cover in combination with the degree of weathering and the vegetation rendered these techniques invalid.

2.2 RADARSAT IMAGERY

The contract specified that high resolution Radarsat imagery would be obtained; therefore ninety-two frames were purchased, providing complete coverage of both the Volta and Keta Basins. Table 4 lists the specification of the frames including the dates of acquisition by the satellite.

Image Date	Orbit	Number of frames	Beam mode	Spatial resolution (m)
28/04/1997	07727	5	F1F	6.25
31/05/1998	13415	11	F5	6.25
18/07/1998	14101	7	F4	6.25
28/07/1998	14244	6	F4F	6.25
04/08/1998	14344	12	F4N	6.25
11/08/1998	14444	3	F4N	6.25
21/08/1998	14587	7	F4N	6.25
28/08/1998	14930	9	F3	6.25
14/09/1998	14930	9	F3	6.25
01/03/1999	17331	10	F2	6.25
06/02/2006	53546	1	F1	6.25
09/02/2006	53589	2	F2	6.25
13/02/2006	53646	2	F4F	6.25
02/03/2006	53889	2	F2F	6.25
05/04/2006	54375	6	F2N	6.25
Total		**92**		

Table 4 Index of Radarsat data acquired for the project.

Each scene was quality-checked statistically and visually before geocorrection. Initial checks of the Radarsat data indicated that rectification using the ephemeris data produced inaccuracies up to 320m so the images were compiled into strips and rectified using GCPs referenced against the Landsat data. An average of 200 GCPs were used per strip resulting in a total number of approximately 3,600 control points to rectify the Radarsat data. The raw Radarsat data required 23 GB of disk space.

After each strip was rectified the imagery was contrast-matched, which is the process that attempts to reduce (or ideally remove) any variations between the strips. This is done using the histogram break-point editor in the digital image processing software, and it requires a substantial input from an experienced image analyst in order to produce a seamless result (Figure 4 B). A seamless mosaic makes the task of interpretation easier because the geologist is not distracted by contrast variations that are due to image variance rather than geological features.

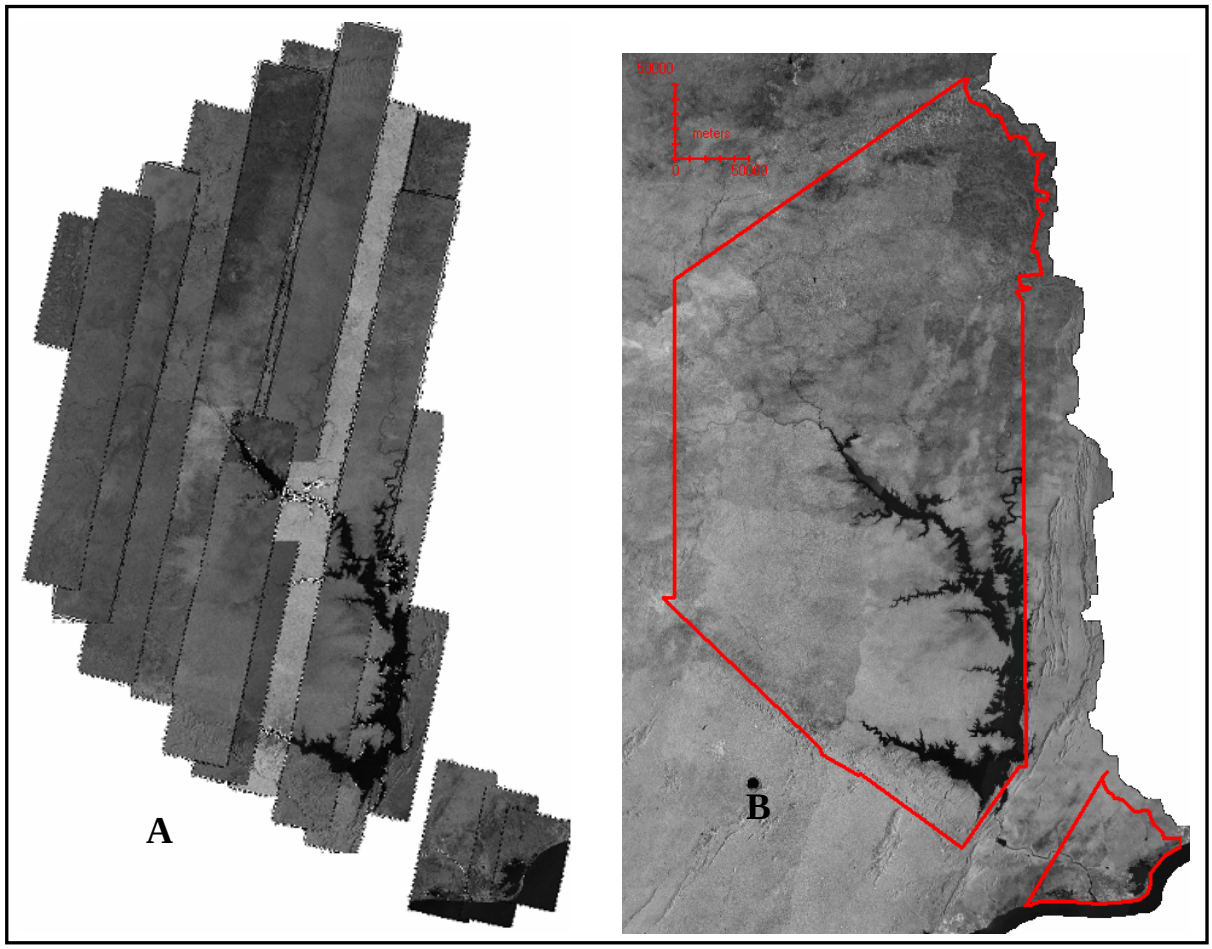

Figure 4 Radarsat imagery; A) fine beam strips (6.25 m resolution) and B) processed mosaic (25 m resolution).

The processed radar images were exported in a compressed format so that they could be viewed and interpreted in the GIS alongside the other raster and vector datasets.

2.3 DIGITAL TERRAIN MODEL

A digital terrain model (DTM) with a 50 m horizontal grid spacing and a vertical accuracy of less than 16m was derived from the Shuttle Radar Topography Mission (SRTM) data. The DTM extends 1km beyond the periphery of the project area and also includes the region between the Volta and Keta Basins so that modelling and interpolations, such as the creation of contours will extend smoothly to the limits of the area. The total area covered by the dataset is 80,440km^2, requiring 355 MB of disk space. The DTM was acquired as a source for metric contours and as a base for geological/geomorphological interpretation. Figure 5 is an illustration of the raw DTM with the basin boundaries delimited in red.

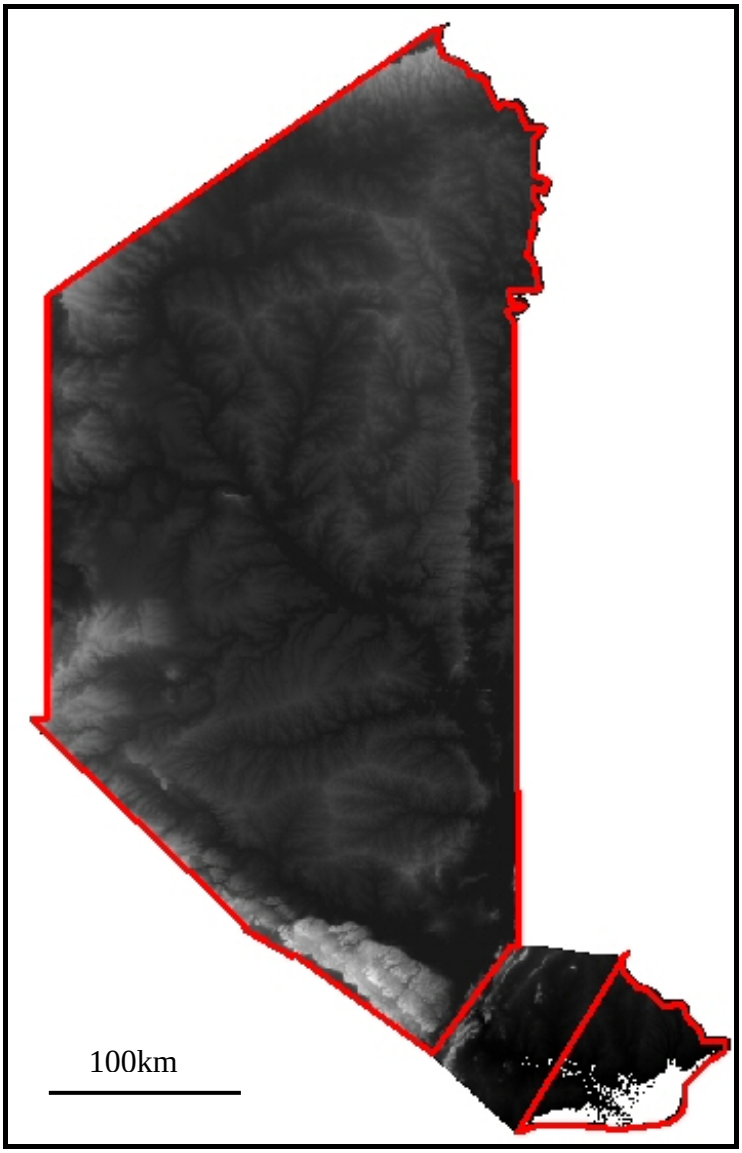

Figure 5 DTM data with the outlines of the Volta and Keta Basins superimposed.

Before the DTM was used to derive new information such as contours and geological features, it was necessary to ascertain and confirm its spatial accuracy, this is explained in detail in Jordan et al (2006) and summarised here. The DTM elevations were compared with those from the differential GPS survey. The difference values were plotted to assess the overall vertical accuracy of the GPS data with respect to the DTM (Figure 6).

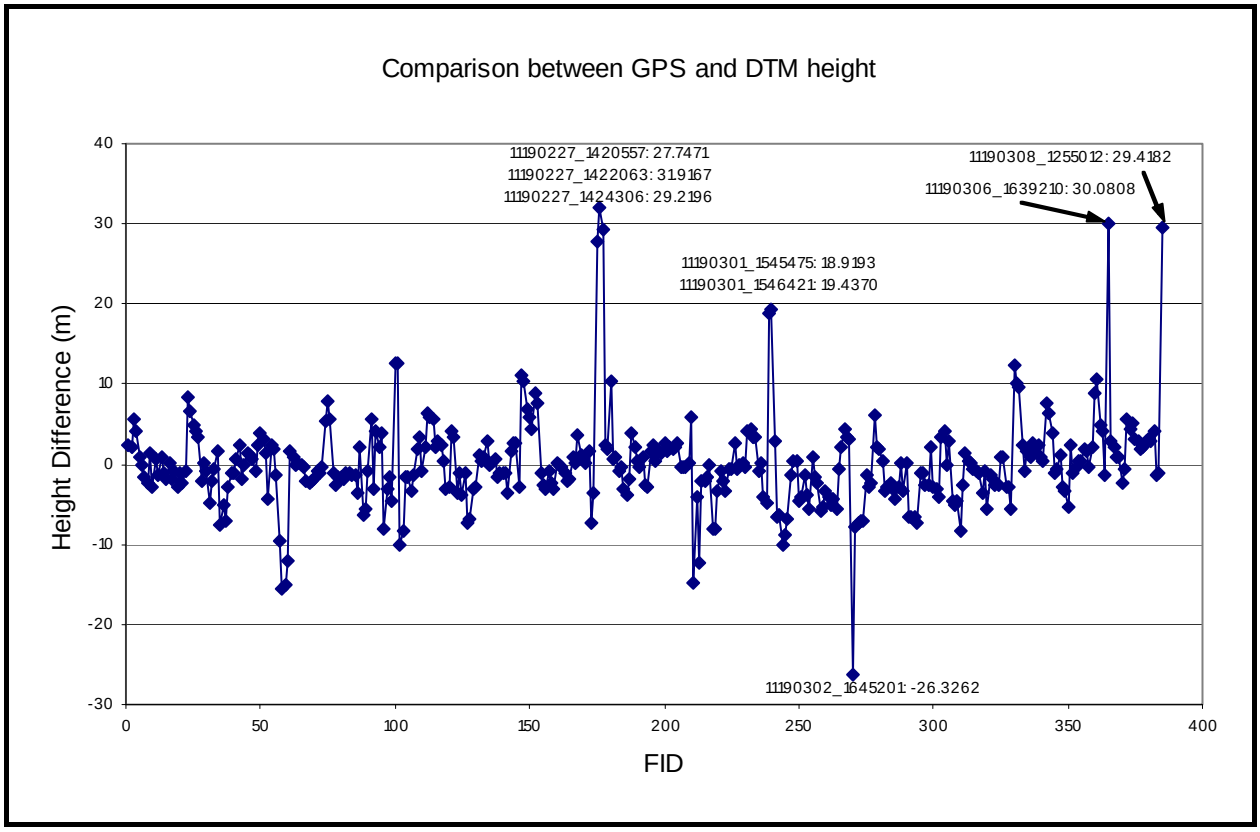

Figure 6 Graph indicating the difference between the GPS and DTM height values.

The figure above indicates that the difference between the GPS and the DTM is within the predicted vertical height accuracy except for eight locations (Table 5). The positional height quality (POSNHGTQTY) of these points is similar to the other GPS points so the height discrepancies cannot be a result of GPS error.

FID	PointID	ELLIPHGT (GPS)	RASTERVALU (DTM)	DIFFERENCE (GPS-DTM)	POSNHGTQTY
174	11190227_1420557	282.3241	254.5770	27.7471	0.912
175	11190227_1422063	286.4937	254.5770	31.9167	1.474
176	11190227_1424306	286.932	257.7123	29.2197	0.857
238	11190301_1545475	114.5331	95.6138	18.9193	2.26
239	11190301_1546421	115.0508	95.6138	19.4370	1.92
270	11190302_1645201	201.6035	227.9297	-26.3262	1.108
364	11190306_1639210	376.1204	346.0396	30.0808	1.661
384	11190308_1255012	269.6565	240.2383	29.4182	1.186

Table 5 Anomalous points and their associated height values.

To test where these errors may originate, each position was checked on the Landsat ETM imagery in order to determine if there were local factors that may have influenced the results. The conclusion is that the seven points above are affected by factors such as proximity to a steep slope, or a tree canopy. The example below (FID 174) highlights this issue. This GPS control point was collected at the edge of a steep slope as shown by the cyan dot on the Landsat imagery at scales of 1:50,000 (left) 1:25,000 (centre) and 1:10,000 (right) and on the accompanying photograph taken in the field. However the DTM has a planimetric accuracy of 50m so the height is an average of the elevation collected on a footprint 50m by 50m which does not match the point measurement taken by the differential GPS in this case.

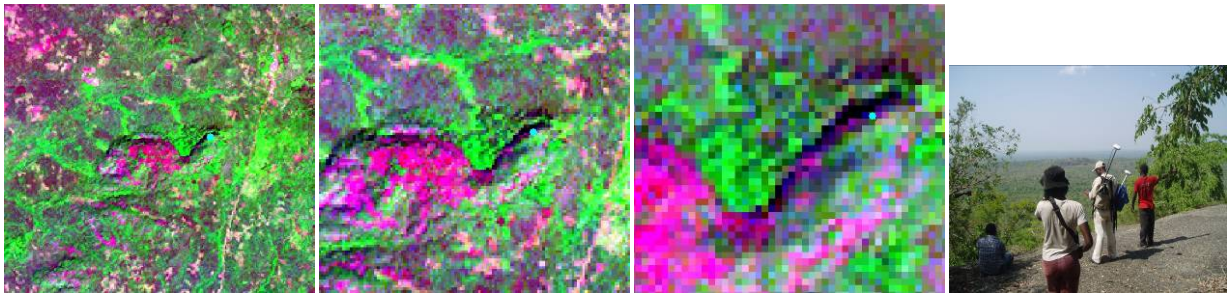

Figure 7 Anomalous GPS point (cyan dot) plotted on the Landsat ETM imagery and photographed in the field.

The DTM was processed to extract geomorphological and geological information once the accuracy of the data was confirmed. A smoothing algorithm was applied to the data to reduce the impact of artefacts on the automatic and manual interpretations. Following this, various derivative images were produced including relief images shaded from various perspectives, as well as slope maps (Figure 8). These maps were used directly to interpret breaks in slope which are used in feature mapping (i.e. using geomorphology to interpret geological structure and lithologies) as well as to determine the texture(s) of the terrain, which also provides valuable information on structure and lithology.

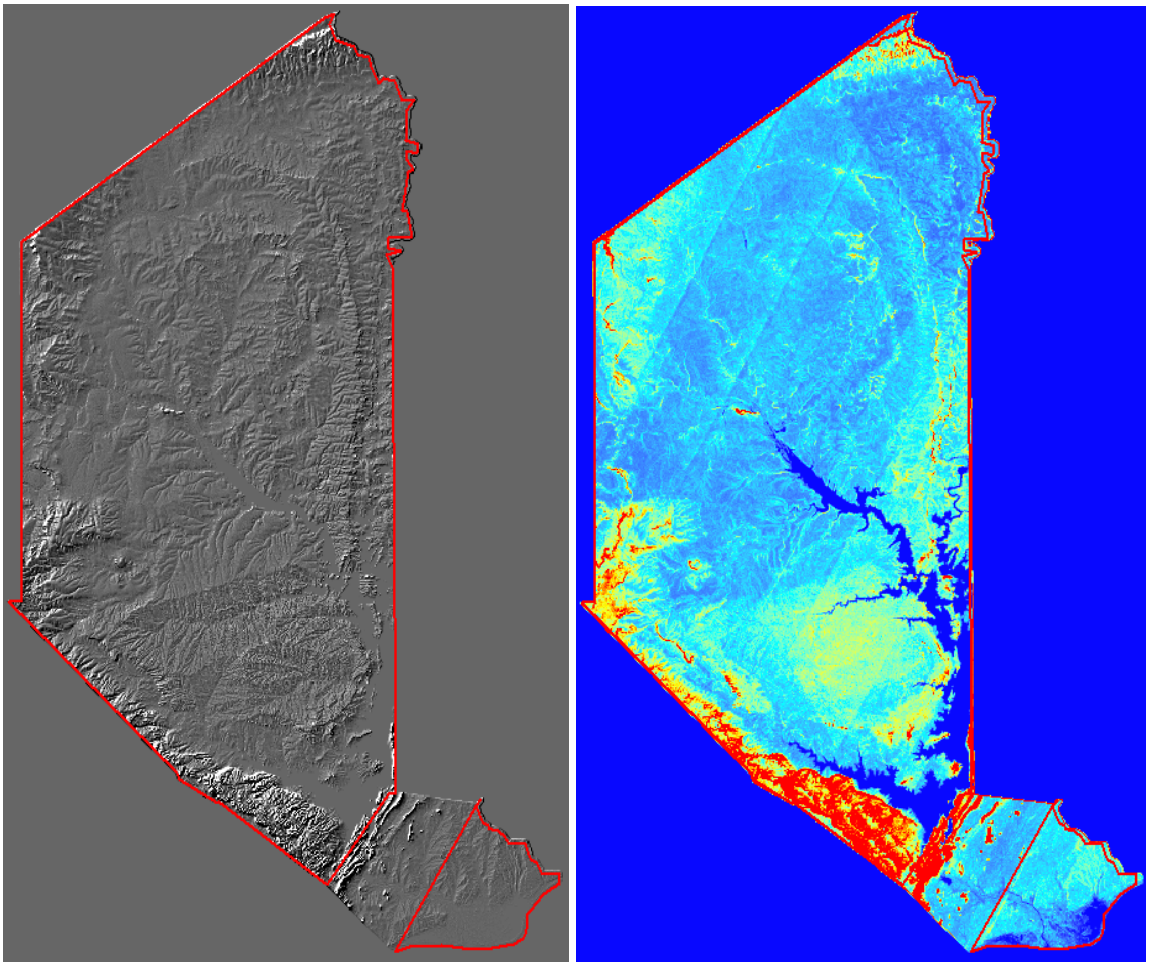

Figure 8 Shaded relief and slope maps derived from the DTM.

Contours at 30m intervals were derived from the smoothed DTM using the Surface Analysis module of the 3D Analyst extension of ArcGIS 9. Contours less than 700m long were deleted automatically as they cannot be distinguished on a map at 1:100,000. An example of the contours produced for the northern tip of the Volta Basin is illustrated in Figure 9. Note that although the contours below are not labelled, they are each labelled on the topographic maps.

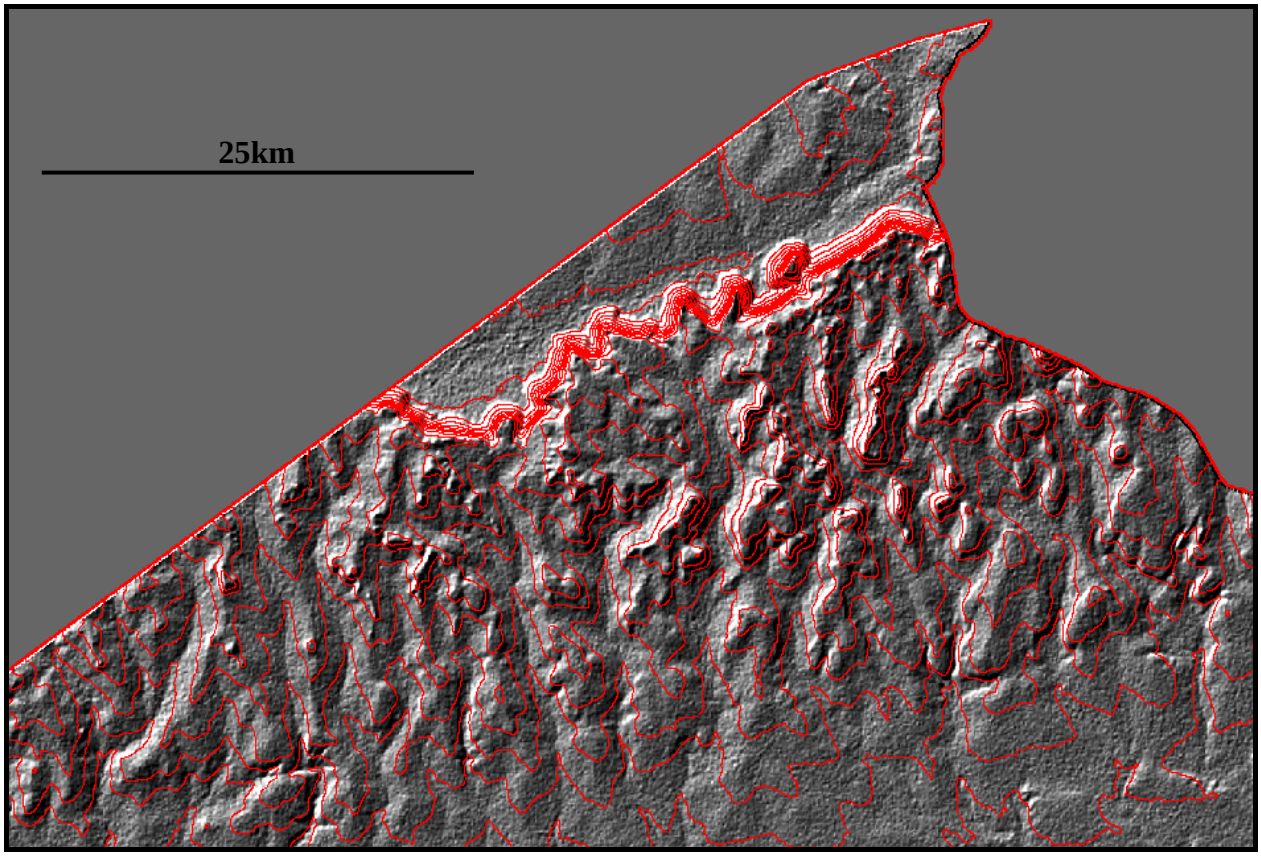

Figure 9 30m contours overlaid onto the DTM for the northern tip of the Volta Basin.

The ability to create perspective views of a terrain is a very powerful tool for geological mapping. In this situation it was also very useful as it was used to exaggerate the vertical display of the low relief areas to highlight geological and geomorphological features. Examples of this will be illustrated in the following section which deals with information extraction (image interpretation) from the remote sensing datasets.

2.4 IMAGE INTERPRETATION

The appearance of the ground surface depends on a complex interaction of a number of factors, the most important of which are climate (both regional and local), tectonic setting, stage of geomorphic development, lithology, and structure (Berrangé, 1991). The climate is controlled by factors such as latitude, altitude and position in the landmass with regard to the surrounding seas or mountain chains. Climate strongly controls the type of vegetation, the nature of erosion (both mechanical and chemical) and so the soil profile. The tectonic setting is related to the geological evolution of the region e.g. an active fold belt versus a stable shield. The stage of geomorphic development is governed by uplift and changes in sea level, while lithology affects the type of soil and the rate of erosion. Each factor acts and reacts with the others, the results combining to determine the appearance of the landscape. This interaction is so complex that similar lithological and structural units can have a wide diversity of appearances across the Volta and Keta Basins. The task of image interpretation was to recognise indicative characteristics on the imagery and correlate them with geological features in advance of field checking.

Structural elements recognisable on the remote sensing imagery include:

i. Bedding – traces and planes;

ii. Lithological units – marker beds and stratigraphic successions;

iii. Lithological boundaries and unconformities;

iv. Fractures – faults, shear zones and joints;

v. Folds;

vi. Mass movement features.

These six features show up on the imagery in the form of planar features and/or lineaments. A lineament in this case is any sensibly straight or slightly curvilinear linear feature that is (or is presumed to be) structurally controlled. It includes alignments of natural features such as stream courses, lakes, hollows, cols, ridges and vegetation. Lineaments frequently represent fractures, but also correspond to bedding, veins, dykes, contacts, unconformities, foliation, or any combination of these. Lines representing man-made or cultural features such as roads, tracks, railways or field boundaries are not considered to be lineaments, although their location may be governed by geological structures e.g. a road along a fault-controlled valley.

An understanding of the bedding is essential for a remote sensing interpretation of the geological structure; although detailed fieldwork is a prerequisite in areas where no bedding can be seen due to deep weathering, cover by superficial deposits, or simply due to lack of bedding in the succession. Bedding manifests itself in various ways on the remote sensing imagery, the clearest being the 'bedding trace', which is the line separating the dip slope from the relatively steeper scarp slope (Figure 10). During Phase 1 of this project, interpretations of the bedrock geology were mainly based on shaded relief imagery derived from the DTM, supplemented by contours (Figure 9). Using this method and the principles explained in the next paragraph, several new geological units were identified and mapped out.

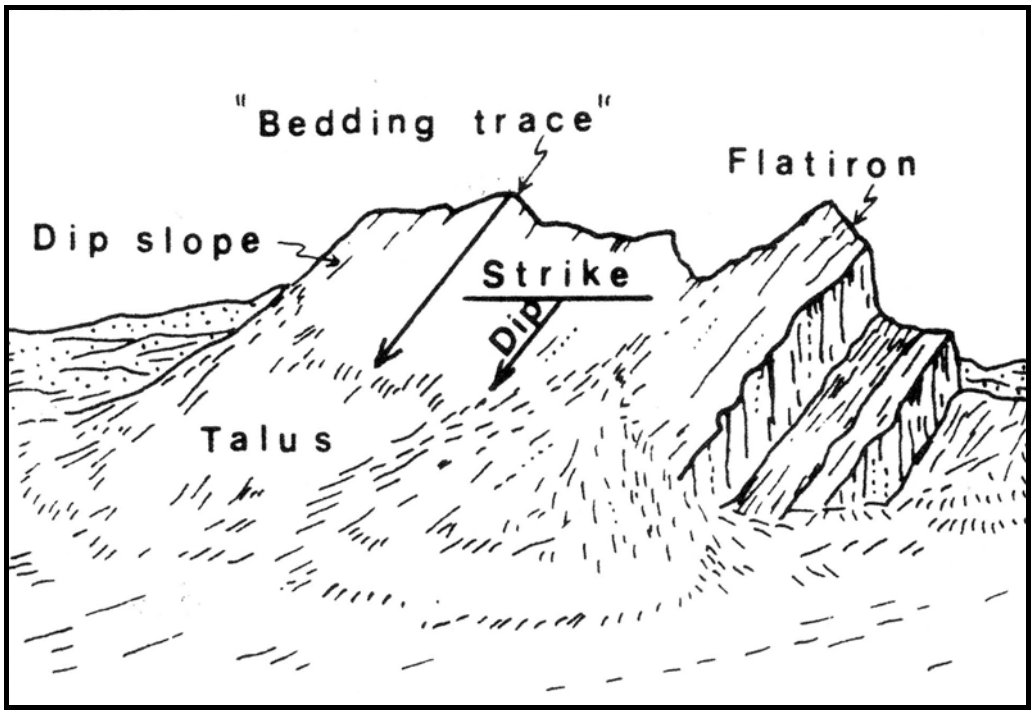

Figure 10 Relationship between strike/dip and the bedding trace (from Berrangé, 1991).

The bedding trace, dip slopes and flatirons illustrated above have been observed on remote sensing imagery of the project area, as shown in the annotated figure below. In this example, the DTM of the Kwahu escarpment is shown in perspective view with the interpreted geology overlaid in semi-transparent colour. The viewer is looking from southeast to northwest parallel to the trend of the bedding trace, i.e. along strike. The dip trend is from left to right i.e. towards the northeast.

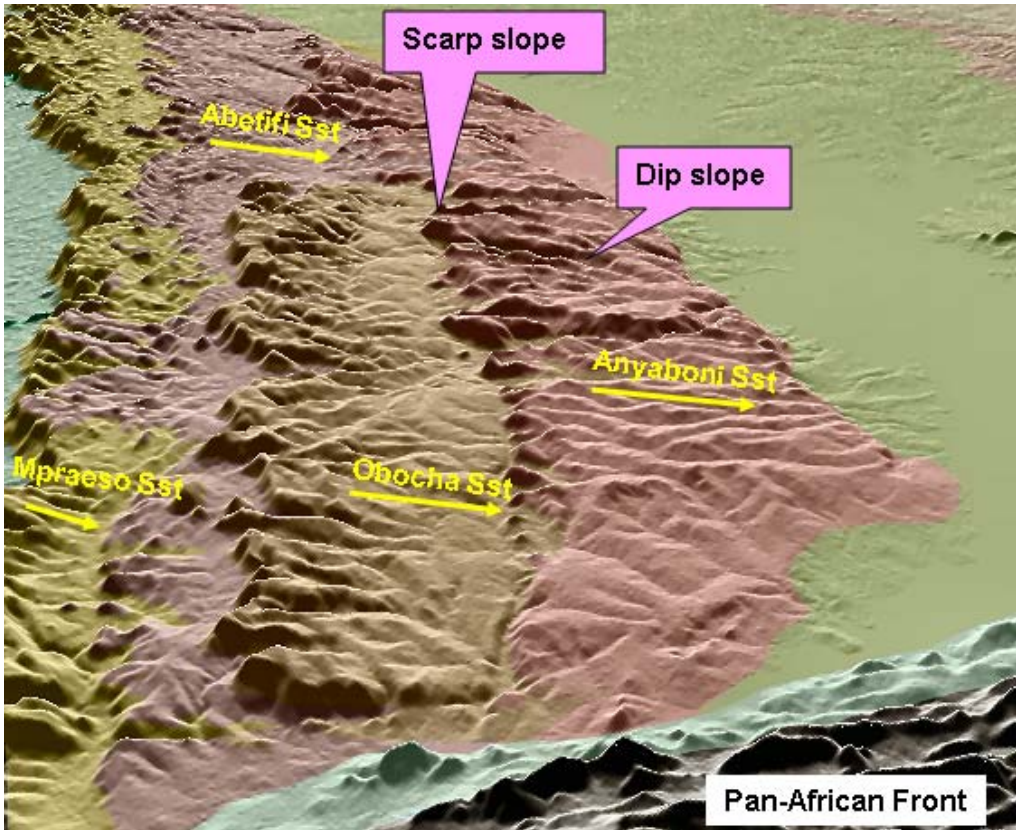

Figure 11 Bedding traces and dip slopes in the Kwahu Group, illustrated on remote sensing imagery, view is towards the NW.

Each of the remote sensing datasets has a specific 'strength' in terms of what geological or geomorphological information it can contribute. The texture of the landscape from the Radarsat and DTM, along with the spectral properties of the Landsat datasets contributed information regarding lithological variations (although this was limited) as well as structural information. An example of the textural information, relating to lithological variations is shown below (Figure 12). In this example, the texture of an area (the Afram Plains) crudely outlined in red is clearly different to the surroundings and this is due to different erosional patterns developing on different lithological units.

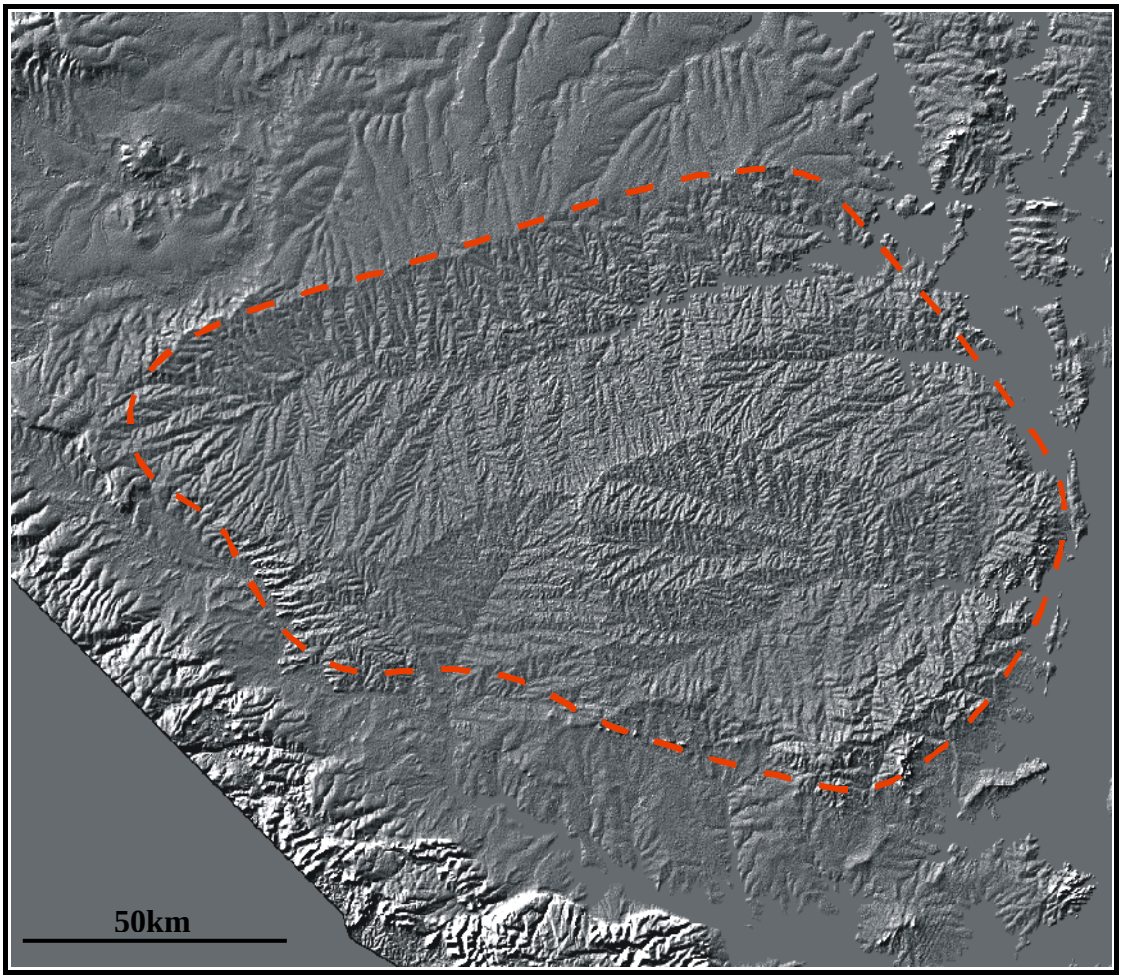

Figure 12 Illustration of different erosion patterns due to different lithological units.

Superficial deposits such as alluvium were also delineated on the remote sensing imagery. A combination of Landsat ETM and the DTM (more specifically a shaded relief derivative of the DTM) were preferred for this interpretation task with the Landsat used to distinguish vegetation changes and the shaded relied used to delineate breaks in slope (e.g. between a flat-lying floodplain and the adjoining deposits). As with all the other interpretative linework, the superficial boundaries were checked in the field where time and access allowed. Figure 13 is a 'screen grab' from the GIS illustrating the alluvial boundaries (red dashed lines) as they were being interpreted from the remote sensing imagery. The image is approximate 25km wide and is situated along the western shores of Lake Volta.

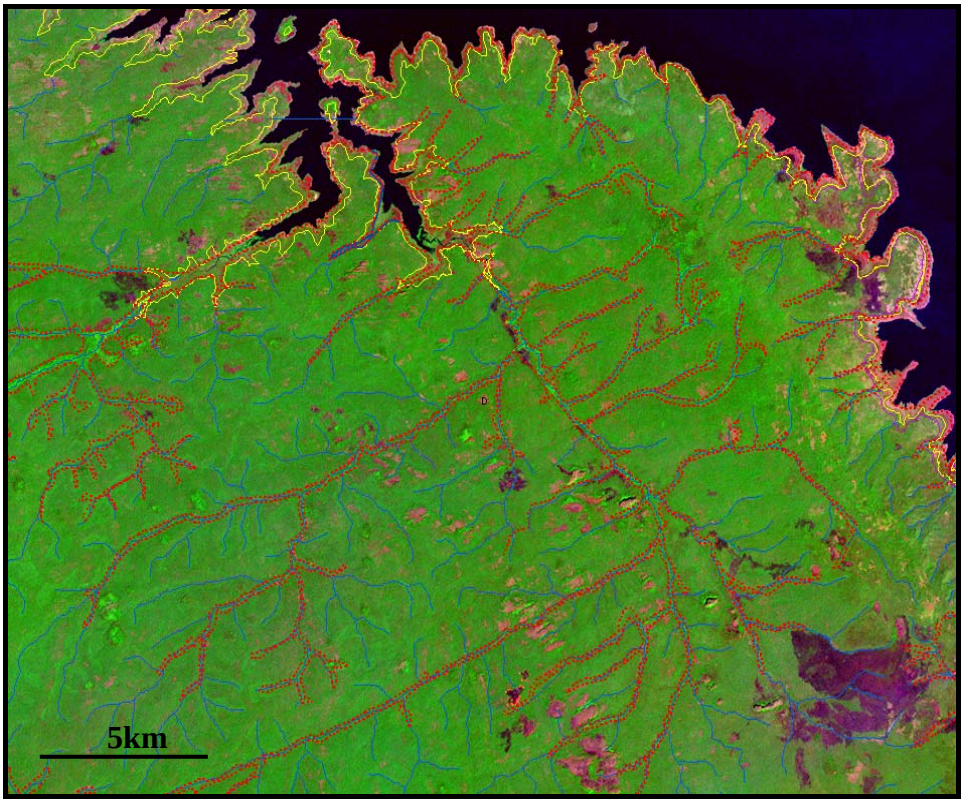

Figure 13 Alluvium (red dashed lines) was digitised from the Landsat and DTM imagery before field checking – image is approximately 25km wide.

All of the datasets in this project were geocorrected, displayed and integrated in a GIS for interpretation. The interpretation was conducted predominantly in the digital environment using 'heads-up' digitising, and the digital linework was taken to the field on tablet PCs and hardcopy plots for corroboration where possible in the time available.

3 Geological Inspection of Outcrops and Morphological Features (Reconnaissance Fieldwork)

BGS staff took part in five visits to Ghana. The first was from the 9th to the 26th of January 2006 but there was no fieldwork component to this visit as it was to review and collect extant data and forge links with counterparts, GSD staff and other relevant organisations such as the University sector. The Table below lists the visits. One trip was used to conduct a differential GPS survey, two were dedicated 'reconnaissance' geological mapping field trips, while the fourth was an excursion (led by BGS) which was part of the Volta Stratigraphic Workshop. During the workshop excursion the opportunity was seized to record additional geological information and discuss geological ideas / models with local and international experts, and for this reason it has been included in this report. Furthermore the additional geological observation points noted during the excursion were added to the fieldwork database and added to the list in the Appendices of this report.

Visit Type	Dates	Number of BGS Field Teams
Data gathering	9/1/06 to 26/1/2006	1
Differential GPS	12/4/06 to 14/3/06	1
Geological mapping	27/9/06 to 28/10/06	2
Geological mapping	4/11/07 to 30/11/07	2
Workshop excursion	14/3/08 to 17/03/08	1

Table 6 BGS field visits to Ghana.

3.1 DIFFERENTIAL GPS SURVEY

The purpose of the differential GPS ground truthing was to undertake a high quality differential survey to allow accurate rectification of the remote sensing data. Control points were acquired at fixed points that could be easily distinguished on the satellite imagery e.g. road intersections. A BGS Leica GS550 GPS was used for the survey in conjunction with an addition module that enabled linkage to the OmniStar system for real-time differential readings. Mr Joehida Quaye (Principal Geologist at the GSD) and Ms Akua Appiah-Akuramaa (Assistant Geologist) accompanied the BGS staff on the field survey which was conducted from the 12th of February until the 14th of March 2006.

The methodology consisted of locating a suitable point on the remote sensing imagery that could be measured on the ground and then occupying that point with the GPS until the software predicted a suitable quality of reception had been gained. It was necessary to remain at each position between 5 and 20 minutes to achieve the accuracy of greater than 1m which was required. The variable time at each site was a factor of the satellite constellation and the level of interference e.g. from tree cover. 269 control points were collected and 5522km were covered during the GPS survey, as illustrated in Figure 14. Another useful outcome was that outcrops seen during the survey were recorded and added to the project GIS to help planning of the fieldwork phase.

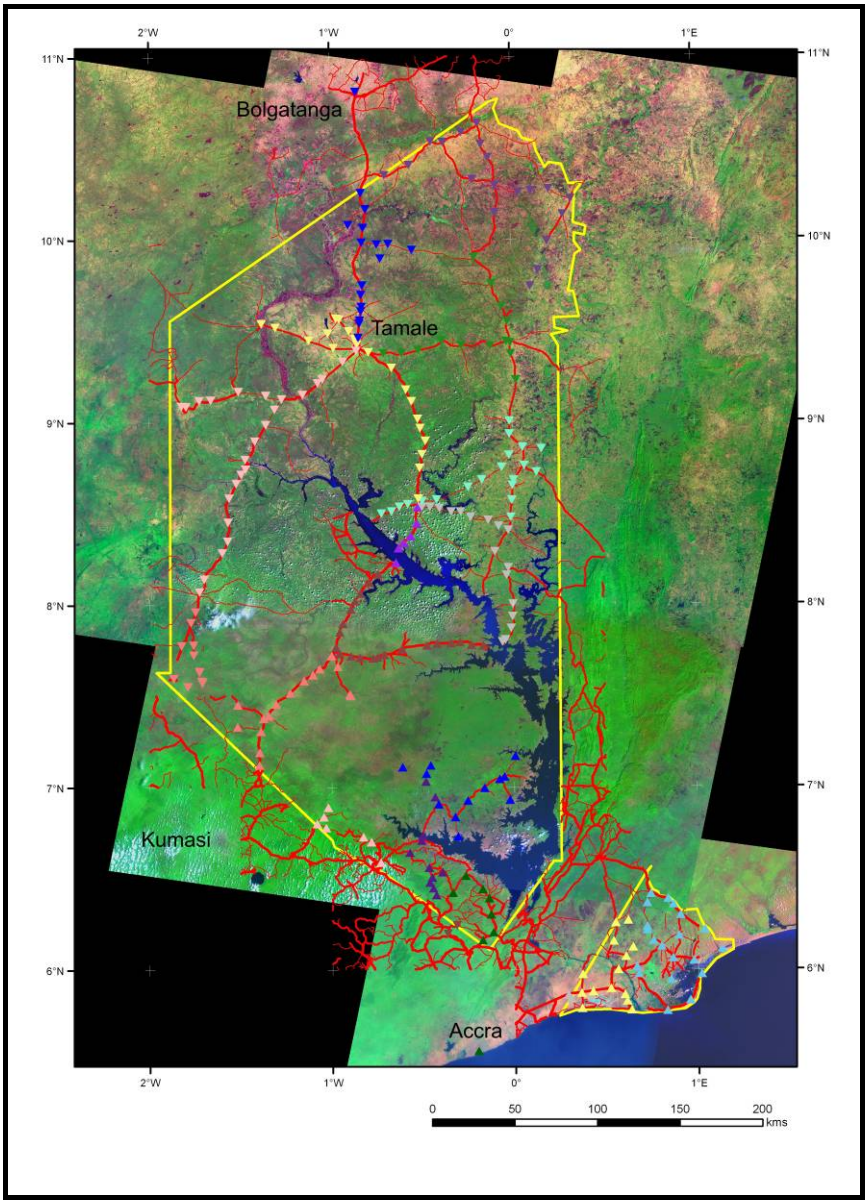

Figure 14 Landsat ETM image with road network and GPS points plotted as triangles.

3.2 RECONNAISSANCE GEOLOGICAL MAPPING

Reconnaissance geological mapping was conducted over two field seasons in September/October 2006 and November 2007. The fieldwork objectives were to verify the image interpretation and conceptual geological model, to visit mineral localities and to examine exposures of as many geological units as possible. Samples were collected for various analyses including thin section, fossil identification and multi-element and fire assay. The GSD counterparts (Mr Quaye and Ms Appiah-Akuramaa) were both in the field for all of the first field season, and each counterpart participated in approximately half of the second field season.

The project areas are characterised by dense vegetation and subdued relief. Apart from the hilly tracts that form the rim to the Volta Basin, there are very few rock exposures. Given such conditions, it is felt that the findings reported here have vindicated the importance of using remote sensing imagery to interpret geology.

The field campaigns in 2006 and 2007 were conducted by two BGS field teams each year, operating in 4x4 vehicles with drivers from the GSD. The vehicles covered a total distance of approximately 24,000 kilometres, and over 700 localities were recorded. Lithological information was mainly obtained from roadside and drainage ditch exposures, but advantage was

also taken of quarry exposures and debris from excavations, particularly for reservoirs, water wells, pit latrines and telecommunication tower construction. A figure showing the distribution of traverse routes and Observation Points (OP's) is provided below. Brief locality details and geological notes made at the OP's are provided in the Appendices.

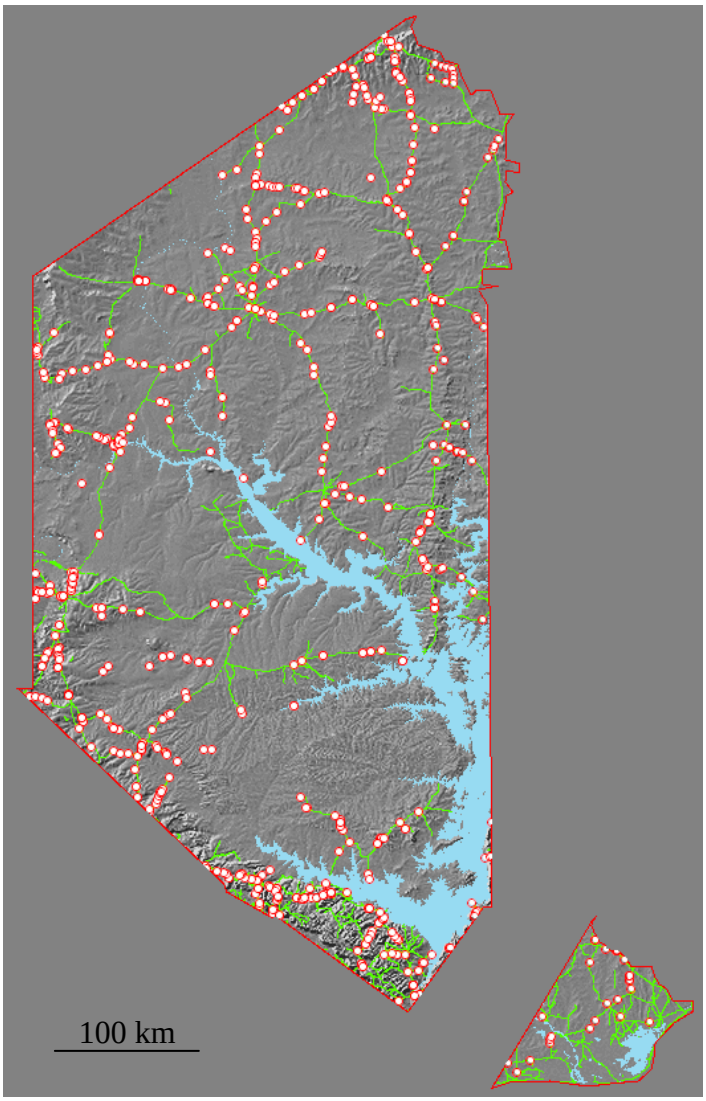

Figure 15 Map showing distribution of access routes in green and Observations Points (OPs) in red.

At each locality a GPS coordinate was logged, and appropriate observations and measurements were taken. These measurements included tectonic and sedimentological structures and certain physical properties (magnetic susceptibility, total gamma count, uranium, potassium and thorium). Rock samples were collected in order to have representative samples from each Formation (where possible) as well as for analyses including thin section, fossil, and Inductively Coupled Plasma with Optical Emission Spectroscopy / Mass Spectrometry (ICPOES/MS) Analysis and fire assay. The field instrument readings are provided in the Appendices and the multi-element analyses are discussed the Mineral Prospectivity Modelling Chapter.

Satellite imagery and DTM data were continually referred to in the field, allowing the integration of lithological and landform observations with features discerned on the imagery. Bedrock and surficial boundaries were verified and revised in the field.

In March 2008 the BGS led a field excursion as part of the Volta Stratigraphic Workshop. The time in the field was limited so we were restricted to the Kwahu escarpment area, along with a traverse via the Adowso Ferry to the Afram Plains area. It was not the intention to conduct new

mapping within the excursion but some new exposures were evident during our traverses so they were logged and added to our database.

The results of the geological field reconnaissance, together with preliminary interpretations of the stratigraphy, sedimentology and structure, are described in the following chapter.

4 Geological Model

The descriptions, interpretations and lithostratigraphy in this section both expand upon, and in many cases replace the preliminary accounts in Section 8 of the Phase 1 Report. It should also be noted that subsequent to the Phase 1 Report being completed, certain of the geological boundaries and lithostratigraphical divisions that appeared on the Phase 1 Geological Interpretation Maps, including the hard-copy set of 1:100 000 scale maps for the Volta Basin issued to the GSD, may have been changed.

4.1 VOLTA BASIN AND PAN-AFRICAN BELT

4.1.1 Palaeoproterozoic basement rocks and the Voltaian unconformity

Basement metamorphic rocks occupy a small part of the Volta Basin project area, cropping out on the lower ground to the south-west of the main escarpment bordering the Kwahu Plateau. They are of Palaeoproterozoic age and were formed during the Birimian tectonic cycle. The main lithologies include phyllites, schists and various metasedimentary rocks interbedded with a ‘greenstone’–type association of metavolcanic and metasedimentary rocks. Both assemblages are intruded by granitoid igneous bodies and were last deformed during the Eburnean orogenic phase, the main events occurring between about 2.13 and 2.0 Ga (Feybesse et al., 2006).

The DTM imagery and airborne geophysical data show that the principal basement elements, which in the Project area include Ashanti and Sefwi belts, are characterized by a dominant north-easterly orientation, also featured in the various structural diagrams in Feybesse et al. (2006). Topographically, this is reflected by prominent granitoid-cored ridges that rise above an otherwise featureless peneplane. Observations made within and outside of the project area suggest that as these ridges encounter the Kwahu Plateau escarpment, they retain their topography and are draped-over by the basal strata of the Voltaian Supergroup. The unconformity surface is therefore highly irregular, at least locally. Such relationships suggest that in part, the modern basement topography reflects that of the Neoproterozoic land surface immediately before deposition of the Voltaian Supergroup. The unconformity is well displayed in a road cutting along the Kwahu Escarpment, between Nkawkaw and Mpraeso, as described below.

4.1.2 Voltaian Supergroup

Sedimentary rocks in the Volta Basin (Figure 16) are currently included within the Voltaian Supergroup, the lithostratigraphy of which is summarized in Table 7. They are lithologically diverse, with mudstones, siltstones, sandstones, conglomerates and limestones all represented. Seismic and geophysical (gravimetric and aeromagnetic) data indicate that the Supergroup has an estimated maximum thickness of 5000 to over 6000 m, according to Anan-Yorke (1971) and Ako and Wellman (1985) respectively. The depth model proposed by the latter authors shows that the Voltaian Supergroup thickens progressively towards the east, where it terminates abruptly against a mountain range in which rocks of the Buem and Togo Formations are exposed (e.g. Grant, 1969). These highlands represent part of a Pan-African orogenic belt, certain components of which probably represent the folded and thrust-imbricated equivalents of Volta Basin sediments.

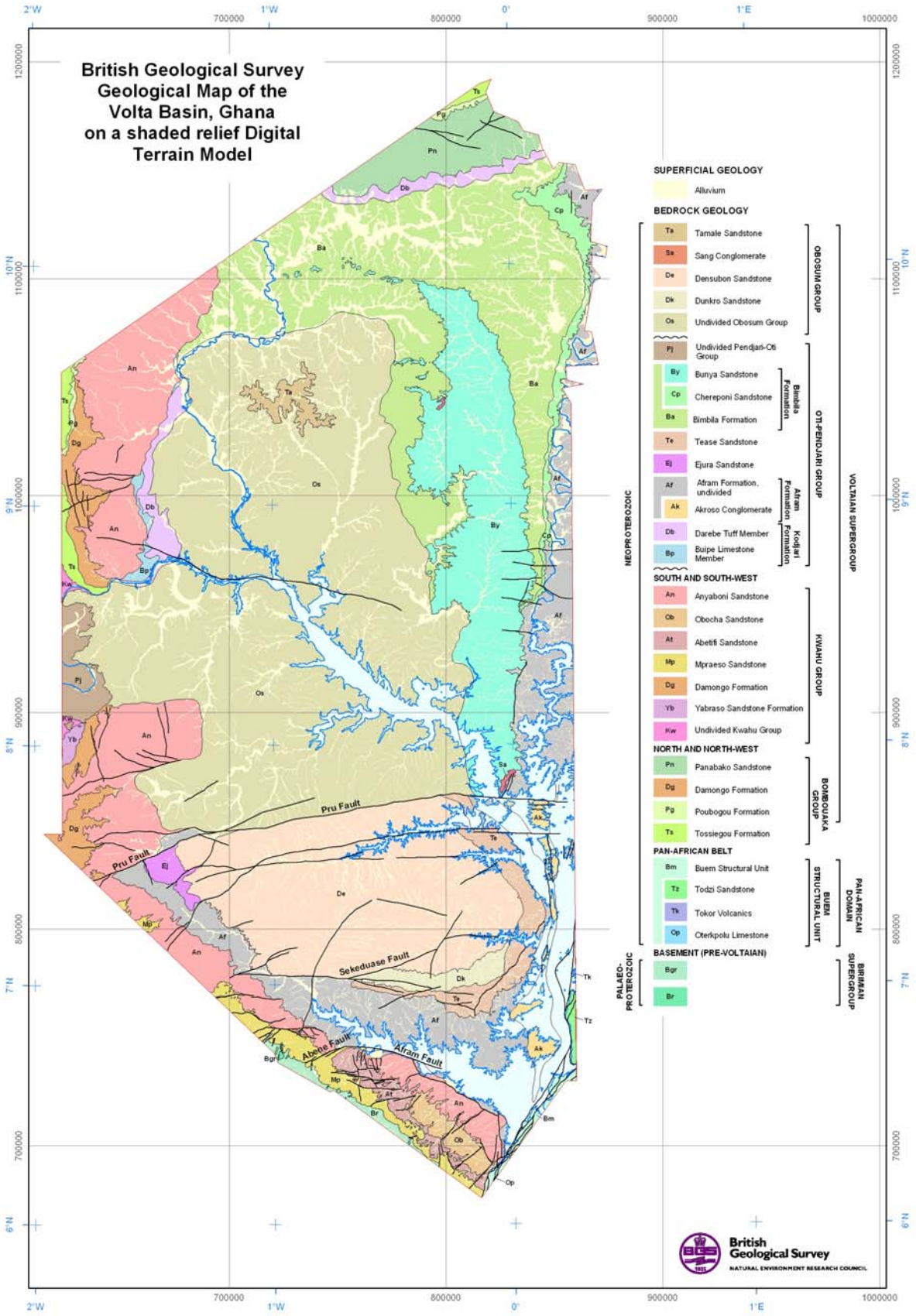

Figure 16 Geological map of the Volta Basin, derived from satellite imagery and subsequent field-checking.

GHANA – FINAL STRATIGRAPHICAL TABLE, BGS/FUGRO Project, Phase 4: UPDATED 2008				
AGE	VOLTA BASIN		**PAN AFRICAN BELT**	KETA BASIN
Quaternary (Holocene)	Alluvium (map-symbols) Alluvial Fan Deposits River Terrace Deposits Quaternary Deposits of uncertain origin			Alluvium (map-symbols) Volta Delta Deposits Tidal Flat Deposits & Salt Pans Shoreface & Beach Deposits Raised Tidal Flat Deposits Raised Beach Deposits River Terrace Deposits
Cenozoic to Pleistocene				Agbakope Sand (**Ag**) Koluedor Gravel (**K**)
Cenozoic	Central Volta Surface: Laterite, including gravels and cover silts/sands (as map-symbol)			Laterite & cemented gravel (not mapped)
Neoproterozoic	VOLTAIAN SUPERGROUP **Obosum Group**: Undivided mudstones, siltstones and sandstones (**Os**) Tamale Sandstone Formation (**Ta**); Sang conglomerate (**Sa**) Densubon Sandstone Formation (**De**) Dunkro Sandstone Formation (**Dk**) **--- UNCONFORMITY--** **Oti - Pendjari Group**: Undivided mudstones, siltstones and sandstones (**Pj**) Bimbila Formation: Undivided mudstones, siltstones and sandstones (**Ba**) Bunya Sandstone Member (**By**) Chereponi Sandstone Member (**Cp** Tease Sandstone Formation (**Te**) Ejura Sandstone Formation (**Ej**) Afram Formation (**Af**): Akroso Conglomerate Member (**Ak**) Kodjari Formation (**Kj**): Darebe Tuff Member (**Db**) Buipe Limestone Member (**Bp**) **-- MAJOR UNCONFORMITY --**		Buem Structural Unit: Undivided mudstones, siltstones and sandstones, locally sheared and foliated **(Bm)** Oterkpolu Limestone Member (**Op**) Todzi sandstones **(Tz)** Tokor volcanics **(Tk)**	
Neoproterozoic	**Kwahu Group**: Anyaboni Sandstone Fm (**An**) Obocha Sandstone Fm (**Ob**) Abetifi Sandstone Fm (**At)** Mpraeso Sandstone Fm (**Mp**) Damongo Formation (**Dg**) Poubougo Formation (**Pg**) Yabraso Sandstone Formation (**Yb**) Undivided mudstones and siltstones (**Kw**)	**Bombouaka Group**: Panabako Sandstone Fm (**Pn**) Poubogou Fm (**Pg**) Tossiegou Fm (**Ts**)		
Palaeoproterozoic	**Birimian Supergroup** Greenstone (**Bgr**) Undivided (**Br**)			**Dahomeyan Complex** Mesocratic orthogneiss (**mgn**) Leucocratic orthogneiss (**lgn**)

Table 7 New lithostratigraphy for the Volta and Keta basins.

(NB: stratigraphical relationships between the Bimbila Formation and the Tease/Ejura formations cannot be established).

4.1.2.1 PREVIOUS WORK AND EVOLUTION OF THE LITHOSTRATIGRAPHY

This section is not intended to provide an exhaustive account of the previous studies. One of its objectives is to trace the origin of certain 'traditional' subdivisions of the Volta Basin sequence which, although now discredited, are nevertheless still being used by some workers.

Early stratigraphical schemes involving 'Upper' and 'Lower' Voltaian

Early geological surveys in the Volta Basin were carried out in support of water supply programmes and the main outcomes were summarised by Junner and Hirst (1946). About 40 000 miles of roads, tracks, rivers and cut lines were traversed, variously by foot, bicycle, road or canoe. Some exposures were described in detail, but are now difficult to trace since their locations often relied on estimates of distances and compass directions from villages, many of which no longer appear on topographical maps. Attempts to establish a basin-wide lithostratigraphy for the Volta Basin succession were undoubtedly hampered by the absence of reliable topographic maps, as well as the paucity of exposure due to the low-lying nature of much of the central part of the basin, and extent of lateritic cover (see Anan-Yorke, 1971). Junner and Hirst nevertheless used the scores of reports that had been produced to derive the lithostratigraphical classification shown below in Table 8.

Sub-group	Symbol	Name and Description of Beds	Estimated Maximum thickness (m)
Upper Voltaian	(V_{3b})	**Upper Sandstone**: Massive, cross-bedded quartz-sandstones containing, in places, beds of shale and mudstone up to at least 30 metres thick	220
	(V_{3a})	**Thin-bedded Sandstone**: Thin-bedded flaggy sandstone, micaceous, ferruginous of feldspathic; clay galls and ripple marks common.	124
Lower Voltaian	(V_{2b})	**Obosum Beds**: Red, green, purple mauve and chocolate coloured arkoses, mudstones and shales, with Sang conglomerate and some limestone and quartz-sandstone. Cross-bedding common in the sandy and pebbly beds	155
	(V_{2a})	**Oti Beds**: Akroso conglomerate, grits and arkose, sandstones, mudstones, shales and limestones. Nodular structures common and yellow-weathering typical	250
	(V_1)	**Basal Sandstones**: Quartz-sandstone and pebbly grits with ripple marks and clay galls.	63

Table 8 Junner & Hirst (1946) classification of the Voltaian sediments.

The important feature of this classification is the stratigraphical status of the quartzose sandstones comprising the 'Upper Sandstone' of the 'Upper Voltaian' (V3) succession. These strata form the elevated rim to the basin, around Gambaga, Damongo, Kintampo and the Kwahu Plateau, due in part to their greater resistance to erosion. Possibly because of their topographic expression, these sandstones were considered to overlie all of the other units and thus represent the youngest phase of sedimentation. Later work summarised below, as well as that carried out by the present authors, has confirmed that these strata, which are now known as the Kwahu and Bombouaka groups (Table 7), in fact represent the *earliest* sedimentation in the basin and thus *underlie* the 'Oti Beds' (now the Oti-Pendjari Group).

Bates (1954) attempted to simplify this classification by suggesting that the Obosum and Oti beds are laterally equivalent and also that the 'Upper Voltaian' rocks should no longer be subdivided (reviewed in Anan-Yorke, 1971). Edmonds (1956), mapping the Gambaga field

sheet, amplified the scheme of Junner and Hirst (1946) by subdividing the sequence into lower, middle and upper subgroups.

During 1962-66, a major integrated programme involving geological, hydrogeological and geophysical studies, including seismic reflection profiling and hydrocarbon exploration drilling, was carried out mainly in the central and northern sectors of the Volta Basin by teams from the USSR (SGG - Soviet Geological Group). Some of the results of this work were presented in a series of publications and internal reports (e.g. Bozhko et al., 1964). Following the enforced and rather sudden departure of the Soviet teams, officers of the Geological Survey of Ghana endeavoured to review this comprehensive data set, much of which was of necessity incomplete and 'raw' in the sense of not having been the subject of detailed interpretations and basin-wide correlations. The review by Anan-Yorke (1971) described how the Soviet geological project divided the western part of the Volta Basin sequence into the units shown in Table 9.

Subgroup	Symbol	Name and Description	Thickness (m)
Upper Voltaian	$Pz_1\ Vt^1_2$	**Upper Massive Sandstone** Quartzose and feldspathic sandstones, fine bedded in the lower 90 metres; massive and cross-bedded in the upper 200 – 300 metres **'Thin-bedded Sandstone Formation'** at the base	(300-400m)
Middle Voltaian	Vt^4_2	**(Tamale) Red Series** Quartzose, feldspathic and poorly sorted sandstones, siltstones, mudstones and conglomerate	(400m)
	Vt^3_2	**Greenish –grey Upper Series** Poorly sorted greenish grey sandstones, siltstones and mudstones with limestone intercalations	(480-660m)
	Vt^2_2	**Variegated Series** (Argillaceous Carbonate Series): Variegated coloured sandstones, siltstones, shales, mudstones with limestones and dolomites.	(400-500m)
	$Pz_1Vt^1_2$	**Conglomeratic Sandstone Series** Tillite – like conglomerates and sandstones.	(120-200m)
Lower Voltaian	$Pz_1\ Vt_1sm$	**Greenish Grey Lower Series** Poorly sorted greenish-grey sandstones, siltstones and shales.	(1000m)
	$Pcm\ Vt^1_1$	**Basal Sandstone Series** Poorly sorted sandstones, siltstones and shales	(400m)

Table 9 Bozhko et al. (1964) classification for the western Volta Basin, as summarized by Anan-Yorke (1971).

Obtaining the original papers by Bozhko and colleagues has proved difficult as most were published in Russia or France. From the synthesis in Table 9, it appears that the Soviet geologists followed the previous practice of designating as 'Upper Voltaian' the quartzose sandstone successions (= 'Upper Massive Sandstone') now referred to the Kwahu Group and the Bombouaka Group, both of which are now known to form part of the earliest phase of sedimentation in the Volta Basin (Table 7).

The classification produced by the review of Anan-Yorke (1971) was based on perceived unconformities and variations in the degree of induration of these strata and incorporates certain modifications to Bozhko's scheme (Table 10). In particular, the 'Upper Voltaian' sandstones were said to be separated from the Middle Voltaian by a distinct unconformity at the base of the 'Tamale Red Beds'. The latter are, however, geographically separated from the supposed 'Upper Voltaian' sandstones of the Kwahu Plateau, Kintampo and Gambaga areas, invalidating this general conclusion for those outcrops. Anan-Yorke's succession would have drawn heavily on the seismic

interpretations and deep drilling results of Bozhko et al (1964; see also, Bozhko, 2008), although some differences are apparent; for example the stratigraphical positioning of the 'Tamale Red Beds' (compare Tables 9 and 10). Anan-Yorke (1971) refuted an alternative stratigraphy, which had by then been erected by Saunders (1970; see below), as being 'unsupported by the field evidence'.

Subgroup	Name and description	Estimated Maximum thickness (m)
Upper Voltaian	Massive cross-bedded sandstones	300
	Thin-bedded sandstones	122
	Tamale Red Beds	406
Middle Voltaian	Upper Green Beds	710
	Afram Shale	532
	Akroso Conglomerate	187
	Lower Green Beds	2000
Lower Voltaian	Basal Sandstone	2000

Table 10 Anan -Yorke (1971) classification of Voltaian Basin strata.

It is noted that Junner and Hirst (1946), Bozhko et al. (1964) and Anan-Yorke (1971) all recognised a 'Basal Sandstone' division (='Lower Voltaian') that underlies all other units and is thickly present at depth (Tables 8 - 10). The convergence of these basal sandstones with the 'Upper Voltaian' sandstones in the western and northern parts of the basin (cross-sections of Junner and Hirst, 1946) was attributed to thinning out of the intervening 'Middle Voltaian'. The present lithostratigraphical scheme (Table 7), however, places the 'Basal Sandstone' and 'Upper Sandstone' together, within both the Kwahu and Bombouaka groups, thereby restricting them to stratigraphical levels below the Oti-Pendjari Group. In the map compiled by Bozhko (Ghana Geological Survey, 1964) it is clear that the 'Middle Voltaian' includes strata of the 'Red Series', which today are included within the Obosum Group, as well as the underlying 'Greenish-Grey Series' now included within the Oti-Pendjari Group.

Moon and Mason (1967), and Mason (1963), working in the south of the basin on the Bompata sheet near Kumasi, followed the general practice of dividing the sequence into 'lower' and 'upper' Voltaian. They evidently assumed that the lowest exposed sandstones around Agogo (which included the 'Agogo Clay Gall Sandstone Formation') overlay the Afram Shales – a reversal of the present stratigraphy shown in Table 7. The lack of field evidence for this relationship i.e. the absence of any exposures of the Afram Shales beneath the Agogo sandstone, was attributed to overstepping of the former by the latter in that particular region. It is noteworthy that Mason (1963) mentioned the occurrence of dune bedding in the 'Chirimfa Arkosic Sandstone' of the 'Upper Voltaian' division. This suggests that the unit may equate with the Anyaboni Sandstone Formation of Saunders (1970, and see below), a conclusion also reached by Blay (1983).

Grant (1969) followed tradition by placing the sandstones occupying the higher ground of the Kwahu Plateau and Kintampo areas at the very top of the Volta Basin succession, within the

'Upper Voltaian', even suggesting that they represented a post-orogenic molasse resting on the 'Obosum Beds'.

Evolution of the modern stratigraphy

Following mapping carried out on the Kwahu Plateau, in the south-east of the Volta Basin, Saunders (1970) produced a stratigraphy that differed radically from the previous classifications discussed above:

Obosum Beds	
Afram Shales	
Anyaboni Formation	Massive feldspathic sandstone (250-300 m)
	Micaceous, thin-bedded sandstone with siltstone and shale at base (130 m)
Kwahu Sandstone	Upper Quartzite; orthoquartzite (300 m)
	Shale (30-130 m)
	Lower Quartzite; thin-bedded, with basal arkose and shales locally (400-500 m)
Unconformity with Palaeoproterozoic basement	

Table 11 Stratigraphy for the SE Volta basin (Saunders, 1970).

The ordering of units shown in Table 11 indicates that Saunders disagreed with the previous assignations for 'Upper Voltaian' sandstones (Tables 8-10). He concluded instead that these strata, which he named as the Kwahu and Anyaboni sandstones, actually underlie the 'Afram Shales' and 'Obosum Beds', also noting that in the south-eastern part of the basin the Anyaboni Sandstone is in tectonic contact with the Afram Shales along the Afram Fault. This displacement has caused the Anyaboni Sandstone to occupy elevated ground (Figure 17), compared to the adjacent Afram Shales outcrop, and this may be one of the reasons why previous workers considered it to be the younger of the two units.

Figure 17 Medium to thickly bedded strata of the Anyaboni Sandstone Formation, viewed looking south-westwards, towards the face of the Afram Fault escarpment (i.e. from OBS JC41)[1]

Anani (1999), in support of Saunders (1970), included the 'Kwahu Sandstone Member' in the lower part of the Voltaian succession, but in another diagram placed the overlying Anyaboni Sandstone in the 'Middle Voltaian', with a tillite/limestone/shale interval occupying the intervening basal part, above the Kwahu Sandstone. It is noteworthy that at the base of the Anyaboni Formation Saunders mapped a sequence of micaceous siltstones and shales, suggesting the possibility that other workers, comparing these lithologies with the Afram Formation, have supposed that the two are lateral equivalents. Such conclusions can be ruled out on stratigraphical grounds by the findings of Saunders (1970) and this survey. In the unit here termed the Kwahu Group (Table 7), however, the mis-correlation of 'shales' with Afram Formation shales, has evidently continued (e.g. Blay, 1983), resulting in the Anyaboni Formation, which is a composite unit with basal 'shales', being placed as 'Upper Voltaian'. In view of this, and in order to prevent further confusion between those advocating either of the schemes proposed by Saunders and Blay, *it is recommended that terms such as 'Lower', 'Middle' and 'Upper' Voltaian should no longer be used.*

The revisions of Saunders (1970) were eventually taken on board by Grant (1973), who stated that the traditional stratigraphy, in particular the status of the 'Upper Voltaian' sandstones of Junner and Hirst (1946), was incorrect and that the latter sandstones in fact constitute part of the basal division of the sequence. Grant (1973) thus affirmed the view of Saunders (1970) that in the extreme south of the basin the 'Lower Voltaian' in effect encompasses the Kwahu and Anyaboni sandstones. Grant further stated that the 'Middle Voltaian (Oti Formation)' lies unconformably on these lower sandstones, and that it commences with basal conglomeratic beds, interpreted as tillites, followed by shales, siltstones, sandstones, limestones and dolomite. This latter sequence is also detailed in Bozhko (1967, 1969a, 1969b). In the southernmost part of the basin, however, both the tillites and the basal unconformity to the 'Middle Voltaian' would

[1] OBS = Field Observation point. See Appendix 1 for details and GPS coordinates

appear to be absent according to Saunders (1970). Grant (1973), quoting a personal communication with Bozhko (1970), suggested that the base of the 'Obosum Formation' (now Obosum Group, Table 7) should be taken below an unconformity surface, marked by the first appearance of red quartzo-feldspathic sandstones.

According to Zitzmann et al. (1997), Bar (1977), working in the southern margin of the basin, found the following units, each separated by an erosional discordance:

Vo	V_7	Dominase Group	Quartz sandstone, white	>80m
Vo	V_6	Asesewa Group	Asesewa sandstone, red-brown	c.200
			Basal conglomerate	
Vm:	V_5	Ejura Group:	Upper sandstone, white, red or grey-green	
			Lower Pelite, red to grey-green, with limestone and chert	120
	V_4	Dente Group	Coarse sandstone, white-yellow	120
	V_3	Akroso Group:	Upper sandstone, arkosic, yellow	>200
			Middle Pelite, grey-green, calcareous interbeds	
			Basal Conglomerate	
Vu	V_2	Afram Group:	Upper pelite, grey-green, including limestone	>100
			Lower Sandstone, white to red	100
	V_1	Koforidua Group:	Upper Banded Pelite, grey to black	50
			Middle sandstone, white, yellow red	100-150
			Basal Pelite, red and grey-green	10

Table 12 Stratigraphical scheme of Bar (1977) according to Zitzmann et al. (1997).

Although the Bar (1977) paper has not been obtained, some elements of this stratigraphy may be identified with that appearing in the present report; for example 'Upper sandstone/Ejura Group' may be equivalent to the Ejura Sandstone of Table 7.

In an MSc Thesis, Affaton (1975) principally described relationships within the 'Pendjari Basin', which is the north-easterly continuation of the Volta Basin in Togo. There, a predominantly south-eastwards-dipping succession was recognised, commencing with quartzose sandstones of the Dapango-Bombouaka Group unconformably overlain by the Pendjari Group (equivalent of the former 'Oti Beds'), the latter commencing with a tillite-carbonate sequence.

Towards the end of the 20th century, lithostratigraphical classifications increasingly reflected the perceived influence of tectonics on sedimentation within the basin. Thus Black (1967), Bozhko (1969b) and Grant (1969) proposed a fundamental linkage between tectonic activity within the Pan-African 'Dahomeyan' belt and deposition farther west within the Volta Basin, the latter author recognising the Obosum Group as representing a post-orogenic molasse-type association. Many of the subsequent lithostratigraphical schemes established by French/West African researchers are somewhat ephemeral, with each new publication incorporating changes to the names and ranks of the various units that have been designated. All of the classifications agree that the basin can be subdivided into three major unconformity-bounded sequences, reflecting that the Voltaian Supergroup was deposited episodically and within a variety of different tectonic settings. Provenance studies (Anani, 1999) and zircon age spectra (Kalsbeek et al., 2008) on the stratigraphically lowermost sandstone sequences, here called the Kwahu and Bombouaka groups (Table 7), are compatible with an initial passive margin setting that prevailed during a very early

phase of regional subsidence within the supercontinent of Rodinia; similar sandstone lithologies are found within within the Pan-African deformed belt along the eastern basin margin (Osae et al., 2006). Some time after this, subsidence and rifting commenced as a prelude to the eventual break-up of Rodinia. Affaton et al (1980) envisaged that initially, passive margin-type sediments were deposited, represented by the lower parts of the Oti-Pendjari Group (Table 7). Closure of the rift, and subsequent uplift of the Pan-African orogenic belt bordering the basin's eastern margin resulted in a transition to a foreland basin receiving flysch (main part of Oti-Pendjari Group) and ultimately, to the deposition of terrestrial molasse of the Obosum Group (see Section 4.1.2.8).

Affaton et al. (1980) discussed the tectono-stratigraphical relationships between the Volta Basin and the deformed rocks of the Pan-African 'Dahomeyide' orogenic belt flanking it to the east. They subdivided the Volta Basin sequence (Table 13) into groups and formations, the names of many being derived from equivalent outcrops in Togo and Benin. For comparative purposes, the previous stratigraphical schemes of Junner and Hirst (1946), Grant (1969) and Bozhko (1969a) were summarized in the form of cross-sections. Affaton et al. did not mention the work of Saunders (1970), but concurred by emphasizing that the basal quartzose sandstones, of the Dapango-Bombouaka Group, are amongst the oldest units present rather than, as supposed by many previous workers, being part of the youngest ('V3') sequence (see also, Affaton, 1975). The geological sketch map provided by Affaton et al. (1980) was based on the work of Sougy (1970), who included what was essentially the outcrop of Bozhko's 'Red Series' within a northerly extension of the Obosum Group. This apart, however, the main outcrops on the map closely resembled previous versions, indicating that the new work had not entailed a significant revision of outcrops in the Ghanaian sector of the basin. Affaton et al. (1980) noted that their Pendjari-Oti Group rests unconformably upon the Dapango-Bombouaka Group, and that the striated pavement on the latter is overlain by a 'triad' of lithologies comprising the Kodjari Formation. This unit commences with a tillite/carbonate succession (Buipe Limestone Member), as also recognised by Leprun and Trompette (1969) and Affaton (1975). Above this is the silicic, tuffaceous Darebe Tuff Member (of this report), the uppermost unit of the Kodjari Formation (Table 7). The Dapango-Bombouaka Group and Pendjari-Oti Group are differentiated on the basis of the major unconformity at the base of the Kodjari Formation. The extent of the erosional unconformity between the two is indicated by the fact that locally, the Pendjari-Oti Group cuts down through the Dapango-Bombouka Group to rest directly on the underlying Birimian basement.

Group	Formation	Description	Estimate Maximum thickness (m)	Possible correlation with Bozhko classification	Correlation with Junner and Hirst (1946)
Obosum Group		Continental sandstones, red shales and siltstones Fluvio-glacial origin?	500?	Upper Voltaian/Obosum	V_{2b} + part of V_3
Pendjari-Oti Group	Pendjari Formation	Silty shales, argillaceous siltstones, sandstones and greywackes. Greenish	4000	Middle Voltaian	V_{2a}
	Kodjari Formation	Argillaceous siltstone, carbonate layer, Lenticular mixite (tillite?)	30?		
Dapango – Bombouaka Group	Panabako Formation	Sandstones and quartzites, medium to coarse grained	400	Part of Upper Voltaian; Lower Voltaian	V_1 + part of V_{2a} + part of V_3
	Poubogou Formation	Shales and siltstones	160		
	Tossiegou Formation	Fine sandstones and quartzites, thin bed of conglomerates and siltstones	500		

Table 13 Stratigraphical correlation proposed by Affaton et al. (1980).

The PhD thesis of Affaton (1990) gives a comprehensive review of previous work in the Volta Basin, together with much new data on the lithology, petrography and structure. It includes a lithostratigraphical scheme (Table 14) in which many existing units were either renamed (from Affaton et al., 1980) or upgraded in rank, with three supergroups now featured: Bombouaka, Pendjari-Oti and Tamale.

A summary of the lithostratigraphy and structure of the Volta Basin, together with an accompanying map, was given in Bertrand-Sarfati et al. (1991); the same lithostratigraphy was used in a companion paper by Affaton et al. (1991). These studies retain the three supergroups of Affaton (1990; see Table 14); however, in a partial reversion to the nomenclature of Affaton et al. (1980) they stated that the Pendjari-Oti Supergroup commences with a newly ranked unit, the Kodjari Group. There is also mention of ‘diamictite’ and ‘partly glacial conglomerates’ at the base of the Tamale Supergroup (Bertrand-Sarfati et al., 1991). A three-phase geodynamic evolution of the basin was proposed, commencing with deposition of craton-margin sandstones (Bombouaka Supergroup) followed by sedimentation marginal to a Pan-African oceanic domain (Pendjari-Oti Supergroup), culminating in the development of a foreland basin into which molassic sediments of the Tamale Supergroup were poured.

The geodynamic evolution of the Volta Basin was discussed further by Deynoux et al. (2006), in the context of wider correlations with sedimentary accumulations in similar basins elsewhere on the West African Craton (e.g. Taoudeni, Tindouf and Bove-Adrar basins; Hoggar-Iforas and anti-Atlas belts). The three major units previously recognised were retained (Bombouaka, Pendjari-Oti, Tamale), but were elevated in rank, from supergroup to megasequence. It was concluded that there are broad similarities in lithofacies between the various basins, with the tillites at the base of the Oti-Pendjari strata representing an excellent ‘marker’ horizon with which to constrain inter-basin correlations. There may, however, have been variations between the basins in the timing of the progression from rift- to collision-related sedimentation.

<table>
<tr><td colspan="2">Affaton et al. 1980</td><td colspan="3">Affaton, 1990</td></tr>
<tr><td colspan="2" rowspan="3">Obosum Group</td><td rowspan="3">Tamale Supergroup</td><td rowspan="3">Kebia Group</td><td>Kebia Formation</td></tr>
<tr><td>Salaga Formation</td></tr>
<tr><td>Sang Formation</td></tr>
<tr><td colspan="2"></td><td>Yendi Group</td><td></td></tr>
<tr><td rowspan="2">Pendjari Group</td><td>Pendjari Formation</td><td rowspan="2">Pendjari-Oti Supergroup (‘Afram Supergroup’)</td><td colspan="2">Oti-Pendjari Formation</td></tr>
<tr><td>Kodjari Formation</td><td rowspan="2">Sud-Banboli Group</td><td>Barkoissi Formation</td></tr>
<tr><td rowspan="6">Dapango-Bombouaka Group</td><td>Panabako Formation</td><td rowspan="6">Bombouaka Supergroup</td><td>Sud-Banboli Formation</td></tr>
<tr><td rowspan="2">Poubougo Formation</td><td rowspan="2">Bombouaka Group</td><td>Panabako Formation</td></tr>
<tr><td>Bogou Formation</td></tr>
<tr><td rowspan="2">Fosse-aux-Lions Group</td><td>Kotiare Formation</td></tr>
<tr><td>Natala Formation</td></tr>
<tr><td rowspan="2">Tossiegou Formation</td><td rowspan="2">Dapaong Group</td><td>Dapaong Formation</td></tr>
<tr><td>Korbongou Formation</td></tr>
</table>

Table 14 Comparison of lithostratigraphical schemes proposed by Affaton et al. (1980) and Affaton (1990).

See also, Table 13.

4.1.2.2 RECOMMENDED LITHOSTRATIGRAPHICAL NOMENCLATURE

The nomenclature for units adopted in this report follows as closely as possible the more recently published schemes discussed above and shown in Tables 13 and 14. It also, however, recognises the practices recommended in the North American Commission on Stratigraphic Nomenclature (NACSN, 1983). This remains the standard reference, offering much practical advice on the naming of units and their placement within a consistent and workable lithostratigraphical heirarchy.

Of particular relevance is the statement in NACSN that the formation is the fundamental unit in lithostratigraphical classification. The report goes on to say that: *No formation is considered valid that cannot be delineated at the scale of geologic mapping practiced in the region where the formation is proposed.* In the case of the current project, the '*scale of mapping practiced*' is basin-wide and the methodologies, discussed in Chapter 2 and 3, have resulted in a generalised, regional-scale stratigraphy based on the delineation of rock units that give rise to features that can be traced effectively on remotely-sensed images. Whilst checking of these features in the field has validated the results of the remote image interpretations, the time constraints during the field programme did not allow for detailed subdivisions to the degree, for example, proposed by Affaton (1990) and shown in Table 14.

With the above constraints in mind, a preliminary stratigraphical table has been constructed for the units that were identified within the Volta Basin and the small part of the adjacent Pan-African orogenic belt in the east (Table 7). Wherever possible, this utilises a modified version of the published terminology of Affaton et al. (1980), at least for units of group rank that can be recognised on the remote imagery. The subsequent classification of Affaton (1990) is not followed here, however, as it was evidently based on detailed field mapping in the Togo/Benin extension of the basin and features a number of units that cannot be distinguished on the scale of the present survey (Table 14). Furthermore in this report, only one 'supergroup' has been erected (Voltaian Supergroup), which covers all of the sedimentary divisions in the Volta Basin. The threefold division into supergroups by Affaton (1990) may be unneccessary and is a somewhat confusing departure from the published nomenclature established by Affaton et al. (1980). It also relegates the importance of the formation as the main mapping unit (NACSN, 1983). An alternative approach, relying on division at the lower end of the hierarchy shown in Table 14, could have been adopted by using the 'member' and then 'bed' rankings, as recommended by NACSN.

As noted above, some of the more recent schemes for subdividing the Volta Basin are inconsistent in their usage of stratigraphical terminology, nor have they benefited from the type of approach used in this report, which has utilised the presence of landform features, enhanced by remote imagery, to trace the extent of individual units throughout the basin. The nomenclature used in Table 7 should nevertheless be regarded as preliminary, and will be finalised only after further work has been conducted and consultations held with the Supervisor (GSD) and the Ghana National Stratigraphical Committee.

In Table 7 the 'Voltaian Supergroup' is the name given to the entire sedimentary sequence within the Volta Basin, overlying Palaeoproterozoic basement and lying to the west of the Pan-African thrust-front. The supergroup is in turn divided into four main groups: the laterally equivalent Kwahu and Bombouaka Groups, which are unconformably overlain by the Oti-Pendjari Group; the latter is in turn unconformably succeeded by the Obosum Group. Note that in Table 7 the name 'Oti-Pendjari' represents a minor modification to 'Pendjari-Oti' as used by Affaton et al (1980). The reversal of these names reflects that by far the largest outcrop of this group lies within Ghana, and much of it was originally termed 'Oti Beds' (e.g. Table 8). The etymology derives from the Pendjari River in Benin, which becomes the Oti River across the border into Togo, to the east of Ghana.

4.1.2.3 KWAHU GROUP

This newly named unit unconformably overlies Palaeoproterozoic, Birimian basement on the Man-Leo Uplift of the West African Craton. It is, in turn, overlain unconformably by the Oti-Pendjari Group. It includes the lowermost, predominantly arenaceous sequences of the Voltaian Supergroup along the southern and western rims of the basin and comprises sedimentary rocks of aeolian, fluvial and shallow marine origin. The Kwahu Group is of equivalent age to strata of the Dapango-Bombouaka Group of Affaton et al. (1980), which crop out along the basin-rim escarpment and in the Gambaga massif of the northern part of the basin. It corresponds to the 'Upper Sandstone', 'Upper Massive Sandstone' and 'Massive cross-bedded sandstones' of the schemes shown in Tables 8-10.

Mapping of the Kwahu Group, and its subdivision into the formations shown in Table 7, mainly depends upon the recognition of a distinctive set of landforms. The principal features, which also define the outcrops and boundaries of individual units, consist of steep erosional scarps, behind the crests of which are long, gentle (<1^{o}) dip slopes. These features are recognisable when viewed from appropriate directions in the field, but can be considerably enhanced by manipulation of the DTM imagery (Figure 11). Field investigations have shown that many of the formations constitute sedimentary packages, the individual parts of which could in future be separated out as members. A typical formation commences with mudstones and siltstones passing up into flaggy, fine-grained sandstones. These in turn pass upwards to a sequence of regularly bedded, predominantly medium-grained sandstones. These lithological variations have influenced the geomorphological evolution of the outcrop; the main process being scarp retreat initiated by differential erosion of the softer, mud-rich basal parts of the formations. The end result of this is the characteristically stepped topography of the Kwahu 'Plateau' (Figure 11), and the trellis drainage pattern of the region which reflects the broadly orthogonal relationship between streams aligned parallel with the strike of bedding along escarpment fronts, and those flowing down the adjoining dip slopes.

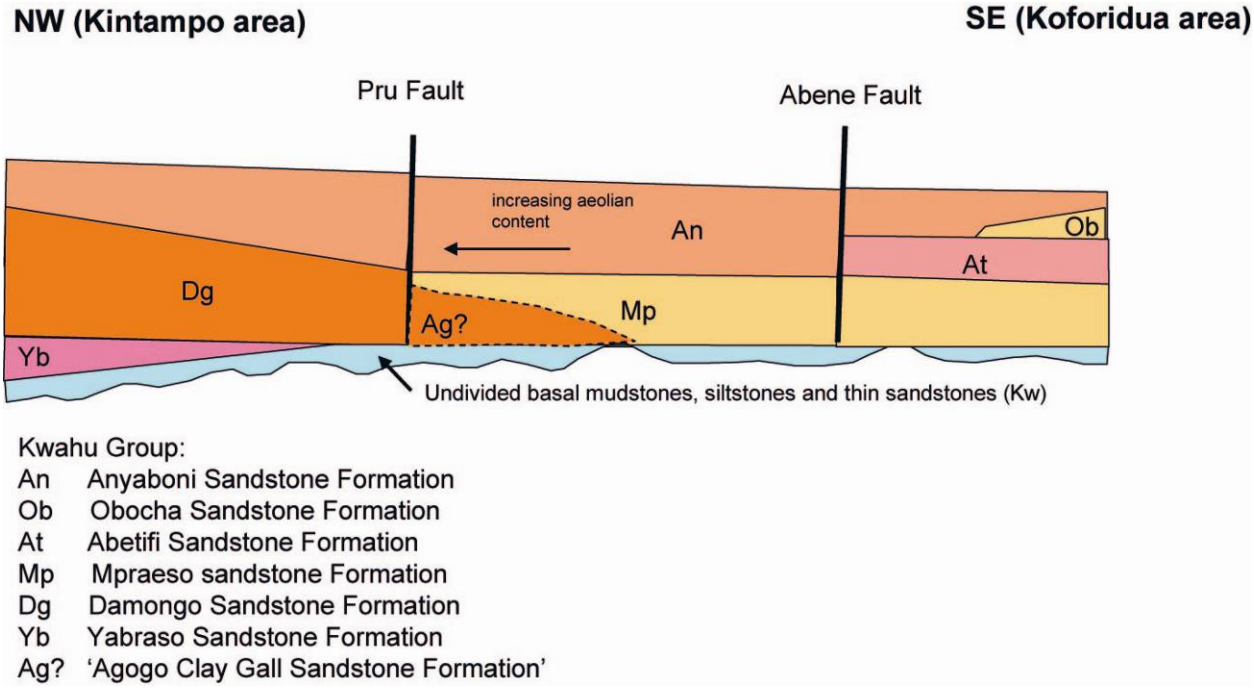

Figure 18 Inferred lateral facies changes in the Kwahu Group (units are not shown to scale).

Mapping suggests that overall, the Kwahu Group changes in thickness and lithological character from the south-east to the north-west of its outcrop area. This is reflected by a north-westwards

reduction in the number of mappable divisions (Figure 18). Syn-depositional movements along structures such as the Abene Fault may have played a role in this transition, but its precise nature requires further and more detailed investigation. Although feature mapping shows that the Obocha Sandstone does wedge out (Figure 11), there is less certainty about the status of the division remaining below the Anyaboni Sandstone. To the north-west of the Abene Fault, this lowest unit could be either the Mpraeso Sandstone (the currently favoured interpretation) or the Abetifi Sandstone, in which case the Mpraeso sandstone would be the unit missing. One further complication is that farther to the north-west, the putative Mpraeso Formation is replaced laterally by the Damongo Formation, as shown in Figure 18. Such variations within the Kwahu Group suggest that the Pru Fault may also have influenced sedimentation.

The lateral changes described above are accompanied by variations in the aggregate thickness of the part of the Kwahu Group within the project area, from about 1000 m in the south-east around Koforidua, to about 450 m between the Abene and Pru faults. North of the latter fault, around Kintampo, the Kwahu Group maintains a thickness of about 450-500 m and a similar value is suggested for the outcrop north of Damongo. It should be noted that in the western and northern parts of the outcrop the Birimian unconformity lies outside of the project area and consequently these thickness estimates are less well constrained.

Yabraso Sandstone Formation

This newly-named unit crops out around and to the south of Yabraso township, 11 km west of Kintampo (Figure 16). It is readily identified on remote images by its broad, smooth dip-slope, which indicates a structural dip of about half a degree towards the east. On the basis of this geometry, the Yabraso Sandstone is inferred to pass beneath the Damongo Formation, which is represented by an eroded escarpment feature farther to the east. Local topographic considerations suggest a thickness of 80-90 m for the formation. To the west, the Yabraso Sandstone overlies argillaceous strata forming the lowest-exposed part of the Kwahu Group in the Project area (‘Kw’ undivided on the map). At OBS JC 303, these underlying beds consist of maroon to pale green, variegated blocky mudstones and siltstones with a very diffuse lamination; their thickness is unknown as they extend outside of the project area.

The Yabraso Sandstone does not appear on the sketch maps shown in Affaton et al. (1980) or Affaton (1990), for example, but its topographical expression is identical to that of the Tossiegou Formation, which crops out 150 km farther north; consequently the two are considered to be equivalent. On the basis of this correlation, it is likely that the formation represents part of the ‘Basal Sandstones’ division in the ‘Lower Voltaian’ of Junner and Hirst (1946; see also tables 8-10). The same sandstone body was named the ‘Fuller Fall Sandstone’ by Kalvig and Vosgerau (2008). It should be noted that a further sandstone, 182 m thick, resting on basement and underlying 123 m of argillaceous strata presumably represented by the ‘Kw’ mudstones referred to above, has been identified in a borehole near Yabraso (No. 8 of Bozhko, 2008). This lower, concealed sandstone, which would presumably crop out to the west of the Project area, has been called the ‘Yabraso Sandstone Formation’ by Kalvig and Vosgerau and is the ‘First Unit’ of Bozhko (2008). It was correlated with the Tossiegou Formation by Kalvig and Vosgerau.

Excellent exposures of the Yabraso Sandstone, as defined here, can be seen to the east of Yabraso, at Fuller Falls. There (OBS JC 306; CT 20), the formation consists of buff-weathering, moderately to well-sorted medium- to coarse-grained quartz arenite in thin to medium beds. Internal structures consist of tabular and planar cross-stratification and some bed surfaces show undulatory to catenary current ripples. One exposure shows herringbone cross-bedding, with four current reversals in one metre of section (Figure 19a). About 5.5 km to the south-west of Yabraso (Obs JC 305; CT 19), roadside pavements show pale cream weathering, thinly bedded, medium to fine-grained quartzose sandstone with basal channel lags containing well rounded quartz granules and pebbles up to 20 mm in diameter (Figure 19b).

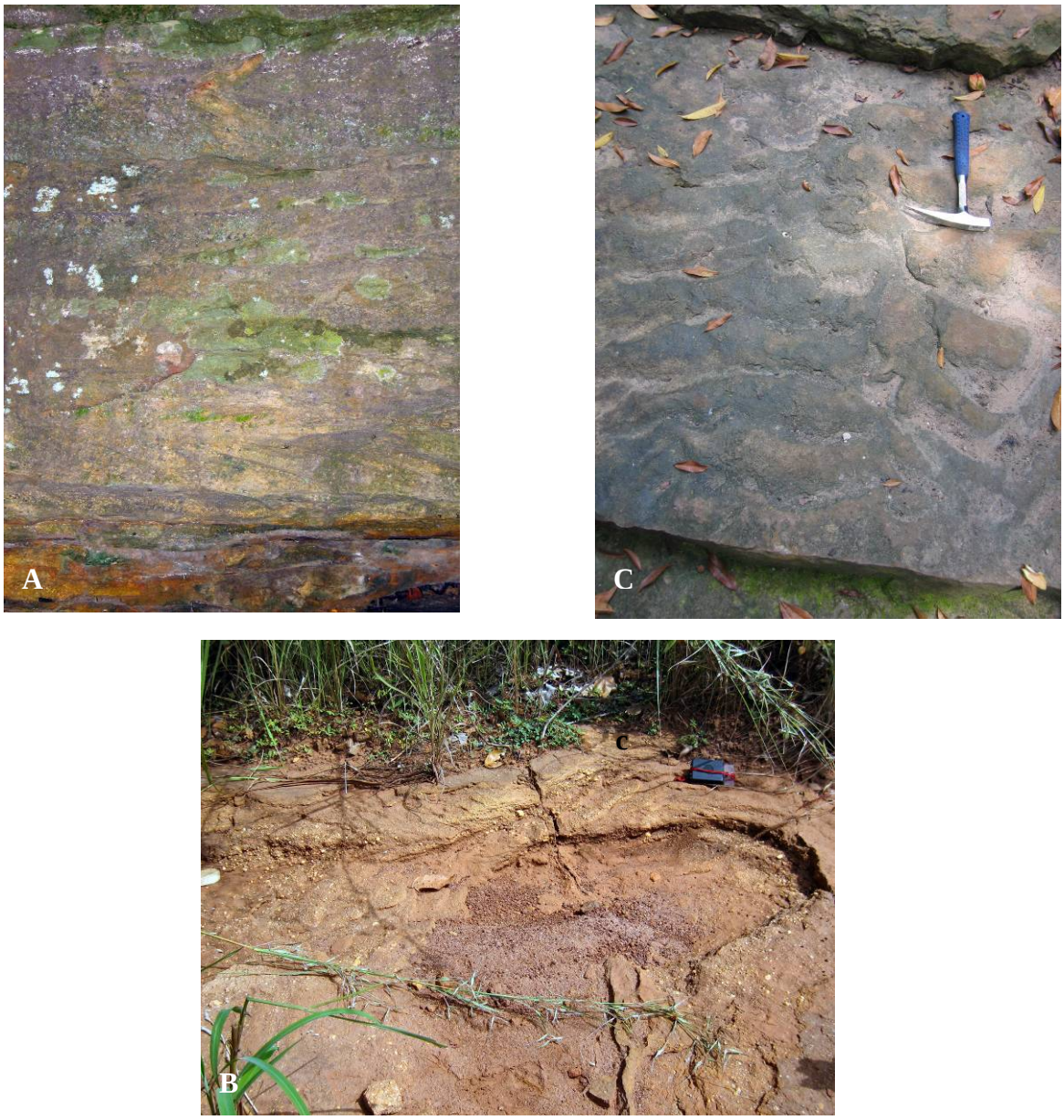

Figure 19 Sections in the Yabraso Sandstone west of Kintampo.
A) Yabraso Sandstone showing herringbone cross-stratification. B) Yabraso Sandstone showing channelised lags with quartz granules and pebble lags. C) Yabraso Sandstone showing current-rippled bed surface.

Only twelve records of palaeocurrent direction were obtained from the Ybraso Sandstone Formation, the majority of these from the excellent exposures at the Fuller Falls, west of Kintampo. Although there are some reversals in current direction between some beds, suggesting bimodal current directions, the current directions recorded are dominantly towards the north and east, with a few measurements uniformly towards the southwest (Figure 20a).

Interpretation: The sedimentary characteristics of the Ybraso Sandstone Formation indicate deposition in a fluvial environment that was also locally and/or temporally affected by shallow marine processes. Much of the style of cross-stratification and the consistent northerly current directions in the sandstone units strongly suggest fluvial flow. Well-rounded pebbles in lags at some localities may represent gravel accumulations in fluvial sand bars. In contrast, the presence of some herring-bone cross-stratification and current ripples on some bed surfaces are more consistent with a tidally-influenced environment. Thus, the depositional environment is a little ambiguous. On balance, a dominantly fluvial setting for the Ybraso Sandstone is preferred, the sediments probably being worked and deposited in a high-energy braid-plain with anastomising

channels that rapidly switch direction. If the tidal influence is also correctly interpreted, then we infer that this braidplain system was near-shore and close to an estuarine environment, such that strong tidal currents, such as those occuring during spring tides, could locally impinge on the the braid plain sediments. Finally, the northerly-directed fluvial currents indicate a northward-prograding largely fluvial system transgressing basin-ward. The wider implications for the depositional history are discussed further below.

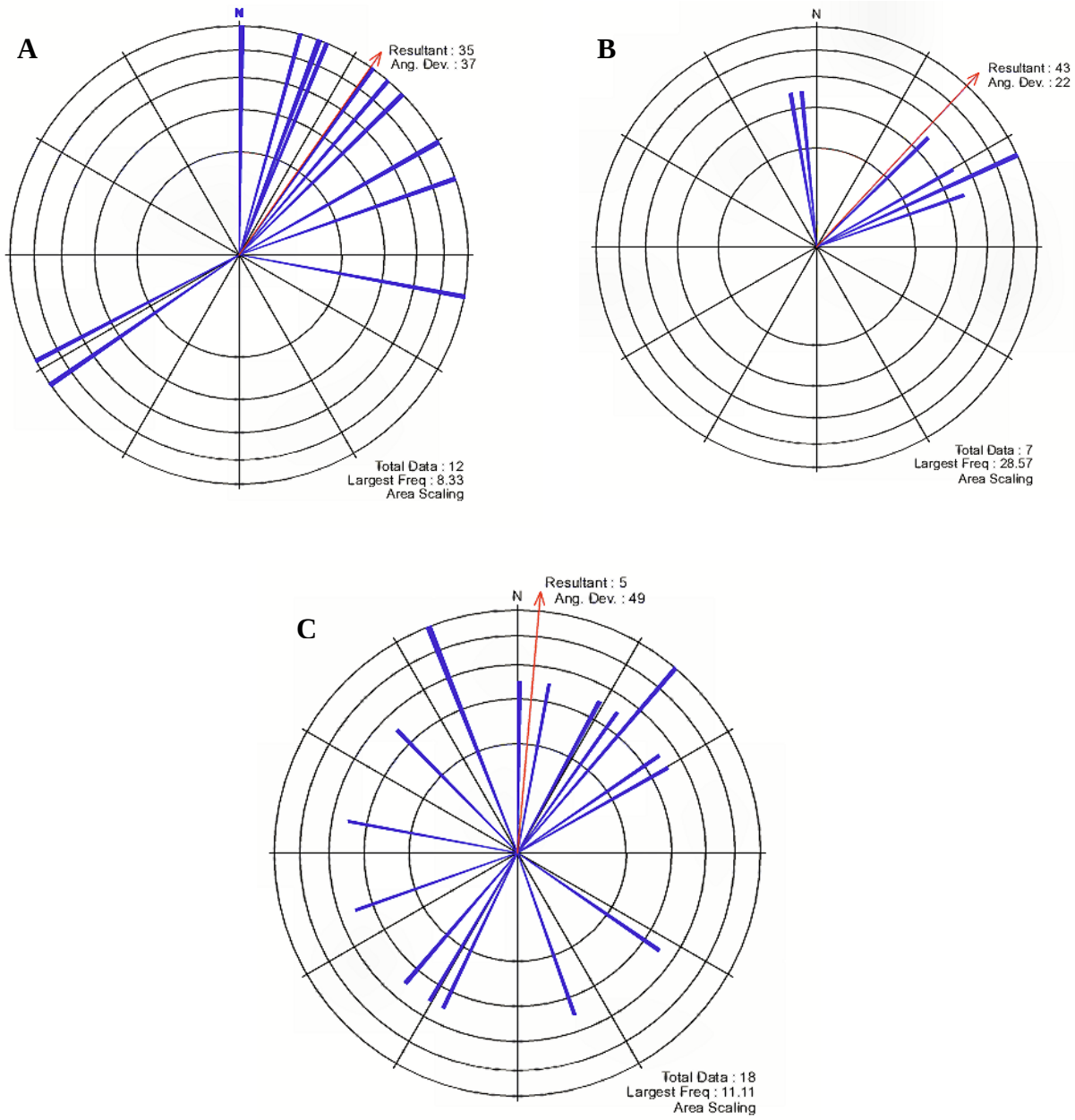

Figure 20 Rose diagrams for palaeocurrent data from the Yabraso, Mpraeso and Abetifi sandstone formations, Kwahu Group. A) Yabraso Sandstone Formation. B) Mpreaso Sandstone Formation. C) Abetifi Sandstone Formation.

Tossiegou Formation

This unit is considered equivalent in age and stratigraphical position to the Yabraso Sandstone Formation, which crops out farther south and is described above. As it is common to both the

Kwahu and Bombouaka groups its lithostratigraphy and correlation will be discussed later, in the section on the Bombouaka Group.

In the Kwahu Group, the formation crops out along the north-western margin of the Project area, about 6.5 km to the west of Damongo. It is recognised by its broad dip-slope, with an eastwards structural dip of about half a degree. This geometry indicates that the unit must pass beneath the Poubougo and Damongo formations.

No exposures were seen during field reconnaissance of the formation's limited outcrop in the north-westernmost part of the Project area (Figure 16). Descriptions of the unit in the Gambaga area are given below, in the section on the Bombouaka Group.

Poubougou Formation

This unit was originally included within the 'Dapango-Bombouaka Group' of Affaton et al. (1980) but is also a component of the lower part of Kwahu Group, as defined here, to the north of Damongo (Figure 16). As its main outcrop is in the Bombouaka Group, however, further descriptions and interpretations are provided in that section (below).

In the north-western outcrop of the Kwahu Group, the Poubougou Formation intervenes between the Tossiegou Formation, below, and overlying strata of the Damongo Formation. Here, it is estimated to be about 30 m thick, and to thin out southwards. The strata seen in the single exposure visited, beside the road (OBS CJ 112) about 750 m west of Larabanga, are from near the top of the formation. They consist of about 6 m of fissile, olive green mudstones and siltstones with thin (c. 5-10 cm) beds of pink-weathering, fine-grained sandstone (Figure 29d).

Damongo Formation

This newly-named unit consists of medium to thinly bedded and flaggy micaceous sandstones, fine-grained sandstones and siltstones. It crops out beneath the Anyaboni Sandstone Formation along the western margin of the Voltaian Supergroup, to the north of the Pru Fault. There, it may replace laterally the quartzose sandstones of the Mpraeso Formation, as described below and summarised in Figure 18. Farther north, the Damongo Formation rests on prominent dip slopes formed by the Yabraso and Tossiegou sandstone formations. The predominantly flaggy and micaceous Damongo lithofacies has been recognised in strata transitional between the Poubougou and Panabako formations in the Gambaga escarpment of the northern Volta Basin. The lithofacies is also very similar to flaggy sandstones that occur just above the mudstone and siltstone-rich basal facies of the Mpraeso Formation (see below). In the Agogo area, flaggy sandstones occupying the same stratigraphical position, and thus the probable equivalents of the Damongo Formation, were named by Mason (1963) as the 'Clay Gall Sandstone Formation', as discussed in the section on the Mpraeso Formation. The Damongo Formation may be equivalent to the 'Lower Kintampo Sandstone Formation' of P. Kalvig (Draft report PK 25/05/07), although in Kalvig and Vosgerau (2008) the equivalent strata were subsumed into a 'Kintampo Sandstone Formation', which also includes the Anyaboni Sandstone of this account.

On DTM shaded relief imagery the Damongo Formation is identified by ground that is devoid of prominent scarp and dip slope features, and is instead characterised by a highly distinctive, dendritic drainage pattern, as to the south of Damongo, west of Kintampo and west of Nkoranza (around OBS CJ 146). The formation is about 100 m thick west of Kintampo and in the Damongo type area. North of the latter it thins and appears to either wedge out or be replaced laterally by the Poubougou Formation.

Because of the susceptibility of this formation to weathering and erosion, good roadside sections were rarely found, and time constraints did not allow for detailed examination of river sections.

Small exposures on the road between Damongo and Larabanga consist of pink weathering flaggy bedded to finely laminated, fine-grained quartzose sandstone interbedded with micaceous, very fine-grained sandstones and siltstones (OBS JC 190). Farther north, diggings around a radio mast were mainly in buff, medium-grained, laminated quartzose sandstone and dark grey to purple fine-grained micaceous sandstones with grey mudflakes; flakes of maroon micaceous siltstone and mudstone were also seen. West of Kintampo (OBS CT21), exposures at the top of the formation, just below the junction with the Anyaboni Sandstone (Figure 21a,b), show fine- to medium-grained, moderately feldspathic, pale buff to variegated sandstone. Some beds exhibit large-scale cross bedding in their lower parts of beds, passing up into a massive sandstone upper part. Structures reminiscent of hummocky cross stratification are also seen.

Figure 21 Sedimentary features in the Damongo Formation. A) Sandstone showing cross-bedding in lower part, Damongo Formation west of Kintampo. B) Fine-scale cross lamination in sandstone of the Damongo Formation west of Kintampo. C) Flaggy, micaceous fine-grained sandstone of the Damongo Formation, roadside north of Kintampo.

At a further locality by the roadside 10 km north of Kintampo (OBS CT 24) strata typical of the Damongo Formation consist of fine-grained, feldspathic and micaceous thin- to medium-bedded sandstones. The beds are tabular to weakly trough cross stratified, and some show cross lamination (Figure 21c).

Interpretation: The Damongo Formation appears to have been deposited in a near-shore fluvial to shallow marine environment. Flaggy and micaceous sandstone with maroon and grey mudflake clasts, coupled with trough and tabular cross-bedding and northerly-directed current flow suggests a fluvial setting for part of the formation. However, other outcrops contain swaly cross-stratification, the presence of which indicates water of sufficient expanse to allow a fetch large enough to generate powerful storm waves. This could have been a coastal, large semi-marine lagoonal (tidal) or lacustrine setting, and there are similarities here with the Ybraso Formation.

Mpraeso Sandstone Formation

The Mpraeso Sandstone Formation represents the lowermost division of the Kwahu Group in the outcrop to the south-east of the Pru Fault (Figure 16). About 400 m thick, it includes an upper component of medium to thickly bedded and cross-bedded quartz arenites that dominate the landscape in the south-eastern part of the Kwahu escarpment (Figure 22a). The quartz-arenites pass downwards, and also laterally north-westwards (Figure 18), into flaggy, micaceous sandstones interbedded with mudstones and siltstones. In the south-eastern part of the outcrop the argillaceous basal facies rests upon the Birimian unconformity surface, which is locally exposed in the Project area. In the pre-1970 schemes of nomenclature, strata of the Mpraeso Sandstone were included within the 'Upper Voltaian' (Tables 8-10). The formation's outcrop closely corresponds to the 'Lower Quartzite' of the 'Kwahu Sandstone' division in the revised lithostratigraphical scheme proposed by Saunders (1970, and Table 11).

In the Bompata NE field sheet, at the north-western extremity of the outcrop, Mason (1963) recognised three divisions within what is here termed the Mpraeso Sandstone Formation. The 'Clay Gall Sandstone Formation' of Agogo occurs at the base, and is overlain by the 'Dente Shale and Siltstone Formation', which is capped by the 'Dente Massive Sandstone'. These components could not be separately mapped by the survey methodologies employed during this current project, and as they appear to occur within one landform unit on the remote imagery they are considered to belong to a single sedimentary cycle, which is encompassed by the Mpraeso Sandstone Formation as defined here.

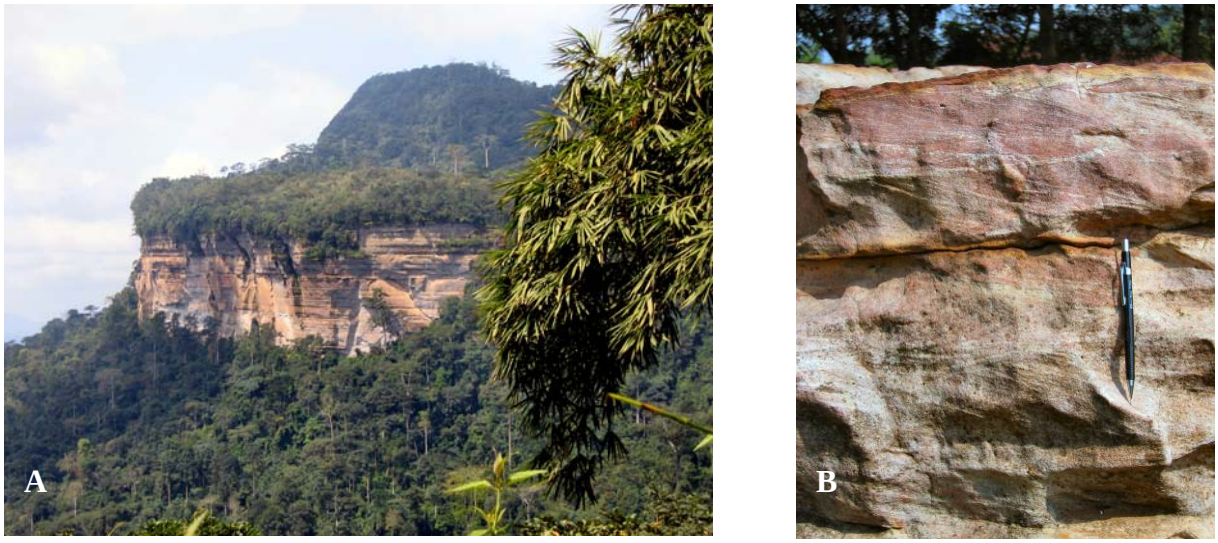

Figure 22 Sedimentary features in the Mpraeso Formation. A) Well-bedded quartz-arenites forming the middle and upper part of the Mpraeso Sandstone in the Kwahu escarpment. View northwards from near OP JC272. B) Mpraeso Sandstone showing planar and trough cross bedding, with herringbone pattern locally developed (near centre of image).

The basal Voltaian unconformity. In a roadside cutting between Nkawkaw and Mpraeso (OBS JC272), an exposure of this unconformity corresponds to the intersection of the Kwahu escarpment with a NE-elongated ridge of Birimian basement. Here, core stones of Birimian granitoid, representing the weathered top of the basement ridge, are mantled by a few metres of mudstone and siltstone forming the local base to the Mpraeso Sandstone (Figure 23). Certain of the mudstone and siltstone beds show flexuring and load structures, features interpreted to result from syn-sedimentary compaction against the irregular Birimian surface.

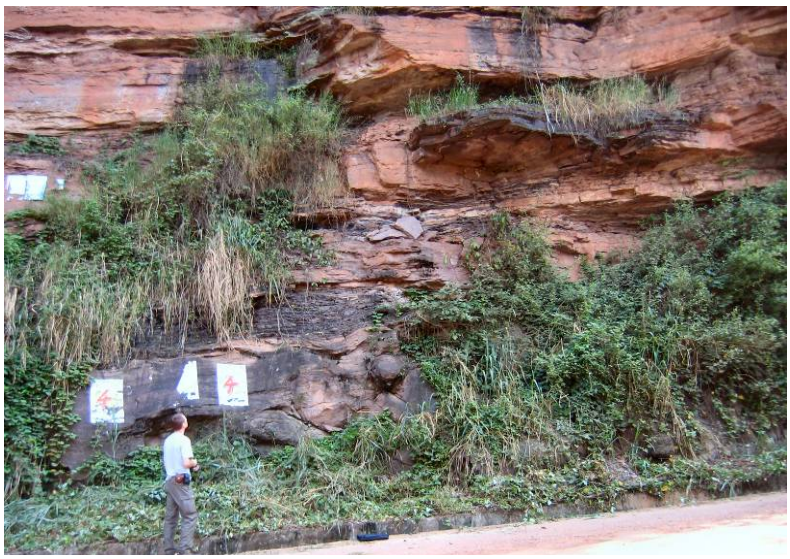

Figure 23 View of the Birimian/Kwahu Group unconformity. View of Birimian unconformity with granitoid core stones (upper right) mantled by variegated and laminated mudstones and siltstones showing load structures (lower right).Lower photo shows incoming of flaggy, micaceous sandstones.

The mudstones and siltstones pass upwards into a succession containing beds of flaggy, micaceous sandstone, which increase in proportion, and become progressively thicker up the section. Due to heavy commercial traffic, this transition was not followed farther up the cutting; however, other accounts (eg Junner and Hirst, 1946) note that this basal flaggy facies is about 60 m thick between Koforidua and Begoro and just over 100 m (350 feet) thick in the escarpment section between Nkawkaw and Mpreaso, below the upper quartz-arenites of the Mpraeso Formation. These flaggy beds are possibly equivalents of the 'Clay Gall Sandstone Formation' of Agogo, named by Mason (1963; see below) in the NE Bompata area. There, they commonly give rise to aprons of low-lying ground along the foot of the Kwahu escarpment, which have proved difficult to separate from the basement outcrop on remote imagery. More detailed investigation may show that the flaggy beds, and units such as the 'Clay Gall Sandstone' may represent a continuation of the lithofacies described (above) for the Damongo Formation.

Exposures in the lower and middle part of the Mpraeso Formation, in the north-west of the outcrop around Agogo township, typically consist of thinly bedded to laminated, fine- to medium-grained sandstone interbedded with grey mudstone and siltstone (OBS JC261); locally the sandstone is laminated and highly micaceous (OBS JC 262), suggesting that it may be a lateral equivalent of the Damongo Formation described above. These flaggy sandstones were named by Mason (1963) as the 'Clay Gall Sandstone Formation' of Agogo, distinguishing them from the overlying beds (see below) of the 'Dente Shale and Siltstone Formation', which is capped by the 'Dente Massive Sandstone', all of these divisions being placed within the 'Lower Voltaian'. According to Mason (1963), the 'Clay Gall Sandstone' reaches a thickness of about 260 m in the Bompata area, suggesting significant lateral variation within the Mpraeso Formation (Figure 18).

Exposures in the upper part of the formation are principally of quartz arenites. In the Bompata NE field sheet these strata were termed the 'Dente Massive Sandstone Formation', and placed within the 'Lower Voltaian' by Mason (1963). The quartz arenites are just over 100 m thick in the Agogo area of the Bompata field sheet, but farther south are estimated to be 200 m thick in prominent exposures along the face of the Kwahu escarpment (Figure 22a). During the current project, these strata were mainly seen in the south-east of the outcrop, in situations close to the top of the Mpraeso Formation as indicated by the morphology of its dip slope. A roadside section (OBS CJ206) exposes flaggy, medium- to coarse-grained sandstone with wave ripples on one bedding plane. Nearby, a more extensive outcrop shows cross bedding, with one very coarse bed containing small pebbles near to the top. In a further exposure (OBS CJ208) of the upper part of the formation, medium- to coarse-grained, locally pebbly sandstones contain abundant cosets of herringbone cross bedding. About 12 km north-east of Koforidua, pink-weathering, pale grey to cream, tabular bedded and cross-laminated quartz arenites are typical of the upper part of the formation. Here, sporadic reversals in current direction give rise to local herringbone patterns of cross-bedding (OBS JC273; Figure 22b).

Interpretation: The highly irregular unconformity surface at the base of the Mpraeso Formation suggests that immediately prior to deposition of the Kwahu Group, the landscape was probably that of a peneplane, with upstanding, NE-trending granitoid ridges. The core stones of weathered basement granitoid indicate a (probable) low-latitude, humid to semi-arid climatic regime.

The depositional environment of the argillaceous beds described at the base of the formation, which overlie Birimian basement, is uncertain. They may represent early lacustrine or deltaic (marginal marine) conditions, which were superseded by fluvial channel environments (micaceous sandstones higher up the escarpment). Samples from the basal mudstone-siltstone facies were investigated for acritarchs, but none were found.

Mason (1963) noted that the lower, 'Clay gall sandstone', included here within the Mpraeso Formation, was thinly bedded, with ripple-marked and locally mudcracked bedding surfaces indicative of shallow water, semi-emergent conditions, possibly along the 'shallow shore of a

large sea or brackish lake'. The overlying and closely similar 'Dente Shale and Siltstone Formation' contained similar sedimentary features which also included raindrop imprints.

Many of the sedimentary features in the Mpraeso Sandstone Formation described above are consistent with a largely fluvial origin. The lateral thickening of argillaceous facies referred to in pervious accounts as clay-gall sandstone also suggests fluvial depositional environments, as does the lack of acritarchs. However, the Formation does appear to become more mature upwards and this, coupled with the presence of herring bone cross-stratification in several outrops indicates a tidal influence. As with other coarsening-upwards units within the Kwahu Group, the evidence suggests a coastal, marginal marine setting in which fluvial sand systems interact with shallow marine processes, especially towards the top of the Formation. This is also consistent with the largely marine character of the overlying Abetifi Sandstone Formation. Only seven measurements of current direction were available for the Mpraeso Formation, all within the upper quartz arenite beds. However, they are broadly the same as those for the Ybraso Formation, showing trends to the north and east (Figure 20b). Zircon age spectra from the Mpreaso Formation presented by Kalsbeek et al. (2008, sample Gh 2) confirm that the formation was deposited shortly after 1000 Ma. It is therefore similar to other components of the Kwahu Group in that it pre-dates units such as the Afram Formation of the Oti-Pendjari Goup, deposited after about 620 Ma (Section 4.1.2.5).

Abetifi Sandstone Formation

This newly named unit is estimated to be between 150 and 200 m thick. It mainly consists of cream to white, medium-grained, cross-bedded quartz arenites and quartzites. The formation's outcrop is limited to the north-west by the Abene and Afram faults (Figure 16). To the south-east, it rests on the dip-slope of the Mpraeso Sandstone and is readily distinguished on remote imagery by its characteristic scarp and dip-slope morphology (Figure 11). The formation corresponds in part to the 'Upper Quartzite' division of the informally named 'Kwahu Sandstone' (Saunders, 1970), although that unit also includes the outcrop of the overlying Obocha Sandstone Formation of this account (see below). Where the Obocha Sandstone has thinned out farther north-west, the Abetifi Sandstone is succeeded by the Anyaboni Sandstone Formation.

As with the other formations of the Kwahu Group, the Abetifi Sandstone sedimentary cycle is inferred to commence with argillaceous strata. Such basal facies were not seen on the traverses taken during the current project. However, on the scarp slope just above the base of the formation near the village of Adokrom, a roadside cutting (OBS JC35) showed a tectonic contact between pale grey quartz arenite and steeply dipping grey, micaceous siltstone, the latter possibly representing an upfaulted sliver of the basal beds.

Strata in the middle to upper part of the formation are well exposed on the steep scarp slope of the formation, about 2.2 km south of Abetifi. Here (OBS CT2), an unusual facies of quartz arenite is developed, consisting of fine- to medium-grained, pale grey sandstone in very tabular beds of thin to medium thickness (Figure 24a). Saw-tooth profiles suggest that these beds are graded, fining upwards. They commonly show internal plane lamination, but some have very gently inclined cross-lamination; other than this, cross-stratification is absent. Certain beds contain gently scoured bases and a slight waviness to bed tops and bases is also apparent.

A roadside traverse east of Abetifi township shows abundant exposures of current-agitated sandstones representing beds close to the top surface of the formation (see also Carney et al. 2008. p.122-126). These are principally very clean quartz-arenites or quartzites, but with some highly micaceous laminae visible in places. Along the small track south of the 'Be A Man' junction (OBS CT3), small crags show hard, pale cream to white sandstones. They vary from medium-grained to very coarse-grained with granules present. Grains are generally very well sorted, with the coarse sand to granule fraction commonly being well rounded. The sandstones are thin to medium bedded and generally trough cross-bedded, with herring-bone cross-

stratification very common (Figure 24b). Farther along the same traverse, pavement exposures of bedding planes (OBS JC282) show medium-grained quartz arenites with interfering sets of current and wave ripples; the axes of trough cross-beds are also commonly seen on the same surface (Figure 24c). North of Begoro, roadside exposures (OBS 371) show pale grey, quartz-rich, medium- to coarse-grained sandstone. Tabular, cross-bedded sandstone is present throughout, with foresets dipping at angles of 10-25^{o}; drag-folding occurs in some beds, implying rapid sedimentation.

Figure 24 Sedimentary features in the Abetifi Sandstone. A) Thin-bedded tabular facies, from middle/upper part of theAbetifi Sandstone Formation. B) Herringbone cross-bedding near top of Abetifi Sandstone. C) Abetifi Sandstone bedding plane showing ripple marks and trough cross-stratification (to left of hammer head).

Interpretation: The nature of the sediment and the sedimentary structures in the Abetifi Sandstone indicate deposition in a generally shallow, high-energy marine environment. Many of the features are consistent with a shore-face setting and the extensive planar feature top-surface to the formation seen east of Abetifi implies an extensive, prograding shore-face system. The thin, tabular beds seen in the quarries south of Abetifi are interpreted to be turbidites, probably deposited down the apron of a delta front.

This unit, comprising sedimentary rocks deposited mainly in shallow marine environments, has a more complex distribution of palaeocurrent data than the underlying Mpraeso Formation. There is strong bi-modality in the data and there are two sets of bimodal data (Figure 20c). The dominant directions are towards the northeast and southwest; however, there also consistent north-north-westerly and south-south-easterly directed of trends. In exposures, sedimentological evidence of tidal flow is common (e.g. herringbone cross-stratification) and the dominant northeast and southwest trends are considered to be due to this process. The NNW-SSE set of trends are also

likely to be due largely to tidal flow, but the c. 70° divergence between these and the NE-SW direction indicates a change in coastline orientation, either locally (e.g. a stongly indented coastline) or a change in orientation with time. Limited control on the level in the succession at which the data were measured makes it difficult to assess the latter possibility, but it should be considered. Furthermore, the dominant trend in each of the two bimodal sets is to the north, indicating dominant palaeoflow to the north. When considered together with the palaeoflow evidence from the Mpraeso and Ybraso formations, it is clear that, overall, sediment transport and dispersal is to the north, ultimately towards the Taoudeni Basin in central/western Sahara. Zircon age spectra from the Abetifi Formation presented by Kalsbeek et al. (2008, sample Gh 3) confirm that the formation was deposited shortly after 1000 Ma, and is similar to other components of the Kwahu Group in that it pre-dates units such as the Afram Formation of the Oti-Pendjari Goup.

Obocha Sandstone Formation

As with other units of the Kwahu Group, this newly-defined formation is identified on remotely-sensed imagery by its topography, which consists of a prominent escarpment and dip slope (Figure 11). It reaches a maximum thickness of 200 – 250 m, but, on the basis of its topographic features, the formation wedges out to the north-west (Figure 18). The Obocha Sandstone forms part of the 'Upper Quartzite' of the 'Kwahu sandstone', as informally named by Saunders (1970). It also encompasses the outcrop of the 'Quartz sandstones' component of the 'Kwahu Sandstone Member' ('Lower Voltaian Formation') of Anani (1999).

As with the other divisions of the Kwahu Group, the sedimentary cycle represented by the Obocha Sandstone commences with argillaceous beds. These were visited at a single locality (OBS JC375) in landslipped ground along the foot of the Obocha Sandstone escarpment, about 15.5 km north-east of Koforidua. Here, a small scar and erosional gullies on the adjacent track (Figure 25) expose several metres of green-grey to brick red, micaceous, blocky to laminated mudstones and siltstones. These strata contain sporadic dark grey concretions consisting of phosphate-cemented mudstone and siltstone.

Quartz arenites forming the upper part of the Obocha Sandstone were not well exposed on the traverses undertaken for this project. A roadside pavement (e.g. OBS JC33) shows quartzitic sandstones, with common coarse sand and granules in a medium-grained matrix. This poor degree of sorting is typical of many other exposures of the Obocha Sandstone. A further locality (OBS JC36) exposes flaggy bedded to finely laminated quartz arenites, with some rippled bed tops. Two fining-up sequences were noted, each about 80 cms thick, their flaggy bases showing thin (1-2 cm) quartz granule layers and lenticles within medium-grained sandstone. This may be in keeping with the observation by Anani (1999), that on the Obocha sandstone outcrop many thickly bedded quartz arenites are underlain by granule conglomerates.

Petrographic studies on quartz arenite samples collected from the Obocha Sandstone outcrop by Anani (1999) showed a predominance of non-undulatory quartz grains, indicative of mainly plutonic, granitic source rocks. Tourmaline grain compositions indicated a similar provenance, although with a minor contribution from metasediments. Anani suggested that these sandstones were derived from the craton interior, attributing their compositional maturity to severe chemical weathering. Such a conclusion is in keeping with the observation of core stones on weathered basement rocks below the Voltaian unconformity (see above: Mpraeso Sandstone).

Figure 25 Exposures of mudstones and siltstones at the base of the Obocha Sandstone. The hill in the background represents the erosional escarpment of the formation, which is capped by quartz-arenites.

Interpretation: The presence of phosphate-cemented nodules in the argillaceous rocks at the base of the formation implies a marine setting. Higher up-section, the poorly sorted but fining upward quartz arenite beds indicate rapid deposition, possibly from turbidity currents, whilst the general coarsening upwards of the Formation as a whole indicates a prograding system. Thus we favour a marine setting for the Formation, possibly in a prograding delta front that reworks sediment from a hinterland where weathering and sedimentary processes have produced lithologically mature sediment.

Anyaboni Sandstone Formation

The name for this stratigraphically youngest unit of the Kwahu Group is taken from the 'Anyaboni Formation', which was first identified by Saunders (1970) in the south-eastern part of the Volta Basin. In the current project, landform analysis (Figure 11) has enabled the formation's outcrop to be traced around the southern and western margins of the Project area across a total strike length of about 520 km (Figure 16). The Anyaboni Formation is about 150-200 m thick on average and includes a spectrum of lithologies. Argillaceous and micaceous strata lie at the base, passing upwards into grey to pink, medium-grained sandstones with mainly subarkosic compositions (Anani, 1999) and an aeolian component. The formation was originally included within the outcrop of 'V3' or 'Upper Sandstone' of Junner and Hirst (1946, and see Tables 8-10). As also noted by Blay (1983), it broadly corresponds to the 'Chirimfa Beds', which were mapped at the top of the 'Upper Voltaian' north of Agogo, in the NE Bompata field sheet (Mason, 1963). Blay's conclusion, however, that the Anyaboni Formation overlies the Afram Formation is incorrect and resulted from a mis-correlation of the latter with mudstones forming the basal part of the Anyaboni sedimentary sequence (see also below: *interpretation)*. In the west of its outcrop, the unit is equivalent to the upper part of the 'Kintampo Sandstone Formation' of Kalvig and Vosgerau (2008).

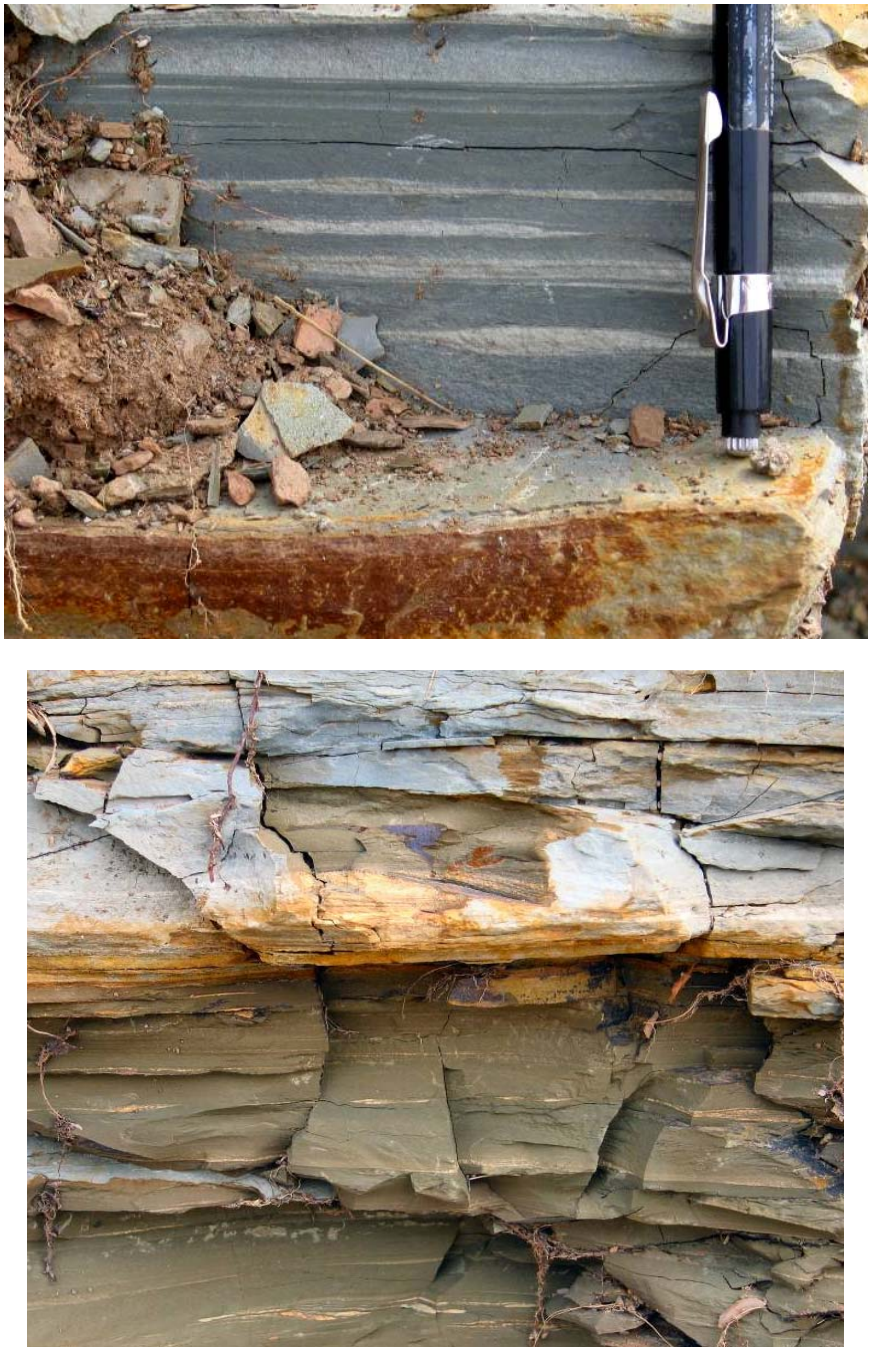

Figure 26 Mudstones and siltstones at the base of the Anyaboni Formation. Upper photo shows pale grey siltstone laminae with a graded bed at the top. Bottom photo shows a channelised bed (centre right) and discontinuous siltstone lenticles (middle and lower parts of photo).

The basal beds of the Anyaboni Sandstone are exposed at the back of a small quarry excavated into the foot of the Anyaboni scarp feature, to the east of the Abetifi-Adowso road (OBS JC374). The actual contact with the underlying Abetifi Sandstone Formation was not seen; however, ripple-marked quartz-arenite representing the top-surface of the latter was exposed on the quarry floor at about the same level as the Anyaboni formational base, suggesting that contact is a very sharp sedimentological break. In the quarry the basal beds of the Anyaboni Formation consist of at least 4 m of grey mudstone and siltstone (Figure 26), the former weathering to green-grey or khaki colours. The mudstone and siltstone beds are laminated, with mica coatings present on most laminae surfaces. The siltstone component consists of pale grey laminae, wisps and

lenticles; some of these outline starved wave-ripples, and there are sporadic graded beds of very fine-grained sandstone fining upwards to siltstone. Fallen slabs feature symmetrical wave-rippled top surfaces, some small-amplitude (c. 1-1.5 cm) examples of which show chevron upbuilding internal structure. Strata slightly higher in the succession were exposed in the road about 20 km east of Abetifi (OBS JC284) as purple-grey, very fine-grained, highly micaceous feldspathic sandstone (Carney et al., 2008, p.126) with some local fine-scale cross-lamination. This lithofacies is similar to that described by Saunders (1970) for the 'lower member' of the Anyaboni Formation, which together with basal shales and siltstones was estimated to be 130 m thick in the south-east of the outcrop. It is also very similar to the 'Chirimfa Shale and Siltstone Formation', which was mapped by Mason (1963) as a c. 60 m- thick sequence in the NE Bompata field sheet, to the north of Agogo. Mason noted in this unit the presence of variegation (red, green and purple) and the very high proportions of clastic biotite and muscovite.

Figure 27 Sedimentary features in the Anyaboni Formation. A) Plane-laminated arkosic sandstone beds in the lower/middle part of the Anyaboni Formation. B) Fluviatile sandstones in upper part of the Anyaboni Formation. C) Dune bedding in upper part of the Anyaboni Formation. D) Anyaboni Formation showing dune bedded sandstones succeeded by more thinly bedded, fluviatile sandstones.

In the south-east of the outcrop, beds in the lower to middle part of the formation are exposed in a roadside section 25 kn east of Abetifi (OBS JC285). They consist of red-weathering, fine- to medium-grained arkosic sandstones in tabular beds. Faint parallel lamination and low-angle cross-lamination are seen in parts. Bed tops and bases are very sharp and planar (Figure 27a).

The upper component of the Anyaboni Formation consists of medium-grained, subarkosic sandstones, mainly of fluviatile origin in the south-east, but with an increasing proportion of aeolian dune-bedded sandstone as the formation is traced to the west and north. High on a valley side about 24 km east of Abetifi (OBS JC 288) the fluviatile facies of the Anyaboni Formation is exposed as crags in red, medium- to thickly bedded arkosic sandstones (Figure 27b). The sandstones are either plane-bedded or cross-bedded, with some overturned bedding seen. Some of the beds are separated by thin (1-3 cm), discontinuous partings of purple, highly micaceous siltstone. Arkosic sandstone debris in the gully below these crags shows a wide range of sedimentary rock-types and structures appropriate to fluvial and possibly aeolian environments. They include beds with sporadic green or maroon mudflakes and mudflake-conglomerates. Most of the sandstone debris is plane-laminated to cross-laminated, some boulders suggesting the presence of beds up to 2 m thick. The debris includes sandstone with ‘pinstripe’ lamination in which rounded, millet seed grains are present.

Farther to the east, roadside exposures (OBS JC286) show feldspathic sandstones that have a striking, purple to grey-green pervasive lamination that is not related to any original sedimentary structures, and which largely obliterates the latter. The lamination has been attributed to incipient silicification, which may pre-date deposition of the Obosum Group (Crowe and Jackson-Hicks, 2008). Features possibly related to this process are seen farther north in the Anyaboni outcrop near the top of the Afram escarpment (OBS JC 38), where crystalline quartz infills numerous veinlets and rims small cavities within the sandstone.

In the south-eastern part of the outcrop, north of Koforidua, Anani (1999) noted the abundance of quartz grains with undulatory extinction in these sandstones. Together with tourmaline compositions, this feature suggested derivation from largely metamorphic source rocks, with a small contribution from granitic terranes. It was suggested that the sandstone compositions reflect derivation from a craton interior, but with local topographic relief perhaps imposed by wrench tectonics.

Aeolian dune bedding within the Anyaboni Formation is present at a number of localities in the north-west of the outcrop; for example, along the Mampon to Ejura road (OBS JC 250) and between Ejura and Nkoranza (OBS JC299; CT13), where roadside cuttings show particularly thick dune bedding (Figure 27c). Farther north, impressive exposures on the Yabraso road about 1.1 km north-west of Kintampo (OBS JC 310, CT 23), show friable, careous-weathering medium-grained arkosic sandstone in 3-4 m thick dune bedded sets overlain by 5-6 m of fluviatile sandstones. The latter are stacked in tabular-planar, unidirectional, cross-bedded sets of medium thickness (Figure 27d), with some cross-beds showing overfolding and slumping. This exposure corresponds to the upper part of the ‘Kintampo Sandstone Formation’ of Kalvig and Vosgerau (2008). A further correlation can be made between the arenaceous upper part of the Anyaboni Formation and the locally dune-bedded strata of the ‘Chirimfa Arkosic Sandstone Formation’, which occur in the hills to the north of Agogo (Mason, 1963).

Interpretation: The argillaceous basal beds of the formation at OBS JC374 were deposited as muds and silts in low-energy environments starved of clastic input. The occurrence of symmetrical wave ripples indicates shallow water in which sediment was affected by wind-driven waves. Other styles of cross-lamination and isolated, fine grained sand laminae in muddy rocks indicate tidal or other currents, probably in a shallow marine setting. However, the main part of the Anyaboni Sandstone comprises terrestrial, fluvial red-bed and aeolian facies. The fluvial facies were most likely deposited in braided river systems and there is evidence for some very large channel systems, as can be seen in the main escarpment looking southwards from the Adowso ferry landing and Adowso-Abetifi road. The large-scale aeolian dune facies are

restricted to the northwestern part of the outcrop. However, developed within these dune systems and also present in the outcrops east of Abetifi are very thick bedded, plane-laminated units that exhibit pin-stripe lamination. These units are interpreted as wet aeolian dune systems in which aeolian deposition is controlled by the height of the water table, leading either to accumulation, bypass or erosion (e.g. Crabaugh & Kocurek 1993), depending on the level within the sediment of the capillary fringe. Such wet aeolian systems form interdune flats. Aeolian deposits would have been common in the Neoproterozoic in the absence of plantae and were perhaps particularly common in coastal settings where sand supply was abundant. A number of modern analogues exist, where aeolian dunes interact with rivers (Langford 1989). A feature is the development of ephemeral lagoonal flood basins or playas dammed by the dunes in which sediment may accumulate before the lagoons either dry up or overflow the dune dams. The mudflakes noted in some of the sandstones may have originated in such shallow lagoons. The presence in many sandstone beds of well-rounded grains is also consistent with aeolian working of at least some of the sand. As with other units in which aeolian deposits have been identified, the restriction of the aeolian deposits to the western part of the outcrop indicates a general but clearly consistent geographical differentiation in facies: more commonly marine in the southeast, more commonly terrestrial in the west. The implications of this with regard to palaeogeography during deposition of the Kwahu Group will now be discussed.

The mainly fluvial palaeocurrent data recorded from the Anyaboni Formation are dominated by a north-westerly and a north-easterly trend (Figure 28a). There is a minor south-westerly component that may be bimodal with the main north-westerly trend. Once again, it is clear that the dominant sediment transport path was towards the north.

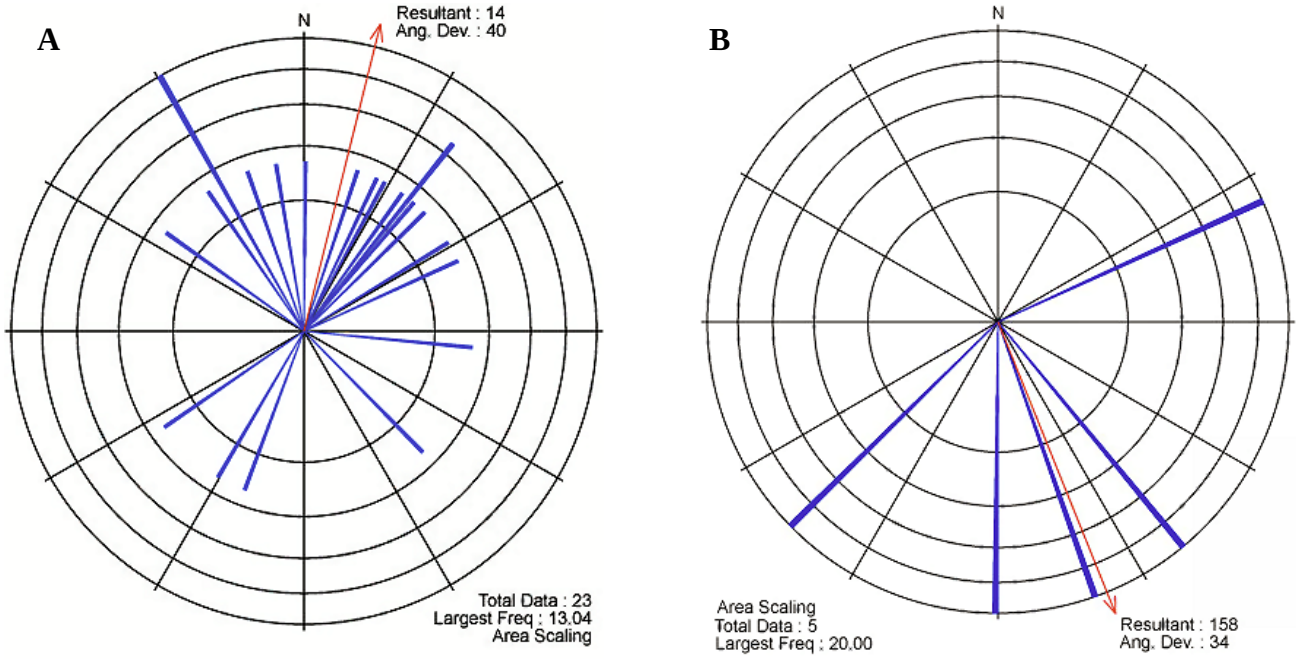

Figure 28 Fluvial and Aeolian palaeocurrent data from the Anyaboni Sandstone Formation. A) Fluvial palaeocurrent data from the Anyaboni Sandstone. B) Aeolian palaeocurrent data from the Anyaboni Sandstone

Not unsurprisingly, the aeolian palaeocurrent data indicate a different story. Although the data are fewer in number, the dominant trend is towards the south-southeast, with two measurements indicating transport to the east and the southwest (Figure 28b); these are opposite to the bulk of the fluvial and tidal data for underlying formations. The aeolian deposits are concentrated in the west of the outcrop of the Anyaboni Sandstone Formation and the data suggest dominantly south-easterly winds. How this relates to craton and basin geometries, or to palaeolatitudes, in terms of prevailing climate patterns is unclear from these and other limited data, but a more

detailed study might reveal how climate systems worked around the West African Craton during early Neoproterozoic time.

Zircon age spectra from the 'Kintampo Sandstone', equivalent to the Anyaboni Formation of this account, confirm that these strata were deposited shortly after 1000 Ma, and therefore are of a similar age to older components of the Kwahu Group (Akah, 2008). These data reinforce the inclusion of the Anyaboni Formation within the Kwahu Group, contrary to the conclusions of Blay (1983) that the formation post-dates the 'Afram Shales'. In this account the latter form part of the Oti-Pendjari Group, the age of which post-dates the Marinoan glacial deposits (Kodjari Formation), dated at 635-620 Ma (Section 4.1.2.5).

4.1.2.4 BOMBOUAKA GROUP

This group rests on Birimian basement and is in turn overlain by the Oti-Pendjari Group, a stratigraphical position identical to that of the age-equivalent Kwahu Group. Its outcrop is restricted to the northern extremity of the project area (Figure 16), where it is contiguous with the succession in Togo named as the 'Dapango-Bombouaka Group' (Affaton et al., 1980), subsequently revised to the 'Bombouaka Supergroup' (Affaton, 1990; 2008).

The subdivisions of the Bombouaka Group in this report (Table 7) essentially follow those of Affaton et al. (1980), as summarised in Table 7. Only the middle and upper parts of the group occur within the Project area, representing an aggregate minimum thickness of about 300 m. The various subdivisions shown in Table 7 were delineated on the basis of remote imagery interpretations supported by limited field checking, as explained in the section introducing the Kwahu Group.

Tossiegou Formation

The name for this unit is taken from Affaton et al. (1980) who mainly based their work on the contiguous exposures in Togo/Benin. Subsequently, however, Affaton (1990) renamed it as the 'Dapaong Group' (Table 14). Only the upper division of this new group ('Dapaong Formation') is likely to be present in the Project area; and to the east of Ghana this is described (Affaton, 1990) as consisting of alternations between ripple-marked quartzites, siltstones and shales. In the report of Junner and Hirst (1946), these strata were evidently all included within the 'Basal Sandstones' division (Table 8). They correspond to the 'Lower Voltaian' sandstones mapped by Edmonds (1956) in the Bawku-Gambaga area, and also perhaps to the 'Shishie Sandstone Formation' of Ayite et al. (2008).

In the Project area the formation occurs in the lower ground to the north of the Gambaga escarpment. Remote imagery shows that this outcrop represents a broad dip slope, inclined southwards and thus passing beneath the Poubougo Formation, the latter cropping out along the middle and lower parts of the Gambaga escarpment. No exposures were seen during the fieldwork. However, from this general area of outcrop Edmonds (1956) described both feldspathic and 'clean' quartzitic sandstones, commonly ripple-marked and including coarse-grained sandstones and 'grits'. Junner and Hirst (1946) noted quartzose, locally micaceous sandstones with subordinate beds of mudstone and conglomerate, conforming perhaps to the description by Affaton (1990) of the Dapaong Formation in Togo/ Benin.

Poubougou Formation

The name for this unit is taken from Affaton et al. (1980). It was later split between three formations and two groups (Affaton, 1990), as shown in Table 14, but such a detailed division cannot be substantiated and used by the current project because of the large-scale survey methods employed (Chapter 3). The Poubougou Formation mainly consists of mudstones and siltstones with thin sandstone beds. It is found only in the north and north-west of the Project area, where it overlies the dip-slope of the Tossiegou Formation and underlies with a gradational

contact, the Panabako Formation (north) and Damongo Formation (Kwahu Group north-western outcrop; see above). These strata were referred to the 'Middle Voltaian' by Edmonds (1956), and to the 'Nakpanduri Mudstone Formation' by Ayite et al. (2008).

In the Project area, strata conforming to the Poubougou Formation according to Affaton et al. (1980) were examined in roadside cuttings on the Gambaga escarpment, just below the Panabako Formation (OBS CJ 79). There, the formation is estimated to be about 170 m thick. Its middle and lower parts (Figure 29a) consist of green-grey, micaceous mudstones and siltstones, commonly with a 'papery' fissility. Harder and less fissile intercalations of siltstone and fine-grained sandstone stand out as ribs; they typically have sharp top surfaces and undulatory, slightly channelised bases, the latter in places showing spectacular load structures (Figure 29b). These argillaceous beds are also present beneath the Damongo Formation in the north-west of the Project ares (see above; Kwahu Group). In the Gambuga escarpment they are estimated to be 130 m thick according to Edmonds (1956). Their passage into overlying beds of the Panabako Formation is gradational over some 20-30 m of stratigraphical thickness; by upwards increase in the proportion of sandstone intercalations (Figure 29c) at the expense of the mudstone and siltstone component. In this upper part of the formation, the sandstones are typically grey-green and flaggy, with micaceous laminae and partings. Many are plane-laminated but some wavy and possibly hummocky lamination was also noted. Certain sandstones contain mudclasts and intraformational mudclast breccia layers.

Interpretation: The gradual increase in number and thickness of sandstone beds in the Poubougou Formation indicates a prograding sand source. It is probable that this is a type of delta system, and that the mudstones and siltstones are likely to be marine in origin, probably deposited on the toe of the delta. The fine-grained sandstone beds were likely to have been deposited by turbidity currents generated by storms or possibly earthquakes. Thus, the overlying Panabako Formation represents the proximal delta sandstones that prograded out over the earlier argillaceous rocks. The thin-bedded sandstones could represent over-bank flood sands in a fluvial system but, given the overall nature of the facies, this is considered less likely than the inferred marine origin. The corollary of the above interpretation is that the interpreted delta represents a marine front to the dominantly fluvial sedimentation seen to the south in the stratigraphical equivalent units of the Kwahu Group.

Figure 29 Sedimentary features in the Poubougou Formation. A) Mudstones, siltstones and thin sandstones near the top of the Poubougou Formation, Gambaga escarpment. B) Complex load structure at the base of a fine-grained sandstone bed near the top of the Poubougou Formation, Gambaga escarpment. C) Flaggy to thin-bedded sandstones at the gradational contact between the Poubougou and Panabako formations, top of Gambaga escarpment. D) Olive green mudstones and thin sandstones of the Poubougou Formation; escarpment north of Damongo. Note load structures at base of sandstone bed above hammer head.

Panabako Formation

This formation represents the topmost component of the Bombouaka Group (Table 7). It mainly consists of quartz arenites similar to, and probably age-equivalents of, the Mpraeso, Abetifi and Obocha sandstone formations in the Kwahu Group farther south. Its name is taken from Affaton et al. (1980; 1990), as shown in Table 13, and the same nomenclature was adopted by Viljoen et al. (2008). The formation is estimated to be 150-200 m thick and, from DTM imagery, to comprise two main (and as yet unnamed) sandstone sequences, the upper of which forms a series of erosional ‘sugarloaf’ cappings to the basal sandstone. It is noted that the Oti-Pendjari Group overlies the gentle southwards dip-slope of the older sandstone, indicating that at least some of the upper beds were removed prior to deposition of that group. The gradational passage between the formation and the underlying Poubougou Formation is described above.

In previous accounts (Junner and Hirst, 1946; Edmonds, 1956) the formation was included within the ‘V3’ or ‘Upper Voltaian’ (Tables 8-10 and discussion in text). More recently it has been referred to as the ‘Upper Nakpanduri Sandstone Formation’ (Ayite et al., 2008).

A roadside exposure in the south-west of the outcrop (OBS CT 35) shows sandstones that are very reminiscent of the top part of the Abetifi Sandstone Formation. They are hard and well-cemented, white, locally stained ochre, medium-grained and well sorted quartz arenites or quartzites, with minor contents of feldspar. The strata are thin-bedded, with possible swales and hummocks, and locally show trough cross-stratification. Farther to the north-east, by the side of the Walewale to Gambaga road, exposures (OBS CT 36) are in fine- to medium-grained weakly feldspathic quartz arenites, with sparse heavy minerals. The sandstones are laminated in broad, shallow, swaly or trough-like structures with unidirectional cross-stratification. Farther along the same road (OBS JC 138), quartz arenites of the formation are moderately feldspathic and medium-grained, with some fine-grained and coarse-grained, locally gritty layers. They occur in tabular cross-stratified beds, the latter locally overturned (Figure 30a); plane laminated beds commonly intervene between the cross-stratified sets (Figure 30b). North-east of the latter locality, a further exposure (OBS CT 37) is in moderately feldspathic, medium- and fine-grained quartz arenite showing low-angle cross-bedded sets (Figure 30c) that are in angular contact with beds in the lower part of the section. They pass up into tabular bedded sandstone with a parting lineation on some bed surfaces.

Viljoen et al. (2008) noted similar features in quartz arenites and subarkoses of the Panabako Formation to those described above. They also found poorly preserved herringbone cross-bedding and possible tidal bundles and reactivated surfaces; *Skolithos* burrows were well developed in places. They concluded that the formation was deposited in shallow marine, beach, tidal, lagoonal and estuarine sedimentary environments.

Interpretation: The evidence from the sediment and the sedimentary structures in the rocks suggest deposition in dynamic, marginal environments where a range of processes operated, as described by Viljoen et al (op cit.). The features seen in the good outcrops at OBS JC138 are consistent with deposition in a Gilbert delta; such deltas commonly form as fan deltas in water, where a narrow source exits into a wider basin. Gilbert deltas typically have a thick development of planar foresets forming the delta slope with the delta top at water-level. At the outcrops, the foresets are overlain by thinner top-sets of cross-bedded sandstone – again typical of Gilbert deltas. The presence of overturned cross-beds indicates drag folding during rapid deposition of sand. Gilbert deltas are not diagnostic of marine or non-marine environments; however, the switching direction of cross-stratification, and possible hummocky stratification suggests, in part, a near shore environment, possibly mid- to lower shoreface. Thus, the sandstones in the Panaboko Formation are interpreted to reflect a highly dynamic, prograding depositional system where marginal fluvial and marine processes interacted.

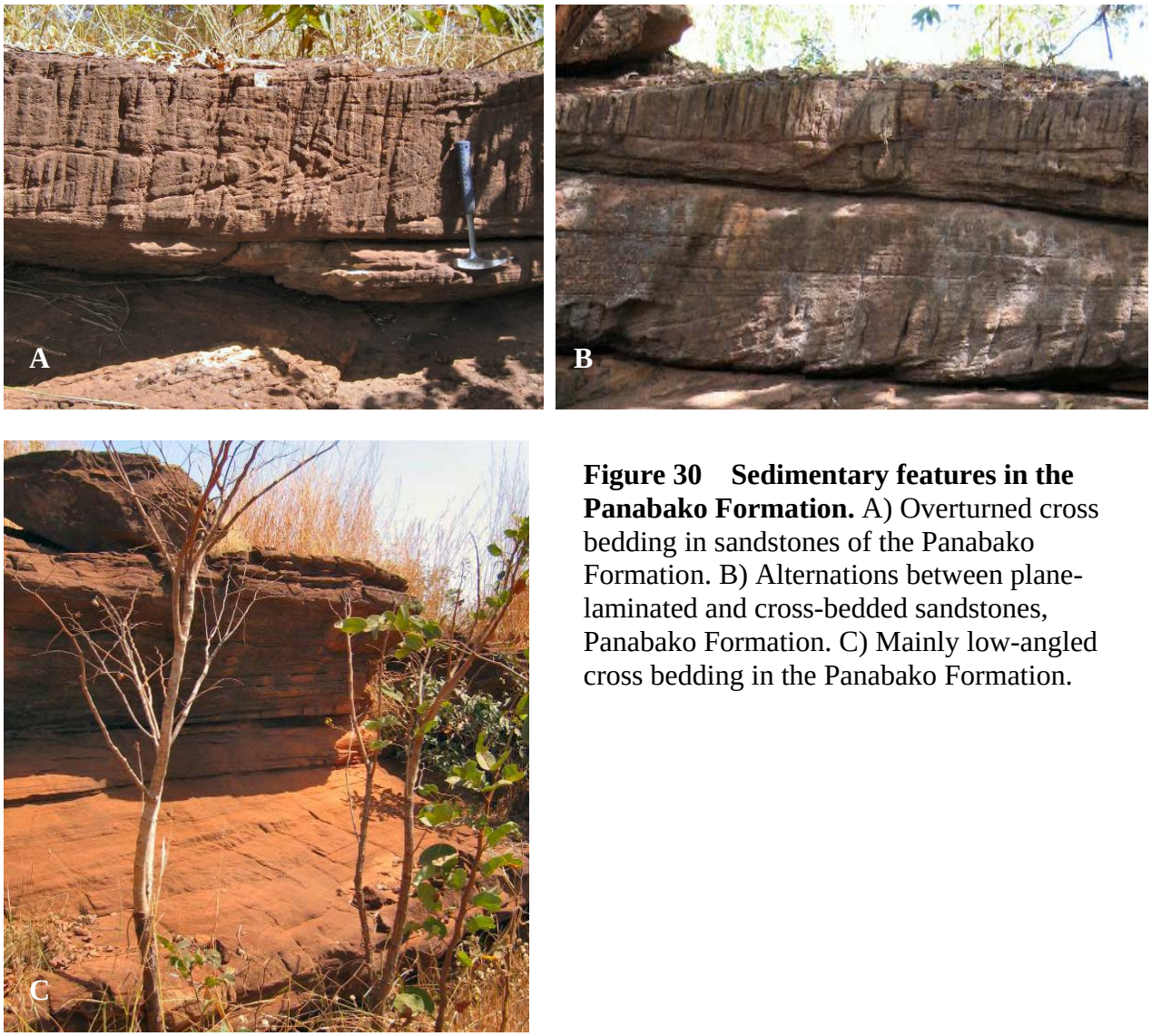

Figure 30 Sedimentary features in the Panabako Formation. A) Overturned cross bedding in sandstones of the Panabako Formation. B) Alternations between plane-laminated and cross-bedded sandstones, Panabako Formation. C) Mainly low-angled cross bedding in the Panabako Formation.

Overall interpretation of the Kwahu and Bombouaka groups

The sedimentary rocks of the Kwahu and Bombouaka groups present tantalising glimpses into the palaeogeography and depositional environments. What emerges from the cumulative evidence is a system that largely reflects deposition in marginal environments from fluvial through to shallow marine, from large-scale ergs to marine delta fronts or slopes. In many of the formations, there is strong evidence for deposition in shallow water and many include evidence for both fluvial and shallow marine depositional and erosional processes in the same or nearby exposures. Erg systems are generally confined to the western part of the outcrop of the Kwahu Group in the youngest unit, the Anyaboni Sandstone, whilst marine deposits appear to be more common in southeastern areas, indicating asymmetry to the basin. This asymmetry is consistent with the successive disappearance of some Kwahu Group units towards the west and northwest; for example, the Mpraeso and Abetifi formations, and with an overall decrease in the group's thickness in those directions. Such regional trends may in part be fault-controlled, as shown in Figure 18.

The implied asymmetry of the Volta Basin during Kwahu and Bombouaka group time probably reflects the fact that the basin as seen today is all that remains of a much broader marine gulf on the eastern side of the West African Craton (WAC) in early Neoproterozoic time, given that the eastern side of the basin is now defined structurally by an orogenic front. We envisage a coastal system for the Kwahu and Bombouaka groups in which rivers drained orthogonally off the WAC,

interacting with shallow marine and erg systems on a very broad coastal plain based on eroded and peneplaned Birimian basement. This coastal plain probably also included a broad fluvial braid-plain draining northwards (present day orientation) that carried long-travelled sediment from Amazonia and reworked locally-derived fluvial and aeolian sediment from the WAC. The presence of Grenville ages in zircon populations in samples from the Kwahu and Bombouaka groups is intriguing (Kalsbeek et al., 2008; Akah, 2008). In most Neoproterozoic crustal reconstructions of the putative Rodinian supercontinent, the Grenville orogen closest to the Volta Basin is the Sunsas Orogen, now located on the western margin of Amazonia. In reconstructions to date, the minimum distance between this orogen and the Volta Basin is of the order of thousands kilometres.

Coarsening upward sequences are characteristic of the formations, their bases defined by argillaceous successions that are succeeded by sandstones of various sorts. We suggest that the argillaceous units are likely to represent flooding events in most cases. However, the argillaceous sediments at the base of the Anyaboni Formation that succeed the Abetifi Formation are interpreted to reflect the establishment of estuarine conditions and may actually indicate a basinward migration of semi-marine to fluvial facies over shoreface deposits. This may reflect a lowering in sea level, and so the base of the Anyaboni Formation may represent a true sequence boundary. This would be consistent with the subsequent development of terrestrial red-bed fluvial facies throughout much of the remaining Anyaboni Formation. However, while it is tempting to consider the flooding events in terms of the Exxon Sequence Stratigraphy model, based on erosional sequence boundaries, this may not be appropriate. Rather, the Galloway model of dividing sequences based on flooding events may be a more profitable framework within which to consider Kwahu Group sedimentation and lithostratigraphy.

4.1.2.5 OTI-PENDJARI GROUP

This group rests with profound unconformity on the Kwahu and Bombouaka groups, and is in turn unconformably overlain by the Obosum Group. It includes certain of the ‘Middle Voltaian’ divisions proposed by Anan-Yorke (1971, and Table 10), and most of the ‘Pendjari Group’ of Affaton et al. (1980, Table 14). The group occupies a broad, asymmetrical trough, its strata thickening from zero in the west, to about 2700 m in the east (e.g. Affaton, 2008). In that part of the Volta Basin, and particularly in the sector occupied by the Oti and (flooded) Volta valleys, the strata become increasingly folded and flexured, before being terminated against the frontal thrust systems of the Pan-African ‘Dahomeyide’ orogenic belt (Bertrand-Sarfati et al, 1991; Affaton, 2008).

The nomenclature and etymology of the group is discussed in Section 4.1.2.2, and its division into formations and members is shown in Table 7. The strata mainly consist of mudstones and siltstones, commonly grey-green but locally with ‘red beds’, together with sporadic limestones and conglomerates. The youngest recognised unit, here termed the Bimbila Formation, has a higher arenaceous content and includes prominent beds of turbiditic sandstone, some of which form important stratigraphical and structural markers.

The unconformity that defines the base of the group spans about 350 m.y. of geological time (see section 4.1.2.8). During that period, strata of the Kwahu and Bombouaka groups were eroded into wide palaeovalleys that were subsequently infilled by the Oti-Pendjari and Obosum groups. Such erosion would have mainly taken place during the Cryogenian Period of Late Neoproterozoic time and so may have involved processes associated with ‘icehouse’ climatic conditions. While deposits of the c. 720-710 Ma Sturtian icehouse (e.g. Knoll, 2000) have not, apparently, been preserved, tillites related to glaciation during the Marinoan icehouse interval (630-620 Ma; Knoll et al., 2004) are locally present at the base of the Oti-Pendjari Group. In Togo, these tillites overlie a striated pavement developed on underlying sandstones of the Bombouaka Group (Leprun and Trompette, 1969).

Owing to the relatively soft, erodible nature of the infilling Oti-Pendjari and Obosum strata, the original palaeovalleys are currently being re-excavated, notably by the trunk streams of the White and Black Volta rivers. This process has partially exhumed certain upstanding Neoproterozoic landscape elements, represented by massifs formed by the underlying Kwahu and Bombouaka groups, which now form the low hill ranges marginal to the Volta Basin around Gambaga, Damongo and the Kintampo-Kwahu area (Figure 16). Away from these palaeovalleys, and from displacements such as the Afram Fault (Figure 17), DTM imagery and profiles derived from Fugro EM data (e.g. cross section 4 of the Intrabasin Interpretation Map) show that the Oti-Pendjari Group overlies gently dipping strata of the Kwahu Group, which in the south and west consist of the Anyaboni Formation. Such relationships, together with zircon chronological age spectra (Kalsbeek et al., 2008; Akah, 2008) favour the lithostratigraphical interpretations of Saunders (1970) and Affaton et al. (1980), and this account, rather than those of Blay (1983) as discussed in Section 4.1.2.1.

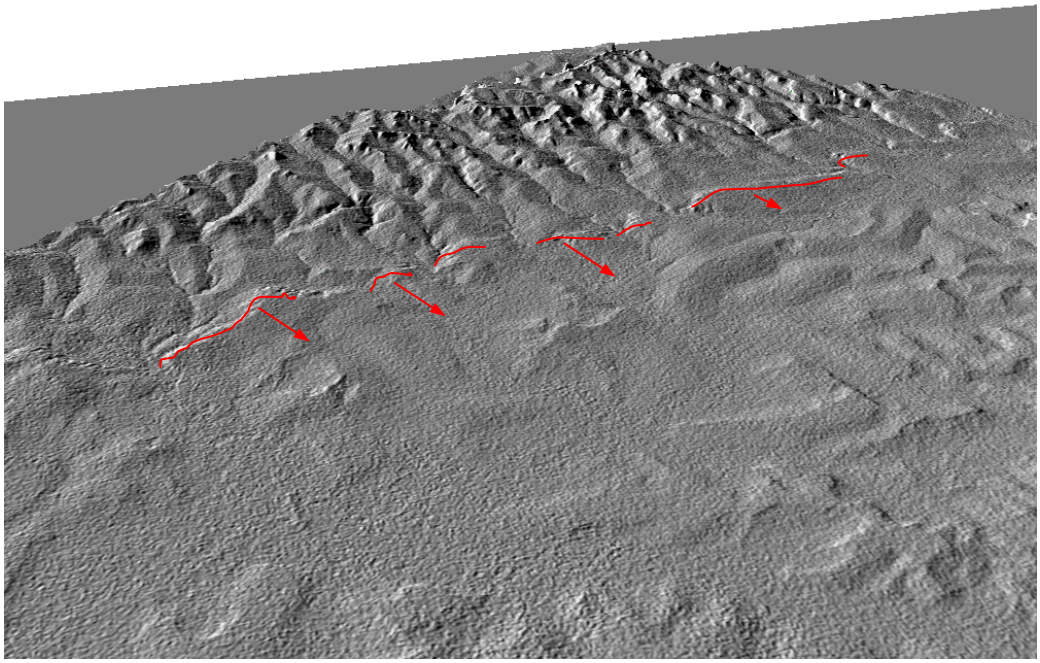

Figure 31 DTM shaded relief perspective looking northeast. The escarpment formed by the Darebe Tuff Member and the latter's generalised dip direction (red arrows) are shown.

Kodjari Formation

The name Kodjari Formation follows the usage of Affaton et al. (1980); however in Affaton (1990) the unit was renamed as the 'Sud-Banboli Group' (Table 14). The formation represents a distinctive 'triad' of lithologies, consisting of a basal tillite, not differentiated separately in this study, overlain by a 'cap-carbonate' sequence (Buipe Limestone Member), which in turn is succeeded by laminated tuffs and ash-rich siltstones (='silexites' of Affaton et al., 1980), here named the Darebe Tuff Member. The siliceous nature of the Darebe Tuff renders it resistant to erosion, relative to overlying beds of the Oti-Pendjari Group, enabling its northern outcrop to be recognised as a prominent cuesta consisting of a low escarpment, surmounting underlying strata (Panabako Formation) of the Bombouaka Group, and a narrow, southerly inclined dip-slope (Figure 31). This feature is the most important criterion for mapping the outcrop of the Kodjari Formation using the methods employed for this project. The same feature, although more subdued, can be recognised around Buipe, in the north-west of the basin, but its absence farther south suggests that in those areas the Darebe Tuff, and possibly other members of the Kodjari Formation, may not be present. It is noted, however, that in the Afram valley outcrop debris from

a well digging (OP/JC249) close to where the Afram Formation is inferred to unconformably overlie the Anyaboni Sandstone showed abundant fragments of non-laminated, pink and yellow chert. This suggests that silicification of the type described (below) from the Daboya area may be widespread along the unconformity between the Bombouaka-Kwahu groups and overlying Oti-Pendjari Group in the southern part of the basin.

Buipe Limestone Member. This unit is here named from its type area to the west of Buipe township, where trial pitting and quarrying activities have provided good sections. The outcrop in this area is partly based on the sketch map provided by Mitchell (1960), with modifications to the eastern boundary where the Darebe Tuff feature can be recognised from the project's DTM imagery (see above). The member appears to crop out intermittently at the base of the Oti-Pendjari Group throughout the northwestern and northern parts of the Project area, although it is generally poorly exposed.

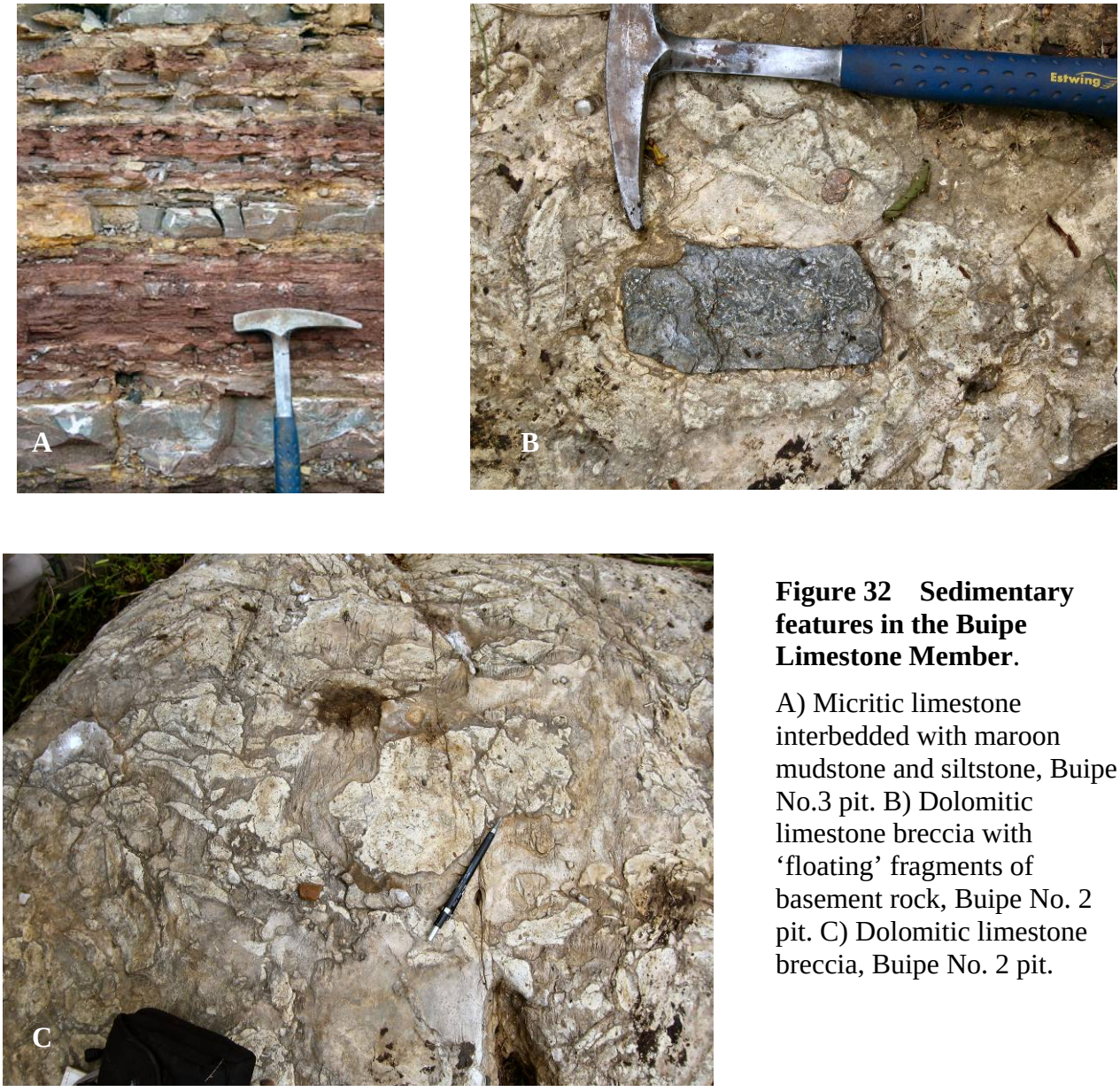

Figure 32 Sedimentary features in the Buipe Limestone Member.

A) Micritic limestone interbedded with maroon mudstone and siltstone, Buipe No.3 pit. B) Dolomitic limestone breccia with 'floating' fragments of basement rock, Buipe No. 2 pit. C) Dolomitic limestone breccia, Buipe No. 2 pit.

In the Buipe No.3 limestone quarry (OBS JC197), the lithology consists of pale grey or blue-grey, laminated, thinly bedded or massive micritic limestone with regular alternations of dark maroon, finely laminated ('papery') micaceous siltstone (Figure 32a). The tops of some limestone beds are ripple-marked, and are pock-marked by small pits resembling halite

pseudomorphs. These beds pass downwards to yellow, thinly bedded, dolostones. Nearby, in Buipe No.1 Quarry (OBS JC200), exposures are in massive dolomitic limestone breccia with sporadic 'floating' pebbles and cobbles of basement rock (Figures 32b and c); the lithology is illustrated further in the Mineral Occurrences section of the Phase 1 report.

A borehole at Buipe intersected 110 m of conglomeratic strata, which Bozhko (2008) named the 'Buipe Formation'. The lower 62 m consisted of a 'tillite-like conglomerate' consisting of various basement rock fragments enclosed within an unsorted, quartzitic to feldspathic sandy matrix. This appears to grade downwards, possibly through a weathering zone, into bedded sandstones, which here are correlated with the Anyaboni Sandstone. In the upper 48 m of this sequence, similar basement clasts are enclosed within a dark green, argillaceous matrix suggesting a more typical 'tillite' lithology. The overlying carbonates in the Buipe borehole were included by Bozhko within a 'Prang Formation', but no details or thicknesses were given save that the carbonates may be less than 6 m thick. It was noted that farther east, in the Prang borehole, dolomitic carbonates overlie sandstone with no obvious tillite present.

A detailed study of lithologies from the base of the Kodjari Formation at Buipe was undertaken by Nédélec et al. (2007), although information on the nature or whereabouts of their stratigraphical section was not given. The Buipe Member was described as being 25 m thick, commencing with about 11.5 m of yellow to pale pink dolostone with fenestral, birds-eye and peloidal structures indicative of microbial activity. There is an upwards transition into shales with beds of pure limestone, the latter, being recrystallized, showing no primary sedimentary features. The tillite outcrops around Buipe were described as being discontinuous, but no descriptions were given.

About 85 km north of Buipe, further exposures in the Buipe Limestone Member were visited at the Daboya landing, on the west bank of the Black Volta (OBS JC166, 323; CT 29, 30). Here, about 1.5 m of cream-grey, predominantly fine-grained barite-veined dolostones are exposed. Beds average 20-30 cm in thickness and most show internal lamination. Many beds contain diffuse, matrix-supported conglomeratic layers or lenticles (Figure 33a), the latter in the form of troughs with channelised bases. The larger clasts consist of quartz, chert and various metamorphic rock-types. The lower exposed part of the section consists of at least 55 cm of pale yellow dolostone or calcareous sandstone with abundant medium quartz grains. Local dips of 20-30^{o} to north or north-east are anomalous, and may suggest syn-sedimentary slumping.

Some 150 m upstream of the Daboya landing, riverside crags (OBS JC 324) expose the unconformable contact between the Buipe Limestone Member and underlying aeolian dune-bedded quartz arenite of the Anyaboni Sandstone. The succession, shown in Figure 33b, illustrates an unconformity surface with a local marked palaeo-relief of about 1.5 m. The lower part of the section is the unconformity surface, which here consists of chert-veined Anyaboni Sandstone. Tillite might be expected to be present above the Anyaboni Sandstone, and may be represented here by a diamicton consisting of massive, pale yellow, calcareous sandstone with sporadic 'floating' clasts that include Anyaboni Sandstone (Figure 33c). Succeeding the diamicton is a thin lenticle of pale grey mudflake conglomerate. Overlying this, the basal carbonate unit is composed of laminated, ooidal limestone.

The limestone exposures around Daboya possess locally high magnetic susceptibility values (Appendix 6; OBS JC 167, 168), suggesting a means for further delimiting the limestone outcrop in this densely vegetated terrain.

No exposures of the Buipe Limestone Member were found in the northernmost outcrop of the Kodjari Formation, south of Gambaga, where the carbonates have been commercially prospected around Bongo-Da (see Mineral Occurrences section). In this general area, however, the equivalent strata, named as the Buipe Formation, have recently been re-surveyed by Viljoen et al. (2008). The unit is described as consisting of a white to pink, laminated to bedded dolostone interbedded with sandstone and shale. Structures include pseudo-tepees, synsedimentary breccias, folding and symmetrical ripple marks. The tillite locally exposed beneath the

carbonates was named by Viljoen et al. as the Kudjawen Formation, and is described as a calcitic diamictite.

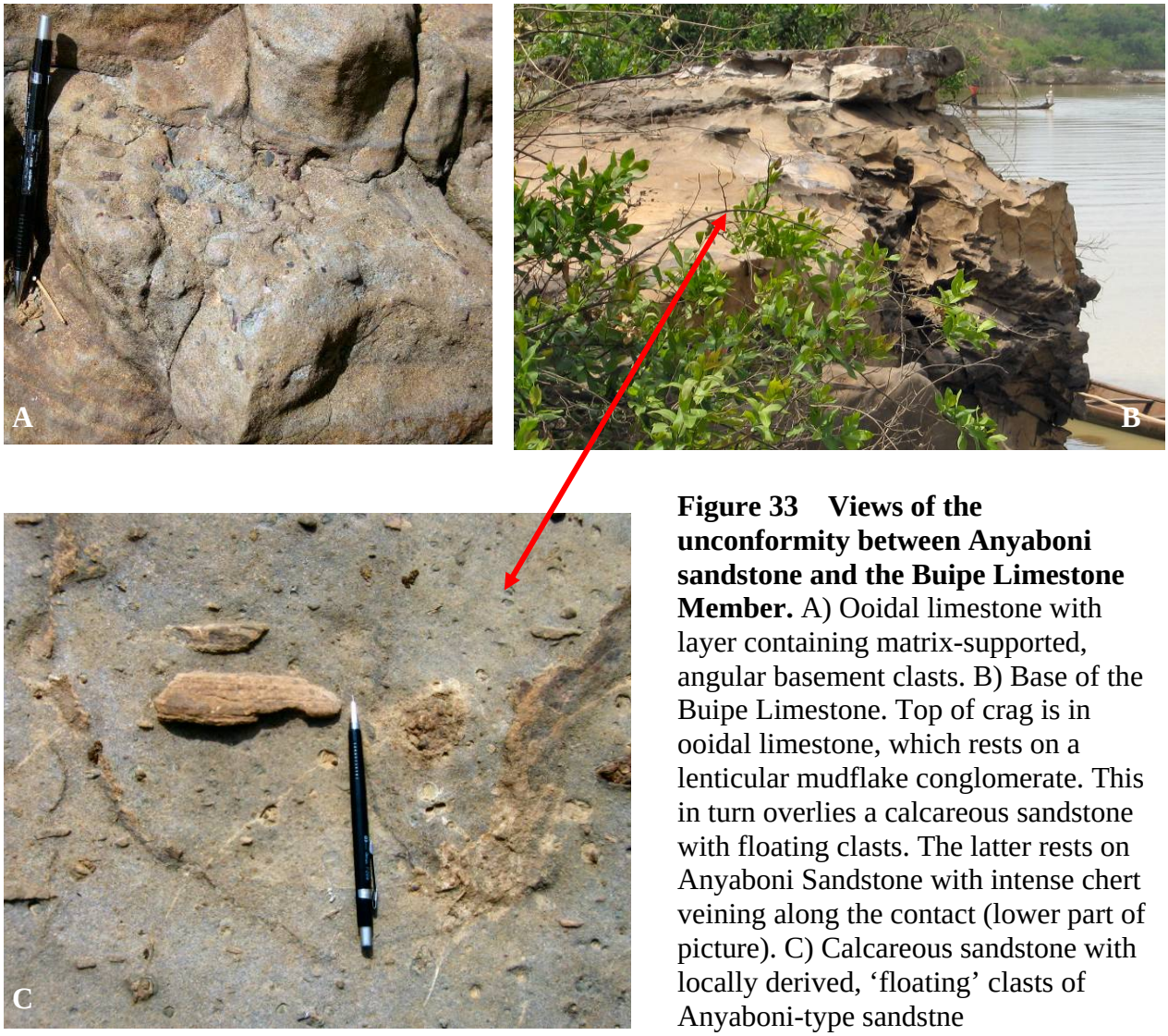

Figure 33 Views of the unconformity between Anyaboni sandstone and the Buipe Limestone Member. A) Ooidal limestone with layer containing matrix-supported, angular basement clasts. B) Base of the Buipe Limestone. Top of crag is in ooidal limestone, which rests on a lenticular mudflake conglomerate. This in turn overlies a calcareous sandstone with floating clasts. The latter rests on Anyaboni Sandstone with intense chert veining along the contact (lower part of picture). C) Calcareous sandstone with locally derived, 'floating' clasts of Anyaboni-type sandstne

Interpretation: In the Daboya exposures the tillite basal to the Buipe Limestone Member either is not present or is replaced by a sandy diamicton, the latter possibly representing part of a glacial outwash apron. The remainder of the formation represents a classic 'cap-carbonate' lithological association, deposited following global 'icehouse' conditions, evidence for which is provided by the basal tillite observed elsewhere in the Buipe outcrop. Nédélec et al. (2007) concluded that the Buipe carbonates were deposited in peritidal environments, analogous to modern littoral lagoons or sabkhas, in warm to semi-arid conditions. Geochemical profiles and carbon and oxygen isotope profiles through the carbonate sequence were interpreted to indicate the action of bacterial sulphate reduction. The glacial event that deposited the basal tillite was considered to have been either Sturtian or Marinoan in age. Equivalent carbonates at the base of the Oti-Pendjari Group in Togo were studied by Porter et al. (2004), who concluded that the lithological characters and stable isotope variations were typical of carbonates overlying the Marinoan tillite elsewhere in the world, rather than being related to the much earlier Sturtian glacial event. The Marinoan glaciation is believed to have occurred at about 620-635 Ma, and it defines the commencement of the Ediacaran Period of Late Neoproterozoic time (Knoll et al., 2004). This is therefore taken to be the maximum age for strata of the Oti-Pendjari Group as defined in Table 7.

The association between thin limestones and interbedded maroon, papery shales observed at the Buipe No.3 quarry during the present project is suggestive of a low-relief, terrestrial environment, with the limestones representing deposition in ephemeral bodies of water. However, a marine origin as proposed by Nédélec et al. (2007) cannot be ruled out and more work would be needed to establish the origin of this particular lithofacies.

The locally high magnetic susceptibility of the Buipe Member, measured during this Project at Daboya, though not at Buipe, is comparable to the lower parts of the Doushanto (Ediacaran) cap carbonate sequence in China, which was attributed by Wu et al. (2005) to an abundance of insoluble siliciclastic material derived from the underlying tillite. The possibility that glacial influences overlapped with deposition of the basal beds at Daboya and Buipe is further suggested by the local presence of extraclasts, either as discrete cobbles (?dropstones) or concentrated in layers within the carbonates.

Darebe Tuff Member. This resistant unit is readily identified by its classic 'flatiron' features on the DTM (Figure 31), their relief suggesting a thickness of about 20 m. In the field, the member is mainly seen as distinctive tabular debris on roads and in cuttings, but was seldom found in situ. These fragments consist of pale grey, highly siliceous ('flinty'), finely laminated vitric tuff or tuffaceous siltstone, which is deeply weathered to brown and crimson colours (OP/JC126). Samples from the latter locality, which is from the northern (Gambaga area) outcrop, were found to contain microscopic slivers of microcrystalline quartzo-feldspathic material interpreted to be recrystallized volcanic ash shards (Figure 34); these are separated by turbid, brown, grainy material. A gradual transition upwards, from Buipe Limestone into Darebe Tuff, is suggested by fragments recovered from around a water well (OP/JC196) near Buipe, which consist of brown-weathering, laminated siliceous siltstone (?tuffaceous) with discontinuous layers and doggers of blue-grey micritic limestone.

A sample of Darebe Tuff was submitted for heavy mineral separation followed by geochronological dating at the NERC Isotope Geoscience Laboratory, BGS. The LA-ICP-MS facility was used to screen the zircons for age populations, particularly for ages less than ca. 635 Ma, which is the maximum age constraint inferred from the correlation of the underlying Buipe Mimestone Member with the Marinoan glaciation. The preliminary results produced 6 grains with ID-TIMS ages of less than 635 Ma, and from this population the most accurate maximum U-Pb age constraint was 601.3 $\pm$ 2.0 Ma (written communication D. Condon, 2008).

Interpretation: The presence of shards of devitrified glass indicates a significant contribution to the sediment by volcanic ash fall-out, although the fine-grained nature of the lithologies suggests that the source(s) lay at some distance from the Project area. The matrix between the shards may represent clay minerals derived from the submarine breakdown of finely comminuted ash. The high silica content, evidenced by the fact that the fresh, grey tuff scratches steel, may be due to the abundance of tridymite in the volcanic ash, a feature that has been observed in certain modern explosive eruptions involving dacitic or rhyolitic magmas. Siliceous rocks, interpreted as bedded chert ('silexite') have been described from this stratigraphical horizon in Togo (e.g. Porter et al., 2004), as have 'ignimbrites with quartz shards' (Affaton et al., 1980). The occurrence may suggest that the regional subsidence leading to accumulation of the Oti-Pendjari Group was accompanied by significant volcanic activity somewhere in the hinterland to the Volta Basin.

It is possible that the Darebe Tuff may be the distal equivalent of volcanic rocks farther east within the Pan-African structural domain around Tiele, in neighbouring Benin (Affaton et al., 1997). These contain basalts, but also include rhyolites, which can give rise to explosive eruptions producing ash clouds that could have supplied pyroclastic material to the Darebe Tuff. The Tiele volcanics are suggested by Affaton et al. to have arisen along a passive margin undergoing rifting, a similar scenario to that envisaged for the more alkaline Tokor Volcanics, which crop out farther south in the Ghana sector of the orogenic belt (Section 4.1.2.7.). Neither volcanic assemblage has been directly dated by U-Pb techniques, but both are clearly pre-

orogenic associations and must therefore precede tectonic uplift and exhumation of deep crustal lithologies within the Pan-African belt, an event that has yielded U-Pb titanite ages of 586-578 Ma (Attoh et al., 2007). Thus the 601 Ma age of the Darebe Tuff may plausibly date volcanism associated with the onset of pre-orogenic rifting along the eastern margin of the Volta Basin. The problem is discussed more fully in section 4.1.2.8.

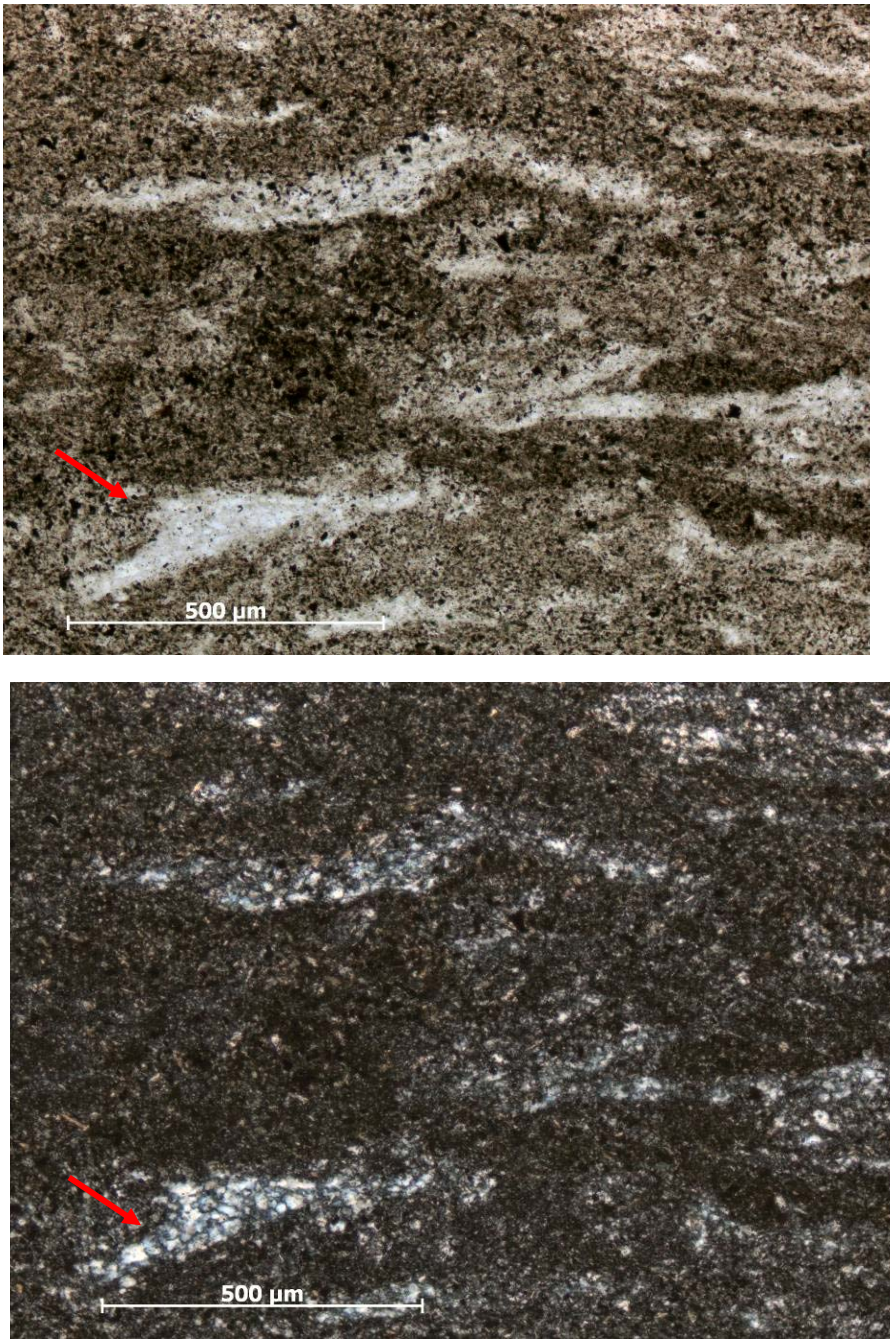

Figure 34 Photomicrographs of Darebe Tuff , in PPL (top) and cross polarized light (below). The red arrows indicate selected volcanic ash shards, which show microcrystalline textures typical of devitrified glass. The incurved left-hand margin of the lower shard is interpreted tobe part of the wall of a gas bubble.

Afram Formation

This formation was included by Junner and Hirst (1946) within the 'Oti Beds' of the 'Lower Voltaian' (Table 8), and is in part represented by the 'Afram Shale Formation' and 'Lower

Green Beds' of the Middle Voltaian in the classification of Anan-Yorke (1971; Table 10). Blay (1983) included the 'Afram Shales' within the 'Middle Voltaian'; however, as discussed in section 4.1.2.1 the mis-correlation of the Afram Shales with mudstones and siltstones at the base of the Anyaboni Formation led to erroneous conclusions; for example, that the Anyaboni Formation and Obosum strata were synchronous. The latter suggestion is refuted by the stratigraphical correlations based on field work and DTM imagery presented here, and also by zircon age spectra presented by Kalsbeek et al. (2008) and Akah (2008). The unit is not well exposed and in order to fulfil one of the objectives of this project, which is to produce a workable geological map, its outcrop against adjacent units was taken at 'mappable' boundaries. These are based in part upon features recognised on DTM imagery, but which should also be identifiable in the field (Figure 16). In the south, the formation's outcrop follows the Afram River valley, where it either overlies the dip slope of the Anyaboni Sandstone Formation, or is in tectonic contact with the latter along the Afram Fault. On the northern side of the valley the formation is overlain by prominent, feature-forming units such as the Ejura and Tease sandstone formations, and by the unconformable Obosum Group. In the east of the Volta Basin, the formation crops out in the lower ground along the floor of the Oti River valley, where it is overlain by the Chereponi Sandstone Member and, in the south, the Bunya Sandstone Member of the Bimbila Formation, both of which form prominent features and are of a distinctive lithology. Correspondence between the strata in the Afram and Oti valleys is reinforced by the compositional similarities implied by the formation's predominantly grey colouration on Fugro gamma-spectrometry ternary images (Crowe and Jackson-Hicks, 2008).

The Afram Formation mainly consists of olive green to grey mudstones and siltstones, but with 'red beds' developed near the top of the unit in the western part of the Afram River valley (Figure 43). It also contains limestone beds, and there is a thick development of rudaceous strata named as the *Akroso Conglomerate Member*.

Owing to the erodibility of the formation, and its tendency to weather to an ochreous ferruginous duricrust, exposures were only sporadically encountered during the field phase of this project. In the Oti valley outcrop, to the east of the Oti River south of Damanku village, roadside sections (OBS CJ236) expose 2m of olive green siltstone interbedded with fine-grained, grey, lithic sandstone and papery laminated mudstones, the latter with mudcrack structures. The thicker (several cm) sandstone beds locally contain mudflakes, show ripple-drift cross-lamination and faint, low-angle cross-lamination, the latter indicating currents towards the south (180^{o}). The strata here are affected by minor folding (Figure 35a). Further exposures in the Oti valley at Dambai (OBS JC350) and near Ayiramo village (OBS JC 351) show very similar strata consisting of green to brown-weathering laminated siltstones and mudstones interbedded with green-grey, fine-grained, highly immature feldspathic sandstones.

In the Afram valley outcrop, exposures to the north of Lake Volta, by the side of the road (OBS CJ8) are in pale green-grey, khaki-weathering, laminated micaceous mudstones and siltstones typical of the Afram Formation (Figure 35b). Limestone beds up to 9 m thick are intercalated in the Afram Formation along the River Fo, to the south-west of Tease, but they were not visited during this project and very few details are available. Farther west along the Afram valley, the formation takes on an increasingly variegated appearance, with red, brown or purple mudstones and siltstones more commonly seen. For example, diggings for a tank in Aframso village (OBS JC259) produced debris of finely laminated, grey/yellow/purple, non-micaceous mudstones as well as dark grey/purple, poorly sorted, medium-grained micaceous and feldspathic sandstone. Reddening of the succession is particularly noticeable farther west, in roadside exposures near the top of the formation, immediately beneath the Ejura Sandstone (OBS JC53; 297). The succession there (Figure 35c) consists of red-brown to maroon, rarely green-grey, laminated, non-micaceous mudstones with sporadic thin (0.5-3cm), hard beds of grey-green dolomitic siltstone; the latter reacting weakly when treated with dilute HCl. The dolomitic beds show climbing ripple cross-lamination, with one current direction measured towards the northeast (036^{o}). Fine-scale textures reminiscent of algal mats were noted on some bed surfaces. The

persistence of this ‘red bed’ facies is suggested by an exposure (OBS CJ158) of green and maroon mudstones on the scarp slope just below the Densubon Sandstone of the Obosum Group, 13.6 km farther east.

It is possible that the Afram Formation may correspond, at least in part, to strata penetrated at depth in exploration boreholes and named as the ‘Prang Formation’ by Bozhko (2008). These strata show variegation in chocolate, brown, green and grey colours. They consist of shales and mudstones together with subordinate siltstones and fine-grained sandstones; the latter contain numerous white, pink or brown carbonate. The Prang Formation passes down into predominantly green-grey shales and mudstones interbedded with turbiditic sandstones (Yendi Formation). Borehole log correlations indicate that the Prang Formation thickens progressively from west (c. 70 m) to east (530 m) in the central part of the basin.

Akroso Conglomerate Member. This unit is now mostly inaccessible, on small islands in Lake Volta, and was not visited during the project. Its outcrop, shown on the accompanying map (Figure 16), is referenced in from previous geological maps of the Volta Basin, which suggest that it occupies an interval in the upper preserved part of the Afram Formation. From the account of Anan-Yorke (1971), it is clear that some workers have included conglomerates found far to the west, in the Daboya area, within this unit. In this account, the Daboya conglomerates are placed within the Obosum Group, and thus are younger in age.

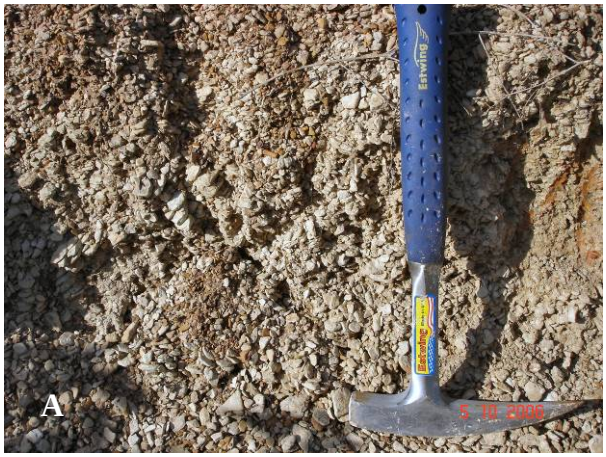

Figure 35 Sedimentary features in the Afram Formation. A) Afram Formation siltstones affected by a minor fold verging to S 160. B) Afram Formation mudstones and siltstones. C) ‘Red-bed’ facies of Afram Formation, showing red brown mudstones and siltstones with grey-green, hard, dolomitic siltstone beds.

In the Oti valley type area (now partially submerged beneath Lake Volta) the conglomerates appear to be lensoid in form, pinching out laterally. There may also be a structural explanation for this outcrop geometry, however, given the close proximity of the member to the Pan-African thrust front farther east, and the fact that the member appears to form the core to an anticline (Junner and Hirst, 1946, and see introduction to section 4.1.2.7: Buem Structural Unit). Previous workers noted that some conglomerate beds are up to 60 m thick, but there are also thinner

conglomerates that are interleaved with beds of grey-brown sandy mudstone and green, brown and mauve arkosic sandstone or pebbly sandstone. The conglomerates are usually described as massive, unsorted aggregations of well-rounded pebbles and boulders measuring up to 0.6 m in dimension in a matrix of arkosic sandstone. Most of the clasts consist of brown and green feldspathic sandstone, and there are generally only minor proportions of granite, porphyry, chert, jasper, phyllite limestone and quartz (Junner and Hirst, 1946). Anan-Yorke (1971) noted two localities where the predominant clast types of 'green arkosic sandstone and quartzite', are lithologically similar to the matrix of the conglomerate.

Interpretation: The Afram Formation (as mapped) is, from a lithological perspective, asymmetric in the distribution of the lithologies and facies across the Volta Basin. The fine-grained, grey-green clastic rocks in the east and north (Oti valley outcrop) may represent the earliest distal marine flysch derived from the advancing Pan-African orogen. The depositional setting is, however, equivocal, based on the field evidence available to date. Given that there are terrestrial red shales and thin dolomitic siltstones and limestones in the south and west, the grey-green siltstones and mudstones may represent an extensive and quiescent marginal shallow marine facies.

In its southern, Afram valley outcrop, the Afram Formation becomes increasingly variegated towards the west, a trend culminating in the outcrops south of Ejura where laminated, red-brown mudstones at the top of the formation suggest deposition in arid environments. Periodic sheetfloods, followed by evaporation in playa lakes, are represented by the thin beds of ripple cross-laminated dolomitic siltstone. A younger analogue for this part of the sequence would be the continental, arid-climate Triassic strata of the Mercia Mudstone Group (formerly 'Keuper Marl'), in the UK. The facies change within the Afram Formation, from deep-water flysch to probable terrestrial red-beds, indicates a westwards shallowing of this part of the Volta Basin.

In the south-east of the outcrop, the coarser, arkosic and conglomeratic facies assigned to the *Akroso Conglomerate Member* was not visited and therefore is poorly understood, as are its field relations with adjacent lithologies. Previous descriptions suggest it may represent proximal, conglomerate-rich flysch derived from the advancing Pan-African orogenic front. High-energy environments are envisaged for these beds, which were most likely deposited within submarine debris flow aprons. The reported predominance of green arkosic sandstone clasts that are lithologically similar to the conglomerate matrix suggests a strong intraformational component. Their rounding could indicate derivation from an earlier part of the Volta Basin sequence that was lithified, uplifted and reworked along shorelines or river systems adjacent to the Pan-African Front, prior to being recycled back into the basin as conglomerates. The basement-derived clast-types provide the evidence that the conglomerates were deposited contemporaneously with tectonic uplift of Dahomeyan basement terranes in the adjacent Pan-African orogenic belt.

Ejura Sandstone Formation

This unit extends for a short distance laterally (east-west, about 30 km), relative to many other formations of the Volta Basin, but where fully developed it forms a prominent SW-facing escarpment feature surmounting the Afram Formation in the north-western part of the Afram valley outcrop (Figure 36a). The topography of this escarpment suggests that the formation is about 80-100 m thick. Behind (i.e. to the north-east of) the escarpment, a dissected dip-slope feature occupying the Pru Forest Reserve indicates that the Ejura Sandstone passes beneath the Densubon Sandstone Formation of the Obosum Group, rather than overlying the latter. In consequence, it does not correlate with units such as the Tamale Sandstone farther north, as implied by the sketch maps of previous workers (e.g. Affaton et al., 1980).

In the Phase 1 Report of this project, the Ejura Sandstone was placed at the base of the Obosum Group. However, since it and similar strata of the Tease Sandstone Formation (see below) lack the highly feldspathic and lithics-rich composition of sandstones in that group, and have a

partially marine rather than a purely terrestrial origin, they are now regarded as the uppermost stratigraphical components of the Oti-Pendjari Group.

In the Ejura escarpment section (OBS JC 54, CT11; Figure 36c), the sandstone is a very clean quartzite, medium- to locally coarse-grained and with thin to medium width tabular bedding and some trough cross-bedding. Figure 37a shows a summary sketch abstracted from Figure 36c to highlight some unusual features of the lithology. Locally, the bed-tops show ripple marks; however, these ripples are unusual in that they do not appear to be cross laminated internally, but are draped by successsive beds of thin sandstone of approximately equal thickness. It is difficult to see these as deformation structures, as the sandstone in the core of the ripples is clearly variable in thickness. They may be antidunes formed during high current flow and high sediment load. The bases of some beds are erosional, and hummocky, downlapping bedforms are also locally present. Similar quartz-rich sandstones are exposed farther along the escarpment to the north-west (OBS JC298, CT 12); they are white to pale cream coloured, fine- to coarse-grained and locally gritty with moderate sorting. The beds here are thin to very thin and tabular to weakly lenticular, with wavy form in places and with trough cross bedding locally developed (Figure 36b). Trough-like erosion channels are developed at the bases of some beds. Cross-lamination is only sporadically developed; some individual beds locally show grading, but most appear massive.

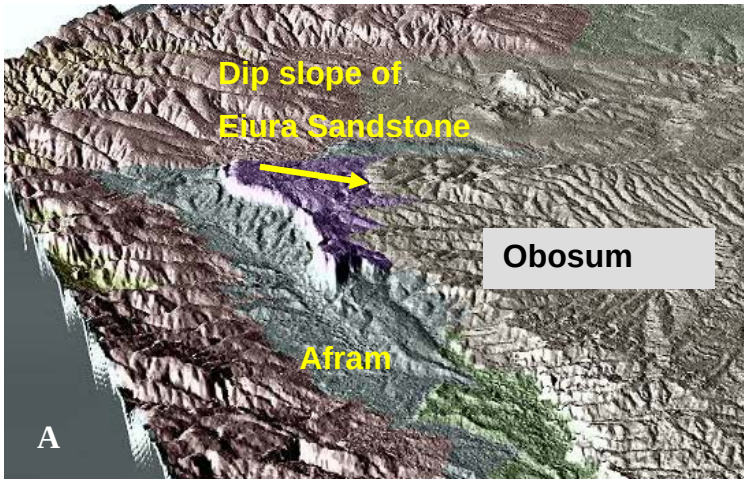

Figure 36 Sedimentary features in the Ejura Sandstone Formation. A) Oblique view of DTM, looking north-west and showing the escarpment and north-east inclined dip slope of the Ejura Sandstone. B) Thin, tabular bed-forms. C) Asymmetrical folds in bedding.

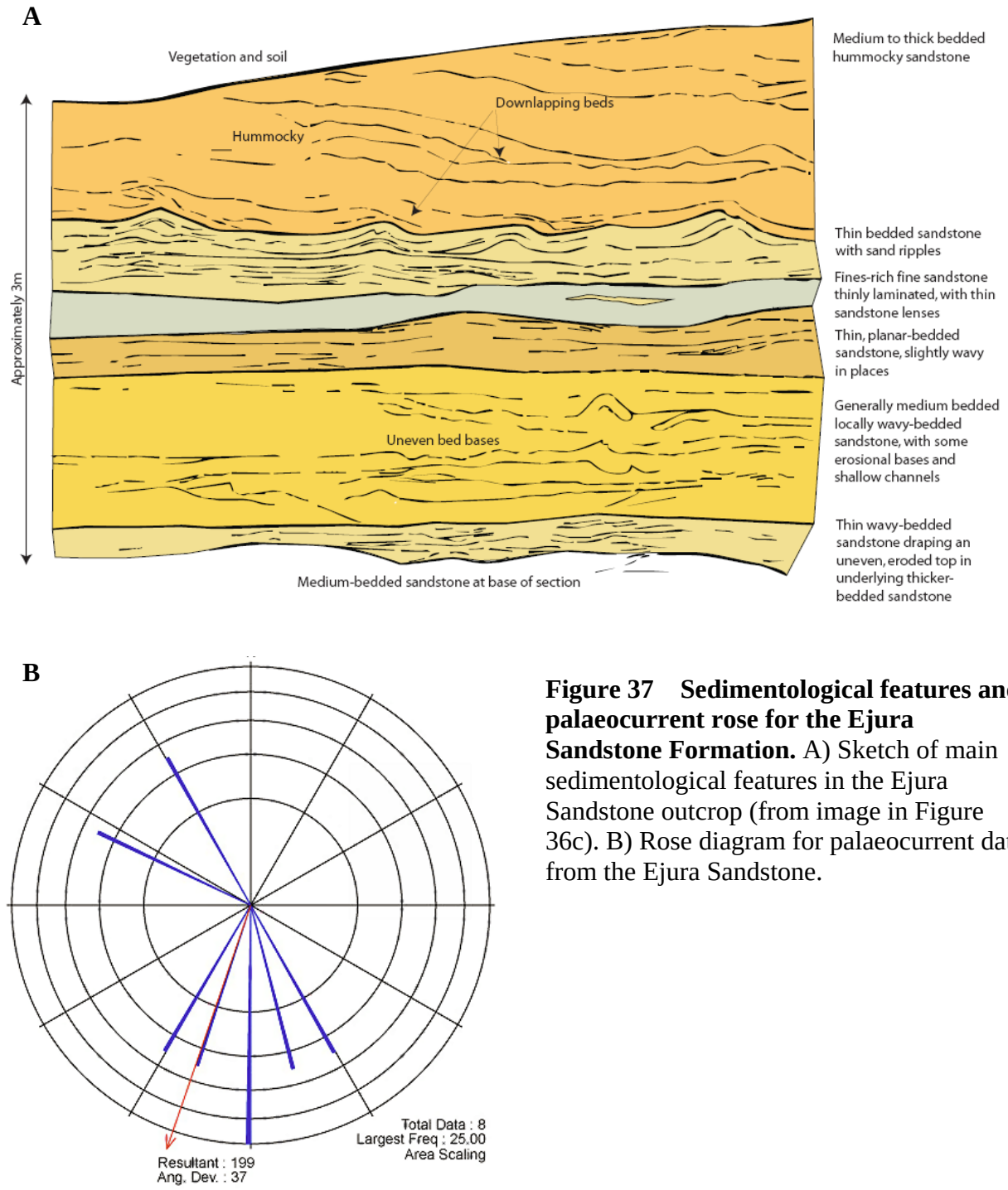

Figure 37 Sedimentological features and palaeocurrent rose for the Ejura Sandstone Formation. A) Sketch of main sedimentological features in the Ejura Sandstone outcrop (from image in Figure 36c). B) Rose diagram for palaeocurrent data from the Ejura Sandstone.

Interpretation: The lithologies in the Ejura Sandstone exposed in the outcrop shown in Figure 36c are considered to have formed in a mid to lower shoreface setting, deposited and worked by storm waves and possibly tides. The beds shown in Figure 36b are much more planar and tabular in appearance than those seen at OBS JC298 and may represent marine delta foreset beds. The high degree of maturity is also considered to indicate a marine depositional environment for these rocks.

Palaeocurrent data are limited for this formation, but the dominant direction is towards the south (Figure 37b), with a couple of measurements indicating north-westerly palaeoflow. The southerly palaeoflow contrasts markedly with the dominantly northerly palaeoflow in the formations of the Kwahu Group and indicates very different flow regimes and palaoeslope, at least locally, within this part of the Oti-Pendjari Group.

Tease Sandstone Formation

This unit occupies the southern and eastern rims of the Obosum Syncline and is regarded as a correlative of the Ejura Sandstone, as discussed above. Like the Ejura Sandstone it overlies the Afram Formation, its resistance to erosion resulting in prominent escarpment and dip slope features that allow it to be traced on DTM imagery (Figure 38a). Using these features as a guide, a thickness of about 80-100 m can be estimated for the unit, in reasonable agreement with the findings of a water borehole at Tease (Asare and Klitten, 2008), which proved 82 m of 'quartzitic' sandstone underlain by fine-grained sandstone and siltstone (?of the Afram Formation); no further descriptions were given. The narrow westerly extension of the Tease Sandstone outcrop along the southern rim of the Obosum Syncline, shown on the sketch map (Figure 16), is uncertain; it is based on a line of small hills, which presumably indicate the presence of resistant strata. These topographical features, however, may also represent a southern extension of the Dunkro Sandstone, which in this case would have overstepped the Tease Sandstone to rest directly on the Afram Formation.

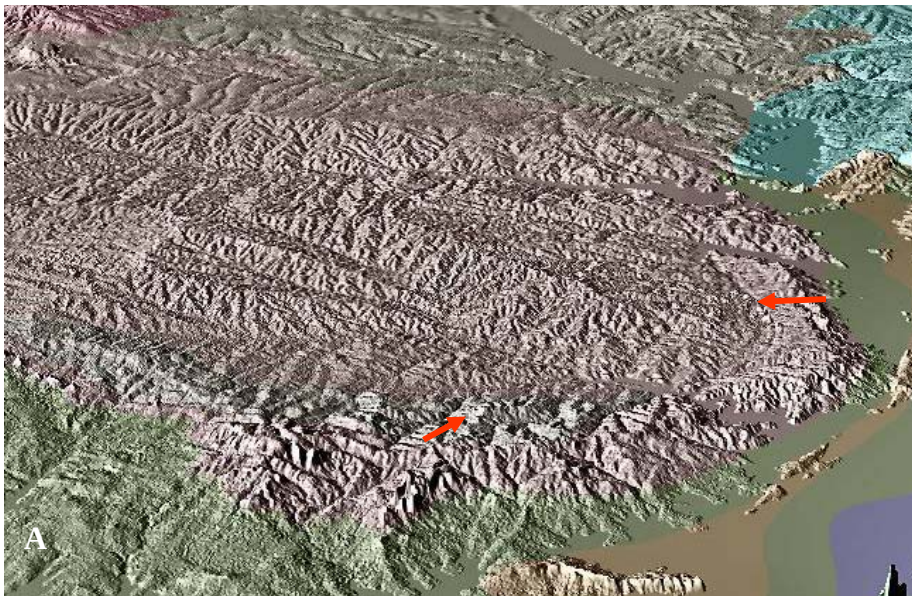

Figure 38 DTM image and sedimentary structures in the Tease Sandstone Formation. A) Oblique view of the Obosum Syncline, looking NNW, showing the dip slope (red arrows) of the Tease Sandstone Formation. B) Herring-bone cross bedding in the Tease Sandstone.

By the roadside south of Tease village (OBS JC293, CT8), the formation consists of pale grey, well-cemented, medium- to coarse-grained feldspathic quartz arenite. Thin trough cross-beds with herring-bone form are prominently developed (Figure 38b), and show palaeocurrents to the N and SW. Dark grey heavy minerals are concentrated along certain bed or lamina surfaces. At Tease village (OBS JC263) the sandstones are pale grey and quartz-rich. However, feldspar is present, as well as 'millet seed' quartz grains. Most sandstones are medium-grained and moderately well sorted, but some coarse-grained to granule-size lenses, and mudflakes, are also present. Cross-bedding with herring-bone pattern is developed locally. The bedding here is steeply dipping in places, and parts of the succession are affected by low-angle syn-sedimentary faults resembling small thrusts with a southwards transport direction. The steeply dipping bedding and syn-sedimentary faulting may indicate the onset of tectonic instability prior to deposition of the overlying and unconformable Obosum Group.

Interpretation: The exposures of the Tease Sandstone seen during the fieldwork suggest deposition in a shallow marine setting subject to tidal flow. The few current indicators that were measured indicate palaeoflows towards the southeast, southwest and north-northwest, similar to flow directions measured for the Ejura Sandstone. The presence of millet seed sand grains indicates an aeolian source for at least some of the sand in this unit, but this is unsurprising, given that there was no vegetation to stabilise sediment in flood-plains or vegetated marginal marine dunes. The appearance of these quartz-rich, current-agitated sandstones at the top of the Oti-Pendjari Group is puzzling. They may represent an episode of more extensive reworking on or close to a transient shoreline, as the accommodation space decreased towards the end of the marine phase of the Voltaian foreland basin. This could have been a prelude to mild deformation and partial basin inversion, just before deposition of the terrestrial molasse represented by the Obosum Group. A shallow-water, possibly nearshore depositional setting for the Tease Sandstone is consistent with this interpretation, with the laterally equivalent strata of the Ejura Sandstone representing a lower shoreface environment.

One of the major problems that remains unresolved is the stratigraphical relationship between the Tease Sandstone and units of the Oti-Pendjari Group farther north, such as the Bimbila Formation. The critical localities around and to the south of Kete Krachi are flooded by Lake Volta, and were inaccessible given the time constraints imposed on fieldwork during the present project.

Bimbila Formation

This formation was included within the 'Oti Beds' of the 'Lower Voltaian' (Table 8), as designated by Junner and Hirst (1946), and is in part represented by the 'Upper Green Beds' of Anan-Yorke (1971; Table 10). It is not well exposed, but those sections that were visited suggest that it is fairly homogeneous lithologically, consisting of green-grey mudstones and siltstones with common beds of green-grey, highly immature, feldspathic and lithics-rich sandstones. Two sandstone units are thick enough to form prominent stratigraphical markers that can be recognised both on DTM imagery and in the field: the Chereponi Sandstone Member forms a readily mappable basal division resting on the Afram Formation, whilst the Bunya Sandstone Member forms the exposed top of the formation across an extensive area.

The stratigraphical separation between the two sandstone members narrows and eventually disappears as their outcrops merge together southwards, indicating a progressive thinning of the Bimbila Formation in that direction. In the south of the outcrop the Bunya Sandstone is possibly overstepped by the Obosum Group, although the relationships between the various units in the Kete Krachi area are not clear on DTM imagery. The western and northern junction between the Bimbila Formation and the overlying and unconformable strata of the Obosum Group is similarly ill defined, but broadly corresponds to that depicted for the 'Pendjari-Oti Group' on the sketch map provided by Affaton et al. (1980).

In many lithological respects, these strata resemble the underlying Afram Formation. Significant compositional differences between the two units are nevertheless suggested by Fugro gamma-spectrometry ternary images, in which the Bimbila Formation is characterised by predominantly turquoise-green to blue-green colours, indicative of relatively high Th and U contents, in contrast to the dark grey colours over the Afram Formation (Crowe and Jackson-Hicks, 2008).

The Bimbila Formation, as defined here, corresponds to at least part of the 'Nasia Formation', a unit encountered in several deep exploration boreholes (Bozhko, 2008), and which was also previously referred to as the 'Greenish-grey Upper Series' (Table 9). In the boreholes, Bozhko described these strata as consisting of a lower sequence of monotonous shales, mudstones, siltstones and sandstones of turbiditic character; and an upper more arenaceous sequence. The Nasia borehole proved a maximum thickness of 539 m for these two units. The same strata mapped at surface in the northern (Gambaga) outcrop were named by Viljoen et al. (2008) as the 'Nasia Formation', and described as consisting of green-grey mudstones interbedded with greywackes. The overlying sandstones of the Gusiegu Formation; (Viljoen et al, *op cit*) may well correlate with the Bunya Sandstone Member as defined in this account.

Undivided beds of the Bimbila Formation. In the north-western part of the outcrop, on the Tamale-Walewale road, cellphone mast diggings in the formation just south of Diari village (OBS JC 328) showed pale green, fine-grained and highly immature (lithic and feldspar-rich) sandstones in which grains of green jasper and dark grey ?spinel are visible; grey mudflakes are also present, as are some highly micaceous laminae. A thin section of this sandstone (Figure 41a) contains abundant angular to subangular grains of feldspar (plagioclase and K-feldspar), and lithic grains that include clinopyroxene, hornblende, chlorite, various phyllite lithologies and microcrystalline quartz (probably jasper), all indicating a source that includes mafic lithologies. Farther north, at Nasia (OBS JC 339), mast diggings brought up debris of khaki, micaceous siltstones. In the eastern part of the outcrop, exposures by the side of the road between Gushiegu and Nakpandura reveal a sequence consisting of interbedded mudstones, siltstones and sandstones. At OBS JC339 the sandstones are pale green, micaceous, rich in feldspar and lithic fragments, and are interbedded with pale green, highly micaceous laminated siltstone. Farther south, at OBS JC340, riverbed exposures show pale green-grey, micaceous, very fine-grained siltstone in thin, tabular beds with wind-rippled tops. Some very low angle cross-bedding is visible here, with currents towards the west; up-section bedding becomes increasingly flaggy and plane-laminated. Just below the escarpment formed by the overlying Bunya sandstone (OBS CJ62) there are several 1-3 m thick ribs of olive green, fine-grained, micaceous and felsdpathic sandstone in the road.

About 2 km to the east of Yendi, just beyond the base of the Bunya Sandstone escarpment, the streambed around a water well to the north of the road (OBS JC110) exposes pavements in subhorizontal, medium- to thinly-bedded, grey-green micaceous siltstones and very fine-grained, feldspathic sandstones (Figure 39a), the latter commonly with rippled bed-tops. In the wall of the well, locally-derived slabs of grey micaceous siltstone are plastered with branching, bulbous organic impressions (Figure 39b). They resemble microbial, *Kinneyia*-type 'wrinkle structures' described from shallow-water Late Neoproterozoic strata in Namibia (Hantzschel and Reineck, 1968; Scheiber et al., 2007), although many appear to radiate outwards from foci, which is a feature that could be attributed to growth rather than deformation. The impressions partially overprint an elongated ribbed or segmented form, with a faint midline visible, which is possibly a vendobiont and has some similarities to *Corumbella*, an Ediacaran fossil that has been reported from SW Brazil and western USA (Babcock et al., 2005). In situ exposures of fine-grained sandstone at this locality additionally show bed tops with possible microbial build-up structures akin to siliciclastic stromatolites (Figure 39c). A more thorough search of exposures in the streambeds around this locality could well reveal further Ediacaran fossils.

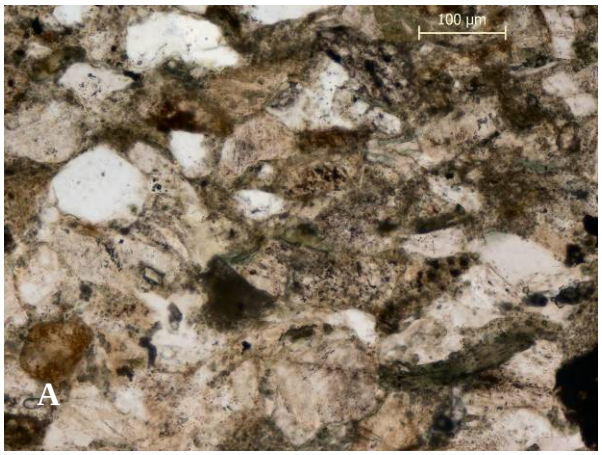

Figure 39 Photomicrograph and organic impressions, Bimbila Formation. A) Detail of feldspar- and lithics-rich sandstone (plane-polarized light). B) Microbial structures on sandstone bed-top. Note the ribbed ? vendobiont to lower right. C) Microbial build-up structures on sandstone bed-top.

Chereponi Sandstone Member. This sandstone is somewhat arbitrarily taken as the mappable base to the Bimbila Formation. It overlies the Afram Formation and can be traced over a strike-length of about 210 km along the margins of the Afram River floodplain. The feature formed by the sandstone resembles that of a dissected escarpment with a narrow, westerly-inclined dip slope, the latter only rarely preserved. A thickness of about 40-60 m is estimated from topographical considerations.

In many respects, this sandstone is lithologically identical to the Bunya Sandstone (see below), and to the thinner sandstone beds in the Bimbila Formation described above. It is named from its exposures (OBS CJ55) around the eponymous township, which show that it consists of dark olive green to grey, fine-grained micaceous and lithics-rich sandstone, typically with onion-skin weathering. On the road about 11 km south-east of Nakpayili village, exposures (OBS CJ 235) are in hard, possibly siliceous, fine-to medium-grained olive green to grey arkosic sandstone with sporadic green mudflakes. The sandstone is compositionally immature, with many angular grains, some of which are of green jasper. The Chereponi Sandstone merges with the overlying Bunya sandstone in the southernmost part of its outcrop (Figure 16).

Bunya Sandstone Member. This is the youngest exposed division of the Bimbila Formation and can be traced on DTM imagery over a total strike length of about 300 km. Topographical evidence suggest that the formation averages about 50 m in thickness. The features shown on the DTM (Figure 40a) include east- and west-facing marginal escarpments and dip-slopes which, where not dissected, are inclined inwards towards an axis represented by the valley of the Daka River. This outlines a structure named the Daka Syncline. In the north of the outcrop, the axis of this syncline curves westwards and here, the Bunya Sandstone is seen as a series of disconnected outliers or ‘keels’, which are the evidence for the continuation of the synclinal structure.

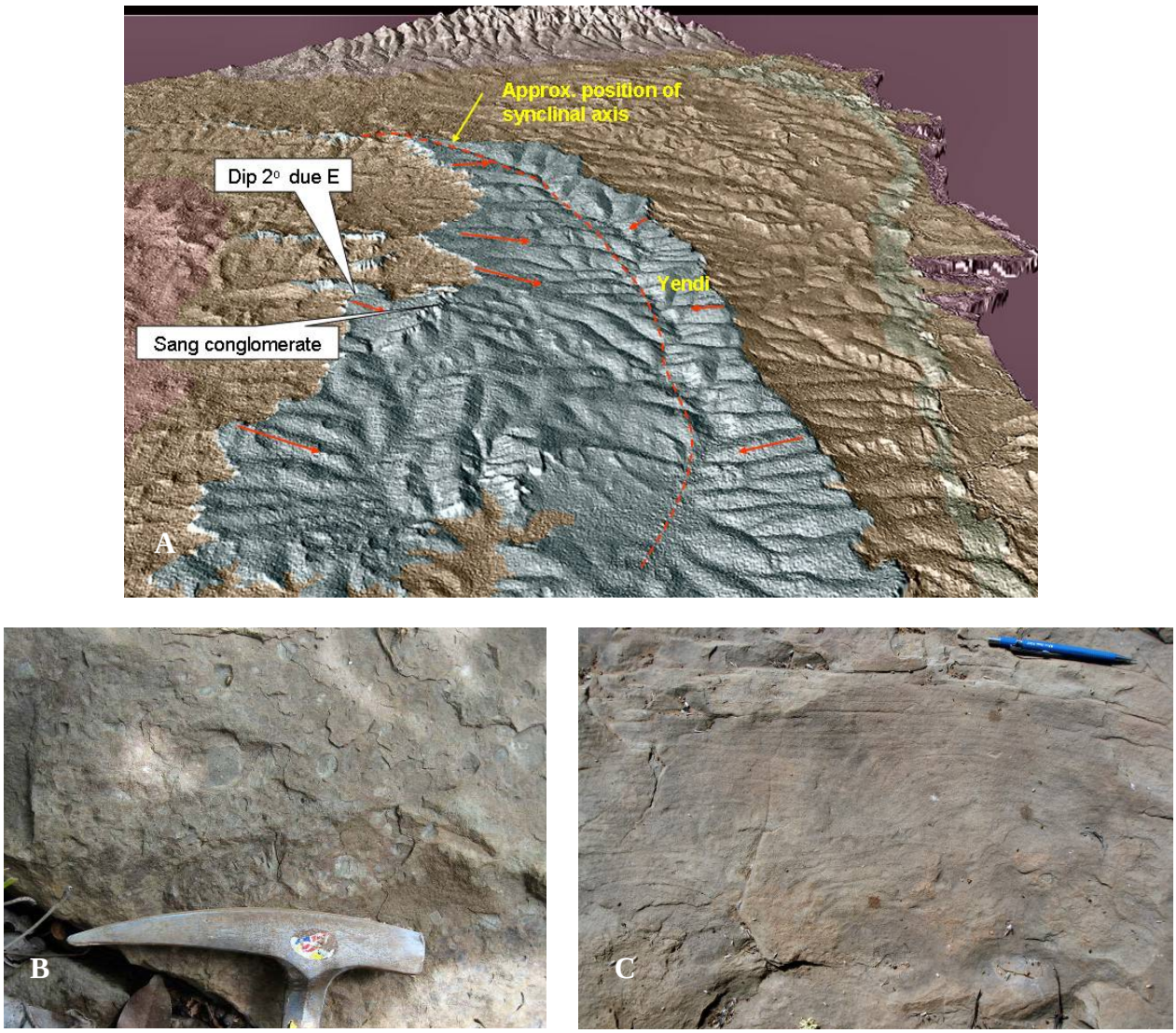

Figure 40 DTM image and sedimentary features in the Bunya Sandstone Member.
A) Oblique view of DTM looking northwards, showing the Bunya Sandstone (blue-green) and axis of the Daka Syncline. Note the opposing escarpment features, to east and west of the outcrop. Structural dips are indicated by the red arrows. B) Typical Bunya Sandstone, here with abundant mudlfakes. C) Bunya Sandstone, showing contorted thick lamination.

The synclinal structure outlined above does not appear on Fugro airborne electromagnetic time-domain (GEOTEM) data (Kalvig, 2008), which suggest that the Bunya Sandstone dips uniformly westwards. To address this problem, particular attention was paid to a roadside cutting through the unit along the crest of the escarpment that forms the western edge of the Daka Syncline. Field measurements demonstrated that here, the bedding indeed dips eastwards, albeit at very shallow angles (measured at c. 2°; Figure 40a), thus proving the existence of this contentious limb of the syncline (see also, Figure 43). At this locality (OBS JC106) maroon, green and grey, slightly micaceous siltstones overlie a sandstone bed. The latter is grey-green, medium-grained, micaceous and poorly sorted, being rich in feldspar and lithic grains. Maroon mudflakes are also present on some bedding planes. The sandstone is thinly stratified in part, with some top surfaces showing ripple marking. It also shows normal grading, coarsening down over 0.3 m to feldspathic sandstone containing granules of quartz, red jasper and metavolcanic lithologies in a pinkish-grey, argillaceous matrix.

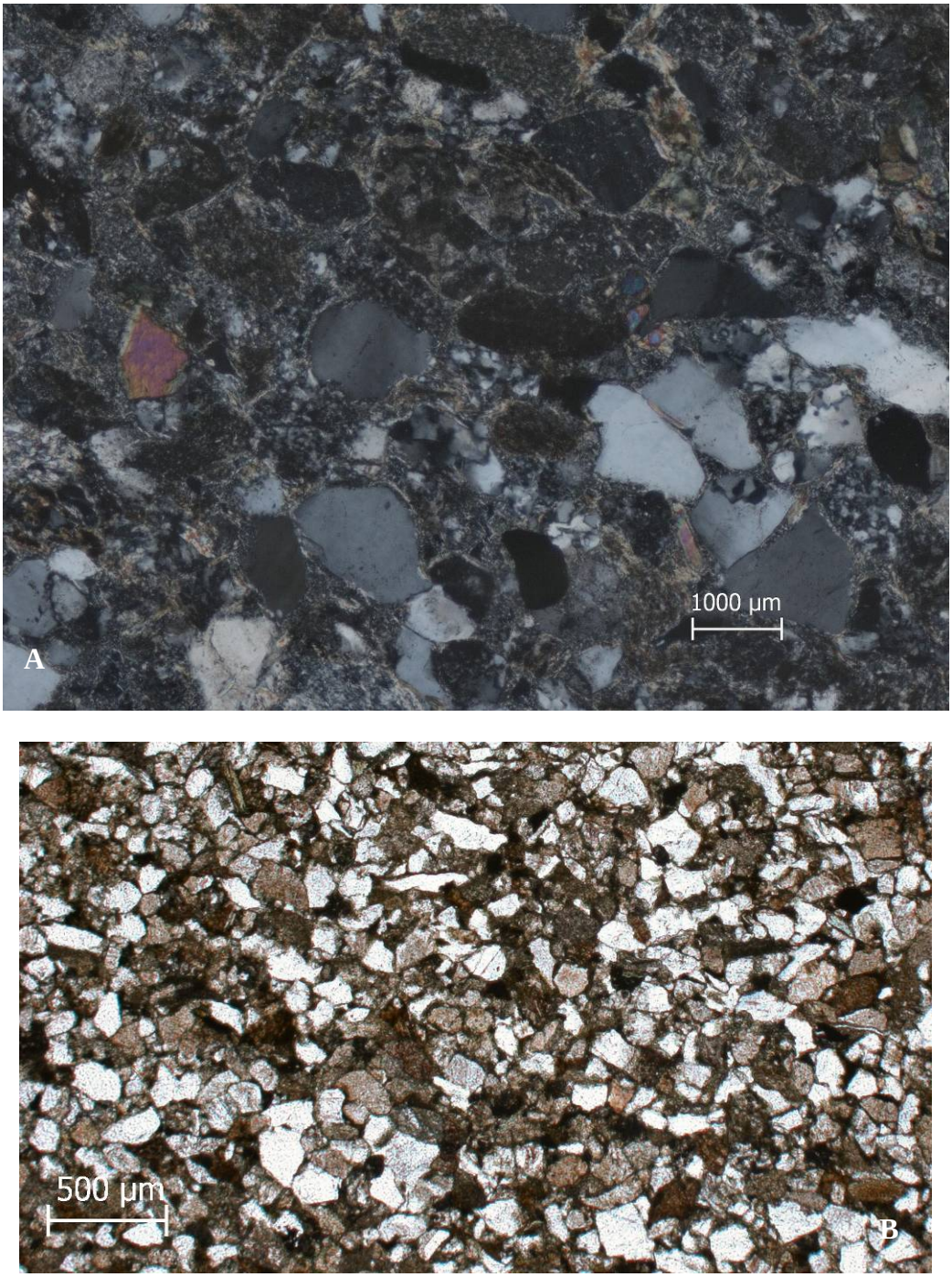

Figure 41 Photomicrographs of sandstones in the Bimbila Formation.
A) Photomicrograph of lithic-rich sandstone in the Bimbila Formation (undivided beds). Note abundant grains of microcrystalline quartz (?jasper or chert) and clinopyroxene (red/blue colours). B) Photomicrograph of Bunya Sandstone. Note angularity of grains, abundance of feldspar (brownish, turbid crystals) and lithic material (dark brown, grainy) (plane-polarised light).

At the type locality in Bunya village (OBS JC349), a series of small, rounded tors expose green-grey, feldspathic and lithics-rich sandstone. In places the lithology is massive, but some exposures show large scour structures defined by arcuate lamination. These indicate a range of current directions between SSW and NNW. In the northern part of the village, bedding and lamination dip at various angles and are locally subvertical, indicating syn-sedimentary slumping. About 16.5 km south of Bunya, a roadside exposure (OBS JC88) shows typical green-grey Bunya sandstone with thin beds and lenticles of mudflake conglomerate (Figure. 40b). In thin section (Figure 41b), the

component grains are angular with low sphericity; quartz is subordinate to feldspar (plagioclase and orthoclase) and lithic grains, the latter including metamorphic rock-types. At a locality about 32 km south of Yendi (OBS CJ232), pavement exposures show fine- to medium-grained khaki to grey sandstone with mica and feldspar and orange mineral grains, which are possibly jasper, together with dark, mica-rich laminae. Sedimentary structures noted here include broad swales and hummocks and bedding is locally disturbed and convoluted, suggesting loading or water-escape (Figure 40c). In the southernmost exposure of Bunya Sandstone visited, about 22.4 km north of Kete Krachi, roadside pavements (OBS JC 344) show green-grey, fine to medium-grained, highly feldspathic sandstone with green mudflakes concentrated along certain laminae. In places, dispersed subangular to angular granules and small pebbles of basement rocks produce a diamict. North of Yendi, and about 3 kilometres east of Nakpayili, roadside ditch sections (OBS CJ25) show about 4 m of pale olive-green, fine-grained micaceous sandstone passing down to sandstone with interbedded weathered bands of olive green siltstone and sporadic comglomeratic beds. The sandstone is locally flaggy, with possible ripple-drift lamination, indicating palaeocurrent flow towards the NW.

In the north-western part of the Bunya Sandstone outcrop, an outlier on the road between Tamale and Walewale exposed (OBS CT34) undulating pavements in greenish grey, very fine grained, feldspathic, micaceous and lithic sandstone. Structures include trough bedding, with shallow scoops containing cross-stratified strata. The topmost hed here is a c. 0.3 m thick tabular sheet sandstone, very hard and fine-grained, with trough cross sets suggesting current flow towards the S and SSW. No grading was seen at this locality.

Deep boreholes on the Bunya Sandstone outcrop at ‘Wulasi’ (now Wulensi) and Yendi intersected 383 m and 286 m, respectively, of strata named by Bozhko (2008) as the ‘Nasia Formation’. These strata, which overlie the ‘Prang Formation’ of Bozhko (2008), were said to mainly consist of greenish grey mudstones, siltstones and sandstones, the latter of turbiditic character. It was noted that sandstones become predominant higher up in the boreholes, which is the part of the sequence most likely to correlate with the Bimbila Formation as defined here.

Field determinations indicate that the Bunya Sandstone has significantly raised magnetic susceptibility values, compared to other Oti-Pendjari Group lithologies. This may be due to an increased abundance of magnetite, which in turn indicates the more mafic nature of the source rocks that were currently being unroofed farther to the east.

Interpretation: The Bimbila Formation comprises a range of lithologies with a range of sedimentary structures. The overriding feature is the immaturity of the clastic rocks, with clear evidence for derivation from mafic and metamorphic sources. The presence of jasper fragments could suggest input from weathered oceanic crust, possibly from an ophiolitic source. However, thick sequences of ferruginous quartzite and jasper, as well as limestones with red and white jasper nodules, have also been found in association with alkaline volcanic rocks of the Tokor Volcanics (Section 4.1.2.7.), in the Pan-African domain to the east of the Bunya Sandstone outcrop (Jones, 1990). Deeper parts of the succession, as encountered in boreholes, and some of the few exposures in the north, contain rocks that indicate deposition by turbidite flows in deeper water. As described above, however, some exposures contain evidence for shallow water deposition, particularly those near the exposed top of the Bimbila Formation containing soft-bodied and trace fossils and algal lamination. The general impression, therefore, is of a shallowing-upward succession. This might include immature fluvial deposits at the very top of the formation. The sedimentary rocks are considered to have been derived from the advancing Pan-African orogenic front to the east, and thus deposited in a foreland basin setting. The detrital zircon geochronological studies of Kalsbeek et al. (2008), which include a sample (Gh 21) of the Bunya Sandstone, provide further evidence for this Pan-African source region. The Bimbila Formation is regarded as representing the marine flysch phase of the foreland basin fill, and it is possible that major sandstone units, such as the Chereponi and Bunya members, reflect stages of accelerated uplift within that domain, perhaps corresponding to nappe emplacements. Although

passage into fluvial rocks at the top of the formation suggests the transition into the terrestrial molasse stage of the foreland basin development, the final stages of the formation are probably not seen as those strata would have been eroded prior to the deposition of the overlying and clearly molassic, terrestrial red-bed Obosum Group.

The change to southerly and westerly sediment transport indicated in the Ejura Sandstone Formation data (Figure 37b) is highlighted much more strongly in the data for the Bimbila Formation (Figure 42a). Palaeoflow directions are dominantly towards the southwestern hemisphere, ranging from 120° to about 300°; only two measurements indicate northerly flow. Such a change in sediment flow-paths is considered to represent the onset of medium and far-field effects of the Pan-African orogeny as it encroached on the basin succession from the east (as now configured). In addition, the generally south-westerly palaeoflow suggests that flow was confined to some extent, following a direction approximately parallel to the orogenic front, although the more westerly directions indicate flow away from the orogen, as might be expected intuitively.

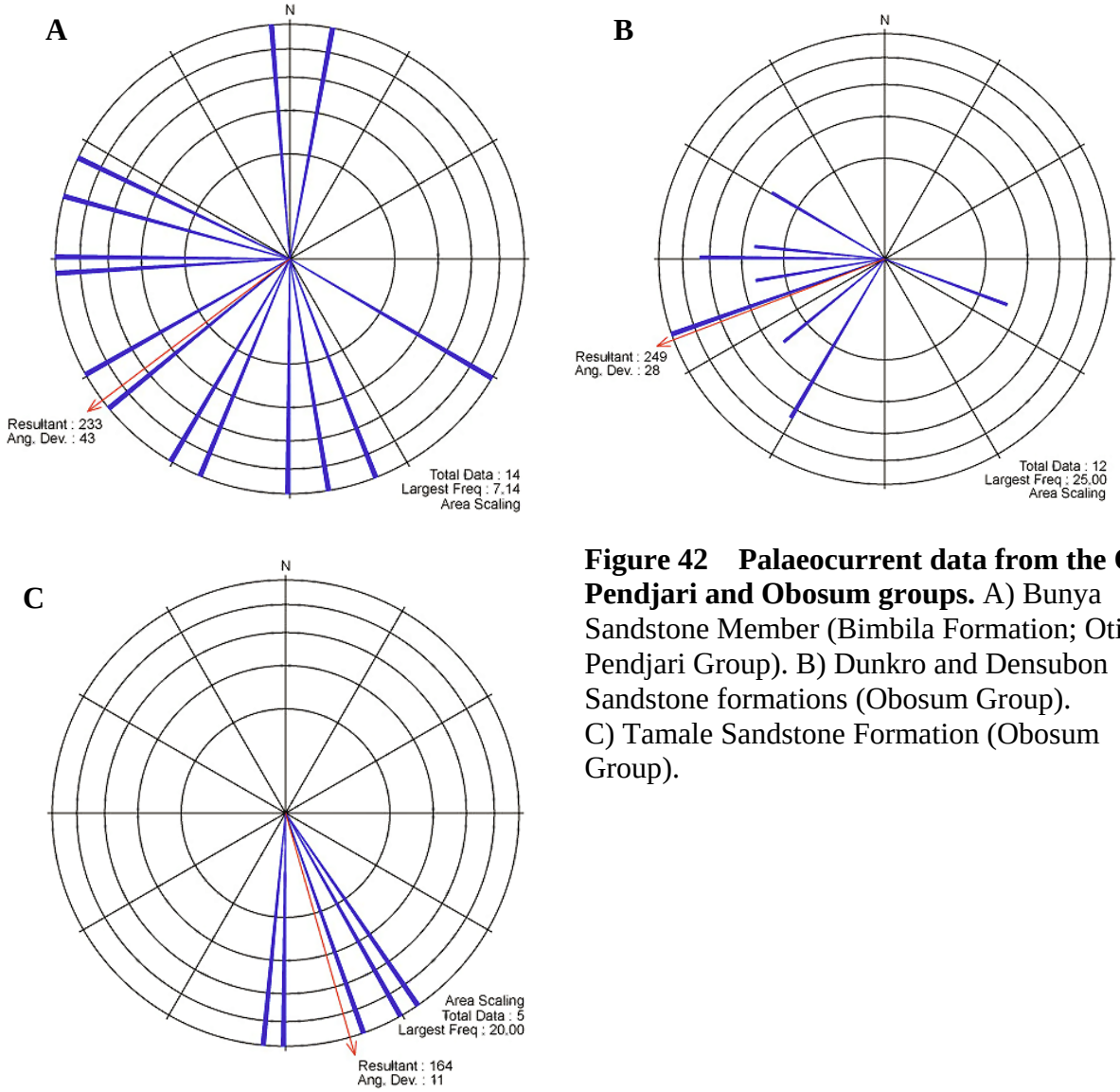

Figure 42 Palaeocurrent data from the Oti-Pendjari and Obosum groups. A) Bunya Sandstone Member (Bimbila Formation; Oti-Pendjari Group). B) Dunkro and Densubon Sandstone formations (Obosum Group). C) Tamale Sandstone Formation (Obosum Group).

4.1.2.6 OBOSUM GROUP

The Obosum Group is the youngest lithostratigraphical component of the Volta Basin sedimentary fill. It unconformably overlies the Oti-Pendjari Group and in the west of the basin it may locally overstep those strata to rest on the Kwahu Group. The group is in part equivalent to the 'Obosum Beds' of Junner and Hirst (1946), although these were placed at the top of their 'Lower Voltaian' division (Table 8). It was included within the 'Tamale Red Beds' of the 'Upper Voltaian' by Anan-Yorke (1971; Table 10). The name 'Obosum Group' was established by Affaton et al. (1980) and, as that unit is not capable of significant further subdivision, this name is preferred to the term 'Tamale Supergroup', subsequently adopted by Affaton (1990).

The distribution of the group as determined during this Project (Figure 16) is broadly similar to that proposed by Affaton et al. (1980). Although most workers recognise that the group mainly comprises detritus derived from the Pan-African orogenic belt to the east, its outcrop does not abut against the Pan-African frontal thrusts, nor can the strata be proved to thicken eastwards. Instead, the Obosum Group occupies relatively shallow, synclinal troughs developed in the central and western parts of the basin, behind (ie to the west of) structures such as the Daka Syncline, as shown in Figure 43. This suggests that flexuring and uplift along the eastern part of the Volta basin may have preceded, and also possibly accompanied, deposition of the Obosum Group, reducing its potential to be preserved in that area and accounting for its apparent disconnection with the Pan-African source region. One structure implicated in this marginal uplift is the Akroso Anticline, discussed in the next section.

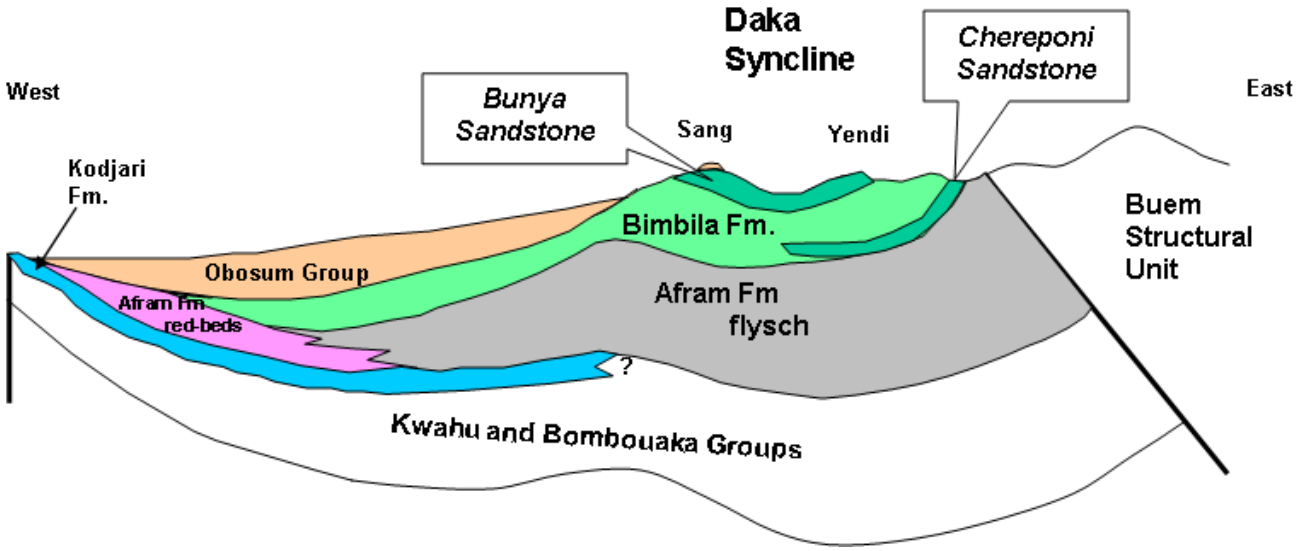

Figure 43 Conjectural section across the northern part of the Volta Basin (not to scale).

Two broad associations of lithologies have been recognised within the Obosum Group. North of the east-west trending Pru Fault, the *undivided beds of the Obosum Group* mainly consist of a flysch-type association of variegated mudstones, siltstones and sandstones, with sporadic but highly distinctive beds of pebble conglomerate. In this part of the outcrop the terrain is gently undulating and extensively lateritised, hence there are few outstanding features by which individual components – or the limits of the group - can be reliably mapped using DTM imagery. Two components are nevertheless distinguishable; the *Tamale Sandstone Formation* and the *Sang Conglomerate.* To the south of the Pru Fault the strata mainly consist of highly immature, molasse-type sandstones and conglomerates of the *Dunkro Sandstone* and *Densubon Sandstone* formations. Those units occupy a structural trough, the Obosum Syncline (Figure 38a), which is partially confined between east-west fault systems. On the DTM their outcrop is characterised by

a highly distinctive, strongly lineated texture etched out by the dendritic drainage systems of that region.

It should be noted that the Pru Fault ceases to have a surface expression to the east of the Pru River, hence the demarcation between the two Obosum Group components proposed here is somewhat arbitrary. It is nevertheless supported by colour contrasts shown on Fugro ternary radiometric imagery (Crowe and Jackson – Hicks, 2008). The highly feldspathic and lithic-rich Densubon and Dunkro sandstones of the southern outcrop are characterised by strong red colours, indicative relatively high proportions of K, whereas the more argillaceous, undivided beds of the northern outcrop show grey, turquoise and green colours. The latter could suggest relatively higher proportions of Th and U, although this colouring may also at least in part reflect the more extensive and deeper weathering developed across that part of the outcrop, on which a morphological feature termed the 'Central Volta Surface' is developed (see section on the Cenozoic geology, below). On Fugro GEOTEM electromagnetic time-domain profiles, the junction between the two areas of Obosum Group outcrop is broadly coincident with a sharp, vertical colour boundary suggesting a major structural control, either by the Pru Fault or related displacements that run parallel to it.

Undivided beds of the Obosum Group, cropping out to the north of the Pru Fault, were observed in small roadside exposures, or as debris brought up during diggings for mast foundations. Laminated and highly variegated (yellow/brown/grey/purple/green) micaceous calcareous mudstones and siltstones (Figure 44a) were found by the side of the Tamale to Daboya road (OBS JC172, CT31). About 15 km to the west, strata inferred to represent part of the westernmost, feather-edge of the Obosum Group were encountered in gullies by the roadside about 3.4 km due east of the Daboya landing (OBS JC320; CT 27, 28). They consist of purplish grey, micaceous siltstone and very fine-grained sandstone, the latter finely laminated in planar beds. Overlying these strata is a thick, micaceous and argillaceous sandstone unit, with a convoluted or channelled base and with local, diffuse, upwards coarsening packages internally. Thin limestone beds are intercalated in the siltstone sequences; they were investigated for acritarchs, but none were found. In one part of this exposure a thin (c. 0.4 m) matrix-supported pebble conglomerate is intercalated between maroon siltstone, above, and maroon/green variegated mudstone and siltstone with lenticular sandstone beds below. Pebbles in the conglomerate (Figure 44b) are of various basement metamorphic rock types, but also include much quartz and quartzite, banded chert and green chert, porphyritic andesite or microdiorite and a green metavolcanic lithology. In the north-west of the Obosum Group (OBS CJ 42) a further conglomerate bed is interbedded with fine-grained, dark grey, argillaceous sandstone. Both these occurrences are of identical lithology to the Sang Conglomerate, described below. Other conglomerate localities along the Volta River near Daboya were described by Junner and Hirst (1946), in their section on the Sang Conglomerate.

A deep borehole in Tamale encountered 408 m of predominantly red and purple coloured strata, called the 'Third Unit' by Bozhko (2008) and here tentatively correlated with the Obosum Group:

Depth (m)	**Description**
0-131	Shales and mudstones interbedded with siltstones and sandstones
131-296	Fine- to medium-grained polymictic sandstones, argillaceous, with numerous flakes of micaceous shale. The lowermost beds include conglomerates with basement clasts in a sandstone matrix
296-408	Shales and mudstones interbedded with subordinate siltstones and sandstones

As indicated by this borehole, sandstones evidently form an important part of the northern Obosum Group succession. Although they do not produce good topographical features on DTM imagery, Fugro ternary radiometric imagery (Crowe and Jackson-Hicks, 2008) shows arcuate, red-coloured features to the north of Tamale, which may represent sandstone outcrops. Sandstone is exposed at various places around Tamale; for example, in a reservoir north of the Tamale-Kintampo road (OBS JC 92), large slabs consist of pale buff to yellow, fine-grained, micaceous and quartzose sandstone with planar lamination and with a parting lineation on some surfaces. Other features noted here include mudclasts and ripple-drift cross-lamination. By the side of the Tamale-Walewale road there are a number of exposures in grey to pink-weathering feldspathic quartz arenites, some with well-rounded 'millet seed' grains. At one of these localities (OBS JC 160), close to the inferred northern margin of the Obosum Group, debris in a trench consists of very fine-grained, cream to purplish grey-weathered micaceous sandstone with ripple-drift cross lamination, flaser bedding, 'hummocky' cross-stratification and, in the more argillaceous sandstone layers, mudcracked top-surfaces. Very similar sandstones, seen in mast diggings, about 2 km farther south (OBS JC327), are purplish grey, micaceous and very fine-grained with flute casts, load structures, rippled tops and mud flakes. Closer to Tamale, the floor of a laterite pit (JC162, CT33) exposes pale grey, massive, medium-grained quartzitic sandstone with common well rounded 'millet seed' grains. Nearby, a hydrological borehole at the village of Libga encountered 'lithified arkosic sandstone' to a depth of 30 m (Lutz et al., 2007).

In the southern outcrop, a hand-dug well by the Tamale road 9.7 km north of Salaga (OBS JC316) yielded abundant flaky debris of finely laminated, variegated (maroon/grey/green) micaceous siltstones with ripple-drift cross-lamination. 30 kms to the north (OBS JC 317), roadside mast diggings are of maroon/green-grey, locally papery, laminated mudstones and siltstones together with 1-2cm thick tabular fragments of green-grey, fine-grained sandstone. About 29 km north of Atebubu (OBS CT 25), streambed exposures show drab grey, plane bedded siltstones with some dewatering structures preserved in the upper bed (Figure 44c). The underlying beds are planar laminated, with nodular weathering, and show slight upwards coarsening.

Interpretation: The dominantly fine-grained, variegated rocks of the undivided northern Obosum Group succession have many features consistent with shallow water deposition and intermittent subaerial exposure. The assemblage may be transitional from a flysch-like, but shallow marine setting into a shallow, dominantly fresh water environment with ephemeral lacustrine, estuarine and fluvial systems. The lack of acritarchs suggests a non-marine setting, though this is not conclusive because of the small sample set. The sandstone units may represent the more actively fluvial domains and/or sheet floods, whilst the presence of millet-seed sand grains indicates an aeolian source for some of the sand. Again, aeolian material would be consistent with a largely terrestrial setting. Mud cracks and mud flakes and limestone- bearing or calcareous horizons indicate periodic dessication. Thus, the undivided part of the Obosum Group may be transitional from the underlying flysch-like deposits of the Bimbila Formation (even though they are separated by an unconformity) into the more classically molassic deposits of the Dunkro and Densubon formations in the south and the Tamale and Sang units in the north.

Tamale Sandstone Formation. This unit forms the higher ground on which Tamale itself is located. Its intricate outcrop was traced by reconnaissance field survey, using as a guide the presence of scarp-like features on the DTM, the latter reflecting the erosion of strata forming a local capping to the Obosum Group. Very few in situ exposures of the sandstone were visited. Close to the GSD office in Tamale (OBS JC319) there are pavements in red, medium-grained, moderately well-sorted quartz-rich sandstone with rounded to subangular grains. The main structure consists of large-scale trough cross-bedding, indicative of currents towards the south and south-east (Figure 42c). On the Daboya road about 20 km west of Tamale centre, roadside exposures (OBS JC175) show pink-weathering, flaggy, very finely laminated sandstone and siltstone with partings of grey mudstone; ripple-drift cross-lamination was noted. About 300-400 m to the east, medium-bedded red-pink weathering micaceous sandstone crops out. About 3 km

to the north of this, pond excavations (OBS CJ 100) produced boulders of fine-grained, dark red to purple, well cemented quartz sandstone. On the Walewale road, about 10.5 km north of Tamale centre, a roadside cutting (OBS JC164) is marked by debris of laminated, dark grey to dark maroon, fine-grained sandstone and siltstone; lunate and sinuous crested ripple marks were seen on some bedding surfaces.

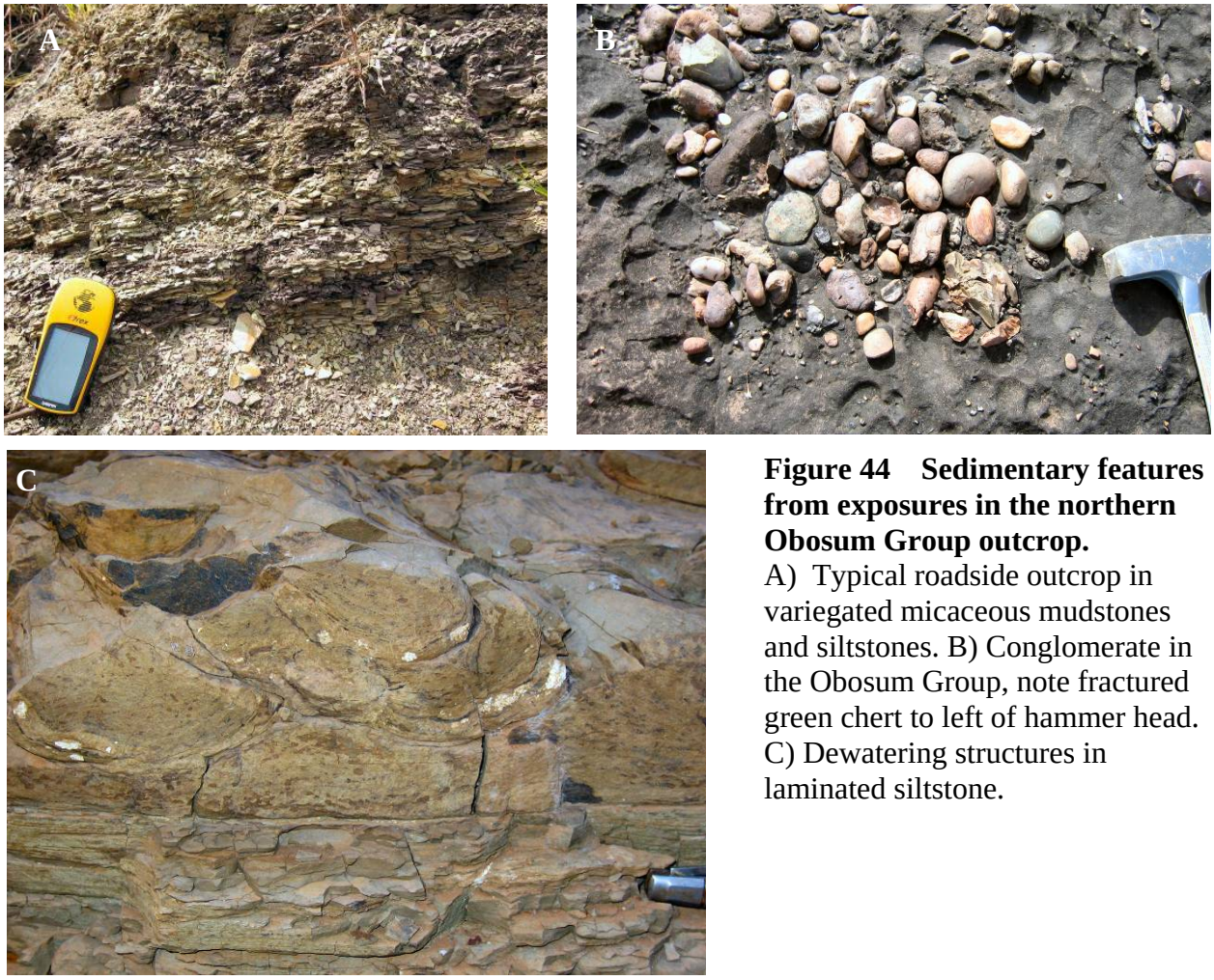

Figure 44 Sedimentary features from exposures in the northern Obosum Group outcrop.
A) Typical roadside outcrop in variegated micaceous mudstones and siltstones. B) Conglomerate in the Obosum Group, note fractured green chert to left of hammer head. C) Dewatering structures in laminated siltstone.

Interpretation: The Tamale Sandstone is interpreted to be a classic fluvial red-bed deposit, representing molasse derived from the Pan African orogen. It was probably much more extensive than its current extent, but has been removed by erosion. It may be that other small outliers of this unit remain to be delineated in the region, but such outcrops would only be found through further, more detailed mapping.

Sang Conglomerate (informal name). This highly distinctive lithology was described by Junner and Hirst (1946), who considered the best exposures to be around the village of Sang, on the Tamale-Yendi road. Its outcrop has been traced on DTM imagery, with some difficulty, as a series of low hills to the west and south of Sang (Figure 40a). On such topographic considerations, as well as the local abundance of pebbles in lateritised bedrock, also noted by Junner and Hirst (1946), the conglomerate is suggested to rest unconformably on the Bunya Sandstone. Good exposures of the latter occur to the south (OBS JC325) and west (OBS JC106; see above, Oti-Pendjari Group), further constraining the Sang Conglomerate outcrop. A number of other localities for the conglomerate were described by Junner and Hirst by reference to village names, none of which could be located during the present study.

At its type locality in shallow, roadside workings (OBS JC 107), the exposed part of the unit consists of massive, well-cemented cobble and pebble conglomerate, up to 1.5 m thick (Figure 45a).There are also exposures of weathered green-grey sandstone with layers and lenticles containing granules and pebbles. The pebbles include quartz and quartzitic sandstone, and there are many of 'basement' derivation that include green metavolcanic rocks, red jasper, porphyritic dacite, garnetiferous psammite and various types of schist and phyllite. They are locally closely packed, but mostly are supported within a dark grey, pink or purple, poorly sorted, coarse sand to granule grade matrix (Figure 45b).

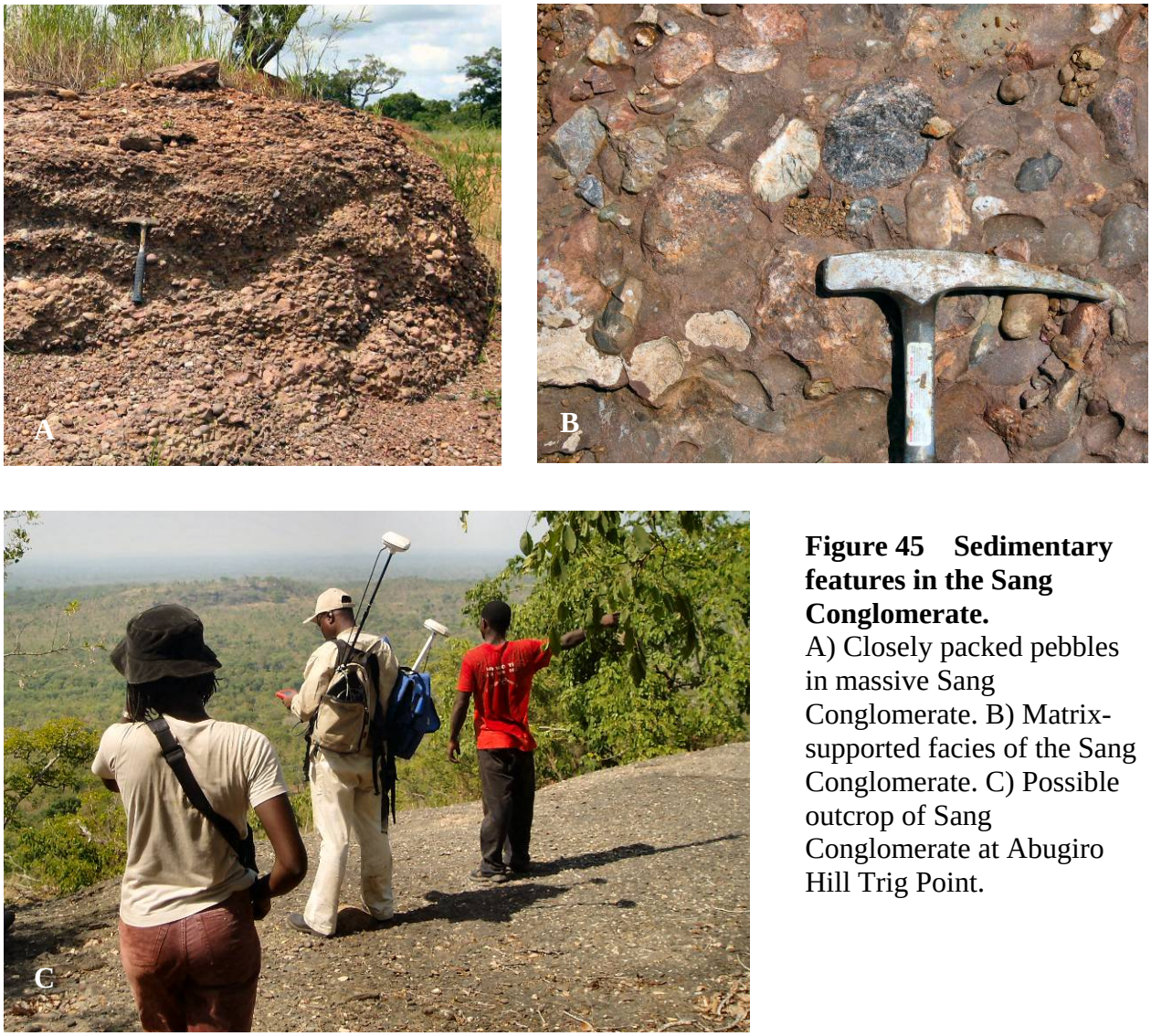

Figure 45 Sedimentary features in the Sang Conglomerate.
A) Closely packed pebbles in massive Sang Conglomerate. B) Matrix-supported facies of the Sang Conglomerate. C) Possible outcrop of Sang Conglomerate at Abugiro Hill Trig Point.

A further exposure of massive, dark grey conglomerate with basement pebbles (Figure 45c) was noted at the Trig Point on Abugiro Hill (GPS: 11190227, 1420557), about 7.8 km north of Kete Krachi. This locality was visited during the GPS reconnaissance survey phase of the project, but not investigated during either of the two visits to validate the geological map and its correlation with the Sang Conglomerate is therefore tentative. Its outcrop does, however, coincide with a series of low hills surmounting the Bunya sandstone, as at the Sang locality.

Interpretation: The Sang Conglomerate represents terrestrial red-bed deposits, with a highly oxidised matrix. The unit possibly represents river gravels, and its scattered outcrops are perhaps the remnants of once-more extensive braided, high-energy fluvial systems that carried molassic debris westwards from the Pan African orogen in to the central parts of the Volta Basin.

Dunkro Sandstone Formation. This unit consists of red to pink, highly immature (feldspar and lithics-rich) sandstones and conglomerates. It crops out in the southern part of the Obosum Syncline, where it is inferred to overlie and perhaps to overstep (see above) the Tease Sandstone, the latter marking the top of the Oti-Pendjari Group. The Dunkro Sandstone is in turn overlain by the Densubon Sandstone of the Obosum Group; however, it does not form good features on the DTM and its outcrop is largely inferred from the findings of hydrogeological boreholes. In these provings, feldspathic conglomeratic sandstones, typical of the Dunkro Sandstone defined here, were penetrated across a wide area, as summarised in Davies and Cobbing (2002).

Figure 46 Sedimentary features in the Dunkro Sandstone Formation. A) Abundant, coarse, highly angular feldspar (pink) and lithic grains in Dunkro Sandstone. B) Matrix-supported conglomeratic sandstone, as above, with channelised conglomeratic lag in lower part. C) Oversteepened cross-bedding in Dunkro Sandstone. D) 'Floating' boulder of Dahomeyan grey gneiss in massive Dunkro Sandstone.

The Dunkro Sandstone is well exposed on prominent koppies (OBS CJ162; JC290) to the west of the road leading northwards to Kwaikesi. These crags are in red, medium to coarse grained, highly feldspathic and lithics-rich sandstone (Figure 46a). Conglomeratic layers with maroon mudflakes are present, as are 1-2 m thick layers of poorly sorted cobble conglomerate. The conglomeratic beds are typically massive and matrix-supported, and some appear to infill scoured-out channels (Figure 46b). The massive, pebbly sandstones are in several metres-thick units, but more thinly bedded sandstones locally show lateral accretion surfaces and cross-bedding, with current directions towards the west and south-west. Cross-beds are locally oversteepened (Figure 46c) and in places the bedding is chaotic, suggestive of syn-sedimentary slumping. Clasts in the conglomerates are subangular to well-rounded, with moderate sphericity;

they include green chert, various granitoid lithologies and dark green-grey porphyritic volcanic rock. In one part of the exposure, massive sandstone contains a ‘floating’ boulder of Dahomeyan-type grey mesocratic gneiss (Figure 46d; compare with Figure 56).

Very similar lithologies can be viewed in several roadside exposures farther north; for example, at OBS CJ163, JC 291 and CT 7 where there are pavements in red, coarse-grained, feldspar-lithics rich sandstone with sporadic 'floating' pebbles and trough-like pebbly lags. The clasts here include pink porphyritic ?microgranite and foliated ?metasedimentary lithologies.

Densubon Sandstone Formation. This unit crops out in the central part of the Obosum Syncline, which is an area largely inaccessible to vehicular traversing at the time of the field visits. It overlies the Dunkro Sandstone, but to the west it cuts down through it to rest on the Afram and Ejura formations (Oti-Pendjari Group). The lithologies typically consist of pink to grey feldspathic sandstone with subordinate beds of brown mudstone and siltstone; red or green mudflakes are commonly present. In the south-eastern part of the Obosum Syncline, about 5.7 km south of Densubon, roadside exposures (OBS JC 292) show pink, medium- to fine-grained, highly micaceous arkosic sandstone with local trough cross-lamination indicating currents to the south-west and south-south-west; some mudflakes were present. Similar sandstones occur about 750 m to the south (OBS CJ 166).

Along the escarpment marking the formation’s southern limit, and its junction with the underlying Afram Formation, exposures (OBS CJ156) show maroon, fine-grained, thinly bedded sandstone (Figure 47). Farther to the north-west, exposures (OBS JC 55) along the Ejura-Atebubu road are in pink, fine-grained, micaceous and feldspathic quartzose sandstone with fine-scale trough cross lamination indicating currents in the south-east to south-west quadrant; some beds contain flakes and rounded pellets of maroon mudstone. A possibly more immature facies, noted about 1.4 km north-east along the road (OBS CJ216), consists of dark red, fine- to medium- grained feldspathic and lithic-rich sandstone with mudstone flakes. Pebbles are concentrated in the upper parts of some beds, with laminae of grey, micaceous sandstone at the base. Cross bedding indicates currents towards the west. Nearer to the northern rim of the Obosum Syncline at Seneso village (OBS CJ218), the exposures show red to grey, medium-grained sandstones with minor ripple-drift structures picked out by micaceous cross-lamination. About 27 km east of here, by the village of Dogweme (OBS CJ20), the formation consists of flaggy, red, thinly bedded medium-grained sandstone with ripple-marked bedding surfaces indicating currents towards the west.

Figure 47 Thinly bedded Densubon Sandstone.

Interpretation of the Dunkro and Densubon sandstones: The sandstone lithofacies in these two formations is typical of fluvial red-bed successions. Deposition was rapid, and possibly involved ephemeral flash-flood, wadi, alluvial fan and sheetflood environments as well as more persistent braided stream environments. The range of lithoclasts, including high grade gneissose rocks, clearly indicates derivation from the Pan African orogen, as a terrestrial molasse fill to this southern part of the foreland basin to the orogen. It is possible that the basin was beginning to lose its definition by this stage, with very large fans and sheets of sandstone and conglomerate developing in front of and adjacent to the orogen.

Although widely separated, the common red-bed characteristics of the Tamale, Sang, Dunkro and Densubon units indicate that they are broadly contemporaneous and represent the final stages of infilling of the Volta Basin. The preservation of the thicker red-bed sequences to the south of the Pru Fault may be due to syn- or post-depositional faulting and/or more marked basin inversion to the north.

The limited paleaocurrent data for the Dunkro and Densubon sandstone formations (Figure 42b) reveal dominantly west-south-westerly palaeoflow, which is consistent with the hypothesis that these sediments were derived from the Pan African orogen to the east. It appears from a comparison of Figures 42a and b that the general palaeoslope continued to be orientated towards the southwest from Oti-Pendjari Group time through into at least the early part of Obosum Group time. There may have been a change in slope the upper part of the Obosum Group, as data for the Tamale Sandstone suggest a change to south-south-easterly palaeoflow (Figure 42c). However, since the data are very limited and were sampled from a small area of outcrop, the possibility cannot be ruled out that the Tamale directions represent local flow variation in the north of the basin.

4.1.2.7 BUEM STRUCTURAL UNIT (PAN-AFRICAN DOMAIN)

The Buem Structural Unit, defined by Affaton (1975), contains rocks that crop out within the northerly extension of the Akwapim mountain range, in the south-eastern corner of the Project area. This strongly folded and thrust-imbricated terrain forms part of the Pan-African ‘Dahomeyide’ orogenic belt (Figure 16). It constitutes the westernmost part of the Dahomeyide ‘Zone I’ according to Affaton et al. (1991), which includes quartzitic rocks that have long been thought to represent the highly faulted and folded equivalents of the older Volta Basin strata exposed in the Kwahu Plateau area (e.g. Saunders, 1970). Although this correlation was mainly based on lithological characteristics, it is supported by comparisons between detrital zircon age spectra of sandstones from the Volta Basin and Buem Structural Unit (Kalsbeek et al., 2008; Buem sample Gh5). The Buem Unit may also contain fault-slices with rocks equivalent in age to the Oti-Pendjari Group, however. A further thrust-bounded component of ‘Zone I’, the Atacora Structural Unit (Tiele Unit of Affaton, et al., 1980), is located a small distance farther to the east, outside of the Project area. In that unit, the metamorphic grade is higher than in the Buem (mesozonal as opposed to high-anchizonal), and although quartzitic strata similar to the Kwahu and Bombouaka groups are present, they are tectonically interleaved with fault-bounded slices of Dahomeyan basement rocks (Affaton et al., 1980).

The western edge of the Buem Unit, and of the Pan-African orogenic belt, is inferred to be delimited by a major structure, here termed the ‘Pan-African frontal thrust’. Although exposures of this structure have not been observed, its position is clearly defined in the southernmost part of the Project area, where there is a sharp contrast between gently-dipping Kwahu Group strata and the rugged, strongly lineated Pan-African domain to the east (Figure 48a). The precise location of the frontal thrust is uncertain where it is hidden beneath Lake Volta. Prior to this area being flooded, however, geological surveys in the Volta River valley showed that the Akroso Conglomerate outcrop represents the core of an asymmetric anticline, with strata on the steeper eastern limb dipping at angles of between 40^{o} and 55^{o} in easterly directions (Figure 48b). This geometry suggests that the Oti-Pendjari Group is up-arched against the putative Pan-African

frontal thrust (Figure 16). Farther north, most workers place the frontal thrust on the western side of the Tokor Volcanics outcrop (e.g. Affaton et al., 1980), as shown in Figure 48a, indicating that the volcanics are part of the Buem Unit. An alternative suggestion by Jones (1990), however, is that the Tokor Volcanics lie conformably above the Akroso Conglomerate on the eastern limb of the Akroso Anticline. This interpretation would place at least the western part of the volcanic sequence within the Oti-Pendjari Group, with the Pan-African frontal thrust located in the hill ranges to the east of the lake. One problem with this interpretation is that there are no volcanic rocks on the opposite, western limb of the anticline, although it might be argued that they were removed prior to deposition of the unconformable Obosum Group.

Remote images show that the Buem Structural Unit forms a distinctive terrain characterised by numerous NNE-trending lineaments, which are expressed topographically by narrow ridges and intervening valleys (Figure 48b). Exposures reveal that the valleys are occupied by cataclastic rocks and phyllonites, which indicate the presence of high-angle reverse faults and/or imbricate thrusts. The ridges between these structures are comprised of locally folded, but not pervasively foliated, sedimentary rocks, which include quartz arenites similar to those seen within the Kwahu Group, as noted above. There are also volcaniclastic sandstones (*Todzi sandstones*) and associated basic volcanic rocks (*Tokor volcanics*), neither of which occur in the Kwahu or Oti-Pendjari groups of the Volta Basin. Exposures of the *Oterkpolu Limestone Member* in Oterkpolu Quarry show spectacular arrays of reclined folds and thrusts that demonstrate a westwards tectonic transport direction for the Buem Structural Unit.

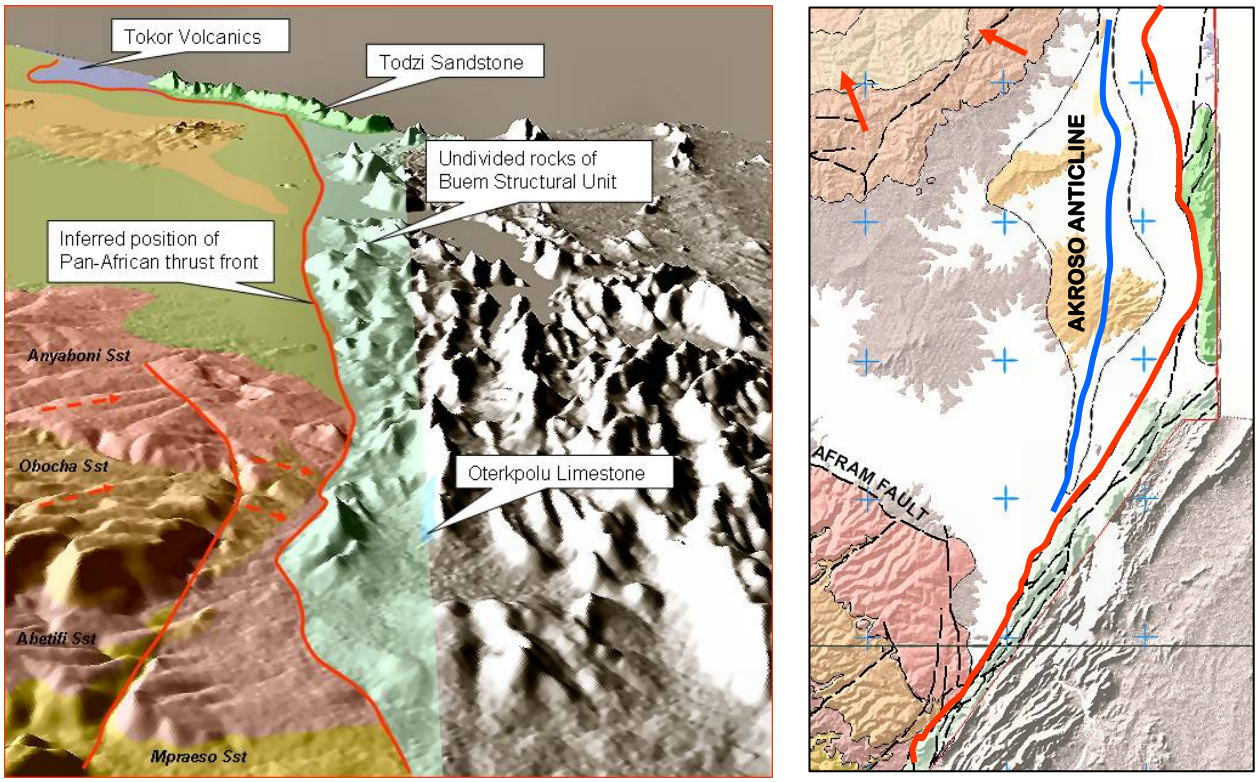

Figure 48 Structures at the eastern margin of the Volta Basin. A) Oblique view of DTM looking north, showing junction between the Buem Structural Unit and Kwahu Group. Dips in latter shown by red dashed arrows. B) Extract from 1:250 000 map showing the main structural elements along the Pan-African thrust front in the south- east of the Project area.

Pan-African thrust Major anticline Regional dip

Undivided rocks of the Buem Structural Unit. These strata form the southernmost part of the Buem Unit in the Project area. They crop out within a terrain of NNE-trending lineaments

bounded to the west by the Pan-African frontal thrust. Hard, pale grey quartz arenite is exposed by the road along the side of a valley about 0.5 km north-east of Boso village (OBS JC 359). Although not pervasively foliated, these rocks are fractured and a cataclastic zone is present. The latter is overprinted by a later generation of spaced fractures trending roughly east-west (100^{o}). About 2.3 km north-east of here, exposures (OBS JC 358) along the valley floor, where a fault is postulated to be present, show the same quartz arenite lithology converted to a very strongly foliated protomylonite that is interbedded with silver-grey phyllonite, the latter injected by quartz veins showing folding and partial transposition into the foliation. The foliation here is flat-lying, possibly due to re-folding, with a weakly developed S-C fabric suggesting a top-to-the-south-east direction of tectonic transport. This is opposite to the tectonic transport direction normally ascribed to the Dahomey belt, and may suggest a subsequent phase of relaxation due to orogenic collapse. About 660 m along the valley to the north-east, in the village of Kpalima (OBS JC 357), the same fault zone is represented by silvery grey phyllonite; the foliation dips south-eastwards at 40^{o} and is cut by multiple generations of quartz veining. The foliation is mildly crenulated along a later set of cm-spaced fractures trending 128^{o}.

Farther to the south-west, quartz-arenites are exposed by the roadside close to the crest of Teteampa ridge, one of the features that characterise the terrain of the Buem Structural Unit. On the north-west side of the ridge (OBS JC361), white, thinly bedded, fine-grained quartz arenite is intercalated within grey, laminated, fine-grained micaceous sandstones, silver-grey siltstones and papery mudstones. The siltstones locally show complex oscillating cross lamination and there are also lenticular ?winnowed quartz-granule lags with mudflakes on some laminae. Although these strata show no penetrative foliation, they are locally crumpled below a minor, bedding-related decollement structure (Figure 49a). About 0.4 km to the south-east across the ridge crest (OBS JC 360), there are ribs of foliated white quartz arenite. Nearby slabs consist of very coarse-grained or granule sandstone with well rounded quartz grains. Farther to the south-east, and across a valley inferred to be occupied by a fault or thrust zone, strata occupying a structurally higher position within the Buem thrust-stack are exposed in a village (OBS JC 362). They are of a different type of lithology, strongly resembling the Anyaboni Sandstone of the Kwahu Group. In one part of the exposure the sandstone is feldspathic, micaceous, and fine-to medium-grained with purple/maroon weathering colours; it passes up into a yellow to pale cream, micaceous, thinly trough cross-bedded sandstone.

Close to the southern termination of the Project area, a cutting on the Oterkpolu to Odumasi road (OBS JC24; CT42) exposes a thinly bedded to laminated sequence of grey-green, fine-grained, micaceous, lithic-rich sandstones interbedded with 'papery' laminated mudstones and siltstones. The sandstones are weakly trough cross bedded and syn-sedimentary slump folding was noted in some very fine-grained beds. This succession bears some resemblance to the turbiditic beds of the Bimbila Formation (Oti-Pendjari Group), but could also be similar to facies found at the base of certain Kwahu Group units; for example, the Mpraeso or Anyaboni formations. The whole sequence is part of an inclined fold with an axial surface dipping towards the south-east, indicative of a north-westwards tectonic transport direction (Figure 49b). Minor folds and decollements in the upper limb are consistent with this geometry. This exposure is located to the south of an area mapped by Saunders (1970) as comprising interthrusted slices of Anyaboni Sandstone and various other Kwahu Group quartz arenites.

Interpretation. Very few localities were visited in these strata; however, they mostly appear to consist of mature quartz-arenites, smilar to the Mpraeso, Abetifi and Obocha sandstone formations of the Kwahu Group, as well as feldspathic sandstones closely resembling the Anyaboni Sandstone. It is noted that elsewhere in the Buem Unit, Kalsbeek et al. (2008) identified sandstones with zircon age spectra similar to the Kwahu and Bombouaka groups, confirming the presence of these older Voltaian strata in this structural domain.

Figure 49 Structures and lithologies in the Buem Structural Unit. A) Thinly-bedded quartz arenite and siltstone with local tight folding. Vergence is towards the NNW (340º). B) Thinly-bedded sandstones and siltstones showing NW verging fold.

Oterkpolu Limestone Member. This unit is located at the extreme south-eastern limit of the project area (Figure 48a), its outcrop suggesting that in comparison to the lithologies described above at OBS JC24, it may occupy a higher structural position within the Buem thrust-stack. In Oterkpolu Quarry (OBS JC269), the sequence consists of blue-grey, hard, massive to laminated micritic limestones that are silicified in part. The limestones feature ripple marked bed-tops and are thinly interbedded with maroon, laminated siltstones (Figure 50a), an association strongly reminiscent of that seen in the Buipe Limestone Member (Oti-Pendjari Group, Figure 32a); thin, phyllitic partings are also present. The beds lying topographically above the carbonate sequence, and exposed above the current back wall of the quarry, consist of yellow-cream siltstones with intercalated cms-thick beds of a hard, maroon, fine-grained siliceous lithology (=Darebe Tuff?). This in turn is overlain by medium-grained, white to pink-weathering, laminated quartzose sandstone.

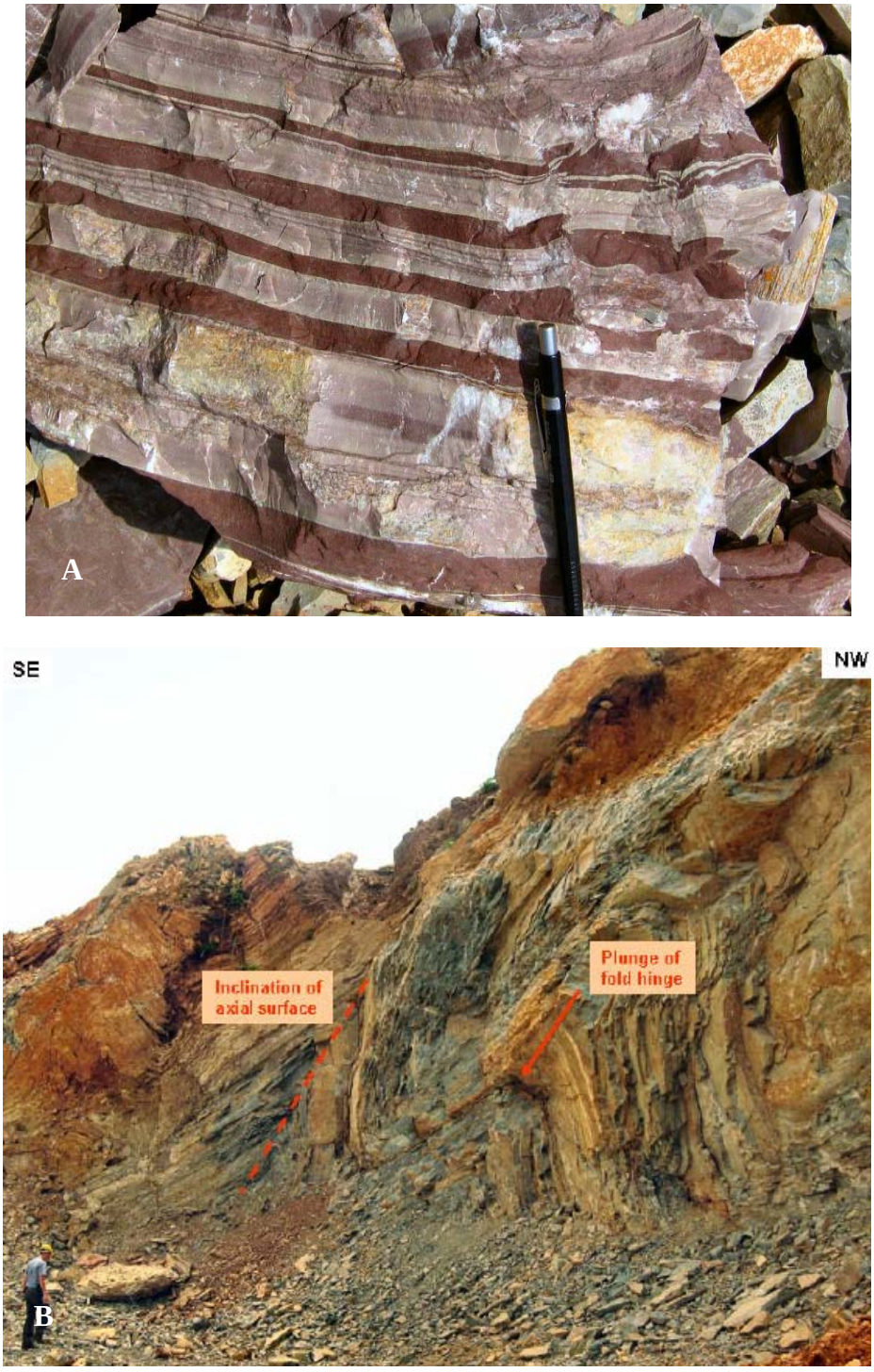

Figure 50 Limestone Member at Oterkpolu quarry. A) Oterkpolu Limestone, showing interbedded maroon siltstone. Note low-angle truncations of the laminae and syn-sedimentary microthrust structures. B) Reclined fold with south-plunging hinge, in Oterkpolu Quarry.

In the quarry the Oterkpolu Limestone is disposed within a series of north-westwards-verging reclined folds with axial surfaces dipping about 40-50^{o} to the south-east and hinges plunging at 15^{o} due south, as shown in Figure 50b. The folding is accompanied by imbrication along a series of decollement planes that also dip consistently to the south-east. The structural observations from this quarry are consistent with a north-westerly direction of tectonic transport within this part of the Buem Structural Unit.

Interpretation: Ripple-marked top-surfaces suggest that the Oterkpolu Limestone Member was deposited in wind-or current-agitated environments, implying relatively shallow waters. The

association between ripple-marked limestones and maroon siltstones is reminiscent of that seen in the Buipe Limestone Member. Should this tentative correlation be confirmed, it would indicate that this part of the Buem Structural Unit includes tectonic slivers of basal Oti-Pendjari Group strata.

Todzi Sandstone. This informally named unit corresponds to sandstones that occupy the rugged, southernmost part of the north-trending Kpandu Range, an outcrop area that includes igneous rocks of the Tokor Volcanics. The very limited exposures visited suggest that at least some of these sandstones are quartzitic. Others, however, include diamictons and there are feldspathic varieties with volcanic detritus. The Todzi Sandstone outcrop is bounded to the west by the Pan-African frontal thrust, the inferred position of which broadly coincides with the eastern margin of Lake Volta. Studies of LANDSAT and DTM (Radarsat and SRTM) imagery suggest that the sandstones occupy a NNE-trending synform, the culmination of which occurs on Tuhorihome Hill, in the south of the outcrop. The synform can be interpreted as part of a klippen, the remnant of a tectonic sliver that has cut down through the sandstones described above, and which is in turn overridden by the basal thrust of the Atacora Structural Unit located to the east of the Project area, as shown in Figure 51a.

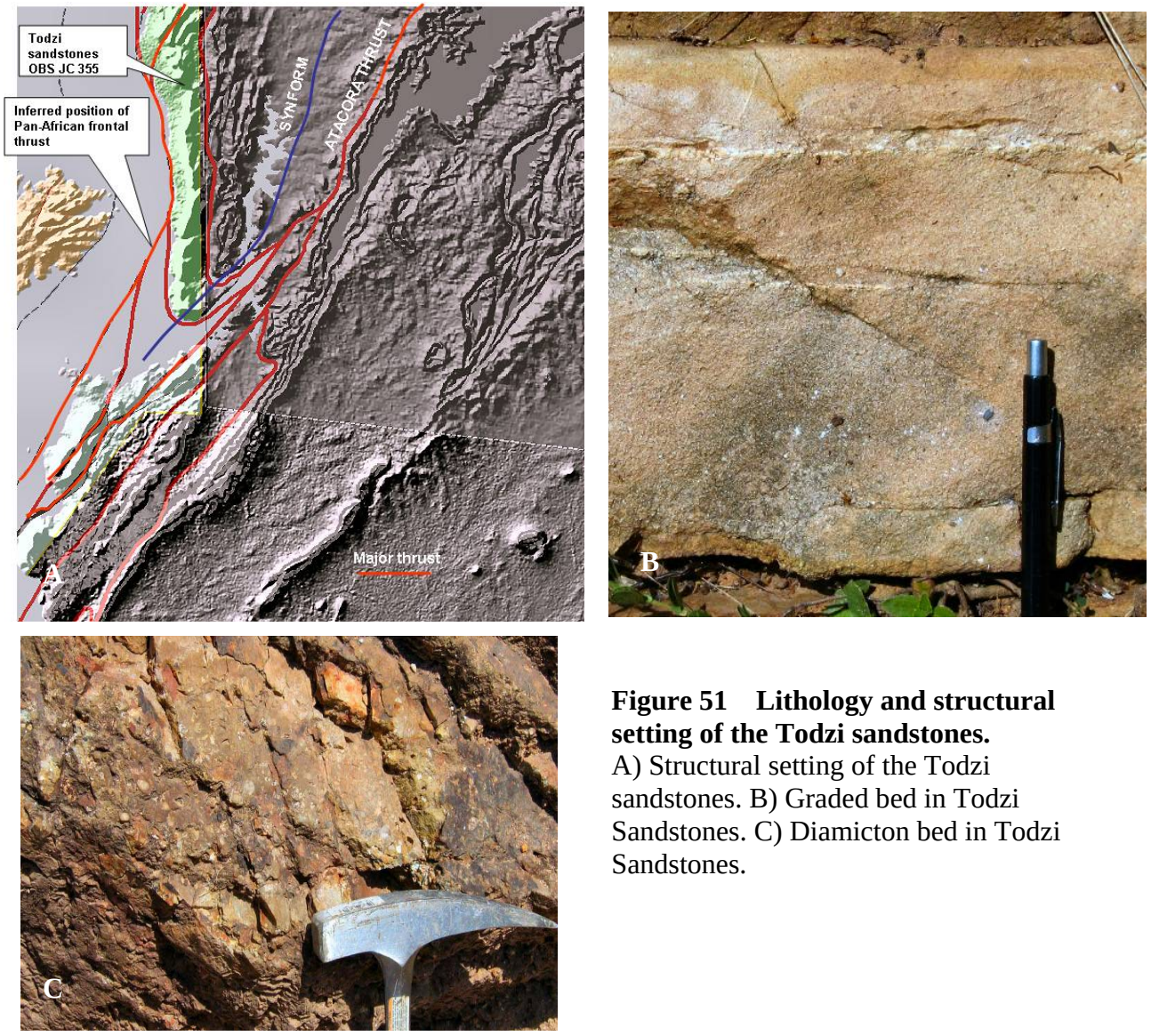

Figure 51 Lithology and structural setting of the Todzi sandstones.
A) Structural setting of the Todzi sandstones. B) Graded bed in Todzi Sandstones. C) Diamicton bed in Todzi Sandstones.

Roadside exposures (OBS JC 353) show a varied succession that includes white to pale grey, massive, medium-bedded sandstones. Granules and angular, small-pebble size fragments are distributed through a medium-grained matrix of feldspathic quartz arenite, indicative of low degrees of sorting. They include white, clay mineral-altered ?feldspars, some of which have subhedral outlines; fine-grained grey-green ?volcanic lithologies; and Fe-Ti oxide grains. A cataclastic zone occurs along the contact with overlying medium-bedded, lithic-rich sandstones showing normal grading (Figure 51b). About 700 m farther to the west, a small roadside quarry (OBS JC 355) exposes sheared and brecciated, white quartz arenites. A diamicton bed, which is 10-20 cm in thickness and highly lenticular, is included in this succession. It consists of small, angular fragments of white to pink, clay mineral-altered feldspar, grey-green basic volcanic rocks, cream chert, mudstone and quartz pebbles set in an olive-green, mud-rich matrix (Figure 51c).

Interpretation: This very preliminary study suggests that the Todzi Sandstone comprises a tectonically bounded package within the Buem Unit, interleaved between the Pan-African frontal thrust and the basal thrust of the Atacora Structural Unit. Although the succession contains quartz arenites, not all of its components are directly comparable to the Kwahu Group. In particular, certain of the more feldspathic beds are poorly sorted and contain detrital constituents, such as volcanic rocks and chert, not found in that group.

Provenance studies were carried out by Osae et al. (2006) on three feldspathic sandstones from the Kpandu Hills, just outside of the project area. They included mixing calculations performed on the two main types of sandstone that were identified. The results suggested that quartz arenites were composed of about 98% Birimian and 2% 'Buem volcanics' detritus, whereas feldspathic arenites could be modelled by a mixture of 30% Birimian granitoids, 20% Birimian metasediments and 50% Buem volcanics. This latter variety may be comparable to the feldspathic sandstones with diamicton beds and volcanic debris described above. It was concluded that these sandstones were deposited within a passive margin tectonic setting, receiving large amounts of mature detritus from hinterland areas. More recent geochemical studies (Huntsman-Mapila et al., 2009) have, however, indicated that sediments previously considered to be of 'passive margin' affinity may have been deposited within a wide spectrum of environments that include intracontinental rift systems. Thus, when re-plotted on the discriminant function and REE diagrams of Huntsman-Mapila et al., the Todzi sandstones sampled by Osae et al. fall within the field of sandstones from the Okavango delta in Botswana, which represent deposition within a early-developing ('nascent') rift.

The occurrence of poorly sorted, massive to normally graded sandstones and mud-matrix-rich diamicton suggests deposition in an unstable slope setting. The close spatial association of these sandstones with the Tokor Volcanics (see below), combined with the detrital provenance studies described above, further indicates deposition within a young intracontinental rift receiving detritus contributed from the Birimian hinterland and basic volcanic edifices. These strata were subsequently incorporated into the Pan-African thrust stack during the end-stages of compression and closure in this sector of the Volta Basin.

Tokor Volcanics. These volcanic rocks are located about 3 km due north of the inferred outcrop of Todzi Sandstones (Figure 48a), in a similar structural position, and possibly part of the same tectonic package as that unit (see above). As noted in the introduction to this section, the position of the Pan-African frontal thrust is based on the assumption that the Tokor Volcanics represent part of the Buem Structural Unit, rather than the autochthonous Volta Basin sequence. Jones (1990) followed Grant (1969), however, in suggesting that the Buem and Volta Basin sequences (including the Akroso Conglomerate described in section 4.1.2.5.) were essentially conformable and/or lateral equivalents. There is very little field evidence available, to confirm or refute this alternative model, although most recent workers consider that these volcanics lie within the Buem Unit and are bounded to the west by the Pan-African frontal thrust (e.g. Osae et al., 2006).

Only a very small outcrop of Tokor Volcanics is present in the Project area, adjoining the eastern shore of Lake Volta. Small, rubbly exposures of these rocks were visited (OBS JC 352) by the lake side east of the Project area boundary, close to the village of Tokor and about 4.3 km due west of Kpandu. The exposures are in a black, fine-grained rock with common to abundant vesicles and a few percent of white amygdales; chloritised phenocrysts, possibly of olivine, were noted in similar exposures nearby. A thin section shows small quartz amygdales, and larger amygdales of calcite lined with granular quartz aggregates. Very sporadic, small, chloritised mafic pseudomorphs have outlines suggestive of both olivine and clinopyroxene. The groundmass is exceedingly fine-grained, consisting of abundant Fe-Ti oxide granules and a felt of plagioclase microlites, the latter forming an orthogonal network possibly indicative of quench induced crystallisation. In the nearby market area, abundant sandstone fragments may represent debris derived by mass-wasting from the ridge about 1.5 km to the east.

The volcanic rocks described above are from an outcrop previously mapped by Jones (1990) as consisting of hawaiite lava with pillowed structure in places. Jones' sketch map shows that the volcanics continue northwards as narrow belt (c. 0.5-2.7 km width), largely outside the project area. The sandstones described by Jones (1990) as being associated with the volcanics, and in places interleaved with them, consist of quartz arenites and feldspathic varieties, some of which grade into conglomerates with pebbles of quartz, phyllite and plutonic rocks. Wackestones and 'mixtites' were also noted by Jones, an association evocative of the Todzi Sandstone outcrop farther south (see above).

Interpretation. Jones (1990) concluded that the rocks here termed the Tokor Volcanics constitute a consanguineous alkaline, undersaturated magmatic suite in which hawaiites, mugearites, trachytes and phonolitic trachytes are all represented as lavas. Olivine-phyric basaltic agglomerates, tuffs and hyaloclastites are also present, and in places the lavas are pillowed, indicating eruption into water. Chemical compositions (Jones, 1990) show that the Tokor Volcanic suite is both olivine- and nepheline-normative. Immobile trace element analyses were presented by Jones to show the consanguinity and magmatic affinities of the volcanics, but this data was not used to characterise the tectonic setting other than to furnish a general conclusion that eruption may have occurred within a rift zone. Alkali basaltic volcanism commonly occurs within immature, intracontinental rift systems, which is in keeping with an interpretation of the Buem Unit as the tectonically telescoped remnant of an extensional basin that developed along the junction between Birimian basement of the Leo Shield and Dahomeyan basement of the Benin Shield (e.g. Dallmeyer and Lecorche (1991), prior to Pan-African orogenesis. On a cautionary note, however, Glazner and Bartley (1994) give examples of alkali magmas generated in contractional or transpressional tectonic settings.

Volcanic rocks occupying a similar structural datum along the western margin of the Buem Structural Unit crop out about 420 km to the NNE of the Tokor Volcanics outcrop, around Tiele in Togo. These, however, are of a different magmatic lineage, ranging from tholeiitic basalts through to andesites and rhyolites (Affaton et al., 1997). Trace element discriminant diagrams suggest that the Tiele mafic lavas have E-type MORB chemical signatures, and are free from crustal contamination; they were generated in a region of strongly attenuated continental lithosphere, and given their association with feldspathic quartz arenites, shales and siltstones, a passive margin tectonic setting was considered likely. This environment, and range of compositions, is analogous with certain modern examples of basalt-rhyolite volcanism in advanced rift settings, such as the Afar-Red Sea region of Ethiopia (Ayalew et. al., 2002). The geochemical evidence of the Ghana and Togo volcanic provinces therefore suggests that the early palaeogeography of the Buem margin to the Volta Basin could have involved incipient extension within an intracontinental rift or transpressional zone (Tokor Volcanics), which propagated northwards into a rifted passive margin setting (Tiele Volcanics of Togo sector). Jones (1990) considered an eruptive age of 600-650 Ma to be possible for the Tokor volcanic rocks. Although neither association has yet been dated by U-Pb or Pb-Pb systematics, they must

pre-date tectonic uplift and exhumation of deep crustal lithologies within the Pan-African belt, an event that has yielded U-Pb titanite ages of 586-578 Ma (Attoh et al., 2007).

The sandstones associated with the Tokor Volcanics were suggested by Jones (*op cit*) to have been deposited in alluvial fan environments. However, the presence of graded bedding in the closely associated strata of the Todzi Sandstone suggests deposition in deeper water, possibly in fan deltas. This would be consistent with the presence of pillow lavas in the Tokor Volcanics described by Jones, and with the suggestion (above) of a young rift setting. This is reinforced by the findings of the provenance mixing models of Osae et al. (2006), discussed above, which included three feldspathic sandstones from the Kpandu Hills, to the east of (i.e. structurally and/or stratigraphically above) the Tokor Volcanics outcrop. The rift margin faults were possibly reactivated, with reversed movement, during Pan-African west-directed compression (Section 4.1.2.8), telescoping the Tokor Volcanics together with the Todzi Sandstone on to the autochthonous part of the Volta Basin sequence.

4.1.2.8 AGE AND EVOLUTION OF THE VOLTAIAN SUPERGROUP AND BUEM STRUCTURAL UNIT

Studies to determine the absolute age of Volta Basin sedimentary sequences have been hampered by the lack of reliable material with which to conduct geochronological analyses. In the case of the lowermost sequences (the Kwahu and Bombouaka groups), direct dating by Rb/Sr isotopic determinations on clay minerals from shales in the Togo outcrop of the Fosse-aux-Lions Group (=Poubougou Formation of this account, see Table 14) suggest an age of 993 $\pm$65 Ma (Clauer and Deynoux, 1987). Although the error range of this method is rather large, the determination is supported by the detrital zircon age spectra (Pb-Pb; LA-SF-ICP-MS method) of quartz arenites from the Kwahu and Bombouaka groups (Kalsbeek et al., 2008; Akah, 2008), which suggest deposition shortly after 1000 Ma.

For the basal part of the Oti-Pendjari Group, Barfod et al. (2004) have reported a Lu-Hf age of 576 $\pm$ 13 Ma from phosphorites capping the Buipe Limestone Member of the Kodjari Formation in Togo. This contradicts the findings of Clauer and Deynoux (1987), who determined a much older Rb/Sr age of 660 $\pm$ 9 Ma for clay minerals in shales from an horizon 1000 m stratigraphically above the Kodjari formation i.e. probably within the Afram or Bimbila formations of this account. This latter age is at odds with the suggestion that the carbonates of the Buipe Limestone Member are related to the Marinoan glaciation (Porter et al., 2004), as discussed in section 4.1.2.5., which would give a maximum age of c. 620-635 Ma for the commencement of the Oti-Pendjari Group. On the basis of this, the age of c. 576 Ma determined by Barfod et al. (*op cit*) would appear to be rather young, although it could be accounted for by a minor non-sequence, or a condensed sequence, within the topmost part of the Buipe Limestone Member.

As discussed previously (Section 4.1.2.5), age-dating undertaken as part of this Project on the youngest post-635 Ma zircon population from the Darebe Tuff constrains the commencement of deposition in the uppermost Kodjari Formation to 601.3 $\pm$ 2.0 Ma (U-Pb; LA-ICP-MS method; written communication D. Condon, 2008). This age is in good agreement with the value of around 600 Ma determined for the youngest parts of zircon age spectra obtained from elsewhere in the Oti-Pendjari Group (Pb-Pb; LA-SF-ICP-MS method by Kalsbeek et al., 2008). It should be noted, however, that these ages reflect the *availability* of zircons within the hinterland to the Oti-Pendjari depo-system; hence, deposition could have commenced earlier, between say 620-635 Ma and 600 Ma, but such an age range would only be recorded if new zircons were being formed and made available during that interval. The source of the c. 600 Ma zircons is important to age interpretations based on detrital components, and in the context of Volta Basin geology there are two possibilities. One possibility is that some of the c. 600 Ma zircons reflect derivation from pyroclastic falls that accompanied volcanism during the pre-orogenic phase of rifting that occurred along the eastern margin of the basin. Such

volcanism is confirmed by volcanic rocks found in the Buem Structural Unit of the Pan-African orogenic belt at Tiele (Benin) and around Kpandu in Ghana (Tokor Volcanics; Section 4.1.2.7.). Their eruption must pre-date the compressional phase of the orogen, which is signalled by the fabrics associated with tectonic exhumation of deep crustal lithologies, an event that has yielded U-Pb titanite ages of 586-578 Ma (Attoh et al., 2007). A second possibility is that the c. 600 Ma zircons actually date the inception of the tectonic uplift referred to previously. In that case, the youngest zircons would reflect the unroofing of thrust-slices containing igneous and/or high-grade metamorphic lithologies newly formed or remobilised during the earliest stages of the Pan-African orogeny.

Biostratigraphical data has to date has relied on the occurrence of stromatolites and acritarchs in the Oti-Pendjari Group. The assemblage described by Amard and Affaton (1984) suggested a rather vaguely defined 'terminal Proterozoic' age for the base of the group. Much the same conclusion, of a 'Vendian' age, was reached by surveys of acritarchs in deep boreholes (e.g. Bozhko, 2008). During the Phase 1 field visit of the present Project, organic impressions were found (OP/JC110) within strata of the Bimbila Formation stratigraphically positioned just below the Bunya Sandstone and thus close to the erosional top of the Oti-Pendjari Group. The impressions (Bimbila Formation: Section 4.1.2.5.) strongly resemble 'wrinkle structures' and the organism *Corumbella*. These are typically found in strata containing the Ediacaran biota, which is dated to between about 575 and 542 Ma (Knoll et al., 2004). These fossils, together with the less age-diagnostic acritarch information, preclude the possibility of a Phanerozoic age for any part of the Oti-Pendjari Group.

There are no reliable age constraints for deposition of the Obosum Group; most workers consider that latest Neoproterozoic or even earliest Cambrian ages are equally plausible.

The evolution of the Pan-African orogenic belt, which contains the Buem Structural Unit of this Project area, has important implications for the development of the adjacent Volta Basin as a foreland basin. As noted earlier (Section 4.1.2.1), this linkage between the two tectonic domains has been developed through the work of Black (1967), Bozhko (1969b), Grant (1969) and Saunders (1970), among others, culminating in the models of Affaton et al. (1980, *et seq*). In Ghana, U-Pb age determinations have been conducted on HP granulites from the Atacora Structural Unit, immediately east of the Buem Unit. The results show evidence for a deep crustal, high-pressure event at 610 $\pm$ 2 Ma (Attoh et al., 1991) and 613 $\pm$ 1 Ma (Affaton et al., 2000). The time of exhumation of these granulites was determined by the $^{40}Ar/^{39}Ar$ method on hornblende separates to be between 587 and 567 Ma (Attoh et al., 1997). An almost identical U-Pb titanite age-range of 586-578 Ma was determined by Attoh et al. (2007) for this event, which probably records the initial and main phases of westwards transport and thrust-emplacement of nappes along the eastern margin of the basin.

In summary, the following sequence of events is suggested for the Volta Basin and adjacent Pan-African domain:

1. Deposition of the stratigraphically lowermost sequences, of the Kwahu and Bombouaka groups (Table 7), shortly after 1000 Ma. The sediments were laid down within a passive margin setting that prevailed during regional subsidence within the supercontinent of Rodinia. Detritus was supplied by major river systems flowing northwards (present-day geography) from Amazonia and subsequently reworked in nearshore and terrestrial (Anyaboni Sandstone) environments. The depositional basin was developed across a peneplaned surface on Birimian basement in which, however, some upstanding elements remained.

2. The Kwahu/Bombouaka basin was subsequently uplifted and subjected to erosion, perhaps for some 200-300 million years spanning the Tonian and Cryogenian periods of Neoproterozoic time. At the end of this hiatus, the resistant quartz-arenites of the Kwahu and Bombouaka groups had been carved into isolated uplands represented by the Kwahu-Kintampo, Damongo and Gambaga massifs. The possibility that faulting occurred at some stage during this long period is suggested by features such as the straightness of the easterly-trending Oti-Pendjari Group

unconformity as mapped along the northern and southern margins of the massif containing Kwahu Group strata, to the northeast and southeast of Kintampo.

3. Resumption of deposition broadly coincided with the Marinoan global glaciation event, dated at 635-620 Ma. Regional subsidence may have commenced prior to this, however, in order to create the conditions for preservation of the tillites and the overlying Buipe Limestone cap-carbonates in the Kodjari Formation of the Oti-Pendjari Group.

4. At this time, or shortly after, an intracontinental rift zone was initiated along the site of what is now the Pan-African deformed margin to the Volta Basin. Rifting was probably facilitated by a zone of structural weakness marking the NNE-trending boundary between the Birimian and Dahomeyan Palaeoproterozoic basement terranes.

5. Localised 'hot-spot' volcanism was superimposed within two sectors of the rift system. In the south, predominantly basic alkaline lavas of the Tokor Volcanics indicate magma generation within a very young, 'nascent' rift. Farther north, in Togo and Benin, the volcanic sequence around Tiele was tholeiitic in character and produced basic volcanic rocks with MORB-type geochemistry indicative of a more advanced stage of rifting. The Darebe Tuff of the Kodjari Formation arguably represents the distal deposits of this early rift-related volcanism. Its age is to some extent constrained to about 601 Ma by geochronological analysis undertaken for this Project (written communication D. Condon, 2008; see discussion above), and could be part of the event that fragmented the Rodinia supercontinent.

6. Rifting was accompanied by general subsidence and deposition of the early part of the Oti-Pendjari Group, possibly within a passive margin setting.

7. Rifting had terminated by about 586 Ma, which is the earliest date for the initiation of compression along the adjacent Pan-African orogenic belt; an event signified by the geochronological analysis of minerals interpreted to have formed during the exhumation of deep crustal lithologies (e.g. Attoh et al., 1997). This date also marks the onset of the early convergent stage of foreland basin tectonic development in the Volta Basin. The first unroofing of thrust sheets along the Pan-African orogen is indicated by marine deposition of the Akroso Conglomerate Member, in the Afram Formation. Regionally within the Afram Formation, the westwards shallowing of lithofacies reflects increasing asymmetry of the foreland basin, concomitant with tectonic loading of its eastern, orogenic margin as the nappes were transported westwards and stacked on top of each other.

8. The marine turbidites in the Bimbila Formation, with their abundant Pan-African-derived detritus, indicate a continuation of foreland basin sedimentation. The generally south-westerly palaeoflow recorded at this time suggests that flow followed a direction approximately parallel to the Pan-African orogenic front, although the more westerly directions also indicate flow away from the orogen. It is possible here that the deposition of major (mappable) sedimentary units, such as the Akroso Conglomerate and the Bunya and Chereponi sandstones, corresponded to individual stages of nappe emplacement within the adjacent Pan-African system.

9. Oti-Pendjari Group deposition was terminated by movements that uplifted and flexed parts of the foreland basin. Structures formed at this time included the Akroso Anticline and Daka Syncline. This deformation was transmitted from the Pan-African orogenic belt and probably represents a decrease in shortening rates, which perhaps was consequent upon locking up of the thrust systems.

10. Non-marine clastic sedimentation in the Obosum Group represents the late convergent stage of foreland basin development. It occurred within new basins, the axes of which were located farther to the west of the deepest, eastern part of the preceding foreland basin. The Obosum basins were fed from westerly-flowing, high-energy depositional systems, such as alluvial fans and braided rivers, emanating from a mountain front of considerable relief. The date of this marked sedimentological change within the Volta Basin cannot be determined from the basin itself, but could be inferred from the late-orogenic cooling history of the adjacent Pan-African belt. Although a review of Rb-Sr ages in the 'Dahomeyides' is given in Affaton et al. (1991), and

some K/Ar age determinations on volcanics are presented by Jones (1990), few conclusions can be drawn from such non-specific studies.

11. During a later, Phanerozoic phase of deformation an intense system of fractures, dominated by E-W and NE-SW trends, was formed across the basin. The fracture system is particularly well displayed on DTM imagery of major arenaceous units, such as the Bunya Sandstone and the Dunkro and Densubon sandstone formations, but is obviously pervasive throughout other types of lithologies. It is also expressed as lineaments on Fugro ternary radiometric images (Crowe and Jackson-Hicks, 2008). At exposure scale the fractures are generally spaced at 20-50 cms. They are observed to cross-cut, and thus to post-date, Pan-African ductile deformational fabrics associated with thrust-faulting in the Buem Structural Unit (OBS JC359). Major brittle displacements, such as the Pru and Afram faults, appear to be related to this fracture system, but also curve into more northeasterly trending faults. The latter trend may be controlled by the reactivation of Birimian basement structures, such as the bounding shear systems of the Sefwi Belt, outside of the Project area (Crowe and Jackson-Hicks, 2008). The age of this fracturing and faulting is not known, nor is its relationship to the regional silicification event described above (Section 4.1.2.3., Anyaboni Sandstone) and discussed by Crowe and Jackson Hicks (2008). It appears to relate geometrically, at least, to offshore Mesozoic transform structures, such as the Romanche Fracture Zone (e.g. Attoh and Brown, 2008), associated with Gondwana break-up.

4.1.2.9 CENOZOIC DEPOSITS

A lateritic duricrust, averaging between 1 and 2 m thick, is ubiquitously developed on interfluves and in most gently sloping, undissected parts of the Voltaian Basin. In the central parts, a subhorizontal landform – termed the '*Central Volta Surface'* - has been developed on the softer mudrocks of the Oti-Pendjari Group. The distribution of this landform is shown on the relevant geological maps. Its edges correspond to the bedrock outcrop on valley sides or, where dissection does not occur and laterite cover is continuous, to a concave slope-break marking a change to higher ground. Thus on maps, the Central Volta Surface does not necessarily correspond to the full extent of the lateritic cover.

In places, clast-supported gravels with basement pebbles occur in association with laterite. These intra-laterite gravels are possibly the deposits of former fluvial channel systems, but some may represent the in situ replacement of bedrock conglomerate. In south-western parts of the Central Volta Surface temporary excavations suggest that the laterite, at least 2 m thick, can be erosively overlain by up to 3 m of red, poorly sorted, structureless silty clay with detrital quartz granules and sporadic pebbles (OBS JC212). The origin of these supra-laterite deposits is not known, but they may relate to the laterisation of conglomeratic or pebbly bedrocks.

A typical lateritic profile on mudrocks (OBS JC78) is about 2 m thick. It consists of an upper, hard, iron-cemented layer about 1 m in thickness, which passes down to a more friable laterite with voids lined with clay minerals. This in turn grades down into weathered bedrock consisting of soft, pale grey clay with brown ferruginous mottles and flaky mudstone lithorelicts. On harder lithologies such as sandstone, the upper c. 20 cms of bedrock is commonly spheroidally weathered and sharply overlain by laterite.

A long and complex history of duricrust formation is typical of most African regions. A geochronological study by Vasconcelos et al. (1994) suggested that for West Africa, the last pervasive oxidation event of this type occurred during the Late Miocene, about 13 Ma.

4.1.2.10 QUATERNARY DEPOSITS

Quaternary Deposits in the Volta Basin are limited to alluvium, alluvial fans and river terraces.

Alluvium is found throughout the basin, forming a complex network of sand and gravel deposits, the most extensive of which are associated with the floodplains and main channels of the Volta (Figure 16). Close to the river an unvegetated zone of active deposition and erosion, representing the main channel, can be identified, which appears purple on the false colour Landsat imagery (Figure 52). On the ground, the edges of many floodplains are not sharply defined, but instead are very gentle slopes. It is therefore unlikely that fieldwork will result in a major improvement to floodplain delineation based on LANDSAT imagery.

The floodplain distribution mapped out by the Project agrees well with the inundation limits of the 2007 flooding in Ghana mapped by various agencies using satellite imagery (Figure 53). The new mapping can therefore be used to delineate areas within the Volta catchment that are vulnerable to fluvial flooding.

Alluvial Fan Deposits, including talus deposits and rockfalls, extensively mantle the major escarpments; only a few have been digitized for this Project.

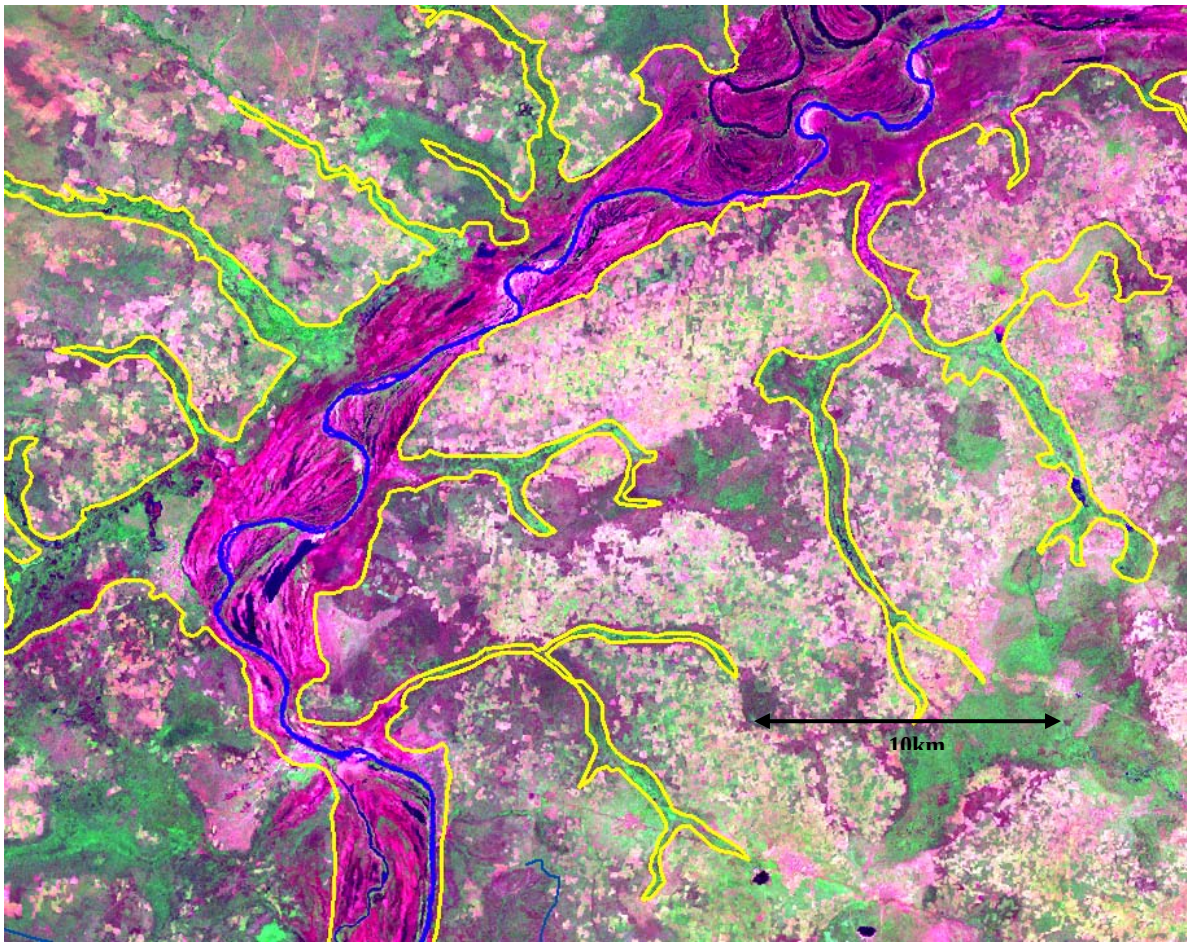

Figure 52 Alluvium boundaries (shown in yellow), mapped along the White Volta around Daboya using Landsat 741 imagery.

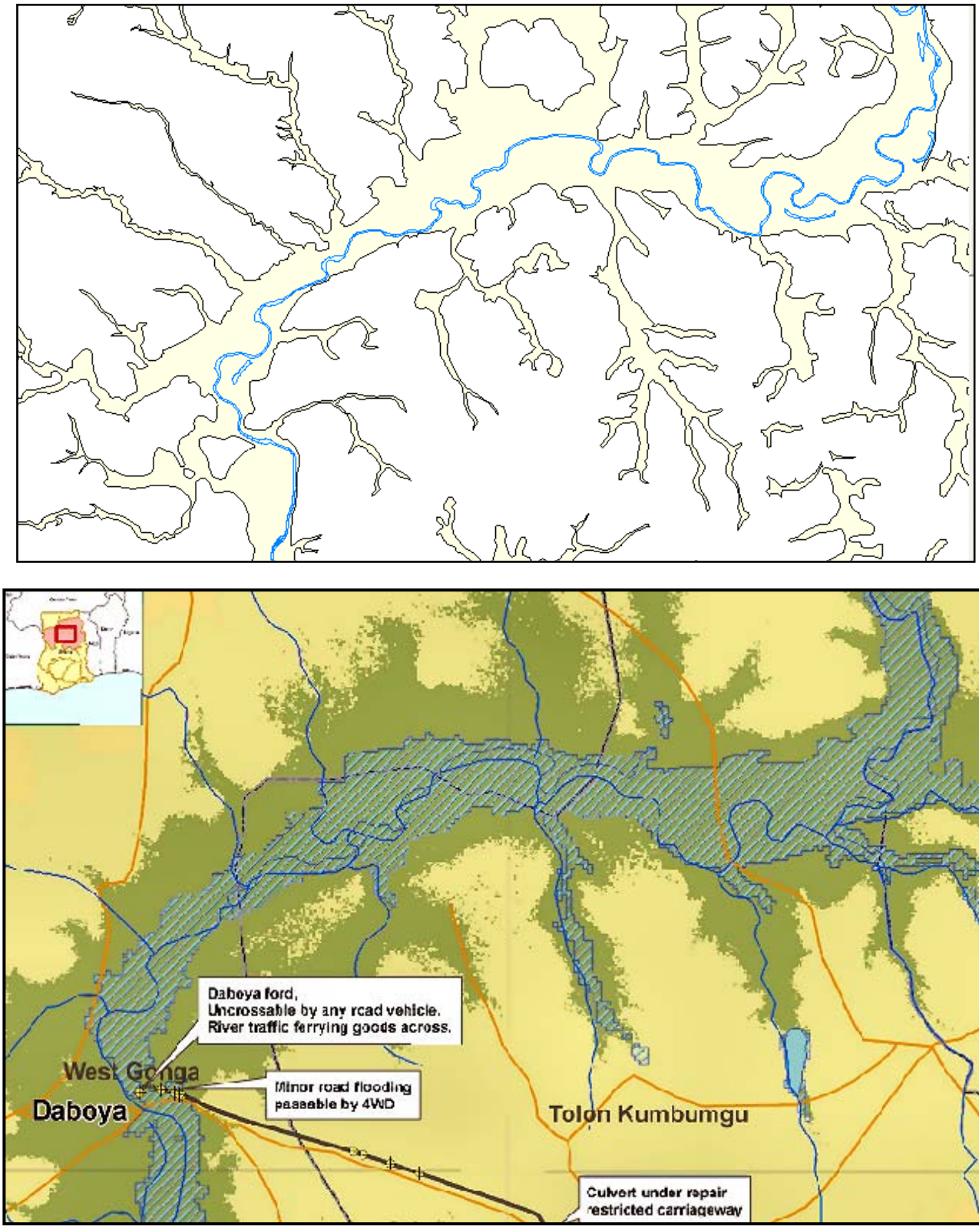

Figure 53 Comparison of mapped floodplains with actual extent of 2007 flooding. The top map showing Quaternary alluvium in yellow, the lower map showing extent of flooding in 2007 (diagonal shading).

River Terrace Deposits have been identified at certain localities along the Volta. Near Ntereso, close to the Volta crossing, 3 m of rounded cemented gravels were exposed in a small quarry (Figure 54), and are thought to represent the deposits of a high terrace.

Figure 54 Terrace gravels near Ntereso (OBS CJ108).

4.2 KETA BASIN GEOLOGY

The strata constituting the onshore part of the Keta Basin, described here, represent the attenuated, northern margin of a considerably larger and deeper depositional basin that in part reflects differential subsidence related to the Mesozoic break-up of Gondwana. This event was controlled by the impingement onto the West African continental margin of major oceanic transform shear zones, such as the Romanche Fracture Zone. Offshore seismic profiles reviewed by Attoh and Brown (2008) show that the pre-rift (pre-break up) sequence consists of Devonian to Carboniferous strata deposited on Palaeproterozoic basement. The syn-break up sequence consists of Cretaceous (Aptian to Albian) siliciclastic strata, of continental facies.

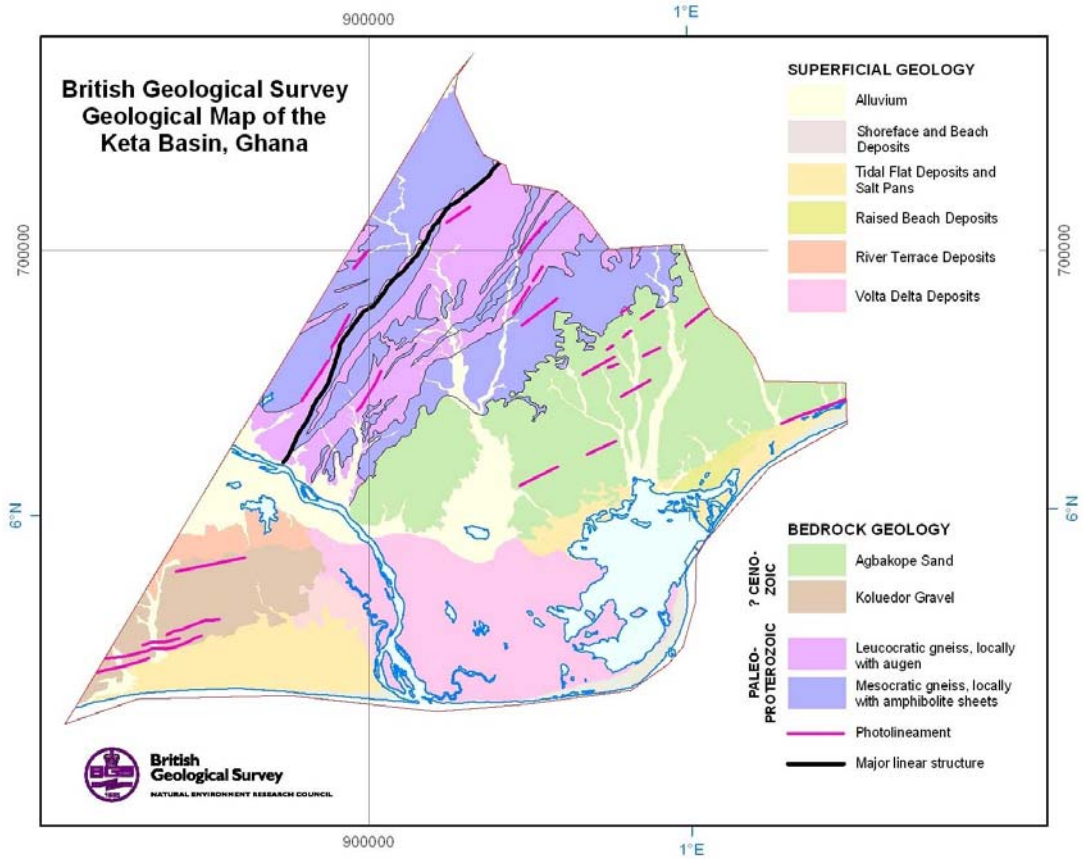

Figure 55 Geological map of the Keta Basin.

For the onshore part of the Keta Basin (Figure 55), the present project has recognised a number of informally named stratigraphical units, as shown in Table 7.

4.2.1 Dahomeyan Complex

These basement metamorphic rocks correspond to lithotectonic Zone III of the 'Dahomeyide Orogen' as described in Affaton et al. (1991). According to the latter review, the main lithologies in this area are likely to include granites, orthogneisses and migmatitic rocks with amphibolite-granulite metamorphic grades. Detailed U-Pb isotopic investigations have not yet been carried out in this area, but it is likely that at least some of the lithologies described below are of Palaeoproterozoic age (c. 2100-1700 Ma), with fabrics imposed during the Eburnean tectonothermal event. The extent of subsequent reworking during the Kibaran (c.1400-1000 Ma) and/or Pan-African (c.700-550 Ma) episodes remains to be determined.

Two assemblages of predominantly amphibolite-grade lithologies were recognised in the Keta project area. They occupy elongated outcrops, parallel with the north-easterly structural grain, but as they were nowhere seen in contact in the field their age relationships are unclear.

Mesocratic gneiss forms distinctive belts of low-lying terrain on the DTM imagery, with few features visible in the field. Outcrops of mesocratic gneiss show up as grey areas on radiometric (Total Gamma Count) imagery; however, these areas also contain narrow, discontinuous tracts that have red tones and which are elongated in a north-easterly direction. At OBS JC13, which coincides with one of the red stripes on the imagery, debris recovered from around a pit latrine consisted of grey-green, possibly granulitic gneiss, with quartz-?K-feldspar and garnet. Extensive exposures of typical mesocratic gneiss form the series of knolls centred on OBS JC15. The lithology is characterised by subvertical mineralogical layering (Figure 56) variously coloured white, pale grey, dark grey or black. These variations depend on the relative proportions of quartz, feldspars, hornblende and biotite; garnet is a rare, sporadic constituent (OBS JC17). Extreme mineralogical end-members consist of rare, mm- to cm-wide amphibolite layers and more extensive and diffuse segregation layers of quartzo-feldspathic pegmatite. Later generations of pegmatite occur as sheets cutting across the gneissic fabrics. The subvertical gneissic layering locally contains intrafolial isoclinal folds, with vergence indicating sinistral shear (OBS JC17). Elsewhere, it is cross-cut by ductile high-strain zones ranging from a few centimetres to metres-wide; these are subvertical and orientated at ~038^{o} (OBS JC15), parallel with the local Dahomeyan structural grain. Similar ductile zones, corresponding to strongly foliated and grain-size reduced mesocratic gneiss with refolded amphibolite sheets, were observed in a quarry at OBS JC22.

Figure 56 Mesocratic gneiss with an early folded fabric cross-cut by ductile high-strain zones trending 038^{o} in centre of picture. View is towards the south-west (OBS JC15).

Leucocratic gneiss forms belts of more upstanding terrain on the DTM. It also corresponds to the pale blue or white-coloured domains on total count radiometric imagery. The main lithology is pale grey to cream in colour and of paragneissic aspect, although no garnetiferous or aluminosilicate-rich gneisses were seen. Its strong foliation is generally subvertical, and consists of layers 1-2 cm wide rich in quartz and feldspars alternating with thinner (1-10 mm) and more sporadic mesocratic layers in which biotite is prominent (Figure 57). As with mesocratic gneiss there is an abundance of intrafolial, isoclinal folds, many of which, as at OBS JC18 & 19, indicate a dextral sense of relative movement (given the subvertical attitude of the foliation). Augen textures are locally developed (OBS JC 19 & 23); the augen consist of coarse, quartz-feldspar aggregates, suggesting that they represent relicts of earlier generation pegmatitic material, rather than being megacrysts. At one locality (OBS JC21) the main foliation, striking at 036-038^{o}, is displaced along sinuous, pegmatite-filled ductile zones of refoliation orientated at 180-160^{o}.

Basement structure. The Dahomeyan Complex has a strongly bimodal lithological layering defined at regional scale by alternating outcrops of mesocratic and leucocratic gneiss. Studies of the few exposures available suggest that these north-easterly trending outcrops may at least in part reflect a younger phase of fabric re-orientation along ductile high-strain zones. In the north-west of the project area, interpretations of DTM remote imagery, combined with radiometric (Total Count) imagery suggest the presence of a north-east trending tectonic discontinuity, corresponding to the major linear structure shown on Figure 55. To the north-west of this discontinuity, features on the remote images interpreted as large-scale gneissose layering outline a major isoclinal fold of several kilometres amplitude. The fold has a subvertical axis, orientated parallel with the regional north-easterly foliation. Vergence towards the south-west is indicated by closures defining the fold nose. This geometry could suggest either a) sinistral strike-slip displacement along the tectonic discontinuity noted above, or b) the discontinuity represents an early zone of south-west directed thrusting, subsequently rotated to the vertical.

Figure 57 Leucocratic gneiss at OBS JC18. The pencil rests on a late-stage pegmatite sheet View is towards the south-west.

4.2.2 Pre-Quaternary (?Cenozoic) deposits

The DTM shows that in the south-east of the project area, the basement rocks are mantled by an extensive pre-Quaternary cover sequence. These deposits, here termed the Koluedor Gravel and Agbakope Sand form sheet-like outcrops, dissected by modern drainage and with upper surfaces sloping very gently to the south-east (i.e. seawards). Both units share similar features on the DTM and total count radiometric imagery, but they differ from each other in lithology and possibly in age.

The *Koluedor Gravel*, named after the eponymous township, crops out to the south-west of the Volta River. It is well exposed in roadside cuttings (OBS JC3) to the east of Koluedor, where it consists of a red to yellow, generally unconsolidated, poorly sorted, structureless, pebbly sand overlain by iron-cemented deflation gravel (Figure 58). Red-brown sandy gravel was noted farther west (OBS JC1), with rounded to subangular pebbles of vein quartz derived from the basement. Topographic considerations suggest that the Koluedor Gravel is between 10-15 m thick and lies at a maximum elevation of about 45 m. The fact that it is overlain by iron-cemented deflation gravels, of lateritic affinity, suggests that it is pre-Late Miocene in age (Section 4.1.2.9). A swarm of parallel photolineaments close to the south-eastern, seaward margin (Figure 55) is an important structural feature of the Koluedor Gravel outcrop. These photolineaments are represented on the ground by a series of low, densely vegetated ridges and are interpreted as neotectonic faults. Their east-north-east orientation is parallel with the seaward margin of the Koluedor Sand outcrop, and with major Atlantic oceanic transform faults, such as the Romanche Fracture Zone. The photolineaments are also in line with the surface extrapolation of the major syn-Cretaceous break-up fault, hidden beneath Volta delta alluvium but shown on the seismic cross section of Akpati (1975; fig. 7).

Figure 58 Koluedor Gravel overlain by lateritic deflation gravel at OBS JC3.

The *Agbakope Sand* crops out extensively to the north-east of the Volta River and is named after Agbakope township. Where seen it is a red to cream, medium-grained, extremely well sorted, non-pebbly sand that is locally dug for brick-making (Figure 59). In a quarry section (OBS JC22) it is seen to sharply overlie Dahomeyan mesocratic gneiss. The deposit is estimated to be between 20-25 m thick, and attains a maximum elevation of about 67 m.

The correlation of this unit is uncertain; on SRTM imagery it appears to be co-extensive with the topographical expression of units mapped farther east in Togo as ‘e1’ through to ‘e4’ (Palaeocene to Eocene); however, the continuity is to some extent obscured by drainage courses near to the national border. On the other hand, this unit does not appear to be overlain by laterite and thus may be of post-Miocene age. Should the latter case be confirmed, deposition possibly occurred during a regression of the sea in Pliocene through to Pleistocene times (Akpati, 1975). DTM imagery indicates that like the Koluedor Gravel, the Agbakope sand is traversed by ENE-trending photolineaments, indicative of very young tectonic activity in this region.

Figure 59 Excavation for brick-making in Agbakope Sand (OP/JC7).

4.2.3 Duricrust deposits

A duricrust composed of red-brown laterite is ubiquitous as a patchy veneer to the basement and pre-Quaternary rocks, but was not mappable. A long and complex history of duricrust formation is typical of most African regions, as discussed in Section 4.1.2.9.

4.2.4 Quaternary Deposits

Quaternary deposits are most widely represented by *Alluvium*, representing the floodplain deposits of the Volta River, its tributaries and other minor drainage channels. At the surface, alluvium mainly consists of cream to pale yellow silty clay overbank deposits, which generally show as green or magenta tones on Landsat 741 imagery (Figure 60). Sand bars of the braided

channel systems are represented by anastomosing, lozenge-shaped areas coloured pink to magenta on the imagery.

Volta Delta Deposits were not visited in the field, but are readily identified on Landsat imagery, which shows a complex system of sand bars anastomosed by fluvial and estuarine channels (Figure 60). *Tidal Flat Deposits and Salt Pans* are dominated by salt-impregnated marginal marine muds and silts. They show on Landsat imagery as dark magenta areas (the tidal flats) anastomosed by pale pink areas representing tidal 'creeks' (Figure 60). The Tidal Flat Deposits and adjacent lagoon margins (turquoise areas at lower left of Figure 60) have been extensively modified by the construction of salt pans. *Shoreface and Beach Deposits*, possibly representing a barrier beach complex, form a discontinuous, narrow coastal strip (Figure 60) that includes the ground on which the township of Keta has been developed. A small area tentatively identified as *Raised Tidal Flat Deposits*, lying at elevations of 4-7 m, has been recognised just to the north of the area shown as Tidal Flat deposits in Figure 60. *Raised Beach Deposits* are recognised from the Landsat imagery in the eastern part of the Keta coastal complex. Though now located about 2.8 km inland, this outcrop is characterised by shoreline-parallel ridges indicative of tidal and longshore current action. *River Terrace Deposits* are tentatively identified in ground intervening between the Volta floodplain and Koluedor Gravel outcrop. They occupy a flat-lying area, raised several metres above floodplain level and underlain by pale brown to blue-grey silty clay (OBS's/JC4 & 5).

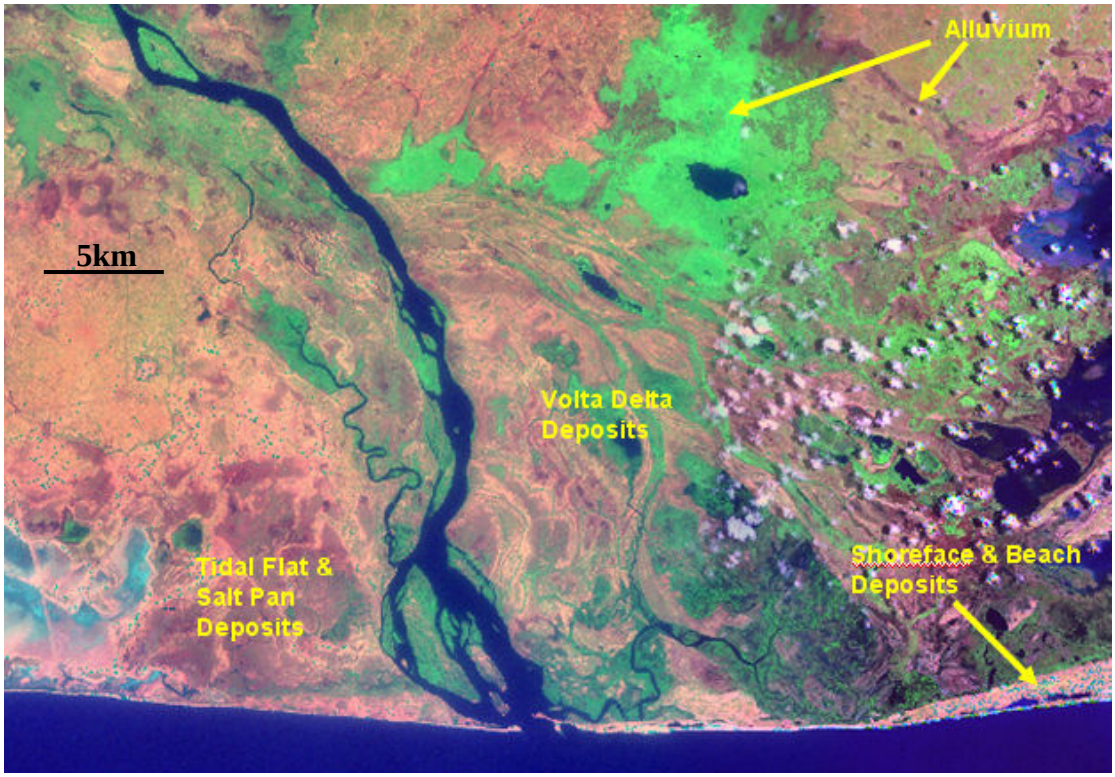

Figure 60 Landsat view of some Quaternary deposits in the Keta project area.

5 Mineral Prospectivity Modelling

This section deals with the economic minerals of the Volta and Keta basins. It is intended to supplement the original chapter on minerals in the phase 1 report (Jordan et al., 2006).

The sequence of economic minerals work in Phase 4 was as follows:

- October 2007 - Utilisation of the available datasets to form basic models in order to generate initial exploration targets.
- November 2007 - Prospecting and mapping in Ghana, following up initial exploration targets.
- December 2007 - Analysis of prospecting samples obtained from field work carried out in both seasons 2006 and 2007
- February 2008 - Post-field work prospectivity analysis using current datasets and latest geological interpretation.
- March 2008 - Results and methodology presentation at a work shop in Accra, Ghana.
- April 2008 - Report and map production, first draft
- June 2008 - Report and map production, second draft

The following text describes the latest prospectivity modelling that has been carried out over the project area in Ghana. Through the use of prospectivity modelling it is intended that specific areas will be highlighted as prospective for a number of selected mineral commodities.

5.1 INTRODUCING PROSPECTIVITY ANALYSIS

During the last few years, there has been an extremely rapid advance in processing power and storage capacity in personal computers. This has corresponded to a dramatic advance in the capability of software packages available to run on these powerful, relatively cheap computers. One area that has advanced dramatically has been the ability to handle spatial data, specifically on Geographic Information System (GIS) platforms.

Emerging from earlier CAD (Computer Aided Design) packages, Geographic Information Systems are essential tools for management and integration of the large amounts of spatial data used in mineral exploration. In its basic use, GIS can be utilized to display large amounts of different data sets or used to present properties of the data. An approach such as this gives a geoscientist the tools required to analyse the interaction between the different data types, which is indispensable in understanding geological processes.

Advanced uses of GIS involve mathematical calculations between the data layers in order to display relationships between the data, or amalgamating the datasets to produce supplementary datasets. Prospectivity analysis is an advanced use of GIS software.

5.2 WHAT IS PROSPECTIVITY ANALYSIS?

Prospectivity analysis is the analysis of multiple digital datasets (e.g. geophysics, geochemistry and geology) in order to identify favourable areas for deposits of mineral commodities, based upon predefined deposit characteristics. Using specific software, the datasets can be utilised, based upon either, the known parameters of a particular mineral deposit model or *trained* to look for similar types of known mineral deposits. The software enables large geographical areas and large amounts of data can be employed to define target areas that are prospective for mineralisation to occur. The end product is usually a *Prospectivity Map* that can assist the 'explorationist' in their search for economic deposits of minerals. The prospectivity analysis method can be applied at all the scales in the exploration cycle, from regional to target scale, however, it is optimally suited to regional and exploration licence scale.

5.2.1 Methodology / Procedures

Once the area for the study / exploration has been agreed, a review of the range of possibilities for mineralisation to exist can be considered. This is based upon known types of mineral deposits that exist elsewhere, either locally, regionally or globally. Some of the important definitions of terms used throughout this method follow.

A ***Mineral Deposit*** is a mass of naturally occurring minerals of sufficient size and concentration to have economic value, at a given point in time.

A ***Mineral Deposit Model*** (MDM) is a synthesis of large amounts of data, systematically arranged, that defines common characteristics for a particular class of mineral occurrence / deposit. Both descriptive and genetic aspects of the deposit form the basis for the MDM. It can be used as a classification method for deposit types, however, its function extends into providing exploration criteria for locating other deposits of comparable type.

Exploration Data are all the datasets that are available to the 'explorationist'.

Exploration Model is the synthesis of the available exploration data with the current understanding of the MDM for a particular deposit style, within the defined limits of the study area.

Prospectivity Map resultant output that displays the relative prospectivity within the study area based on the type of mineral deposit sought, the available data and the data integration technique chosen (see following section).

The relationship between these terms is represented is represented in Figure 61.

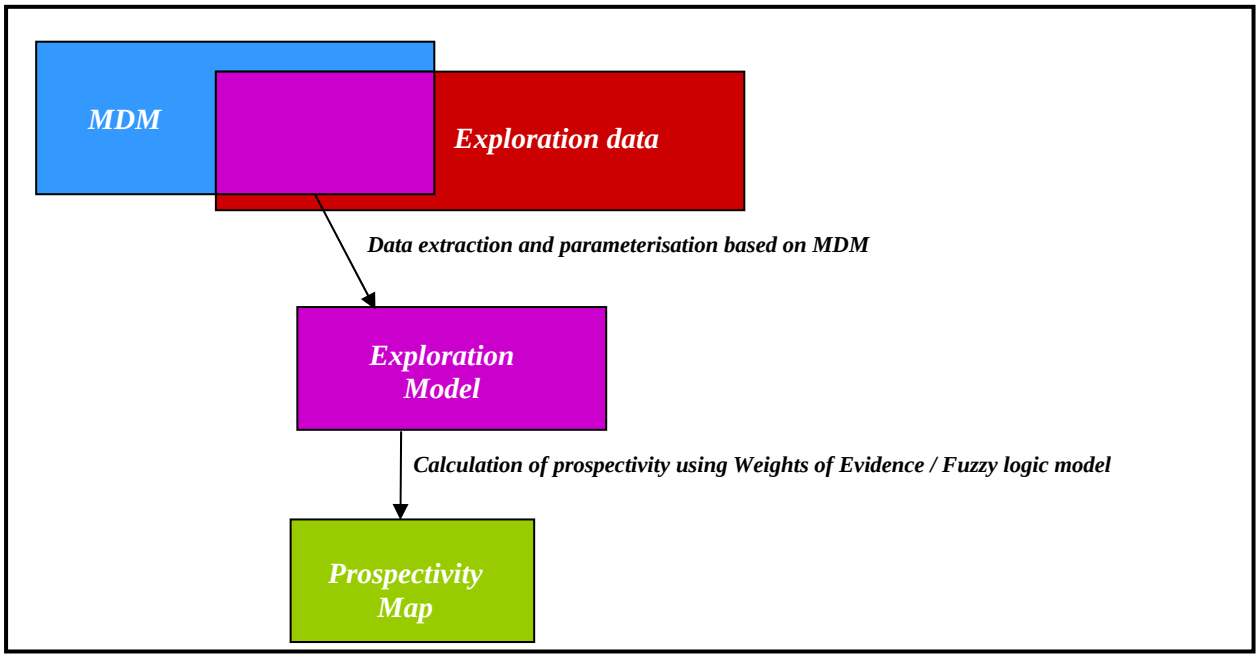

Figure 61 Generalised methodology for Prospectivity Analysis.

5.2.1.1 STAGES

Although Figure 61 graphically demonstrates the generalized process, an explanation of the stages involved is needed.

Selection of target mineralisation

The specific mineral to be explored for is determined through an understanding of the geology of the study area, evidence for occurrence in the study area or evidence for occurrence in a similar area elsewhere in a similar tectonic, sedimentary, igneous or metamorphic terrane or environment.

Review of Mineral Deposit Model(s) to determine key parameter indicators

Using a variety of sources, including many of the main Geological Surveys, geological texts and journals, the specific Mineral Deposit Model can be chosen. From this the key parameter indicators (i.e. specific identifiable / measurable factors), including the physical properties, can be selected.

Assessment of available exploration data to determine its capability to provide key indicators

Not every mineral deposit model can be modelled using the available data. Deposit scale, deposit form, geochemical properties, geophysical properties, etc. may not be measurable using the available datasets. The key exploration data is identified and selected for the modelling

Data processing, interpretation and analysis to extract key indicators

The selected exploration data may need additional processing to make it suitable for modelling. Datasets may require reduction or clipping to the study area dimensions, re-gridded and re-interpreted before converting them into software compatible formats. Common processing includes the *buffering* of line-work and point data to enable it to have a wider yet progressively decreasing influence; or the *gridding* of point data to form a contoured map of similar values.

Assignment of weights of influence to key indicators (expert parameterisation)

Each of the datasets is given a value of weighting. It is these values that are used in the calculation to determine the prospectivity. Weightings indicate relative importance between the different datasets as well as between the buffers/ gridded contours on each specific dataset. The relative values are determined from the mineral deposit model, specific geological knowledge on a deposit or on the reliability of a specific dataset.

Calculation of a prospectivity

There are two modelling methods which are used to integrate the data:

- Data-driven modelling, which are probability-based techniques using the spatial distribution of *known* mineral occurrences. This modelling aims to *train* the datasets to a specific type of exploration model based on the known occurrences. There are two sub groups, Weights of Evidence and Logistic Regression.
- Knowledge driven modelling, which explore the relationship between spatial exploration data sets and the mineral deposit model (MDM). It is used when none or limited number known mineral occurrences are known. This modelling is *subjective* in that the 'explorationist' determines the relative significance of the exploration datasets, then assigns a *significance* weighting based on the exploration model (interpreted MDM). There are two sub groups, Fuzzy Logic and Neural Network. The method applied to this study area was Fuzzy Logic.

5.2.1.2 FUZZY LOGIC

As described above, Fuzzy Logic is a subjective form of modelling with specific weightings given to the various datasets by the exploration geologist. The weightings are between 0-1 and are defined as the *Fuzzy Membership* of the dataset. The dataset are then combined using Fuzzy Logic operators to produce a prospectivity map. A summary of each operator is:

- *Fuzzy AND* is used when two pieces of evidence must be present together for a hypothesis to be true. The evidence with the smallest fuzzy membership controls the output.
- *Fuzzy OR* is used to combine two pieces of evidence where any existence of positive evidence is favourable to the hypothesis. The evidence with the largest fuzzy membership controls the output.
- *Fuzzy PRODUCT* multiplies all the evidence layers. However it produces a decreasive result as the values are less than 1.
- *Fuzzy SUM* causes the all the evidence to reinforce each other piece of evidence, hence the result is increasive.
- *Fuzzy GAMMA* is used to compromise between the decreasive *PRODUCT* and the increasive *SUM*. All evidence is used in the calculation but the reinforcing influence is controlled by the *GAMMA* figure given.

For a complete review of this technique refer to Bonham-Carter (1994).

5.2.2 Software used

Arc spatial Data Modeller or ArcSDM is the software used this process. It runs in Arcview or ArcGIS through the Spatial Analysis extension. This software was developed by the United States and Canadian Federal Geological Surveys in association with a number of mining companies. ArcSDM is a collection of geo-processing tools for adding categorical maps with interval, ordinal, or ratio scale maps to produce a predictive map of where something of interest is likely to occur.

ArcSDM provides 6 methods of prospectivity analysis:

- Weights of evidence (Normal)
- Weights of evidence (Expert)
- Logistic regression
- Neural Network (Supervised)
- Neural Network (Unsupervised)
- Fuzzy Logic

5.3 PROSPECTIVITY ANALYSIS OVER THE PROJECT AREAS

Gold, phosphates, and uranium were chosen to be modelled using the Prospectivity Analysis software. These commodities were selected due to their economic importance in West Africa. This is not intended to be an exhaustive list of commodities likely to occur in the project area, rather a subset of commodities that lend themselves readily to Prospectivity Analysis in this area, utilising the data currently available. In addition diamonds will be discussed in terms of prospectivity however they were not modelled.

5.4 THE DATA AVAILABLE

Two major types of data were used in the production of the prospectivity maps; geological mapping line-work and geophysics. The data was supplied in ArcGIS format and no further interpretation occurred in the prospectivity analysis other than isolating subsets of the datasets that were deemed suitable for the mineral deposit models.

5.4.1 Geological mapping linework

During phase 1 and 4 of the project, involving two extended field visits by BGS staff, the stratigraphy was reinterpreted and geological maps drawn. Fault line work and formation boundaries were subsequently used in the prospectivity modelling.

5.4.2 Geophysical interpretation

The airborne surveys carried out over the study area included magnetics, radiometrics and electromagnetics.

5.4.2.1 MAGNETICS

High resolution Magnetics was flown and the processed data interpreted, defining:

Interpreted dykes

Geological boundary-confident interpretation

Geological boundary-inferred interpretation

Geological boundary-transitional

Major fault- confident interpretation

Major fault- inferred interpretation

Minor ductile shear- inferred interpretation

Minor fault- inferred interpretation

Minor fault- confident interpretation

Thrust fault- inferred interpretation

5.4.2.2 RADIOMETRICS

Total count, uranium, thorium and potassium data was measured. The data was compiled into a raster image over the entire area. The calculated uranium and the total count were subsequently used in the prospectivity analysis.

5.4.2.3 ELECTROMAGNETICS

A very coarse regional grid was flown and at the time of the prospectivity analysis no EM was used.

5.4.2.4 MINERAL OCCURRENCES

As part of the phase one, and appearing in the subsequent report (Jordan et al., 2006), a list of the known mineral occurrences was compiled. For the purposes of the prospectivity analysis this data was only used for verification purposes and not incorporated into the analysis calculations. As the mineral occurrences were not very numerous or easily substantiated, they would not provide a reliable dataset.

5.5 GOLD

Gold is an established, well traded, store of value or wealth. Often, it is seen as a safe back up in times of crisis, and in this current global economic environment, its price is likely to reflect this, making finding it a priority for the mining industry. Gold is used in the jewellery and in the electronics industries.

Ghana is the 2nd largest gold producer in Africa, after South Africa. Between the years 2001 and 2005 the average annual output of 68t of metal was produced, this being 30% larger than the next major producer, Mali (Hetherington et al. 2008). With increasing uncertainty in global economies and energy shortages in the southern region of Africa, Ghana is well placed to supply the projected demand for gold.

5.6 OCCURRENCE OF GOLD IN GHANA

Gold is the major commodity mined and explored for in Ghana. Currently, no mining or exploration licences exist over the Neoproterozoic Volta and Keta basins for gold; however, the new airborne geophysics clearly displays the continuation of the important basement structures associated with the known deposit beneath these extensive cover sediments.

There are 4 important types of gold deposits in Ghana (see *Gold Deposits of Ghana 2002*).

5.6.1 Birimian hosted deposits

Also recognised as Ashanti-type, these deposits consist of multiple stages of quartz vein development with associated disseminated sulphides, occupying zones along NE-NNE trending structural corridors (known as belts) in the Birimian Mesoproterozoic basement. The host rocks are interbedded argillites, greywackes and volcaniclastic units. The veins extend for large distances and may be discreet narrow structures or form as complex stockworks. The quartz tends to be dark grey with visible gold and arsenopyrite / pyrite. The gangue commonly includes chlorite, carbonate and carbonaceous matter. It is this carbonaceous matter existing as graphite that gives the veins a grey hue. Associated with these auriferous veins are disseminated sulphides that can contain significant grades of gold locked up within the sulphides. Examples of this type of deposit include the active Obuasi mine and Bogoso-Prestea mining district (see Figure 62 to Figure 64). Although both these example are situated in the southern most Ashanti belt there are a number of further examples that appear to be similarly constrained by NE-NNE trending corridors, further to the north.

Genesis of these deposits is thought to relate to a hydrothermal event in the Eburnian orogeny, circa 2063+/-9a Ma (Pigois et al., 2003).

Figure 62 Bogoso Mine. This is now closed.

Figure 63 Bogoso Mine. Mineralisation in the base of the pit.

Figure 64 Prestea Mine. Currently active and producing gold concentrate.

5.6.2 Tarkwaian hosted deposits

Within the Tarkwaian group of southern Ghana gold occurs in paleoplacers and to a lesser degree within veins. It was these paleoplacers that have originally attracted the most interest in exploration and have produced in excess of 10 million oz of gold. The gold occurs associated with the thin bedded, well rounded conglomerates and is believed to be either sourced from gold lodes related to an early compressional phase of the Eburnian orogeny or an intrusion, circa 2200-2100Ma.

5.6.3 Alluvial Gold deposits

Early gold production from Ghana concentrated on streams and rivers draining the prospective basement areas. Currently there are many small operations focusing on quaternary and recent gravels, containing substantial amounts of gold eroded from the basement.

5.6.4 Intrusive associated deposits

This is a minor deposit style in Ghana, however, there are significant gold occurrences associated with intermediate to felsic intrusives. At Bibiani, for example, an auriferous vein is hosted in a granitoid body intruding the Birimian basement.

5.6.5 Occurrences in the Study Area

None of the various types of gold deposits found in Ghana have been found and mined in the Volta or Keta basins. However, a small number of occurrences have been documented,

including the Oboase hydrothermal vein and the Ejuanema placer (see Figure 65). It is reported (Junner 1935) that small amounts of gold were located in the conglomerates and volcanic rocks of the Buem series as well as in the Voltaian and Akwapimium conglomerates.

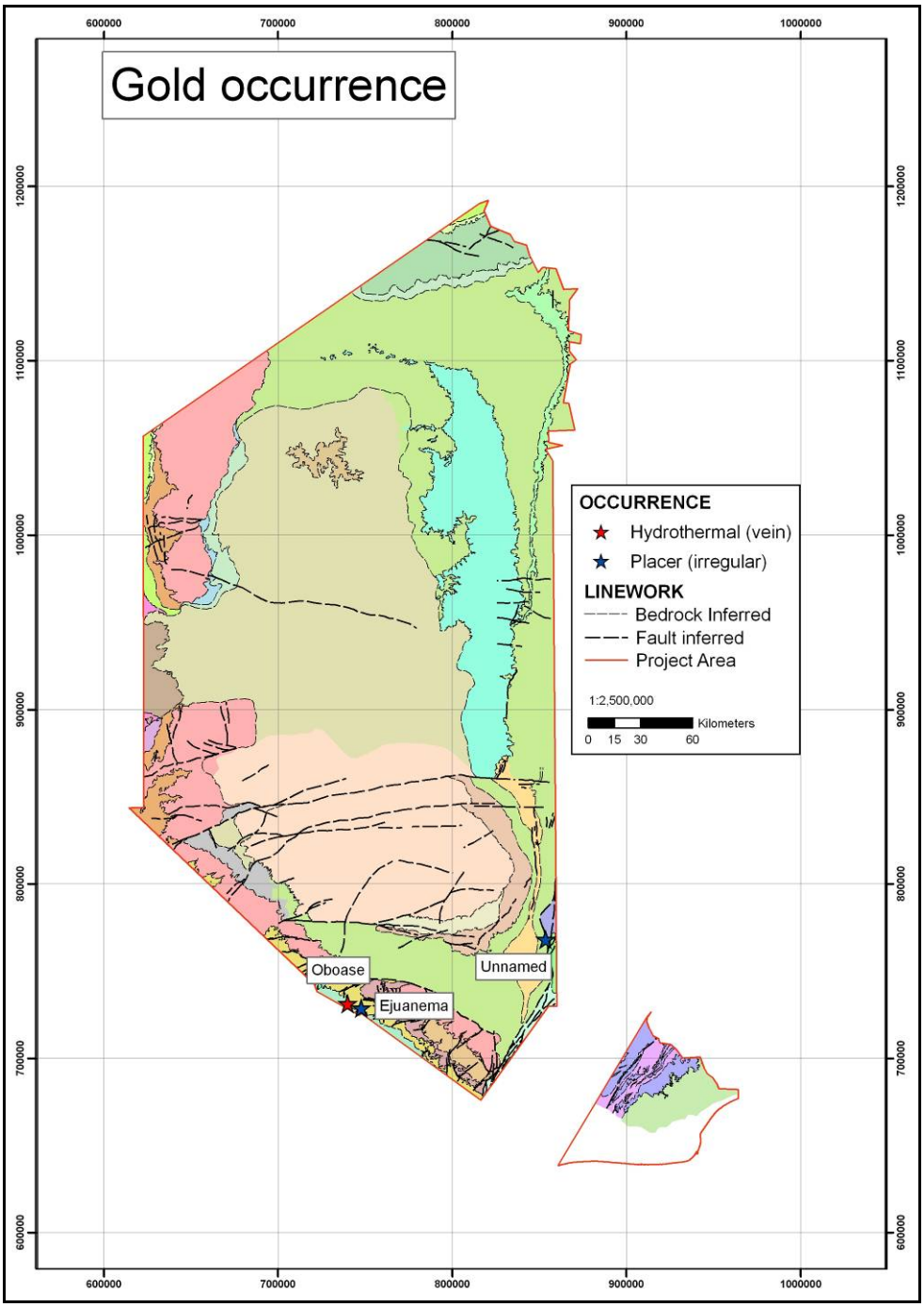

Figure 65 Gold occurrences in the Volta and Keta Basins, overlaid on a generalized geology map.

5.7 GOLD IN WEST AFRICA

Gold is being mined from a number of deposit styles across West Africa. The following text summaries some of these (see *The Geological atlas of Africa*, 2006, for a useful summary).

5.7.1 Benin

In Benin, to the east of Ghana, gold occurs in a variety of host rocks. The quartzites of the Togo group in the NW of the country have been found to be auriferous, encouraging a number

exploration companies to explore the potential. In addition to this, gold mineralisation has been identified in the Atacora and Alibori regions, in hard rock and alluvial deposits. Current gold production in Benin is small and associated with artisanal mining.

5.7.2 Burkina Faso

There are many gold occurrences of similar style to those hosted in the Ghanaian basement and within alluvial concentrations in quaternary or younger gravels. Areas of known gold occurrences include Poura, Dori-Yalago, Aribinda, Essakane, Yako-Kaya-Ouahigouya and Kwademen. There has been much mine development in recent years with two projects, Youga mine and the Taparko-Bouroum mine now reporting gold production. Further gold projects are in the pipeline, the most advanced being the Essakane deposit.

5.7.3 Côte d'Ivoire

There are many examples of gold occurrences in the Côte d'Ivoire, with many of the deposit types similar to those found in Ghana, including economical deposits within quartz veins, disseminated sulphide bodies and placers. There is currently one mine operational in the Côte d'Ivoire, Ity mine, situated in the west of the country. The gold production has seen a fall from 3.6 tonnes of gold in 2001 to 1.5 tonnes in 2005 (Benham et al. 2007).

5.7.4 Mali

Mali is a very important gold producer with a mining history dating back to 1433. In 2006 62 t (2Moz) was produced, extracted from six producing mining operations (Hetherington et al. 2008). The gold is associated with the Paleoproterozoic Greenstone belts.

In addition to those highlighted above Guinea, Niger, Senegal, Sierra Leone and Togo all have deposits of gold commonly associated with the greenstone belts.

As noted above, gold deposits occur throughout West Africa, however as in Ghana none have been found in the Neoproterozoic to Palaeozoic basin sediments that overlie the Mesoproterozoic and Paleoproterozoic basement rocks.

5.8 DEPOSIT MODELS THAT APPLY TO THIS MINERALISATION

There are a number of major types of gold deposit models that are seen in West Africa. Orogenic and placer types are discussed in the following section.

5.8.1 Orogenic gold deposits

Orogenic gold deposits are typified by quartz-carbonate-dominant vein systems associated with deformed metamorphic terranes of all ages. They are also known as greenstone-hosted deposits or mesothermal gold deposits. Mineralisation displays strong structural controls at a variety of scales. In a global context, these deposits are the second most important source of gold, after palaeoplacers, such as the Witwatersrand Palaeoplacers in South Africa. Table 15 lists some of the main characteristics of these deposits.

Orogenic gold deposits - typical characteristics

- Occur within a collisional tectonic regime.
- Can occur proximal to major accretionary boundary structures.
- Associated with ‘first-order’ transcrustal structures and related high angle ‘second-order faults’.
- Commonly hosted in rocks of greenschist metamorphic grade.
- Mineralisation is post-peak metamorphism (i.e. late syncollisional).
- May have an association with late syncollisional, intermediate to felsic magmatism.
- Tabular veins in more competent lithologies with veinlets and stringers forming stockworks in less competent units.
- Ore mineralogy is typically gold, pyrite, arsenopyrite, native gold, Cu, Pb, Zn and Sb sulphides.
- Gangue mineralogy is dominated by quartz ± carbonate, feldspar, mica
- Wall-rock alteration is common.
- Geochemical anomalies in rock, soil, stream-sediments, with elevated values for Au, Ag, As, Sb, K, Li, Bi, W, Te, Cu, Pb, Zn, Cd.
- Mineralisation is associated with metamorphic fluids.
- The fluids are C-O-H ± N, near-neutral to low pH, and low salinity.

Table 15 Main characteristics of Orogenic gold deposits.

5.8.2 Paleoplacers / Modern placer deposits

Paleoplacers and their modern equivalents, Holocene placers deposits, are the most economically important gold deposits, accounting for the majority of the world reserves. Table 16 lists some of the main characteristics of these deposits.

Paleoplacers / Modern Placer deposits – typical characteristics

- Concentrations occur along erosional surfaces at the base of channel sequences.
- Well sorted, fine to coarse-grained sands and well rounded, imbricated and clast-supported gravels are the most common hosts.
- Paleorelief and source of gold are important controlling factors with gold collecting in natural hollows and trenches.
- Ore mineralogy includes detrital gold, platinum group elements and other heavy minerals.
- A highly variable deposit and laterally discontinuous form but commonly lens shaped less than 2m in thickness.
- Commonly tertiary and Pleistocene. Older deposits are rare; however, one notable exception is the Proterozoic Witwatersrand deposit in South Africa.
- Elevated values for Au, Ag, Hg, As, Cu, Fe, Mn, Ti, U or Cr in stream sediments.
- The paleochannels may have distinct geophysical properties due to concentrations of heavy minerals in the channels. Radiometrics can be used to locate surface deposits if there is a uranium association.

Table 16 Main characteristics of placer deposits.

5.9 PROSPECTIVITY MODELLING OF GOLD

In the study area both types of deposit described above, or a variation, could exist in the study area.

5.9.1 Orogenic Gold

This section will discuss the modelling of an Orogenic Gold model over the study area, specifically the Volta region. However, two caveats should be noted before the modelling plan is discussed.

Age — This deposit style has not been found elsewhere in West Africa within similar stratigraphy. Without doubt, an important economic deposit in Ghana, so to locate them in the study area would be a very important discovery. However, they do appear to be restricted to Archean and Paleoproterozoic sequences and it is very unlikely that they exist in the Neoproterozoic to Palaeozoic basin sediments. There is the possibility that fluids could be activated along later faulting and be deposited in younger sequences during the Pan African event. The model will work on this premise.

Within the study area there is a slice of Birimian stratigraphy. No model is needed to establish that this is the most prospective area for locating gold related to this deposit style.

Cover thickness — The fact that within the Volta basin the sediments can be up to 5 km thick has not been factored into the final map; however, one improvement of the model would be to use depth to basement as a variable in the final determination of prospectivity.

5.9.1.1 MODEL OUTLINE

In Orogenic Gold deposits structure plays an important role. In the Proterozoic basement a range of structural orientations are significant in the location of deposits. Taking evidence from a range of areas, including Obuasi mine, Bogoso mine and Bibiani belt, it would appear that N to NE structural corridors play a significant part in focusing mineralization. Additionally, cross cutting structures may help to localise the mineralization. To enable remobilisation into the cover sequences, a later orogenic event would have to generate hydrothermal fluids that remove the gold from the basement and transfer it via structures to the cover stratigraphy. The Pan African orogenic event may act as this event.

5.9.1.2 MODELLING PLAN:

This is the generalised outline of the modelling process applicable to the Orogenic Gold.

The two major steps in this model are:

A. Locate areas within the underlying basement where gold deposits may occur.

B. Locate areas in the overlying cover sequences where gold could be remobilized to.

Exploration data to be used:

- Magnetic basement lineaments.
- Mapped faults in the cover stratigraphy.

Exploration Model:

The shortage of known gold occurrences / deposits within the area that could be used as a training set limits our analysis to be *Knowledge driven modelling* using Fuzzy Logic. The following tasks are required.

1. Extract all the N to E trending basement structures (basement corridors).
2. Locate intersections of these selected structures with other basement structures.
3. Run spatial modelling software to produce a prospectivity map of favourable basement corridors.
4. Model the results of this map with the mapped faults in the cover to produce a prospectivity map of potential remobilised basement gold in the Voltaian area.

5.9.1.3 METHOD

The sequence leading to the output of the map can be generalised as follows:

1. *Target* - Orogenic Gold in the basement remobilised into cover sequences.
2. *MDM* - refer to Figure 61
3. *Exploration data used* - Magnetic basement lineaments; mapped faults in the cover stratigraphy. The following processing was applied to the data:
    - Extraction of all magnetic lineaments striking between north and east; Multi-ring buffering of selected faults depending the confidence of interpretation and the suitability of the fault to the deposit model type:

      10 km buffer width (1km spacing) for the major confident faults and shears

      7 km buffer width (1km spacing) for the inferred faults and shears

7 km buffer width (1km spacing) for the minor confident faults

4 km buffer width (1km spacing) for the inferred minor faults

- Combine all the magnetic lineaments (unbuffered) using Fuzzy logic within the study area. If Fuzzy gamma is used the output will display a raster map that has values for each cell. The value of the cell will be determined by the amount of intersections of magnetic lineaments. Each of the intersections can then be buffered to give it a progressive influence on the model:

  3 km buffer (single buffer) around each intersection

- All the mapped faults in the cover stratigraphy were buffered using a 5 km buffer (1 km spacing between the buffering rings).

4. At this stage in the sequence Fuzzy membership values were given to the buffered datasets:

   - *Magnetic lineaments: Confident faults/ shears* were given values between 0.99 for the closest and 0.10 for the furthest buffers. The software generates linear interpolation between the outer and inner buffers.
   - *Magnetic lineaments: Inferred faults /shears* were given values between 0.70 for the closest buffered ring and 0.10 for the furthest buffers. The software generates linear interpolation between the outer and inner buffers.
   - *Magnetic lineaments: Buffered intersections* were given a fuzzy membership of 0.05.
   - Mapped Faults: values between 0.50 for the closest buffered ring and 0.20 for the furthest. The software generates linear interpolation between the outer and inner buffers.

5. The selected magnetic lineaments were initially modelled together to give an initial output of favourable structures using the fuzzy OR operator. This was then modelled with the lineament intersections using the fuzzy GAMMA operator. The resultant map was combined with the buffered mapped faults using the Fuzzy GAMMA operator. The flow diagram in Figure 66 demonstrates the operation.

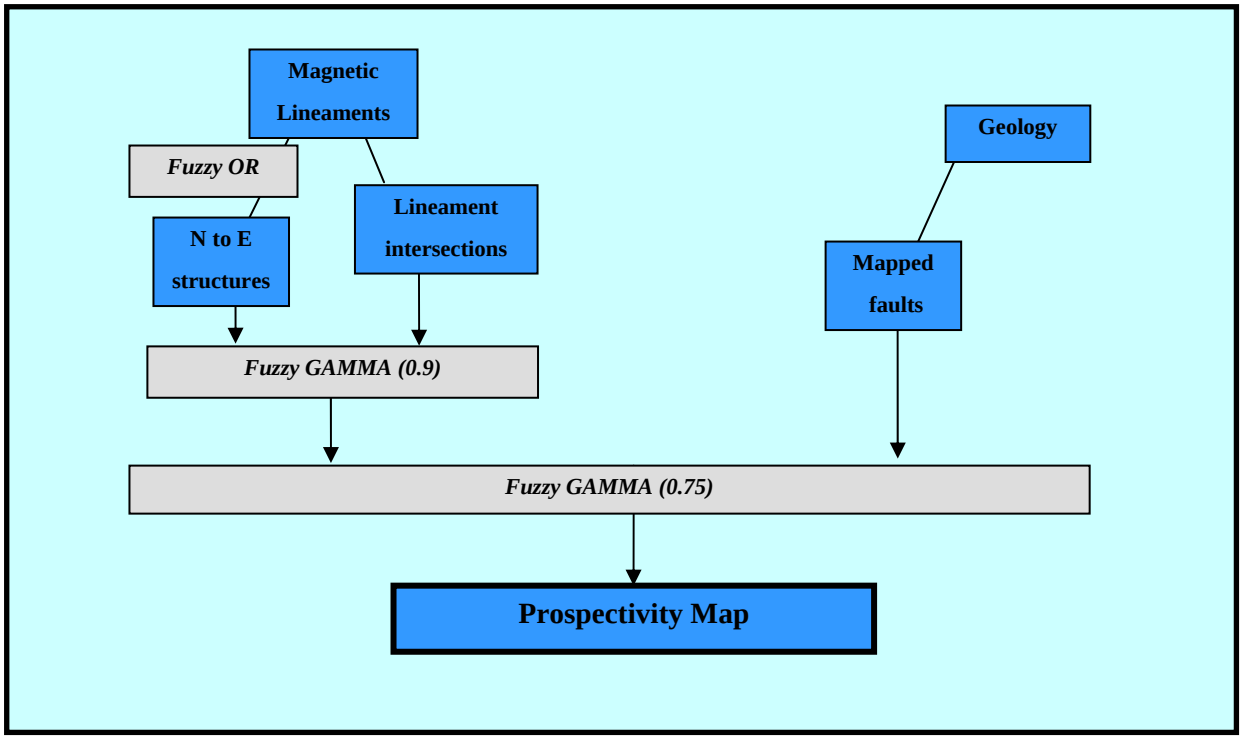

Figure 66 A flow diagram of the mathematical operations for the Orogenic Gold Model.

5.9.1.4 RESULTS

The resulting prospectivity map displays the range of prospectivity over the Volta area for a model of gold remobilisation from favourable basement zones into the overlaying sediments. Using the Fuzzy Logic Gamma operator to combine the intermediate maps, the modelling recognises the fact that all the evidence is important and has a function in the model, as well as acknowledging the nature of the data as being interpretive and not a measured value. See Figure 67 to Figure 71 which display the results for the model.

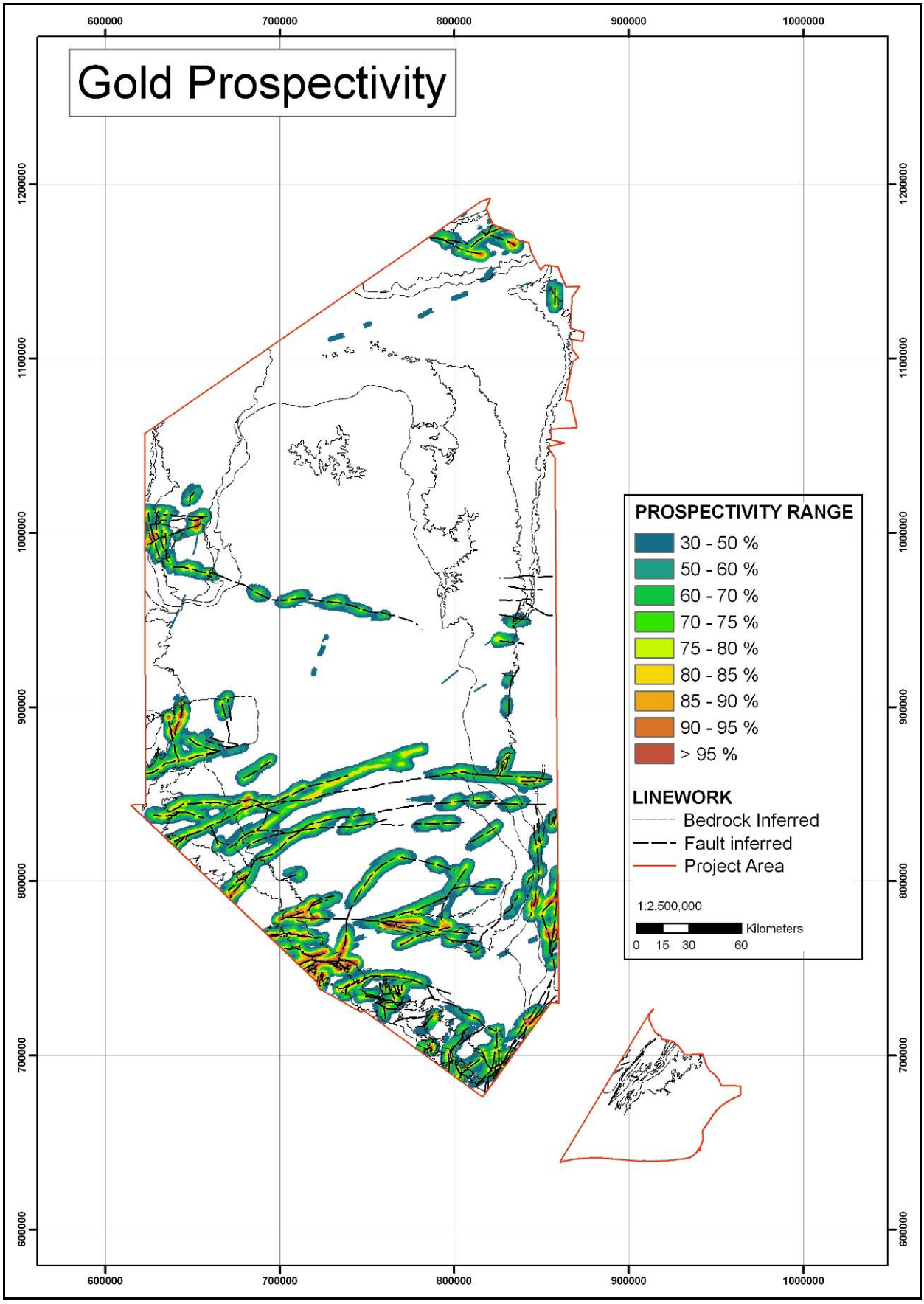

Figure 67 Gold prospectivity map of the Volta and Keta Basins.

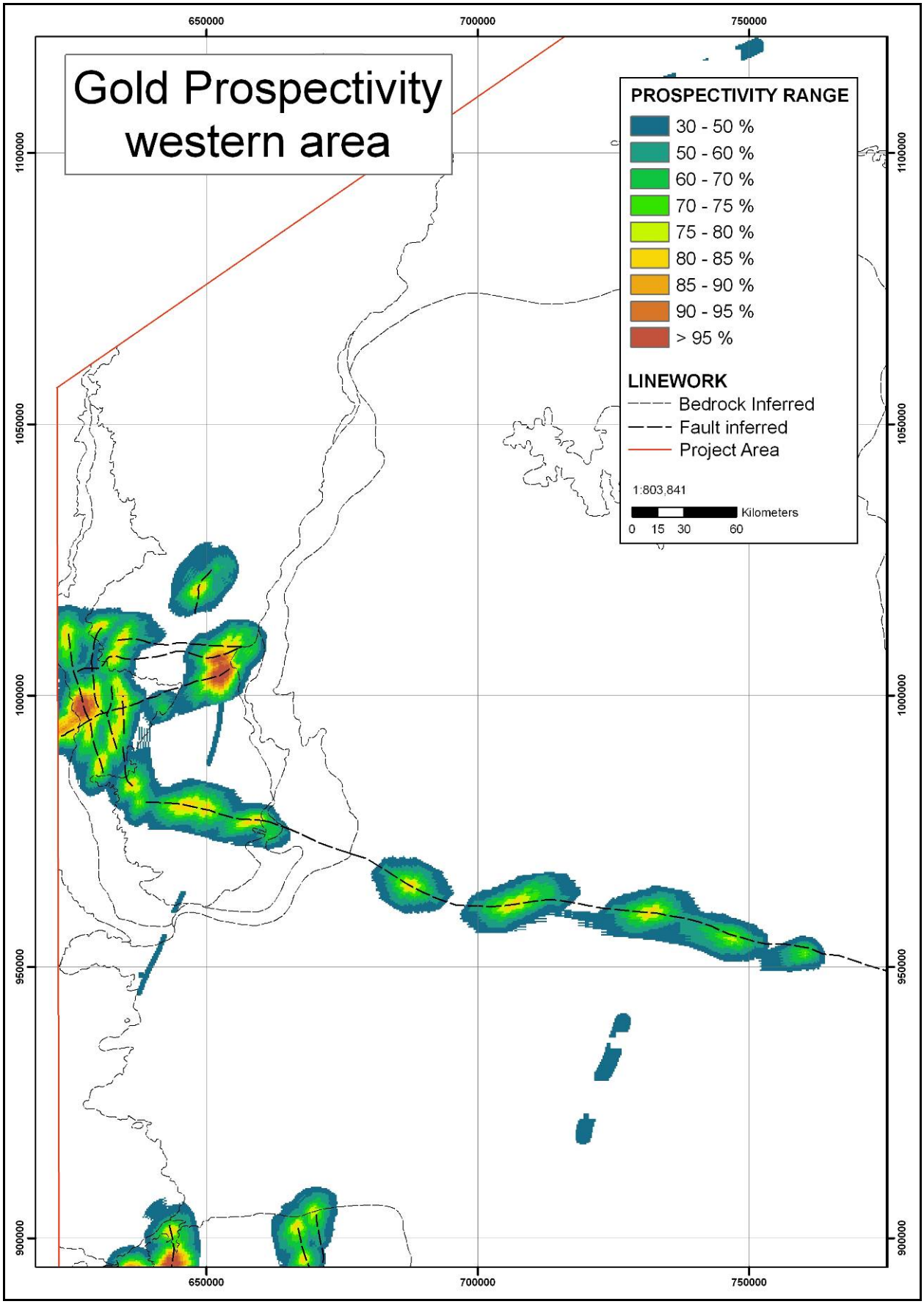

Figure 68 Gold prospectivity map of the west Volta Basin.

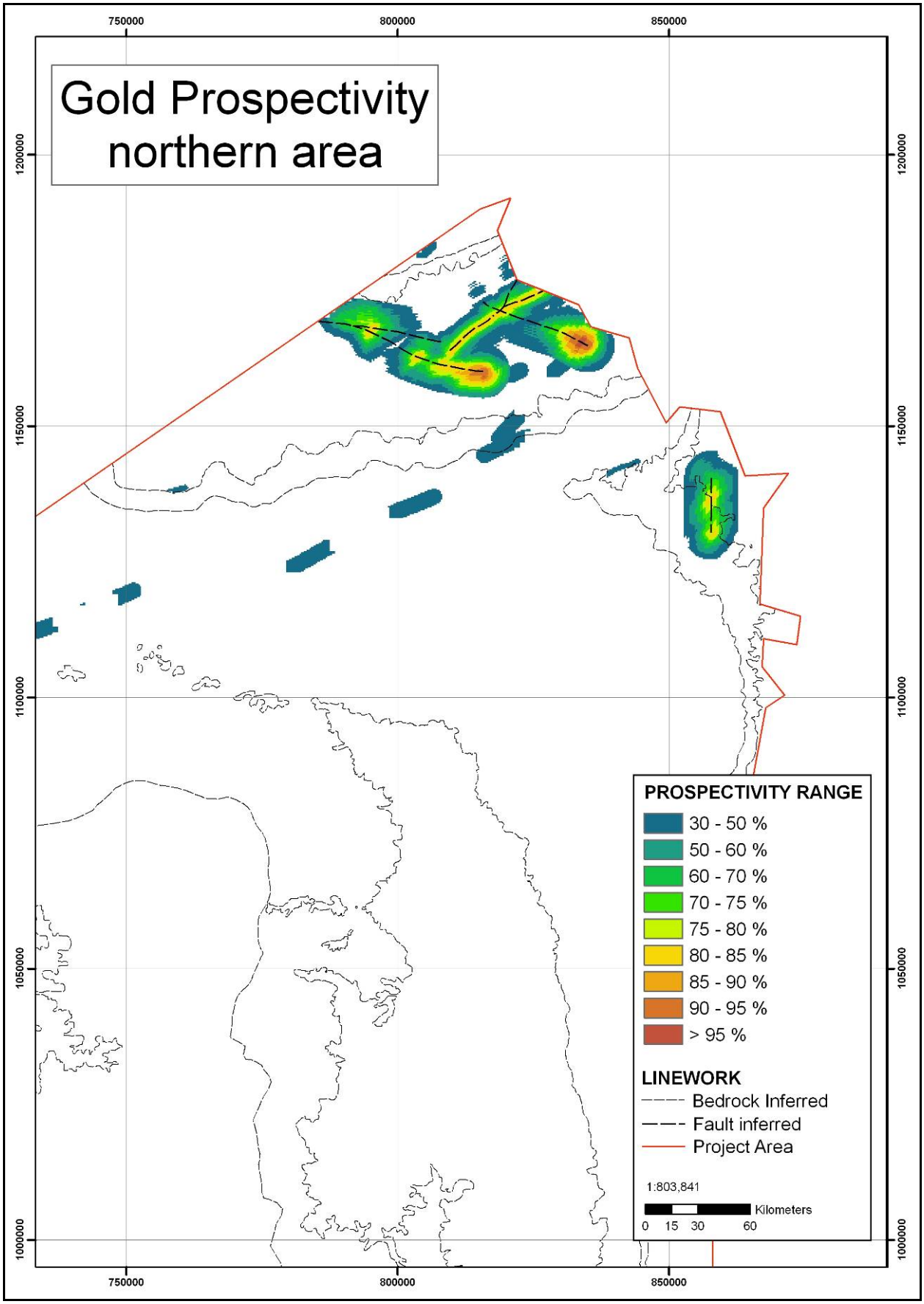

Figure 69 Gold prospectivity map of the north Volta Basin.

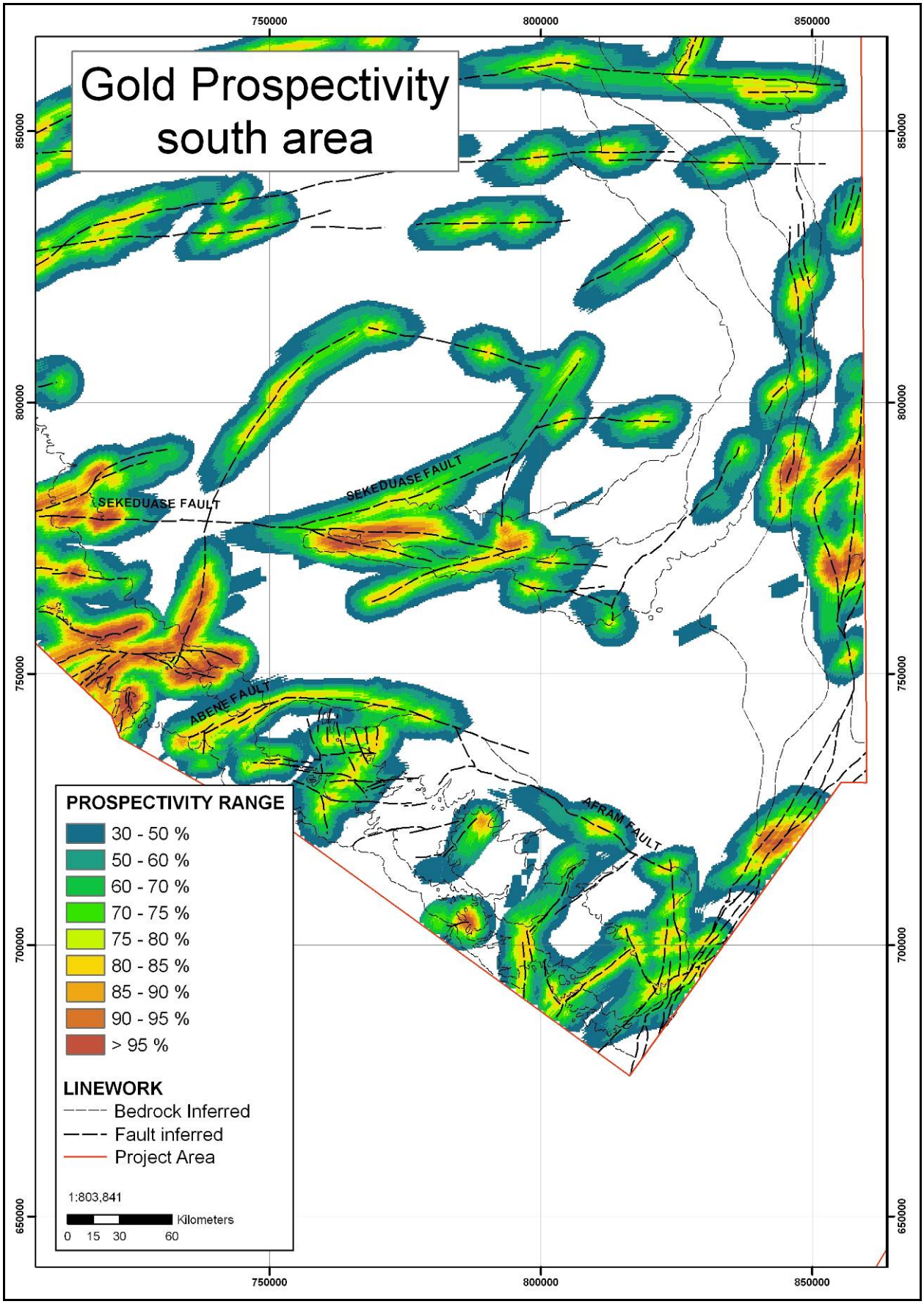

Figure 70 Gold prospectivity map of the south Volta Basin.

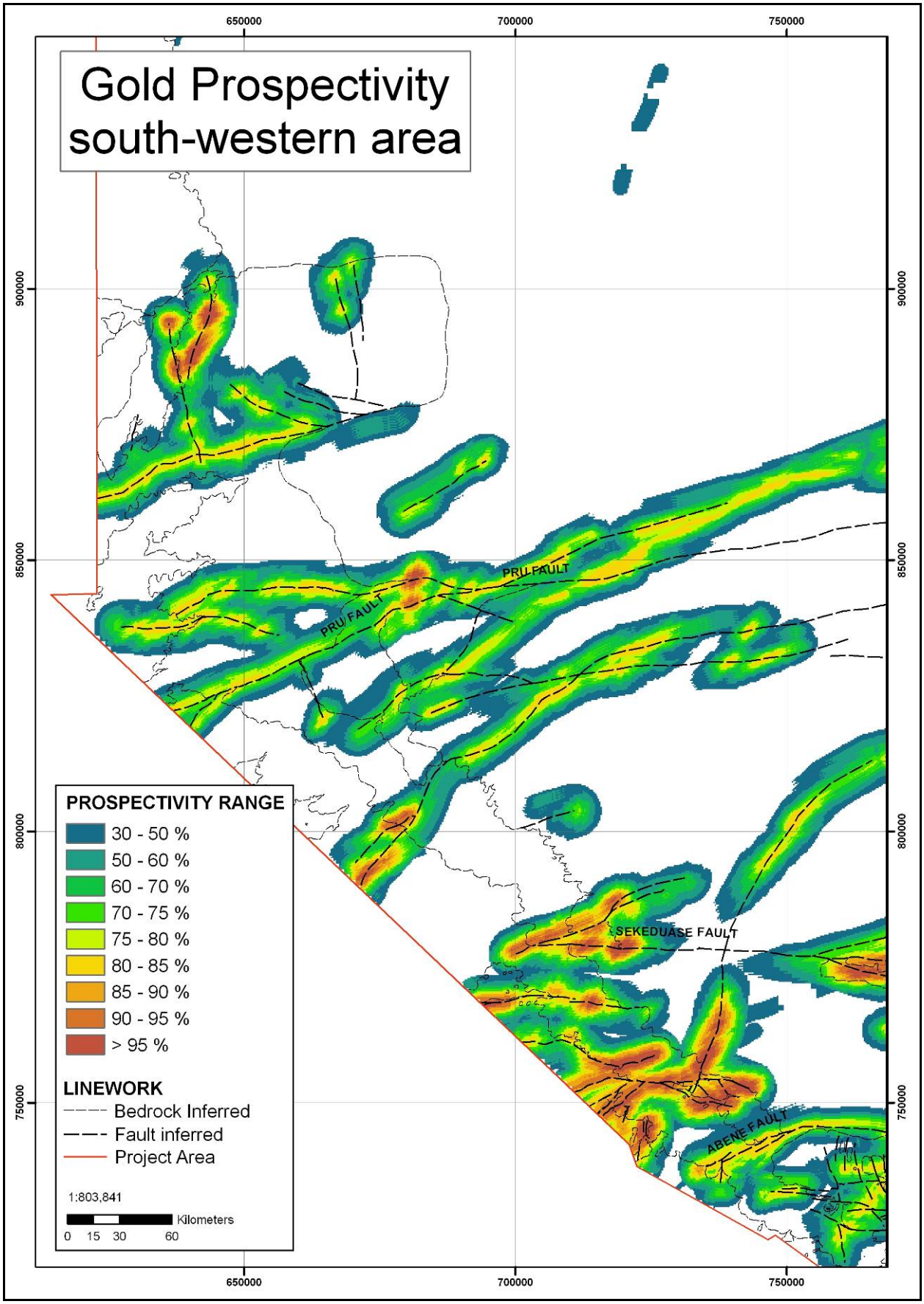

Figure 71 Gold prospectivity map of the southwest Volta Basin.

5.9.2 Placer deposits

With the currently available data, there is no exploration model that can be used to generate a prospectivity map for these types of deposits within the study area.

5.9.2.1 CHANNEL LOCATION AND DELINEATION

The scale of the deposits and the available data make modelling these difficult at this regional scale. Ground based geophysics (e.g. radar, magnetics or seismics) and local geochemical sampling would both be suitable for the location and delineation of these deposits. This data does not exist currently.

5.9.2.2 GEOLOGY

A mentioned above, minor gold has been located in the basal conglomerates of the Voltaian sediments. The new mapping will help in defining these favourable geological areas which may host deposits. At the base of the Bombouaka and Kwahu groups, mapped as age-equivalents groups that lie unconformably on the basement, gold bearing basal conglomerates may occur. The Tossiegou formation is close to the base of the Bombouaka while Yabraso Sandstone and Damongo Formation (where former is not present) would similarly form the base of the Kwahu group. In the south the Mpreaso Sandstone forms the base in of the Kwahu group. So it is over these formations that geochemistry and detailed mapping could be used to generate exploration targets.

This sequence can be identified in the mapped geology dataset, so in theory, a model can be applied. However, at this stage, it is considered that this model would not add any additional knowledge, other than identifying the location of the suitable stratigraphy.

5.9.2.3 SCOPE

The scope for substantial deposits of paleoplacer gold deposits has not been fully tested. Although outcrops of the basal conglomerates were not located, in the prospecting sampling a float sample of quartz pebble conglomerate was located in the south of the project area. The sample contained 13 ppb Au. Although this sample value is disappointing, it is the most significant gold value obtained from all the samples and should not be overlooked.

5.10 URANIUM

Uranium is primarily used as a fuel in nuclear power generation. With the current concern over energy supply and excessive CO_2 production there is likely to be an increased demand for uranium in the near future.

There is no uranium production in Ghana. However, within Western Africa, there are important uranium mines and deposits and moreover uranium exploration in this region is increasing. With increasing uncertainty in global energy supplies this commodity is likely become more important in the global commodity marketplace. In addition many uranium deposits previously considered uneconomic, e.g. pegmatites, may become economic as demand increases.

5.11 OCCURRENCE OF URANIUM IN GHANA

The only recorded uranium in Ghana is within pegmatites in the Cape Coast Granite on the southern coast. There are four localities at Ejaa, Akrobadzi, Haseode and Amoada.

5.11.1 International Uranium Resources Evaluations Project (IUREP) report

This report, on work carried out in 1982, reviewed the current knowledge concerning the possible existence of uranium in Ghana. The report summarised the potential for each of the major rock types to host uranium deposits. Key points (Kesse, 1985):

- Dahomeyan System - Major uranium target due to its occurrence in the Panafrican-Brazlian mobile belt.
- Togo series and Buem Formation - no potential.
- Voltaian System - Similar age to the Taoudeni Basin in Guinea that hosts uranium deposits.
- Eburnean Granites - Host to the known deposits and may host further similar types.
- Tarkwaian system - The conglomerates have the potential to host uranium similar to the paleoplacers deposits in South Africa.
- Coastal basins - low potential.
- Palaeozoic Accraian and Sekondian series - low potential.
- Cretaceous and Tertiary basins - low potential.
- Birimian System - low potential.

Importantly this IUREP highlights that the Voltaian Basin has the potential to host uranium deposits.

5.11.2 Occurrences in the Study Area

There are no occurrences noted within the study area.

5.12 URANIUM IN WEST AFRICA

5.12.1 Burkina Faso

Within Burkina Faso there is increased interest in uranium exploration, with a number of exploration licences held and others impending. Some of this interest is due to strong uranium anomalies from the N-S structure on the edge of the granitic body of Bossié in SW Burkina Faso.

5.12.2 Mali

There are a number of companies currently active, exploring for various uranium deposit types including paleochannel-hosted uranium and uranium bearing pegmatites. The Falea area, which covers 150 km² of the Falea-North Guinea-Senegal basin, is a Neoproterozoic sedimentary basin marked by significant radiometric anomalies. Here, drilling has identified copper and uranium mineralization, associated with stromatolites in sandstones and shales.

5.12.3 Niger

Niger is Africa's leading uranium producing nation. A number of companies have been mining uranium since 1971 and past production from the two operating mines exceeds 100,000 tonnes of uranium. In 2006, production from these two mines, one near Arlit and the other near to Akouta, exceeded 3,434 tonnes (Hetherington et al. 2008). Niger remains one of the world's largest uranium producers, contributing approximately 7.5% of annual world production. The host rocks are arenites, of Carboniferous to Cretaceous age, deposited in fluvial to deltaic environments. The source of the uranium is considered to be from the basement.

5.12.4 Togo

In the 1960's, a small uranium resource was outlined by drilling, near to the major regional centre of Lama-Kara in the north of Togo. The prospect is currently being revisited, undergoing modern exploration and assessment.

5.13 DEPOSIT MODELS THAT APPLY TO THIS MINERALISATION

There are a number of deposits styles that occur throughout West Africa, however, three deposit styles could be applied to this project area.

5.13.1 Sandstone hosted uranium

Accounting for approximately 18% of global uranium resources, this important type of uranium deposit occurs in a number of countries. The main producer is the USA, from the Western Cordillera region. In Africa, Niger has significant sandstone deposits and, significantly, to this study, within the Neoproterozoic Franceville Basin in Gabon, there are a number of uranium deposits of this style. Table 17 outlines some of the main characteristics of this deposit style.

Sandstone hosted uranium

Typical features of these deposits include:

- Occur in intracratonic basins filled with flat-laying continental fluvial sandstones.
- Occur adjacent to fault zones as these may provide conduits for reducing solutions.
- Commonly post-Silurian, however, older deposits do occur proximal to reducing agents.
- Uranium sourced from adjacent igneous rocks.
- Deposits occur due to chemical traps in the form of oxidation-reduction fronts, commonly associated with organic matter.
- Three types of deposit: Roll Front, Tabular deposits, tectonic/lithologic.
- Mineralogy includes Uraninite, coffinite, and pyrite in organic-rich horizons.

Table 17 Main characteristics of sandstone hosted uranium.

5.13.2 Paleoplacers / Modern Placers deposits

Uranium is commonly a by product of paleoplacers Au deposits such as the Witwatersrand in South Africa. The deposit properties have been listed in Table 17 above. These account for 13% of the global uranium production.

5.13.3 Unconformity related uranium

This type of deposit is the most important producer of uranium, accounting for approximately 33% of the global production. The most significant are within the Athabasca basin uranium district in Canada and within a number of mining districts in Australia. Table 18 outlines some of the main characteristics of this deposit style.

Unconformity related uranium

Typical features of these deposits include:

- Occur within intracratonic sedimentary basins.
- Occur below, above or straddling unconformities over Archean / Paleoproterozoic igneous and metamorphic rocks.
- Generally deposits occur in sandstones, Proterozoic in age.
- Metal rich oxidised fluids migrate along the unconformity until a suitable reducing environment is reached. Deposits occur at this REDOX (reducing – oxidizing) boundary.
- The deposit scale is up to few kilometres in dimension, as tabular, pencil shaped or irregular shaped forms.
- Deposits may occur in structures proximal to the unconformity.
- Commonly, the ore is made up of pitchblende and coffinite; however, complex deposits occur with other metallic minerals, including gold.
- Anomalous zones of U, Ni, Co, As, Pb and Cu are good indicators in geochemical surveys.
- Commonly alteration is present in the form of chloritization, hematization, kaolinization, illitization and silification.

Table 18 Main characteristics of unconformity related uranium.

5.14 PROSPECTIVITY MODELLING OF URANIUM

As discussed in the section above, concluded within the IUREP report, there is the potential for the Volta basin to host uranium deposits. The basins of the study area overlay the basement which appears to have uranium sources as indicated by the exploration successes in neighbouring countries. However, questions still exist as whether the sandstones within the basins are suitable and if the geology has suitable REDOX boundaries. Modelling the currently available data will provide some areas for ground follow up.

5.14.1 Sandstone-hosted Uranium

This section will discuss the modelling of Sandstone hosted uranium over the study area. However, two caveats should be noted before the modelling plan is discussed.

5.14.1.1 CAVEATS

A. *Suitability of the Geophysics;* Airborne radiometrics was used to determine areas of anomalous uranium. This method is suitable for the search for near surface deposits only, due to the limited penetration of the detectors.

B. *Geology;* both the Anyaboni Formation and the Obosum Group, in the south of the project area, are either continental or fluvial and could act as hosts to the mineralization. This is based on the current understanding of the geology. The model assumes that these are the most prospective sandstones in the study area.

5.14.1.2 MODEL OUTLINE

The model is based on a typical Sandstone-hosted uranium deposit profile with a possible source being the basement granites and suitable host sandstones being both the Anyaiboni Formation and the Obosum Group. Transport and focusing of the fluids is along the faults mapped in the cover sequence.

5.14.1.3 MODELLING PLAN

The two major steps in this model are:

A. Locate prospective stratigraphy in the project area. Both the Anyaboni Formation and the Obosum Group, in the south of the project area, are either continental or fluvial and could act as hosts to the mineralization. Granites in Burkina Faso could act as source rocks.

B. Locate areas in the overlying cover where there is raised radioactivity proximal to faults that could be acting as conduits for the fluids.

Exploration data to be used:

- Mapped geology over the Volta project area.
- Uranium radiometrics.
- Mapped structures in the overlaying basin sandstones.

Exploration Model:

The shortage of known gold occurrences / deposits within the area that could be used as a training set limits our analysis to be knowledge driven modelling.

1. Extract the favourable stratigraphy.
2. Model the favourable geology with buffered faults. This will give geological favourable areas.
3. Model these geological favourable areas with the uranium values of the radiometrics.
4. Create a prospectivity map of potential sandstone-hosted uranium in the Voltaian project area.

5.14.1.4 METHOD

The sequence leading to the output of the prospectivity map can be generalised as follows:

1. Target – Sandstone hosted uranium.
2. MDM – refer to Figure 61.

3. Exploration data to be used - mapped geology over the Volta project area; uranium radiometrics; mapped structures in the overlaying basin sandstones.
    - The mapped faults were buffered to 5 km (0.5km ring spacing).
    - The Anyaboni Formation and the Obosum Group were clipped from the other groups.
4. Fuzzy membership values were given to the datasets:
    - Favourable geology was given a value of 0.25.
    - Buffered faults were given values between 0.25 for the closest and 0.10 for the furthest buffers. The software generates linear interpolation between the outer and inner buffers.
    - The uranium was given values between 0.05 and 0.01 depending on the measures value. The software generates linear interpolation between the outer and inner buffers.
5. The mapped faults were initially modelled with the favourable geology to produce a map of favourable geological areas. This was achieved using the Fuzzy operator AND. The resultant map was then modelled with the radiometric uranium using the Fuzzy operator SUM. This produced a prospectivity map of potential Sandstone-hosted uranium in the Voltaian project area. Figure 72 displays the mathematical operation for the Sandstone-hosted uranium Model.

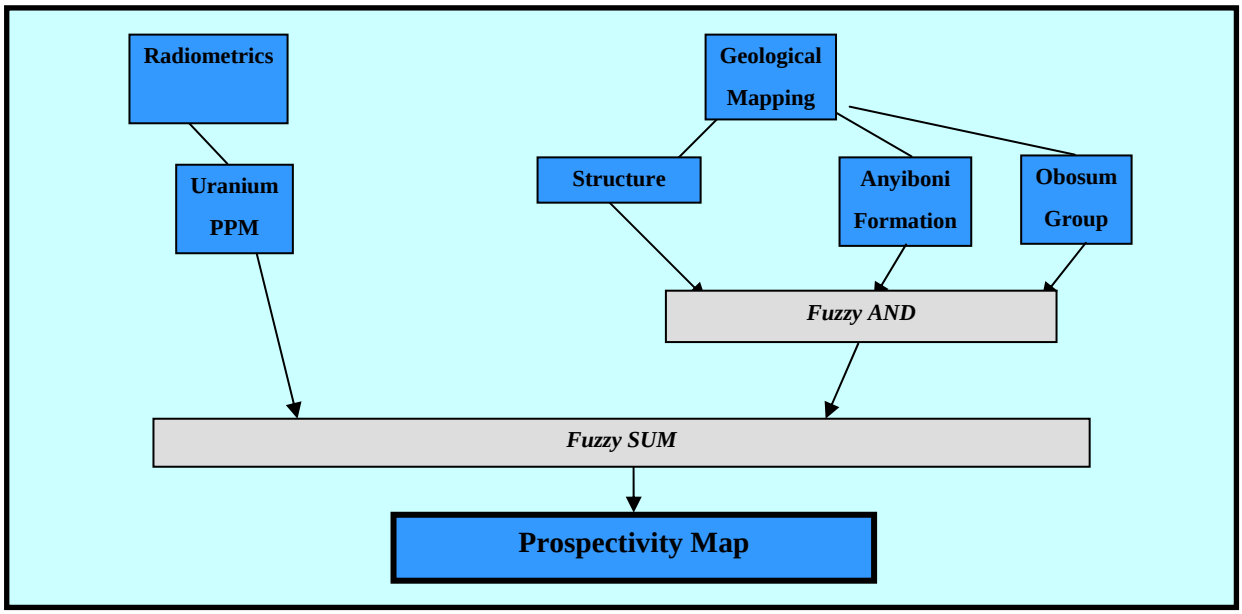

Figure 72 A flow diagram of the mathematical operations for the Sandstone-hosted Uranium Model.

5.14.1.5 RESULTS

The resulting prospectivity map displays the range of prospectivity over the Volta area for a model of uranium mineralization in favourable basin sediments. Using the Fuzzy Logic SUM operator to combine the intermediate maps, each piece of evidence reinforces the accompanying evidence causing an increasive result. Figure 73 to Figure 77 display the results for the model.

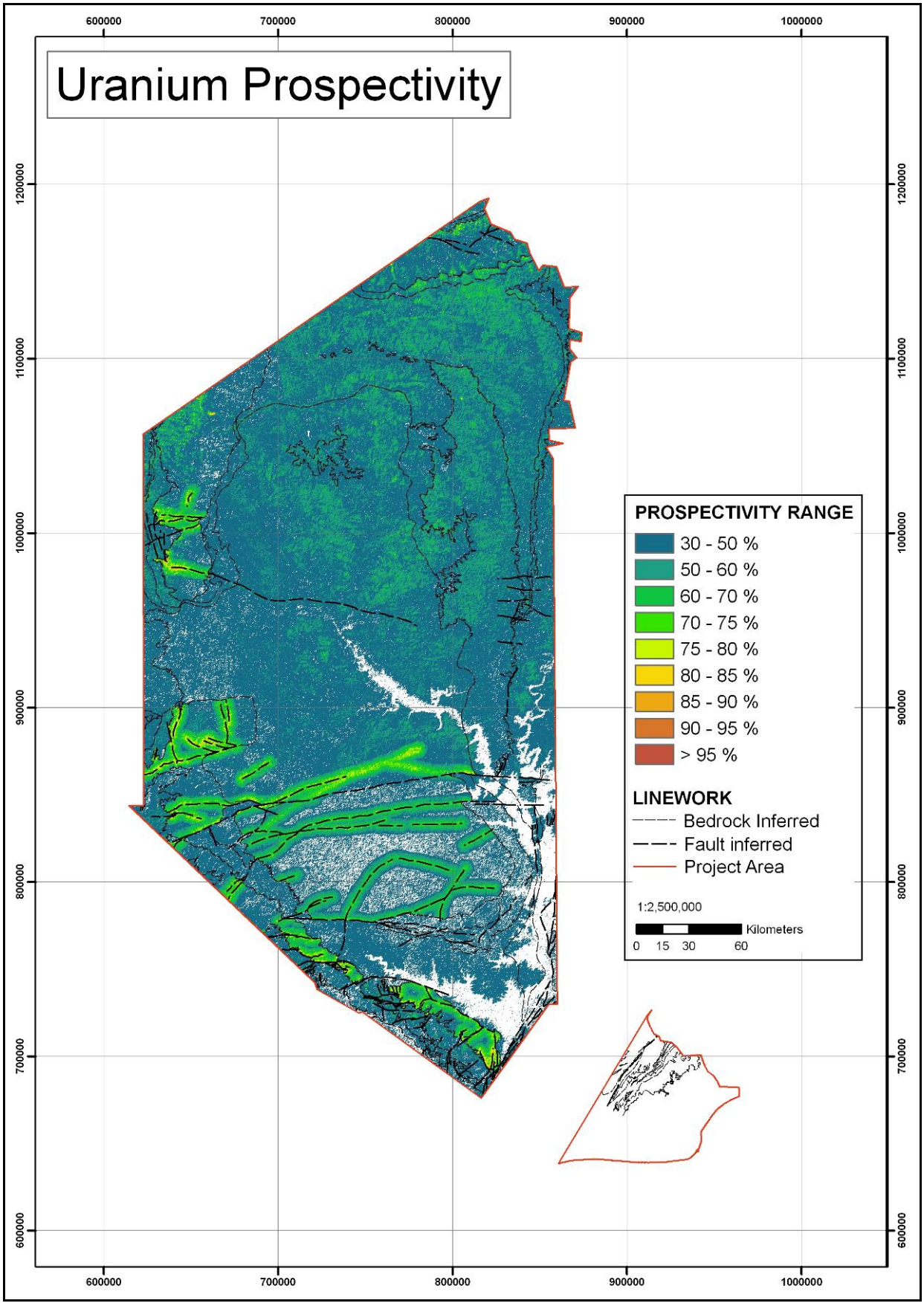

Figure 73 Uranium prospectivity map of the Volta Basin.

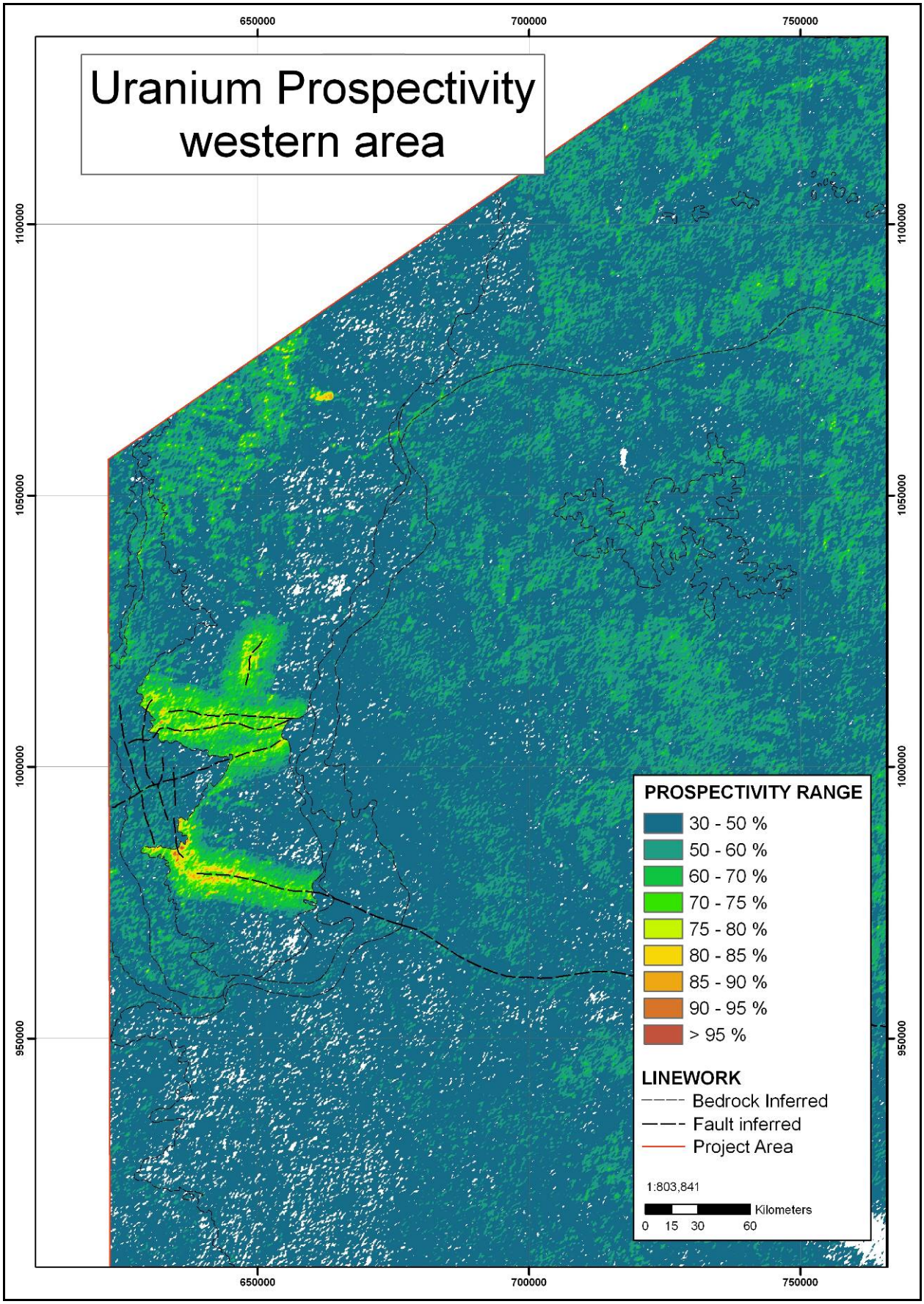

Figure 74 Uranium prospectivity map of the western Volta Basin.

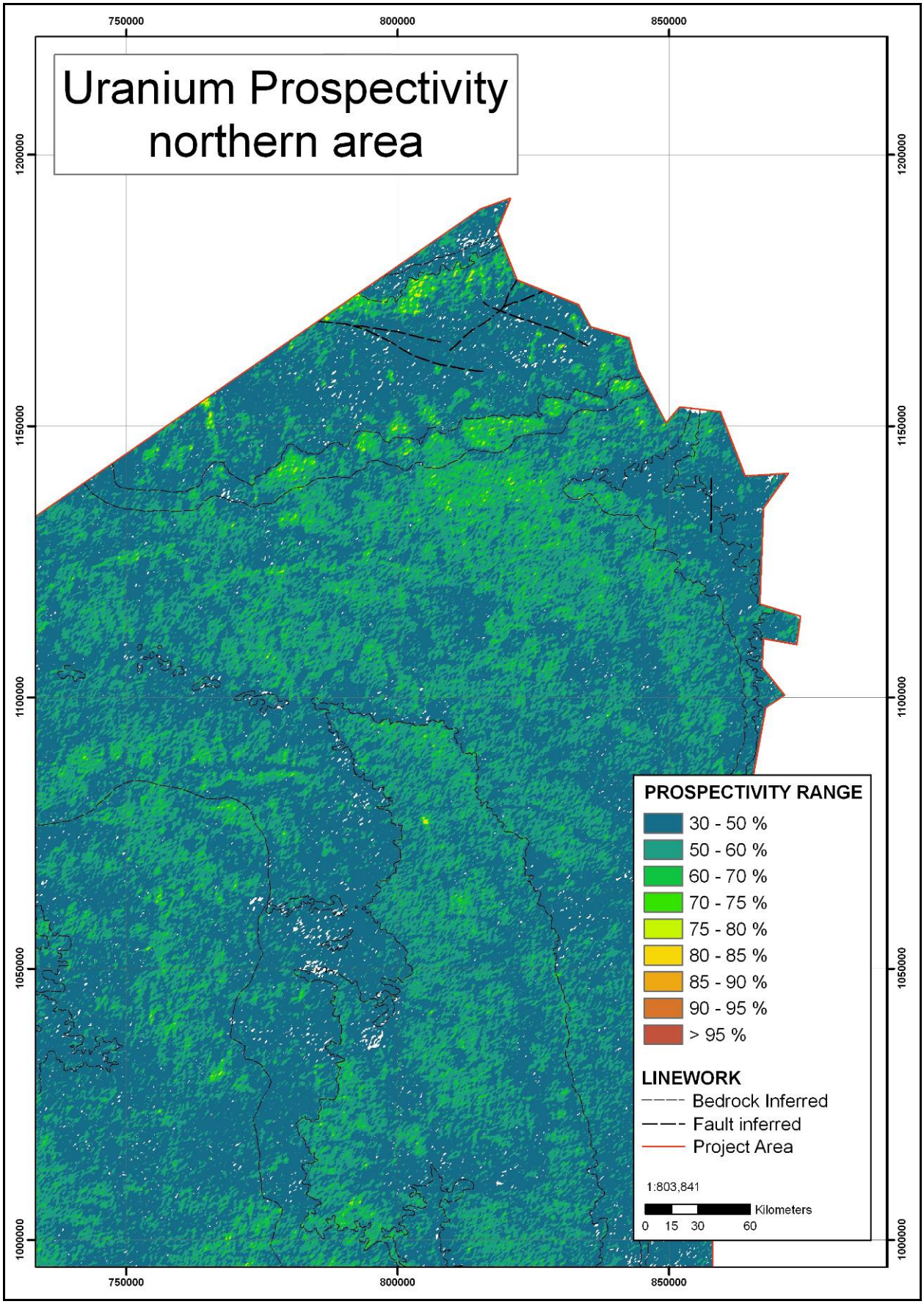

Figure 75 Uranium prospectivity map of the northern Volta Basin.

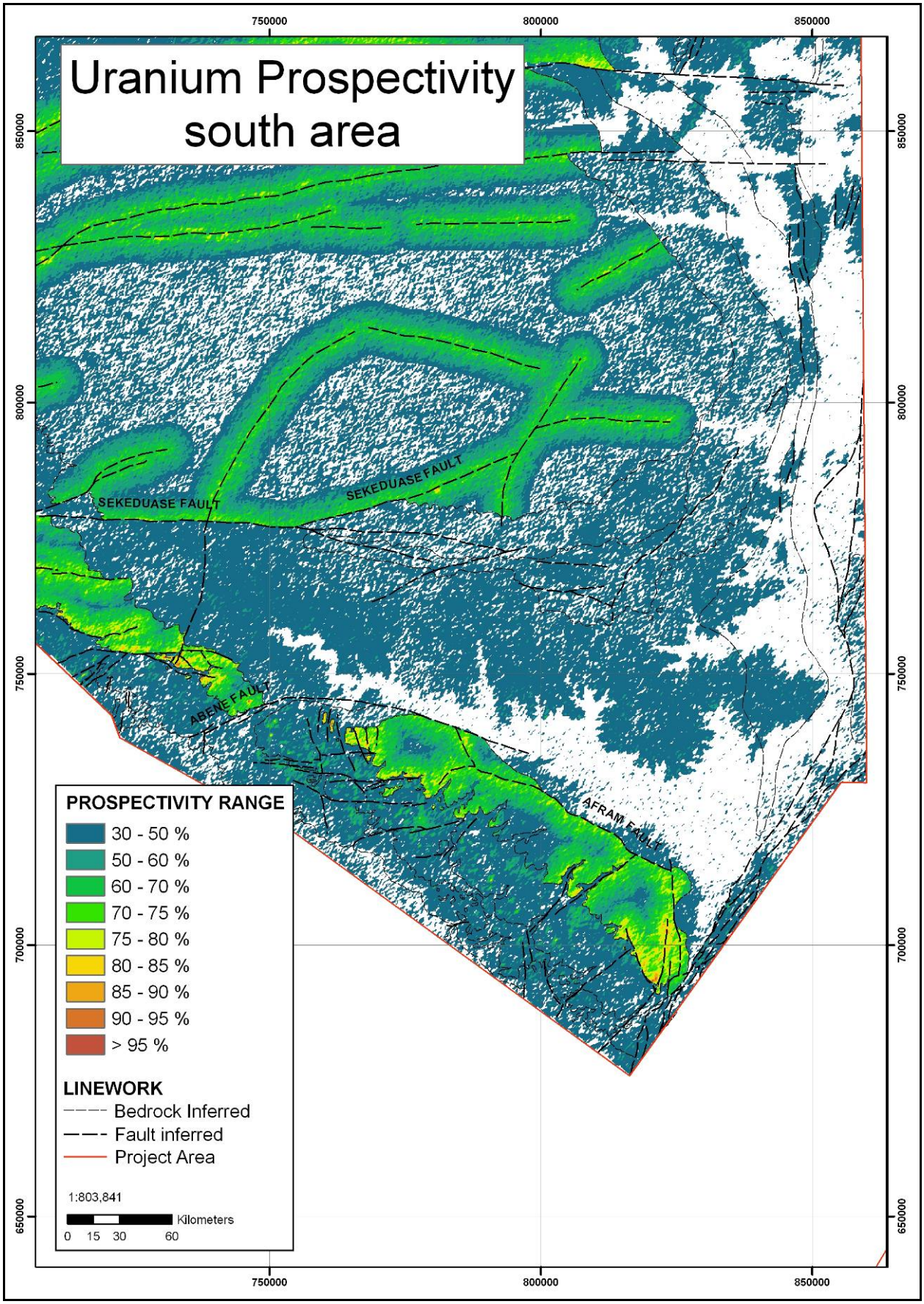

Figure 76 Uranium prospectivity map of the southern Volta Basin.

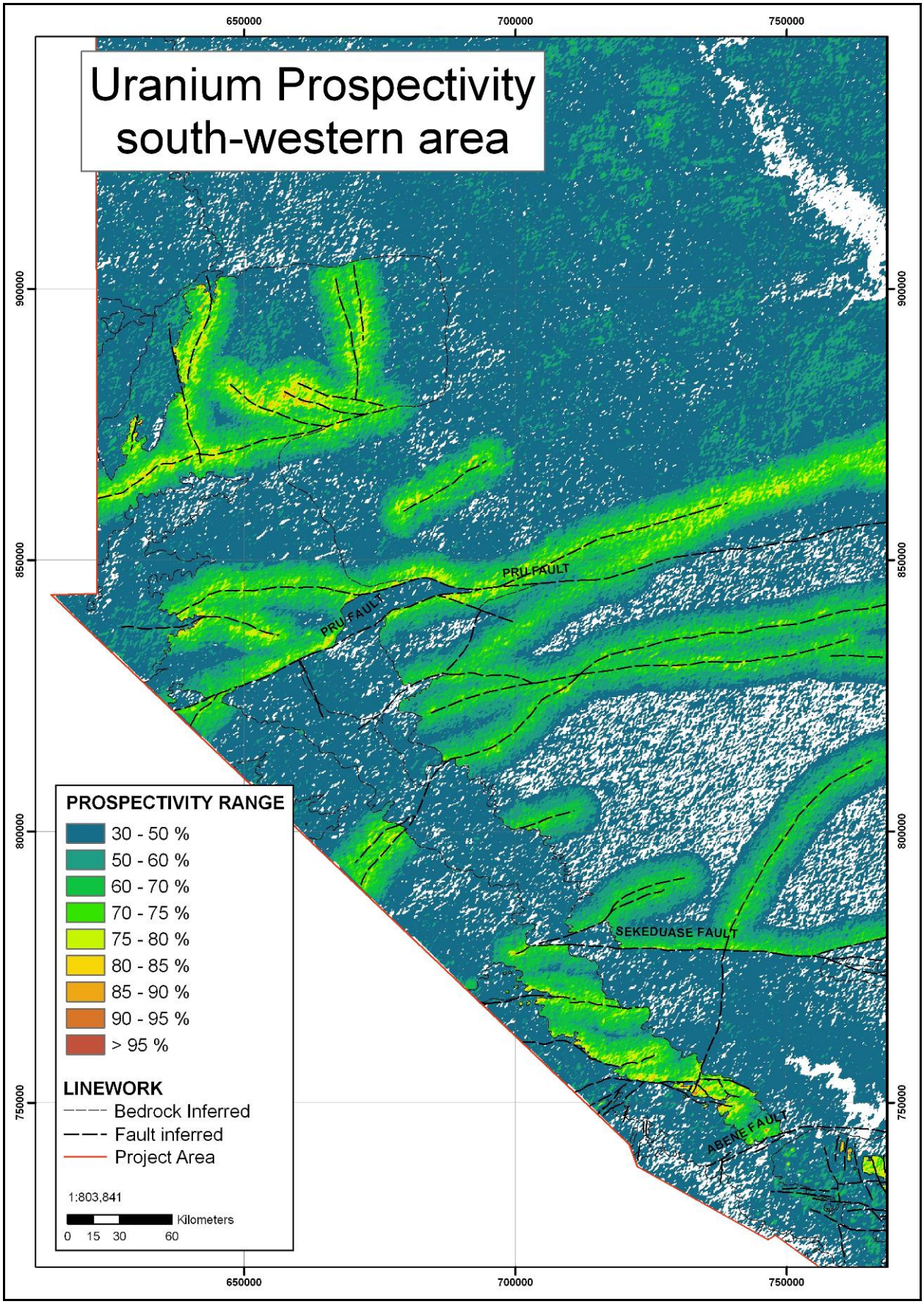

Figure 77 Uranium prospectivity map of the south-western Volta Basin.

5.15 PHOSPHATE

As phosphate is used in the production of plant fertilisers and as an additive in animal feedstock, the demand is likely to rise as the need for food to feed the growing global population increases.

Within West and North Africa, phosphate is a very important commodity, specifically with Togo, Senegal, Egypt and Morocco all having very significant mines and deposits. Although no phosphate mining occurs in Ghana, minor deposits have been identified within the Volta and Keta Basins (Figure 78) within similar phosphate-hosting strata to neighbouring Togo, Burkina Faso, Benin and Niger.

5.16 OCCURRENCE OF PHOSPHATES IN GHANA

Although phosphates occur in a number of areas throughout Ghana there is no current commercial extraction.

5.16.1 Keta basin

In neighbouring country of Togo, the large Hahotoe phosphate deposit is hosted in Eocene sediments. Following the discovery that these Eocene host sediments also extended into the Keta basin, exploration was initiated to discover similar deposits (Kesse, 1985). Unfortunately, results were disappointing with samples showing less than 5% P_2O_5, with occasional highs up to 55%. For commercial purposes phosphates deposits are generally expected to have values between 15-30% P_2O_5. See Figure 78 for the location of this minor deposit.

5.16.2 Volta Basin

In the Volta Basin, there are some minor occurrences associated with barites, hosted within middle Voltaian limestones of the Daboya area. However, samples analysed came back with low values of less than 3% P_2O_5. See Figure 78 for the location of this occurrence. In the north eastern end of the Volta basin, outside Ghana located near to the boundaries of Benin and Niger, there are deposits with substantial resources up to 100Mt of ore, grading between 15% and 30% P_2O_5 (Wright et al., 1985).

5.16.3 Other areas

In the Sekondi area SW Ghana, phosphate bearing nodules occur within Devonian shales. Additionally, there are minor igneous-related phosphates associated with pegmatites, occurring in the Bole and Anobabo areas of northern Ghana.

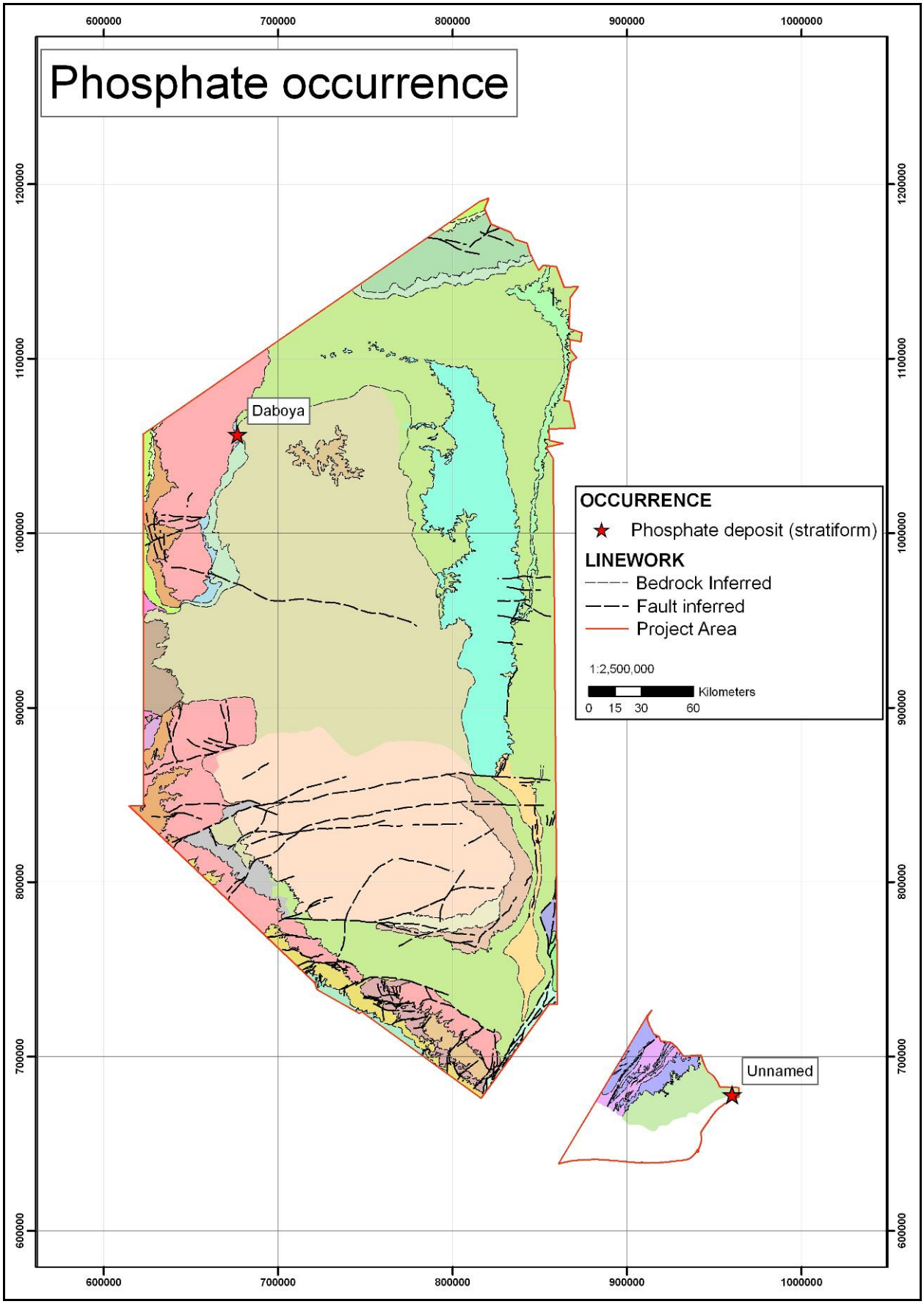

Figure 78 Phosphate occurrences in the Volta and Keta Basins, overlaid on a generalized gelogy map.

5.17 PHOSPHATES IN WEST AFRICA

As indicated above, phosphates are an important commodity in West Africa, as highlighted by Senegal, which produced on average 1.3Mt / y between 2002 and 2006 (Hetherington et al. 2008). In addition to the main producers, Togo and Senegal, countries such as Benin, Guinea-Bissau and Mali are all recognised as having significant phosphate potential.

5.17.1 Burkina Faso

There are several phosphate deposits in the SE of Burkina Faso, hosted within the Kodjari Formation of the Pendjari series. The Kodjari deposit (Trompette, 1989) and the associated Arli prospect are typically fine grained and well sorted, interpreted as shallow marine platform deposits.

5.17.2 Niger

Within Niger, there are two deposits of significance. The Tapoa deposit is hosted by Volta group sediments of Neoproterozoic to Cambrian aged sediments and contains proven resources of 207m at a grade of 23% P_2O_5 (Schluter, 2006). The deposit is up to 40m thick with intercalations of shale and siltstone (Trompette, 1989). The much younger, Tahoua deposit is hosted in Palaeocene to Eocene sediments and has reserves of 7.4Mt about 30% P_2O_5 (Schluter, 2006).

5.17.3 Togo

Between 2001 and 2005 Togo produced an average of 1.2 Mt of phosphate rock (Hetherington et al. 2008). The phosphate is found in Eocene deposits in the Hahotoe-Akoumape and at Dagbati areas. The principle deposit is Hahotoe, 35 km northeast of the capital Lome, and is currently an active mine. In addition to these deposits, within the older Neoproterozoic sequence, there are also deposits of phosphates, however these have not been exploited or assessed.

5.18 DEPOSIT MODELS THAT APPLY TO THIS MINERALISATION

Approximately 75% of global phosphate resources are within sedimentary, marine phosphate rock deposits, while 15% are sourced from igneous hosts. The remainder is from weathered deposits and guano accumulations (van Straaten, 2002). Table 19 lists the characteristics of the sedimentary hosted phosphate deposits.

Typical features for sedimentary hosted phosphate deposits include:

- Occur in upwelling areas within basins, with good connection to the open sea.
- The tectonic setting is on intra-plate shelves and platforms.
- Deposition occurs in warm latitudes, mostly between the 40th parallels.
- Deposits can occur in a range of rock types, including phosphorite, marl, shale, chert, limestone, dolomite, and volcanic materials.
- Age of host ranges from Precambrian through to Miocene.
- Principle mineralogy includes apatite and fluorapatite.
- The deposit form varies, with sedimentary layering of pellets, nodules, phosphatized shell and bone material all common.
- Individual beds may be a metre or more thick and may extend over hundreds of km^2.
- Geochemical anomalous zones of P, N, F, C, and U.
- Some deposits may be anomalously radioactive.

Table 19 Typical characteristics of sedimentary hosted phosphate deposits.

5.19 PROSPECTIVITY MODELLING OF PHOSPHATES

5.19.1 Sedimentary Phosphate deposits

This section will discuss the modelling of sedimentary-hosted Phosphate deposits over the study area, specifically the Volta region. However, two should be considered before the modelling plan is discussed.

A. *Geology;* As the model is based on the most recent mapped geological understanding in the Volta and Keta basins, it is necessary to mention the lack of outcrop or section in many parts of the study area. This factor causes difficulty in the mapping and determining of exact contacts.

B. *Radioactivity;* Not all phosphate deposits have associated raised radioactivity, but for the purposes of this model it is assumed that they do. In the absence of geochemistry, this assumption aims to utilise as many of the available datasets as possible.

5.19.1.1 MODELLING OUTLINE

The model is based on the Sedimentary-hosted Phosphate deposit profile. It aims to locate the similar stratigraphy that is known to host phosphate deposits in Burkina Faso and identity within these rock packages areas of raised radioactivity.

5.19.1.2 MODELLING PLAN

This is the generalised outline of the modelling process applicable to the Sedimentary-hosted phosphate model.

A. Locate prospective stratigraphy in the Volta Project area. The Pendjari group is of similar age to the deposits in Burkina Faso, with specifically, the Kodjari Formation the most prospective.

B. Locate areas in the overlying favourable geology where there is raised radioactivity.

Exploration data to be used:

- Mapped geology over the Volta project area.
- Total Count Radiometrics.

Exploration Model:

The shortage of known phosphate occurrences / deposits within the area that could be used as a training set, limits our analysis to be Knowledge driven modelling (using Fuzzy Logic).

1. Extract the favourable stratigraphy.
2. Model this favourable geology with the Total Count from the radiometrics
3. Create a prospectivity map of potential Sedimentary-hosted phosphate in the Voltaian project area.

5.19.1.3 METHOD

The sequence leading to the output of the map can be generalised as follows:

1. Target – Sedimentary-hosted Phosphate deposits hosted in the Voltaian sediments of east central Ghana.
2. MDM - refer to Figure 61
3. Exploration data used - Mapped geology over the Volta project area; Total count Radiometrics. The following processing was applied to the data:
    - Extraction of the Pendjari group from the rest of the geology.
4. Fuzzy membership values were given to the datasets:
    - *Geology:* Kodjari Formation (Darebe Tuff Member and Buipe Limestone Member) was given a Fuzzy Membership of 0.7; the rest of the Pendjari group, undivided, was given a value of 0.45. All other geology was given a nominal value of 0.01.
    - *Total Count Radiometrics:* The uranium was given values between 0.7 and 0.1 depending on the measures value. All areas with no data were given a nominal value of 0.01.
5. The geology and the total-count radiometrics were modelled together using the Fuzzy Operator AND. This operator Fuzzy AND produces a prospectivity map that recognises that all data must be present to produce a favourable result. The flow diagram in Figure 79 demonstrates operation.

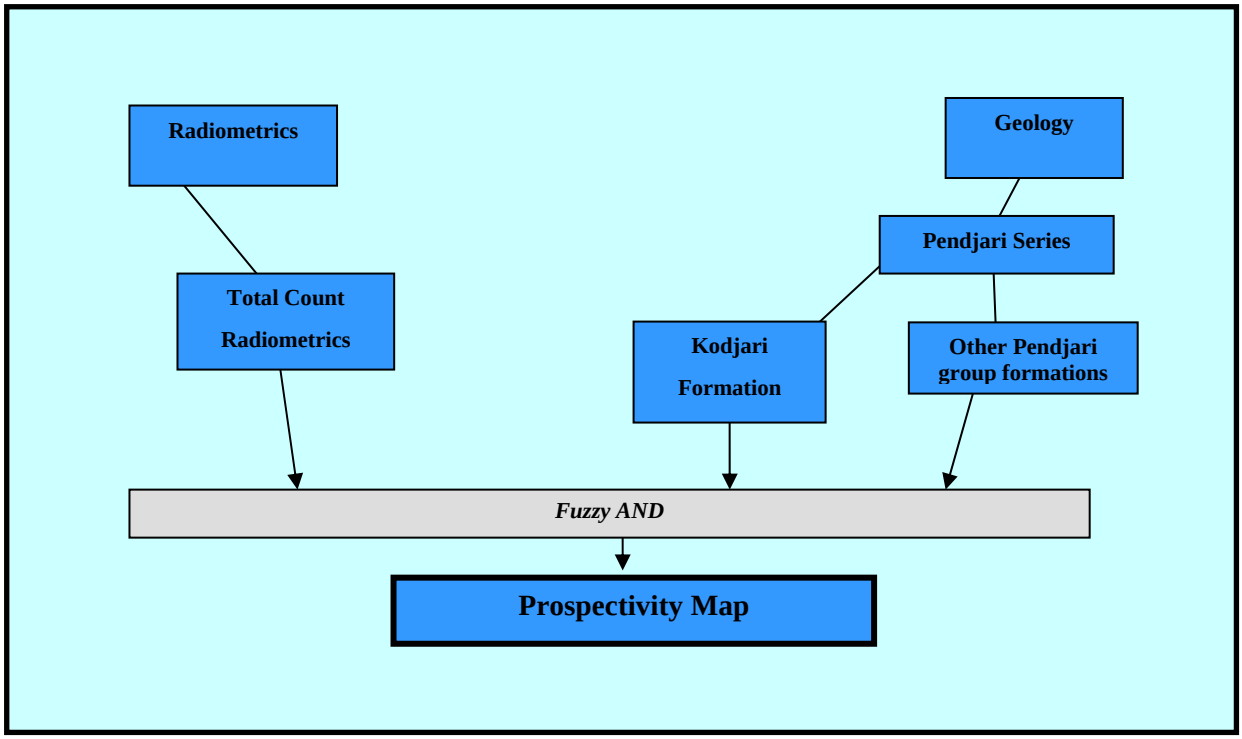

Figure 79 A flow diagram of the mathematical operations for the sedimentary hosted phosphate model.

5.19.1.4 RESULTS

The resulting prospectivity map displays the range of prospectivity over the Volta area for a model of Sedimentary-hosted phosphate deposits. Figure 80 to Figure 82 display the results for the model.

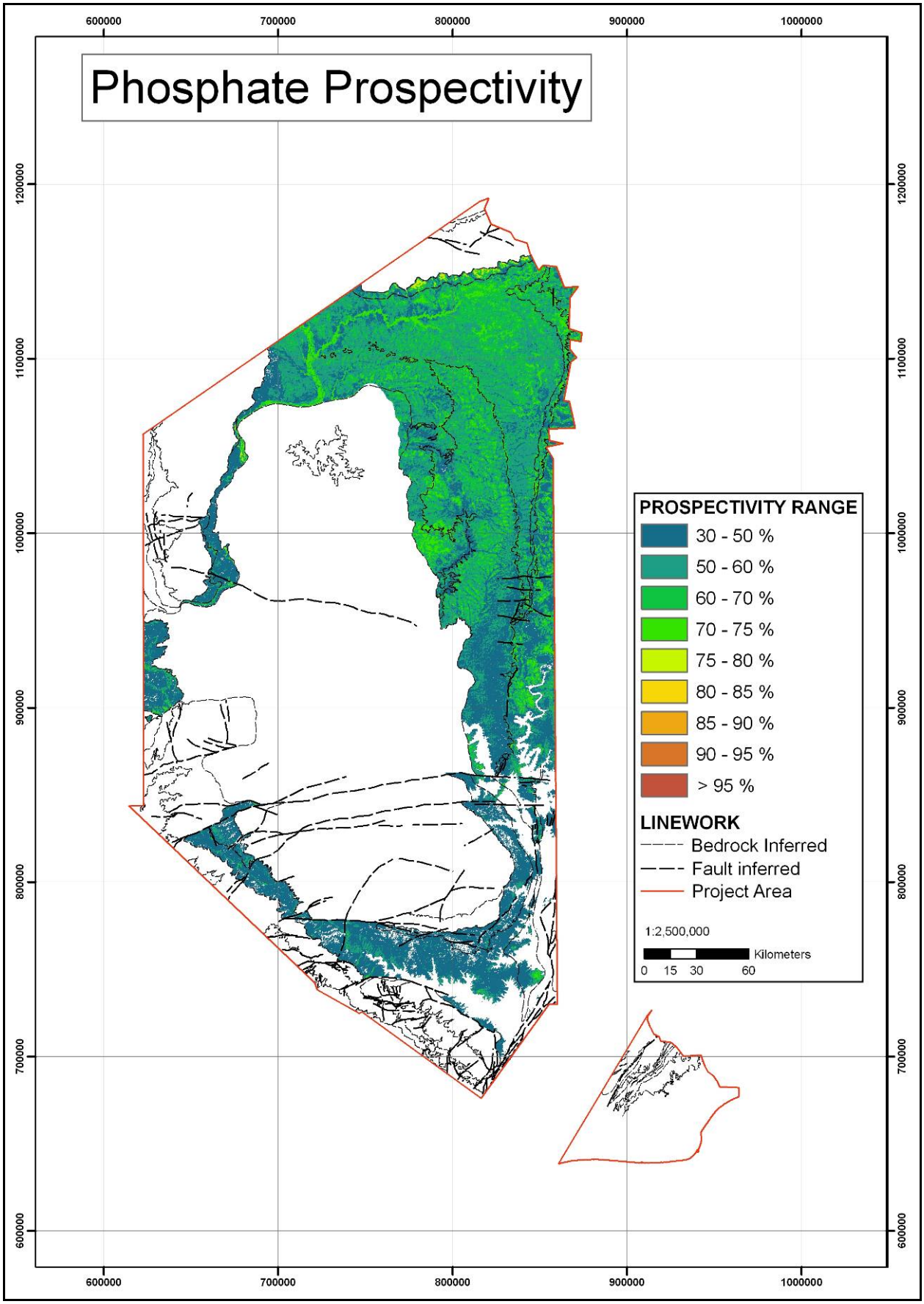

Figure 80 Phosphate prospectivity map of the Volta and Keta Basins.

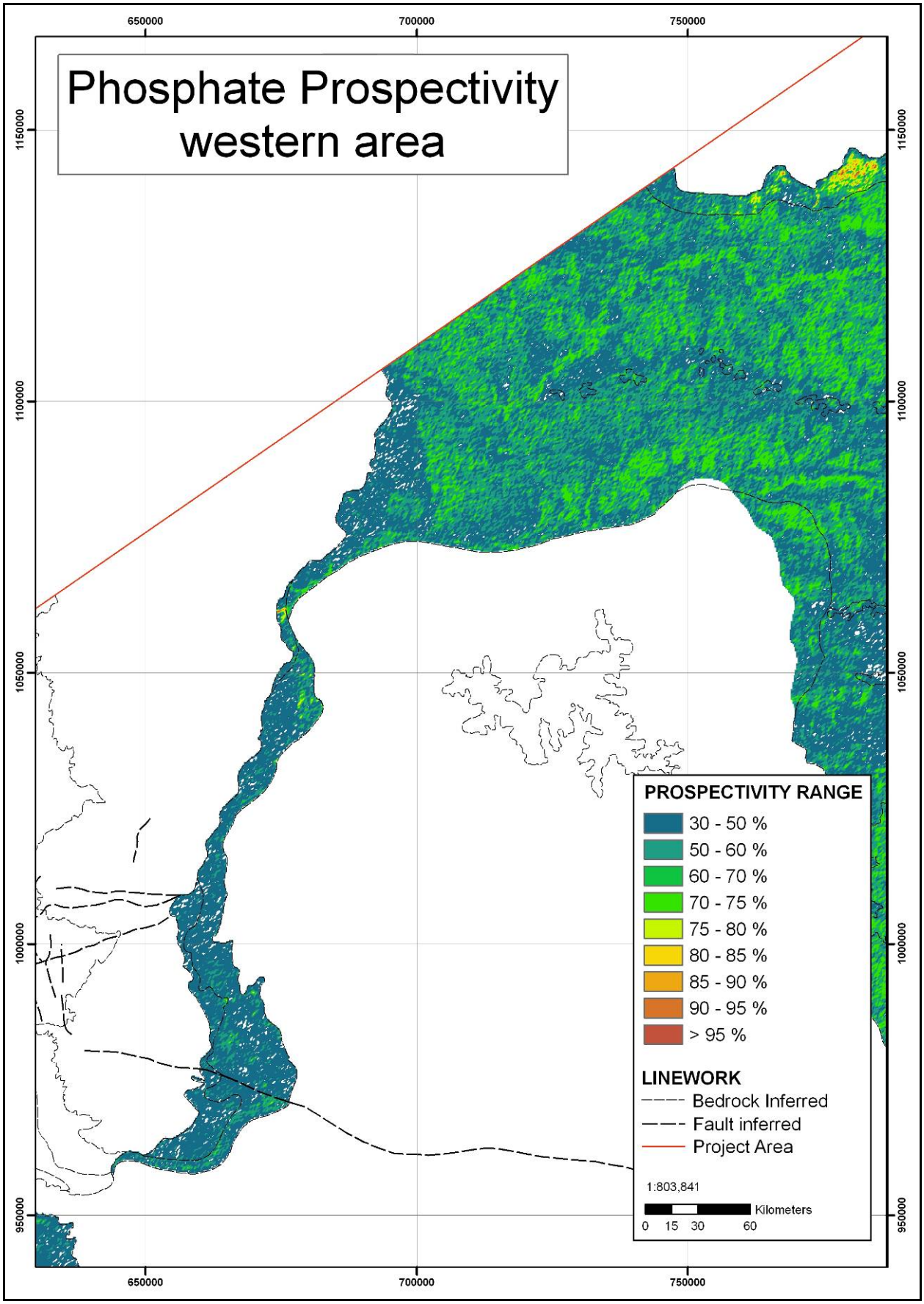

Figure 81 Phosphate prospectivity map of the western Volta Basin.

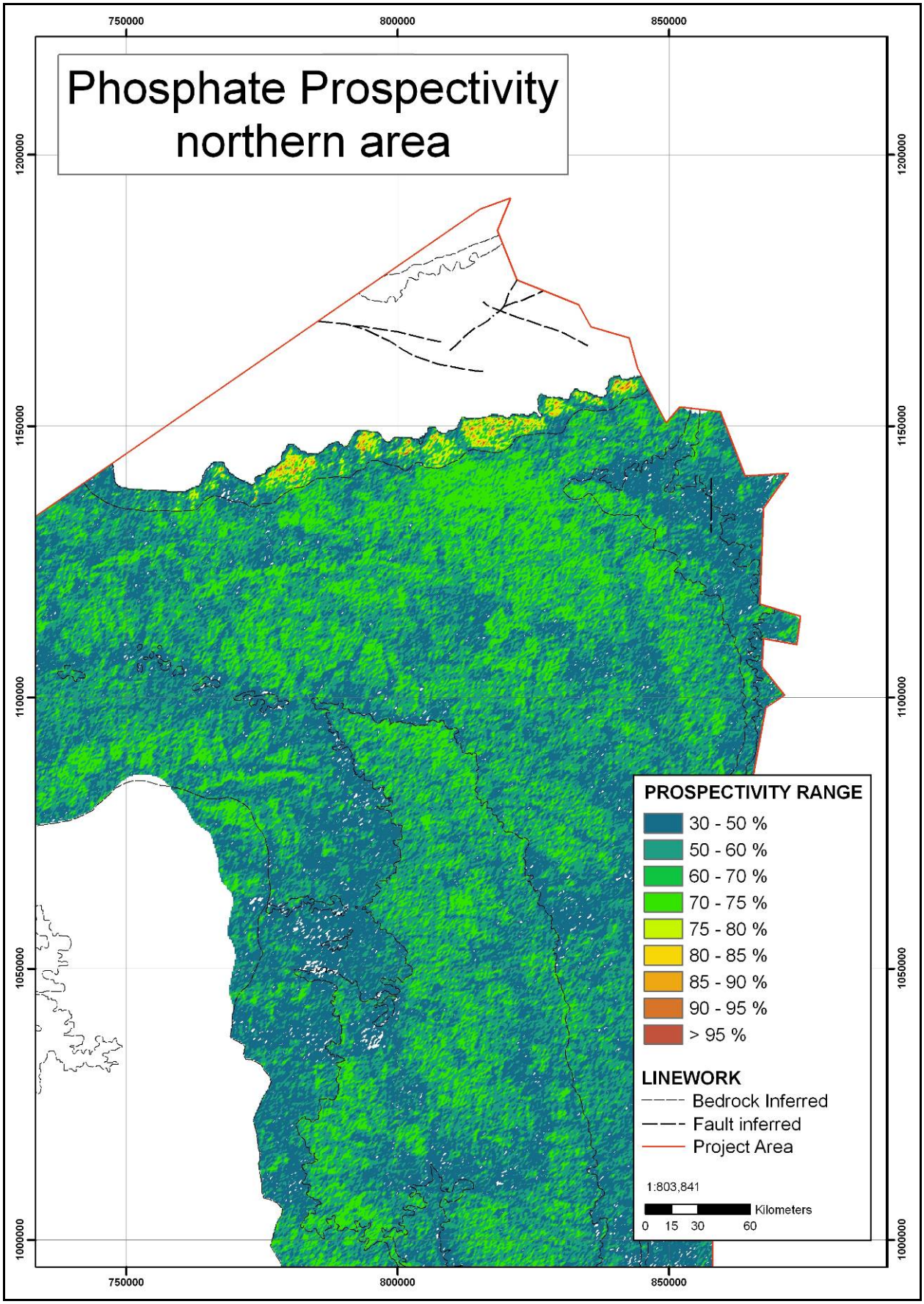

Figure 82 Phosphate prospectivity map of the northern Volta Basin.

5.20 DIAMONDS

Alluvial diamonds have been known in Ghana since 1919. Junner (1943) documents the history of diamond discoveries in Ghana up until the mid 1950s. Kesse (1985) provides an excellent account of diamond discoveries, exploitation and production in Ghana and gives a description of the two principal diamond fields: the Birim in the Eastern Region and the Bonsa field in the Western Region, both outside the Voltaian and Keta Basins. The Birim diamond field, located in the Birim River Valley in the Eastern Region, overlies Birimian rocks. The Bonsa diamond field, located in the valley flats of the Bonsa River and its tributary in the Western Region of Ghana, overlies the Tarkwaian Kawere conglomerates (Tarkwaian). The diamonds occur in gravels in the beds and flats of the Birim and Bonsa Rivers and their tributaries. Both fields lie outside the study area. A number of isolated diamonds have been discovered elsewhere throughout Ghana including in the Western Province, in the north around Bolgatanga, in the Worawora area on the border with Togo and a scattering in the Voltaian Basin area.

Ghanaian diamonds are relatively small and of moderate quality rendering them most suitable for industrial applications. Ghana's diamond production is increasing for the first time in many years, with the largest producer being state owned Ghana Consolidated Diamonds (GCD).

5.21 OCCURRENCE OF DIAMONDS IN GHANA

All of the production to date has been from alluvial deposits, which overlie Birimian, and to a lesser extent, Tarkwaian rocks. There are currently two main diamond fields in Ghana, Birim and Bonsa, producing approximately 1m carats per year (Benham et al. 2007). The government owned, Ghana Consolidated Diamonds Ltd, is the main producer, with the remainder being produced by small (artisanal) and medium scale operations. Diamonds have been found throughout Ghana and are not limited to the known fields.

The source of the diamonds is undetermined, however, it is inferred that the diamonds found in Ghana are Precambrian (Tompkins et al., 1984) These were transported from the north for considerable distances in old river gravels, and that the kimberlites from which they came might have been destroyed during the Eburnean Orogeny or may be present under Voltaian sediments.

5.21.1 Occurrences in the Study Area

A number of isolated diamond occurrences have been reported in areas underlain by Voltaian strata and the Buem Formation (Figure 83). However, no systematic exploration for diamonds has been conducted in these areas.

In 1919, the Geological Survey of Ghana found two small diamonds in the gravels of the Aboabo Su, north-east of Obusuman, near the confluence of the Volta and Obosum rivers (Mangoase). This area has since been inundated by Lake Volta. In 1936, diamonds of larger than average size were found in gravels in the Obosumanu River and in the Afram River near Mankrong (Nketepa) during large scale tests carried out by CAST (Consolidated African Selection Trust Limited). The streams drain large outcrops of coarse conglomerate at the base of the Voltaian system. In the north of the Voltaian Basin, near Gambaga, two large diamonds, one 10.5 carats and the other 7.5 carats, were found in 1936 in the gravels of the White Volta. Voltaian sandstones that, in places, contain quartz pebbles are the dominant lithology in the area, and Birimian metamorphic and granitic rocks and Pleistocene terrace gravels are found upstream.

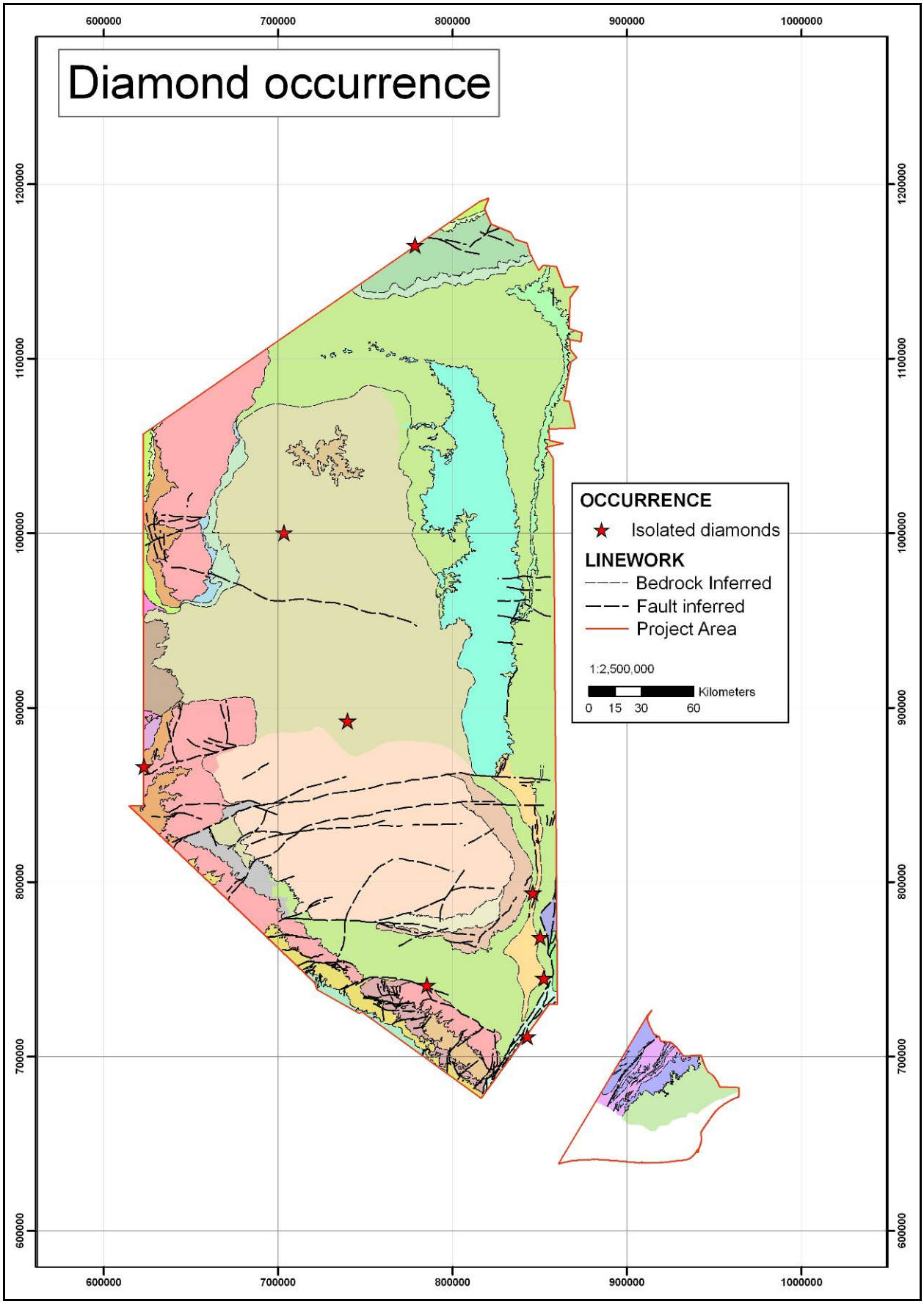

Figure 83 Diamond occurrences in the Volta and Keta Basins, on a generalized geology map.

Isolated diamonds have been found in the Yoko Su River between Wenchi and Kintampo (Amoama and Agyima), where the gravels consist mainly of well-rounded quartz pebbles

derived from pebbly beds near the base of the Voltaian. Further isolated discoveries were made at Basare, Txosor and Tsyame Sa, all of which have been immersed by Lake Volta.

In 1994, diamonds were discovered to the east of the Volta Basin, in the Worawora and Jasikan areas, by the activities of registered and illegal small-scale miners. Details concerning grade or production levels are not available but the size of the diamonds from this area is reportedly much larger than those from the Bonsa and Birimian fields. A license has been granted for prospecting in the area. This area extends from Ho in the south to Worawora in the north, underlain by rocks of the Buem Formation.

The primary source of diamonds in Ghana has long been debated and has yet to be conclusively identified. Until recently, no kimberlites or traces of kimberlitic minerals were located in Birimian metasediments or the Tarkwaian rocks which underlie the diamond fields of Ghana. This implies the diamonds are not of local origin but were transported for considerable distances in sheets of old river gravels. In 1984, Tompkins and Haggerty inferred that the diamonds found in Ghana are Precambrian and several explanations have been proposed to explain their occurrence. They postulated that the diamonds are not locally derived but are transported from the north over considerable distances in old river gravels, and that the kimberlites from which they may be derived may have been destroyed during the Eburnean Orogeny, or may be hidden under Voltaian strata.

Hastings (1983), attributed the emplacement of kimberlites in West Africa to oceanic rifting. Geophysical data available at the time, although not bearing directly on the origin of diamond deposits in Ghana, supports the hypothesis of Eburnean rifting. The kimberlites of the Cote d'Ivoire have yielded radiometric dates of about 1430 Ma and occur on the flanks of postulated Eburnean rifts. Kimberlites in Mali have yielded younger dates of about 1070 Ma (this in fact suggests a Kibaran event).

During the Eburnean, thick new continental crust is thought to have been produced and subsequent extension of this new craton may have resulted in diatreme activity. This is considered to be the source of diamond bearing kimberlites in Cote d'Ivoire and Mali. The emplacement of kimberlitic diatremes may also have occurred in Ghana, the erosion of which may be a source of alluvial diamonds within the Neoproterozoic sedimentary units of the Voltaian Basin.

In Sierra Leone and Guinea, kimberlites, based on age and geographic location, are more likely associated with the Mesozoic opening of the Atlantic, yielding dates broadly in the range of 80-140 Ma. These hypotheses could conceivably be applied to prospecting for diamonds in Ghana. For example, in northern Ghana, near the Burkina Faso border, a Mesozoic kimberlite has been reported, (Wright et al., 1985) and it is inferred to lie along the north-eastern extension of the same oceanic fracture zone on which the kimberlitic intrusions in Sierra Leone and northern Cote d'Ivoire are located. Other Atlantic fracture zones, such as the St. Paul fracture, which intersects the coast near Abidjan, could extend into Ghana.

However, recent research by Canales and Norman (2003) revealed that diamonds from the Akwatia diamond field, north of the Birim diamond field, are different from other diamonds found in Ghana as they show no evidence of transport, lack kimberlitic indicator minerals and are associated with metamorphosed ultramafic rocks with a composition resembling komatiite or boninite. The ultramafic rocks are associated with arc sediments contained within or intruded into Birimian metasedimentary rocks including turbidities, phyllites and greywackes. The diamondiferous rocks are actinolite/tremolite schists and actinolite rocks with little or no schistocity and distinctive clastic texture, containing clasts of phyllite and carbon. The clastic units are elongate and contained within the actinolite schist. Major and trace element analysis of these rocks suggest a suite of rocks similar to the diamond-bearing volcaniclastic komatites of French Guiana and/or the metamorphosed suit of komatiite/ boninite type rocks of the Wawa (Superior Province) greenstone belts (Canales and Norman, 2003). Furthermore, diamondiferous

dykes at Mitzic, Gabon, and Bobi, Cote d'Ivoire, termed "metakimberlites" are highly altered and sheared, with an appearance of talc schist (Bardet, 1974).

It is thought that diamond deposits in the Akwatia field represent some of the oldest diamond deposits that have been found and there is little doubt that Akwatia is a residual deposit. In April 2006, Paramount Mining reported the recovery of diamonds from a hard rock source from a site within the Osenase project; south of the Akwatia diamond field (Paramount Mining, 2006) diamonds are reported to occur within heavily lateritised ultramafic rocks. Initial field observations, in particular the visual appearance and mode of emplacement of the rocks, show a strong resemblance to meta-kimberlite, however, more detailed investigations are required.

The West African Craton includes the Man Archon and the Ebumean Proton. Diamondiferous kimberlite pipes and dykes are located on the Man Archon in Sierra Leone, Guinea, Liberia and Mali. Alluvial deposits immediately downstream from kimberlites are mined in Sierra Leone, Guinea and Liberia. Additionally occurrences of pipes and alluvials are being evaluated in Mali. Lamproite dykes located on the Eburnean Proton in Ivory Coast were mined in the past and large alluvial deposits, which cannot be traced to their primary host rock, are mined in Ghana and Ivory Coast.

Since the Archean there have been a number of periods of concentrated Kimberlite intrusion, including 1000Myr, 500Myr, Devonian and throughout the Mesozoic / Cenozoic eras. The intrusions intrude stable continental crust, >2500Myr, commonly within thick Archean - Proterozoic shields. These phases of intrusion are related to plume activity, or low plate velocity, when uninterrupted mantle convection gave rise to partial melting and volatile production. Epeirogenic movements (vertical) may create fractures that allow the kimberlites to rise to the near surface. Figure 84 shows two crustal scale structures, possibly dykes or faults that may be indicating epeirogenic movement.

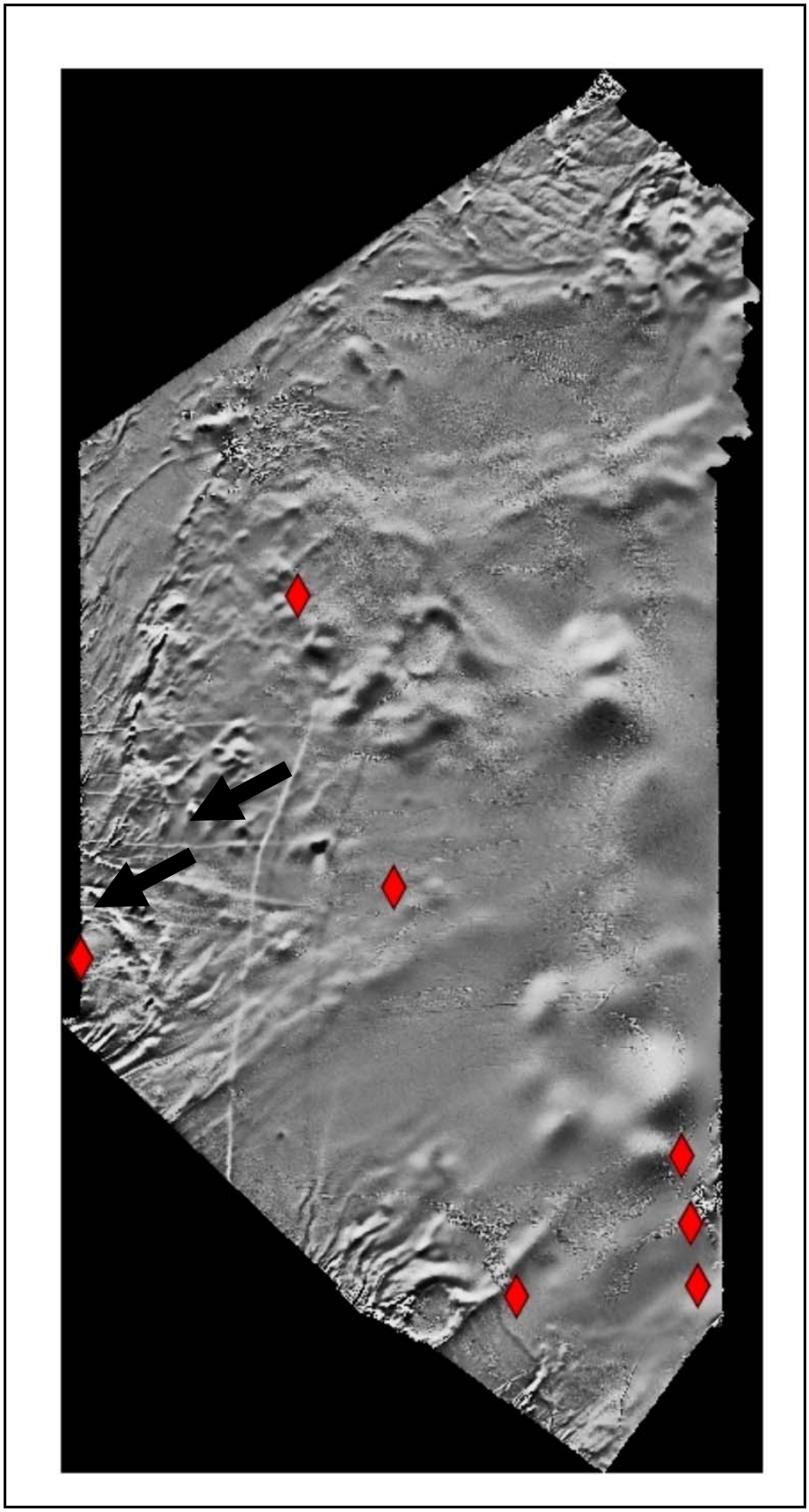

Figure 84 Crustal scale structures in the Volta Basin which may facilitate kimberlite emplacement.

These structures (being studied by Fugro as part of this project) may facilitate kimberlite emplacement and Table 20 lists the characteristics of the Mineral Deposit Model (MDM) for Kimberlite diamonds.

Diamonds

Typical features of these deposits include:

- Occur in Kimberlites, with surface expressions up to 146 hectares.
- Can occur in any age of stratigraphy other than Archean.
- Regions underlain by stable Archean cratons.
- Alteration may include serpentinization, silicication or bleaching.
- Weather to 'yellow ground', clay rich material.
- Kimberlites occur in clusters.
- Intrusions regionally controlled by major transcrustal faults and shears and the intersections of these.
- Raised Ti, Cr, Ni, Mg, Ba and Nb in soils, however this is similar to other alkaline rocks.
- Kimberlites may show magnetic highs or lows depending on the contrast with the local host rocks. Electrical methods may pick up weathered clay rich, yellow ground. Gravity is also used, with weathered kimberlites showing lows and fresh kimberlites displaying distinct highs.

Table 20 Mineral Deposit Model (MDM) for Kimberlite diamonds.

5.22 MINERAL PROSPECTING AND SAMPLING IN THE FIELD

Fieldwork was carried out over two seasons in 2006 and 2007. This enabled the collection of data from the various offices in Ghana that may be applicable to Mineral Deposits in the Volta and Keta Basins, field follow up of this data, and prospecting in the field. In addition to this, lithogeochemistry sampling was undertaken and a small amount of ground geophysics was carried out. The next section discusses this field work.

5.23 PROSPECTING / SAMPLING

As part of the exercise to map the geology of the Ghanaian Volta and Keta Basins, there was an opportunity to follow up some of the mineral occurrences compiled in the Phase 1 report (Jordan et al, 2006). This process involved the prospecting in the vicinity of the mapped occurrence, and where applicable, the rock sampling of mineralisation (Figure 85 and Figure 86). The fieldwork also allowed prospecting / sampling of areas that appeared altered or mineralized.

Figure 85 Sampling quartz veins in the Pan African deformed rocks.

Figure 86 Following up alluvial gold occurrences by panning.

Table 21 lists the samples taken for further analysis and Figure 87 displays their locations. The analysis and results will be discussed later in this Section.

SAMPLE ID	DESCRIPTION	TYPE
pmcd1	Quartz vein material with no visible sulphides	In situ
pmcd2	Breccia fault zone within silicified E-W fault, iron oxide staining	In situ
pmcd3	Bleached sandstone from fault zone with no visible sulphides	In situ
pmcd4	Quartz pebble conglomerate (basal conglomerate)	In situ
pmcd5	Highly magnetic medium grained sandstoneproximal to a large regional structure	In situ
pmcd6	Bunya sandstone, coarse grit with volcanic and mafic materials, highly magnetic	In situ
pmcd8	Alluvial channel gravel, partially consolidated	In situ
pmcd9	Faulted area with bleached zone and iron oxide staining	In situ
pmcd10	Vuggy quartz vein taken from a phyinite shear zone	In situ
pmcd11	Quartz veinlet stockwork near to shear area with minor iron oxide staining	In situ
pmcd12	Iron oxide stained quartzite with two minor cross-cutting veinlets	In situ
pmcd13	Vuggy quartz veinlets in fold nose	In situ
pmcd14	Minor hematite veinlet in a coarse sandstone	In situ
pmcd15	Sandstone with a veinlet of hematite	float
CJ17	Laminated siltstone with manganese	In situ
CJ21	Laminated siltstone with manganese	In situ
FMG5	Laterite - sampled to check average Fe and Al content in laterite	In situ
FMG7	Siltstone with total count > 45	In situ
FMG8	Manganese laminations/layers in siltstone from quarry on outskirts of Tamale	In situ
FMG9	Mudstone - green/anoxic conditions. Manganese horizons. Water dam diggings	Grab
FMG10	Conglomerate horizon in sandstone. Possible Tertiary weathering channel fill? Near to laterite quarry.	In situ
FMG11	Baryte blades in grey ooid limestone from Daboya	In situ
FMG12	Grey sandy limestone with mag. susp. > 10	Chip in situ
FMG13	Chip sample of chert/baryte stockwork veins with possible heavy minerals, Daboya	Chip in situ
FMG14	Dark grey limestone with ooids. Mag. susp. = 48. Finely laminated. Upstream from Daboya.	In situ
FMG15	Grey laminated limestone, Daboya, from a adjacent to boat slipway	In situ
FMG16	Yellow dolomitic limestone with interbedded micrite and siltstones. Former 6 lens sampled. Buipe trial quarry 3	Chip in situ
FMG17	Finely laminated micrite & dolomitic limestone. Latter sampled.Buipe trial quarry 2	In situ
FMG18	Brecciated dolomitic limestone with large baryte flower structures (20cm x 10cm) Buipe trial quarry 1	In situ
FMG19	Frequent 0.5-2cm Mn rich horizons in sandstone with surface displays dendritic and blebs of possible pyrolusit	Grab
FMG20	Silicious sandstone with very fine grained tarnished metallic minerals possibly of copper magnetite and galena	Grab
FMG21	Maroon mudstone with a raised total count	In situ
FMG22	Micaceous sandstone with a raised total count and dendritic manganese.	In situ
FMG23	mm scale sub-vertical quartz veins in arenaceous sandstone	Chip in situ
	Total number of samples	**34**

Table 21 List of samples taken for further analysis.

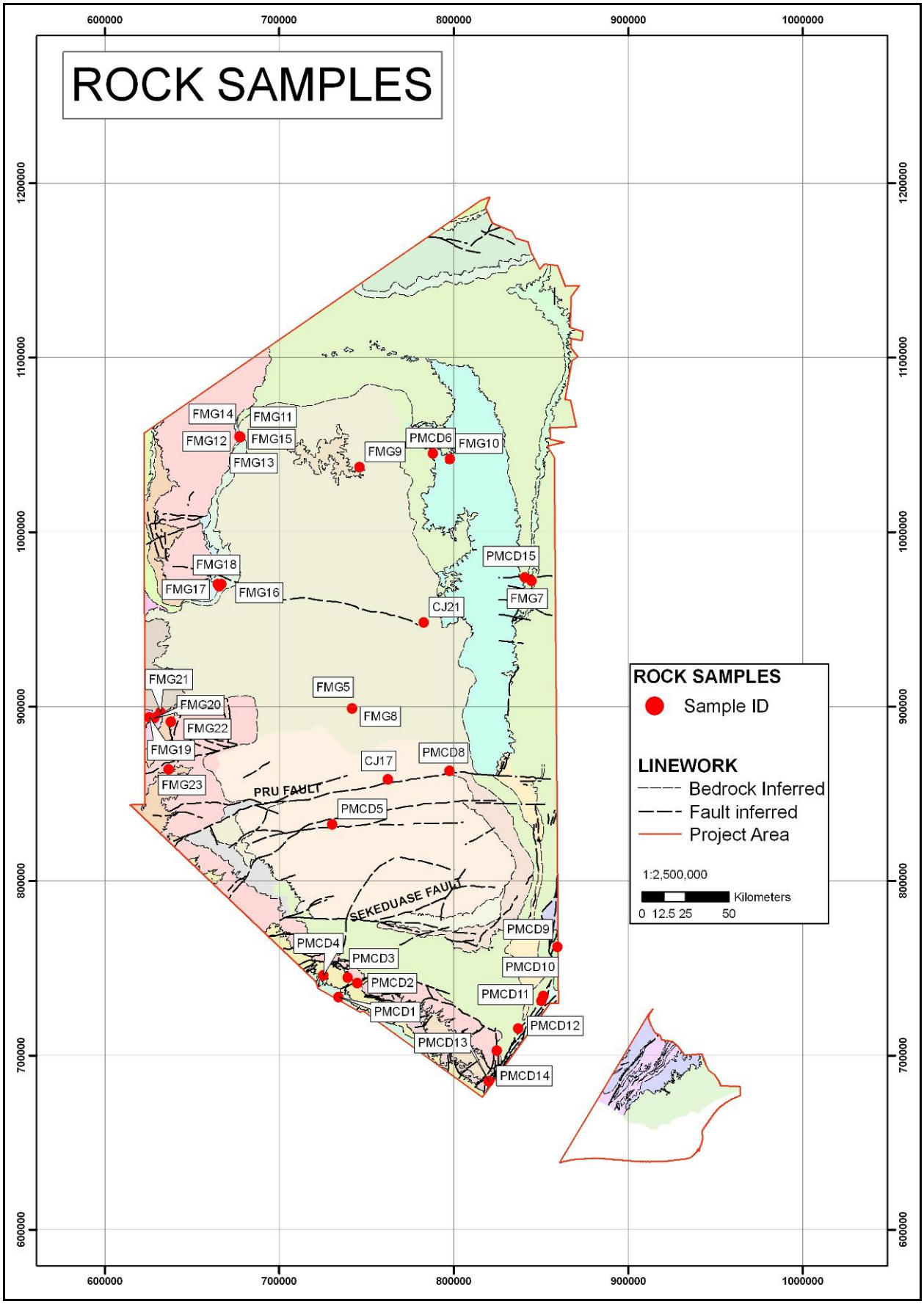

Figure 87 Locations of rocks sampled for further analysis.

5.24 ANALYSIS

The samples were initially crushed at the GSD (Figure 88) then analysed for multi-element signatures including gold.

5.24.1 Sample preparation

This was completed at the Geological Survey Department, in Accra. The rock samples were crushed and sieved to 100 grams of <75 microns in diameter in the new facility on site. The samples were then posted back to the BGS Keyworth office.

Figure 88 Sample preparation at the Geological Survey Department, Accra.

5.24.2 Geochemical Analysis

After a tendering process, the OMAC Laboratories Ltd., Co. Galway, Ireland was selected to carry out the analysis.

The samples were subject to Inductively Coupled Plasma with Optical Emission Spectroscopy / Mass Spectrometry (ICPOES/MS) Analysis after multi acid digestion (46 elements) and fire assay with lead collection and AA finish (for gold).

The combination of ICP OES and MS techniques is very useful for determining an extremely wide range of elements from major components to very low detection limits (typically sub ppb) with high accuracy and precision. It is a technique commonly used by exploration, geological and environmental organisations. Fire assay is considered the most reliable method for accurately determining the content of gold, silver, and platinum-group metals (except osmium and ruthenium) in ores or concentrates.

5.24.3 Results

Table 22 shows the gold fire assay results while Table 23 to Table 26 list the ICPOES/MS results.

SAMPLE ID	Auppb		Auppb Repeat	
pmcd1	-2			
pmcd2	-2			
pmcd3	-2			
pmcd4	13			
pmcd5	-2			
pmcd6	2			
pmcd8	-2			
pmcd9	-2			
pmcd10	-2			
pmcd11	-2			
pmcd12	-2		-2	*(48.50g)*
pmcd13	-2			
pmcd14	-2			
pmcd15	-2			
CJ17	-2			
CJ21	-2			
FMG5	-2			
FMG7	-2			
FMG8	-2			
FMG9	-2	*(44.00g)*		
FMG10	-2		6	*(48.00g)*
FMG11	-2			
FMG12	-2			
FMG13	-7	*(15.00g)*		
FMG14	-2			
FMG15	-2			
FMG16	-2			
FMG17	-2			
FMG18	-2			
FMG19	-2		-3	*(31.00g)*
FMG20	-11	*(9.00g)*		
FMG21	-3	*(31.50g)*		
FMG22	-2			
FMG23	-5	*(20.50g)*		

Table 22 Gold Fire assay results.

SAMPLE ID	Ag	Al	As	Ba	Be	Bi	Ca	Cd	Ce	Co	Cr	Cu
	ppm	%	ppm	ppm	ppm	ppm	%	ppm	ppm	ppm	ppm	ppm
pmcd1	<0.5	1.71	2.2	108	<1	<0.05	0.03	<0.02	3.8	1.7	48	16.6
pmcd2	<0.5	1.13	5.3	26	<1	<0.05	0.01	<0.02	12.0	1.3	38	8.8
pmcd3	<0.5	3.52	7.9	43	<1	<0.05	<0.01	0.06	70.1	7.4	31	16.7
pmcd4	<0.5	3.02	3.8	1340	1	<0.05	0.02	<0.02	65.2	14.6	64	7.3
pmcd5	<0.5	9.82	1.4	570	2	0.09	3.06	0.07	202.2	32.5	66	37.7
pmcd6	<0.5	7.56	4.8	505	3	0.10	1.32	0.06	75.4	15.0	94	35.7
pmcd8	<0.5	5.44	4.0	201	<1	0.14	0.07	0.03	80.0	9.8	82	33.1
pmcd9	<0.5	6.30	5.4	193	1	0.07	0.05	0.04	21.0	3.2	59	15.6
pmcd10	<0.5	2.77	0.9	444	<1	0.11	0.03	0.03	15.4	22.7	80	29.4
pmcd11	<0.5	2.19	0.3	211	<1	<0.05	0.11	0.03	17.2	2.3	55	16.9
pmcd11repeat	<0.5	2.21	0.5	210	<1	<0.05	0.11	0.03	18.5	2.2	56	16.8
pmcd12	<0.5	3.52	3.5	186	<1	0.06	0.02	0.07	56.9	1.3	28	10.3
pmcd13	<0.5	6.68	7.0	434	2	0.18	0.17	0.12	58.1	13.3	46	15.8
pmcd14	<0.5	3.65	1.1	796	1	<0.05	0.02	<0.02	32.9	2.8	37	11.5
pmcd15	<0.5	4.87	6.7	674	3	0.39	0.04	0.03	225.1	11.2	42	19.5
CJ17	<0.5	8.71	24.0	620	3	0.25	0.28	0.06	61.4	20.6	87	43.4
CJ21	<0.5	6.61	4.0	607	2	0.24	0.36	0.08	66.6	11.6	51	27.0
FMG5	<0.5	4.52	29.8	1444	3	0.19	0.05	0.04	158.2	226.0	98	61.0
FMG7	<0.5	8.70	7.6	581	3	0.28	0.18	0.05	61.0	14.7	76	37.5
FMG8	<0.5	4.73	3.6	1165	2	<0.05	0.46	0.06	80.9	26.2	33	18.5
FMG9	<0.5	5.66	5.0	347	2	0.17	0.16	0.04	79.8	14.8	56	25.0
FMG9repeat	<0.5	5.67	5.8	345	2	0.17	0.16	0.04	82.8	14.9	55	25.9
FMG10	<0.5	7.61	5.7	613	2	0.13	1.69	0.20	93.0	19.8	101	37.6
FMG11	<0.5	0.45	2.6	310	<1	<0.05	19.25	0.07	62.4	11.3	179	17.2
FMG12	<0.5	0.92	2.0	1049	1	<0.05	18.15	0.06	143.9	21.2	532	19.2
FMG13	<0.5	1.05	5.1	10556	2	<0.05	5.72	0.09	63.8	33.5	206	59.6
FMG14	<0.5	1.16	4.5	310	2	<0.05	13.63	0.11	141.7	38.7	555	24.6
FMG15	<0.5	1.73	3.3	17759	2	<0.05	9.70	0.08	133.8	53.0	543	70.7
FMG16	<0.5	0.76	3.4	1539	<1	<0.05	33.43	0.58	12.3	3.7	21	9.6
FMG17	<0.5	0.92	2.5	410	<1	<0.05	31.79	0.92	11.5	3.1	18	7.2
FMG18	<0.5	0.60	19.0	7796	1	<0.05	26.89	1.73	38.7	8.8	12	28.7
FMG19	<0.5	8.03	2.6	1472	1	0.18	0.32	0.05	83.7	4.3	73	7.5
FMG19repeat	<0.5	7.93	3.0	1437	1	0.18	0.29	0.06	77.2	4.3	62	6.9
FMG20	<0.5	1.25	2.1	142	<1	<0.05	0.07	0.02	39.1	1.8	44	60.4
FMG21	<0.5	7.43	14.2	685	3	0.51	0.45	0.08	50.5	12.2	43	50.9
FMG22	<0.5	6.81	2.8	1033	2	0.19	0.16	0.16	147.2	6.2	52	29.1
FMG23	<0.5	4.08	3.3	308	<1	0.06	1.69	0.09	50.9	3.3	24	47.3

Table 23 ICPOES/MS results 1.

SAMPLE ID	Fe	Ga	Ge	Hg	K	La	Li	Mg	Mn	Mo	Na	Nb
	%	ppm	ppm	ppm	%	ppm	ppm	%	ppm	ppm	%	ppm
pmcd1	1.42	5.1	0.7	0.03	0.31	1.9	<2	0.07	269	2.63	0.05	0.89
pmcd2	2.80	2.6	0.8	0.01	0.26	6.8	10	0.03	146	1.02	<0.01	1.06
pmcd3	10.20	6.4	0.9	0.02	0.55	19.4	17	0.12	2824	1.07	<0.01	2.82
pmcd4	3.02	10.7	0.9	0.02	1.25	31.4	<2	0.07	288	1.14	0.07	1.77
pmcd5	4.14	23.3	1.9	0.02	0.97	206.4	17	1.54	2182	0.54	1.74	8.86
pmcd6	4.55	19.4	1.7	0.02	1.03	34.7	26	1.22	1177	0.76	2.15	10.27
pmcd8	4.97	14.3	1.5	0.02	0.55	21.1	11	0.21	743	1.42	0.02	8.85
pmcd9	7.85	14.2	1.3	0.02	0.79	13.8	10	0.23	202	1.82	0.02	5.31
pmcd10	2.21	6.8	1.1	0.02	0.60	6.2	20	0.20	2664	2.19	0.28	1.98
pmcd11	1.22	6.1	1.0	0.02	0.77	9.4	9	0.17	351	1.39	0.28	1.86
pmcd11repeat	1.21	6.1	1.0	0.02	0.77	10.0	9	0.17	348	1.35	0.28	1.90
pmcd12	1.67	8.8	1.2	0.01	1.31	29.5	12	0.17	93	1.01	0.01	4.03
pmcd13	4.62	20.3	1.5	0.01	2.36	27.4	35	1.36	576	0.38	1.19	8.61
pmcd14	3.50	8.6	1.2	0.03	3.41	16.5	3	0.06	212	0.93	0.08	3.82
pmcd15	19.04	18.0	1.8	0.03	1.99	161.1	11	0.15	312	1.53	0.01	4.56
CJ17	4.52	25.1	2.1	0.02	2.55	30.2	45	1.59	1088	0.57	0.74	11.18
CJ21	3.07	16.8	1.9	0.02	1.84	27.9	40	0.82	3282	0.35	1.91	10.84
FMG5	16.18	15.7	1.3	0.02	0.57	16.4	29	0.19	11086	3.55	0.02	15.99
FMG7	4.62	25.9	2.1	0.01	2.54	58.5	39	1.22	636	0.30	0.80	13.45
FMG8	2.04	10.8	1.5	0.03	1.07	31.2	15	0.26	3607	0.65	1.17	4.21
FMG9	3.16	15.6	1.7	0.02	0.98	39.3	34	0.31	636	0.78	0.08	18.47
FMG9repeat	3.17	15.8	1.6	0.03	0.98	39.4	34	0.31	632	0.81	0.08	18.45
FMG10	4.78	22.9	2.0	0.02	1.08	79.5	26	1.29	2309	0.88	2.12	11.92
FMG11	2.98	3.4	0.6	0.04	0.16	35.3	6	8.42	2928	0.36	0.02	28.48
FMG12	6.38	7.4	1.6	0.04	0.33	75.5	7	7.50	2714	0.40	0.02	18.12
FMG13	7.03	8.7	1.3	0.02	0.34	33.0	14	2.83	3519	1.79	0.05	35.01
FMG14	7.46	11.8	1.4	0.05	0.48	79.1	11	6.89	2505	0.65	0.03	20.95
FMG15	8.61	13.2	1.1	0.04	0.04	69.5	94	7.17	1740	0.56	0.03	12.68
FMG16	0.53	4.8	0.2	0.03	0.27	7.2	3	0.26	858	0.22	0.04	0.98
FMG17	0.56	2.9	0.2	0.03	0.27	7.1	3	0.38	710	0.13	0.03	2.23
FMG18	2.12	6.3	0.3	0.05	0.15	43.4	3	4.34	2572	10.40	0.05	0.84
FMG19	2.44	15.9	1.3	0.06	5.85	37.7	5	0.41	147	0.65	0.11	11.43
FMG19repeat	2.42	16.4	1.3	0.03	5.76	35.6	5	0.40	141	0.51	0.11	10.81
FMG20	0.81	3.3	0.8	0.04	0.26	18.1	7	0.04	195	1.14	0.04	1.50
FMG21	4.21	22.4	2.6	0.03	2.84	39.7	28	1.31	683	0.81	1.58	9.78
FMG22	1.29	17.8	1.6	0.04	5.10	67.5	9	0.37	507	0.49	0.12	19.06
FMG23	0.91	8.2	0.9	0.03	0.11	23.6	6	0.07	674	0.59	0.01	5.70

Table 24 ICPOES/MS results 2.

SAMPLE ID	Ni	P	Pb	Rb	Re	S	Sb	Sc	Se	Sn	Sr	Ta
	ppm	%	ppm	ppm	ppm	%	ppm	ppm	ppm	ppm	ppm	ppm
pmcd1	15.3	0.003	1.1	11.6	0.002	<0.01	0.13	2.1	0.9	0.2	19	<0.05
pmcd2	8.4	0.020	3.5	13.1	0.002	<0.01	0.28	1.2	0.8	0.3	15	0.08
pmcd3	16.7	0.011	13.9	23.1	<0.002	<0.01	0.40	5.5	1.1	0.6	21	0.22
pmcd4	26.5	0.018	14.6	50.8	<0.002	<0.01	0.45	5.5	0.8	0.5	133	0.14
pmcd5	47.2	0.076	12.7	44.7	0.002	<0.01	0.29	15.4	1.0	1.2	354	0.74
pmcd6	115.7	0.099	10.8	47.7	0.002	<0.01	0.35	14.9	1.0	1.3	228	0.84
pmcd8	27.1	0.011	15.9	52.1	0.002	<0.01	0.54	5.8	1.0	1.1	17	0.66
pmcd9	13.5	0.024	11.6	49.9	<0.002	<0.01	0.70	5.1	1.5	0.8	35	0.43
pmcd10	40.6	0.012	42.5	31.1	0.002	<0.01	0.16	3.7	0.7	0.5	23	0.14
pmcd11	18.2	0.055	5.4	37.8	0.002	<0.01	0.12	1.7	0.5	0.4	29	0.15
pmcd11repeat	17.6	0.056	5.3	37.2	<0.002	<0.01	0.09	1.7	0.5	0.4	33	0.16
pmcd12	8.4	0.019	15.7	65.9	0.002	<0.01	0.50	2.9	0.8	0.7	28	0.32
pmcd13	26.8	0.049	43.8	133.0	0.002	<0.01	0.54	8.8	0.6	2.2	52	0.78
pmcd14	16.3	0.032	19.0	145.7	<0.002	<0.01	0.21	1.5	<0.5	0.7	63	0.35
pmcd15	39.9	0.074	88.6	99.9	0.004	<0.01	3.46	8.0	0.6	0.8	114	0.47
CJ17	103.7	0.072	14.5	153.7	0.002	<0.01	0.85	14.8	0.6	2.0	75	0.83
CJ21	40.0	0.093	22.1	108.9	0.002	<0.01	0.75	8.8	0.6	1.8	101	0.86
FMG5	55.2	0.024	110.9	45.1	0.004	<0.01	1.72	6.8	0.9	1.3	16	1.14
FMG7	53.1	0.036	16.6	148.4	0.004	<0.01	1.00	13.7	0.6	2.2	72	1.07
FMG8	17.6	0.014	25.3	52.0	<0.002	<0.01	0.24	5.7	<0.5	0.6	68	0.32
FMG9	23.9	0.035	16.2	83.9	<0.002	0.02	0.45	10.2	0.7	1.5	51	1.29
FMG9repeat	24.2	0.035	16.6	85.0	<0.002	0.02	0.46	10.0	0.8	1.5	52	1.33
FMG10	54.3	0.117	12.5	47.6	0.002	<0.01	0.42	16.2	0.8	1.4	219	0.93
FMG11	158.0	0.069	4.9	10.4	<0.002	<0.01	0.12	3.6	<0.5	0.3	94	1.68
FMG12	308.7	0.211	12.4	21.5	0.002	0.03	0.17	7.5	0.5	0.6	107	1.47
FMG13	259.1	0.083	9.2	23.1	0.002	0.27	0.49	4.3	<0.5	0.6	65	2.59
FMG14	467.4	0.158	15.6	29.5	0.002	0.01	0.13	9.5	<0.5	0.9	88	1.70
FMG15	430.7	0.114	15.5	3.0	0.004	0.50	<0.05	9.7	<0.5	0.9	409	1.08
FMG16	9.1	0.055	3.4	13.3	0.004	0.06	<0.05	1.4	<0.5	<0.2	82	<0.05
FMG17	11.9	0.067	2.1	13.0	0.004	0.01	0.10	1.7	<0.5	<0.2	58	0.12
FMG18	21.8	0.426	13.3	8.1	0.002	0.22	0.69	1.9	0.7	<0.2	142	0.07
FMG19	15.9	0.052	19.8	254.2	<0.002	<0.01	0.71	5.8	<0.5	2.0	148	1.10
FMG19repeat	14.4	0.048	19.9	252.3	<0.002	<0.01	0.68	5.2	1.0	2.0	143	1.04
FMG20	14.6	0.012	9.9	14.9	0.002	<0.01	0.24	1.3	0.6	0.4	33	0.10
FMG21	51.9	0.054	23.1	144.1	0.004	<0.01	1.67	12.0	0.7	1.7	136	0.71
FMG22	13.1	0.034	27.5	224.2	0.004	<0.01	0.87	8.8	0.9	2.5	96	1.50
FMG23	8.0	0.197	35.6	6.5	0.002	0.02	0.30	3.5	0.8	0.6	76	0.40

Table 25 ICPOES/MS results 3.

SAMPLE ID	Te	Th	Ti	Tl	U	V	W	Y	Zn	Zr
	ppm	ppm	ppm	ppm	ppm	ppm	ppm	ppm	ppm	ppm
pmcd1	<0.05	0.5	365	0.09	0.2	26	0.6	0.9	9.6	9
pmcd2	<0.05	2.1	438	0.09	0.7	19	0.1	3.8	33.7	82
pmcd3	<0.05	6.7	911	0.13	2.1	29	0.2	12.4	139.3	207
pmcd4	<0.05	5.4	1083	0.33	0.6	60	1.0	6.0	14.2	91
pmcd5	0.11	10.3	5035	0.29	1.7	83	0.7	51.9	75.5	91
pmcd6	0.10	12.1	5418	0.23	1.2	112	0.7	58.3	107.4	102
pmcd8	<0.05	8.5	3146	0.28	1.5	100	0.7	8.5	29.2	121
pmcd9	0.06	5.9	1957	0.28	1.3	90	0.5	6.7	17.4	147
pmcd10	<0.05	2.0	881	0.22	0.4	28	0.4	2.9	26.3	37
pmcd11	<0.05	2.8	732	0.19	0.6	19	0.4	4.1	25.3	76
pmcd11repeat	<0.05	3.2	787	0.16	0.7	18	0.4	4.2	26.0	84
pmcd12	0.06	13.5	1403	0.36	2.5	23	0.5	24.8	13.9	460
pmcd13	0.07	12.0	3389	0.73	2.8	64	1.2	17.8	115.5	190
pmcd14	<0.05	9.1	1104	0.70	1.3	25	0.2	7.2	18.2	73
pmcd15	0.05	18.4	1571	0.57	3.7	330	2.6	17.6	49.6	135
CJ17	0.11	10.1	4490	0.67	1.9	111	1.5	31.6	132.5	132
CJ21	0.06	14.1	4121	0.54	2.4	65	1.6	20.5	79.2	241
FMG5	0.17	9.9	6038	0.66	3.3	250	1.7	7.7	19.9	126
FMG7	0.08	13.0	5192	0.82	2.4	109	1.8	27.1	106.5	182
FMG8	<0.05	6.7	1681	0.42	1.8	37	0.5	16.5	24.3	200
FMG9	<0.05	14.2	5960	0.43	2.8	76	1.7	19.5	25.2	165
FMG9repeat	<0.05	13.9	5829	0.46	2.8	76	1.7	19.5	25.2	161
FMG10	0.11	13.5	6459	0.25	2.7	126	1.1	41.0	92.8	143
FMG11	0.76	2.6	3878	0.10	0.9	50	0.3	3.1	42.1	42
FMG12	0.77	9.0	10229	0.11	2.4	63	0.1	5.9	103.4	73
FMG13	0.22	4.0	5630	0.13	3.9	338	0.3	4.8	60.7	74
FMG14	0.67	9.8	16389	0.13	3.9	167	<0.1	8.2	222.7	138
FMG15	0.51	11.6	15898	0.05	3.8	120	<0.1	8.5	108.2	142
FMG16	0.42	0.8	329	0.07	0.4	26	<0.1	5.2	13.4	12
FMG17	0.42	1.0	585	0.06	0.4	17	0.2	5.6	17.7	16
FMG18	0.59	0.9	274	0.16	1.5	45	0.2	56.0	101.6	9
FMG19	0.06	24.1	3743	1.38	3.5	36	1.1	24.5	40.4	313
FMG19repeat	0.06	21.5	3616	1.37	3.4	37	1.1	24.2	41.3	310
FMG20	<0.05	1.7	611	0.18	1.0	16	0.3	4.4	35.9	63
FMG21	0.10	9.6	4309	0.60	1.9	85	2.0	18.8	105.9	151
FMG22	0.16	39.4	8638	1.19	7.6	64	1.2	71.6	42.1	1046
FMG23	0.07	5.7	1365	0.39	1.3	20	0.3	10.5	36.6	147

Table 26 ICPOES/MS results 4.

Au

As discussed previously, the only gold sampled was from the basal conglomerates in the south of the study area (Figure 89), with sample *PMCD4* having a result of 13ppb. This is an indication of movement of gold within these basal conglomerates and should be followed up to locate outcrop and favourable channels where gold might collect.

Ba

Two samples displayed high barium results, FMG13 and FMG15, showing 1.1% and 1.7% respectfully. Both of these were from the Daboya area. As reported in the phase one report (Jordan et al., 2006), Daboya has been investigated, by various government bodies in the past, which located barite values up to 20%.

Fe

As the study area has extensive laterite deposits it would be expected that some samples might display raised or very deficient iron content. The laterite that was sampled, FMG5, had a value of 16.2% Fe. This is significant but not likely to be economic. The highest Fe sampled was from sample pmcd15, described as sandstone with a 1.5cm veinlet of hematite (possibly some magnetite). This contained 19% Fe.

P

The highest phosphorous content, 0.5% was recorded in the limestone from the Buipe trail quarry, from sample FMG18. This is low; however, this is an indication of the prospectivity of the Kodjari Formation to host phosphate deposits.

Ti

There are three samples, taken from the Kodjari formation, FMG12, FMG14 and FMG15 that have raised Ti, showing values of 1.0%, 1.6% and 1.6% respectfully. This is due to the collection of heavy minerals, likely to be rutile and ilmenite, within the limestone, as a result of erosion of an igneous complex. Significantly, a high Fe content, likely to be magnetite related, as indicated by the raised magnetic susceptibility, is measured at these locations. The nature of the intrusion is uncertain, however, high Ti values can be associated with kimberlites, possibly explaining some of the alluvial diamonds recorded in the Volta Basin. Within these samples there is also high chromium, again associated with kimberlites.

Figure 89 The subcrop of the basal conglomerate.

5.25 GROUND GAMMA SPECTROMETER

As part of the second phase of field work, a hand held gamma-ray spectrometer was used to obtain the total count, uranium, potassium and thorium from field locations. This tool acted as a ground follow up of anomalous uranium values indicated in the airborne radiometrics.

The instrument used was the GRM-260 gamma-ray spectrometer, which is designed for field operation to determine the radionuclides in rocks soil and water. The instrument is based on the capture of emitted gamma quanta from the source in the meter by the sample or outcrop. Radioactivity in rocks is caused by one or more of the three natural sources in rocks, potassium (^{40}K), Thorium (^{232}Th) or Uranium (^{238}U). The GRM-260 gamma-ray spectrometer measures the K fraction directly but indirectly measures the U fraction as ^{214}Bi and the Thorium fraction as ^{208}Tl. The readings measured are displayed in Figure 90.

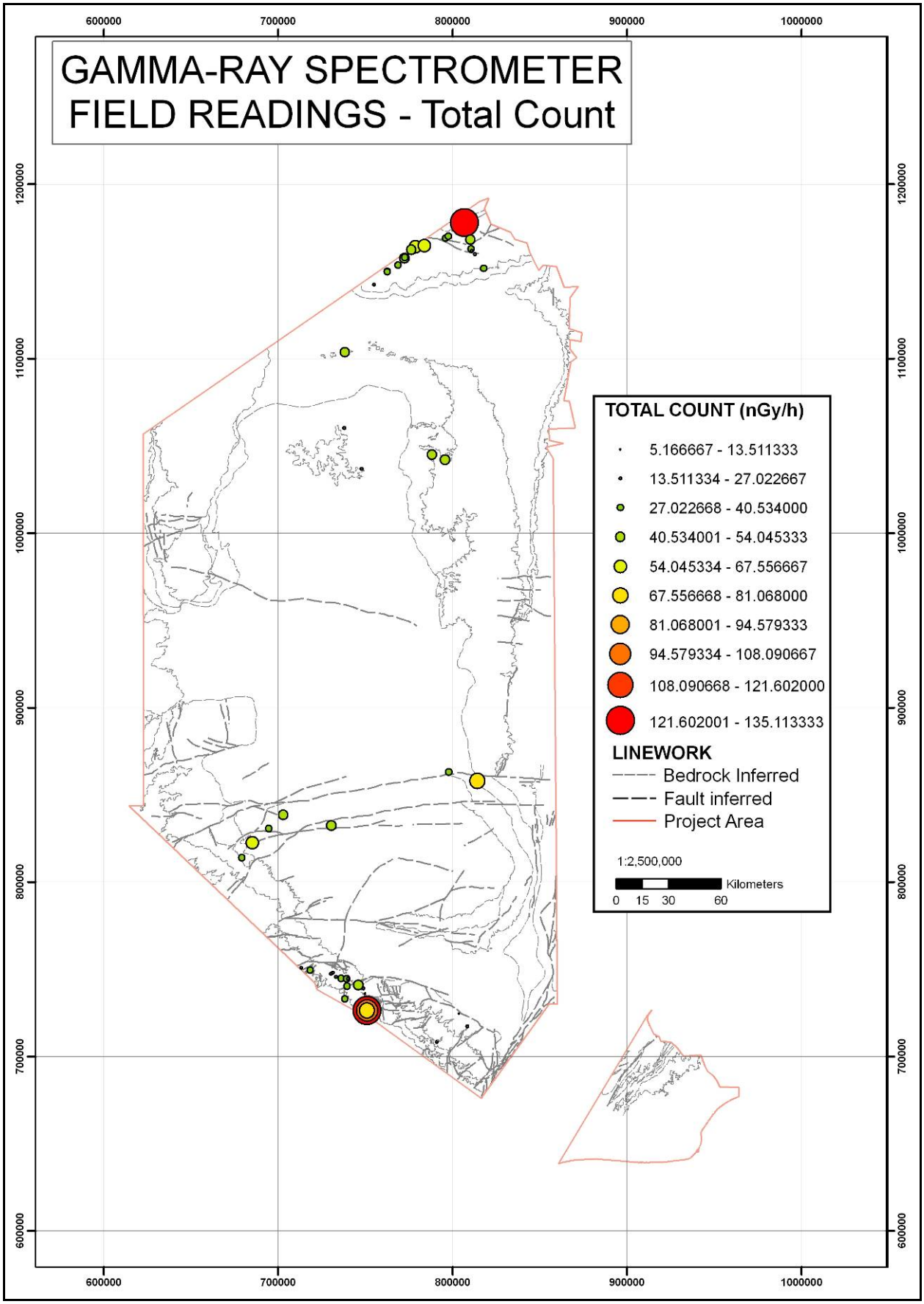

Figure 90 Total count Gamma-Ray spectrometer results.

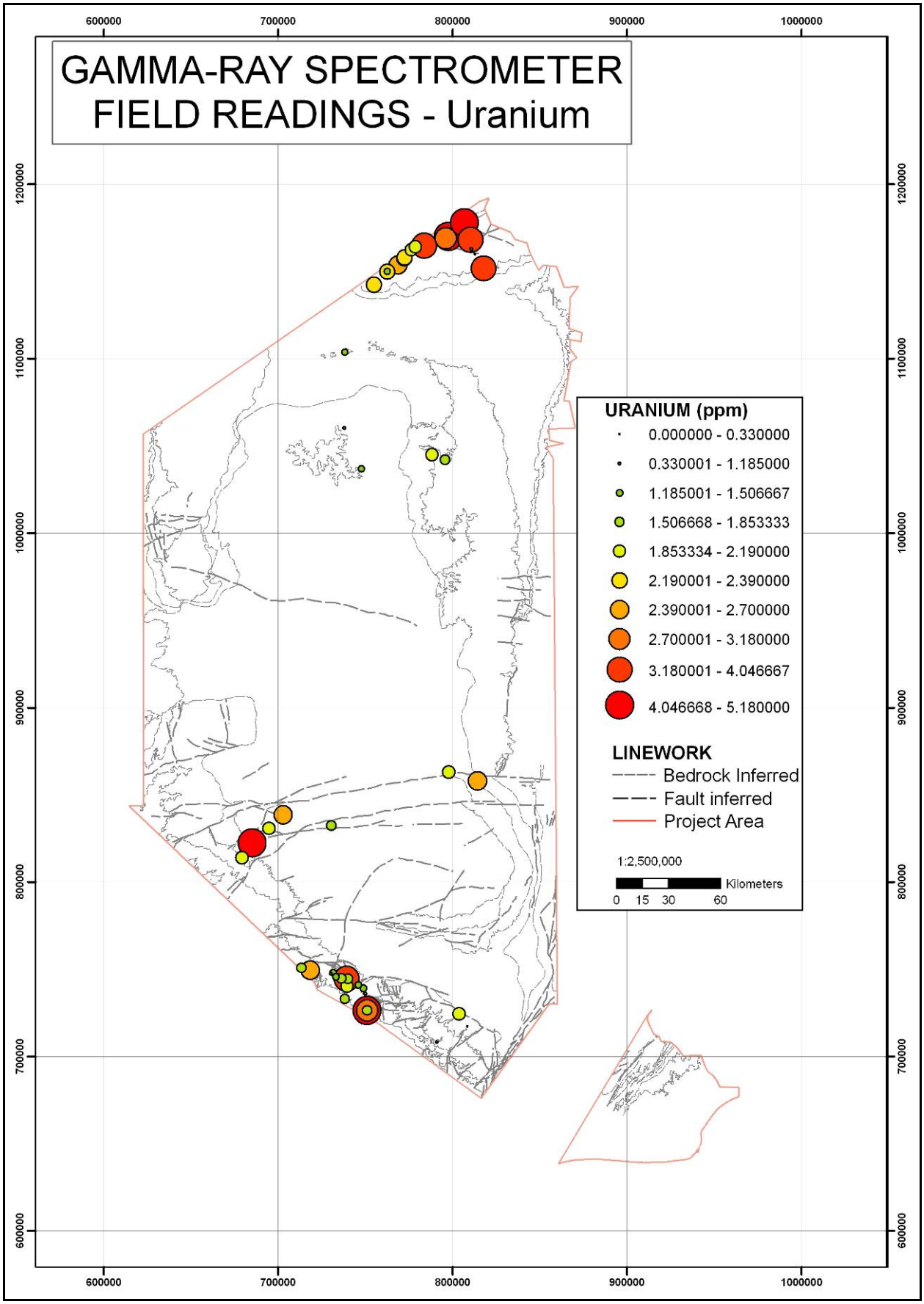

Figure 91 Uranium Gamma-Ray spectrometer results.

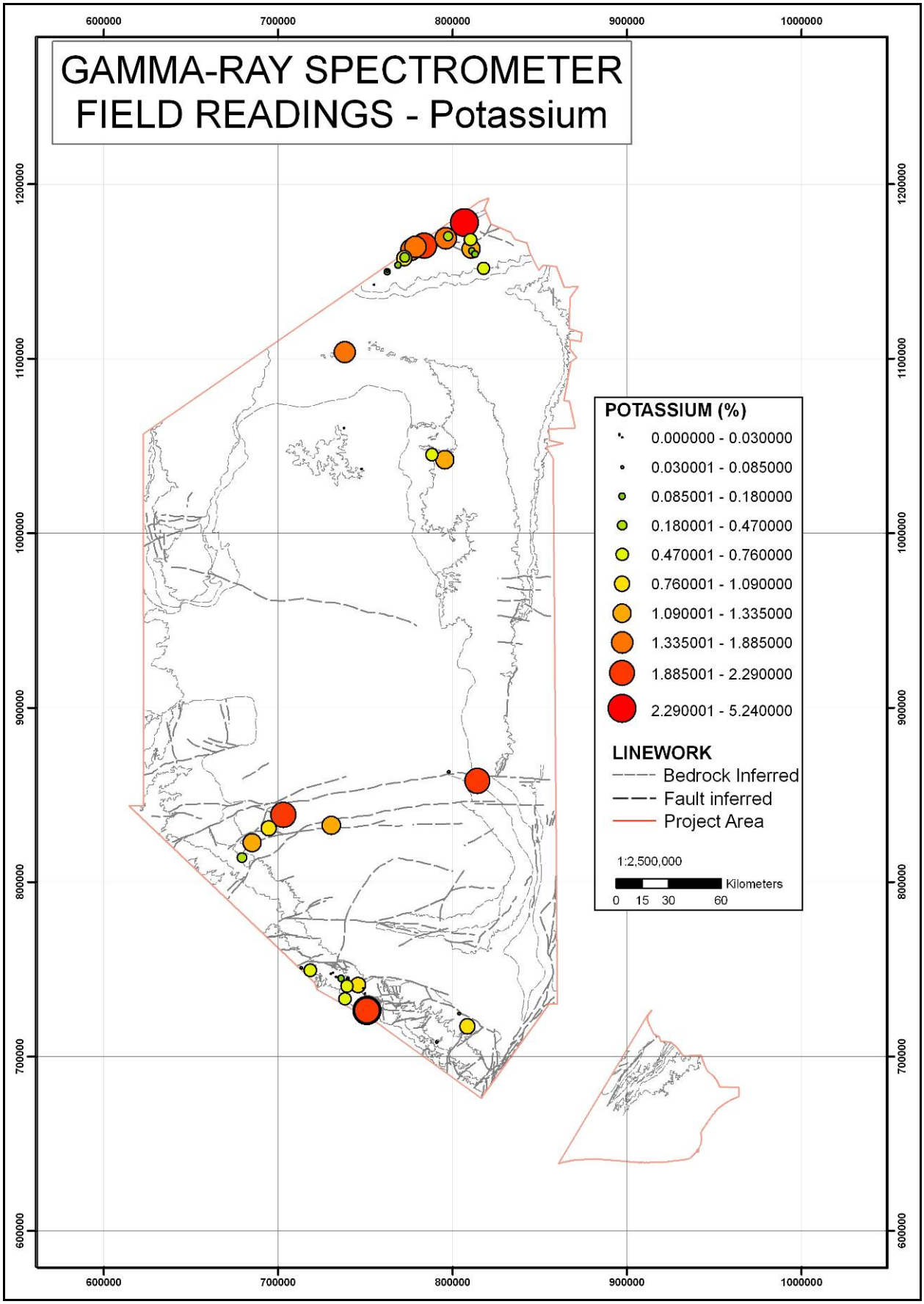

Figure 92 Potassium Gamma-Ray spectrometer results.

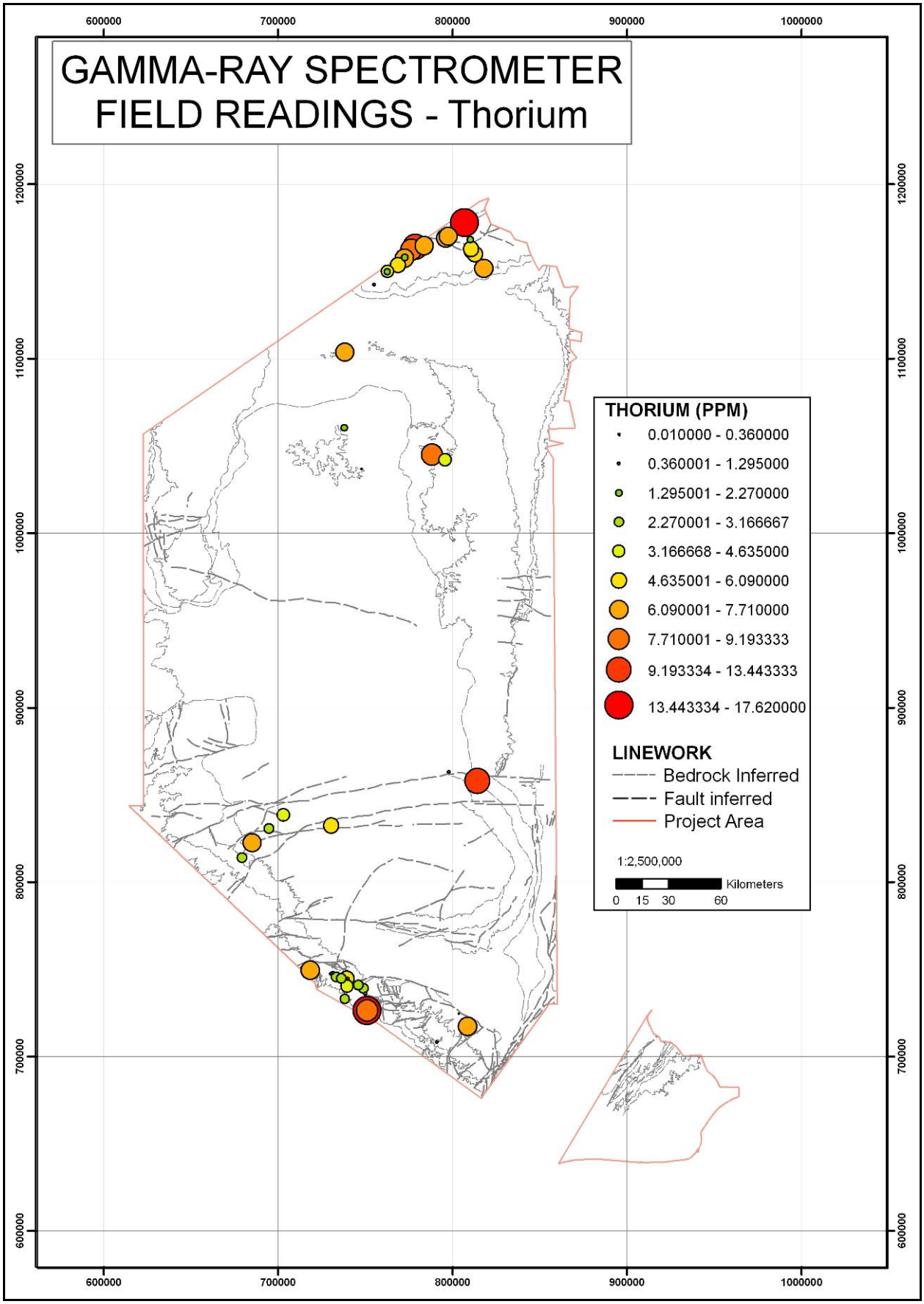

Figure 93 Thorium Gamma-Ray spectrometer results.

5.26 CONCLUSIONS

The previous Sections document prospectivity modelling over the Volta Basin, Ghana, for gold, uranium and phosphates. The data used was the newly acquired geological mapping and airborne geophysics.

The prospectivity models are limited and could be improved with additional data and interpretation.

5.27 GOLD

Locating gold in the Volta basin would be a very important discovery in terms of improving the economic potential of the area. The modelling applied was limited to structural related deposit and did not apply to other, stratigraphical related, deposits such as placers.

Primary deposits: There is potential for primary gold deposits to occur in the Volta basin, as there has been a very significant tectonic event to the east, in the form of the Pan African. Fluids may have remobilised gold from the basement into structures in the cover sediments.

Secondary deposits (placers): A systematic stream sediment with panning survey is a proven way to locate these deposits. However, in the case of the basal conglomerates, systematic mapping of the geology, could be used to determine localities where heavy mineral paleotopographic traps would occur. This could be followed up with an extensive sampling program of soils over the mapped lithologies, and where applicable, outcrop lithogeochemical sampling.

Other areas highlighted in the prospectivity maps should be followed up with additional stream sediment sampling / panning, as well as prospecting to locate areas of mineralisation.

5.28 URANIUM

Areas highlighted in the prospectivity maps should be followed up with additional stream sediment sampling / panning, as well as prospecting to locate areas of mineralisation. Further focused ground Gamma Spectrometry may assist in the location of uranium concentrations.

5.29 PHOSPHATE

Follow up some of the areas highlighted in the modelling specifically those within the favourable geology. Additionally, systematic outcrop lithogeochemical sampling should be utilised to identify areas of increased phosphate.

5.30 DIAMONDS

There are a number of diamonds that have been located in the Volta basin, making the area prospective for alluvial diamonds, if not primary diamonds. The two major structures seen in the basement (Figure 84) may indicate possible environments for kimberlite emplacement. The high Ti and Cr values seen in a number of samples (from the Kodjari Formation) may be an indication of kimberlites; however, these are also indicative of all alkaline intrusions. Systematic sampling of this stratigraphy with a microscopical search for diamonds and diamond indicator minerals should be undertaken.

6 Map Production

The map products consist of 1:100,000 scale topographic and preliminary interpretative geological maps which were delivered in paper and digital form at the end of Phase 1, along with 1:250,000 scale geological maps delivered at the end of the project. The 1:100,000 scale topographic and geological maps were produced by BGS, while the final 1:250,000 geology maps were produced by Fugro, using a combination of geophysical interpretations and updated BGS linework.

Forty-nine 1:100,000 sheets are required for complete coverage of the project area. The map production process for both of these outputs is outlined below. The complete GIS and associated Geodatabase from which the maps were derived, along with PDF versions of the maps and hardcopy prints were delivered to the GSD at the end of Phase 1. The BGS did not produce formal hardcopies of the subsequent 1:250,000 geology maps, but we provided our updated GIS (with linework appropriate to publication at 1:250,000 scale) to Fugro and to the GSD, as contractually agreed.

To clarify the Ghanaian department names in an effort to avoid confusion below, the Geological Survey is officially called the Geological Survey Department (GSD) while the 'ordnance survey' is called the Ghana Survey Department; in this text the Geological Survey Department is abbreviated to GSD and the Ghana Survey Department is abbreviated to the Survey Dept.

6.1 TOPOGRAPHIC MAPS

Digital topographic data from the Survey Dept formed the basis of our 1:100,000 outputs. The Survey Dept maps were updated with information concerning infrastructure such as roads, railways and airstrips, and cultural features such as towns / villages where appropriate using information visible on the satellite imagery and data from the dGPS survey. The GSD already had some topographic data, in DXF format (probably from a CAD original) and the additional data required for the project were obtained in Arc Interchange format by BGS staff on a visit to the Survey Dept.

The Survey Dept 1:100,000 topography sheets are numbered in a system based on their latitude and longitude. For example 0601 has a lower left corner coordinate 06°N and 01°W. Each degree square is split into 4 quadrants; A, B, C and D. The quadrants cover the NW, NE, SW and SE respectively. There are four quarter-degree tiles in each quadrant, numbered 1, 2, 3 and 4 and covering the NW, NE, SW and SE quadrants respectively.

The GSD reports and maps cover the same areas as the Survey Dept sheet areas but have their own naming and numbering index system. The GSD numbers start in the south and increase northwards. For example the Survey Dept half-degree square covered by 0601A sheets 1, 2, 3 and 4 is called Abetifi by the GSD (Figure 94). Survey Dept sheets 0601A 1, 2, 3 and 4 represent GSD sheets 135, 136, 133 and 134 respectively. GSD Bulletins cover the individual sheets and there are 1:100,000 maps for some of these. The GSD quarter-degree numbering system only covers those sheets south of the 7°30' line of latitude. North of that the GSD uses either half-degree or full degree squares and maps for these sheets are at 1:250,000 or larger scales.

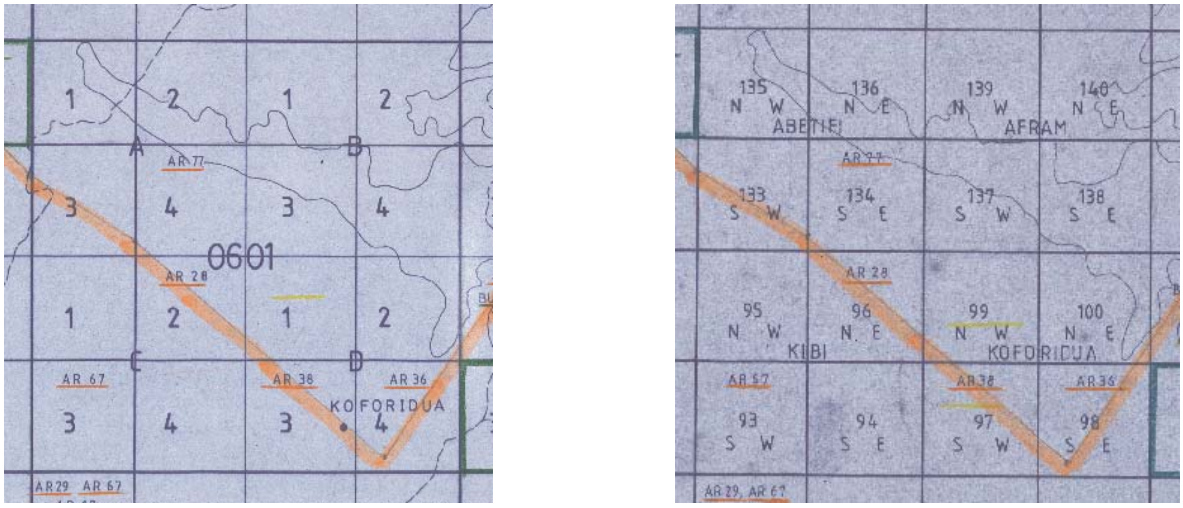

Figure 94 Survey Dept 1:100k numbering (left); GSD numbering and naming (right).

The Survey Dept topographic data for each quarter degree square was provided to BGS as DXF files compressed in zipped format. Unfortunately we received no hard copies or scans of the printed 1:100,000 Survey Department maps to see the layout style the Survey Dept uses. The DXF files were transformed into shapefiles, with a folder for each of the layer type. These layers are named cult_pol, cultural, forest, hydro, hypso, landform, neat, sd50k, text, transport and utility. Only one sheet remained unavailable, 0900A, and our counterparts were requested to obtain this from the Survey Dept in June 2006.

It is important to note that many of the sheets have no layers for certain features, either because there those features are absent in that sheet area or because that information in unavailable. For example there are many areas with no utility layer. This is possibly because there are no electricity supply lines or pipelines in those areas.

An ArcGIS MXD project file was created and all the separate layers were added, still in their original Accra Ghana coordinate system. Subsequently all the data from all the individual sheets were merged into one shapefile for each of the feature types required on the final maps. Some of the feature types had point, line and polygon features and others only had one or two of these. For example in the hydro layer we used the polylines that included the watercourses and initially considered using the polygons that included the marsh and flood land areas. The merged data were then reprojected into the UTM projection using the agreed three-parameter transformation of dx = -199, dy = 32 and dz = 322.

The next task was to check the quality of the merged shapefiles by looking at the data in situ and the attribute tables. Some amendments were required to attribute the data:

- In the transport polyline files the track and trail attributes were a different naming convention for the same type of feature.
- The Neatline and SD50k data are only sheet boundaries for survey department sheets and was not used.
- We did not need the hypso polyline and polygon layers, as we used the contours derived from the DTM on the final maps.
- Merged all the other layers; cult_poly, cultural, forest, landform, text, transport and utility but did not use the landform data as the coverage was not consistent across the area.
- Gave these merged files names such as Hydro_Polyline_merge_utm30.shp

Ground control points that were collected in WGS84 UTM format during the differential GPS survey were used to corroborate the locational accuracy of the transformed vector linework (as well as the elevation accuracy of the DTM). Figure 95 illustrates a selection of control points collected at road junctions in the Afram Plains area showing correlation with the GPS control points.

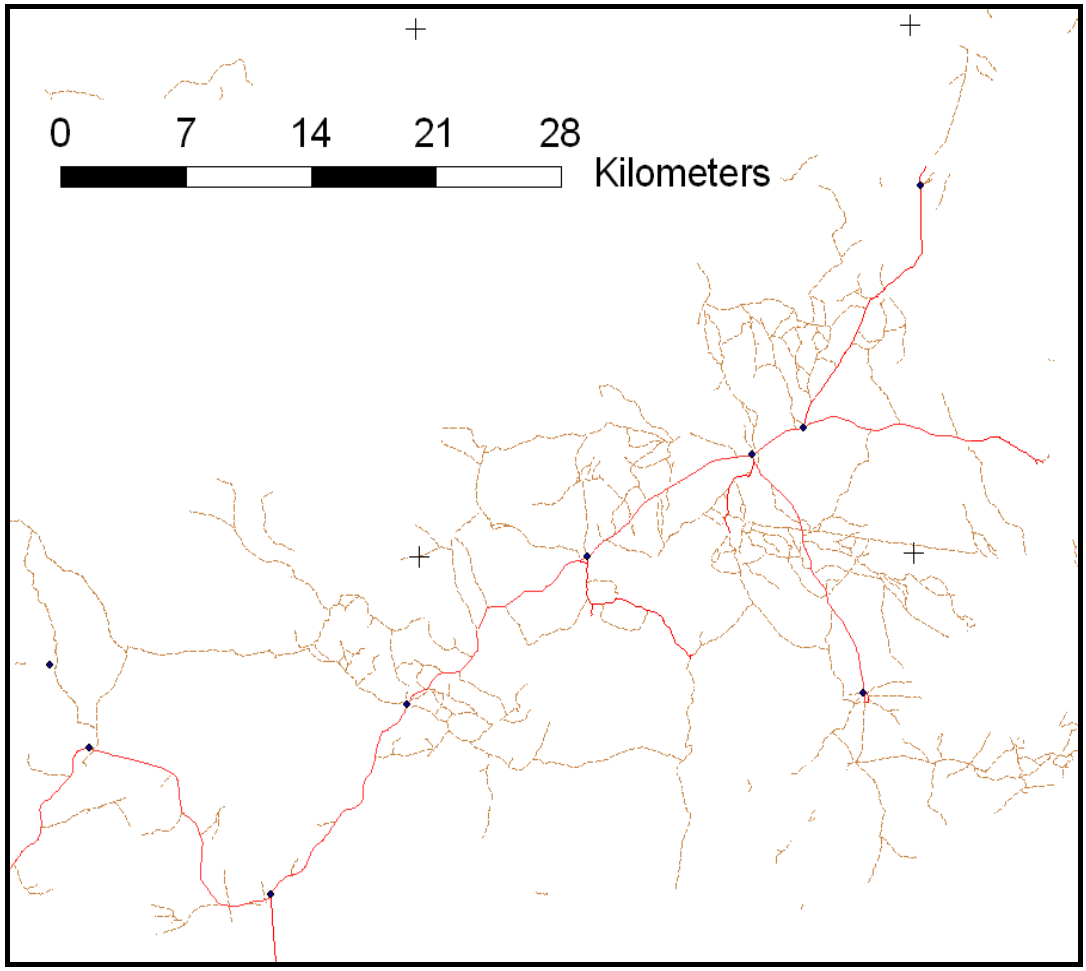

Figure 95 Example of differential GPS points overlaid onto topographic data.

As the text for all of the features was stored in the text point file there were two labelling options. The first was to add labels automatically and then move the point feature to the correct position so that the labels are correctly positioned at 1:100,000 scale. The second was to add the labels, save them as an annotation layer and then edit their positions. The first option was the most efficient and therefore the one chosen for this project.

There were several challenges to overcome with the data. In several layers there were features along the map boundary called Neatline that had to be deleted. In the hydro polygon file we had hoped to use the polygons for Marsh and Floodland areas but these when the polygons were compared to the polyline layer it became evident that not all the areas bounded by Marsh or Floodland lines had been polygonised on the polygon layer. Shoreline and coastline features in the polylines file were required as boundaries of geological polygons. However not all the shoreline or coastline features were large enough to have colour fill at 1:100,000 and these were deleted. Small dams that were too small to be distinguished against the geology were reattributed as SmallDam. The shoreline and coastline features were checked and made contiguous by renaming any parts that had been attributed wrongly. They were then saved out as new shapefiles for merging with the geology linework. The component layers for the 1:100,000 topographic maps are outlined in the Appendices.

All the new main and minor roads that could be distinguished on the satellite images were digitised and merged with the existing database to update, correct or replace existing data where appropriate. Furthermore, the existing cultural layer contained individual buildings which could not be shown at 1:100,000 so this layer was edited and a new village symbol was added where appropriate. The Ghana Survey maps were used as a guide to this new set of topographic maps, with the addition of some extra features from the remote sensing imagery where suitable. The final legend is shown below (Figure 96).

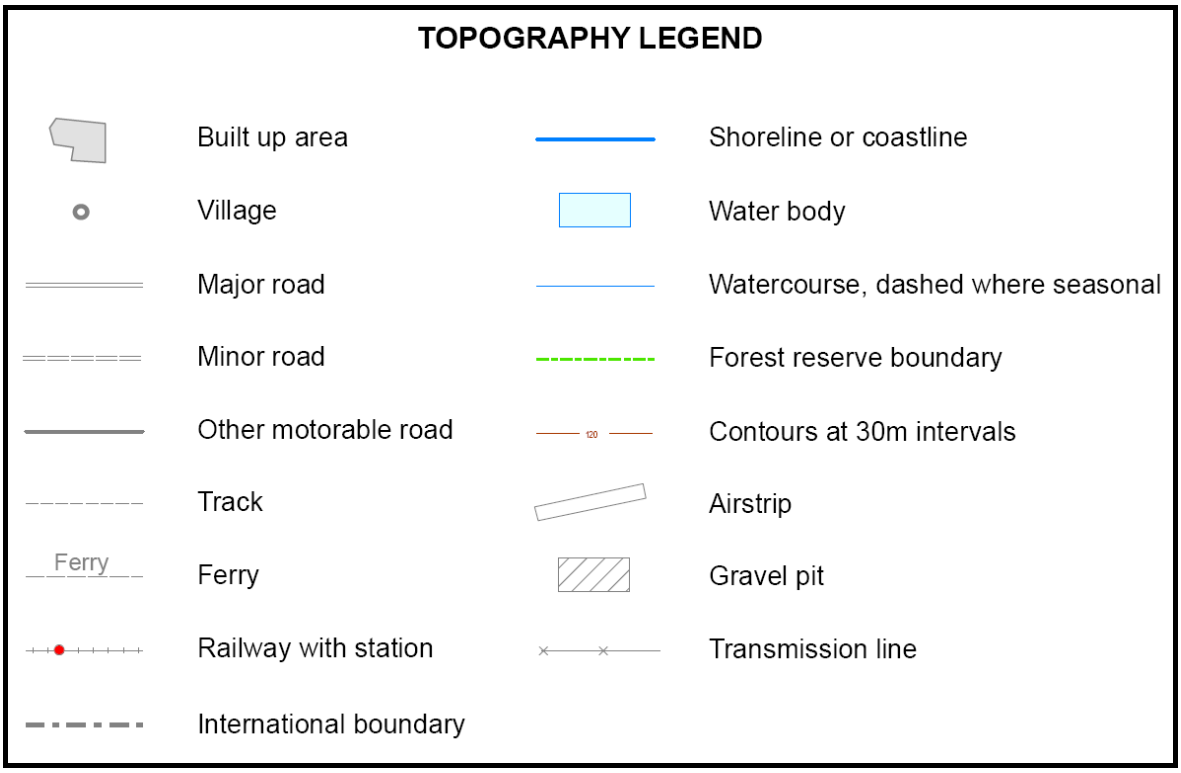

Figure 96 1:100,000 topographic map legend.

The contours were created at 30m intervals, as specified in the contract. They were derived from a DTM with a 50m x,y resolution and a vertical accuracy of 16m. Contours less than 700m in length were removed as they were too small to show at 1:100000 scale, while contour values are only shown on contours greater than 1500 metres in length.

6.2 PRELIMINARY INTERPRETATIVE GEOLOGICAL MAPS

It is very important to note that the 1:100,000 scale geological maps (produced in the first year of the project) represented a preliminary geological interpretation and they cannot be considered to be geological maps in the conventional sense. The prime reason for this is that the maps were derived from initial interpretations of remotely sensed data, augmented by information from limited reconnaissance fieldwork and further interpretation, rather than conventional mapping. The field reconnaissance consisted of two teams covering 98,000km^2 in four weeks, so while every effort was made to check the geological/geomorphological interpretations as well as the information on the mineral occurrence database, much of the area could not be visited for reasons of time limitations and access logistics. A second period of fieldwork (also with two teams for 4 weeks) was used to update the geological model and linework before the revised GIS was supplied to Fugro for the production of the 1:250,000 geological maps.

As noted previously, the geological / geomorphological interpretation of the remote sensing imagery was conducted digitally by geologists using ‘heads-up’ digitising via a BGS customised interface to ESRI ArcGIS. This linework was checked and enhanced in the field where time and

access allowed, followed by further interpretation of the remote sensing imagery on return from the field. Subsequently cartographers and specialist GIS staff cleaned and enhanced the linework topologically and cartographically (e.g. dangling nodes were identified and cleaned) and transformed into map outputs using ArcGIS functionality. The topographic layer used for location of the geological features on the interpretative geological maps is the one produced by BGS for this project.

The map layouts and design were agreed with the GSD, the geophysics QC Team and Fugro, and this agreement led to the production of ArcGIS MXD templates that were applied in this project. The Phase 1 maps were prepared for printing at 1:100,000 however they could be printed at any scale because they are supplied in digital form, but this is not recommended because of limitations arising from the scales at which data were captured.

7 Training

A training component is important to ensure sustainable development and knowledge transfer, and this project was served by both formal (course-based) and informal (on-the-job) training. The BGS, GSD, GEUS and Fugro staff agreed a training matrix (Table 27) in order to coordinate training between the 'Airborne geophysics survey of the Volta River and Keta Basin' and the 'Provision of quality control services to the airborne geophysical survey' projects to aid sustainability of the methodologies within the GSD. There are clear overlaps between the projects and the importance of providing a framework in which the training components are conducted was agreed.

	GPS Survey techniques - BGS field course	**Introduction to geophysics at BGS, UK**	**Remote Sensing at BGS, UK**	**Remote sensing verification and mapping- BGS field course, Ghana**	**Geophysics processing training at BGS, UK**	**Remote sensing verification and mapping- BGS field course, Ghana**
Dates	**Feb / March 2006**	**Feb / March 2006**	**March 2006**	**October 2006**	**January 2007**	**November 2007**
Wilfred Akah		*				
Abukari Suale					*	
Thomas Akamaluk		*			*	
Samuel Kwabla					*	
Akua Appiah – Akuramaa+	*		*	*		*
Joehida Quaye+	*		*	*		*

Table 27 List of training courses and GSD attendees;

+ denotes the two remote sensing counterparts.

7.1 REMOTE SENSING TRAINING

The first training course consisted of on-the-job training in the techniques and methodologies of conducting a high resolution differential GPS survey of the Voltaian and Keta Basins. The training was attended by Ms Akua Appiah-Akuramaa and Mr Joehida Quaye, the two remote sensing counterparts, as well as representatives of the Project Management Unit (PMU). Training was given within the framework of the GPS survey, which was conducted from the 12th of February to the 14th of March 2006. Instruction was provided to the GSD counterparts while the survey was ongoing thereby providing the trainees with 'real-world' experience of the hardware (Leica GS550 GPS) and associated Omnistar systems.

Ms Appiah-Akuramaa and Mr Quaye also attended two weeks of formal course-based training in remote sensing at the BGS in Nottingham between the 20th and 31st of March 2006. This course included modules on the following topics:

- Fundamentals of remote sensing
- Introduction to digital image processing
- Remote sensing data types: uses and limitations
- Aerial photography and photogeological interpretation
- Optical remote sensing (e.g. Landsat, SPOT)
- Radar remote sensing (e.g. Radarsat)
- High resolution imagery
- Advanced sensors (e.g. hyperspectral)
- Advanced digital image processing
- Geological interpretation
- GIS and map preparation

Training materials and all the presentations given during the course were supplied in digital and hardcopy format including the tailored ERMapper course notes (Jordan, 2006) and ERDAS Imagine notes (Hall et al. 2006). Each of the counterparts was also presented with a textbook (Drury, 2001), chosen as it specifically caters to geological remote sensing. Remote sensing imagery acquired for the Voltaian and Keta Basins was used for the course. As well as the topics noted above, additional training modules consisting of the application of GIS to mineral exploration and the use of a Portable Infrared Mineral Analyser (PIMA) were given.

In addition to the GPS survey, the counterparts also received on-the-job training during the two geological field mapping campaigns. The instruction focussed on field verification of remote sensing data and associated mapping techniques. Figure 97 below illustrates Mr Quaye receiving instruction at an outcrop. The field training included:

- lithological and mineralogical identification and recording;
- guidance on taking structural measurements;
- guidance on using a magnetometer and scintillometer;
- incorporating remote sensing datasets with reconnaissance field mapping.

Figure 97 GSD staff receiving instruction at an outcrop, November 2007.

Ms Appiah-Akuramaa and Mr Quaye were also given 'refresher' training in the use of the ERMapper digital image processing software on return to the GSD following the first reconnaissance mapping campaign. This served to confirm that the software and data were properly loaded on the GSD computer equipment, and that the counterparts were familiar with the process of installing and transferring the software as well as operating it.

7.2 GEOPHYSICS TRAINING

The geophysics training provided by BGS consisted of formal course-based events that were held at BGS Offices in the UK using Ghanaian data wherever possible.

Mr Wilfred Akah and Dr Thomas Akamaluk attended a two week formal training course at the BGS in Nottingham between the 20th of February and the 3rd of March. The first week covered 'Basic Geophysics' including magnetic anomalies from simple geological structures, 2D modelling exercises to show how the shape and amplitude of magnetic anomalies change with latitude, orientation, dip and depth; natural gamma radiation and the radioactivity of common rocks, factors affecting the attenuation of gamma radiation; the electrical conductivity of rocks and minerals and the grading of electromagnetic anomalies; characterisation of the broad range of lithologies encountered in Ghana by their joint magnetic/radiometric/electromagnetic signatures; and the qualitative recognition of faults, dykes and lithological contacts.

The second week of this course was an 'overview of airborne geophysics' and consisted of an outline of airborne geophysical and avionic equipment; magnetic and GPS base stations;

selection of survey parameters (line spacing, line direction, flying height) and effects on anomaly resolution; survey planning and airborne data QC with the aid of Geosoft Airborne QC toolkit.

A second, three-week course was attended by three GSD staff who travelled to the UK for the training (Table 27). This course took place following completion of magnetic and spectrometry data acquisition, and included data processing, data transformation, imaging, interpretation and GIS. The training consisted of:

Week 1: Data processing and introduction to Geosoft Oasis Montaj

An outline of data pre-processing (spike removal, removal of diurnal effects and IGRF, levelling, stripping and height attenuation corrections of radiometric data etc); importing data into a Geosoft database, profile display, data editing, creation of new channels; gridding and map creation, shaded relief with various azimuths and elevations of the illumination source, adding and subtracting grids, linking database, profile and maps.

Week 2: More advanced features of Geosoft

Filtering of magnetic data and various transformations (reduction to the pole, vertical and horizontal gradients, analytical signal, upward continuation and the separation of regional/residual fields to enhance high frequency features); edge detection; depth solutions from profile and gridded data by Euler, Werner, Analytical Signal and Slope de-convolution methods; picking magnetic axes, the preparation of ternary and radioelement ratios maps of radiometric data, the use of magnetic transform images and radioelement maps to characterise various litho-structural provinces.

Week 3: Further modelling, populating a GIS and integrated interpretation

2D and 3D modelling of selected structures, magnetic lineament and signature capture and analysis; principles of GIS (ArcGIS overview, introduction to ArcCatalog & ArcMap, geoprocessing, metadata and data types, symbology, labels and annotation, creating and editing data, topology, tables & queries, layouts, basic customisation, printing and exporting/importing data, extensions); use of GIS for overlaying a broad range of thematic images and observing data correlations; an introduction to prospectivity analysis (involving the inclusion of geochemistry and mineral occurrence data with geophysical data to predict prospective zones/trends etc) (where other relevant data is available); demonstrate the synergy of joint interpretation approaches, integration with known/mapped geology and extension into ‘unknown’ areas

8 Summary

The mineral sector in Ghana has shown significant growth in the past decade thanks to an investor-friendly environment fostered by the Government since the mid 1980's. However the success of this sector, which employs more than 36,000 people and accounts for approx 38% of the total export value is in doubt with rapid depletion of know resources and the lack of discovery of new deposits. Private sector mining operations cannot be sustained, unless the mining institutions improve their operations, provide up-to-date geological and geophysical information to discover new resources and formulate and implement new policies. The European Union has provided funding to the Government of Ghana to support these interventions, under the Mining Sector Support Programme (MSSP).

Recent airborne surveys were carried out in Ghana as part of the Mining Sector Development and Environment Project co-funded by the World Bank and the Nordic Development Fund. However no systematic regional work was carried out in the Volta or Keta Basins, an area of 98,000km^2, primarily because it was believed that the sedimentary rocks did not host economically viable mineral resources.

This report describes the EU-funded work undertaken by BGS between November 2006 and March 2009 in collaboration with Fugro Airborne Surveys Pty Ltd on an airborne geophysical survey and ground reconnaissance mapping campaign of the Volta and Keta Basins. The main beneficiary of this project was the Geological Survey Department, GSD, which received improved facilities and data, while its personnel received hands-on training on modern geological mapping technology. Indirect beneficiaries were other Government Departments such as the Ghana National Petroleum Corporation as well as mining and exploration companies that can follow up the reconnaissance work with detailed exploration work.

The Project was divided into five phases, of which the BGS had input to Phases 1, 4 and 5. Each of the deliverables expected from the BGS input is listed in Table 1. These included acquiring, processing and interpreting satellite imagery, undertaking a differential GPS survey, conducting two geological field reconnaissance campaigns, producing preliminary 1:100,000 geology and topographic maps, working alongside the geophysicists to interpret the geology in light of the fieldwork and the new geological model, providing a fully attributed GIS, and training counterparts both in the field and in the UK. All of the deliverables in the contract, plus additional ones such as contributing to the Voltaian Stratigraphic Workshop were met.

The methodology applied to the work is outlined in Figure 2. The BGS differential GPS survey data were used to geocorrect the DTM and the satellite imagery prior to interpretation for both topographic and geologic data. Following review of existing data, image interpretation and a field campaign, Phase 1 was concluded with the production and delivery of 1:100,000 topographic and preliminary geological maps in paper and digital form.

A substantial revision of the lithostratigraphy of the Volta Basin was undertaken. Initially a desk study reviewed existing information including papers, maps, reports and borehole logs. This was followed by image interpretation and two field mapping campaigns. In the field, the mapping teams recorded geological information at over 700 localities helping us to review and update the known geological model of the area. For example, historically, strata in the Volta Basin have been divided into 'Upper Voltaian' and 'Lower Voltaian' (e.g. Junner & Hirst 1946), often with the addition of a 'Middle Voltaian' unit (e.g. Anan-Yorke 1971). This stratigraphy has persisted and is still being used by some. However, it is largely based on the incorrect assumption that the quartzitic sandstones forming the higher ground bordering the southern, western and northern rims of the Volta Basin are amongst the youngest strata present ('Upper Voltaian'). It became clear that these sequences (now termed the Kwahu and Bombouaka groups) actually represent

the oldest strata, as suggested by Saunders (1970), and subsequently by Affaton (1975), dipping beneath strata in the central part of the Basin.

The mineral prospectivity was conducted by two BGS economic geologists who were involved at all stages of the project including the first visit to Accra to compile data, and the two field mapping campaigns. Jordan et al (2006) addresses the relevant mineral occurrences in the study area including gold, diamonds, bauxite, phosphate, limestone, baryte, silica sand, common salt, jasper, ilmenite and rutile, noting previously-known occurrences, their geological context and our exploration methodology. Mineral prospectivity modelling (an advanced form of computer modelling) was used to undertake prospectivity analysis for gold, uranium, phosphate and diamonds, the results of which are detailed in this report. Due to the lack of known deposits in the study area a knowledge-driven fuzzy logic technique was applied using all available data including the airborne geophysics. The results are displayed in map form, highlighting areas where we recommend follow up with techniques such as stream sampling and-or panning associated with detailed geological mapping.

Various maps were delivered to the client and customer in both paper and digital form. Two types of map were produced by BGS in Phase 1; 1:100,000 topographic maps, and 1:100,000 preliminary geological maps. There were forty-nine of each. As well as the paper plots and digital PDF maps, BGS also provided the full GIS and Geodatabase so that the GSD staff could update/modify the maps and produce derived outputs as required. The GIS included all of the raw and processed Landsat, Radarsat and SRTM satellite imagery. A commercial copy of the image processing software ERMapper was also installed and tested on one of the GSD computers so that the imagery can continue to be used for any geoscience application after this project has finished.

A set of 1:250,000 geological maps is the final map deliverable, and these will be produced by Fugro, using a combination of BGS geological data and Fugro geophysical interpretations.

In order to ensure sustainable development, an important component of any EU-funded project, the BGS were pleased to lead a series of formal and informal training courses (Table 27). Three formal courses were held at the BGS offices, one in remote sensing, and two in geophysics. Satellite and airborne data from this project was used in these courses to ensure relevance, whilst customised training manuals and textbooks were provided to the attendees. The formal courses were supplemented by informal training including practical hand-on instruction in GPS surveying, geological field mapping and field instrumentation such as the GRM-260 gamma-ray spectrometer.

The methodology applied in this project is outlined in Figure 2. It is a system used by BGS internationally and is founded on a thorough understanding of 3D geology and its surface expression i.e. how to interpret subsurface geology from the surface morphology; a process termed ‘feature mapping’. Following a review of existing data (maps, reports, memoirs, borehole logs etc.) a remote sensing interpretation was applied iteratively with focussed field reconnaissance and sampling to revise the maps. This enabled us to map the Volta and Keta Basins in the time available and to substantially upgrade the geological understanding of the area in the process. Furthermore, the fact that the workflow is digital also allowed the data to be incorporated via complex computer modelling for prospectivity modelling. Maps were produced that identify regions where exploration (including detailed mapping, stream sediment sampling etc.) is recommended as a follow-up to our regional mapping approach.

As well as completing all of the contractual requirements of the project, the BGS also provided a large contribution to the Voltaian Basin Workshop. Two BGS staff attended, and gave five presentations, chaired a session, and led the field excursion including producing the field guide published in Kaalsbeek (2008). BGS also provided four abstracts to the workshop publication (Carney et al 2008, Jordan at al[1] 2008, Jordan et al [2] 2008 and McDonnell et al 2008).

The desk studies, field surveys, sample analysis results, topographic and geological maps, raw and processed imagery, database, reports, software and trained staff are specific outputs delivered from this project. The GSD now has a wealth of expertise, data and facilities in geophysics, remote sensing and geological mapping which can be used to undertake new mapping projects or for example to advise and assist exploration companies enticed to the area by the high quality regional data. During the course of our work we were approached by mining/quarrying/exploration companies and consultants in Ghana and elsewhere who wanted to purchase copies of the maps and data, and who required consulting expertise. All of these requests were passed to our counterparts at the GSD. We recommend that the maps and data from this project are widely publicised, thereby raising the profile of the GSD and bringing in revenue.

Appendix 1 Geological Field Observations

YEAR	OBS point	X	Y	UTM Zone	Sample number	Description	Measurement s
2006	CJ1	796421	729896	30	CJ 1	Quartzitic sandstone - horizontal laminations, interbedded red and yellow. Pebbly. Vertical escarpment further inland, now level with its base. Approximatly 20m above Lake Volta.	Jointing 200 Strike 200, Dip 14
2006	CJ2	796369	729893	30	CJ 2-3	Contact between basal fine grained red quartz sandstone and medium grained yellow quartz sandstone.	
2006	CJ3	781624	759360	30		Takorout 'limestone quarry'. Filled in with sand/gravel and duricrust. No limestone present. Red quartz sandstone pebbles and duricrust.	
2006	CJ4	802888	766266	30		On rise up to plateau on DTM. Very gradual planar rise, no actual escarpment. Quartz sandstone boulders by roadside.	
2006	CJ5	803077	766538	30	CJ 4	White quartz sandstone with 1cm bedding.	
2006	CJ6	813214	774593	30		2m roadside gravel. Pebble to cobble size with very rounded clasts supported by medium grained sand matrix.	Strike 320, Dip 22
2006	CJ7	822430	779961	30	CJ 5	Dorkorkrom. Med-grained red/grey sandstone.	Joints at 130 and 32
2006	CJ8	787173	764206	30	CJ 6	0.5m roadside section of clast supported grey to light green siltstone. Weathered. Red staining on upper surface of top layer of pebbles.	
2006	CJ9	747370	727420	30		Bauxite adit 4m diameter, circular. Depth unsure but >10m. Nodular bauxite worked for iron by British company - noted on mineral occurrence database.	
2006	CJ10	749575	734285	30		Quartz sandstone, pale yellow.	Primary jointing 140, secondary 224 Strike 140, Dip 8

2006	CJ11	749761	735706	30		Small scale quarrying in quartz sandstone. Surface ripples indicate flow deposition to 192. Ripple frequency 12cm.	Surface ripples indicate flow deposition to 192; Ripple frequency 12cm Primary joint 102, secondary 210 Strike 102, Dip 10
2006	CJ12	745937	740735	30		2m x 4m x 0.5m high section of quartz sandstone, more feldspar, less clean, flaggy.	Ripple frequency of 8 cm, flow to 354. Bed above is 10 cm thick, with a 2 cm frequency, deposited towards 65
2006	CJ13	797751	862924	30		Sand and gravel pit. 5m section of cobbles, rounded, grading up to pebbles with 0.75m laterite soil on top. Minor channel infilling.	NE / SW face planar bedding Strike 325, Dip 24
2006	CJ14	814172	858052	30		Top: 1m poorly sorted pebbly conglomerate. Dominated by pebble clasts with sandstone boulders. Sub-angular clasts, not far travelled. Base: 5m light green grey siltstone, soapy, fissile. Thinly bedded.	Swinging dip Joints 75 and perpendicular Strike 335, Dip 8
2007	CJ14b	814172	858052	30		Top: 1m poorly sorted pebbly conglomerate. Dominated by pebble clasts with sandstone boulders. Sub-angular clasts, not far travelled. Base: 5m light green grey siltstone, soapy, fissile. Thinly bedded.	Joints 75 and perpendicular Strike 140, Dip 9
2006	CJ15	793430	862352	30		Roadside 0.5m silt, no duricrust or pebble cover.	
2006	CJ16	772947	860353	30		Pebbly conglomerate forms road surface, 5m x 20m, same as top of OBS point CJ14.	Unclear joints 350, 92
2006	CJ17	762475	858239	30		Flat (level) area approx. 1km along road, note colour change to pale grey silty sediment on the surface. Alluvial plain or siltstone (weathered)?	
2006	CJ18	758087	855906	30		Floodplain? Fine to med grained red sand with cobbles and boulders of laterite occasionally on the surface. Lighter pink yellow tones on Landsat.	
2006	CJ19	758481	834712	30		Duricrust on road surface 4m x 2m. Duricrust is pebbly possibly derived from a conglomerate. Pebbles thickly coated in iron oxide. 20m to south, and 2m lower is medium grained sandstone, flaggy, dark grey, very thinly bedded. Alluvium boundary starts here.	

2006	CJ20	758239	834890	30		Flaggy red med grained sandstone, thinly bedded.	Surface ripples indicate flow deposition to 300 with a frequency of 5cm Joints 300
2006	CJ21	783006	948162	30		No outcrop. Flat-lying terrain, though on a slight rise here. Surface of dark red med-grained sand. No laterite visible. Looks like gulley run off to the east.	
2006	CJ22	784224	948449	30		Crossed on to very fine grained sand, silty yellow - sediment.	
2006	CJ23	803130	956094	30		Stream section of pebbly lateritic conglomerate. Pseudo horizontal bedding. Notable series of planar dip slopes to NE.	Jointing 340, 106
2006	CJ24	176504	979613	31		Dirty laminated hard pink grey sandstone, fine to medium grained. Contains non silica. Slightly flaggy. Weathers with rounded boulders on surface and onion weathering.	Joints 138 and possibly 50
2006	CJ25	178206	968198	31		Light olive coloured fine grained micaceous sandstone with interbedded weathered bands of olive siltstone. Exposed for 100m along roadside. Top 4m sandstone, base 4m interbedded siltstone sandstone. Note also isolated pebbly conglomerate beds.	Jointing to 2, 182; dip 8 strike 270 Dip alters in little fracture zones e.g. strike 168, dip 29 but joint pattern is constant.
2006	CJ26	182062	966153	31		200m roadside 2d outcrop of micaceous light olive siltstone, thinly bedded. One NW/SE strike has very steep dip to either side.	Variable dip, highly faulted, no measurements
2007	CJ26b	182062	966153	31		200m roadside 2d outcrop of micaceous light olive siltstone, thinly bedded. One NW/SE strike has very steep dip to either side.	Variable dip, highly faulted, no measurements
2006	CJ27	828496	933797	30		8m x 4m outcrop. Pale olive sandstone, weathers to salmon pink. Flaggy. Contains lithics, feldspar and possibly magnetite, so feldspathic arenite. Onion weathering. Cobbles of laterite on surface nearby.	Various jointing 328, 65, 345, 80
2006	CJ28	828225	929919	30		Same lithology as CJ27.	
2006	CJ29	773352	962400	30		Gently undulating topography. No outcrop. Consistent termite mounds from Salaga to here of pale red/yellow fine sand with silt. Laterite common either as cobbles or in situ.	

2006	CJ30	774245	968608	30		Thin red duricrust with laterite boulders on spherical nodular silty olive green sediment.	
2006	CJ31	775975	978711	30		Grey massive mudstone at base grading into grey nodular laterite. Roadside stream section 50m long with 2m drop. 1m red laterite on 85cm grey laterite on 15cm light green mudstone that is weathered with no structures.	
2006	CJ32	777725	982795	30		West of escarpment crest, 50m long section of 10cm thick olive green/grey mudstone. Weathered with no structures.	
2006	CJ33	768743	1005706	30		Flat lying topography. Swampy. Cover of olive green fine sand and silt.	
2006	CJ34	768421	1009504	30		1.5m nodular hard laterite. Formerly used as extraction pit for road construction. Two boulders nearby of dark grey (weathering to purple-red) fine sandstone. Few laminae visible. K feldspar.	
2006	CJ35	761891	1022076	30		Remote sensing interpretation alluvium boundary here is correct.	
2006	CJ36	747452	1034504	30		Very extensive laterite pit, at least 500m x 300m but not deeper than 2.5m. Dark red hard nodular laterite, though note grey mud at base in some ponding areas. Abundant rounded cobbles (corestones) and sub rounded boulders of quartz-feldspathic fine to medium grained yellow sandstone that weathers to dark red. REVISITED 2007	Palaeocurrents 210, 250
2006	CJ37	745870	1052213	30	CJ 7, a, b, c	Outcrop on hill crest. Boulders and outcrop. Pink yellow quartz sandstone with K feldspar. Weathers to dark red. Fine to medium grained, finely laminated, possible mudstone clasts.	
2006	CJ38	747556	1053549	30		Outcrop on hill crest inroad. Yellow/grey fine to medium grained quartz sandstone, micaceous, weathers to dark red. Outcrop extends 30m.	Jointing 12, 116
2006	CJ39	753288	1058921	30		6m long x 1.5m wide roadside weathered olive yellow (banded with pink, k feldspar) fine grained sandstone. Ripple marks on surface, 1cm bedding. No structure measurements possible. Laterite cobbles on roadside.	
2006	CJ40	761144	1062349	30		30m long x 0.5m high roadside cutting. Top 40cm is laterite, hard, nodular pebbly. Light yellow grey, Base:	

						finely laminated red/olive-grey fine grained flaggy sandstone. Variable dip. Yellow/light purple banding 4mm when fresh, darker when weathered.	
2006	CJ41	771067	1066737	30		Coarse red sand with rounded cobbles of quartz. Coincident with 'mainly pebbly sandy beds' on the 1:1m geology map.	
2006	CJ42	772107	1068237	30		Pebbles and cobbles ubiquitous on surface. Sandstone outcropping (0.4m) with beds of rounded quartz pebbles. Sandstone is dark grey (muddy) fine grained, weathering to a reddish grey i.e. beds of sandstone and conglomerate. Bedding appears flat-lying.	Jointing 262, 218
2007	CJ42b	772107	1068237	30		Pebbles and cobbles ubiquitous on surface. Sandstone outcropping (0.4m) with beds of rounded quartz pebbles. Sandstone is dark grey (muddy) fine grained, weathering to a reddish grey i.e. beds of sandstone and conglomerate. Bedding appears flat-lying.	Jointing 262, 218
2006	CJ43	772850	1069327	30		End of pebbles on surface, now at start of plateau.	
2006	CJ44	826769	1060341	30		10m x 6m outcrop of olive green fine to medium grained dirty sandstone. Banding of k feldspar. Flaggy. One mudstone lithic component found. Undulating sub-horizontal surface, possibly bedding? This outcrop is approximately 100m west of the escapement edge and smaller outcrops occur along the edge.	Jointing 185 to 195
2006	CJ45	826971	1060990	30		Just over ridge/escarpment edge is located a fine grained quartz sandstone, olive-tan with 1cm bands of mica. Weathers to dark red.	
2006	CJ46	827038	1061428	30		Roadside gutter section grades from sandstone to siltstone (here) to mudstone 50m further to the NE. Transitional sequence. Siltstone is olive tan weathering to dark brown. Vertical drop along section is less than 2m.	
2006	CJ47	177801	1071822	31		Traversed down the NE edge of 'resistant plateau' that dips planar to NE. Roadside gulley 25m long with 5m clip. Base: finely laminate mudstone with silt, grey-brown, occasionally grey-green. Slaty cleavage, fissile. Top: cover of nodular red hard laterite 0.5m thick at plateau end of exposure.	Strike 50, Dip 3 (base)

2006	CJ48	181764	1077073	31		Fine grained olive green-brown sandstone 4m long roadside gulley, on ridge. Flaggy, breaks into 1cm thick units. Situated 3m to NE is 5cm to 10cm grey slaty mudstone below the sandstone.	
2006	CJ49	181973	1077451	31		Very fine grained olive yellow sandstone. 30m gulley section 0.5m to 1m thick.	Strike 280, Dip 4
2006	CJ50	187606	1094917	31		Roadside stream section 10m long with 1m drop. Olive green horizontally finely laminated siltstone fissile (slaty cleavage). Darker green mudstone interbedded (10cm beds) with siltstone (2-4cm beds).	Jointing at 272 and 202
2006	CJ51	187779	1095314	31		100m NE of OBS point CJ50, bedding better exposed in olive very fine grained sandstone, nearly a Siltstone, interbedded with minor mudstones.	Strike 150, Dip 3
2006	CJ52	188848	1099671	31		Exposure parallel to ridge crest. Fine gained hard quartz green-grey sandstone. Micaceous. Rounded boulders abundant on surface.	Strike 100, Dip 3
2006	CJ53	200584	1117598	31		Roadside stream section 30m long rise of 1m. Slight ridge. Top: flaggy olive green fine grained sandstone, 20cm thick, well jointed onion weathering. Base: 10cm slaty mudstone.	Sandstone jointing 285 and 35 Strike 90, Dip 5
2006	CJ54	203063	1121745	31		Folded pale olive green laminated siltstone (slaty) with interbedded mudstone.	Fold axis 4 degrees, 48 dip to west, 45 to east; fold nose pinches out at surface
2006	CJ55	204180	1123150	31	CJ 8	Continuation of OBS point CJ54 (several 100m to SW). Dark olive green grey fine grained sandstone with mica, dirty, hard. Well developed jointing. Onion weathering.	Jointing 130 and perpendicular
2006	CJ56	206074	1126537	31		40cm of olive green mudstone and siltstone on fine grained olive grey green sandstone. Mudstone: sub-horizontal bedding but open folding is apparent.	
2006	CJ57	821182	1069018	30		10m long section of olive yellow fine grained weathered sandstone with mica. Onion weathering. Weathers to red.	Jointing 100
2006	CJ58	817684	1077969	30		10m x 5m outcrop in field beside road of dark grey, dark green fire grained hard sandstone with some k feldspar and mica. Flaggy with onion weathering. Location is at crest of Oti bed escarpment.	

2006	CJ59	817366	1078973	30		Same as OBS point CJ58	
2006	CJ60	814307	1088719	30		Small road outcrop with sub-angular boulders alongside. Dark olive green fine grained hard fresh sandstone. Feldspar. Massive homogeneous with no mica. On crest of hill.	
2006	CJ61	811247	1091100	30		Same as CJ60 (fine grained olive green sandstone) though slightly lighter colour, again on crest of hill.	
2006	CJ62	806426	1095605	30		Located on the northern edge of Oti bed escarpment. Several small 2m x 2m outcrops of olive green fine grained hard sandstone with mica. Flaggy. Stepped series of drops (breaks in slope) over resistant sandstone beds north to a plain.	
2007	CJ62b	806426	1095605	30		Northern edge of Oti bed escarpment, Several small 2m x 2m outcrops of olive green fine grained hard 'Bunya'-type sandstone with mica. Flaggy. Slightly coarser grained than other sites today. Stepped series of drops (breaks in slope) over resistant sandstone beds north to a plain.	
2006	CJ63	805962	1096391	30		Base: 30cm fine grained olive green hard sandstone. Mid: 1.5m slaty very fine grained olive green sandstone. Top: 20cm fine grained hard sandstone.	Joints parallel and perpendicular to strike Strike 90, Dip 4
2006	CJ64	797976	1107995	30		Boundary to alluvium to the north.	
2006	CJ65	818538	1140835	30		Bedded friable mudstone, various beds of olive, purple, red; 0.7cm; non calcareous. Working pits for material for house construction. 1m over of hard red pebbly laterite. Break of slope here from plateau to plains to the north. Locals report limestone beneath the mudstone.	
2006	CJ66	818252	1147635	30	CJ 9 a and b	1km long road gentle planar dip to the south. 5m outcrop along stream. Salmon pink, fine grained quartz sandstone steeply dipping. 5cm bedding. Bed of dark salmon pink siliceous cherty siltstone with 3mm 4 frequency ripple marks.	Strike 130, Dip 25
2006	CJ67	817818	1151559	30		Same multicoloured bands as OBS point CJ66. Very fine grained pink sandstone/siltstone; gray siliceous; weathers to tan brown. Small soft sediment structures seen throughout including load structures and micro folds.	Minor fractures 105-285, 82 to south Jointing 94 and 4. Dip variable

2006	CJ68	814027	1157726	30		Traversing along road there is a gentle planar dip to south. 1.5m x 0.5m outcrop of loose grained purple/red very hard med to coarse sandstone. 20m further north, 2m outcrop as before but fresher; purple grey, angular grains.	Strike 320, Dip 3
2006	CJ69	812754	1159928	30		White pale yellow medium to coarse grained quartz sandstone; 3m x 1m outcrop; very hard; flaggy.	
2006	CJ70	812009	1160649	30		As OBS point CJ69. Surface weathering to red.	
2006	CJ71	810938	1161880	30		5mm bedded grey med to coarse grained dirty sandstone, flaggy, angular grains.	Cross Bedding 24/275
2006	CJ72	810615	1162623	30		Large area at crest of hill with in situ rock and many boulders. Beds of purple grey and white pale yellow medium grained sandstone. Flaggy, dirty. Purple grey beds have 5mm bedding of pale yellow within. Small scale quarrying. Banding due to alt bands of quartz or mica rich thin beds	Some evidence of a drag fold with a 300 degree direction of drag Strike 305, Dip 12
2006	CJ73	810706	1167673	30		Extensive ridge; several 100m of fine to med grained sandstone. Pale yellow fresh and hard, weathering to red; flaggy. Onion weathering. Lower outcrop has pavement that weathers to resemble karst pavement. Sandy soil.	Joints 150 and 150
2006	CJ74	809960	1170164	30		2m x 0.5m outcrop of very weathered medium grained sandstone. Surface red, inside is a deep yellow. Angular grains. Possibly a weathered version of OBS point CJ73? 0.3m laterite cover.	
2006	CJ75	808749	1175640	30		10m x 5m outcrop on plateau with scattered boulders on surface. Weathered medium grained sandstone, salmon pink at freshest grading to purple when weathered. K feldspar present; flaggy. Bedding apparent on some surfaces.	Jointing 30 and 320
2006	CJ76	796280	1169399	30		Far north of area. 5m to 10m boulders of pale grey hard quartz sandstone weathering to yellow or purple -red. Medium grained, flaggy.	Trough-cross bedding to 320. Other sets 060, 060, 240 General trend on surface bedding to 230
2007	CJ76b	796280	1169399	30		JC REVISITED 2007. Plane to cross-bedded. Some beds up to 2m thick show large scale foresets - may be aeolian with fluvial influence?	

2006	CJ77	797503	1170147	30		Same as OBS point CJ76, but large flat bedding plane. Poorly cemented medium grained feldspar/mica sandstone	Palaeocurrents 300, fractures 90-270, 80 towards N, Cross-bedding 4/240
2007	CJ77b	797503	1170147	30		JC REVISITED 2007. Red weathering, medium grained feldspathic quartz arenite with elephant skin weathering. Possibly fluviatile.	
2006	CJ78	808003	1177839	30		4m high x 200m long exposure in road cutting of very hard fresh white, pale grey, yellow quartz sandstone with mica. Fine to medium grained. Beds 1.5m to 0.3m thick interbedded with very weathered sediment, possibly weathered siltstone. Northern edge of escarpment. Penabako fm?	Cross bedding 8/280 Strike 90, Dip 3
2006	CJ79	806796	1177841	30	CJ 11 of siltstone.	Descending from the north edge of Gambaga escarpment. Passed through sandstone/siltstone beds, now 6m of shaly slaty olive green siltstone + mudstones. Horizontal bedding prevalent. 5 or 10cm beds of very hard fine quartz sandstone approx every 0.5 to 1m, 20% sandstone. Note thick sandstone cap of at least 15m. Possibly Poubougu fm?	
2006	CJ80	804898	1181884	30		Northernmost point. No outcrop. Loose sand laterite with sparse laterite boulders. Topographic surface dips to the south. Possibly Tossiegou fm?	
2006	CJ81	812509	1175283	30		40m long section with 4m rise. Hard pale grey/white fine to med grained quartz sandstone. Weathers to purple; flaggy. Cross bedding present.	Jointing 100 and various orthogonal e.g. 25 Strike 320, Dip 5
2006	CJ82	174083	1166183	31		2m x 2m outcrop of fine to med grained pale grey yellow quartz sandstone with mica. Weathers to pink/red.	
2006	CJ83	177415	1165059	31		Some as OBS point CJ82. But extremely hard. Frequent scattered boulders and outcrops in village.	
2006	CJ84	180035	1164371	31		Same as OBS point CJ82. Weather to purple, plateau cap rock.	
2006	CJ85	182534	1163291	31		Small crop of one bed of extremely hard white quartz sandstone weathering to yellow. Flaggy. Med grained angular grains. Large flat lying area with rare outcrop unlike to north.	

2006	CJ86	183215	1160669	31		Same as OBS point CJ85. Surface weathering like karst. Possibly due to siltstone beds weathered eroded away?	General trend, shallow dip to 210 Jointing 350 and 90 Strike 300, Dip 2
2006	CJ87	183649	1158537	31		Old pit. Siliceous cherty siltstone bedded yellow, olive, red, and maroon; platy. Same lithology continues up the scarp but not on the plateau.	
2006	CJ88	183418	1155793	31		Same as OBS point CJ87. 1m elevation drop on this roadside gutter section.	
2006	CJ89	179217	1156876	31		Same as OBS point CJ86. First occurrence of sandstone heading north from chert ridge.	
2006	CJ90	171658	1159040	31		Same as OBS point CJ86.	
2006	CJ91	721143	1108937	30		Alluvium boundary here, break in slope, correct on remote sensing interpretation.	
2006	CJ92	728509	1111933	30		Old pit. 1m nodular hard red laterite. Flat lying topography. Alluvium present to north and south.	
2006	CJ93	740329	1120225	30		Alluvium boundary on remote sensing interpretation proven correct.	
2006	CJ94	738814	1109910	30		Stepped breaks in slope upwards in southerly direction. This location has flat topography between breaks in slope.	
2006	CJ95	738655	1107551	30		Traversing crest. Possibly remnant of the western end of the Oti Bed syncline? Pit here in hard nodular red laterite. Few scattered boulders of fine grained olive green hard flaggy sandstone. Weathers to red.	
2006	CJ96	738329	1103661	30		20m x 20m with 1m drop outcrop as OBS point CJ95. Note large potholes on surface of lower bed. Dip 2 towards S.	Palaeocurrents 170, 158 Joints 65 and145 Strike 90, Dip 2
2007	CJ96b	738329	1103661	30		JC REVISITED 2007. Massive fractured cream coloured sandstone, immature, fine grained. Large scale trough cross-lamination possibly produced by tidal currents.	
2006	CJ97	734316	1086591	30		Alluvium boundary from Remote sensing interpretation proven here.	

2006	CJ98	722292	1071626	30		Alluvium, silt and fine sand over 2m thick. Mole River.	E-W dextral fractures, 74-254 80 to the N
2006	CJ99	725150	1070230	30		Old pit, 10m x 10m x 2m deep. Many sub angular boulders of hard nodular laterite. Surrounding area generally flat with cobbles of hard laterite on the surface.	
2006	CJ100	713289	1045541	30		Pond dug for cattle watering. Boulders 2m by 1.5m of fine grained dark red-purple hard quartz sandstone. Weathers to lighter yellow colour. Tamale sandstone? 1m cover of hard nodular dark red laterite.	
2006	CJ101	713864	1046104	30		Roadside gutter, 2m long, 0.5m drop. Olive green sandstone, slaty. Weathers to red or black along laminations. Note: lower elevation than OBS point CJ100.	
2006	CJ102	719309	1050333	30		Extensive alluvium, forms marshy ground used for growing rice. Not noted as alluvium on the interpretation.	
2006	CJ103	722533	1054704	30		Pale purple pink fine to medium grained sandstone weathering to yellow. Angular grains and micaceous. Small outcrop on plateau.	
2006	CJ104	713696	1068499	30		Alluvium forms this river bank.	
2006	CJ105	729889	1051483	30		Roadside sub angular/sub rounded boulders of fine to medium grained, weathering to salmon pink-red or buff. Hard quartziferous. Possibly Tamale sandstone?	
2006	CJ106	731611	1049423	30		2m sub angular boulders of dark red purple medium grained sandstone, not very hard. Very like the lithology noted at Tamale stadium. Angular grains clear. Weathered is same colour as fresh. No bedding, massive, homogeneous. Possibly Tamale sandstone?	
2006	CJ107	702539	1011256	30		Alluvium boundary starts 50m south of here.	
2006	CJ108	698822	1009920	30		Mostly maroon or brown occasionally grey/green mudstone interbedded with occasional siltstone (10cm thick). 4m sequence. Cover 2.5m of lateritised gravels - massive, very rounded quartz pebbles with minor sand matrix. Gravels are same elevation as diamond locality to south: placer deposit? Evidence of gravel extraction. Pebbles have been transported down-slope.	

2006	CJ109	680807	1011097	30		Pit for watering cattle. Flat lying topography but No outcrop. 1m of pale buff pebbly laterite with frequent boulders of red nodular laterite.	
2006	CJ110	675130	1011260	30		No outcrop for several km. Very flat top with grey silt cover, no reaction to HCL, aeolian?	
2006	CJ111	673083	1012809	30		1m pebbly laterite at base including rounded quartz pebbles covered by 80cm of pale brown silt.	
2006	CJ112	624580	1019447	30	CJ 12 (mag reading over 50)	2m thinly bedded, laminated olive green siltstone and mudstones. Weathers to maroon brown. Outcrop is on a plain. Possibly Poubogou fm?	
2006	CJ113	625296	1019306	30		Med-grained red sandstone, weathering to yellow. Thinly bedded, flaggy, onion weathering. Numerous exposures in village.	Joints 60 and 150
2006	CJ114	626040	1019846	30		Gutter outcrop on ridge, 20m long, 1m drop. Fine to medium grained purple-grey sandstone, weathers to grey. Sub-angular grains. 10cm bedding, flaggy, hard, micaceous. Some purple grey banding due to weathering.	Joints 40 and 140,
2006	CJ115	634031	1027912	30		2m laminated silt/sand, narrowly distributed along river banks.	
2006	CJ116	715224	965743	30		No outcrop or boulders. Ploughed field of silt with clay and fine sand. Dark brown reddish. Possibly an old terrace?	
2006	CJ117	694173	982422	30		Laterite boulders common beside stream. No outcrop. Surface sediment: brown silt with fine sand. Occasional rounded pebble – possibly linked to road?	
2006	CJ118	692005	991159	30		Pale brown silt with fine sand on hill crest.	
2006	CJ119	688757	991851	30		Plateau of pale red (pinkish) and white silty soil. No laterite boulders here, though abundant to the east. Possibly aeolian?	
2006	CJ120	674462	983783	30		Marshy, frequent ponding. Road on incline to the SW.	
2006	CJ121	673090	978370	30		Limestone mineral occurrence in database; old pit with sand and pebble gravels.	
2006	CJ122	669425	974917	30		Bottom of break in slope; start of alluvium to south.	
2006	CJ123	625261	893922	30		Gutter 20m long, 2m drop. Interbedded grey mudstone and	

						maroon or orange red siltstones. Flaggy, fissile.	
2006	CJ124	625772	893810	30		West slope up to plateau. Base: 1.5m dominated by silicified grey mudstone (10cm beds) interbedded by millimetric bands of mudstone. Top 2m red/grey mudstone dominated by 20cm beds of fissile mudstone with 10cm beds of more siliceous sediment with dendritic patterns of manganese in the cherty beds. Cover of saprolite, possibly once sandstone?	Variable with open folding
2007	CJ124b	625772	893810	30		West slope up to plateau. Base: 1.5m dominated by silicified grey mudstone (10cm beds) interbedded by millimetric bands of mudstone. Top 2m red/grey mudstone dominated by 20cm beds of fissile mudstone with 10cm beds of more siliceous sediment with dendritic patterns of manganese in the cherty beds. Cover of saprolite, once sandstone?	Dip 8, strike 60 variable with open folding
2006	CJ125	628429	893237	30		Near crest of hill up to plateau. Weathered yellow sandstone on roadside. Road surface: very hard silicified medium grained white arenite sandstone. Possibly described as quartzite by original mappers. Slight coarsening upwards. Rare pebbles between 5-10cm beds.	Joints 95 and 5, Strike 52, Dip 2
2006	CJ126	630776	892756	30		10m gutter. Med grained white weathered sandstone, flaggy. Possibly feldspars but too weathered to be certain.	
2006	CJ127	632187	896190	30		Same maroon and grey sequence as OBS point CJ123.	
2006	CJ128	624735	902894	30		Gulley of gravels, top 0.5m is lateritised. Base 2.5m unconsolidated red weathered gravels. Cobbles and pebbles predominantly quartz rounded. Clast supported but matrix of med grained sand. Massive, no grading. Lateritised part could have been mapped previously as conglomerate? Possibly Tossiegou Formation?	
2006	CJ129	632148	896629	30		Same as OBS point CJ123. Contact here from area of no exposure (but pebbles on surface) to west with mudstones siltstones to the east. 35m gutter, 2m drop.	
2006	CJ130	637972	891165	30		Outcrop approximately mid way up escarpment formed by more resistant bed that can be traced approx 100m along contour. 1-2m beds of maroon fine to med grained micaceous sandstone with 1cm beds above interbedded with grey sandstone grading into grey sandstone, then red	

						bed again. Cross bedding of red laminae abundant. Siltstone bed (15cm) seen at base of one red bed.	
2006	CJ131	639014	891193	30		Edge of escarpment. Weathered salmon pink medium grained sandstone. Sub-angular grains. Cross bedding abundant. Same as OBS point CJ132 but weathering to pink; k feldspar.	
2006	CJ132	656470	885418	30		Old excavation pit. 1m nodular hard red laterite but no outcrop.	
2006	CJ133	659092	885255	30		10m gutter. 1m drop. Sub angular grains, medium grained very weathered sandstone. Salmon pink weathering to maroon veneer.	
2006	CJ134	643450	894151	30		Kintampo falls. 10m boulders of medium grained white or pale yellow hard sandstone with sub angular grains.	
2006	CJ135	659056	881304	30		Sandstone scarp - frequent outcrops beside road. Med grained hard massive yellow to white sandstone weathering to red or maroon on surface. Weathering seems to pick out beds at 15cm intervals. Sub-rounded grains, clean arenite.	
2006	CJ136	637010	876160	30		As OBS point CJ135.	Palaeocurrents 90
2007	CJ136b	637010	876160	30		JC REVISITED 2007. Sandstone cream and friable, with large scale trough cross-beds. Possibly fluvial phase.	
2006	CJ137	634721	871012	30		As OBS point CJ135. Weathering to yellow.	
2006	CJ138	631829	863052	30		As OBS point CJ135. Road cutting. Weathering to dark red from light yellow.	
2006	CJ139	630817	861759	30		As OBS point CJ135. Nearly at base of scarp. Orange weathered. Possibly due to Feldspar?	
2006	CJ140	629771	859243	30		Road cutting. Base: 3m med grained (slightly fine than OBS point CJ135) sandstone with white and pale purple bedding. Mid 2m is same but pale purple with yellow beds. Both contain cross bedding trending to the north. Top 2m: red Laterite soil.	Cross bedding trending to the north
2006	CJ141	628292	854974	30		Outcrop on both sides of road, extensive. light red to tan flaggy sandstone. Fine-Med grained. Outcrop forms small hillocks of rock.	

2006	CJ142	628402	854954	30		Across road from OBS point CJ141. Distinctive pinnacle landforms, with intensely weathered surfaces. Fire grained hard red sandstone, sub rounded grains, homogeneous. Minor feldspar.	
2006	CJ143	621522	839131	30		2m of weathered fine grained thinly bedded sandstone. Base: 0.5m dark green interbedded higher with grey/light green to maroon. Top 1m dominated by light green grey. Green grey beds at basal unit have small silt component.	
2006	CJ144	622345	839365	30		1.5m boulders of slightly micaceous fine to med grained hard light red greyish massive sandstone with sub-rounded grains.	
2006	CJ145	625060	839394	30		Near shrine site. Large outcrops of hard grey/white fine grained sandstone. Rounded grains. Clean. Massive. 6m high.	
2006	CJ146	628421	838514	30		On planar slope. 4m (1m high) boulder of fine grained salmons pink hard massive sandstone.	
2006	CJ147	631145	837708	30	CJ 13	Fine grained interbedded hard light maroon, yellow, grey slightly micaceous sandstone. 30m long, 2m drop. Manganese weathering. Flaggy, thinly bedded. Potholes actively forming with running water.	Joints 250 and 350 Strike 10, Dip 5
2006	CJ148	648388	828642	30		Road cutting. Base: 2m dark red weathered (dark yellow or grey when fresh) fine grained sandstone. Cross bedding constant through all of section. 1m laterite cover.	Cross bedding average 10 dip towards 210 Strike 300, Dip 10
2006	CJ149	658522	830273	30		Gutter section. Fine grained light yellow to white weathered sandstone, weathers to dark yellow or red. No mica but flaggy, thinly bedded with folding common, contorted. First folding seen in this area. Well jointed.	Joints 75 and 355
2006	CJ150	661938	827956	30		Grey, weathering to yellow or red. Fine grained hard sandstone. Massive. Jointed but not flaggy.	
2006	CJ151	664401	823648	30		Thinly bedded flaggy, slightly micaceous med grained weathered sandstone. Grey to light yellow, weathering to red.	Strike 104, Dip 4
2006	CJ152	668078	822133	30	CJ 14 (mica vein)	Thinly bedded fine grained micaceous sandstone. Mostly yellow, but grey and maroon bedding. Weathered but hard.	Vein orientation 78

						Several thin near-vertical mica veins.	
2006	CJ153	680015	815364	30		45cm of pink/purple fine grained soft weathered friable micaceous sandstone. 1cm beds of dark yellow weathered medium grained sandstone.	
2006	CJ154	686980	814273	30		8m x 3m flat outcrop of med to coarse grained hard sandstone, massive in appearance. Poorly sorted with grains up to 2mm. Reddish grey to dark red.	
2006	CJ155	687349	813077	30		Hard, coarse grained sandstone. Brownish yellow weathering to dark brown. Poorly sorted.	
2006	CJ156	691485	810675	30		3m upstanding exposure. Fine grained sandstone. Maroon, thinly bedded.	
2006	CJ157	692158	809817	30		Maroon fine grained micaceous sandstone, massive.	Joints 260 and 350
2006	CJ158	692813	809694	30	CJ 15	Scarp slope. Finely laminated purple siltstone and green interbedded mudstones.	
2006	CJ159	697640	806107	30		Maroon, fine grained sandstone.	
2006	CJ160	711499	811925	30		Maroon, fine grained micaceous sandstone.	
2006	CJ161	716063	811928	30		Maroon, fine grained, thinly bedded micaceous sandstone. Contains occasional green mudstone clast.	
2006	CJ162	781996	772367	30		Large upstanding outcrop (inselberg), 15m high 50m wide. Pale grey red-maroon, poorly sorted micaceous sandstone. Lenses of poorly sorted material with clasts of 2-5cm - possibly channel deposits with lags. Clasts typically granite, quartz and sandstone. Clasts of cobble size observed from a distance.	Cross bedding dipping towards West
2006	CJ163	781922	774664	30	CJ 16	Poorly sorted fine to coarse grained feldspar and mica rich immature pink-grey sandstone, occasionally conglomeritic. Rounded quartz and granite pebbles of up to 5cm.	
2006	CJ164	782415	776063	30		1m thick conglomeratic bed, rounded pebble sized clasts of quartz and granite in coarse sandstone matrix, occasionally clast supported. On 0.5m medium to course poorly sorted sandstone, with thin coarse sandstone beds.	
2006	CJ165	779031	778142	30		Pale red-grey fine to coarse grained poorly sorted feldspar rich sandstone with occasional rounded 1cm sized clasts.	

2006	CJ166	764912	781745	30		Fine grained grey-maroon dirty sandstone, feldspar.	
2006	CJ167	761408	787698	30		Marshy ground, western limit of Mpraeso-Afram traverse.	
2006	JC1	204000	649500	31		Red brown poorly sorted small-pebble gravel with red sandy matrix - fragments of vein quartz.	
2006	JC2	208429	645039	31		Views along road over salt lagoon. Ridges/photo lineaments along road to N were in ochreous iron-cemented gravel. Ridges are probably neo-tectonic features.	
2006	JC3	215577	651075	31		Red Fe-cemented gravel in cuttings. Main lithology consists of yellowish clayey sand with sporadic clasts overlain by brown deflation gravel with duricrust remnants.	
2006	JC4	225908	659726	31		20cm of deflation gravel on blue-grey silty clay. Possibly raised estuarine deposit? Part of wetlands area with lagoons.	
2006	JC5	226039	661363	31		Pale grey/brown silty clay of floodplain.	
2006	JC6	226329	662844	31		100m to N of step down from OBS point JC 5. Latter thus a probable terrace. Now on very flat silty floor of floodplain.	
2006	JC7	246097	667124	31		Textured ground on image, similar to OBS point JC3 but now in pale cream, well sorted structureless medium-grained sand. Dug here for brick making.	
2006	JC8	249484	671174	31		Swampy ground - probably alluvium. Shows best on Landsat colour image.	
2006	JC9	262380	672550	31		Smooth textured ground in red medium grained well sorted non-pebbly sand. NB on Landsat images, onshore bars are seen to S.	
2006	JC10	277382	669943	31		Smooth textured ground in red medium grained well sorted non-pebbly sand.	
2006	JC11	260951	681797	31		Red medium-fine sand.	
2006	JC12	267525	687098	31		Base of slope off sand to N. Change to darker soil on basement.	
2006	JC13	267054	691003	31		Dark grey-green coarse, foliated quartzo-felspathic rock (leucocratic gneiss or granulite) with garnet. Possibly K-feldspar also present. As fragments dug from pit latrine.	

2006	JC14	267040	691720	31		Transitional meso-leucocratic gneiss in road. Contains c. 1cm wide quartz-rich bands alternating with mafic layers; small scale isoclinal intrafolial folds verge to SW.	Foliation strikes 032
2006	JC15	267324	694172	31		Large knoll in finely layered mesocratic gneiss with intrafolial folds separated by grain size-reduced straight zones; latter orientated 038. Multiple generations of QF pegmatite, some occupying straightening zones.	
2007	JC15b	267324	694172	31		Large knoll in finely layered mesocratic gneiss with intrafolial folds separated by grain size-reduced straight zones; latter orientated 038. Multiple generations of QF pegmatite, some occupying straightening zones.	
2007	JC15c	267324	694172	31		Large knoll in finely layered mesocratic gneiss with intrafolial folds separated by grain size-reduced straight zones; latter orientated 038. Multiple generations of QF pegmatite, some occupying straightening zones.	
2006	JC16	264647	701848	31		Since change to higher ground traverse is now on red duricrust.	
2006	JC17	261272	707021	31		Thinly layered mesocratic gneiss - more abundant QF layers than OBS point JC15. Vergence of intrafolial drag-folds suggests sinistral shear. Sporadic pink/red garnet.	Foliation 110 and is subvertical
2007	JC17b	261272	707021	31		Thinly layered mesocratic gneiss - more abundant QF layers than OBS point JC15. Vergence of intrafolial drag-folds suggests sinistral shear. Sporadic pink/red garnet.	Foliation 110 and is subvertical
2006	JC18	260441	707012	31		QF leucogneiss with 1-2 cm wide layering of leuco and mafic (q-f-bi-hnb) components. Minor amphibolite layers show folding. Drag folds indicate dextral shear within a foliation of 040 strike. 2-3 cm wide pegmatite veins present.	Drag folds indicate dextral shear within a foliation of 040 strike
2007	JC18b	260441	707012	31		QF leucogneiss with 1-2 cm wide layering of leuco and mafic (q-f-bi-hnb) components. Minor amphibolite layers show folding. Drag folds indicate dextral shear within a foliation of 040 strike. 2-3 cm wide pegmatite veins present.	Drag folds indicate dextral shear within a foliation of 040 strike
2006	JC19	255126	708026	31		Leucocratic augen gneiss. Thinly layered with sporadic 1-2cm quartz-feldspar augen; latter probably relict transposed pegmatite veins. Mafic (amphibolite) layering is	Foliation 019 and is subvertical

						very thin (1-4mm). Strong intrafolial folding gives dextral shear within foliation striking 019 (subvert).	
2006	JC20	249321	712740	31		Small exposure dominantly in mesocratic gneiss with Q/F layering showing minor intrafolial folding.	Foliation 116 and is subvertical
2007	JC20b	249321	712740	31		Small exposure dominantly in mesocratic gneiss with Q/F layering showing minor intrafolial folding.	Foliation 116 and is subvertical
2006	JC21	246960	701202	31		Pale grey leococratic gneiss. Main foliation strikes 036 and is displaced along pegmatite-filled ductile zones of refoliation; latter with sinuous courses orientated 180-160 and with local development of Q/F augen.	Main foliation 036
2006	JC22	255416	679923	31		Quarry in grey mesocratic gneiss, which is grain-size reduced along wide ductile zones trending 039. Narrow amphibolite sheets are folded and transposed into the foliation. Hornblende coarsens to 4mm in pegmatite rich areas. To E of quarry, gneiss is sharply overlain by pale cream sand c. 2m thick.	
2006	JC23	222017	673380	31		Large exposures in quartzofeldspathic gneiss with augen. Late-stage pegmatite veins.	Strong foliation 025
2006	JC24	820215	685071	30		In road cutting. Thinly bedded to laminated sequence of grey-green fine grained micaceous lithic-rich sandstones interbedded with. Papery' laminated mudstone/siltstones. Syn-sedimentary slump folding in sandstones. Sequence is part of an inclined fold with axial surface dipping 30 deg to SE 130 approx. Some minor folding and thrusting of upper limb shows same vergence (i.e. to NW).	
2007	JC24c	820215	685071	30	PMCD13	JC REVISITED 2007. Green-grey, micaceous massive to normally graded sandstone beds possibly resemble sequences in the Bimbila Formation.	
2006	JC25	819936	690226	30		Glassy quartzitic sandstone; pale pink weathering. Thin internal lamination. Studded with 2-4mm ?pink ?garnet	Palaeocurrents 80, fractures trending 155-335 vertical, 220-40 80 towards the north, Main bed-set, Strike 210, Dip 10
2007	JC25b	819936	690226	30		Glassy quartzitic sandstone; pale pink weathering. Thin internal lamination. Studded with 2-4mm ?pink ?garnet	Strike 210, Dip 10

2007	JC25d	819936	690226	30		JC REVISITED 2007. Possible lower shoreface.	
2006	JC26	816808	697251	30		Brown weathering micaceous siltstones, thinly interbedded with brown fine grained micaceous sandstones - lower part of scarp slope sequence.	
2006	JC27	822617	698116	30		In village, small exposures of hard, grey, quartzitic sandstones. Medium bedded and cross bedded.	Foresets dip 30/305
2006	JC28	824774	701997	30		White, friable quartzitic sandstone. Parts of dip slope of about 10-15 to E 100.	Strike 190, Dip 15
2006	JC29	825258	701868	30		Thinly stratified quartz rich sandstone with well-rounded quartz granules prominent. In some layers sporadic quartz pebbles.	
2006	JC30	829222	705973	30		Pale brown sand on flats by lake shore. Possibly old river terrace?	
2006	JC31	811436	705904	30		Finely laminated medium-fine quartzitic sandstone by road.	
2006	JC32	808914	706585	30		Thinly bedded micaceous sandstone interlaminated with micaceous siltstone.	
2006	JC33	804889	705808	30		Pavements in quartzitic sandstone. Poorly sorted, with common coarse sand and granules in medium grained matrix.	
2006	JC34	793001	701249	30		Medium-bedded (20-70cm) quartzitic sandstone; well laminated with planar and trough cross-bedding.	Palaeocurrents 300, 350
2007	JC34b	793001	701249	30		JC REVISITED 2007. Internal plane- and cross-lamination noted. Some herringbone cross-bedding seen in debris, suggesting a marginal tidal influence.	
2006	JC35	793544	700085	30		White, sugary quartzitic sandstone in road cutting; both well laminated and massive beds types, latter up to 2m. Well jointed and fractured with anomalous dip. Fault juxtaposes sandstone with grey micaceous siltstone to SE; latter dip 38/060	Fault 120 Strike 060, Dip 38
2007	JC35b	793544	700085	30		White, sugary quartzitic sandstone in road cutting; both well laminated and massive beds types, latter up to 2m. Well jointed and fractured with anomalous dip. Fault juxtaposes sandstone with grey micaceous siltstone to SE; latter dip 38/060	Fault 120

2006	JC36	795005	711721	30		White/brown weathering thin bedded quartzitic sandstone in road. Ripple marked bed tops indicate currents to W263	Ripple marked bed tops indicate currents to W 263
2007	JC36b	795005	711721	30		JC REVISITED 2007. Flaggy bedded to finely laminated, with some bed tops rippled. 2 fining-up sequences each about 80cms thick - flaggy bases consist of thin (1-2cm) quartz granule layers and lenticles within medium grained sandstone. Sequences may represent small barrier beach bodies.	
2006	JC37	802020	722144	30		Sandstone, quartzitic, medium grained with subrounded/angular quartz grains.	Cross-lamination indicates currents to NE 038
2007	JC37b	802020	722144	30		JC REVISITED 2007. Sandstone is feldspathic with some lithic grains. Some bed tops are wave-rippled. Common tabular planar cross-bedding.	Cross-lamination indicates currents to 038, 095, 058, 018 (trough), 045
2006	JC38	803735	724584	30		White, pure, hard quartzitic sandstone, flaggy to thick bedded, locally trough cross-bedded. Many millet seed grains indicative of aeolian source in part. Large channel seen in crags to south of road. Cut by swarms of 2-4mm quartz-filled fractures with minor displacements - dominant trend is 020.	Palaeocurrents 25
2007	JC38b	803735	724584	30		White, pure, hard quartzitic sandstone, flaggy to thick bedded, locally trough cross-bedded. Many millet seed grains indicative of aeolian source in part. Large channel seen in crags to south of road. Cut by swarms of 2-4mm quartz-filled fractures with minor displacements - dominant trend is 020.	
2006	JC39	804611	724959	30		Erosion gully in 4m of red clayey silt.	
2006	JC40	802843	728072	30		Very flat lying smooth ground sloping gently towards lake. Possibly underlain by pink clayey sand.	
2006	JC41	797058	729866	30		Pavements in white quartzitic sandstone. Intensely fractured and veined along 095 trend. Riedel shears suggest sinistral movement in part. Some veins contain white amorphous material. In places an earlier vein system is seen, trending 120.	Strike 285, Dip 10
2006	JC42	785761	738130	30		White medium grained quartzitic sandstone - sporadic quartz veins trending 040.	

2006	JC43	747215	727433	30		Top of Odvie Anoma Mountain. Large samples of bauxite lying close to tourist centre.	
2006	JC44	750313	726083	30		On road down to base of escarpment. Thinly bedded sandstones and micaceous siltstones pass up to massive/flaggy quartzite.	
2006	JC45	738267	737625	30		In road cutting grey, quartzitic finely laminated sandstone; intensely fractured along N 015.	
2006	JC46	739748	740336	30		Medium grained yellow-weathering quartzitic sandstone.	Wind ripples show 170 wind direction
2007	JC46b	739748	740336	30		CT REVISITED 2007. Flaggy with siltstone flakes.	
2006	JC47	740700	745588	30		Grey thinly bedded highly micaceous siltstone interbedded with cream siltstone.	
2006	JC48	741789	746883	30	JCGH1	Feature is capped by resistant bed composed of grey-pink quartzose sandstone. Only forms small crags of flaggy bedded sandstone (not typical of L Voltaian).	
2006	JC49	745639	749981	30		Long dip slope towards Lake Volta. No exposures, only duricrust. Possibly slight rise about 300m to SW may mark start of 'Obosum' outcrop.	
2006	JC50	736988	744873	30		Roadside pavements in white/yellow hard medium grained quartzitic sandstone.	
2006	JC51	724822	746009	30		Exposure of basement granitoid.	
2006	JC52	677464	787541	30		Red very fine grained sandstone at crest of scarp.	Strike 245, Dip 15
2006	JC53	679349	811303	30		Roadside cutting up scarp in red/pale cream medium/fine thinly bedded sandstone interbedded with pink siltstone - very little mica. Bedding locally subvertical. 300m up scarp, there are cuttings in red-maroon laminated, non-micaceous mudstones with sporadic thin, hard, grey-green? Dolomitic siltstone beds, latter with ripple drift lamination. See also OBS point JC297.	Strike 315, Dip 4
2006	JC54	679215	814031	30		Thinly bedded pink to red weathering, pink/cream medium grained quartzitic sandstone. Has parting of fine grained sandstone with ripple-drift cross-lamination.	Palaeocurrents 210, 150, 180
2007	JC54b	679215	814031	30		JC REVISITED 2007. Shows plane and trough cross-lamination; some bed bases are channelised. Also some	

						lateral accretion surfaces.	
2006	JC55	693310	829645	30		Pink fine grained micaceous sandstone by road. Shows fine scale trough cross-lamination. Some beds contain flakes and rounded pellets of maroon mudstone.	
2006	JC56	714373	857306	30		Extensive laterite along road - seen as blocks scraped from road and in many small quarries.	
2006	JC57	709885	857448	30	JCGH2	Traverse across change from smooth to rougher textured, paler grained terrain on radiometrics.	
2006	JC58	708849	857586	30	JCGH3	In paler terrain, roadside exposure of a different laterite type with pale brown/grey clay mineral aggregates filling interstices between iron-rich areas.	
2006	JC59	703735	858518	30		Small quarry shows 70cm of red laterite on 30+ cm of pale grey carbonate cemented laterite.	
2006	JC60	702657	859568	30		Possible edge of floodplain here - ground rises to W with swampy area to E.	
2006	JC61	694669	860779	30	JCGH4	In roadside ditch; sandstones are medium grained and red-pink. High proportion of well rounded 'millet seed' grains and maroon mudstone clasts.	
2006	JC62	690369	859987	30	JCGH5	Roadside pavements in fine grey muddy sandstone-poorly sorted- may be road material?	
2006	JC63	659724	852522	30		In Droma village; exposures of thin-bedded, variegated (yellow/pink/pale grey) medium/coarse sandstone. Some possible 'millet seed' grains. Has low angle cross-lamination and minor syn-sedimentary slumping. Red mudstone pellets are common. Cut by minor fault trending NE045, which has rotated adjacent bedding parallel to it.	Fault 045
2006	JC64	662660	854960	30		Pit in soft, white, medium grained quartz-rich sand used for road-surfacing. One fragment of grey cemented sandstone bedrock suggests that the soft sand may be decomposed sandstone - no duricrust here.	
2006	JC65	683388	854977	30		Road mainly on laterite with some white sand cover beneath (sand probably part of road-surfacing material).	
2006	JC66	702025	841746	30		On road just below crest of feature; ribs of pink medium/fine quartzose sandstone. Flakes of maroon	

						mudstone on certain bedding planes - otherwise not generally well bedded.	
2006	JC67	727381	873842	30		Floodplain deposits in pale grey mud and silt; nearby, fragments of maroon/grey, finely laminated sandstone probably dug from bridge foundations.	
2006	JC68	732141	882644	30		River Pru floodplain; exposures of pale cream silty clay alluvium.	
2006	JC69	732717	883232	30		At slope break marking edge of floodplain.	
2006	JC70	723630	887653	30		In road drain; Weathering, dark maroon very fine grained highly micaceous sandstone/siltstone; finely laminated in part.	
2006	JC71	679078	883298	30		On dip-slope; drains show soft, cream-grey superficial sand.	
2006	JC72	669960	884636	30		On significant feature, but nothing exposed. Single piece of pink/grey finely laminated sandstone by roadside.	
2006	JC73	741838	897292	30		Traversing higher ground, just above floodplain.	
2006	JC74	741834	898850	30		Thick laterite with white clay impregnations (Fiona sampled). Floodplain is c. 400m to E	
2006	JC75	761411	920043	30		From ferry landing to here, possible terrace. Slope break marking edge of floodplain is c. 300m to N.	
2006	JC76	770823	930814	30		Laterite road on feature; no exposures.	
2006	JC77	779197	943888	30		Roadside exposures in laterite.	
2006	JC78	787079	942602	30		Ditch section in laterite profile. Hard red laterite passes down over 20-30cm to grey clay with oxide nodules. Latter in turn underlain by pale grey clay with relict flakes of olive green/khaki mudstone	
2006	JC79	793239	941121	30		Well digging shows flakes of grey, fissile mudstone.	
2006	JC80	806757	937064	30		Bank of R Daka - 3-4m of pale yellow silty clay. Impassable crossing.	
2006	JC81	829847	969719	30		Road on red laterite - no exposures.	
2006	JC82	175205	969098	31		Green/grey med grained arkosic sandstone with flakes of green-grey mudstone.	

2006	JC83	170934	961417	31		In road, medium grained green-grey sandstone with green-grey mudstone flakes.	
2006	JC84	827194	929719	30		Red silty clay, massive, overlying laterite in roadside section.	
2006	JC85	824149	925830	30		In Bunya village. Medium grained, green-grey, x-stratified sandstone with green-grey mudstone rip-up flakes - forms small koppies.	
2006	JC86	820860	919701	30		In road, large pavements of green-grey, fine-medium grained sandstone; cut by fractures.	Fractures 088
2006	JC87	824523	910828	30		Brown weathering, green-grey cross-laminated sandstone.	
2006	JC88	825307	909575	30	JCGH6	Green-grey medium/fine laminated sandstone with local concentrations of mud-flakes.	
2006	JC89	171981	905408	31		In road, khaki/green finely laminated micaceous mudstone and siltstone.	
2006	JC90	173554	905463	31		Ditch in laminated, highly micaceous variegated mudstones (maroon, pale grey/dark grey/red)	
2006	JC91	183325	900964	31		Finely laminated khaki-green micaceous mudstones; sub-horizontal but locally faulted or flexured.	tectonic dip is 50/190 Strike 280, Dip 50
2006	JC92	728834	1033473	30		SW of Tamale diggings for pond reveal pale buff/yellow, fine grained micaceous sandstone. Planar laminations picked out by Mn staining; some ripple drift cross-laminae.	
2007	JC92b	728834	1033473	30		JC REVISITED 2007. When parting lineation noted suggestive of high-flow regime. Also some slabs with very large mud clast impressions.	
2006	JC93	725897	1030582	30		In small pond - flakes of buff laminated micaceous siltstone.	
2006	JC94	715228	1007442	30		In laterite quarry; flakes of buff/maroon laminated mudstone and larger fragments of buff laminated micaceous sandstone; some Mn impregnations.	
2006	JC95	715355	1005820	30		Bridge excavations-abundant debris of medium grey, laminated micaceous sandstone.	
2006	JC96	721279	993920	30		In road; rib of pale yellow (possibly weathered) fine grained	

						quartzose sandstone.	
2006	JC97	720970	984711	30		Medium grey micaceous siltstone; laminated with some scattered fine sand grains. Interbedded with maroon micaceous mudstone.	
2006	JC98	732416	952655	30		No exposure-end of search for ring structure.	
2006	JC99	734780	1040925	30		New Tamale stadium; abundant fragments of red medium grained sandstone. Angular/sub-rounded oxide-coated grains.	
2006	JC100	740849	1038220	30		Yendi road; from Tamale to here, common debris of red sandstone. Here in river bed, c. 1m of soft, maroon micaceous mudstones interbedded with thin (<10cm) pale green micaceous mudstones. Sequence is folded along sub-horizontal axis trending 165. Adjacent in river bed, pavements in sub-horizontal, flaggy, pale brown-grey micaceous sandstone. May be in contact with mudstones along postulated fault trending c 050.	Fault 050
2006	JC101	746171	1037174	30		Pond diggings in fissile, extremely well laminated buff to very dark grey or grey green, micaceous papery mudstone - probably of anoxic facies; some debris of 'stadium' red sandstone; well sorted and possibly aeolian.	
2006	JC102	747791	1036750	30		On higher ground, exposures of red-weathering, yellow/buff fine/medium/coarse grained stratified sub-arkosic sandstone - some well-rounded 'millet seed' quartz grains. Possible extension of Tamale Sandstone.	Stained joint 70-250 70 towards N
2006	JC103	763603	1037013	30		Scrapings in pebbly laterite with pebbles of quartzite and fragments of quartzose sandstone - latter commonly tabular and of local derivation.	
2006	JC104	766712	1037648	30		Laterite quarry.	
2006	JC105	777282	1040273	30		Pebbly laterite on ridge.	
2007	JC105b	777282	1040273	30		JC REVISITED 2007. Pale green micaceous arkosic sandstones of 'Bunya' type exposed.	
2006	JC106	788040	1045042	30	JCGH7	Scarp of major feature - exposures in green/grey 'Bunya' sandstone. Medium grained and poorly sorted arkosic, micaceous. Thinly stratified and ripple marked; some	Siltstone, Strike 0, Dip 2

						layers with green and maroon mud-flakes. Dip c. 2 to E	
2007	JC106b	788040	1045042	30	JCGH7/PMCD6	JC REVISITED 2007. Cutting widened to show maroon/green/grey slightly micaceous siltstones overlying sandstone; siltstones sampled for acritarchs . Latter is coarse and gritty at base, with granules of red jasper and metavolcanic lithologies; it fines upwards suggesting a turbidite.	Bedding 36 towards 36 Fractures 165-345 dipping 60 w and 70-250 vertical
2006	JC107	798000	1041900	30		Roadside quarry shows cemented cobble and pebble gravel with basement clasts. Unseen contact on weathered green/grey sandstone exposed c. 1m away. In other parts of quarry, sandstone bedrock contains granule layers and conglomeratic lenticles with rounded basement pebbles.	
2007	JC107b	798000	1041900	30		JC REVISITED 2007. Roadside quarry shows cemented cobble and pebble conglomerate up to 1.5m thick, with basement clasts (green metavolcanic, jasper, porphyritic dacite, garnetiferous psammite, schist). Unseen contact on weathered green/grey, locally gritty sandstone in other parts of quarry. Clasts locally supported in poorly sorted coarse sand/granule matrix. Sandstone contains granule layers and conglomeratic lenticles with rounded basement pebbles. Conglomerate weathers down to pebble-rich gravel.	
2006	JC108	820627	1043058	30		Green/grey, medium grained sandstone of 'Bunya' type.	
2006	JC109	175277	1043019	31		In well, flakes of green-grey micaceous siltstone.	
2006	JC110	171843	1044532	31	JCGH 26B	Pavements in grey, thinly bedded micaceous siltstones and very fine grained sandstone around well; some have rippled bed-tops. In wall of well, local slabs of grey micaceous siltstone plastered with branching, bulbous organic impressions - possibly algal colonies or trace fossils.	
2007	JC110b	171843	1044532	31		JC REVISITED 2007. More slabs and debris found, and sampled. Possible stromatolitic structures photographed on one bed.	
2006	JC111	192479	1035334	31		Gnani village. Pavements in green-grey medium grained arkosic sandstone of Bunya type.	

2006	JC112	197049	1029922	31		On slight rise from Oti floodplain - possibly now on terrace.	
2006	JC113	193150	1034119	31		Terrace back-edge - very gentle concave break up to steeper slope on W side.	
2006	JC114	171398	1033217	31		Road south from Yendi to here - only laterite seen.	
2006	JC115	806428	1095605	30		Green-grey medium grained sandstone.	
2006	JC116	813149	1102481	30		From Gushiego to here no exposures, only laterite.	
2006	JC117	816377	1104786	30		On slight rise, exposures in grey-green fine grained micaceous sandstone.	
2006	JC118	816464	1105633	30		Roadside exposures in grey/green, fissile, finely laminated micaceous mudstone and siltstone.	
2006	JC119	818268	1110581	30		Variegated pale cream/pink/grey micaceous mudstone, fissile. Some mud cracks noted.	
2007	JC119b	818268	1110581	30		JC REVISITED 2007. Some tabular fragments of green, highly siliceous fine sandstone/siltstone.	
2006	JC120	818879	1116165	30		Exposures in yellow/green/grey micaceous fine grained sandstone and siltstone; finely interbedded.	
2006	JC121	819579	1124981	30		Green/khaki/maroon finely laminated micaceous mudstone and siltstone with minor thin sandstone beds forming ribs on road from previous point.	
2006	JC122	830461	1133237	30		Variegated red/khaki/green micaceous mudstones and silty mudstones.	
2006	JC123	804499	1143118	30		No exposures from JC122 to here. Here, floodplain c. 200m wide.	
2006	JC124	803339	1143561	30		Diggings from bridge in flinty, crimson-weathering very finely laminated, siliceous mudstone/siltstone.	
2006	JC125	800078	1143911	30		Bridge diggings in pink/crimson very finely laminated, siliceous siltstone.	
2006	JC126	796543	1147893	30	JCGH8	Red siliceous laminated siltstone with kernels showing that the fresh rock is pale grey and highly siliceous - possibly laminated tuff. Forms flatiron feature.	
2006	JC127	796023	1149861	30		Medium grained buff/white weathering quartz arenite; trough cross-bedded.	Palaeocurrents 30

2006	JC128	800542	1147605	30		On feature; abundant tablets of red weathering, very pale grey finely laminated to massive ('cherty') siliceous mudstone/tuff.	
2006	JC129	793508	1155271	30		Pavements in red weathering quartzitic sandstone with some feldspar grains.	Trough cross-bedded with currents to NE 048
2007	JC129b	793508	1155271	30		Revisited in 2007. Sandstone, slightly feldspathic, medium-grained, well-sorted. Trough cross-bedded throughout	Palaeocurrents 80, 060, 080, 055
2006	JC130	789461	1160270	30		Exposures on dip-slope in yellow-weathering medium grained quartzitic sandstone.	
2006	JC131	788387	1163519	30		Medium grey (yellow weathering) quartzitic sandstone at Chesterfield Lodge Hotel.	
2006	JC132	783613	1164702	30		Med/fine grained yellow weathering quartzitic sandstone in ditch.	
2007	JC132b	783613	1164702	30		JC REVISITED 2007. Very large scale planar lamination and low angle cross-bedding. Sandstone is micaceous with muddy matrix.	
2006	JC133	783776	1164939	30		Outlier on dip slope - in medium grained quartzose sandstone locally well laminated and thickly to thinly bedded.	
2006	JC134	802407	1149721	30		Waterfall in white, quartzitic sandstone.	Trough cross-laminationindicates currents to NE 050
2006	JC135	790627	1154950	30		Pavements in medium/coarse grained quartzitic sandstone.	Cross-bedding indicates currents to NW 330
2006	JC136	788936	1150935	30		Pavements in medium/coarse pink to purple weathering quartzitic sandstone. Fractures oriented 295	Fractures 295
2006	JC137	788093	1146443	30		Subdued feature in pink/brown weathering, grey very finely laminated siliceous mudstone or possibly tuff. Some syn-sedimentary disturbances of laminae	
2006	JC138	776429	1162477	30		Red weathering, white, medium-fine grained quartz-rich sandstone.	Trough cross-laminated with currents to NW 320
2007	JC138b	776429	1162477	30		JC REVISITED 2007. In large faces, drag-folding of planar cross bedding seen. Some plane laminated intervals occur between cross-bed sets.	Palaeocurrents 320, 305, 315, 345

2007	JC138c	776429	1162477	30		CT REVISITED 2007. Sandstone, quartz arenite, moderately feldspathic, medium grained with some fine and coarse, locally gritty in texture. Tabular cross-stratified beds and plane laminated beds, with palaeocurrent directions towards to the NW. Cross-stratification indicates transport of sediment towards the N. Fluvial beds, with very rapid deposition in delta front followed by prograding shallow fluvial sands, including plane laminated beds deposited in the upper flow regime?	Palaeocurrents 360
2006	JC139	772535	1157893	30		Medium grained brown/yellow weathering quartzitic sandstone.	
2007	JC139b	772535	1157893	30		JC REVISITED 2007. Very little feldspar or clay matrix. Possible planar laminated internal structure and ripple drift cross-lamination.	
2006	JC140	768758	1153465	30		Medium grained feldspathic sandstone.	Cross bedding shows currents to NW 315
2007	JC140b	768758	1153465	30		JC REVISITED 2007. Sandstone strongly arkosic, with a white clayey matrix.	Palaeocurrents 330, 310, 305, 295
2006	JC141	757421	1146839	30		Medium grained yellow weathering, white quartzitic sandstone.	
2006	JC142	738566	1103968	30		At Pigu, ridge in medium/fine green/grey 'Bunya' sandstone.	
2006	JC143	739454	1103797	30		Fine grained green/grey sandstone.	
2006	JC144	741304	1103940	30		For last c. 300m, pavements in green/grey fine grained micaceous sandstone.	
2006	JC145	745193	1103673	30		Over last 50m, fine grained green/grey sandstone.	
2006	JC146	747288	1103032	30		Fine grained green/grey micaceous sandstone.	
2006	JC147	749297	1102697	30		Fine grained green/grey sandstone, intermittently seen from OBS point JC146. Here as a thin bed alternating with yellow/green weathering micaceous siltstone.	
2006	JC148	750609	1102720	30		Extensive exposure of green/grey sandstone. Cut by joints at 090	Joints 090
2006	JC149	758757	1102357	30		Pisegu village; fine grained green/grey sandstone.	Palaeocurrents Cross-lamination

						Green/grey mud-flakes present.	indicates currents to SE120
2006	JC150	759937	1102087	30		In pond, buff micaceous siltstones and silty mudstones.	
2006	JC151	763024	1100987	30		Fine green/grey micaceous sandstone; intermittent from OBS point JC150	
2006	JC152	763378	1100832	30		Fine/med green/grey micaceous sandstone with green/grey mud-flakes.	Cross-laminae indicates currents to SW230
2006	JC153	771302	1099705	30		Fine grained green/grey sandstone.	
2006	JC154	773678	1099854	30		Fine grained green/grey sandstone; common green/grey mudstone rips up flakes. Exposed all way up slope.	Cross laminae indicate currents to N 010
2006	JC155	761652	1093710	30		Only laterite exposed from Sang village to here.	
2006	JC156	749367	1089646	30		Only laterite exposed from OBS point JC155 to here.	
2006	JC157	743554	1084931	30		Only laterite from OBS point JC156. Here an extensive swampy tract planted with rice.	
2006	JC158	738098	1079606	30		Very wide swampy floodplain.	
2006	JC159	739234	1076152	30		Approx back edge of floodplain here.	
2006	JC160	738583	1073879	30		Subdued ridge with exposures of faintly laminated, grey micaceous siltstone.	
2007	JC160b	738583	1073879	30		JC REVISITED 2007. Debris in trench of very fine-grained, cream to purplish grey weathered micaceous sandstone with ripple-drift cross-lamination and hummocky cross-stratification. Flaser structure also seen, as are mud-cracks, latter suggestive of semi-emergent lacustrine or tidal flat environments.	
2006	JC161	738036	1061679	30		Roadside diggings show large slabs of medium grained thickly bedded pink weathering quartz rich sandstone.	
2006	JC162	737865	1060121	30		Pale grey medium grained quartzitic sandstone - common well rounded grains, suggestive of aeolian influence. Forms pavements in floor of laterite quarry.	
2006	JC163	736861	1051347	30		Pond diggings - slabs of laminated dark maroon highly micaceous fine sandstone and siltstone.	
2006	JC164	736643	1050551	30		Cutting shows debris of laminated dark grey/dark maroon fine sandstone and siltstone. Lunate and sinuous crested	

						ripple marks. Also debris of more thickly bedded buff micaceous sandstone.	
2007	JC164b	736643	1050551	30		Cutting shows debris of laminated dark grey/dark maroon fine sandstone and siltstone. Lunate and sinuous crested ripple marks. Also debris of more thickly bedded buff micaceous sandstone.	
2006	JC165	736477	1046474	30		Roadside debris of dark maroon fine grained sandstone in tabular beds up to 20cm thick.	
2006	JC166	677784	1054398	30		Daboya landing, west side. Yellow calcareous dolostones overlain by grey, laminated limestones with lenticles and layers containing basement pebbles. Possibly local faulting.	Strike 235, Dip 30
2006	JC167	677669	1054543	30		Sandy limestone, grey, common quartz grains and granules and pebbles of basement (phyllite etc) + maroon siltstone clasts. Barytes/chert veining.	
2006	JC168	677429	1054668	30		Pavements in pale grey weathering, dark grey limestone. Finely laminated and medium grained with abundant rounded pellets and ooids c. 1mm size. Baryte veining.	
2006	JC169	680988	1054278	30		Roadside ditch in highly micaceous purple/grey/green variegated mudstones and siltstones.	
2006	JC170	681488	1054053	30		Roadside exposures in 3-4m sequence of fissile, laminated, grey/brown/maroon micaceous mudstones; some thicker units of micaceous siltstone.	
2006	JC171	693409	1050224	30		In floor of laterite quarry, flakes of yellow weathering, pale brown micaceous siltstone.	
2006	JC172	695200	1049500	30		Roadside section in extremely well laminated variegated micaceous mudstones (yellow/brown/grey/purple/green). Slightly thicker intercalated beds of pale buff laminated micaceous siltstone. Photo of gentle folding. Maroon beds show pale yellow mottling	
2007	JC172b	695200	1049500	30		Roadside section in extremely well laminated variegated micaceous mudstones (yellow/brown/grey/purple/green). Slightly thicker intercalated beds of pale buff laminated micaceous siltstone. Photo of gentle folding. Maroon beds show pale yellow mottling	

2006	JC173	694710	1049890	30		In ditch, exposures of red-weathering very fine micaceous siltstone. Overlain by 10cms of cobble gravel and then laterite.	
2007	JC173b	694710	1049890	30		JC REVISITED 2007. Ribs of grey weakly calcareous, slightly micaceous siltstone intercalated with buff papery shales as c. 1cm thick beds separated by more massive grey/pink siltstones.	
2006	JC174	704694	1045313	30		In laterite pit, large exposures of well cemented fine/med pale grey sandstone, some beds with mud-flakes. Weathers to brown/pink/crimson and forms crest of a small rise.	
2006	JC175	713462	1042599	30		Roadside exposures of flaggy, very finely laminated sandstone and siltstone. Pink weathering with some grey mudstone laminae/partings; some ripple drift cross-lamination. About 300-400m to E, crest formed by medium bedded red/pink weathering micaceous sandstone.	Palaeocurrents 150
2007	JC175b	713462	1042599	30		JC REVISITED 2007. Immature fine grained sandstone (possibly Tamale Fm) with ripple drift cross-lamination.	
2006	JC176	716456	1041230	30		Abundant chips of red fine micaceous sandstone in road.	
2006	JC177	716947	1041011	30		Abundant tablets of red fine micaceous sandstone.	
2006	JC178	663948	1013604	30		Busunu village - fragments of crimson weathering siliceous, laminated siltstone around water main.	
2006	JC179	662268	1015670	30		Laterite quarry - siliceous siltstone clasts abundant in laterite.	
2006	JC180	663388	1026620	30		Roadside ditch in pink weathering med grained laminated quartzitic sandstone; sub-angular to well rounded grains.	
2006	JC181	663247	1027626	30		On a slope down to floodplain. Exposures of fissile, very finely laminated slightly micaceous olive green mudstone.	
2006	JC182	661629	1012423	30		Well diggings in pale green finely laminated mudstone.	
2006	JC183	661670	1012240	30		Roadside quarry in hard pink/crimson weathering siliceous siltstone.	
2006	JC184	657170	1010524	30		Mast foundations in yellow weathering medium grained sandstone with common white feldspar grains.	

2006	JC185	650650	1008670	30		In road, fine/med yellow weathering quartzitic sandstone.	
2006	JC186	644215	1007684	30		In road; hard silicified fine/med quartzose sandstone; possibly some garnet grains.	
2006	JC187	638375	1006268	30		Med grained quartzitic sandstone.	
2006	JC188	636917	1003827	30		In crags c. 8m of brown weathering cross-bedded sandstone. Sandstones are dark maroon with abundant white feldspars.	Trough cross-beds show currents to NE/028
2006	JC189	629586	1004565	30		Abundant tablets of pink weathering fine/med grained sandstone.	
2006	JC190	628773	1007087	30		Ditch in pink weathering flaggy/laminated, quartzitic fine grained sandstone. Interbedded with micaceous fine sandstones and siltstones.	
2006	JC191	626199	1015739	30		Diggings in mast foundation; show medium grained laminated buff quartzitic sandstone and dark grey/purple fine micaceous sandstones with grey mud-flakes. Also debris of maroon micaceous siltstone and mudstone.	
2006	JC192	625736	1017545	30		In ditch highly micaceous laminated fine sandstone with purple/yellow variegation; micaceous siltstone interbeds.	
2006	JC193	625484	1018745	30		Roadside pavements in very finely laminated fine grained micaceous sandstone; some large mud-flakes.	
2006	JC194	690204	1009021	30		Mast diggings show purple/grey laminated micaceous siltstone and silty mudstone.	
2006	JC195	712345	1018557	30		Mast diggings show fragments of pale buff fine grained quartzitic sandstone (Kurusawa)	
2006	JC196	667623	972565	30		Tank diggings at Bwipe; very finely laminated olive green slightly siliceous mudstones. Concretions and discontinuous layers up to 25cm wide of blue/grey, hard, micritic limestone; some domed mudstone laminae	
2006	JC197	664845	970055	30		Bwipe No 3 Quarry. In blue/grey laminated micritic limestone interbedded with dark maroon laminated papery micaceous siltstones; pass down to yellow dolomitic limestone.	
2006	JC198	665604	968854	30		Bwipe No 2 Quarry. In finely laminated micaceous and	

						dolomitic limestone - see notes.	
2006	JC199	665399	969516	30		Bwipe trial pit. C.3-4m of thinly bedded, laminated blue/grey micrite - very subordinate maroon siltstone intercalations.	
2006	JC200	667014	970120	30		Bwipe No 1 Quarry. Small overgrown quarry in massive dolomitic breccia - sporadic basement pebbles + baryte segregations.	
2006	JC201	667623	970010	30		Nr Bwipe; trench for pipe shows debris of khaki/olive green v. finely laminated siliceous(?) mudstone/siltstone with sporadic micritic limestone concretions. (laminated micrite exposed in the same trench farther W)	
2006	JC202	668153	970375	30		Trench in finely laminated crimson weathering hard siltstones.	
2006	JC203	661836	972612	30		From Bwipe to here, no exposures - here a laterite.	
2006	JC204	660044	972119	30		Limestone blocks in road but possibly not in situ. Black soil typical of the limestone outcrop seen here.	
2006	JC205	657754	973753	30		No exposures from OBS point JC204. Here small fragments of red-weathering sandstone by roadside.	
2006	JC206	657587	973815	30		Laterite with abundant chert fragments.	
2006	JC207	656540	974364	30		Small laterite quarry - minor debris of medium grained quartzitic sandstone.	
2006	JC208	641919	977590	30		No exposures from previous point OBS point JC208.	
2006	JC209	668462	966226	30		Laterite quarry.	
2006	JC210	662780	957822	30		Well debris in pale green/purple-grey laminated mudstone.	
2006	JC211	648827	949458	30		Mast footings show at least 1.2m laterite overlain by 2m red sandy, massive silt/clay with coarse sand grains and granules.	
2006	JC212	657777	923876	30		Mast footings show 4-5m section. At least 2m of laterite at base. Overlain with erosive contact by 3m of poorly sorted, massive red silty clay with abundant quartz grains and scattered pebbles.	
2006	JC213	642956	894021	30		Quartzitic sandstone, medium grained verging to coarse.	Dip 20 to E is too steep to be

						Thinly bedded in 5-20cm units.	regional Strike 0, Dip 20
2006	JC214	643321	895248	30		Medium to coarse pale brown-weathering sandstone; common white feldspar grains. Some beds up to 1.5m thick with internal planar lamination. Intercalations of finely laminated medium grained micaceous sandstone.	
2006	JC215	643572	897696	30		On hill by roadside. Quartz-feldspar sandstone, medium grained, laminated.	
2006	JC216	643521	898712	30		Medium grained quartz rich sandstone. Poorly sorted with medium and fine grains, some of former well rounded. Laminated to thickly parallel bedded. Minor bedding-parallel quartz veins.	
2006	JC217	643731	900910	30		Brown weathering fine grained sandstone; flaggy, with abundant mica on bedding surfaces; some cross-bedding.	Palaeocurrents 55
2006	JC218	657686	922679	30		Mast debris indicates laterite on grey clay - latter probably decomposed mudstone.	
2006	JC219	668179	972390	30		Mast at Bwipe - green/pink hard siliceous siltstone with layers of blue/grey micritic limestone.	
2006	JC220	640901	978087	30		Yellow weathering med arkosic sandstone - very common white feldspar grains. Some green mudstone partings.	Palaeocurrents cross-lamination indicates currents to NW 330
2006	JC221	634981	980755	30		Medium grained quartzitic sandstone in ditch.	
2006	JC222	634232	980840	30		In ditch 1m clayey siltstone overlies clast supported gravel with abundant sandstone fragments.	
2006	JC223	632397	980666	30		V pale grey, laminated, micaceous fine grained sandstone on road.	
2006	JC224	632403	979670	30		Pale grey well laminated fine grained micaceous sandstone.	
2006	JC225	633497	976684	30		Pale grey laminated fine grained micaceous sandstone.	
2006	JC226	633851	975873	30		Pale grey med bedded fine grained micaceous sandstone.	
2006	JC227	636166	970025	30		Pale grey med bedded fine/med sandstone.	
2006	JC228	637504	968122	30		Fine grained highly micaceous laminated to thinly bedded (flaggy) sandstone.	

2006	JC229	635882	965643	30		Pavements in brown weathering fine grained laminated highly micaceous sandstone.	
2006	JC230	634879	965077	30		Very finely laminated micaceous fine grained sandstone, dark maroon to pale grey.	
2006	JC231	669989	971021	30		Olive green finely laminated siliceous mudstones in mast debris.	
2006	JC232	643286	904087	30		In ditch decomposed laterite overlain by red silty clay.	
2006	JC233	644886	903917	30		Well diggings show flakes of papery very finely laminated non-micaceous purple/olive green/pale yellow mudstone. Escarpment to W is developed on this. Across road are laterite quarries.	
2006	JC234	636954	864977	30		Kokuma village. Brown weathering dark grey medium grained quartzitic sandstone with sub-angular to angular grains. Common white feldspar grains. Exposure is laterite-coated.	
2006	JC235	636690	863890	30		Crags in medium grained buff sandstone in massive (2-3m) beds. Common feldspar grains. Photos taken of quartz veins; one set at 144 and a later crosscutting set at 220.	
2006	JC236	636645	860500	30		Deep wash-out shows 4m of red silty clay on laterite.	
2006	JC237	637105	859740	30		Well debris in laminated medium/fine buff/red/green/grey sandstone with some green mud-flakes.	
2006	JC238	636730	858431	30		Crest of small feature in grey med/fine sandstone interbedded with dark maroon finely laminated non micaceous sandstone.	
2006	JC239	636677	854826	30		Crags in brown weathering medium/fine sandstone showing very large scale planar cross-bedding. Interbedded with coarse poorly sorted sandstones that fine up to medium grained planar laminated sandstone.	Palaeocurrents 225, 140 (both wind)
2007	JC239b	636677	854826	30		JC REVISITED 2007. Interpreted as aeolian beds.	
2006	JC240	641970	840561	30		In ditch, finely laminated quartz rich medium grained sandstone with sporadic pebbles and mud-flakes. Thin dark maroon syn-sedimentary dykelets present.	
2006	JC241	642171	840181	30		Fine grained, laminated grey to dark maroon sandstone alternates with more massive med/fine sandstone; c. 20%	Palaeocurrents currents to NW 325

						feldspar grains. Some low-angle cross-lamination.	
2006	JC242	649250	826486	30		In ditch down slope, fractured dark maroon, fissile micaceous very fine sandstone interbedded with thin pale grey medium grained sandstone + maroon micaceous mudstones and siltstones.	Fracture 320. Fault 055. Fold axis 320
2006	JC243	647637	822777	30		Roadside exposures of yellow weathering fine grained sandstone - some feldspar grains.	
2006	JC244	653278	813732	30		Brown weathering medium grained poorly sorted quartzitic sandstone with feldspar grains.	Joints 240
2006	JC245	665193	811663	30		Thick laterite.	
2006	JC246	668463	810275	30		Well diggings show fragments of brown medium grained sandstone.	
2006	JC247	672542	809755	30		Well diggings show small flakes of green/dark purple mudstone/siltstone.	
2006	JC248	677712	808497	30		Well diggings in pale green/dark maroon micaceous siltstone.	
2006	JC249	676237	801639	30		Well diggings show abundant fragments of pink and yellow massive chert. Also fragments of brown medium grained sandstone. One fragment shows sharp contact between chert and sandstone.	
2006	JC250	676546	792956	30		Roadside koppies in brown medium grained sandstone. Some cross-lamination in c. 1.5m thick bed sets.	Palaeocurrents: Wind towards S 160
2007	JC250b	676546	792956	30		JC REVISITED 2007. Photos taken of probable dune bedding; some possible fluvial channelling near top.	
2006	JC251	683458	779955	30		N of Nsuta, in roadside ditch, c. 3m of red weathering medium grained quartzitic sandstone. Lamination picked out by slightly finer grained layers; uncertain whether the structure is tectonic or sedimentary. Overlain by Fe-cemented lateritic gravel with local sandstone clasts.	Palaeocurrents: currents towards SW 200
2006	JC252	683848	781258	30		In road, rib of sheared, very hard white silicified quartz-rich sandstone. Rib trends 270. C. 120m to S, laminated sandstone dips 25 to SW 235.	Strike 145, Dip 25
2006	JC253	686744	784120	30		Red weathering, med/fine grained feldspathic sandstone.	

2006	JC254	687465	786393	30		Red weathering, medium grained feldspathic sandstone. Laminated, with dip of 20 to SE 105. Probably this is cross-bedding since against regional tectonic dip.	Palaeocurrents dipping to SE 105, probably cross-bedding since against regional tectonic dip
2006	JC255	688510	788426	30		In drain, laminated very fine grained sandstone and pale yellow/buff laminated siltstone. Debris of red-weathering, non siliceous fine sandstone.	
2006	JC256	689046	789360	30		Medium grained pale yellow weathering quartz-feldspar (arkosic) sandstones. Sporadic green grains may be glauconite.	
2006	JC257	689041	789891	30		Pavements in pale cream weathering medium/fine grained diffusely laminated sandstone.	
2006	JC258	690232	791688	30		Well diggings - only loose sand seen.	
2006	JC259	693850	797632	30		Aframso: well diggings in grey/yellow/purple non micaceous mudstones with debris also of poorly sorted dark grey/purple medium grained micaceous sandstone with feldspar grains.	
2006	JC260	689462	790120	30		Very common fragments of yellow medium grained sandstone on road, but not seen in situ.	
2006	JC261	712158	751911	30		Agogo; thinly bedded to laminated, fine/medium grained sandstone interbedded with grey mudstone and siltstone.	
2006	JC262	712577	751933	30		Red/brown weathering, thinly bedded to laminated, highly micaceous sandstone - medium to fine grained. Overlain by laterite incorporating local sandstone blocks.	
2006	JC263	803056	766542	30		Tease village; white cross-laminated arkosic sandstone; herringbone pattern locally seen. Mainly medium grained but some very course/granule lenses and mud-flakes. Generally well sorted with coarse 'millet seed' grains; possibly reworked aeolian. Bedding locally disrupted by low-angle, syn-sedimentary thrust-faults with vergence to S 170 (strike 70 and dip of thrust plane 22 to NE). Some steeply-dipping, slumped bedding also noted.	
2006	JC264	815734	771379	30		White, faintly laminated quartzitic sandstone, medium grained and similar to OBS point JC263.	
2006	JC265	815875	771088	30		Grey/pink medium/fine arkosic sandstone.	

2006	JC266	804795	766272	30		White, medium grained quartz-rich sandstone with common white feldspars. Very thinly bedded to laminated.	
2006	JC267	796616	747979	30		Well diggings in flakes of blue-grey finely laminated mudstone.	
2006	JC268	797239	745263	30		Well diggings in hard blue/grey laminated mudstone; slightly micaceous.	
2006	JC269	823331	685522	30		Oterkpolu limestone quarry. Limestone is blue/grey, thinly bedded to laminated and in parts interbedded with maroon siltstone. Information states that limestone is silicified (-possibly the dark grey beds). Some fissile, phyllitic partings. Folded into reclined structures verging to NW; axial surfaces dip c. 40-50 to SE 110 approx with hinges plunging 10-15 to S (see notes). Folded limestone is overlain by sandstone (not visited, but contact appears planar and is possibly a slide).	
2007	JC269c	823331	685522	30		JC REVISITED 2007. Photos taken of laminated maroon calcareous siltstone and blue-grey micritic limestone - some possible syn-sedimentary microfaulting present. Some bed tops are rippled. At top of quarry, limestone passes structurally upwards into foliated yellow-cream siltstone with hard cm-thick maroon highly siliceaou layers. This in turn passes up to white-grey, glassy, medium grained, laminated quartz arenite. JC REVISITED 2008. Sample of mudstone taken for Sm-Nd.	
2007	CJ200	747701	729134	30		Gutter section 20m long with 2m drop. White/pale yellow medium grained sandstone. Flaggy.	Trough cross bedding 45 and 65 e-w vertical fracturing Joints 275
2007	CJ201	747515	728977	30		Over steepened cross bedding to 70 deg, note cross cut by horizontal shears. Laminated mudstone.	Palaeocurrents Over steepened cross bedding 70
2007	CJ202	739895	744586	30		Flaggy coarse grained sandstone. Pale yellow/white, weathering to dark red.	Some fractures seen. 80-280 dip 70 south, n-s dip 60 east Joints 260 and 175
2007	CJ203	739331	744485	30	PMCD3	Flaggy med to coarse grained sandstone in quarry floor, pale yellow/white, weathering to dark red. Discontinuous pebble beds. Shear/fracture zone, bleached and slightly	E-W faults seen. One major 2 cm thick fault trending e-w and two minor faults trending 240-60 and

						softer, aligned 90 deg. Secondary fracture set to 155 deg, riedels suggest sinistral movement.	260-80. Minor fracture seen 318-138 70 to NE, 330-150 80 to NE, 340-160 85 to E, fracture zone 90. Secondary fracture 155
2007	CJ204	736081	744789	30		Flaggy med grained yellow sandstone exposed in a gutter section. Cross bedding suggests palaeocurrent to 60 deg. Cross bedding also to 350 deg in coarse grained sandstone with maroon laminae.	Cross bedding 60 and 350, weak jointing 100-280 and160-340, Joints 100 and 355, weakly jointed. Also to 160 in coarse grained sediment
2007	CJ205	733177	745549	30		Flaggy medium grained sandstone in roadside ditch. Yellow, weathering to red. Laminated, with cross bedding to 355 deg.	Cross bedding 355, small vein in fracture trending 146-316 dipping 85 to N. Second minor set 94-274 85 to N
2007	CJ206	731481	747852	30		Flaggy med to coarse grained sandstone, massive bedded - pale yellow/white, med grained in lower section. Surface wave ripples; approximately palaeocurrent towards 350 deg. 20m to west is a more extensive outcrop, cross bedding towards 25 deg in very coarse bed containing small pebbles. Coarsening upwards.	Wave ripples 350. Cross bedding 25, small fractures, 100-280 dip 60 to south Jointing 200 and 300
2007	CJ207	730925	747968	30		As OBS point CJ206; extensive flaggy coarse grained sandstone.	Small fractures showing traces of Fe staining, vertical 125-305 and 110 to 290
2007	CJ208	730291	747211	30		Med to coarse grained bedded sandstone with pebbly beds. Herring bone cross bedding abundant. Edge of outcrop forms 4-5m high escarpment aligned east west. This locality contains a series of east west aligned escarpments.	Two faults appear in this escarpment trending E-W with a down throw to the north
2007	CJ209	723164	748061	30		Roadside gutter section. Thinly bedded fine grained sandstone. Open folding, with fold hinge aligned N/S. Base is fine grained laminated sandstone, similar to variegated shales/mudstones.	
2007	CJ210	722083	748472	30		Dark maroon med grained sandstone interbedded with thin beds of white sandstone (med grained). Massive.	
2007	CJ211	718381	749423	30		4m section of coarse grained bedded yellow sandstone. 5 beds contain cross bedding towards approx 90 deg. Also herring bone cross bedding in pebbly beds.	Cross bedding 90, some minor fractures, vertical 170-350

2007	CJ212	713265	750758	30		Exposure in a bluff above the road. Horizontally bedded med/coarse grained yellow/grey/light red sandstone.	Cross bedding 300 to 360 Joints 25 and 255 Small fissures at 260
2007	CJ213	679200	814049	30		CJ REVISITED OBS point JC54. Roadside outcrop of flaggy sandstone 10 cm beds.	Possible cross bedding to 165, a number of small fractures observed displaying a vertical E-W trend. A second minor set trending 140 dipping 50 to east
2007	CJ214	685194	822489	30		Massive fine grained quartzitic sandstone in road ditch. Red-brown weathers to grey.	
2007	CJ215	690124	827785	30		Red-brown fine to med grained quartzitic sandstone. Flaggy/thinly bedded, massive. Some thin discontinuous pebbly beds.	Joints seen subvertical trending 70-250, 64-244, 100-280;No visible cross cutting
2007	CJ216	694578	830757	30		Dark red fine to med grained immature sandstone with mudstone flakes. Cross bedding towards 260 deg. Pebbly beds at upper surface. Also laminae of fine grey micaceous sandstone at base.	Cross bedding 260 Joints: 250-70 vertical, 254-74 vertical, 60-240 80-to N, 70-250 80 to N
2007	CJ217	702934	838515	30		As OBS point CJ216 but slightly paler colour.	
2007	CJ218	731634	830856	30		Very weathered medium grained sandstone in roadside ditch. Grey/red in colour. Micaceous with feldspar. Sub-angular quartz gains. Minor ripple drift surface with mica rich laminae. Break of slope; drop off to north at location of fault on BGS map.	Vertical joints 70-250
2007	CJ219	730490	832416	30	PMCD5	As OBS point CJ218 but flaggy. Also, magnetite rich, with very high magnetic susceptibility readings.	Minor joints seen 60-240 vertical
2007	CJ220	814170	858044	30	CJ217	REVISIT of OBS point CJ14. Conglomerate reinterpreted at laterite despite intact cobbles of sandstone. Underlain by olive green horizontally laminated siltstones, with mineralised joints (manganese).	Mn stained joints: N-S vertical, 100-280 85 to north, 154-334 87to E, Joints 350, 90 and 354
2007	CJ221	803101	863678	30		Well chippings - greenish shales with fine laminations. Abundant laterite boulders and pebbles. Much quartz vein material-rounded up to 3cm in thickness.	

2007	CJ222	797764	863023	30	ref Paul.	CJ REVISITED OBS point CJ13. Unconsolidated gravels paleochannel on high ground. Rounded cobbles of quartz, sandstone and metasediments. Quartz 50%, sandstone 25%, other 25%; matrix supported. Imbrications of rod-shaped clasts suggests flow to approx 110 deg. Upper 75cm is dominated by pebbles and slightly laterised, more consolidated.	Palaeocurrents: Flow to 110
2007	CJ223	793397	862344	30		CJ REVISITED OBS point CJ15. Possible boundary of cobbles/pebbles strewn on surface derived from gravels or unconsolidated/unlithified weathered conglomerates.	
2007	CJ16b	772947	860353	30		CJ REVISITED 2007. Laterite, not conglomerate.	
2007	CJ224	774280	939687	30		Laterite extensive in 2m deep pit. Flat terrain surface.	
2007	CJ225	774222	939183	30	CJ218	Well chippings. Grey siltstone/shales. Very finely laminated.	
2007	CJ226	793704	921997	30		Geomorphology note; planar dipping land surface, dipping to river systems. Flat tops are laterite covered. In the valleys there is abundant fine grey sand, possibly derived from clay layer sometimes seen beneath the laterite, or from grey mudstone. Wells do not contain chippings in this area.	
2007	CJ227	777573	981355	30	CJ219	Chippings at radio mast construction. Workers report 1.8m laterite. Chippings of red laminated mudstone, note manganese in laminae and in fractures.	
2007	CJ96b	738329	1103661	30		CJ REVISIT 2007. Olive green flaggy. Base: Trough cross bedding surfaces, probably due to tidal scouring just offshore (estuarine). Top: tabular horizontal bedding, suggest near shore.	
2007	CJ76b	796280	1169399	30		CJ REVISIT 2007. Cross bedding to 60 and 240 deg. Pin-stripe lamination suggest thick aeolian beds interbedded within the fluviatile beds.	Cross bedding 60 and 240
2007	CJ77b	797503	1170147	30		CJ REVISIT 2007. Med grained, quite immature. Feldspatic with clay feldspar matrix. Trough cross stratified to 300 deg. Big braided sandur, not much sand sorting - fluviatile.	Palaeocurrents Trough cross stratified 300
2007	CJ79b	806796	1177841	30		CJ REVISIT 2007. Olive green fine sandstone/siltstones.	

						Siltstones undulating; coarsening upwards with loading structures. Possible prograding system.	
2007	CJ78b	808003	1177839	30		REVISITED site. Med to thinly bedded clean sandstone. Manganese along laminations. Planar laminations, quartz sandstone, grey/white. Palaeocurrent to 40 deg. Possibly inside edge of meander channel (plain laminated, no cross stratification), high energy flow regime in a fluvial environment.	Palaeocurrents 40
2007	CJ228	810107	1168127	30		5m x 3m riverside outcrop at bridge. Quartz sandstone. Pale yellow, weathers to pink-red. Medium grained. Sub-angular grains in a clay matrix (feldspar broken down). Feldspatic, rare mica. Massive.	Minor fractures generally 100-280 vertical
2007	CJ72b	810615	1162623	30		CJ REVISIT 2007. Dark grey to red brown, micaceous and feldspathic, medium grained sandstone. Sub-angular to sub-rounded grains. Clay matrix. Drag fold towards 300 deg, channel above has cross bedding to 250 deg. Environment suggested near shore marine.	Palaeocurrents Cross bedding 250, Drag fold 300
2007	CJ71b	810938	1161880	30		CJ REVISIT 2007. As OBS point CJ72 but less mica. Possible glauconite in laminae; suggest marine environment of deposition.	
2007	CJ67b	817818	1151559	30		CJ REVISIT 2007. Salmon pink very fine siltstone, with rare mud-flakes. Horizontally laminated. Water escape and load structures and drag fold. Yellow sand channel (less than 1cm thick) cuts through the siltstone.	Joints 105 Strike 180, Dip 82
2007	CJ69b	812754	1159928	30		CJ REVISIT 2007. Mature, medium to coarse grained. Quartz sandstone, minor feldspar. White/pale yellow. Coarsens upwards with reduced feldspar and more porous. Massive, aeolian at top.	
2007	CJ229	818205	1148413	30	CJ20	Clinker	
2007	CJ66b	818252	1147635	30		CJ REVISIT 2007. Roadside outcrop of steeply dipping salmon pink to light red cherty fine sandstone, very siliceous. Finely laminated, weathers to white. Thin laterite on top.	
2007	CJ230	171977	1031325	31		Gutter subcrop in Bunya sandstone. Medium grained (sub angular) sandstone. Khaki to light brown with mica and	Fractures vertical 56-236, Dubious jointing 25 and 125, dubious

						feldspar. Clay matrix and massive.	bedding to 245
2007	CJ231	172661	1019077	31		8m x 4m pavement outcrop at school. Fine to medium grained khaki sandstone. Slightly immature. Feldspatic and micaceous with possible jasper. Appears massive. Onion weathering evident.	Two fracture sets vertical, 93-273 and 170-330, Jointing 275. Also at 175 with dip 75 to east Strike 90, Dip 75
2007	CJ232	176238	1013358	31		8m x 5m pavement outcrop. Fine to med grained khaki to grey sandstone with mica and feldspar and an orange mineral possibly jasper, some dark fine beds of mica. Harder than other Bunya so far. Slightly immature with sub-angular grains. Swales and hummocks remnants of near shore marine. Includes mud clasts and mica rich laminae. Photo of load/water escape structures. Convoluted section suggests slumping.	
2007	CJ233	170284	1008187	31		Mast under construction. Khaki to pale brown grey fine to med grained sandstone. Finely laminated, with laminae highlighted by mica. Clay matrix. Feldspatic. Friable when weathered, becoming pale grey/white.	
2007	CJ234	186494	979482	31		Laterite soil with laterite boulders. No rock outcrop.	
2007	CJ25b	178206	968198	31		CJ REVISIT 2007. Bunya sandstone. Oliver green fine grained massive, slightly flaggy sandstone. Suggesting of ripple drift surfaces in plan view. Flow to 295 deg. Bedding dips to 315. Minor mica, otherwise sand.	Palaeocurrents: Flow 295, fractures 50-230 63 to the SE and 40-220 60 to SE, bedding to 315
2007	CJ26c	182062	966153	31		CJ REVISIT 2007. Thinly bedded very fine sandstone/siltstone with mica. Olive green. Coarsens upwards to medium grained sand laminae interbedded in the siltstone. Possibly gradation between Bimbilla and Bunya?	Some evidence of N-S fractures Strike 270, Dip 7
2007	CJ235	185023	965030	31		Outcrop forming ridge. Harder than Bimbilla (slightly siliceous). More feldspar, arkosic. Fine to medium grained olive green to grey. Small lithics, rare mud-flakes. Sub angular grains. Immature. Possible brecciated unit aligned approx 250 deg.	
2007	CJ236	189806	961255	31	CJ21	2m section of olive green siltstone interbedded with fine sands and shales, evidence of drying cracks in the shales - Bimbilla. Manganese oxide staining in laminae and	Dominant fracturing 140-320 85 to the NE, cross laminated to 180. Fold axis is E/W, pressure from N/S

						fractures. Pseudo horizontal bedding and cross laminated to 180 deg, distal sand turbidites suggests basinal marine (CWT). Is this flysch on top of Obosum molasse?	measured at 160
2007	JC270	748765	739108	30		Pale grey, medium-coarse grained quartz-arenite comprising cross-laminated lower part, with some coarse laminae, overlain by c. I m thick channelised med-coarse sandstone with some granule layers. (See OBS point CT 1).	Palaeocurrents 230, 265, 060, 010
2007	JC271	749887	736179	30		Pale grey, medium-grained quartz arenite in regular tabular beds 10-20 cm thick. Very low-angle cross-lamination. Some beds show wavy (rippled) partings. Saw-tooth profile suggests individual beds fine up; most are plane-laminated (CT2)	Palaeocurrents 105, Shallow fractures, major trend is 100 degrees while a minor trend of 005
2007	JC272	750917	726379	30		Road cutting in lower Kwahu escarpment. Shows ridge of spheroidally-weathered granitoid 'draped' by variegated (maroon-pale grey) mudstone; latter show syn-sedimentary disruption and syneuresis. 2 further thin (1-2 m) mudstone beds c. 5 and 15 m higher up, intercalated in flaggy, micaceous siltstone/fine sandstone, which is dominant lithology here.	Small quartz vein (1-2 cm) trending 100-180 with a dip to the south
2007	JC273	740684	731494	30		Angular vein quartz debris, with iron staining and tourmaline. Sugary texture fractured with possible second veining event seen. Likely source is unclear as this may be used as a fill.	
2007	JC274	740151	732856	30		Road cutting in red silty diamicton with abundant boulders of weathered Kwahu Group sandstone - a debris flow deposit from the main escarpment.	
2007	JC275	744932	741447	30	PMCD2	Abene village; coarse sandstone with single-grain granule lags. Prominently fractured and locally a fracture-breccia.	Trending E-W in a vertical section. Minor set of fractures cutting at 70-250. The section appears to be cut by a oblique fault, Fracture trend 265,
2007	JC276	745985	740956	30		Pale grey to cream, tabular bedded medium to fine-grained and cross-laminated quartz arenite.	Cross-lamination 012, 315, 346, 345, 330. Wind ripples to 215
2007	JC277	749331	740463	30		Modak Royal Hotel; Pale grey, coarse-grained quartz arenite c. 1.5m with tabular planar cross-lamination.	Palaeocurrents 334, 342, 320; upper beds: 100, 40, 112

2007	JC278	759473	735312	30		Pale grey, medium-coarse grained quartz arenite, some granule lags; trough cross-laminated.	Palaeocurrents 175, 130, 178, 160, 320
2007	JC279	759495	735181	30		Exposures down small track off main road '(To be a Man' junction). In pale grey, medium-coarse-grained quartz arenite. Thinly bedded with plane and cross-lamination. Some foreset beds coarsen up (avalanche). Currents bimodal resulting in herringbone pattern throughout, but with local predominance of unidirectional bundles.	Palaeocurrents 065, 065,020, 050, 010, 220, 220, 230, 210, 220
2007	JC280	762159	734528	30		Pale grey, medium to coarse-grained quartz arenite - top of Abetifi Sandstone dip slope. Grains are mainly well rounded and spherical; minor proportion are sub-angular.	Palaeocurrents 338, 338, 315, 280
2007	JC281	763026	734620	30		Pavements in pale grey medium-fine-grained quartz arenite forming top of Abetifi dip slope. Some highly micaceous laminae. Shows nests of trough cross-laminae and possible wind ripple.	Troughs to 060
2007	JC281b	763026	734620	30		CT REVISITED 2007. Sandstone, medium grained quartz arenite, mature, but locally micaceous, thin bedded. Very shallow marine sandstone; upper shoreface/broad beach. Possibly subject to sub-aerial exposure at times.	
2007	JC282	763602	735144	30		Pale grey quartz arenite surface showing interference between fluvial and wind ripple sets.	Fluvial to 040; wind to 330
2007	JC283	766912	735699	30		Section through c. 6m of quartz arenite, to top of Abetifi dip slope. Top in coarse-grained sandstone with ripples and trough cross-lamination. Herringbone pattern well-developed on faces viewed from the E.	Palaeocurrents 35 Fractures trend 085, 360, 330, 290
2007	JC284	769493	735452	30	JCGH 009	Just above base of Anyaboni Sandstone Fm; in purple-grey, very fine-grained, highly micaceous sandstone/siltstone. Local fine scale cross-lamination.	Palaeocurrents 235
2007	JC285	774687	737538	30		Lower facies of Anyaboni in thick-bedded (50-70cm) medium-grained arkosic sandstone with internal plane lamination; locally very low-angle, large-scale cross-lamination. Some lower bedding surfaces are erosional.	Palaeocurrents 35
2007	JC285b	774687	737538	30		CT REVISITED 2007. Sandstone, thick-bedded, medium-grained arkosic sandstone with internal plane lamination; locally very low-angle, large-scale cross-lamination. Some lower bedding surfaces are erosional. Depositional	

						environment unclear. Internal lamination suggests upper flow regime fluvial beds.	
2007	JC286	777345	737190	30	JCGH 010	Top of Anyaboni Sandstone in red, medium-grained arkose (c. 20-30% white feldspar grains). Apparently massive. Shows purple-green grey pseudo-lamination probably due to water table fluctuations during diagenesis. In distance to north, white quartz-arenite top-beds noted on Anyaboni.	
2007	JC286b	777345	737190	30		CT REVISITED 2007. Sandstone, red, medium-grained arkose. Apparently massive. Shows purple-green grey pseudo lamination probably due to water table fluctuations during diagenesis. Massive sandstone with little internal variation, but with fine alternating colour bands, interpreted to be due to water surfaces percolating in the rock.	
2007	JC287	777093	738054	30		Apaiska village. In medium-grained, maroon highly arkosic sandstone, very large scale trough cross-bedding.	Palaeocurrents 330, 340, 330, 135
2007	JC287b	777093	738054	30		CT REVISITED 2007. Sandstone, very feldspathic, very thick bedded, with large scale fluvial foresets. Large scale foresets developed in fluvial channel sandstone.	
2007	JC288	773481	736619	30		In middle part of valley side, below crags of red Anyaboni Sandstone, gully contains debris of red cross-laminated to plane-laminated arkose; sporadic layers with red to green, silty mud-flakes. Large-scale cross-bedding seen on opposite valley side. REVISITED IN 2008: Crags at top of gully representing middle to upper part of Anyaboni Sandstone consist of medium-grained arkosic sandstone, either plane-laminated or cross-laminated; some cross-lamination is folded over. Most current directions are to the NE. Between some beds are thin (1-3 cm), discontinuous partings of purple, highly micaceous laminated siltstone or fine sandstone very similar to basal facies seen at OBS point JC 284.	Palaeocurrents 040, 205
2007	JC288b	773481	736619	30		CT REVISITED 2007. Escarpment in thick bedded, red fluvial sandstone. This prominent sequence of fluvial beds is traceable at this level in the Anyaboni Sandstone Fm over a wide area. Extensive fluvial channel sequence; almost certainly braided river system.	
2007	JC289	783167	770025	30		On Kwaikese road, in village pits in red silty gravel - part of	

						thick Quaternary cover.	
2007	JC290	782218	772307	30	JCGH 011	To west of Kwaikese road, c. 15m high koppies in red, medium-coarse grained, highly feldspathic and lithics-rich sandstone. Layers with maroon mud-flakes. One prominent c. 1-2m thick layer of poorly sorted cobble conglomerate (probable debris flow). Some lateral accretion surfaces and cross-lamination; other beds appear massive with 'floating' pebbles. Fragments include green chert, granitoid and metamorphic rocks including typical 'Damomeyan' mesocratic gneiss, and possibly porphyritic volcanic rocks. Some quartzitic pebbles are well-rounded, suggesting previous transport; other types are highly angular.	Palaeocurrents 230, 275
2007	JC290b	782218	772307	30		CT REVISITED 2007. Sandstone, red brown, medium to coarse grained, very immature, feldspathic and lithic rich, very thick bedded, locally chaotic, with slumps. Lenses of coarse, bouldery conglomerate. Facies indicate very rapid deposition in terrestrial environment, probably in flash-floods. Possibly wadi deposits.	
2007	JC291	781931	774671	30		Pavements in feldspar-lithics rich, red sandstone with sporadic 'floating' pebbles and pebble lags. Pebbles include pink porphyritic microgranite (possibly) and foliated metasedimentary lithologies. Pebble lags associated with scour troughs.	Palaeocurrents 250
2007	JC292	764647	782289	30	JCGH 012	Medium-fine grained, highly micaceous arkosic sandstone with local trough cross-lamination; some mud-flakes.	Palaeocurrents 250, 210
2007	JC293	801232	763708	30	JCGH 013	Nearby school, pale grey, medium-coarse grained quartz arenite or sub-arkose. Cross-laminated throughout, with herringbone pattern prominent. Dip 27 to 255 suggests tectonic disturbance close by.	Palaeocurrents 210, 350, strike 345, dip 27 to W Strike 165, Dip 27
2007	JC294	774729	742383	30		Road from Adowso. Cutting on top of Abetifi dip slope in pale grey, medium-fine grained quartz arenite. Mainly plane-laminated throughout 1.5m of section, but sporadic cross-lamination seen. Possibly lower shoreface.	Palaeocurrents 55
2007	JC295	766104	740391	30		Road from Adowso. Near top of Abetifi dip slope, here slightly bevelled by erosion. Pavements in pale grey/cream ripple-marked and cross-laminated quartz arenite. Some	Palaeocurrents 250, 205, 124, 160, 040 (possibly wind ripples?)

						interference ripple structures. Herringbone structure locally seen, although most exposures are of the tops of bedding planes. Boulders of red-weathering Anyaboni Sandstone are present, derived from the escarpment to the south.	
2007	JC296	749249	740452	30		Jamasi-Mampon rd. Fine-grained flaggy sandstones underlain by grey mudstones and siltstones. Cut by normal faults trending N-S.	Faults 180
2007	JC296b	749249	740452	30		CT REVISITED 2007. Sandstone, fine grained, underlain and thinly interbedded with siltstone and silty mudstone. Prominent conjugate set of normal faults well developed here, with a hanging wall syncline developed in the larger fault at the left hand end of the exposure. N-S trending faults indicating ~E-W extension. Age of faulting unknown.	
2007	JC297	679423	811788	30	JCGH 014-015	JC REVISITED JC53. The harder beds are of pale grey-green dolomitic siltstone, weak fizzing with acid. Some climbing ripple cross-lamination. Probably lacustrine-playa lake environments with siltstones representing sheet flood events.	Palaeocurrents 36
2007	JC298	664995	823352	30		Regularly, thinly bedded white quartzitic sandstone, medium grained and locally poorly sorted. Some large-wavelength wave-forms on bed tops and some bed bases are channelised.	Palaeocurrents 330, 295
2007	JC299	648388	828656	30		New cutting on Ejura-Nkoranza road. Red-weathering, pale cream, friable medium-grained sandstone in 2-3m dune beds.	Palaeocurrents 215, 228 (wind)
2007	JC299b	648388	828656	30		CT REVISITED 2007. Sandstone, very mature quartz arenite/quartzite, red-weathering, but creamy white where fresh, friable and poorly cemented, medium grained and well sorted. Cross-sets are bound by angular surfaces and are moderately to steeply inclined, with planar lamination internally. Interpreted to be aeolian or possibly beach-face sandstone deposits.	
2007	JC300	642112	839863	30		North of Nkoranza. Medium grained, friable brown/cream sandstone, red weathering with fine scale Pin-stripe aeolian lamination. In a single bed at least 2m thick.	
2007	JC301	642161	840201	30		New cutting in plane bedded, laminated (aeolian) sandstone, medium grained, well sorted in a bed at least	Palaeocurrents 065 (trough), 020

						3m thick. Rests on thinly bedded to laminated, brown-grey, micaceous fine grained fluvial sandstone with trough cross-lamination.	(wind)
2007	JC302	625786	893811	30		Cutting on crest of feature, in pale cream thinly bedded to laminated pale red-brown siltstone interbedded with pale green mudstone. tectonic dip 1-3 to E.	Strike 0, Dip 3
2007	JC303	627257	893498	30	JCGH 016	Continuation of OBS point JC302. Here maroon/pale green blocky mudstones and siltstones - very diffuse lamination. Sample collected for acritarchs.	
2007	JC304	628429	893246	30		Brown weathering, white quartz arenite with sporadic feldspar grains overlying mudstones of OBS point JC303. Medium grained with some larger well rounded grains (bimodal).	
2007	JC305	624713	890111	30		Pavements in thinly bedded, medium to fine-grained sandstone with lags of well rounded quartzose pebbles and granules.	
2007	JC306	632496	893648	30		Fuller Falls. Well sorted medium-coarse-grained sandstone with sporadic well-rounded grains. Generally thin to medium bedded with cross-bedding and ripple marked bed tops. One exposure shows 4 current reversals in 1 m of section suggestive of herringbone structure and tidal influence.	Palaeocurrents 20, 040, 015, 100, 242, 060, 235, 070, 035, 360,
2007	JC307	637979	891141	30		Thinly bedded to laminated, cream medium to fine-grained sandstone; highly micaceous. In large scale (c. 1.3m) planar cross-bedded sets with erosive bases. Possibly lower shoreface.	Palaeocurrents 20, 315, 280
2007	JC308	638181	891056	30		Medium grained sandstone, very thickly bedded (c. 2m) well laminated to diffuse plane lamination. 'Lower Kintampo'.	
2007	JC309	638954	891221	30		Top of ' Lower Kintampo'. In thin bedded (5-10cm), brown, sub-arkosic, fairly well sorted medium grained sandstone; locally plane laminated.	
2007	JC310	638986	891341	30		Large koppies in friable weathered medium grained sandstone, very thickly bedded. Locally 3-4m thick dune bedded sets but also a significant fluvial interval, with stacked tabular-planar cross-bedded, unidirectional sets,	Palaeocurrents: Fluvial current to 350

						including folded and slumped beds.	
2007	JC311	643608	898599	30		Large koppies in friable weathered medium grained plane laminated sandstone.	
2007	JC312	644311	901662	30		Very finely laminated, pale grey siltstone, siliceous; thin tabular beds (3-6cm) of fine grained quartzose sandstone.	
2007	JC313	644714	901354	30		Small pavement of medium-coarse, poorly sorted pebbly arkosic sandstone. In ditch 30m to N pale grey mudstones show contortion suggesting intervening faulting.	
2007	JC314	659293	885127	30		Medium grained well sorted possibly aeolian sandstone with faint fine-scale cross-lamination. 50m to W vertical bedding suggests a local fault.	Palaeocurrents 320
2007	JC315	716849	887247	30		Nyunsa River bridge. 60cm in very finely laminated green-grey siltstone; not variegated but some shallow load structures; finer grained and more fissile to base.	
2007	JC316	772503	955645	30	JCGH 17	Hand-dug well shows abundant flaky debris of finely laminated maroon-grey-green variegated siltstones, micaceous; minor ripple cross-lamination.	
2007	JC317	777083	984563	30		Mast diggings in maroon/green-grey locally papery laminated mudstones and siltstones. Some 1-2cm thick tabular fragments of green-grey fine-grained sandstone.	
2007	JC318	764664	1018733	30		Bright cinnamon-red flakes of hard, laminated siltstone.	
2007	JC319	738026	1040248	30	JCGH 18	By GSD Tamale, pavements in red, medium-grained, well-sorted quartz-rich sandstone. Some large scale trough cross-bedding; possibly aeolian.	Palaeocurrents 185, 145, 160
2007	JC320	681495	1054168	30	JCGH 19	Not seen previously here, pebble/cobble conglomerate with matrix of fine grained, purple grey arkosic sandstone. Pebbles include banded and green chert, porphyritic andesite/microdiorite, and green metavolcanic. Probably Pan-African source. Conglomerate overlain by maroon siltstone and underlain be maroon/green variegated mudstone and siltstone. Sample is of fine grained sandstone locally seen above conglomerate.	
2007	JC321	681365	1054111	30	JCGH 20	100m past OBS point JC320, drab grey laminated siltstones, weakly calcareous, with mudstone laminae. Intercalated harder thin beds of grey finely laminated silty	

						limestone. Sample collected for acritarchs.	
2007	JC322	678364	1054999	30		Edge of pit in fine to medium grained sandstone. Many grains well rounded suggesting aeolian influence.	Fractures trend 068
2007	JC323	677839	1054359	30		By old Daboya bridge. Very poorly sorted, pale grey ooidal limestone. Angular, tabular sandstone clasts are sporadic and show orientation defining ghost stratification. Steeply dipping and may be part of a slump sheet or debris flow. Dip c. 20 to N 035.	Strike 125, Dip 20
2007	JC324	677698	1054528	30		Upstream of OBS point JC323, base-Pendjari unconformity. Dune-bedded Anyaboni Sandstone sharply overlain by yellow tillite composed of clay-matrix supported sand with sporadic sandstone clasts (c.20cm thick). Latter overlain by pale grey ooidal limestone resting on 2-10cm thick pale grey mud-clast conglomerate. Base of limestone is highly irregular, cutting c. 2m down into Anyaboni Sandstone.	
2007	JC325	799196	1041303	30		Road south of Sang. Pavements and koppies in dark green-grey, highly immature arkosic-lithic sandstone with green mud-flake lenses and sporadic floating pebbles; red jasper granules visible. Locally very low angle cross-lamination.	Palaeocurrents 266
2007	JC326	802819	1027187	30		Medium to fine grained Bunya sandstone as small pavements - looks massive.	
2007	JC327	738045	1072171	30		Mast diggings in purplish-grey, micaceous, very fine-grained sandstone. Some beds show flute casts and rippled tops. Mud-flakes and load structures also seen. Possible turbidite facies - marine phase of Obosum?	
2007	JC328	733468	1091230	30	JCGH 22	Mast diggings in pale green, very fine grained 'Bunya' type sandstone. Highly feldspathic, with jasper grains and dark shiny grains which may be of chrome-spinel. Some grey mud-flakes and highly micaceous laminae.	
2007	JC329	740633	1123808	30		Mast diggings in khaki micaceous siltstone.	
2007	JC330	750535	1132388	30		Well diggings in olive green and purple grey laminated siltstone; some tablets of pale green sandstone.	
2007	JC331	754917	1142338	30		Medium grained, brown weathering, white, hard quartzose	Palaeocurrents 210, 278, 145, 110,

						sandstone. In c. 20cm thick beds showing ubiquitous cross-bedding. Possibly upper shoreface. Cut by haematitic fractures trending 085.	108, 135, 110 Fractures/joints all vertical 80-260, 120-300, 70-250
2007	JC332	752214	1144846	30		In river bed, thinly bedded to laminated, medium grained quartzose sandstone.	
2007	JC333	762582	1149872	30		Slightly feldspathic cream/white, quartzose sandstone, mainly trough cross-laminated throughout, but some planar lamination. Possible swaley bedding, fluviatile.	Palaeocurrents 90, 080, 045, 080, 120 Vertical E-W fractures seen
2007	JC334	772373	1157595	30		Down slope from OBS point JC139, in cream, medium-fine feldspathic quartz arenite, plane laminated; sporadic mica and mud-flakes. One large channel seen, cutting down towards 280 (W). The large-scale plane laminated structure differs from earlier exposures e.g. at OBS point JC331. Possible L. shoreface?	Palaeocurrents Channel to W 280
2007	JC335	778523	1164039	30		Red weathering, medium grained, cream/white feldspathic quartz arenite in very low angle cross-bedded sets; lower plane laminated sets are at least 2m thick. A parting lineation suggests upper flow regime - possibly sheet floods or delta foresets.	Palaeocurrents 80, 030,080
2007	JC336	794261	1153938	30		Pavements in white, medium grained quartz arenite. Moderately well sorted, sub-angular-sub rounded grains; slightly feldspathic. Trough cross-bedded.	Palaeocurrents 90, 85, 75
2007	JC337	818439	1139695	30		Well diggings in dark grey to purplish grey to green, fissile, finely micaceous siltstone.	
2007	JC338	820342	1133799	30	JCGH 25	Very finely laminated, olive green siltstone and mudstone; finely micaceous. Sampled for acritarchs.	
2007	JC339	818863	1116263	30		JC REVISITED OBS point JC120. Pale green, very fine grained, arkosic, micaceous, 'Bunya' type sandstone. Interbedded with highly micaceous, pale green laminated siltstones.	
2007	JC340	806001	1096344	30		In river bed, good exposures of pale green-grey, micaceous very fine grained siltstone. In thin tabular beds with wind-rippled tops. Become more flaggy and plane laminated upwards. Some very low angle cross-bedding	Palaeocurrents 285

						seen.	
2007	JC341	828995	1045207	30		No observation noted.	
2007	JC342	828503	933698	30		Pale green-grey, highly weathered Bunya sandstone. Feldspathic and micaceous; finely plane laminated and cross-laminated.	
2007	JC343	169510	888832	31		As above (OBS point JC342), with sporadic coarse grains and granules of red jasper and granitoid lithologies.	
2007	JC344	830447	885245	30		Green-grey, fine to medium grained highly feldspathic Bunya type sandstone with green mud-flakes concentrated along certain laminae. Possible spinel grains. In places, common dispersed sub-angular to angular granules and small pebbles suggest a diamict produced by mass flow.	
2007	JC345	826529	905145	30		Medium grained highly feldspathic green-grey Bunya type sandstone. High magnetic susceptibility reading.	
2007	JC346	827090	906317	30	JCGH 27	Sample of fresh, grey-green, highly feldspathic Bunya type sandstone. Fine to medium grained with a diffuse plane lamination.	
2007	JC347	824493	910856	30		Massive, green-grey, highly feldspathic Bunya type sandstone.	
2007	JC348	823477	924498	30		Weathered exposures of medium grained, highly feldspathic, diffusely plane laminated Bunya type sandstone.	Bedding strikes 153; dips 2 to E Strike 333, Dip 2
2007	JC349	823819	925299	30		Bunya village: medium grained Bunya Sandstone shows large scour structures defined by arcuate lamination. Slightly farther north in village variable dips to lamination, locally vertical, indicate syn-sedimentary slumping.	Palaeocurrents: Troughs to 355, 240, 210,198
2007	JC350	188916	893235	31		Dumbai village. Exposures in green-grey, fine grained, highly feldspathic, slightly micaceous Bimbila type sandstone interbedded with brown-weathering siltstone. Dip is 8 to E 118	E-W fractures, Cut by fracture trending E 90 Strike 208, Dip 8
2007	JC351	193627	879058	31		Ditch in village shows highly weathered cream-green fine grained, highly immature feldspathic sandstone. Also debris of green-grey siltstone and laminated siltstone/mudstone.	Strike 245, Dip 8

2007	JC352	196876	774355	31	JCGH 28	Western edge of village, small exposures in black basalt/intermediate rock. Common to abundant vesicles, and zeoilte amygdale (3%). In market about 70m to east, abundant sandstone debris.	
2007	JC353	196638	756248	31	PMCD9	In road across ridge, exposures in white/grey medium grained, quartzose, volcaniclastic (epiclastic) sandstone. Common coarse sand to granule size fragments of white/pink clayey-altered feldspars, some sub-hedral; also fragments of dark green altered fine-grained volcanic rock - possible magnetite grains. Pass up to thinly bedded and graded quartz-rich epiclastic sandstone beds. Affected by cataclastic shear zone.	Shear zone present Strike 310, Dip 50
2007	JC354	193455	755709	31		At edge of lake; sporadic showings of pink silt and sandstone-clast gravel. Probably part of an alluvial fan association.	
2007	JC355	195976	756387	31		In quarry, brecciated and sheared, white quartz arenite. Includes a c. 10-20cm thick diamicton - fragments of white/pink, kaolinitised feldspar, pebbles of quartz and basic volcanic rock, and mudstone are set in a muddy, olive green matrix - probable volcaniclastic mudflow or lahar emplaced along shoreline or estuary.	Fractures in the quartzite 80-260 vertical slickensides 130-310 and 60-240 Strike 305, Dip 58
2007	JC356	186176	732680	31		In village, weathered pavements in pale green-grey to khaki, fine grained, slightly micaceous sandstone of Bimbila type. Highly brecciated, and possibly folded.	Main fractures and fold axis 005
2007	JC357	188688	728171	31	PMCD10	In village, silvery grey phyllonite, cut by multiple generations of quartz veining.	Micaceous phyllonite trending 22-202 near to shear zone, Phyllonitic foliation strikes 035 dips 65 to 125. Slightly crenulated by a spaced fracture system 128. Also a sub-horizontal rodding lineation Strike 35, Dip 65
2007	JC358	188389	727596	31		Very strongly foliated, protomylonitic quartz arenite, interbedded with silver-grey phyllonite, latter flat-lying. Weakly developed S-C fabric.	Foliation dips 40 to 145 in quartz arenite. Shear sense apparently top down to SE Strike 55, Dip 40
2007	JC359	187585	725400	31	PMCD11	Hard, grey/white quartz arenite. Fractured but not obviously foliated apart from a cataclastic zone. Foliation in	Late fractures 100

						latter cross cut by later spaced 'Voltaian' fractures.	
2007	JC360	174668	709326	31		In road, ribs of foliated white quartz arenite. Local slabs of very coarse grained or granule sandstone with very well rounded quartz grains. Very similar to Kwahu Group quartz arenites.	Foliation dips 65 to SE 120 Strike 30, Dip 65
2007	JC361	174396	709650	31	PMCD12	Road through ridge, exposures of thin bedded fine grained, white quartz arenite intercalated within grey, laminated, fine grained micaceous sandstones, silver-grey siltstones and papery mudstones. Siltstones locally show complex oscillating cross-lamination suggesting microtidal environments. Also some lenticular winnowed granule lags. Strata are locally crumpled below a bedding-related decollement.	Crumple fold on sandstone/quartzite with a decollment Fold axis plunges 63 to 025; direction of vergence towards 340
2007	JC362	175254	709080	31		Village exposures in dark purplish-maroon, fine to medium grained, micaceous, 'red bed' sandstone with fine-scale lamination. Passes up into cream, fine-grained, slightly micaceous sheet sandstones. Thinly bedded and flat-lying (right way up) with trough cross-bedding visible. Possible Anyaboni Sandstone equivalent.	Palaeocurrents: Troughs to 110 and 140
2007	JC363	815766	706202	30		Pavements and boulders in red/pink, poorly sorted medium grained quartzose sandstone with several percent feldspar. Common well rounded grains. Probably fluviatile.	
2007	JC364	811951	713737	30		Weathered exposures of purplish-grey weathering, medium grained feldspathic sandstone.	
2007	JC365	811453	714430	30		Medium grained, fairly poorly sorted white feldspathic sandstone. Many grains well rounded and spherical. Planar cross-bedding and large scale trough cross-bedding.	Palaeocurrents 040, 358 (trough) 10-190 vertical fractures with Mn infill
2007	JC366	809851	715765	30		Medium grained red weathering feldspathic sandstone.	
2007	JC367	808493	717367	30		White-weathering but highly feldspathic sandstone. White clay mineral derived from feldspar and also present as inter-grain fills.	
2007	JC368	798635	718370	30		Dark maroon, medium grained sandstone - abundant white feldspar grains.	
2007	JC369	797553	716370	30		Maroon sandstone, fine to medium grained. Local	

						concentrations of pebbles consisting of pale grey sandstone and possible pale green volcanic rock.	
2007	JC370	796572	714254	30		Medium grained, white quartz arenite; some quartz grains are large and well rounded indicating moderate to poor sorting. Thinly bedded and laminated throughout.	
2007	JC371	791015	708091	30		In north of Begoro, white, quartz-rich, medium to coarse grained sandstone is cross-bedded throughout. Sets are mainly planar and steeply dipping (10-25). Drag-folding noted in some beds. Possible small prograding delta system.	Palaeocurrents 028, 010, 360, 040, fractures 30-210 dipping 85 to the SE
2007	JC372	809616	679007	30		Roadside stone quarry north of Koforidua. In hard, white, glassy quartz arenite, probably recrystallized. Cut by sets of regularly spaced fractures, with much pink (Fe) and manganese staining.	Tectonic dip 30 to 165. Master fractures 070; a subordinate set at 310 Strike 75, Dip 30
2007	JC373	812456	682292	30		Village exposures in hard, pink/white, medium grained quartz arenite. Shows herringbone cross-bedding.	Palaeocurrents 040, 060, 218, 280, 285, 355, fractures, 115-295 throughout
2007	JC374	764233	740041	30		Small quarry to E of Adowso-Abetifi road, at base of Anyaboni Sandstone feature. Exposes c. 3-4 m of green-weathering, grey, locally finely laminated micaceous mudstones with silty laminae and white, fine sandstone wisps and lenticles. Shows symmetrical wave-ripples, locally with internal chevron-up-building structure. Probable tidal (estuarine) setting. Strongly rippled top of underlying Abetifi Sandstone seen in same quarry.	
2007	JC375	811567	687412	30		Exposure in structurally complex area containing large rotational landslips. Shows green-grey to brick-red, laminated micaceous mudstones and siltstones with large phosphate-cemented concretions. Mudrocks represent the basal facies of a Kwahu sandstone formation, possibly the Obocha Formation. Sandstones higher up are of quartzitic type therefore probably do not belong to Anyaboni Fm.	
2007	CT1	748771	739094	30		Sandstone, medium to coarse grained, pale buff to red-weathering; medium to thick bedded. Quartz arenite to quartzite. Well-rounded granule lags present in the bases of some channels; mostly vein quartz, mature. Mature fluvial sandstones. REVISITED in 2008; one bed with	Cross-bed foresets vary from SW to N; those in lower beds dominantly towards the N

						herringbone cross-stratification, suggesting a tidal channel influence.	
2007	CT2	749816	736192	30		Sandstone, fine to medium grained, quartz-arenite/quartzite. Thin to medium bedded, with very tabular beds. Saw-tooth bed profiles suggest beds fine up. Commonly appear plane-laminated. No good cross-stratification observed, but some beds appear to contain some gentle bases appear to contain some cross lamination. Some bed bases appear erosional/scoured. Marine sandstones, possibly deposited as turbidites worked off a mature quartz-rich shore-face/shelf. Outer shelf slope (but probably not deep).	
2007	CT3	759496	735183	30		Sandstone, hard, pale cream to white quartz-arenite/quartzite, medium to very coarse and granule grained, generally very well sorted. Coarse and granule fraction very well rounded. Thin to medium bedded, generally trough bedded. Herring-bone cross-stratification common. Upper shoreface within tidal zone.	Beds dip very gently towards the NE Strike 120, Dip 2
2007	CT4	762157	734528	30		Sandstone, coarse to very coarse, locally granule grade; quartzite; very well rounded grains, very well sorted. Upper shoreface beach deposits?	Beds dip very gently towards the NE/ENE Strike 170, Dip 2
2007	CT5	763019	734622	30		Sandstone, medium to coarse grained, locally micaceous, planar bedded to small-scale trough cross-bedded. Some wind and current ripples well preserved on bedding surfaces. Fluvial to very shallow marine (intertidal /estuarine).	Palaeocurrents 60
2007	CT6	763603	735143	30		Sandstone, medium to coarse, locally micaceous, with trough cross-stratification seen in plan view, and very good wind-driven current ripples; latter locally interfere with former. Very shallow marine to fluvial; possibly estuarine.	Palaeocurrents 60, 330, Trough cross stratification trend to 060, current ripples trend to 330; latter may be wind driven
2007	CT7	781925	774672	30		CT REVISITED OBS point CJ163. Sandstone, pale pink brown, with locally abundant pebbles of igneous and metamorphic lithologies, SA to WR, granule grade lithic and feldspathic material, coarse sands matrix, A/SR, with abundant feldspar, some mica and lithic fragments. Lithic arkose. Very immature terrestrial fluvial red-beds. Possibly molasse from Dahomeyide orogen.	Palaeocurrents 270, Transport of sediment towards west indicated by trough bedding in plan view

2007	CT8	801269	763747	30		Sandstone, medium to locally coarse grained with some feldspar and ferruginous weathering spots. Trough-bedded with cross-bedding prominent in troughs, commonly herring-bone cross-stratification. Also some plane-laminated beds. Heavy mineral bands prominent on some of the foresets. Mature tidal sandstone; upper shoreface.	
2007	CT9	774719	742739	30		Sandstone, quartzite, fine to medium grained, pale buff in colour. Locally cross-bedded, but dominantly plane laminated in medium and mainly thick beds. Possibly some HCS seen, with shallow swaley lamination. Abetifi sandstone forms platform and scarp here below Anyiboni Sandstone. Lower shoreface sandstone, above storm-wave base.	
2007	CT10	679428	811799	30	CTGH1	Siltstone, mudstone and fine grained sandstone, maroon to pale green grey, laminated to thin bedded. Some thin dolomitic siltstone/fine sandstone beds in shallow depressions, Some ripple cross lamination. Probably fluviatile to lacustrine with ephemeral ponding to give carbonate-cemented siltstones.	Palaeocurrents 36, Beds dip very gently to the NE Strike 120, Dip 2
2007	CT11	679216	814019	30		Sandstone, very clean quartzite, medium to locally course grained, tabular to trough cross bedded, thin to medium bedded. Locally rippled bed tops; possibly some standing wave ripples - steep sided, symmetric. Trough beds 2-3 time thicker than tabular beds.	Palaeocurrents 180, Beds dip gently towards N by about 5 degrees Strike 90, Dip 5
2007	CT12	664994	823357	30		Sandstone, white to pale creamy coloured, fine to coarse, locally gritty, quartz rich, SA/WR grains, with pale creamy matrix filling pore space; moderately sorted, poorly cemented. Beds tabular to weakly lenticular with wavy form in places. Locally some trough bedding developed, thin to very thin bedded. Some cross-lamination, but rare. Individual beds appear graded locally, but most appear massive. Possibly lower shoreface? This may represent tabular beds deposited as storm deposits with some current induced trough bedding.	Beds dip gently to moderately to ESE Strike 25, Dip 7
2007	CT13	648396	828657	30		Sandstone, red-weathering, medium grained, very thick bedded in dune cross-bedded. Pale cream where fresh. Erg dry dune system.	

2007	CT14	642118	839862	30		Sandstone, very to extremely thickly bedded, plane laminated with pinstripe lamination. Fine grained quartz rich, with careous weathering in upper part of outcrop. Interpreted as an aeolian sand body deposited in a 'wet dune' environment with an elevated water table.	
2007	CT15	642162	840209	30		Sandstone, very thick bedded, with large aeolian dune foresets overlies trough cross bedded and cross stratified sandstone that in turn overlies more dune bedded sandstone. Dominantly a dune system with some fluvial sands.	Palaeocurrents 65
2007	CT16	636679	854846	30		Sandstone, pale ochre, soft and poorly cemented, medium to coarse grained with some WR granules forming fine bimodal lag. Careous weathering in places. Very thick bedded, with large-scale (2m+) dune foresets. Erg dune system - dry dunes.	Palaeocurrents towards S
2007	CT17	625781	893813	30		Siltstone with thin mudstone interbeds; possibly some very fine grained sandstone interbeds that are weathering pale green grey, but orange-brown internally. Plane laminated, massive, fissile. Beds tabular, planar. About 500m east of this outcrop, similar sequence seen, but here mudstone/siltstone darker green and purplish grey. Possibly marine; sample collected by JC for acritarchs.	
2007	CT18	628434	893229	30		Sandstone, quartzite, fine grained matrix with WR quartz granules/coarse grains. Looks bimodal, well cemented, hard and white where fresh. No bedding seen, but sandstone outcrop just upslope is thin bedded.	
2007	CT19	624718	890114	30		Sandstone, pale cream weathering, ochreous, quartzite with SA/WR quartz granules and pebbles up to 20mm in diameter. Pebble rich units are deposited in channels/scours. Gravelly fluvial facies.	
2007	CT20	632517	893649	30		Sandstone, thin to medium bedded, medium to coarse grained, with WR coarse to granule grade quartz. Quartzite weathers buff/ochre. Tabular beds, planar or tabular cross stratified. Good wavy to linguoid current ripples developed on one bed surface. Plane laminated beds may indicate upper flow regime deposition. Fluvial sandstones, possibly with some tidal influence near top.	Palaeocurrents NNE - NE

2007	CT21	637985	891151	30		Sandstone, fine to medium grained, moderately feldspathic, pale buff to variegated. Some large scale cross-bedding in lower parts of beds, passing into massive sandstone in upper part. Possible hummocky cross-stratification at lower outcrop and fine grained sandstone consistent with lower shoreface sands.	
2007	CT22	638938	891224	30		Sandstone, medium grained feldspathic, poorly cemented, thin, plane laminated beds. Grains SA/SR. Beds tabular, laterally extensive, but generally massive in appearance. Sand is well sorted.	Beds dip very gently E Strike 0, Dip 2
2007	CT23	638938	891224	30		Sandstone, medium to coarse, thin laminated in large dune foresets and tabular cross-stratified sandstone in middle part of outcrop. Poorly cemented quartz arenite/quartzite. Dunes appear to come in again in upper part of outcrop. Dune dominated system with intermittent fluvial sandstone.	Palaeocurrents: Uniformly to N
2007	CT24	643735	900907	30		Sandstone, feldspathic and micaceous; black mica flakes abundant, weathered and poorly cemented. Cross laminated, thin to medium bedded, tabular to weakly trough cross stratified. Fluvial sandstone; this unit assigned tentatively to the Damongo Formation.	Palaeocurrents 55, Beds generally horizontal
2007	CT25	716859	887251	30		Siltstone, drab grey, plane bedded with some dewatering structures preserved in upper bed. Underlying beds are planar laminated, with nodular weathering. Beds at top slightly coarser. Lacustrine mudstone and siltstone.	
2007	CT26	738027	1040247	30		Sandstone, red, quartz arenite/quartzite with haematite cement/grain coating. Polished, fine-medium SA/SR sand with faceted faces imparting sparkly appearance. Large scale foresets in plan view indicate aeolian origin. Aeolian dune system.	Palaeocurrents 180
2007	CT27	681487	1054057	30		Siltstone and very fine grained sandstone, micaceous, purplish grey, fine laminated in planar beds, overlain by thick micaceous muddy sandstone that has a convoluted or channelled base. Sandstone has local coarsening upward packages, but boundaries between packages are poorly defined. Fluvial sands overlying lacustrine deposits, possibly with loading of sand down into mud/silt.	
2007	CT28	681366	1054115	30		Muddy siltstone and thin limestone, moderate to vigorous	

						reaction with 10%HCl. Not clear if siltstone and limestone are marine. Sample for acritarchs collected by JC.	
2007	CT29	677790	1054427	30	CTGH2	Dolostone, oolitic, with extra and intraclasts and slump structures in places. Possibly some algal oncoids. With chert veins and barite in cavities. Sample of oolitic dolostone for thin section. Dolomitised oolite limestone with slumps including clasts of extraneous siliciclastic material.	
2007	CT30	677852	1054367	30		Dolostone, oolitic, with A/SA clasts of sandstone, chert and some intraclasts. Clasts are disorientated and float in the oolite matrix. Just upstream at OBS point JC324, dolostone overlies dune bedded quartz arenite. Unconformity between Pendjari and Bombouaka groups. Tillite supposed to be at this level, but not observed; could be in pockets and angular clasts in oolite may well be derived from tillite during deposition of the oolite itself. The dolostone at the unconformity represents a shoaling, transgressive deposit, drowning a dune sandstone surface. Marked palaeo-relief is indicated at the Daboya locality. The oolite with clasts is structureless and is interpreted as a slumped deposit, possibly resulting from slope failure of unstable glaciomarine debris. This rock is not a basal conglomerate in the conventional sense. Up-dip, the oolite becomes bedded, but the dip of the beds contrasts with the flat topography of the unconformity at OBS point JC324, suggesting that the steep dip could be an oolite dune foreset dip slope.	Palaeocurrents: Dune foresets dip towards S
2007	CT31	694798	1049802	30		CT REVISITED OBS point CJ96. Thin bedded mudstone/fine siltstone and calcareous siltstone, pale grey, laminated. Just west of this outcrop (~30m), the section shows maroon and grey-green fine laminated mudstone and siltstone, with thin beds of calcareous siltstone. Not clear if these are freshwater lacustine deposits or deeper marine muds and silts. Sample collected for acritarchs.	
2007	CT32	799204	1041303	30		Sandstone, fine to medium grained, locally coarse with some granules and fine gravel lags. Feldspathic and lithic and very immature. Reddish grey-brown colour and spotted locally with manganese. Clayey cement/matrix. Some mud-flake (green-grey) clasts in one unit. Very shallow dish shape to some beds, weakly flaggy, locally	Palaeocurrents to W

						more planar bedded. Bedding very poorly developed throughout, with exfoliating whale-back form to many outcrops. Environment difficult to determine, but suggest these are terrestrial sandstones deposited very rapidly as sheet floods. Possibly could also be inner estuary.	
2007	CT33	737867	1060129	30		Sandstone, quartzite, medium grained, SA/R/WR, trace feldspar. A small amount of haematite cement present, but generally poorly sorted. Appears massive in outcrop, no section seen, so bedding not readily assessable. Thought to be aeolian.	E-W fracture displaying a jog indicating a dextral strike, 64-244 80S, 170-350 85W, possible some evidence of N-S cutting the E-W
2007	CT34	738331	1103658	30		Sandstone, greenish grey, very fine grained, feldspathic, micaceous and lithic. Trough bedded, with shallow scoops containing cross-stratified strata. Top bed of outcrop is massive, c. 30 cm thick tabular sheet sandstone, very hard and fine grained. Trough cross sets suggest flow towards the S and SSW. Weathering patterns indicated that some more planar beds are thinly laminated internally. Muddy estuarine facies, possibly subjected to tidal flow. Poor maturity and matrix rich character consistent with storage of sediment in estuarine setting. No graded beds seen and these beds very unlikely to be turbidites. Immaturity of rock and possible presence of mafic/ultra mafic material (e.g. suspected spinel, etc) suggests erosion of such rocks in source region (possibly Buem Formation, Pan African front). Assigned to Bimbila Formation.	Palaeocurrents S, SSW, Bedding dips gently SE Strike 45, Dip 2
2007	CT35	754916	1142340	30		Sandstone, quartz arenite/quartzite (minor feldspar), hard and well-cemented, white, locally stained ochre. Thin bedded with what appear to be swales and hummocks and locally trough cross-stratified strata. Medium grained, well sorted, SA/SR grains. Difficult to tell precisely, as no good bed sections are visible. However, switching direction of cross-stratification and possible hummocky stratification suggests a near shore environment, possible mid to lower shoreface. This unit is very reminiscent of the top part of the Abetifi Sandstone Formation. Assigned currently to the Panabako Formation, within the Bombouaka Group.	
2007	CT36	762582	1149872	30		CT REVISITED OBS point JC333. Sandstone, quartz arenite, weakly feldspathic, with sparse heavy minerals; well-cemented. Fine-medium grained, thin laminated in	Palaeocurrents 90

						broad, shallow, swaley/trough-like structures. Genesis not clear. Suggest the bedforms would appear as tabular to trough bedded, with unidirectional cross-stratification. Suggest these are fluvial in origin.	
2007	CT37	778511	1164042	30		Sandstone, moderately feldspathic, medium and fine grained quartz arenite. Low angle cross sets have angular contacts in beds in lower part of section, passing up into tabular bedded sandstone with parting lineation on some bed surfaces. Delta front sandstone, overlain by tabular sheet sandstone, possibly deposited in upper flow regime.	
2007	CT38	828502	933699	30		Sandstone, fine grained, weathering drab ochre, very feldspathic, matrix rich, highly immature; harder and more siliceous beds also present. Peculiar spheroidal weathering patterns suggest beds massive, homogeneous, forming core-stone like masses. Bedding difficult to discern, but some cross-lamination developed in places. This is the Bimbila Formation. First-cycle detritus, inferred to be marine, probably deposited by density and debris flows.	
2007	CT39	830451	885250	30		Sandstone, weathering buff greenish colour (drab) with abundant feldspar and lithic grains with quartz. Mud-flakes common in top of layering in road. 10m down road to S, saprolitic material is pebbly, with scattered SA/A clasts up to fine gravel size, labile lithologies and some dark red jasper, indicating possibly mafic volcanic source. Diamictic (not tillite). Bimbila Formation.	
2007	CT40	823482	924497	30		CT REVISITED OBS point JC348. Sandstone, fine grained, ochre-weathering, immature, very feldspathic. Thin bedded on top, thicker bedded and massive beneath. Bimbila Formation (Bunya Sandstone Member). Probably turbiditic.	Strike 333, Dip 2
2007	CT41	213087	906906	31		Purple mudstone and cherty rock, dismembered by shear zone. Deep marine mudstone and chert.	
2007	CT42	820184	685029	30		Sandstone, drab olive colour, fine grained, tabular to locally weakly trough bedded, interbedded with finer sandy siltstone, fine laminated internally. Small slump structures developed locally. Some beds more quartz rich and siliceous. No cleavage development or obvious	Fractures 06/360

						metamorphism. Folds developed here are west-vergent, with internal surface dislocations. Beds dip very steeply west on the west side of the outcrop. Lithology is similar to the Bunya Sandstone (Bimbila Formation). Beds look like turbidites.	
2007	PD4	750877	726414	30		50 cm shale band lying just above the basement. Possible lacustine deposit from the basement.	
2007	PD5	750870	726416	30		Thickly bedded sandstone draped over the basement.	
2007	PD8	738260	732857	30		Large outcrop (possible subcrop) of sandstone. Hematite cement. Likely to be saphrolite.	
2007	PD9	739571	740244	30		Roadside sandstone outcrop.	
2007	PD12	747614	729047	30		Flaggy sandstone.	E-W vertical fracturing
2007	PD13	747683	728646	30		Following up mineral database alluvial gold claim. No evidence found.	
2007	PD14	733934	733375	30	PMCD1	Basement saphrolite.	
2007	PD23	725334	745900	30	PMCD4	Pebble conglomerate.	A number of small veins 80-260 dipping 59 south and 20 cm vein dipping 58 towards the north
2007	PD39	795650	1042055	30		Clast supported conglomerate overlain by sandstone. Clasts of metasediments, jasper, vein quartz, quartzites.	
2007	PD40	795650	1042155	30		Sandstone outcrop.	Joints 110-290 85 S, 106-286 85s
2007	PD48	762543	1149815	30		Mature sandstone with silica cement, with cross bedding, dipping 80 approx to the east.	Dextral fault with jog, E-W vertical offset of 0.7 m
2007	PD49	768726	1153446	30		Cream coloured med. grained feldspathic sandstone, less siliceous that OBS point PD48.	
2007	PD50	772634	1157999	30		Roadside subcrop-possibly disturbed, white mature sandstone.	
2007	PD53	778572	1164066	30		Roadside stepped outcrop of a immature fine-grained white sandstone. Containing feldspar, some jasper and mica.	Dipping gently to the NE
2007	PD54	783755	1164650	30		Roadside outcrop, fine grained feldspar rich sandstone, white with some mica.	some minor fractures, N-S 80 towards the east

2007	PD66	172472	1029582	31		Many boulders of massive sandstone in village on hill top.	
2007	PD90	803655	724576	30		Roadside outcrop of a white quartzite (massive bedded) with evidence of cubic / angular pseudomorphs. Interpreted as halite clasts.	
2007	PD92	795010	711730	30		Finely bedded white quartz-rich well sorted fine grained sandstone with some mud clasts.	

Appendix 2 Bulk geochemical analysis samples, including coordinates and description

Sample ID	OBS point	X	Y	UTM Zone	Sample description	Sample Type	Analysis
FMG5	JC74	741834	898850	30	Laterite - sampled to check average Fe and Al content in laterite.	In situ	ICPOES/MS with Fire Assay
FMG7	CJ25	178206	968198	30	Siltstone with total count > 45	In situ	ICPOES/MS with Fire Assay
FMG8	JC92	741834	898850	30	Manganese laminations/layers in siltstone. Quarry on outskirts of Tamale.	In situ	ICPOES/MS with Fire Assay
FMG9	JC101	746171	1037174	30	Mudstone - green/anoxic conditions. Manganese horizons. Water dam diggings.	Grab	ICPOES/MS with Fire Assay
FMG10	JC107	798000	1041900	30	Conglomerate horizon in sandstone. Tertiary weathering channel fill? U? Au? Laterite quarry.	In situ	ICPOES/MS with Fire Assay
FMG11	JC168	677429	1054668	30	Baryte blades in grey ooid limestone Daboya.	In situ	ICPOES/MS with Fire Assay
FMG12	JC167	677669	1054543	30	Grey sandy limestone with magnetic susceptibly> 10. Possibly magnetite associated with baryte.	Chip in situ	ICPOES/MS with Fire Assay
FMG13	JC167	677669	1054543	30	Chip sample of chert/baryte stockwork veins with possible heavy minerals.	Chip in situ	ICPOES/MS with Fire Assay
FMG14	JC168	677429	1054668	30	Dark grey limestone with ooids. Magnetic susceptibly = 48. Finely laminated. Upstream from Daboya.	In situ	ICPOES/MS with Fire Assay
FMG15	JC166	677784	1054398	30	Grey laminated limestone, at Daboya, adjacent to boat slipway.	In situ	ICPOES/MS with Fire Assay
FMG16	JC197	664845	970055	30	Yellow dolomitic limestone with interbedded micrite and siltstones. Former *6 lens* sampled. Buipe trial quarry 3.	Chip in situ	ICPOES/MS with Fire Assay
FMG17	JC198	665604	968854	30	Finely laminated micrite & dolomitic limestone. Latter sampled. Buipe trial quarry 2.	In situ	ICPOES/MS with Fire Assay
FMG18	JC200	667014	970120	30	Brecciated dolomitic limestone with large baryte flower	In situ	ICPOES/MS with

					structures (20cm x 10cm). Buipe trial quarry 1		Fire Assay
FMG19	CJ124	625772	893810	30	Frequent 0.5-2cm Mn rich horizons in sandstone. Surface displays dendritic and blebs of possibly pyrolusite.	Grab	ICPOES/MS with Fire Assay
FMG20	CJ125	628429	893237	30	Siliceous sandstone with very fine grained tarnished metallic minerals (Possibly Copper). There maybe magnetite and galena also.	Grab	ICPOES/MS with Fire Assay
FMG21	CJ129	632148	896629	30	Maroon mudstone. Total count=51.0 in road drain.	In situ	ICPOES/MS with Fire Assay
FMG22	CJ130	637972	891165	30	Micaceous sandstone with a total count of 56.2. Roadside cliff section. Dendritic manganese.	In situ	ICPOES/MS with Fire Assay
FMG23	JC235	636690	863890	30	MM scale sub-vertical 220 and 144 quartz veins in sandstone (arenaceous). Large exposure.	Chip in situ	ICPOES/MS with Fire Assay
pmcd1	PD14	733934	733375	30	Quartz vein material, no visible sulphides.	In situ	ICPOES/MS with Fire Assay
pmcd2	JC275	744915	741427	30	Breccia fault zone associated with a silicified E-W fault. Quartz Fe staining sampled.	In situ	ICPOES/MS with Fire Assay
pmcd3	CJ203	739291	744556	30	Bleached sandstone from fault zone, no visible sulphides.	In situ	ICPOES/MS with Fire Assay
pmcd4	PD23	725334	745900	30	Basal conglomerate, quartz pebble conglomerate.	In situ	ICPOES/MS with Fire Assay
pmcd5	CJ219	730492	832412	30	Highly magnetic medium grained sandstone, near to Pru fault.	In situ	ICPOES/MS with Fire Assay
pmcd6	JC106b	788240	1045081	30	Bunya sandstone, coarse grit with volcanic and mafic materials, highly magnetic.	In situ	ICPOES/MS with Fire Assay
pmcd8	PD35	797765	863018	30	Alluvial channel gravel.	In situ	ICPOES/MS with Fire Assay
pmcd9	JC353	196632	756242	31	Faulted zone with bleached zone and much iron staining.	In situ	ICPOES/MS with Fire Assay
pmcd10	JC357	188688	728171	31	Vuggy quartz vein taken from a shear zone.	In situ	ICPOES/MS with Fire Assay
pmcd11	JC359	187586	725395	31	Quartz veinlet stock-work near to sheared area with	In situ	ICPOES/MS with

					some Fe staining.		Fire Assay
pmcd12	JC361	174353	709649	31	Fe stained quartzite with two small cross-cutting veinlets	In situ	ICPOES/MS with Fire Assay
pmcd13	JC24c	820189	685045	30	Vuggy quartz veinlets in fold nose.	In situ	ICPOES/MS with Fire Assay
pmcd14		824777	702694	30	Small Fe veinlet in a coarse sandstone.	In situ	ICPOES/MS with Fire Assay
pmcd15		181987	966220	31	Sandstone with a Fe rich band.	float	ICPOES/MS with Fire Assay
CJ17	CJ17	762475	858239	30	Laminated siltstone with manganese.	In situ	ICPOES/MS with Fire Assay
CJ21	CJ21	783006	948162	30	Laminated siltstone with manganese.	In situ	ICPOES/MS with Fire Assay
JCGH 006	JC 88	825307	909575	30	Green-grey medium/fine laminated sandstone with local concentrations of mud-flakes	In situ	Thin Section
JCGH 010	JC 286	777345	737190	30	Medium-grained arkose (c. 20-30% white feldspar grains).	In situ	Thin Section
JCGH 011	JC 290	782218	772307	30	Obosum Group; red, medium-coarse grained, highly feldspathic sandstone.	In situ	Thin Section
JCGH 016	JC 303	627257	893498	30	Maroon/pale green blocky mudstones and siltstones.	In situ	Biostrat
JCGH 19	JC 320	681495	1054168	30	Maroon /green variegated mudstone & siltstone.	In situ	Thin Section
JCGH 20	JC 321	681365	1054111	30	Grey laminated siltstones, weakly calcareous, with mudstone laminae.	In situ	Biostrat
JCGH 21	JC106	788040	1045042	30	Micaceous siltstone associated with green/grey 'Bunya' sandstone	In situ	Biostrat
JCGH 22	JC 328	733468	1091230	30	Pale green, very fine grained 'Bunya' type sandstone.	In situ	Thin Section
JCGH 24	JC126	796543	1147893	30	Red/grey siliceous tuff (Darebe Member)	In situ	Thin Section
JCGH 25	JC 338	820342	1133799	30	Olive green siltstone and mudstone; finely micaceous.	In situ	Biostrat
JCGH 26 B	JC110	171843	1044532	31	Grey, thinly bedded micaceous siltstones with branching, bulbous organic impressions.	In situ	Thin Section

JCGH 27	JC 346	827090	906317	30	Grey-green, highly feldspathic Bunya type sandstone.	In situ	
JCGH 28	JC 352	196876	774355	31	Black basalt/intermediate rock.	In situ	Thin Section

Appendix 3 Bulk geochemical analysis samples, ICPOES/MS with Fire Assay results

SAMPLE ID	Au	Au repeat	Ag	Al	As	Ba	Be	Bi	Ca
	ppb	ppb	ppm	%	ppm	ppm	ppm	ppm	%
pmcd1	-2		<0.5	1.71	2.2	108	<1	<0.05	0.03
pmcd2	-2		<0.5	1.13	5.3	26	<1	<0.05	0.01
pmcd3	-2		<0.5	3.52	7.9	43	<1	<0.05	<0.01
pmcd4	13		<0.5	3.02	3.8	1340	1	<0.05	0.02
pmcd5	-2		<0.5	9.82	1.4	570	2	0.09	3.06
pmcd6	2		<0.5	7.56	4.8	505	3	0.10	1.32
pmcd8	-2		<0.5	5.44	4.0	201	<1	0.14	0.07
pmcd9	-2		<0.5	6.30	5.4	193	1	0.07	0.05
pmcd10	-2		<0.5	2.77	0.9	444	<1	0.11	0.03
pmcd11	-2		<0.5	2.19	0.3	211	<1	<0.05	0.11
pmcd11repeat			<0.5	2.21	0.5	210	<1	<0.05	0.11
pmcd12	-2	-2	<0.5	3.52	3.5	186	<1	0.06	0.02
pmcd13	-2		<0.5	6.68	7.0	434	2	0.18	0.17
pmcd14	-2		<0.5	3.65	1.1	796	1	<0.05	0.02
pmcd15	-2		<0.5	4.87	6.7	674	3	0.39	0.04
CJ17	-2		<0.5	8.71	24.0	620	3	0.25	0.28
CJ21	-2		<0.5	6.61	4.0	607	2	0.24	0.36
FMG5	-2		<0.5	4.52	29.8	1444	3	0.19	0.05
FMG7	-2		<0.5	8.70	7.6	581	3	0.28	0.18
FMG8	-2		<0.5	4.73	3.6	1165	2	<0.05	0.46
FMG9	-2		<0.5	5.66	5.0	347	2	0.17	0.16

FMG9repeat			<0.5	5.67	5.8	345	2	0.17	0.16
FMG10	-2	6	<0.5	7.61	5.7	613	2	0.13	1.69
FMG11	-2		<0.5	0.45	2.6	310	<1	<0.05	19.25
FMG12	-2		<0.5	0.92	2.0	1049	1	<0.05	18.15
FMG13	-7		<0.5	1.05	5.1	10556	2	<0.05	5.72
FMG14	-2		<0.5	1.16	4.5	310	2	<0.05	13.63
FMG15	-2		<0.5	1.73	3.3	17759	2	<0.05	9.70
FMG16	-2		<0.5	0.76	3.4	1539	<1	<0.05	33.43
FMG17	-2		<0.5	0.92	2.5	410	<1	<0.05	31.79
FMG18	-2		<0.5	0.60	19.0	7796	1	<0.05	26.89
FMG19	-2	-3	<0.5	8.03	2.6	1472	1	0.18	0.32
FMG19repeat			<0.5	7.93	3.0	1437	1	0.18	0.29
FMG20	-11		<0.5	1.25	2.1	142	<1	<0.05	0.07
FMG21	-3		<0.5	7.43	14.2	685	3	0.51	0.45
FMG22	-2		<0.5	6.81	2.8	1033	2	0.19	0.16
FMG23	-5		<0.5	4.08	3.3	308	<1	0.06	1.69

SAMPLE ID	Cd	Ce	Co	Cr	Cu	Fe	Ga	Ge	Hg
	ppm	ppm	ppm	ppm	ppm	%	ppm	ppm	ppm
pmcd1	<0.02	3.8	1.7	48	16.6	1.42	5.1	0.7	0.03
pmcd2	<0.02	12.0	1.3	38	8.8	2.80	2.6	0.8	0.01
pmcd3	0.06	70.1	7.4	31	16.7	10.20	6.4	0.9	0.02
pmcd4	<0.02	65.2	14.6	64	7.3	3.02	10.7	0.9	0.02
pmcd5	0.07	202.2	32.5	66	37.7	4.14	23.3	1.9	0.02
pmcd6	0.06	75.4	15.0	94	35.7	4.55	19.4	1.7	0.02
pmcd8	0.03	80.0	9.8	82	33.1	4.97	14.3	1.5	0.02
pmcd9	0.04	21.0	3.2	59	15.6	7.85	14.2	1.3	0.02
pmcd10	0.03	15.4	22.7	80	29.4	2.21	6.8	1.1	0.02
pmcd11	0.03	17.2	2.3	55	16.9	1.22	6.1	1.0	0.02
pmcd11repeat	0.03	18.5	2.2	56	16.8	1.21	6.1	1.0	0.02
pmcd12	0.07	56.9	1.3	28	10.3	1.67	8.8	1.2	0.01
pmcd13	0.12	58.1	13.3	46	15.8	4.62	20.3	1.5	0.01
pmcd14	<0.02	32.9	2.8	37	11.5	3.50	8.6	1.2	0.03
pmcd15	0.03	225.1	11.2	42	19.5	19.04	18.0	1.8	0.03
CJ17	0.06	61.4	20.6	87	43.4	4.52	25.1	2.1	0.02
CJ21	0.08	66.6	11.6	51	27.0	3.07	16.8	1.9	0.02
FMG5	0.04	158.2	226.0	98	61.0	16.18	15.7	1.3	0.02
FMG7	0.05	61.0	14.7	76	37.5	4.62	25.9	2.1	0.01
FMG8	0.06	80.9	26.2	33	18.5	2.04	10.8	1.5	0.03
FMG9	0.04	79.8	14.8	56	25.0	3.16	15.6	1.7	0.02
FMG9repeat	0.04	82.8	14.9	55	25.9	3.17	15.8	1.6	0.03
FMG10	0.20	93.0	19.8	101	37.6	4.78	22.9	2.0	0.02

FMG11	0.07	62.4	11.3	179	17.2	2.98	3.4	0.6	0.04
FMG12	0.06	143.9	21.2	532	19.2	6.38	7.4	1.6	0.04
FMG13	0.09	63.8	33.5	206	59.6	7.03	8.7	1.3	0.02
FMG14	0.11	141.7	38.7	555	24.6	7.46	11.8	1.4	0.05
FMG15	0.08	133.8	53.0	543	70.7	8.61	13.2	1.1	0.04
FMG16	0.58	12.3	3.7	21	9.6	0.53	4.8	0.2	0.03
FMG17	0.92	11.5	3.1	18	7.2	0.56	2.9	0.2	0.03
FMG18	1.73	38.7	8.8	12	28.7	2.12	6.3	0.3	0.05
FMG19	0.05	83.7	4.3	73	7.5	2.44	15.9	1.3	0.06
FMG19repeat	0.06	77.2	4.3	62	6.9	2.42	16.4	1.3	0.03
FMG20	0.02	39.1	1.8	44	60.4	0.81	3.3	0.8	0.04
FMG21	0.08	50.5	12.2	43	50.9	4.21	22.4	2.6	0.03
FMG22	0.16	147.2	6.2	52	29.1	1.29	17.8	1.6	0.04
FMG23	0.09	50.9	3.3	24	47.3	0.91	8.2	0.9	0.03

SAMPLE ID	K	La	Li	Mg	Mn	Mo	Na	Nb	Ni
	%	ppm	ppm	%	ppm	ppm	%	ppm	ppm
pmcd1	0.31	1.9	<2	0.07	269	2.63	0.05	0.89	15.3
pmcd2	0.26	6.8	10	0.03	146	1.02	<0.01	1.06	8.4
pmcd3	0.55	19.4	17	0.12	2824	1.07	<0.01	2.82	16.7
pmcd4	1.25	31.4	<2	0.07	288	1.14	0.07	1.77	26.5
pmcd5	0.97	206.4	17	1.54	2182	0.54	1.74	8.86	47.2
pmcd6	1.03	34.7	26	1.22	1177	0.76	2.15	10.27	115.7
pmcd8	0.55	21.1	11	0.21	743	1.42	0.02	8.85	27.1
pmcd9	0.79	13.8	10	0.23	202	1.82	0.02	5.31	13.5
pmcd10	0.60	6.2	20	0.20	2664	2.19	0.28	1.98	40.6
pmcd11	0.77	9.4	9	0.17	351	1.39	0.28	1.86	18.2
pmcd11repeat	0.77	10.0	9	0.17	348	1.35	0.28	1.90	17.6
pmcd12	1.31	29.5	12	0.17	93	1.01	0.01	4.03	8.4
pmcd13	2.36	27.4	35	1.36	576	0.38	1.19	8.61	26.8
pmcd14	3.41	16.5	3	0.06	212	0.93	0.08	3.82	16.3
pmcd15	1.99	161.1	11	0.15	312	1.53	0.01	4.56	39.9
CJ17	2.55	30.2	45	1.59	1088	0.57	0.74	11.18	103.7
CJ21	1.84	27.9	40	0.82	3282	0.35	1.91	10.84	40.0
FMG5	0.57	16.4	29	0.19	11086	3.55	0.02	15.99	55.2
FMG7	2.54	58.5	39	1.22	636	0.30	0.80	13.45	53.1
FMG8	1.07	31.2	15	0.26	3607	0.65	1.17	4.21	17.6
FMG9	0.98	39.3	34	0.31	636	0.78	0.08	18.47	23.9
FMG9repeat	0.98	39.4	34	0.31	632	0.81	0.08	18.45	24.2
FMG10	1.08	79.5	26	1.29	2309	0.88	2.12	11.92	54.3

FMG11	0.16	35.3	6	8.42	2928	0.36	0.02	28.48	158.0
FMG12	0.33	75.5	7	7.50	2714	0.40	0.02	18.12	308.7
FMG13	0.34	33.0	14	2.83	3519	1.79	0.05	35.01	259.1
FMG14	0.48	79.1	11	6.89	2505	0.65	0.03	20.95	467.4
FMG15	0.04	69.5	94	7.17	1740	0.56	0.03	12.68	430.7
FMG16	0.27	7.2	3	0.26	858	0.22	0.04	0.98	9.1
FMG17	0.27	7.1	3	0.38	710	0.13	0.03	2.23	11.9
FMG18	0.15	43.4	3	4.34	2572	10.40	0.05	0.84	21.8
FMG19	5.85	37.7	5	0.41	147	0.65	0.11	11.43	15.9
FMG19repeat	5.76	35.6	5	0.40	141	0.51	0.11	10.81	14.4
FMG20	0.26	18.1	7	0.04	195	1.14	0.04	1.50	14.6
FMG21	2.84	39.7	28	1.31	683	0.81	1.58	9.78	51.9
FMG22	5.10	67.5	9	0.37	507	0.49	0.12	19.06	13.1
FMG23	0.11	23.6	6	0.07	674	0.59	0.01	5.70	8.0

SAMPLE ID	P	Pb	Rb	Re	S	Sb	Sc	Se	Sn
	%	ppm	ppm	ppm	%	ppm	ppm	ppm	ppm
pmcd1	0.003	1.1	11.6	0.002	<0.01	0.13	2.1	0.9	0.2
pmcd2	0.020	3.5	13.1	0.002	<0.01	0.28	1.2	0.8	0.3
pmcd3	0.011	13.9	23.1	<0.002	<0.01	0.40	5.5	1.1	0.6
pmcd4	0.018	14.6	50.8	<0.002	<0.01	0.45	5.5	0.8	0.5
pmcd5	0.076	12.7	44.7	0.002	<0.01	0.29	15.4	1.0	1.2
pmcd6	0.099	10.8	47.7	0.002	<0.01	0.35	14.9	1.0	1.3
pmcd8	0.011	15.9	52.1	0.002	<0.01	0.54	5.8	1.0	1.1
pmcd9	0.024	11.6	49.9	<0.002	<0.01	0.70	5.1	1.5	0.8
pmcd10	0.012	42.5	31.1	0.002	<0.01	0.16	3.7	0.7	0.5
pmcd11	0.055	5.4	37.8	0.002	<0.01	0.12	1.7	0.5	0.4
pmcd11repeat	0.056	5.3	37.2	<0.002	<0.01	0.09	1.7	0.5	0.4
pmcd12	0.019	15.7	65.9	0.002	<0.01	0.50	2.9	0.8	0.7
pmcd13	0.049	43.8	133.0	0.002	<0.01	0.54	8.8	0.6	2.2
pmcd14	0.032	19.0	145.7	<0.002	<0.01	0.21	1.5	<0.5	0.7
pmcd15	0.074	88.6	99.9	0.004	<0.01	3.46	8.0	0.6	0.8
CJ17	0.072	14.5	153.7	0.002	<0.01	0.85	14.8	0.6	2.0
CJ21	0.093	22.1	108.9	0.002	<0.01	0.75	8.8	0.6	1.8
FMG5	0.024	110.9	45.1	0.004	<0.01	1.72	6.8	0.9	1.3
FMG7	0.036	16.6	148.4	0.004	<0.01	1.00	13.7	0.6	2.2
FMG8	0.014	25.3	52.0	<0.002	<0.01	0.24	5.7	<0.5	0.6
FMG9	0.035	16.2	83.9	<0.002	0.02	0.45	10.2	0.7	1.5
FMG9repeat	0.035	16.6	85.0	<0.002	0.02	0.46	10.0	0.8	1.5
FMG10	0.117	12.5	47.6	0.002	<0.01	0.42	16.2	0.8	1.4

FMG11	0.069	4.9	10.4	<0.002	<0.01	0.12	3.6	<0.5	0.3
FMG12	0.211	12.4	21.5	0.002	0.03	0.17	7.5	0.5	0.6
FMG13	0.083	9.2	23.1	0.002	0.27	0.49	4.3	<0.5	0.6
FMG14	0.158	15.6	29.5	0.002	0.01	0.13	9.5	<0.5	0.9
FMG15	0.114	15.5	3.0	0.004	0.50	<0.05	9.7	<0.5	0.9
FMG16	0.055	3.4	13.3	0.004	0.06	<0.05	1.4	<0.5	<0.2
FMG17	0.067	2.1	13.0	0.004	0.01	0.10	1.7	<0.5	<0.2
FMG18	0.426	13.3	8.1	0.002	0.22	0.69	1.9	0.7	<0.2
FMG19	0.052	19.8	254.2	<0.002	<0.01	0.71	5.8	<0.5	2.0
FMG19repeat	0.048	19.9	252.3	<0.002	<0.01	0.68	5.2	1.0	2.0
FMG20	0.012	9.9	14.9	0.002	<0.01	0.24	1.3	0.6	0.4
FMG21	0.054	23.1	144.1	0.004	<0.01	1.67	12.0	0.7	1.7
FMG22	0.034	27.5	224.2	0.004	<0.01	0.87	8.8	0.9	2.5
FMG23	0.197	35.6	6.5	0.002	0.02	0.30	3.5	0.8	0.6

SAMPLE ID	Sr	Ta	Te	Th	Ti	Tl	U	V	W
	ppm	ppm	ppm	ppm	ppm	ppm	ppm	ppm	ppm
pmcd1	19	<0.05	<0.05	0.5	365	0.09	0.2	26	0.6
pmcd2	15	0.08	<0.05	2.1	438	0.09	0.7	19	0.1
pmcd3	21	0.22	<0.05	6.7	911	0.13	2.1	29	0.2
pmcd4	133	0.14	<0.05	5.4	1083	0.33	0.6	60	1.0
pmcd5	354	0.74	0.11	10.3	5035	0.29	1.7	83	0.7
pmcd6	228	0.84	0.10	12.1	5418	0.23	1.2	112	0.7
pmcd8	17	0.66	<0.05	8.5	3146	0.28	1.5	100	0.7
pmcd9	35	0.43	0.06	5.9	1957	0.28	1.3	90	0.5
pmcd10	23	0.14	<0.05	2.0	881	0.22	0.4	28	0.4
pmcd11	29	0.15	<0.05	2.8	732	0.19	0.6	19	0.4
pmcd11repeat	33	0.16	<0.05	3.2	787	0.16	0.7	18	0.4
pmcd12	28	0.32	0.06	13.5	1403	0.36	2.5	23	0.5
pmcd13	52	0.78	0.07	12.0	3389	0.73	2.8	64	1.2
pmcd14	63	0.35	<0.05	9.1	1104	0.70	1.3	25	0.2
pmcd15	114	0.47	0.05	18.4	1571	0.57	3.7	330	2.6
CJ17	75	0.83	0.11	10.1	4490	0.67	1.9	111	1.5
CJ21	101	0.86	0.06	14.1	4121	0.54	2.4	65	1.6
FMG5	16	1.14	0.17	9.9	6038	0.66	3.3	250	1.7
FMG7	72	1.07	0.08	13.0	5192	0.82	2.4	109	1.8
FMG8	68	0.32	<0.05	6.7	1681	0.42	1.8	37	0.5
FMG9	51	1.29	<0.05	14.2	5960	0.43	2.8	76	1.7
FMG9repeat	52	1.33	<0.05	13.9	5829	0.46	2.8	76	1.7
FMG10	219	0.93	0.11	13.5	6459	0.25	2.7	126	1.1

FMG11	94	1.68	0.76	2.6	3878	0.10	0.9	50	0.3
FMG12	107	1.47	0.77	9.0	10229	0.11	2.4	63	0.1
FMG13	65	2.59	0.22	4.0	5630	0.13	3.9	338	0.3
FMG14	88	1.70	0.67	9.8	16389	0.13	3.9	167	<0.1
FMG15	409	1.08	0.51	11.6	15898	0.05	3.8	120	<0.1
FMG16	82	<0.05	0.42	0.8	329	0.07	0.4	26	<0.1
FMG17	58	0.12	0.42	1.0	585	0.06	0.4	17	0.2
FMG18	142	0.07	0.59	0.9	274	0.16	1.5	45	0.2
FMG19	148	1.10	0.06	24.1	3743	1.38	3.5	36	1.1
FMG19repeat	143	1.04	0.06	21.5	3616	1.37	3.4	37	1.1
FMG20	33	0.10	<0.05	1.7	611	0.18	1.0	16	0.3
FMG21	136	0.71	0.10	9.6	4309	0.60	1.9	85	2.0
FMG22	96	1.50	0.16	39.4	8638	1.19	7.6	64	1.2
FMG23	76	0.40	0.07	5.7	1365	0.39	1.3	20	0.3

SAMPLE ID	Y	Zn	Zr
	ppm	ppm	ppm
pmcd1	0.9	9.6	9
pmcd2	3.8	33.7	82
pmcd3	12.4	139.3	207
pmcd4	6.0	14.2	91
pmcd5	51.9	75.5	91
pmcd6	58.3	107.4	102
pmcd8	8.5	29.2	121
pmcd9	6.7	17.4	147
pmcd10	2.9	26.3	37
pmcd11	4.1	25.3	76
pmcd11repeat	4.2	26.0	84
pmcd12	24.8	13.9	460
pmcd13	17.8	115.5	190
pmcd14	7.2	18.2	73
pmcd15	17.6	49.6	135
CJ17	31.6	132.5	132
CJ21	20.5	79.2	241
FMG5	7.7	19.9	126
FMG7	27.1	106.5	182
FMG8	16.5	24.3	200
FMG9	19.5	25.2	165
FMG9repeat	19.5	25.2	161
FMG10	41.0	92.8	143

FMG11	3.1	42.1	42
FMG12	5.9	103.4	73
FMG13	4.8	60.7	74
FMG14	8.2	222.7	138
FMG15	8.5	108.2	142
FMG16	5.2	13.4	12
FMG17	5.6	17.7	16
FMG18	56.0	101.6	9
FMG19	24.5	40.4	313
FMG19repeat	24.2	41.3	310
FMG20	4.4	35.9	63
FMG21	18.8	105.9	151
FMG22	71.6	42.1	1046
FMG23	10.5	36.6	147

Appendix 4 GR-110 Scintillometer total count radiometric readings

OBS point	X	Y	UTM Zone	Total count: Min	Total count: Max	Total count: Average
CJ10	749575	734285	30	11.5	13.1	12.3
CJ11	749761	735706	30	7.3	8.6	7.95
CJ12	745937	740735	30	18	20	19
CJ23	803130	956094	30	37	39.2	38.1
CJ24	176504	979613	31	28	35	31.5
CJ25	178206	968198	31	29	37.8	33.4
CJ26	182062	966153	31	46.6	53	49.8
CJ27	828496	933797	30	26.9	28.9	27.9
CJ28	828225	929919	30	23.5	27.5	25.5
CJ37	745870	1052213	30	14.7	20.5	17.6
CJ38	747556	1053549	30	11.1	12.7	11.9
CJ39	753288	1058921	30	24.5	27.2	25.85
CJ42	772107	1068237	30	29.7	37.1	33.4
CJ42b	772107	1068237	30	27.3	32.7	30
CJ44	826769	1060341	30	27	31.1	29.05
CJ45	826971	1060990	30	24.1	28.4	26.25
CJ48	181764	1077073	31	25.3	29.3	27.3
CJ49	181973	1077451	31	28.6	29.1	28.85
CJ50	187606	1094917	31	42.7	43.4	43.05
CJ51	187779	1095314	31	35.3	37.2	36.25
CJ52	188848	1099671	31	23.8	25.8	24.8
CJ53	200584	1117598	31	28.3	30.5	29.4

CJ54	203063	1121745	31	34.4	37.7	36.05
CJ55	204180	1123150	31	28.7	29.7	29.2
CJ56	206074	1126537	31	33.5	37.5	35.5
CJ57	821182	1069018	30	39.7	44.8	42.25
CJ58	817684	1077969	30	28.8	32.2	30.5
CJ59	817366	1078973	30	33.6	34.6	34.1
CJ60	814307	1088719	30	30.1	34.3	32.2
CJ61	811247	1091100	30	31.3	36.7	34
CJ62	806426	1095605	30	29.2	32.8	31
CJ62b	806426	1095605	30	24	45	34.5
CJ63	805962	1096391	30	30.1	34.3	32.2
CJ66	818252	1147635	30	27.4	32.2	29.8
CJ67	817818	1151559	30	26.3	28.3	27.3
CJ68	814027	1157726	30	14.1	18.7	16.4
CJ69	812754	1159928	30	11.9	13.7	12.8
CJ71	810938	1161880	30	17.4	20.2	18.8
CJ72	810615	1162623	30	31.1	35.2	33.15
CJ73	810706	1167673	30	19.6	23.2	21.4
CJ74	809960	1170164	30	13.8	18.4	16.1
CJ75	808749	1175640	30	39.2	41.3	40.25
CJ76	796280	1169399	30	38.4	39.9	39.15
CJ77	797503	1170147	30	39.2	41.5	40.35
CJ78	808003	1177839	30	31.4	37.6	34.5
CJ79	806796	1177841	30	76.8	80.8	78.8
CJ81	812509	1175283	30	18.7	24.2	21.45
CJ82	174083	1166183	31	14.3	15.9	15.1

CJ83	177415	1165059	31	17.8	19.9	18.85
CJ84	180035	1164371	31	10.2	11.2	10.7
CJ85	182534	1163291	31	18.5	20	19.25
CJ86	183215	1160669	31	9	11.2	10.1
CJ87	183649	1158537	31	20.2	25.2	22.7
CJ88	183418	1155793	31	20.5	22.5	21.5
CJ89	179217	1156876	31	10.2	13	11.6
CJ90	171658	1159040	31	12.3	14.3	13.3
CJ96	738329	1103661	30	29.6	30.9	30.25
CJ100	713289	1045541	30	14.2	23.6	18.9
CJ101	713864	1046104	30	23.5	28.1	25.8
CJ103	722533	1054704	30	14.9	17.7	16.3
CJ112	624580	1019447	30	56	63	59.5
CJ113	625296	1019306	30	29.1	29.3	29.2
CJ114	626040	1019846	30	4.7	6.8	5.75
CJ123	625261	893922	30	30.2	36	33.1
CJ124	625772	893810	30	36.3	36.3	36.3
CJ125	628429	893237	30	15.5	15.5	15.5
CJ126	630776	892756	30	11.3	11.3	11.3
CJ127	632187	896190	30	18.6	18.6	18.6
CJ135	659056	881304	30	11.1	11.7	11.4
CJ136	637010	876160	30	10.6	10.8	10.7
CJ141	628292	854974	30	7.6	8.6	8.1
CJ142	628402	854954	30	8.3	9.5	8.9
CJ143	621522	839131	30	36.8	39.2	38
CJ145	625060	839394	30	8.4	10.4	9.4

CJ147	631145	837708	30	46.8	50.8	48.8
CJ149	658522	830273	30	15.5	19.3	17.4
CJ150	661938	827956	30	15.4	17	16.2
CJ151	664401	823648	30	9.8	12.2	11
CJ152	668078	822133	30	9.5	11.5	10.5
CJ153	680015	815364	30	18.7	21.8	20.25
CJ154	686980	814273	30	8.6	9.2	8.9
CJ155	687349	813077	30	9.1	10.7	9.9
CJ156	691485	810675	30	22.3	23.7	23
CJ157	692158	809817	30	23.5	26.1	24.8
CJ158	692813	809694	30	46.1	57.1	51.6
CJ160	711499	811925	30	38.2	41.4	39.8
CJ161	716063	811928	30	46.3	50.1	48.2
CJ162	781996	772367	30	28.9	30.1	29.5
CJ163	781922	774664	30	23.1	26.7	24.9
CJ164	782415	776063	30	23	26	24.5
CJ165	779031	778142	30	21.7	25.5	23.6
CJ166	764912	781745	30	28.2	33.2	30.7
JC14	267040	691720	31	11.8	14.2	13
JC15	267324	694172	31	12.2	15	13.6
JC15b	267324	694172	31	14.9	15.5	15.2
JC18	260441	707012	31	19.4	22.7	21.05
JC18b	260441	707012	31	33	35.8	34.4
JC19	255126	708026	31	39.3	46.7	43
JC20	249321	712740	31	30.5	36.4	33.45
JC21	246960	701202	31	44.4	49.4	46.9

JC22	255416	679923	31	22.9	26.7	24.8
JC23	222017	673380	31	63.5	69.1	66.3
JC24	820215	685071	30	67.7	73.1	70.4
JC25	819936	690226	30	12.4	15.4	13.9
JC26	816808	697251	30	12.2	14.7	13.45
JC27	822617	698116	30	25.2	26.7	25.95
JC28	824774	701997	30	20.4	21.2	20.8
JC29	825258	701868	30	26.2	27.8	27
JC31	811436	705904	30	55.2	66.7	60.95
JC33	804889	705808	30	12.8	16.2	14.5
JC34	793001	701249	30	14.2	14.2	14.2
JC35	793544	700085	30	19.9	19.9	19.9
JC35b	793544	700085	30	66	73.3	69.65
JC36	795005	711721	30	13.4	16.4	14.9
JC37	802020	722144	30	13.2	19	16.1
JC38	803735	724584	30	8.7	8.7	8.7
JC40	802843	728072	30	8.6	9.6	9.1
JC41	797058	729866	30	7.5	7.5	7.5
JC46	739748	740336	30	6.3	8.6	7.45
JC70	723630	887653	30	29.7	38.9	34.3
JC127	796023	1149861	30	7	20	13.5
JC129b	793508	1155271	30	7	15	11
JC138b	776429	1162477	30			0.046
JC166	677784	1054398	30	33.4	33.6	33.5
JC166b	677784	1054398	30	18.3	21.3	19.8
JC166c	677784	1054398	30	10.1	13.7	11.9

JC167	677669	1054543	30	20.9	22.4	21.65
JC168	677429	1054668	30	17.7	18.7	18.2
JC269	823331	685522	30	24.5	30.5	27.5
JC269b	823331	685522	30	17.4	21.4	19.4
JC270	748765	739108	30			20
JC279	759495	735181	30			10
JC284	769493	735452	30			40
JC286	777345	737190	30			15
JC290	782218	772307	30	30	35	32.5
JC291	781931	774671	30	23	30	26.5
JC292	764647	782289	30	25	50	37.5
JC293	801232	763708	30	4	9	6.5
JC297	679423	811788	30	50	75	62.5
JC298	664995	823352	30	7	16	11.5
JC305	624713	890111	30	8	14	11
JC306	632496	893648	30	6	10	8
JC308	638181	891056	30	31	48	39.5
JC315	716849	887247	30	20	36	28
JC319	738026	1040248	30	8	15	11.5
JC336	794261	1153938	30	3	18	10.5
JC338	820342	1133799	30	27	39	33
JC339	818863	1116263	30	20	40	30
JC340	806001	1096344	30	16	35	25.5
JC342	828503	933698	30	23	45	34
JC344	830447	885245	30	20	30	25
JC345	826529	905145	30	17	33	25

JC346	827090	906317	30	22	38	30
JC347	824493	910856	30	22	30	26
JC348	823477	924498	30	16	30	23

Appendix 5 GRM-260 gamma-ray spectrometer radiometric readings

OBS point	X	Y	UTM Zone	K	U	Th	Total Count
CJ67	817818	1151559	30	0.63	3.27	7.10	34.62
CJ72	810615	1162623	30	1.30	1.18	6.09	36.64
CJ76b	796280	1169399	30	1.84	2.95	7.23	37.91
CJ77	797503	1170147	30	0.39	4.46	7.53	36.94
CJ79	806796	1177841	30	5.24	5.18	17.62	125.32
CJ96b	738329	1103661	30	1.61	1.37	6.60	52.84
JC102	747791	1036750	30	0.00	1.41	0.09	16.09
JC106b	788040	1045042	30	0.76	2.15	8.98	50.71
JC152	763378	1100832	30	1.89	1.99	8.08	52.24
JC264	815734	771379	30	0.05	1.61	1.20	25.05
JC265	815875	771088	30	0.01	3.30	5.68	31.12
JC266	804795	766272	30	0.16	1.65	2.48	30.52
JC267	796616	747979	30	0.02	1.43	2.68	21.37
JC268	797239	745263	30	0.00	1.26	0.98	15.31
JC269b	823331	685522	30	0.02	1.03	1.07	19.69
CJ201	747515	728977	30	0.67	2.70	7.42	38.20
CJ202	739895	744586	30	0.06	1.74	0.01	19.20
CJ203	739331	744485	30	0.47	2.16	2.99	34.12

CJ204	736081	744789	30	1.21	4.79	6.94	54.17
CJ206	731481	747852	30	1.09	2.06	2.95	34.62
CJ207	730925	747968	30	2.28	2.58	4.64	47.90
CJ209	723164	748061	30	1.23	1.74	5.63	43.38
CJ210	722083	748472	30	2.22	2.47	10.43	69.46
CJ212	713265	750758	30	0.09	1.94	1.30	30.48
CJ228	810107	1168127	30	0.68	3.37	1.92	42.04
CJ71b	810938	1161880	30	0.18	0.33	5.72	16.02
CJ69b	812754	1159928	30	0.18	0.33	5.72	16.02
CJ231	172661	1019077	31	1.95	2.90	5.82	53.31
CJ232	176238	1013358	31	1.81	2.80	6.09	53.56
CJ25b	178206	968198	31	1.62	3.03	11.11	51.55
CJ26c	182062	966153	31	2.29	2.37	11.60	46.57
CJ235	185023	965030	31	1.05	2.60	6.77	48.00
JC270	748765	739108	30	0.03	1.34	3.17	21.72
JC271	749887	736179	30	0.00	0.96	0.65	5.17
JC272	750917	726379	30	4.63	3.18	9.19	95.62
JC276	745985	740956	30	1.03	1.51	2.76	42.35
JC331	754917	1142338	30	0.03	2.27	0.77	17.83
JC333	762582	1149872	30	0.07	1.28	3.62	28.04
JC334	772373	1157595	30	0.99	2.34	7.06	47.64
JC367	808493	717367	30	1.02	0.00	7.71	26.62
JC371	791015	708091	30	0.07	1.12	1.28	15.97
CT33	737867	1060129	30	0.02	1.19	1.55	15.84
PD4	750877	726414	30	5.11	5.13	16.08	135.11
PD5	750870	726416	30	2.13	1.85	8.01	71.20

PD8	738260	732857	30	0.62	1.70	2.85	30.57
PD9	739571	740244	30	0.64	2.10	3.91	39.16
PD39	795650	1042055	30	1.34	1.69	3.96	40.93
PD48	762543	1149815	30	0.12	2.26	2.27	30.12
PD49	768726	1153446	30	0.14	2.59	5.92	32.32
PD50	772634	1157999	30	0.47	2.39	1.73	32.61
PD53	778572	1164066	30	1.53	2.10	13.44	66.26
PD54	783755	1164650	30	2.02	4.05	7.32	56.43
PD90	803655	724576	30	0.05	2.19	0.36	5.33

Appendix 6 Magnetic susceptibility measurements, listed by observation point

OBS point	X	Y	UTM Zone	Description	Mag. Susp.1	Mag. Susp.2	Mag. Susp.3	Mag. Susp.4	Mag. Susp.5	Average
CJ10	749575	734285	30	Quartz sandstone, pale yellow.	-0.008	0.012	0.033	0.007		0.011
CJ11	749761	735706	30	Small scale quarrying in quartz sandstone. Surface ripples indicate flow deposition to 192. Ripple frequency 12cm.	-0.011	0.005	0.41	0.06		0.116
CJ12	745937	740735	30	2m x 4m x 0.5m high section of quartz sandstone, more feldspar, less clean, flaggy. Red.	0.001	0.093	0.015			0.036
CJ14	814172	858052	30	Top: 1m poorly sorted pebbly conglomerate. Dominated by pebble clasts with sandstone boulders. Sub-angular clasts, not far travelled. Base: 5m light green grey siltstone, soapy, fissile. Thinly bedded.	1.49	1.13	1.03			1.217
CJ14b	814172	858052	30	As OBS point CJ14.	0.219	0.244	0.211			0.225
CJ16	772947	860353	30	Pebbly conglomerate forms road surface, 5m x 20m, same as top of CJ14	1.02	1.13	1.903			1.351
CJ19	758481	834712	30	Duricrust on road surface 4m x 2m. Duricrust is pebbly possibly derived from a conglomerate. Pebbles thickly coated in iron oxide. 20m to south, and 2m lower is medium grained sandstone, flaggy, dark grey, very thinly bedded. Alluvium boundary starts here.	0.082	0.144	0.267			0.164
CJ20	758239	834890	30	Flaggy red med grained sandstone, thinly bedded. Surface ripples indicate flow deposition to 300° frequency of 5cm.	0.068	0.172	0.319			0.186
CJ23	803130	956094	30	Stream section of pebbly lateritic conglomerate. Pseudo horizontal bedding. Note series of planar dip slopes to NE.	0.347	0.479	0.396			0.407
CJ24	176504	979613	31	Dirty laminated hard pink grey sandstone, fine to medium grained. Contains non silica. Slightly flaggy. Weathers with rounded boulders on surface and onion weathering.	0.188	0.291	0.173			0.217
CJ25	178206	968198	31	Light olive coloured fine grained micaceous sandstone with interbedded weathered bands of olive siltstone. Exposed for 100m along roadside. Top 4m sandstone, base 4m interbedded siltstone sandstone. Note also	0.135	0.194	0.179			0.169

				isolated pebbly conglomerate beds.						
CJ26	182062	966153	31	200m roadside 2d outcrop of micaceous light olive siltstone, thinly bedded. One NW/SE strike has very steep dip to either side.	0.162					0.162
CJ26b	182062	966153	31	As OBS point CJ 26.	0.471	0.321				0.396
CJ27	828496	933797	30	8m x 4m outcrop. Pale olive sandstone, weathers to salmon pink. Flaggy. Contains lithics, feldspar and possibly magnetite, so feldspathic arenite. Onion weathering. Cobbles of laterite on surface nearby.	0.207	0.265	0.227			0.233
CJ28	828225	929919	30	Same lithology as CJ27.	0.186	0.237	0.228			0.217
CJ62b	806426	1095605	30	Northern edge of Oti bed escarpment, Several small 2m x 2m outcrops of olive green fine grained hard 'Bunya'-type sandstone with mica. Flaggy. Slightly coarser grained than other sites today. Stepped series of drops (breaks in slope) over resistant sandstone beds north to a plain.	1.29	1.18	1.16	1.3	1.22	1.230
CJ67	817818	1151559	30	Same multicoloured bands as CJ66. Very fine grained pink sandstone/siltstone, gray siliceous, weathers to tan brown, small soft sediment structures seen throughout including load structures and micro folds.						0.126
CJ72	810615	1162623	30	Large area at crest of hill with in situ rock and many boulders. Beds of purple grey and white pale yellow medium grained sandstone. Flaggy, dirty. Purple grey beds have 5mm bedding of pale yellow within. Small scale quarrying. Banding due to alt bands of quartz or mica rich thin beds						0.065
CJ76b	796280	1169399	30	JC REVISITED 2007. Plane- to cross-bedded. Some beds up to 2m thick show large scale foresets - may be aeolian with fluvial influence?						0.068
CJ77	797503	1170147	30	Same as CJ76, but large flat bedding plane. Poorly cemented medium grained feldspar/mica sandstone						0.048
CJ79	806796	1177841	30	Descending north edge of Gambaga escarpment. Passed through sandstone/siltstone beds, now 6m of shaly slaty olive green siltstone + mudstones. Horizontal bedding prevalent. 5 or 10cm beds of very hard fine quartz sandstone approx every 0.5 to 1m, 20% sandstone. Note						0.207

				thick sandstone cap of at least 15m. Possibly the Poubougu Fm						
CJ96b	738329	1103661	30	JC REVISITED 2007. Massive fractured cream coloured sandstone, immature, fine grained. Saw large scale trough cross-lamination possibly produced by tidal currents.						0.8714
JC1	204000	649500	31	Red brown poorly sorted small-pebble gravel with red sandy matrix - fragments of vein quartz.	0.043					0.043
JC14	267040	691720	31	Transitional meso-leucocratic gneiss in road. Contains c. 1cm wide quartz-rich bands alternating with mafic layers; small scale isoclinal intrafolial folds verge to SW.	0.187	0.19	0.089			0.155
JC15	267324	694172	31	Large knoll in finely layered mesocratic gneiss with intrafolial folds separated by grain size-reduced straight zones; latter orientated 038. Multiple generations of QF pegmatite, some occupying straightening zones.	0.087					0.087
JC15b	267324	694172	31	As OBS point JC 15.	1.87					1.870
JC15c	267324	694172	31	As OBS point JC 15.	0.486	0.201				0.344
JC17	261272	707021	31	Thinly layered mesocratic gneiss - more abundant QF layers than (15). Vergence of intrafolial drag-folds suggests sinistral shear. Sporadic pink/red garnet.	0.081	0.239	0.036			0.119
JC17b	261272	707021	31	As OBS point JC 17.	0.227	0.427				0.327
JC18	260441	707012	31	QF leucogneiss with 1-2 cm wide layering of leuco and mafic (q-f-bi-hnb) components. Minor amphibolite layers show folding. Drag folds indicate dextral shear within a foliation of 040 strike. 2-3 cm wide pegmatite veins present.	0.255	0.311	0.181	0.289		0.259
JC18b	260441	707012	31	As OBS point JC 18.	-0.009	-0.006				-0.008
JC19	255126	708026	31	Leucocratic augen gneiss. Thinly layered with sporadic 1-2cm quartz-feldspar augen; latter probably relict transposed pegmatite veins. Mafic (amphibolite) layering is very thin (1-4mm). Strong intrafolial folding gives dextral shear within foliation striking 019 (subvert).	0.052	19.02	0.132	0.06	0.106	3.874
JC20	249321	712740	31	Small exposure dominantly in mesocratic gneiss with Q/F layering showing minor intrafolial folding.	0.126	0.177	0.135			0.146

JC20b	249321	712740	31	As OBS point JC 20.	0.291					0.291
JC21	246960	701202	31	Pale grey leococratic gneiss. Main foliation strikes 036 and is displaced along pegmatite-filled ductile zones of refoliation; latter with sinuous courses orientated 180-160 and with local development of Q/F augen.	0.146	0.149	0.196	0.179	0.125	0.159
JC22	255416	679923	31	Quarry in grey mesocratic gneiss, which is grain-size reduced along wide ductile zones trending 039. Narrow amphibolite sheets are folded and transposed into the foliation. Hornblende coarsens to 4mm in pegmatite rich areas. To E of quarry, gneiss is sharply overlain by pale cream sand c. 2m thick.	2.55	7.08				4.815
JC23	222017	673380	31	Large exposures in quartz-feldspathic gneiss with augen. Late-stage pegmatite veins.	0.153	0.105	0.096	0.124	0.153	0.126
JC24	820215	685071	30	In road cutting. Thinly bedded to laminated sequence of grey-green fine grained micaceous lithic-rich sandstones interbedded with. Papery' laminated mudstone/siltstones. Syn-sedimentary slump folding in sandstones. Sequence is part of an inclined fold with axial surface dipping 30 deg to SE 130 approx. Some minor folding and thrusting of upper limb shows same vergence (i.e. to NW).	0.078	0.027	0.119			0.075
JC24b	820215	685071	30	As OBS point JC 24.	0.103					0.103
JC24c	820215	685071	30	JC REVISITED 2007. Green-grey, micaceous massive to normally graded sandstone beds possibly resemble sequences in the Bimbila Formation.						0.136
JC25	819936	690226	30	Glassy quartzitic sandstone; pale pink weathering. Thin internal lamination. Studded with 2-4mm pink minerals, possibly garnet.	-0.01	-0.004	-0.001			-0.005
JC25b	819936	690226	30	As OBS point JC 25.	0.036					0.036
JC25c	819936	690226	30	As OBS point JC 25.	0.006					0.006
JC26	816808	697251	30	Brown weathering micaceous siltstones, thinly interbedded with brown fine grained micaceous sandstones - lower part of scarp slope sequence.	0.203	0.067	0.27			0.180
JC27	822617	698116	30	In village, small exposures of hard, grey, quartzitic sandstones. Medium bedded and cross bedded.	0.012	0.024	0.016	0.035		0.022

JC28	824774	701997	30	White, friable quartzitic sandstone. Part of dip slope of about 10-15 to E 100.	0.094	0.155	0.191	0.053		0.123
JC29	825258	701868	30	Thinly stratified quartz rich sandstone with well-rounded quartz granules prominent. In some layers sporadic quartz pebbles.	0.035	0.049	0.056			0.047
JC30	829222	705973	30	Pale brown sand on flats by lake shore. Possibly an old river terrace?	0.048	0.058				0.053
JC33	804889	705808	30	Pavements in quartzitic sandstone. Poorly sorted, with common coarse sand and granules in medium grained matrix.	0.027	0.065	0.047			0.046
JC34	793001	701249	30	Medium-bedded (20-70cm) quartzitic sandstone; well laminated with planar and trough cross-bedding.	0.013	0.018	0.013			0.015
JC35	793544	700085	30	White, sugary quartzitic sandstone in road cutting; both well laminated and massive beds types, latter up to 2m. Well jointed and fractured with anomalous dip. Fault juxtaposes sandstone with grey micaceous siltstone to SE; latter dip 38/060	0.074	0.063	0.014	0.018		0.042
JC35b	793544	700085	30	As OBS point JC 35.	0.131	0.218	0.425			0.258
JC36	795005	711721	30	White/brown weathering thin bedded quartzitic sandstone in road. Ripple marked bed tops indicate currents to W263	0.044	0.019	0.031	0.042		0.034
JC37	802020	722144	30	Sandstone, quartzitic, medium grained with subrounded/angular quartz grains.	0.042	-0.01	0.026			0.019
JC38	803735	724584	30	White, pure, hard quartzitic sandstone, flaggy to thick bedded, locally trough cross-bedded. Many millet seed grains indicative of aeolian source in part. Large channel seen in crags to south of road. Cut by swarms of 2-4mm quartz-filled fractures with minor displacements - dominant trend is 020.	-0.009	-0.004	0.002			-0.004
JC38b	803735	724584	30	As OBS point JC 38.	0.083	0.021	0.013			0.039
JC41	797058	729866	30	Pavements in white quartzitic sandstone. Intensely fractured and veined along a 095 trend. Riedel shears suggest sinistral movement in part. Some veins contain white amorphous material. In places an earlier vein system is seen, trending 120.	-0.01	0.032	0.015			0.012

JC41a	797058	729866	30	As OBS point JC 41.	0.203	0.008				0.106
JC42	785761	738130	30	White medium grained quartzitic sandstone - sporadic quartz veins trending 040.	-0.021	-0.005	-0.012			-0.013
JC70	723630	887653	30	In road drain; exposures of spheroidally. Weathering, dark maroon very fine grained highly micaceous sandstone/siltstone; finely laminated in part.	0.249	0.153	0.205			0.202
JC96	721279	993920	30	In road; rib of pale yellow (weathered) fine grained quartzose sandstone.	0.026	0.323	0.058			0.136
JC97	720970	984711	30	Medium grey micaceous siltstone; laminated with some scattered fine sand grains. Interbedded with maroon micaceous mudstone.	1.42	0.665				1.043
JC100	740849	1038220	30	Yendi road; from Tamale to here, common debris of red sandstone. Here in river bed, c. 1m of soft, maroon micaceous mudstones interbedded with thin (<10cm) pale green micaceous mudstones. Sequence is folded along sub-horizontal axis trending 165. Adjacent in river bed, pavements in sub-horizontal, flaggy, pale brown-grey micaceous sandstone. May be in contact with mudstones along postulated fault trending c 050.	0.163	0.253	0.214			0.210
JC102	747791	1036750	30	Exposures of red-weathering, yellow/ buff fine/medium/coarse grained stratified sub-arkosic sandstone - some well-rounded 'millet seed' quartz grains. Possible extension of Tamale Sandstone.						0.145
JC105b	777282	1040273	30	JC REVISITED 2007. Pale green micaceous arkosic sandstones of 'Bunya' type exposed.						0.195
JC106	788040	1045042	30	Scarp of major feature - exposures in green/grey 'Bunya' sandstone. Medium grained and poorly sorted arkosic, micaceous. Thinly stratified and ripple marked; some layers with green and maroon mud-flakes. Dip c. 2 to E	3.87	4.89	4.64			4.467
JC106b	788040	1045042	30	JC REVISITED 2007. Cutting widened to show maroon/green-grey slightly micaceous siltstones overlying sandstone; siltstones sampled for acritarchs (see OBS point JC21). Latter is coarse and gritty at base, with granules of red jasper and metavolcanic lithologies; it fines upwards suggesting a turbidite.						6.463

JC108	820627	1043058	30	Green/grey, medium grained sandstone of 'Bunya' type.	1.66	1.77	1.53			1.653
JC109	175277	1043019	31	In well, flakes of green-grey micaceous siltstone.	1.24	1.13	0.915			1.095
JC109b	175277	1043019	31	As OBS point JC 109.	1.55	0.992	0.71			1.084
JC109c	175277	1043019	31	As OBS point JC 109.	0.876	0.671	0.773			0.773
JC115	806428	1095605	30	Green-grey medium grained sandstone.	1.09	1.16	0.937			1.062
JC119	818268	1110581	30	Variegated pale cream/pink/grey micaceous mudstone, fissile. Some mud-cracks noted.	0.491	0.464	0.49			0.482
JC120	818879	1116165	30	Exposures in yellow/green/grey micaceous fine grained sandstone and siltstone; finely interbedded.	1.23	2.26	1.91			1.800
JC121	819579	1124981	30	Green/khaki/maroon finely laminated micaceous mudstone and siltstone with minor thin sandstone beds forming ribs on road from previous point.	1.54	0.82	0.154			0.838
JC122	830461	1133237	30	Variegated red/khaki/green micaceous mudstones and silty mudstones.	0.137	0.271	0.173			0.194
JC127	796023	1149861	30	Medium grained buff/white weathering quartz arenite; trough cross-bedded.	0.009	0.014	0.012	0.009	0.018	0.012
JC129	793508	1155271	30	Pavements in red weathering quartzitic sandstone with some feldspar grains.	0.012	0.029	0.042			0.028
JC129b	793508	1155271	30	Revisited in 2007. Sandstone, slightly feldspathic, medium-grained, well-sorted. Trough cross-bedded throughout.	0.033	0.058	0.009	0.044	0.064	0.042
JC130	789461	1160270	30	Exposures on dip-slope in yellow-weathering medium grained quartzitic sandstone.	0.08	0.054	0.046			0.060
JC131	788387	1163519	30	Medium grey (yellow weathering) quartzitic sandstone at Chesterfield Lodge Hotel.	0.012	0.016	0.01			0.013
JC132	783613	1164702	30	Med/fine grained yellow weathering quartzitic sandstone in ditch.	0.037	0.029	0.052			0.039
JC133	783776	1164939	30	Outlier on dip slope - in medium grained quartzose sandstone locally well laminated and thickly to thinly bedded.	0.032	0.017	0.084			0.044
JC135	790627	1154950	30	Pavements in medium/coarse grained quartzitic sandstone.	0.025	0.028	0.012			0.022

JC136	788936	1150935	30	Pavements in medium/coarse pink to purple weathering quartzitic sandstone. Fractures oriented 295.	0.024	0.043	0.044			0.037
JC138	776429	1162477	30	Red weathering, white, medium-fine grained quartz-rich sandstone.	0.029	0.034	0.081			0.048
JC139	772535	1157893	30	Medium grained brown/yellow weathering quartzitic sandstone.	0.03	0.037	0.041			0.036
JC140	768758	1153465	30	Medium grained feldspathic sandstone.	0.072	0.086	0.072			0.077
JC141	757421	1146839	30	Medium grained yellow weathering, white quartzitic sandstone.	0.033	0.011	0.019			0.021
JC142	738566	1103968	30	At Pigu, ridge in medium/fine green/grey 'Bunya' sandstone.	0.987	0.993	1.11			1.030
JC145	745193	1103673	30	Fine grained green/grey sandstone.	0.91	1.62	1.78			1.437
JC148	750609	1102720	30	Extensive exposure of green/grey sandstone. Cut by joints at 090.	0.867	0.772	0.927			0.855
JC149	758757	1102357	30	Pisegu village; fine grained green/grey sandstone. Green/grey mud-flakes present.	0.887	1.05	0.899			0.945
JC151	763024	1100987	30	Fine green/grey micaceous sandstone.	0.633	0.753	0.933			0.773
JC152	763378	1100832	30	Fine/med green/grey micaceous sandstone with green/grey mud-flakes.	1.17	0.934	1.02			1.041
JC153	771302	1099705	30	Fine grained green/grey sandstone.	1.03	0.941	0.818			0.930
JC154	773678	1099854	30	Fine grained green/grey sandstone; common green/grey mudstone rip-up flakes. Exposed all way up slope.	1.01	0.889	1.01			0.970
JC156	749367	1089646	30	Only laterite exposed.						0.077
JC158	738098	1079606	30	Very wide swampy floodplain.						0.021
JC159	739234	1076152	30	Approximate back edge of floodplain here.						1.03
JC160	738583	1073879	30	Subdued ridge with exposures of faintly laminated, grey micaceous siltstone.	1.23	1.12	1.09			1.147
JC161	738036	1061679	30	Roadside diggings show large slabs of medium grained thickly bedded pink weathering quartz rich sandstone.						1.437
JC162	737865	1060121	30	Pale grey medium grained quartzitic sandstone - common well rounded grains, suggestive of aeolian influence.	0.008	0.091	0.05			0.050

				Forms pavements in floor of laterite quarry.						
JC164	736643	1050551	30	Cutting shows debris of laminated dark grey/dark maroon fine sandstone and siltstone. Lunate and sinuous crested ripple marks. Also debris of more thickly bedded buff micaceous sandstone.	1.12	2.21	2.07			1.800
JC164b	736643	1050551	30	Cutting shows debris of laminated dark grey/dark maroon fine sandstone and siltstone. Lunate and sinuous crested ripple marks. Also debris of more thickly bedded buff micaceous sandstone.	3.88	4.15	4.35			4.127
JC166	677784	1054398	30	Daboya landing, west side. Yellow calcareous dolostones overlain by grey, laminated limestones with lenticles and layers containing basement pebbles - see notes. Possibly local faulting.						0.773
JC166b	677784	1054398	30	As OBS point JC 166.						1.041
JC166c	677784	1054398	30	As OBS point JC 166.						0.93
JC167	677669	1054543	30	Sandy limestone, grey, common quartz grains and granules and pebbles of basement (phyllite etc) + maroon siltstone clasts. Barytes/chert veining.	40.3	48.8	48.5			45.867
JC167b	677669	1054543	30	As OBS point JC 167.	2.11	4.17	7.78			4.687
JC168	677429	1054668	30	Pavements in pale grey weathering, dark grey limestone. Finely laminated and medium grained with abundant rounded pellets and ooids c. 1mm size. Baryte veining.	18.01	14.6	18.4	10.9		15.478
JC168b	677429	1054668	30	As OBS point JC 168.	2	1.08	4.87			2.650
JC170	681488	1054053	30	Roadside exposures in 3-4m sequence of fissile, laminated, grey/brown/maroon micaceous mudstones; some thicker units of micaceous siltstone.	0.451	0.603	0.634			0.563
JC171	693409	1050224	30	In floor of laterite quarry, flakes of yellow weathering, pale brown micaceous siltstone.						1.147
JC172	695200	1049500	30	Roadside section in extremely well laminated variegated micaceous mudstones (yellow/brown/grey/purple/green). Slightly thicker intercalated beds of pale buff laminated micaceous siltstone.	1.02	1.02	1.2			1.080
JC172b	695200	1049500	30	As OBS point JC 172.	0.18	0.132	0.148			0.153

JC173	694710	1049890	30	In ditch, exposures of red-weathering very fine micaceous siltstone. Overlain by 10cms of cobble gravel and then laterite.	1.06	1.19	1.13			1.127
JC174	704694	1045313	30	In laterite pit, large exposures of well cemented fine/med pale grey sandstone, some beds with mud-flakes. Weathers to brown/pink/crimson and forms crest of a small rise.	0.066	0.168	0.061			0.098
JC175	713462	1042599	30	Roadside exposures of flaggy, very finely laminated sandstone and siltstone. Pink weathering with some grey mudstone laminae/partings; some ripple drift cross-lamination. About 300-400m to E, crest formed by medium bedded red/pink weathering micaceous sandstone.	0.136	0.134	0.139			0.136
JC176	716456	1041230	30	Abundant chips of red fine micaceous sandstone in road.	0.171	0.262	0.223			0.219
JC179	662268	1015670	30	Laterite quarry - siliceous siltstone clasts abundant in laterite.						45.867
JC180	663388	1026620	30	Roadside ditch in pink weathering med grained laminated quartzitic sandstone; sub-angular to well rounded grains.	0.12	0.075	0.012			0.069
JC181	663247	1027626	30	On a slope down to floodplain. Exposures of fissile, very finely laminated slightly micaceous olive green mudstone.						15.478
JC182	661629	1012423	30	Well diggings in pale green finely laminated mudstone.						2.65
JC183	661670	1012240	30	Roadside quarry in hard pink/crimson weathering siliceous siltstone.	0.076	0.09	0.078			0.081
JC184	657170	1010524	30	Mast foundations in yellow weathering medium grained sandstone with common white feldspar grains.						0.563
JC186	644215	1007684	30	In road; hard silicified fine/med quartzose sandstone; possibly some garnet grains.						1.08
JC187	638375	1006268	30	Med grained quartzitic sandstone.	0.003	0.05	0.096			0.050
JC188	636917	1003827	30	Crags of ~8m of brown weathering cross-bedded sandstone. Sandstones are dark maroon with abundant white feldspars.						1.127
JC190	628773	1007087	30	Pink weathered flaggy/laminated, quartzitic fine grained sandstone. Interbedded with micaceous fine sandstones and siltstones.	0.055	0.057	0.052			0.055

JC191	626199	1015739	30	Diggings in mast foundation; show medium grained laminated buff quartzitic sandstone and dark grey/purple fine micaceous sandstones with grey mud-flakes. Also debris of maroon micaceous siltstone and mudstone.						0.136
JC192	625736	1017545	30	In ditch highly micaceous laminated fine sandstone with purple/yellow variegation; micaceous siltstone interbeds.	0.119	0.187	0.13			0.145
JC193	625484	1018745	30	Roadside pavements in very finely laminated fine grained micaceous sandstone; some large mud-flakes.	0.079	0.086	0.095			0.087
JC197	664845	970055	30	Bwipe No 3 Quarry. In blue/grey laminated micritic limestone interbedded with dark maroon laminated papery micaceous siltstones; pass down to yellow dolomitic limestone.						0.069
JC198	665604	968854	30	Bwipe No 2 Quarry. In finely laminated micaceous and dolomitic limestone.	-0.003	-0.009	-0.012			-0.008
JC200	667014	970120	30	Bwipe No 1 Quarry. Small overgrown quarry in massive dolomitic breccia - sporadic basement pebbles + baryte segregations.						0.081
JC204	660044	972119	30	Limestone blocks in road but possibly not in situ. Black soil typical of the limestone outcrop seen here.						0.05
JC207	656540	974364	30	Small laterite quarry - minor debris of medium grained quartzitic sandstone.						0.055
JC209	668462	966226	30	Laterite quarry.						0.145
JC210	662780	957822	30	Well debris in pale green/purple-grey laminated mudstone.						0.087
JC215	643572	897696	30	On hill by roadside. Quartz-feldspar sandstone, medium grained, laminated.						-0.008
JC231	669989	971021	30	Olive green finely laminated siliceous mudstones in mast debris.						0.009
JC232	643286	904087	30	In ditch decomposed laterite overlain by red silty clay.						0.04
JC233	644886	903917	30	Well diggings show flakes of papery very finely laminated non-micaceous purple/olive green/pale yellow mudstone. Escarpment to W is developed on this. Across road are laterite quarries.						0.122
JC234	636954	864977	30	Kokuma village. Brown weathering dark grey medium	0.168	0.203	0.214			0.195

				grained quartzitic sandstone with sub-angular to angular grains. Common white feldspar grains. Exposure is laterite-coated.						
JC235	636690	863890	30	Crags in medium grained buff sandstone in massive (2-3m) beds. Common feldspar grains. Photos taken of quartz veins; one set at 144 and a later crosscutting set at 220.						0.018
JC238	636730	858431	30	Crest of small feature in grey med/fine sandstone interbedded with dark maroon finely laminated non micaceous sandstone.	0.093	0.051	0.005			0.050
JC239	636677	854826	30	Crags in brown weathering medium/fine sandstone showing very large scale planar cross-bedding. Interbedded with coarse poorly sorted sandstones that fine up to medium grained planar laminated sandstone.	0.04	0.23	0.157			0.142
JC240	641970	840561	30	In ditch, finely laminated quartz rich medium grained sandstone with sporadic pebbles and mud-flakes. Thin dark maroon syn-sedimentary dykelets present.	-0.018	0	0.045			0.009
JC241	642171	840181	30	Fine grained, laminated grey to dark maroon sandstone alternates with more massive med/fine sandstone; ~ 20% feldspar grains. Some low-angle cross-lamination.	0.03	0.051	0.039			0.040
JC242	649250	826486	30	In ditch down slope, fractured dark maroon, fissile micaceous very fine sandstone interbedded with thin pale grey med sandstone + maroon micaceous mudstones and siltstones. Common fracture trend is 320 with a small fault trending 055. Slight folding along axis trending 320.	0.149	0.122	0.094			0.122
JC243	647637	822777	30	Roadside exposures of yellow weathering fine grained sandstone - some feldspar grains.	1.14	1.1	1.33			1.190
JC244	653278	813732	30	Brown weathering medium grained poorly sorted quartzitic sandstone with feldspar grains.	0.026	0.023	0.006			0.018
JC245	665193	811663	30	Thick laterite.						0.098
JC246	668463	810275	30	Well diggings show fragments of brown medium grained sandstone.						0.101
JC247	672542	809755	30	Well diggings show small flakes of green/dark purple mudstone/siltstone.						0.058

JC248	677712	808497	30	Well diggings in pale green/dark maroon micaceous siltstone.						-0.005
JC251	683458	779955	30	N of Nsuta, in roadside ditch, c. 3m of red weathering medium grained quartzitic sandstone. Lamination picked out by slightly finer grained layers; uncertain whether the structure is tectonic or sedimentary. Overlain by Fe-cemented lateritic gravel with local sandstone clasts.	0.026	0.093	0.018			0.046
JC252	683848	781258	30	In road, rib of sheared, very hard white silicified quartz-rich sandstone. Rib trends 270. C. 120m to S, laminated sandstone dips 25 to SW 235.	0.032	0.012	0.021			0.022
JC253	686744	784120	30	Red weathering, med/fine grained feldspathic sandstone.	0.022	0.028	0.077			0.042
JC254	687465	786393	30	Red weathering, medium grained feldspathic sandstone. Laminated, with dip of 20 to SE 105. Probably this is cross-bedding as it is against regional tectonic dip.	0.153	0.12	0.022			0.098
JC255	688510	788426	30	In drain, laminated very fine grained sandstone and pale yellow/-buff laminated siltstone. Debris of red-weathering, non siliceous fine sandstone.	0.126	0.106	0.071			0.101
JC256	689046	789360	30	Medium grained pale yellow weathering quartz-feldspar (arkosic) sandstones. Sporadic green grains may be glauconite.	0.04	0.057	0.076			0.058
JC257	689041	789891	30	Pavements in pale cream weathering medium/fine grained diffusely laminated sandstone.	-0.002	-0.005	-0.009			-0.005
JC261	712158	751911	30	Agogo; thinly bedded to laminated, fine/medium grained sandstone interbedded with grey mudstone and siltstone.	0.091	0.025	0.012			0.043
JC262	712577	751933	30	Red/brown weathering, thinly bedded to laminated, highly micaceous sandstone - medium to fine grained. Overlain by laterite incorporating local sandstone blocks.	0.035	0.135	0.08			0.083
JC263	803056	766542	30	Tease village; white cross-laminated arkosic sandstone; herringbone pattern locally seen. Mainly medium grained but some very coarse/granule lenses and mud-flakes. Generally well sorted with coarse 'millet seed' grains; possibly reworked aeolian. Bedding locally disrupted by low-angle, syn-sedimentary thrust-faults with vergence to S 170 (strike 70 and dip of thrust plane 22 to NE). Some steeply-dipping, slumped bedding also noted.	0.064	0.001	0.031			0.032

JC264	815734	771379	30	White, faintly laminated quartzitic sandstone, medium grained and similar to previous obs.	0.039	0.027	0.05			0.039
JC265	815875	771088	30	Grey/pink medium/fine arkosic sandstone.	0.11	0.134	0.107			0.117
JC266	804795	766272	30	White, medium grained quartz-rich sandstone with common white feldspars. Very thinly bedded to laminated.	-0.006	-0.04	-0.051			-0.032
JC267	796616	747979	30	Well diggings in flakes of blue-grey finely laminated mudstone.						0.072
JC268	797239	745263	30	Well diggings in hard blue/grey laminated mudstone; slightly micaceous.						0.03
JC269b	823331	685522	30	Oterkpolu limestone quarry. Limestone is blue/grey, thinly bedded to laminated and in parts interbedded with maroon siltstone. Quarry geologist says limestone is silicified (-possibly the dark grey beds). Some fissile, phyllitic partings. Folded into reclined structures verging to NW; axial surfaces dip c. 40-50 to SE 110 with hinges plunging 10-15 to S. Folded limestone is overlain by sandstone.						0.044
CJ201	747515	728977	30	Over steepened cross bedding to 70, note cross cut by horizontal shears. Laminated mudstone.						0.03
CJ202	739895	744586	30	Flaggy coarse grained sandstone. Pale yellow/white, weathering to dark red.						0.035556
CJ203	739331	744485	30	Flaggy medium to coarse grained sandstone in quarry floor, pale yellow/white, weathering to dark red. Discontinuous pebble beds. Shear/fracture zone, bleached and slightly softer, aligned 90 secondary fracture set to 155, riedels suggest sinistral movement.						0.042222
CJ204	736081	744789	30	Flaggy med grained yellow sandstone exposed in a gutter section. Cross bedding suggests palaeocurrent to 60 deg. Cross bedding also to 350 deg in coarse grained sandstone with maroon laminae.						0.132857
CJ206	731481	747852	30	Flaggy med to coarse grained sandstone, massive bedded - pale yellow/white, med grained in lower section. Surface wave ripples, approximate palaeocurrent direction towards 350 deg. 20m to west is a more extensive outcrop, cross bedding towards 25 in very coarse bed containing small pebbles. Coarsening upwards.						0.22

CJ207	730925	747968	30	As OBS point CJ 206; extensive flaggy coarse grained sandstone.						0.0933
CJ209	723164	748061	30	Roadside gutter section. Thinly bedded fine grained sandstone. Open folding, with fold hinge aligned N/S. Base is fine grained laminated sandstone, similar to variegated shales/mudstones.						0.6572
CJ210	722083	748472	30	Dark maroon med grained sandstone interbedded with thin beds of white sandstone (medium grained). Massive.						0.165
CJ212	713265	750758	30	Exposure in a bluff above the road. Horizontally bedded medium/coarse grained yellow/grey/light red sandstone.						0.74
CJ216	694578	830757	30	Dark red fine to med grained immature sandstone with mudstone flakes. Cross bedding towards 260. Pebbly beds at upper surface. Also laminae of fine grey micaceous sandstone at base.						0.195
CJ220	814170	858044	30	Conglomerate reinterpreted as laterite despite intact cobbles of sandstone. Underlain by olive green horizontally laminated siltstones, with mineralised joints (manganese).						0.05
CJ221	803101	863678	30	Well chippings - greenish shales with fine laminations. Abundant laterite boulders and pebbles. Much quartz vein material-rounded up to 3cm in thickness.						0.142
CJ228	810107	1168127	30	5m x 3m riverside outcrop at bridge. Quartz sandstone. Pale yellow, weathers to pinking red. Medium grained. Sub-angular grains in a clay matrix (feldspar broken down). Feldspatic, rare mica. Massive.						0.05
CJ71b	810938	1161880	30	CJ REVISITED 2007. As OBS point CJ72 but less mica. Possible glauconite in laminae; suggest marine environment of deposition.						0.04
CJ69b	812754	1159928	30	CJ REVISITED 2007. Mature, medium to coarse grained. Quartz sandstone, minor feldspar. White/pale yellow. Coarsens upwards with reduced feldspar and more porous. Massive, aeolian at top.						0.04
CJ66b	818252	1147635	30	CJ REVISITED 2007. Roadside outcrop of steeply dipping salmon pink to light red cherty fine sandstone, very siliceous. Finely laminated, weathers to white. Thin						0.251

				laterite on top.						
CJ230	171977	1031325	31	Gutter subcrop in Bunya sandstone. Medium grained (sub angular) sandstone. Khaki to light brown with mica and feldspar. Clay matrix and massive.						0.25
CJ231	172661	1019077	31	8m x 4m pavement outcrop at school. Fine to med grained khaki sandstone. Slightly immature. Feldspatic and micaceous with possible jasper. Appears massive. Onion weathering.						3.93
CJ232	176238	1013358	31	8m x 5m pavement outcrop. Fine to medium grained khaki to grey sandstone with mica and feldspar and a orange mineral possibly jasper, some dark fine beds of mica. Harder than other Bunya so far. Slightly immature with sub-angular grains. Swales and hummocks, possibly remnants of near shore marine. Includes mud clasts and mica rich laminae. Photo of load/water escape structures. Convoluted section suggests slumping.						0.346
CJ25b	178206	968198	31	CJ REVISITED 2007. Bunya sandstone. Oliver green fine grained massive, slightly flaggy sandstone. Suggesting of ripple drift surfaces in plan view. Flow to 295. Bedding dips to 315. Minor mica, otherwise sand.						0.2
CJ26c	182062	966153	31	CJ REVISITED 2007. Thinly bedded very fine sandstone/siltstone with mica. Olive green. Coarsens upwards to med grained sand laminae interbedded in the siltstone. Possibly a gradation between Bimbilla and Bunya.						0.26
CJ235	185023	965030	31	Outcrop in Cp forming ridge. Harder than Bimbilla (slightly siliceous). More feldspar, arkosic. Fine to med grained olive green to grey. Small lithics, rare mud-flakes. Sub angular grains. Immature. Possible brecciated unit aligned approximately 250. Possible jasper clasts.						0.436
CJ236	189806	961255	31	2m section of olive green siltstone interbedded with fine sands and shales, evidence of drying cracks in the shales - Bimbilla. Manganese oxide staining in laminae and fractures. Pseudo-horizontal bedding and cross laminated to 180 deg, distal sand turbidites suggests basinal marine (CWT). This is possibly flysch on top of Obosum molasse.						0.1828

JC270	748765	739108	30	Pale grey, medium-coarse grained quartz-arenite comprising cross-laminated lower part, with some coarse laminae; overlain by ~ I m thick channelised med-coarse sandstone with some granule layers. (see OBS point CT 1).						0.061429
JC271	749887	736179	30	Pale grey, medium-grained quartz arenite in regular tabular beds 10-20 cm thick. Very low-angle cross-lamination. Some beds show wavy (rippled) partings. Saw-tooth profile suggests individual beds fine up; most are plane-laminated (see OBS point CT2)						0.0275
JC272	750917	726379	30	Road cutting in lower Kwahu escarpment. Shows ridge of spheroidally-weathered granitoid 'draped' by variegated (maroon-pale grey) mudstone; latter show syn-sedimentary disruption and syneuresis. 2 further thin (1-2 m) mudstone beds c. 5 and 15 m higher up, intercalated in flaggy, micaceous siltstone/fine sandstone, which is dominant lithology here.						0.174545
JC276	745985	740956	30	Pale grey to cream, tabular bedded medium to fine-grained and cross-laminated quartz arenite.						0.07
JC290	782218	772307	30	To west of Kwaikese road, c. 15m high koppies in red, medium-coarse grained, highly feldspathic and lithics-rich sandstone. Layers with maroon mud-flakes. One prominent c. 1-2m thick layer of poorly sorted cobble conglomerate (probable debris flow). Some lateral accretion surfaces and cross-lamination; other beds appear massive with 'floating' pebbles. Fragments include green chert, granitoid and metamorphic rocks including typical 'Damomeyan' mesocratic gneiss, and possibly porphyritic volcanic rocks. Some quartzitic pebbles are well-rounded, suggesting previous transport; other types are highly angular.	0.061	0.113	0.11	0.108	0.106	0.100
JC291	781931	774671	30	Pavements in feldspar-lithics rich, red sandstone with sporadic 'floating' pebbles and pebble lags. Pebbles include pink porphyritic microgranite (possibly) and foliated metasedimentary lithologies. Pebble lags associated with scour troughs.	0.099	0.088	0.097	0.101	0.187	0.114
JC292	764647	782289	30	Medium-fine grained, highly micaceous arkosic sandstone	0.133	0.111	0.11	0.079	0.053	0.097

				with local trough cross-lamination; some mud-flakes.						
JC293	801232	763708	30	Next to school, pale grey, medium-coarse grained quartz arenite or sub-arkose. Cross-laminated throughout, with herringbone pattern prominent. Dip 27 to 255 suggests tectonic disturbance close by.	0.017	0.028	0.089	0.093		0.057
JC297	679423	811788	30	JC REVISITED OBS point JC53. The harder beds are of pale grey-green dolomitic siltstone, weak fizzing with acid. Some climbing ripple cross-lamination. Probably lacustrine-playa lake environments with siltstones representing sheet-flood events.	0.14	0.078	0.089	0.118	0.086	0.102
JC298	664995	823352	30	Regularly, thinly bedded white quartzitic sandstone, medium grained and locally poorly sorted. Some large-wavelength wave-forms on bed tops and some bed bases are channelised.	0.022	0.028	0.012	0.015	0.038	0.023
JC305	624713	890111	30	Pavements in thinly bedded, medium to fine-grained sandstone with lags of well rounded quartzose pebbles and granules.	0.139	0.125	0.033	0.041	0.019	0.071
JC306	632496	893648	30	Fuller Falls. Well sorted medium-coarse-grained sandstone with sporadic well-rounded grains. Generally thin to medium bedded with cross-bedding and ripple marked bed tops. One exposure shows 4 current reversals in 1 m of section suggestive of herringbone structure and tidal influence.	0.002	0.003	0.001	0.002		0.002
JC308	638181	891056	30	Medium grained sandstone, very thickly bedded (c. 2m) well laminated to diffuse plane lamination. 'Lower Kintampo'.	0.007	0.01	0.337	0.21	0.143	0.141
JC315	716849	887247	30	Nyunsa River bridge. C. 60cm in very finely laminated green-grey siltstone; not variegated but some shallow load structures; finer grained and more fissile to base.	0.626	0.669	0.661	0.568	0.674	0.640
JC319	738026	1040248	30	By Geological Survey Dept., Tamale, pavements in red, medium-grained, well-sorted quartz-rich sandstone. Some large scale trough cross-bedding; possibly aeolian.	0.448	0.394	0.338	0.262	0.364	0.361
JC327	738045	1072171	30	Mast diggings in purplish-grey, micaceous, very fine-grained sandstone. Some beds show flute casts and rippled tops. Mud-flakes and load structures also seen.						1.348

				Possible turbidite facies - marine phase of Obosum.						
JC328	733468	1091230	30	Mast diggings in pale green, very fine grained 'Bunya' type sandstone. Highly feldspathic, with jasper grains and dark shiny grains which may be of chrome-spinel. Some grey mud-flakes and highly micaceous laminae.						0.54
JC331	754917	1142338	30	Medium grained, brown weathering, white, hard quartzose sandstone. In c. 20cm thick beds showing cross-bedding. Possibly upper shoreface. Cut by haematitic fractures trending 085.						0.257
JC333	762582	1149872	30	Slightly feldspathic cream/white, quartzose sandstone, mainly trough cross-laminated throughout, but some planar lamination. Possible swaley bedding.						0.0766
JC334	772373	1157595	30	Down slope from OBS point JC139, in cream, medium-fine feldspathic quartz arenite, plane laminated; sporadic mica and mud-flakes. One large channel seen, cutting down to W 280. The large-scale plane laminated structure differs from earlier exposures e.g. at OBS point JC331. Possible lower shoreface.						0.034
JC338	820342	1133799	30	Very finely laminated, olive green siltstone and mudstone; finely micaceous.	0.22	0.217	0.166	0.204	0.216	0.205
JC339	818863	1116263	30	JC REVISITED OBS point JC120. Pale green, very fine grained, arkosic, micaceous, 'Bunya' type sandstone. Interbedded with highly micaceous, pale green laminated siltstones.	0.958	0.932	0.838	0.942	0.934	0.921
JC340	806001	1096344	30	In river bed, good exposures of pale green-grey, micaceous very fine grained siltstone. In thin tabular beds with wind-rippled tops. Becoming more flaggy and plane laminated upwards. Some very low angle cross-bedding seen.	0.147	0.098	0.177	0.175	0.145	0.148
JC342	828503	933698	30	Pale green-grey, highly weathered Bunya sandstone. Feldspathic and micaceous; finely plane laminated and cross-laminated.	0.129	0.113	0.128	0.132	0.128	0.126
JC344	830447	885245	30	Green-grey, fine to medium grained highly feldspathic Bunya type sandstone with green mud-flakes concentrated along certain laminae. Possible spinel grains. In places, common dispersed sub-angular to	0.202	0.377	0.208	0.327	0.328	0.288

				angular granules and small pebbles suggest a diamict produced by mass flow.						
JC345	826529	905145	30	Medium grained highly feldspathic green-grey Bunya type sandstone.	8.06	7.06	8.08	6.39	5.83	7.084
JC346	827090	906317	30	Sample of fresh, grey-green, highly feldspathic Bunya type sandstone. Fine to medium grained with a diffuse plane lamination.	0.268	0.207	0.231	0.225	0.272	0.241
JC347	824493	910856	30	Massive, green-grey, highly feldspathic Bunya type sandstone.	0.377	0.342	0.339	0.342	0.457	0.371
JC348	823477	924498	30	Weathered exposures of medium grained, highly feldspathic, diffusely plane laminated Bunya type sandstone.	0.136	0.123	0.127	0.138	0.138	0.132
JC350	188916	893235	31	Dumbai village. Exposures in green-grey, fine grained, highly feldspathic, slightly micaceous Bimbila type sandstone interbedded with brown-weathering siltstone. Dip is 8 to E 118						0.18
JC353	196638	756248	31	In road across ridge, exposures in white/grey medium grained, quartzose, volcaniclastic (epiclastic) sandstone. Common coarse sand to granule size fragments of white/pink clayey-altered feldspars, some sub-hedral; also fragments of dark green altered fine-grained volcanic rock - possible magnetite grains. Pass up to thinly bedded and graded quartz-rich epiclastic sandstone beds. Dip is 50 to 220. Affected by cataclastic shear zone.						0.096
JC358	188389	727596	31	Very strongly foliated, protomylonitic quartz arenite, interbedded with silver-grey phyllonite, latter flat-lying. Weakly developed S-C fabric.						0.064
JC359	187585	725400	31	Hard, grey/white quartz arenite. Fractured but not obviously foliated apart from a cataclastic zone. Foliation in latter cross cut by later spaced 'Voltaian' fractures.						0.04
JC360	174668	709326	31	In road, ribs of foliated white quartz arenite. Local slabs of very coarse grained or granule sandstone with very well rounded quartz grains. Very similar to Kwahu Group quartz arenites.						0.46
JC363	815766	706202	30	Pavements and boulders in red/pink, poorly sorted						0.06

				medium grained quartzose sandstone with several percent feldspar. Common well rounded grains. Probably fluviatile.						
JC365	811453	714430	30	Medium grained, fairly poorly sorted white feldspathic sandstone. Many grains well rounded and spherical. Planar cross-bedding and large scale trough cross-bedding.						0.044
JC367	808493	717367	30	White-weathering but highly feldspathic sandstone. White clay mineral derived from feldspar and also present as intergrain fills.						0.05
JC371	791015	708091	30	In north of Begoro, white, quartz-rich, medium to coarse grained sandstone is cross-bedded throughout. Sets are mainly planar and steeply dipping (10-25). Drag-folding noted in some beds. Possible small prograding delta system.						0.03
JC373	812456	682292	30	Village exposures in hard, pink/white, medium grained quartz arenite. Shows herringbone cross-bedding.						0.02
CT32	799204	1041303	30	Sandstone, fine to medium grained, locally coarse with some granules and fine gravel lags. Feldspathic and lithic and very immature. Reddish grey-brown colour and spotted locally with manganese. Clayey cement/matrix. Some mud-flake (green-grey) clasts in one unit. Very shallow dish shape to some beds, weakly flaggy, locally more planar bedded. Bedding very poorly developed throughout, with exfoliating whale-back form to many outcrops. Environment difficult to determine, but suggest these are terrestrial sandstones deposited very rapidly as sheet floods. Could also be inner estuary.						5.431
CT33	737867	1060129	30	Sandstone, quartzite, medium grained, SA/R/WR, trace feldspar. A small amount of haematite cement present, but generally poorly sorted. Appears massive in outcrop, no section seen, so bedding not readily assessable. Thought to be aeolian.						0.065
PD4	750877	726414	30	50 cm shale band lying just above the basement. Possible lacustine deposit from the basement						0.1275
PD5	750870	726416	30	Thickly bedded sandstone draped over the basement						0.07

PD8	738260	732857	30	Large outcrop (possible subcrop) of sandstone. Hematite cement. Likely to be saphrolite						0.185
PD9	739571	740244	30	Roadside sandstone outcrop.						0.15875
PD23	725334	745900	30	Pebble conglomerate.						0.391667
PD39	795650	1042055	30	Clast supported conglomerate overlain by sandstone. Clasts of metasediments, jasper, vein quartz, quartzites						1.595
PD40	795650	1042155	30	Sandstone outcrop						6.82
PD48	762543	1149815	30	Mature sandstone with silica cement, with cross bedding, dipping 80 approx to the east						0.06
PD49	768726	1153446	30	Cream coloured medium grained feldspathic sandstone.						0.1
PD50	772634	1157999	30	Roadside subcrop-possibly disturbed, white mature sandstone.						0.044
PD53	778572	1164066	30	Roadside stepped outcrop of a immature fine-grained white sandstone. Containing feldspar, some jasper and mica.						0.066
PD54	783755	1164650	30	Roadside outcrop, fine grained feldspar rich sandstone, white with some mica.						0.0566
PD90	803655	724576	30	Roadside outcrop of a white quartzite (massive bedded) with evidence of cubic / angular psueudomorphs. Interpreted as halite clasts.						0.033

Appendix 7 Component layers of the geology and topographic maps

Text			
Layer name	**Ghana_BGS_Text_Annotation_utm30Dec06.shp**		
Type	Shapefile	Point	Comment
Symbology	Unique values		
Text	Label (using Maplex)	Yes	Water Features: Arial italic 8.25 pt, offset 1pt Rotated using Angle field Colour (RGB) 0,92,230 Forest reserves: Arial 8pt, offset 1pt Colour (RGB) 56,168,0 Lower case and Upper case villages: Arial 8pt, offset 4pt Colour (RGB) 130,130,130 All use Best Position
	Colour (RGB)	78,78,78	

Cultural political - polygons			
Layer name	**Ghana_BGS_Cult_Pol_Polygon_utm30Dec06.shp**		
Type	Shapefile	Polygon	Comment
Symbology	Unique values		
BuiltUpArea	Label (using Maplex)	No	
	Symbol	Simple fill	
	Fill Colour (RGB)	225,225,225	
	Outline Colour (RGB)	130,130,130	
	Outline Width (mm)	0.15	
Gravelpit	Label (using Maplex)	No	
	Symbol	Line fill	Width 0.1; Angle 45°; Separation 1.5
	Line Colour (RGB)	130,130,130	
	Outline Colour (RGB)	130,130,130	
	Outline Width (mm)	0.15	

Cultural - points			
Layer name	**Ghana_BGS_Cultural_Point_utm30Dec06.shp**		
Type	Shapefile	Point	Comment
Symbology	Unique values		
Village	Label (using Maplex)	No	
	Symbol	Simple marker	Circle; Size 2
	Fill Colour (RGB)	None	
	Outline Colour (RGB)	104,104,104	
	Outline Width (mm)	0.5	
Mineral Area	Label (using Maplex)	No	
	Symbol	Character marker	ESRI Cartography, Unicode 204, Size 4
	Colour (RGB)	130,130,130	
RailwayStation	Label (using Maplex)	No	
	Symbol	Simple marker	Circle; Size 2
	Fill Colour (RGB)	255,0,0	
	Outline Colour (RGB)	130,130,130	

Cultural - polylines			
Layer name	**Ghana_BGS_Cultural_Polyline_utm30Dec06**		
Type	Shapefile	Polyline	Comment
Symbology	Unique values		
InternatBound	Label (using Maplex)	No	
	Symbol	Cartographic	6:2:2:2 Dash:gap:dash:gap
	Colour (RGB)	130,130,130	
	Width (mm)	0.5	

Cultural – polygons			
Layer name	**Ghana_BGS_Cultural_Polygon_utm30Dec06**		
Type	Shapefile	Polygon	Comment
Symbology	Unique values		
Quarry	Label (using Maplex)	No	

Cultural – polygons			
Layer name	**Ghana_BGS_Cultural_Polygon_utm30Dec06**		
	Symbol	Line fill	Width 0.1; Angle 45°; Separation 1.5
	Line Colour (RGB)	130,130,130	
	Outline Colour (RGB)	130,130,130	
	Outline Width (mm)	0.15	

Transport – roads			
Layer name	**Ghana_BGS_Transport_Polyline_utm30Dec06**		
Type	Shapefile	Polyline	Comment
Symbology	Unique values		
Major road	Label (using Maplex)	No	
	Symbol	Cartographic	Cased road, 0.1mm lines offset by 0.25mm
	Colour (RGB)	130,130,130	
Minor road	Label (using Maplex)	No	
	Symbol	Cartographic	Cased road, 0.1mm lines offset by 0.25mm. 6:1 dash:gap
	Colour (RGB)	130,130,130	
Other motorable road	Label (using Maplex)	No	
	Symbol	Simple	
	Colour (RGB)	130,130,130	
	Width (mm)	0.2	

Transport – other lines			
Layer name	**Ghana_BGS_Transport_Polyline_utm30Dec06**		
Type	Shapefile	Polyline	Comment
Symbology	Unique values		
Airstrip	Label (using Maplex)	No	
	Symbol	Simple	
	Colour (RGB)	130,130,130	
	Width (mm)	0.1	
Ferry	Label (using Maplex)	No	
	Symbol	Cartographic	6:1 dash:gap

Transport – other lines			
Layer name	**Ghana_BGS_Transport_Polyline_utm30Dec06**		
	Colour (RGB)	130,130,130	
	Width	0.15	
Railway	Label (using Maplex)	No	
	Symbol	Cartographic	Line is Simple, 0.15mm. Hash symbol is 0.5mm with gap:dash:gap of 2:1:2
	Colour (RGB)	130,130,130	
	Width (mm)	0.15	
Track and trail	Label (using Maplex)	No	
	Symbol	Cartographic	4:1 dash:gap
	Colour (RGB)	130,130,130	
	Width (mm)	0.1	

Forest - polylines			
Layer name	**Ghana_BGS_Forest_Polyline_utm30Dec06**		
Type	Shapefile	Polyline	Comment
Symbology	Unique values		
InternatBound	Label (using Maplex)	No	
	Symbol	Cartographic	4:1:2:1 Dash:gap:dash:gap
	Colour (RGB)	76,230,0	
	Width (mm)	0.25	

Utilities			
Layer name	**Ghana_BGS_Utility_Polyline_utm30Dec06**		
Type	Shapefile	Point	Comment
Symbology	Unique values		
Transmlines	Label (using Maplex)	No	
	Symbol	Marker	Simple line with 1.5mm marker line symbol (ESRI Default Marker Unicode 68) spaced every 20pt
	Colour (RGB)	130,130,130	
	Width (mm)	0.25	

Hydrology - rivers			
Layer name	**Ghana_BGS_Hydro_Polyline_utm30Dec06**		
Type	Shapefile	Polyline	Comment
Symbology	Unique values		
Damtoscale	Label (using Maplex)	No	
	Symbol	Simple line	
	Colour (RGB)	130,130,130	
	Width (mm)	0.2	
SmallDam	Label	No	
	Symbol	Simple line	
	Colour (RGB)	0,128,255	
	Width (mm)	0.2	
Watercourse and WatercourseVS	Label	No	
	Symbol	Simple line	
	Colour (RGB)	0,128,255	
	Width (mm)	0.15	
WatercourseBoundary	As Watercourse	0.2	
WatercourseIndef	Label	No	
	Symbol	Cartographic	5:1 dash:gap
	Colour (RGB)	0,128,255	
	Width (mm)	0.15	

Hydrology - shoreline			
Layer name	**Ghana_BGS_Shoreline_Polyline_merge_utm30Dec06**		
Type	Feature Class	Polyline	Comment
Symbology	Unique values		
Shoreline, ShorelineNonColour and ShorelineVS	Label (using Maplex)	No	
	Symbol	Simple line	
	Colour (RGB)	0,128,255	
	Width (mm)	0.2	

Hydrology - coastline			
Layer name	**Ghana_BGS_Coastline_Polyline_utm30Dec06**		
Type	Feature Class	Polyline	Comment
Symbology	Unique values		
Coastline and CoastlineNonCol	Label (using Maplex)	No	
	Symbol	Simple line	
	Colour (RGB)	0,128,255	
	Width (mm)	0.2	

Contours			
Layer name	**Ghana_BGS_ContoursNorth_utm30Dec06 and Ghana_BGS_ContoursSouth_utm30Dec06**		
Type	Feature class	Polyline	Comment
Symbology	Single symbol		

	Label (using Maplex)	Yes	Some contours form shapes that are too small to label. Use this expression in the label dialogue to only label contours with a length greater than 1500m:
			Function FindLabel ([CONTOUR], [Shape_Leng])
			if [Shape_Leng] > 1500 then
			FindLabel = [CONTOUR]
			end if
			End Function
			Arial narrow 5pt
			Colour (RGB) 168,56,0
			Straight and centred on line
			At best position on line
			Aligned to direction of line
			White Halo mask, size 0.5

	Symbol	Simple line	
	Colour (RGB)	168,56,0	
	Width (mm)	0.1	

The geology layers and their symbology are as follows:

Lineaments			
Layer name	**Ghana_BGS_Lineaments_utm30Dec06**		
Type	Feature class	Polyline	Comment
Symbology	Single symbol		
	Label (using Maplex)	No	
	Symbol	Simple	

	Colour (RGB)	255,0,0	
	Width (mm)	0.3	

Geomorphology lines			
Layer name	**Ghana_BGS_GeomorphologyLines_utm30Dec06**		
Type	Feature class	Polyline	Comment
Symbology	Single symbol		
	Label (using Maplex)	No	
	Symbol	Cartographic	5:1 Dash:gap
	Colour (RGB)	0,77,168	
	Width (mm)	0.25	

Superficial lines			
Layer name	**Ghana_BGS_SuperficialLines_utm30Dec06**		
Type	Feature class	Polyline	Comment
Symbology	Single symbol		
	Label (using Maplex)	No	
	Symbol	Simple	
	Colour (RGB)	0,0,0	
	Width (mm)	0.1	

Bedrock lines			
Layer name	**Ghana_BGS_BedrockLines_utm30Dec06**		
Type	Feature class	Polyline	Comment
Symbology	Unique values		
Bedrock inferred	Label (using Maplex)	No	
	Symbol	Cartographic	7:1 Dash:gap
	Colour (RGB)	0,0,0	
	Width (mm)	0.2	
Fault	Label (using Maplex)	Yes	Using LABEL field Arial 8pt bold Colour (RGB) 0,0,0 Curved, above line, offset 2pt
	Symbol	Simple	
	Colour (RGB)	0,0,0	

	Width (mm)	0.35	
Fault inferred	Label (using Maplex)	Yes	Using LABEL field Arial 8pt bold Colour (RGB) 0,0,0 Curved, above line, offset 2pt
	Symbol	Cartographic	12:2 Dash:gap
	Colour (RGB)	0,0,0	
	Width (mm)	0.35	
Fault tick	Label (using Maplex)	Yes	
	Symbol	Simple	
	Colour (RGB)	0,0,0	
	Width (mm)	0.35	

Laterite polygons			
Layer name	**Ghana_BGS_LateritePolygon_utm30Dec06**		
Type	Feature class	Polygon	Comment
Symbology	Single symbol		
	Label (using Maplex)	No	
	Fill Symbol	Simple marker	0.7mm white dot 45° grid
	Line Colour (RGB)	255,255,255	
	Line Width (mm)	0.1	

Superficial polygons			
Layer name	**Ghana_BGS_SuperficialPolygon_utm30Dec06**		
Type	Feature class	Polygon	Comment
Symbology	Unique values		
	Label (using Maplex)	No	
	Fill Symbol	Simple	
	Line Colour (RGB)	Null	
	Width (mm)	Null	

Bedrock polygons	
Layer name	**Ghana_BGS_BedrockPolygon_utm30Dec06**

Type	Feature class	Polygon	Comment
Symbology	Unique values		
	Label (using Maplex)	No	
	Fill Symbol	Simple	
	Line Colour (RGB)	Null	
	Width (mm)	Null	

Water polygons			
Layer name	**Ghana_BGS_WaterPolygon_utm30Dec06**		
Type	Feature class	Polygon	Comment
Symbology	Unique values		
	Label (using Maplex)	No	
	Fill Symbol	Simple	
	Line Colour (RGB)	Null	
	Width (mm)	Null	

Table showing the attributes of the geological polygon features.

AGE	CODE	UNIT_NAME	DESCRIPTION	MEMBER	FORMATION	GROUP	SUPERGROUP	Comment	Red	Green	Blue
QUATERNARY	ALV	Alluvium							255	255	224
QUATERNARY	ALV	Alluvium	Locally including lacustrine and estuarine deposits					Fluvial and Deltaic Deposits, Keta	255	255	224
QUATERNARY	ALF	Alluvial Fan Deposits							255	201	224
QUATERNARY	VDD	Volta Delta Deposits						Fluvial and Deltaic Deposits, Keta	255	237	201
QUATERNARY	TF	Tidal Flat Deposits and Salt Pans						Marine and Coastal Zone Deposits, Keta	255	255	176
QUATERNARY	BD	Shoreface and Beach Deposits						Marine and Coastal Zone Deposits, Keta	237	224	201
QUATERNARY	RTF	Raised Tidal Flat Deposits						Raised Marine Deposits, Keta	255	224	224
QUATERNARY	RBD	Raised Beach Deposits						Raised Marine Deposits, Keta	237	237	148
QUATERNARY	RTF	River Terrace Deposits							255	237	201
QUATERNARY	Q	Quaternary deposits of uncertain origin							201	237	224
?CENOZOIC	Ag	Agbakope Sand	Pale grey to cream, structureless, medium-grained sand					Keta	224	224	201
?CENOZOIC	K	Koluedor Gravel	Red pebbly sand and gravel, locally overlain by laterite					Keta	237	255	237
CENOZOIC	CVS	Central Volta Surface	Subdued, dissected landform veneered by lateritic duricrust with associated deposits of cemented gravel; locally covered by red, poorly sorted sand					White hold out mask	255	255	255
NEOPROTEROZOIC	Ta	Tamale Sandstone Formation	Red to brown medium-grained sandstone		Tamale	OBOSUM	VOLTAIAN		255	148	201

AGE	CODE	UNIT_NAME	DESCRIPTION	MEMBER	FORMATION	GROUP	SUPERGROUP	Comment	Red	Green	Blue
NEOPROTEROZOIC	De	Densubon Sandstone Formation	Red, brown and grey fine- to medium-grained feldspathic sandstone; subordinate beds of brown mudstone and siltstone		Densubon Sandstone	OBOSUM	VOLTAIAN		255	176	237
NEOPROTEROZOIC	Dk	Dunkro Sandstone Formation	Grey, red and maroon very poorly sandstone and conglomerate; pebbles of quartzite and angular to subangular fragments of chert, granite, volcanic rock and various gneissose metamorphic lithologies		Dunkro Sandstone	OBOSUM	VOLTAIAN		224	148	237
NEOPROTEROZOIC	Te	Tease Sandstone Formation	White, grey and pink, thinly bedded to laminated sandstone; locally coarse-grained		Tease Sandstone	OTI--PENDJARI	VOLTAIAN		255	148	237
NEOPROTEROZOIC	Ej	Ejura Sandstone Formation	Pale grey to cream, thinly bedded fine-to medium-grained sandstone,		Ejura Sandstone	OTI--PENDJARI	VOLTAIAN		237	148	255
NEOPROTEROZOIC	By	Bunya Sandstone Member	Green-grey, medium-grained sandstone, weakly micaceous, with mudstone flakes	Bunya Sandstone	Bimbila	OTI--PENDJARI	VOLTAIAN		148	255	224
NEOPROTEROZOIC	Cp	Chereponi Sandstone Member	Green-grey, medium-grained, micaceous sandstone	Chereponi Sandstone	Bimbila	OTI--PENDJARI	VOLTAIAN		176	255	176
NEOPROTEROZOIC	Ak	Akroso Conglomeratic Member	Pebbly, arkosic sandstone and conglomerate with clasts up to boulder size. Includes intraformational pebbles of greenarkosic sandstone together with pebbles of chert, jasper, granite and metamorphic rocks (not visited)	Akroso Conglomeratic	Afram	OTI--PENDJARI	VOLTAIAN		255	224	148
NEOPROTEROZOIC	Ba	Bimbila Formation Undivided	Grey to olive green, weakly micaceous mudstone and siltstone with thin beds of green-grey arkosic, lithic	Undivided	Bimbila	OTI--PENDJARI	VOLTAIAN		201	237	148

AGE	CODE	UNIT_NAME	DESCRIPTION	MEMBER	FORMATION	GROUP	SUPERGROUP	Comment	Red	Green	Blue
			sandstone								
NEOPROTEROZOIC	Yb	Yabraso Sandstone Formation	White, medium-grained, cross-bedded, flaggy quartzose sandstone; locally coarse-grained	Yabraso Sandstone	Yabraso Sandstone	KWAHU	VOLTAIAN		224	176	224
NEOPROTEROZOIC	Af	Afram Formation Undivided	Mainly mudstones and siltstones, commonly grey-green and micaceous; locallt variegated in red, grey and green. Sporadic beds of limestone	Undivided	Afram	OTI--PENDJARI	VOLTAIAN		201	201	201
NEOPROTEROZOIC	Db	Darebe Tuff Member	Pale grey, flinty, laminated vitric tuff, weathering to brown and crimson	Darebe Tuff	Kodjari	OTI--PENDJARI	VOLTAIAN		237	201	255
NEOPROTEROZOIC	Bp	Buipe Limestone Member	Pale grey, thinly bedded to massive micritic limestone and sandy limestone passing down to dolomitic limestone; locally peloidal and pebbly. Interbedded with maroon siltstone. Basal tillite (not shown on maps)	Buipe Limestone	Kodjari	OTI--PENDJARI	VOLTAIAN		176	224	237
NEOPROTEROZOIC	An	Anyaboni Sandstone Formation	Pale grey to red, thickly dune-bedded to cross-bedded medium-grained arkosic sandstone; becoming finer grained, with mudrocks and micaceous, flaggy sandstones towards the base		Anyaboni Sandstone	KWAHU	VOLTAIAN		255	176	176
NEOPROTEROZOIC	Ob	Obocha Sandstone Formation	Pale grey, locally brown-weathering, thickly bedded to cross-bedded medium-grained quartzose sandstone; becoming finer grained, with mudrocks and micaceous, flaggy sandstones towards		Obocha Sandstone	KWAHU	VOLTAIAN		237	201	148

AGE	CODE	UNIT_NAME	DESCRIPTION	MEMBER	FORMATION	GROUP	SUPERGROUP	Comment	Red	Green	Blue
			the base								
NEOPROTEROZOIC	At	Abetifi Sandstone Formation	Pale grey, thickly bedded to cross-bedded quartzose sandstone, locally flaggy and interbedded with grey micaceous siltstone		Abetifi Sandstone	KWAHU	VOLTAIAN	Basal Sandstone	224	176	176
NEOPROTEROZOIC	Mp	Mpraeso Sandstone Formation	Pale grey, locally brown weathering, thickly bedded to cross-bedded medium-grained quartzose sandstone becoming finer grained, with mudrocks and micaceous, flaggy sandstones towards the base		Mpraeso Sandstone	KWAHU	VOLTAIAN	Basal Sandstone	237	224	117
NEOPROTEROZOIC	Pn	Panabako Sandstone Formation	Pale grey, yellow to pink-weathering, medium-grained quartzose sandstone; commonly cross-bedded		Panabako Sandstone	BOMBOUAKA	VOLTAIAN	Basal Sandstone	176	224	176
NEOPROTEROZOIC	Dg	Damongo Formation	Pale grey to yellow, flaggy to laminated, fine- to medium-grained micaceous sandstone		Damongo	BOMBOUAKA	VOLTAIAN	Basal Sandstone	237	176	117
NEOPROTEROZOIC	Pg	Poubogou Formation	Olive green mudstone and siltstone with sharp-based, thin beds of sandstone		Poubogou	BOMBOUAKA	VOLTAIAN	Basal Sandstone	225	255	176
NEOPROTEROZOIC	Ts	Tossiegou Formation	Fine-grained sandstone, locally pebbly		Tossiegou	BOMBOUAKA	VOLTAIAN	Basal Sandstone	210	255	117
NEOPROTEROZOIC	Bm	Buem Structural Unit	Undivided quartz arenites and fine-grained sandstones		Buem		BUEM STRUCTURAL UNIT	Pan-African domain	201	255	224
NEOPROTEROZOIC	Op	Oterkpolu Limestone Mermber	Pale grey, thinly bedded micritic limestone and yellow dolomitic limestone with subordinate intercalations of maroon siltstone	Oterkpolu Limestone	Buem		BUEM STRUCTURAL UNIT	Pan-African domain	148	224	255

AGE	CODE	UNIT_NAME	DESCRIPTION	MEMBER	FORMATION	GROUP	SUPERGROUP	Comment	Red	Green	Blue
PALAEOPROTEROZOIC	lgn		Leucocratic gneiss, locally with augen				DAHOMEYAN COMPLEX	Keta	176	176	255
PALAEOPROTEROZOIC	mgn		Mesocratic gneiss, locally with amphibolite sheets				DAHOMEYAN COMPLEX	Keta	237	176	255
PALAEOPROTEROZOIC	Bgr		Mainly granitoid rocks				BIRIMIAN		117	237	176
PALAEOPROTEROZOIC	Br		Undivided; mainly metasedimentary and metavolcanic rocks				BIRIMIAN		176	237	201
Man Made	MM	Man Made	Area of infilled ground					Made Ground hatch symbol	255	255	255
Unknown	UB	Unknown bedrock	Unknown bedrock					Keta area - bedrock below Superficial	255	255	255
NEOPROTEROZOIC	Kw	Undivided Kwahu Group	Undivided mudstones and siltstones			KWAHU	VOLTAIAN		255	148	224
NEOPROTEROZOIC	Os	Undivided Obosum Group	Undivided mudstones, siltstones and sandstones			OBOSUM	VOLTAIAN		224	176	176
NEOPROTEROZOIC	Tz	Todzi sandstones	Pale grey arenites, (?) volcaniclastic sandstones and diamictons	Todzi sandstones			BUEM STRUCTURAL UNIT	Pan-African domain	148	255	148
NEOPROTEROZOIC	Tk	Tokor volcanics	Amygdaloidal and basic intermediate volcanic rocks				BUEM STRUCTURAL UNIT	Pan-African domain	201	176	237
NEOPROTEROZOIC	Pj	Undivided	Undivided mudstones, siltstones and sandstones			OTI--PENDJARI	VOLTAIAN		201	176	148
NEOPROTEROZOIC	Sa	Sang Conglomerate	Conglomerate, poorly sorted; large and small pebbles of quartzite, granite, chert and metamorphic lithologies in a red to purple coarse-grained matrix of arkosic sandstone			OBOSUM	VOLTAIAN		237	148	117

References

British Geological Survey holds most of the references listed below, and copies may be obtained via the library service subject to copyright legislation (contact libuser@bgs.ac.uk for details). The library catalogue is available at: http://geolib.bgs.ac.uk.

Acheampong, S.Y. and Hess, J.W. (2000) Origin of the shallow groundwater system in the southern Voltaian Sedimentary Basin of Ghana: an isotopic approach, *Journal of Hydrology*, 233, p37-53

Affaton, P. (1975) Etudes géologique et structurale du Nord-Ouest Dahomey, du Nord Togo et du Sud-Est de la Haute-Volta: Lab. Sci. Terre St-Jerome Travaux, Marseille, France, no. 10, 201pp

Affaton, P. (1990) Le basin des Volta (Afrique de l'Ouest): une marge passive, d'age proterozoique superieur, tectonisee au Panafricain (600± 50 Ma). These Doct. Sc. Fac. Sci, St-Jerome, Marseille, France, 462pp

Affaton, P. (2008) Lithostratigraphy of the Volta Basin and related structural units. In: Kalsbeek (ed). *The Voltaian Basin, Ghana, Workshop and Excursion*, March 10-17, 2008, Abstract Volume pp. 13-17. GEUS 136pp ISBN 987-87-7871-233-2

Affaton, P., Aguirre, L, and Menot, R-P. (1997). Thermal and geodynamic setting of the Buem volcanic rocks near Tiele, Northwest Benin, West Africa. *Precambrian Research*, 82, p 191-209

Affaton, P., Kroner, A., and Seddoh, K.F. (2000) Pan-African granulite formation in the Kabye massif of northern Togo (West Africa): Pb-Pb zircon ages. *International Journal of Earth Sciences*, 88, 778-790.

Affaton, P. Rahaman, M.A. Trompette, R. and Sougy, J. (1991) The Dahomeyide orogen: tectonothermal evolution and relationships with the Volta Basin, In: Dallmeyer, R.D. and Lécorché (eds). *The West African Orogens and Circum-Atlantic Correlatives*, p107-122

Affaton, P. Sougy, J. and Trompette, R. (1980) The tectono-stratigraphic relationships between the Upper Precambrian and Lower Paleozoic Volta basin and the Pan African Dahomeyide orogenic belt (West Africa). *American Journal of Science,* 280, p224-248

Akah, A.K. (2008) Detrital zircon chronology by LA-ICP-MS: Voltaian sediments from the Gambaga and Kintampo massifs. In: Kalsbeek (ed). *The Voltaian Basin, Ghana, Workshop and Excursion*, March 10-17, 2008, Abstract Volume pp. 55-56. GEUS 136pp ISBN 987-87-7871-233-2

Ako, J.A and Wellmann, P. (1985) The margin of the West African craton: the Voltaian Basin, *Journal of the Geological Society London*, 142, p625-632

Akpati, B.A. (1975) Geological structure and evolution of Keta Basin. *Ghana Geological Survey, Rep. 75/3*

Amard, B. and Affaton, P. (1984) Decouverte de *Chuaria circularis* (acritarchs) dans la bassin de Volta. Age proterozoique terminal de la Pendjari et de la tillite sous-jacent. *C R Academie Science* de Paris, 299 II (14), p975-980

Anani, C. (1999) Sandstone petrology and provenance of the Neoproterozoic Voltaian Group in the southeastern Voltaian Basin, Ghana, *Sedimentary Geology*, 129, p83-98

Anan-Yorke, R. (1971) Geology of the Voltaian Basin – *Special Bulletin of the Geological Survey Department*: 29pp, 6 figs: Accra

Anan-Yorke, R. (1974) Phosphate evaluation project. Report to Director, Geological Survey of Ghana 1966-67. Unpublished Report 15pp

Asare, E, and Klitten, K. (2008) In: Kalsbeek (ed). The Voltaian Basin, Ghana, Workshop and Excursion, March 10-17, 2008, Abstract Volume pp. 61-65. GEUS 136pp ISBN 987-87-7871-233-2

Attoh, K., and Brown, L. (2008) Deep structure of the southeastern margin of the West African Craton from seismic reflection data, offshore Ghana. In: Ennih, N., and Liegeois, J-P (eds). *The Boundaries of the West African Craton*. Geological Society of London Special Publication, 297, p 499-508

Attoh, K., Hawkins, D., and Bowring, S. (1991) U-Pb zircon ages of gneisses from the Pan-African Dahomeyide orogen, West Africa. *EOS Transactions of the American Geophysical Union*, 72, S299.

Attoh, K. Dallmeyer, R.D. and Affaton, P. (1997) Chronology of nappe assembly in the Pan-African Dahomeyide orogen, West Africa: evidence from $^{40}Ar/^{39}Ar$ mineral ages. *Precambrian Research*, 82, p153-171

Attoh, K, Corfu, F, and Nude, P.M. (2007) U-Pb zircon age of deformed carbonatite and alkaline rocks in the Pan-African Dahomeyide suture zone, West Africa. *Precambrian Research,* 155, p 251-260

Ayalew, D., Barbey, P., Marty, B., Reisberg, L., Yirgu, G, and Pik, R. (2002) Source, genesis, and timing of giant ignimbrite deposits associated with Ethiopian continental flood basalts. *Geochimica et Cosmochimica Acta*, 66, p 1429-1448.

Babcock, l.E., Grunow, A.M., Sadowski, G.R, and Leslie, S.A. (2005) *Corumbella*, an Ediacaran-grade organism from the Late Neoproterozoic of Brazil. *Palaeogeography, Palaeoclimatology, Palaeoecology,* 220, p 7-18.

Bar, P. (1977) Geologische Entwicklung der jungprakambrisch-altpalaozoischen Schichtfolgen im sudlichen Randgebiet des Volta-_Beckens (Ghana, W-Afrika) – Giessener Geol. Schr.,m 12: 21-56, 6 Abb.:Giessen

Barfod, G.H., Vervoort, J.D., Montanez, I.P. and Riebold, S. (2004) Lu-Hf geochronology of phosphates in ancient sediments, Goldschmidt Conference Abstract, Copenhagen, Denmark June p 5–11.

Barning, K. (1997) Industrial Mineral Resources of Ghana. Minerals Commission, Ghana

Bardet, (1974) The geology of diamonds: kimberlites of West Africa. Mem. BRGM 83 (1974) p178-212

Bates, D.A. (1954) Geological map of Ghana

Bell, S.W. (1964) Some comments on the tillites from the Buem formation of Upper Precambrian age, from the Volta region of Ghana, West Africa: Geological Magazine, v.101, p564-565

Benham A J, Brown, T J, MacKenzie A C and Idoine N E, 2007. British Geological Survey, African Mineral Production 2001–2005

Berrangé, J.P. (1991) Aerial photography, photogeological interpretation and mapping: course notes. *British Geological Survey Technical Report WC/91/36.* 75pp

Bertrand-Sarfati, J, Moussine-Pouchkine, A, Affaton, P, Trompette, R, and Bellion, Y. 1991. Cover sequences of the West African Craton. In: R.D. Dallmeyer and J.P. Lecorche (eds) The West African orogens and circum-Atlantic correlatives, pp. 74-82. Springer-Verlag: Berlin Heidelberg

Black, R. (1967) Sur l'ordonnance des chaines metamorphiques en Afrique Occidentale: *Chronique Mines et Recherché Miniere*, no. 364, p225-238.

Blay, P.K. (1983) The stratigraphic correlation of the Afram Shales of Ghana, West Africa. *Journal of African Earth Sciences*, v 1, p9-16.

Bonham-Carter, G.F. (1994). Geographic Information Systems for Geoscientists, Modelling with GIS. Pergamon, Oxford, 398pp

Bozhko, N.A. (1967) The stratigraphy and tectonics of the Voltaian basin, and the Akwapim-Togo (Atacorian) fold belt: *NEDRA*, v 17, p20-26

Bozhko, N.A. (1969a) Concerning the existence of a Riphean geosynclial area in West Africa: *Izvestija Vysshih Uchebnya Zavedenij Geologija i Razvedka*, no. 5, p21-26

Bozhko, N.A. (1969b) Stratigraphy and tectonics of the Voltaian basin. V. Coll. Geol. Afric., Clermont-Ferrand, 9-12 avril. Resume des Comm : *Ann. Faculty Science University of Clermont Ferrand*, no 41, Geol. et Miner., 19, p3-4

Bozhko, N.A. (1994) Program of joint Ghana-Russian comprehensive geological studies in the central and eastern parts of Ghana. Ghana Geological Survey Special Report, p 6 - 9 (unpublished)

Bozhko, N.A. (2008). Stratigraphy of the Volta Basin on evidence derived from borehole drillings. In: Kalsbeek (ed) *The Voltaian Basin, Ghana Workshop and Excursion*, March 10-17, 2008, Abstract Volume. pp 7-12. ISBN 978-87-7871-233-2

Bozhko, N.A. et al, (1964) Geological Report on the Volta Basin Ghana (unpublished)

Canales, D.G. and Norman, D. I. (2003) The Akwatia diamond field, Ghana, West Africa – Source rocks, accessed April 2003, at URL:

www.gsa.confex.com/gsa/2003AM/finalprogram/abstract_63618.htm

Carney J, Jordan C.J., and Thomas C.W. (2008) Voltaian Basin Workshop, March 2008, Accra: Field excursion guide and notes. In: Kalsbeek (ed) The Voltaian Basin, Ghana Workshop and Excursion, March 10-17, 2008, Abstract Volume. pp 107-132. ISBN 978-87-7871-233-2

Crabaugh, M. & Kocurek, G. (1993). Entrada Sandstone: an example of a wet aeolian system. In: *The Dynamics and Environmental Context of Aeolian Sedimentary Systems* (edited by Pye, K.). *Geological Society Special Publication* 72. The Geological Society, London, p 103-126.

Clauer, N. Caby, R. Jeannette, D. and Trompette, R. (1982) Geochronology of sedimentary and metasedimentary Precambrian rocks of the west African craton. *Precambrian Research*, 18, p53-72

Clauer, N, and Deynoux, M. (1987) New information on the probable isotopic age of the Late Proterozoic glaciation in West Africa. *Precambrian Research*, 37, p 89-94.

Cooper, V.G.G. (1926) *Ann. Rept. Gold Coast Geological Survey*, April 1925 - March 1926, p13 – 15

Crowe, W.A, and Jackson-Hicks, S. (2008) In: Kalsbeek (ed). *The Voltaian Basin, Ghana, Workshop and Excursion*, March 10-17, 2008, Abstract Volume pp. 31-38. GEUS 136pp ISBN 987-87-7871-233-2

Dallmeyer, R.D., and Lecorche, J.P. (1991) Introduction. In: Dallmeyer, R.D. and Lécorché (Eds). *The West African Orogens and Circum-Atlantic Correlatives*, p 3-5

Davies, J. and Cobbing, J. (2002) Low-permeability rocks in sub-Saharan Africa: An assessment of the hydrogeology of the Afram Plains, Eastern region, Ghana. *British Geological Survey, Internal Report*, CR/02/137N

Deynoux, M, Affaton, A, Trompette, R, and Villeneuve, M. (2006). Pan-African tectonic evolution and glacial events registered in Neoproterozoic to Cambrian cratonic and foreland basins of West Africa. *Journal of African Earth Sciences*, 46, 397-426.

Drury, S.A. (2001). Image interpretation in Geology. 3rd Edition. Blackwell Science. 304pp

Edmonds, E.A. (1956) The Geology of the Bawku – Gambaga Area. Gold Coast Geological Survey Bull. No.19, 54pp

Feybesse, J-L, Billa, M, Guerrot, C, Duguey, E, Lescuyer, J-L, Milesi, J-P. and Bouchot, V. (2006). The palaeoproterozoic Ghanaian province: geodynamic model and ore controls, including stress modeling. *Precambrian Research*, 149, p 149-196.

Gaisie A, J. S. and Winter (1974) Tillites in the Togo formation in Ghana. *Geological Magazine*, 111, p253-254

Glazner, A.F., and Bartley, J.M. (1994) Eruption of alkalic basalts during crustal shortening in southern California. *Tectonics,* 13, p 493-498

Grant, N.K. (1967) Complete late Pre-Cambrian to early Palaeozoic orogenic cycle in Ghana, Togo and Dahomey. *Nature*, 215, p609-610

Grant, N.K. (1969) The Late Precambrian to Early Paleozoic Pan – African Orogeny in Ghana, Togo, Dahomey and Nigeria: *Geol. Soc. America Bull*., 80, p45 – 56.

Grant, N.K. (1973) Orogeny and Reactivation to the West and Southeast of the West African Craton. In: *The Ocean Basins and Margins: Volume 1 The South Atlantic*, Nairn E.M and Stehli, G.F. (eds), p447-485

Griffis, R.J. and Agezo, F.L. (2000) Mineral Occurrences and exploration potential of Northern Ghana. Minerals Commission

Hall, M. Bateson, L. and Jordan, C.J. (2006) ERDAS Imagine 8.5 & 8.6 training manual. *British Geological Survey Internal Report.* 71pp

Hall, A.M., Thomas, M.F. and. Thorp M.B (1985) Late Quaternary alluvial placer development in the humid tropics: the case of the Birim Diamond Placer, Ghana. *Journal of the Geological Society of London*, 142, p777-778

Hantzschel, W, and reineck, H-E. (1968) Fazies-Untersuchungen im hettangium von helmstedt (Niedersachsen). *Mitt. Geol. Staatsinst. Hamburg*, 37, p 5-39

Hastings, D.A. (1983) On the tectonics and metallogenesis of West Africa; a model incorporating new geophysical data. *Geoexploration*, 20, p 295-327

Hetherington L.E., Brown, T.J., Benham A.J., Bide T., Lusty P.A.J., Hards V.L., Hannis S.D., Idoine N.E., MacKenzie A.C. (2008). British Geological Survey, World Mineral Production 2002–2006

Huntsman-Mapila, P., Tiercelin, J-J., Benoit, M., Ringrose, S, B., Diskin, S., Cotton, J, and Hemond, C. (2009) Sediment geochemistry and tectonic setting: Application of discrimination diagrams to early stages of intracontinental rift evolution, with examples from the Okavango and southern Tanganyika rift basins. *Journal of African Earth Sciences*, 53, p33-44.

Iddrisu Y. (1987) Rock phosphate prospects in Ghana. In: Wachira JK and AJG Notholt (eds) Agrogeology in Africa. Commonwealth Science Council, Technical Publication Series 226: p 67-76

Jones, W.B. (1990) The Buem volcanic and associated sedimentary rocks, Ghana: a field and geochemical investigation. *Journal of African Earth Sciences*, 11, p 373-383

Jordan C.J. (2006) Introduction to ERMapper 7 for satellite image processing – Ghana Airborne Geophysics Project. *British Geological Survey Internal Report*. 24pp

Jordan C.J., Carney J.N., McEvoy F.M., Turner P., Hall M., Bateson L.B., Thomas C.W. and McManus K. (2006) Ghana airborne geophysics project: BGS Phase 1 Report. Financed by the 8th European Development Fund to the Government of Ghana, Project No. 8 ACP GH 027/13, under the Mining Sector Support Programme. British Geological Survey Commissioned Report, CR/06/235. 167pp.

[1]Jordan C.J., Carney J.N., Thomas C.W. and McDonnell P. (2008) Application of remote sensing and field mapping to a revision of the geology of the Volta Basin. In: Kalsbeek (ed) *The Voltaian Basin, Ghana Workshop and Excursion,* March 10-17, 2008, Abstract Volume. pp 87-90. ISBN 978-87-7871-233-2.

[2]Jordan C.J., Carney J.N., Turner P., Bateson L., McDonnell P. and Thomas C.W. (2008) Application of digital data to the Airborne Geophysics Project in the Volta Basin. In: Kalsbeek (ed) *The Voltaian Basin, Ghana Workshop and Excursion*, March 10-17, 2008, Abstract Volume. pp 91-94. ISBN 978-87-7871-233-2.

Junner, N.R. (1935) Gold in the Gold Coast. Gold Coast Geological Survey Memoirs, Accra.

Junner, N.R. (1940) Geology of the Gold Coast and Western Togoland, with revised geological map. (1:1 000 000) *Gold Coast Geological Survey Department Bulletin*, No.11, 40pp

Junner, N.R. (1943), The diamond deposits of the Gold Coast with notes on other diamond deposits in West Africa: *Gold Coast Geological Survey Department Bulletin,* No.12, 55pp

Junner, N.R and Hirst, T. (1946) The geology and hydrogeology of the Volta Basin. *Mem. Gold Coast Geological Survey*, 8, 50pp.

Junner, N.R. and Service, H. (1936) The Geology and Hydrogeology of the Voltaian Basin. *Gold Coast Geological Survey Mem.* 8, 51pp.

Kalsbeek F (2008) The Voltaian Basin, Ghana, Workshop and Excursion, March 10-17, 2008, Abstract Volume. GEUS 136pp ISBN 987-87-7871-233-2

Kalsbeek F., Frei, D. and Affaton, P. (2008) Detrital zircon ages from the Volta Basin and adjoining Pan-African thrust sheets in Ghana. In: Kalsbeek (ed). *The Voltaian Basin, Ghana, Workshop and Excursion*, March 10-17, 2008, Abstract Volume pp. 51-53. GEUS 136pp ISBN 987-87-7871-233-2.

Kalvig, P. (2008) A conceptual geological model of the Voltaian basin, derived from image interpretation and field mapping) In: Kalsbeek (ed). *The Voltaian Basin, Ghana, Workshop and Excursion*, March 10-17, 2008, Abstract Volume pp. 25-31. GEUS 136pp ISBN 987-87-7871-233-2

Kalvig, P, and Vosgerau, H.J. (2008) Lithostratigraphy of the Neoproterozoic Kintampo Massif. In: Kalsbeek (ed). *The Voltaian Basin, Ghana, Workshop and Excursion*, March 10-17, 2008, Abstract Volume pp. 45-50. GEUS 136pp ISBN 987-87-7871-233-2.

Lutz, A, Thomas, J.M, Pohll, G, and McKay, W.A. (2007). Groundwater resource sustainability in the Nabogo Basin of Ghana. *Journal of African Earth Sciences,* 49, 61-70.

Van Kauwenbergh, S.J. Johnson, A.K.C. McClellan, G.H. and Mueller H.W. (1991). Evaluation of the underdeveloped phosphate deposits of the Volta Basin and West Africa; Benin, Burkina Faso, Ghana, Mali, Mauritania and Niger. International Fertilizer Development Centre, Muscle Shoals, Alabama, USA, 237pp. 1991)

Kesse, G.O. (1974) Bauxite deposits of Ghana. Geological Survey Report No 75/2

Kesse, G.O. (1985) The Mineral and Rock Resources of Ghana, Balkema, Rotterdam, 610pp

Knoll, A.H. (2000) Learning to tell Neoproterozoic time. *Precambrian Research*, 100, p 3-20.

Knoll, A.H, Walter, M.R, Narbonne, G.M, and Christie-Blick, N. (2004) A new period of time for the geologic time scale. *Science*, 305, p 621-622.

Langford, R. P. (1989) Fluvial-aeolian interactions: Part I, modern systems. *Sedimentology,* 36, 1023-1035.

Leprun, J.C. and Trompette, R. (1969) Subdivision du Voltaïen du massif de Gobnangou (République de Haute-Volta) en deux séries discordantes séparées par une tillit d'âge éocambrien probable: Acad Sci. Paris Compte rendu, D v. 269, p. 3251-3261

Leube, A., Hirdes, W. Mauer, B. and Kesse, G. O. (1990) The Early Proterozoic Birimian Supergroup of Ghana and some aspects of its associated gold mineralisation. *Precambrian Research*, 46, p 139-165

Mason, D. (1963) The Geology of the ¼º Field Sheets No. 132 – Bompata N.E. *Ghana Geological Survey Bull*. No. 33, 31 pp

Mathers, S.J. and Northolt, A.J.G. (1994) Industrial minerals in developing countries. *British Geological Survey: Geosciences in international development Series*, No. 18, 272 pp

McDonnell P, Jordan C J, Carney J, and Thomas C (2008) Mineral prospectivity modelling in Ghana's Volta Basin, utilizing ArcSDM to model geological and geophysical data. In: Kalsbeek (ed) *The Voltaian Basin, Ghana Workshop and Excursion*, March 10-17, 2008, Abstract Volume. pp 95-98. ISBN 978-87-7871-233-2

Minerals Commission (2002) Gold Deposits of Ghana, Minerals Commission, Accra, Ghana

Mitchell, J. (1960) Limestones of Ghana, *Ghana Geological Survey Bulletin* No. 23

Moon, P.A. and Mason, D., 1967: The Geology of the ¼º Field Sheets Nos. 129 and 131, Bompata S.W. and N.W. *Ghana Geological Survey Bulletin,* 31, 45 pp

North American Commission on Stratigraphic Nomenclature (1983). In: *American Association of Petroleum Geologists Bulletin*. V.63 No.5, pp. 841-875.

Nédélec, A. Affaton, P. France-Lanord, C. Charrière, A. and Alvaro, J. (2007) Sedimentology and chemostratigraphy of the Bwipe Neoproterozoic cap dolostones (Ghana, Volta Basin): a record of microbial activity in a peritidal environment. *C. R. Geoscience*, 339 (2007) p 223-239

Osae, S. Asiedu, D.K. Banoeng-Yakubo, B. Koeberl, C. and Dampare, S.B. (2006) Provenance and tectonic setting of Late Proterozoic Buem sandstones of southeastern Ghana: Evidence from geochemistry and detrital modes. *Journal of African Earth Sciences*, 44, p85-96

Paramount Mining (2006). Article access at www.paramountmining.com/ghana.html, November 2006

Petters, S.W. (1991) *Regional Geology of Africa*. Lecture notes in Earth Sciences 40, Springer, Berlin, p 296-302.

Pigois, J.-P., Groves, D. L., Fletcher, I. R., McNaughton, N. J., and Snee, L.
W. (2003), Age constraints on Tarkwaian palaeoplacer and lode-gold formation
in the Tarkwa-Damang district, SW Ghana: Mineralium Deposita, v.38, p. 695–714

Porter, S.M., Knoll, A.H. and Affaton, P. (2004). Chemostratigraphy of Neoproterozoic cap carbonates from the Volta Basin, West Africa. *Precambrian Research*, 130, 99-112.

Saunders, S.R. (1970) Early Paleozoic Orogeny in Ghana: Foreland Stratigraphy and Structure. *Geol. Soc. America Bull*., 81, p.233 – 240

Scheiber, J. and 6 others (eds) (2007) *Atlas of microbial mat features preserved within the clastic rock record.* Elsevier, 324 pp.

Schlutter, T. (2006) Geological Atlas of Africa, with Notes on Stratigraphy, Economic Geology, Geohazards and Geosites of Each Country

Shackleton, R.M. (1971) On the south-eastern increase in deformation and metamorphism at the margin of the Pan-African domain in Ghana: Leeds University Research. Inst. African Geology, 15th, Annual Report., p2-7

Sheldon, R.P. (1986) Potential phosphate resource assessment of Ghana. Unpublished report to United Nations Department of Technical Cooperation for Development, 33pp

Sougy, J. (1970) Le basin de la Volta et son contexte (Ghana, Niger, Togo, Dahomey, Haute Volta). Etude bibliographique interpretee. *Travaux des Laboratoires des Sciences de la Terre* St-Jerome, Marseille, X-12, 78pp.

Soviet Geological Survey Team (1964-66) Geological Map of the West Part of Ghana, scale 1:250,000, Geological Survey Department Ghana

van Straaten, P. (2002) Rocks for Crops: Agrominerals of sub-Saharan Africa. ICRAF, Nairobi, Kenya, 338pp.

Tompkins, L.A., and Haggerty, S.E., 1984, The Koidu Kimberlite Complex, Sierra Leone, geological setting, petrology, and mineral chemistry, In Kornprobst, J., (ed.), *Kimberlites and Related Rocks*: Amsterdam, Elsevier, 466 p.

Trompette, R. (1969) Les stromatolites du “Precambrien superieur” de l’Adrar de Mauritania (Sahara occidental): *Sedimentology*, v.13 p123-154

Trompette, R. (1986) Phosphorites of the Northern Volta Basin. In Notholt AJG, Sheldon RP and DF Davidson (eds). *Phosphate deposits of the world. Vol. 2: Phosphate rock resources*, Cambridge University Press, Cambridge, UK, p214-218

Vasconcelos, P.M. Brimhall, G.H. Becker, T.A. and Renne, P.R. (1994) $^{40}Ar/^{39}Ar$ analysis of supergene jarosite and alunite: Implications to the palaeoweathering history of western USA and West Africa. *Geochimica et Cosmochimica Acta*, 58, p401-420

Viljoen, J.H.A, Gyapong, W, Le Berre, W, Reddering, J.S.V, Thomas, E, and Atta-Ntim, K. (2008) Geology of Sheet 1001D South of Gambaga. In: Kalsbeek (ed). *The Voltaian Basin, Ghana, Workshop and Excursion* March 10-17, 2008, Abstract Volume pp. 39-40. GEUS 136pp ISBN 987-87-7871-233-2.

Watt, D.S. (1977) Premause-1 Well resume. *Unpublished report of SHELL International*, The Hague, Netherlands.

Watts, Griffis and McQuat Ltd., (1995) Recommendations for regional surveys and government policy initiatives to stimulate mineral exploration in Ghana – Data evaluation phase: Final Report; Ghana mineral resource assessment project; unpublished report, 93pp

Wright, J. B. Hastings, D.A. and Jones W.B. (1985) Geology and Mineral Deposits of West Africa. London: Allen and Unwin, 189 pp

Wu, H, Zhang, S, Jiang, G, and Li, Haiyan. (2005) Magnetic susceptibility variations of the Ediacaran cap carbonates in the Yangtze platform and their implications for palaeoclimate. *Chinese Journal of Oceanology and Limnology*, 23, p 291-298

Zitzmann, A. Kiessling, R. and Loh, G. (1997) Geology of the Bui Belt Area in Ghana, *Geologisches Jahrbuch*, Reihe B, Heft 88, p 7-111